

DIGITAL ACCESS TO SCHOLARSHIP AT HARVARD
DASH.HARVARD.EDU

HARVARD LIBRARY


Stereo- and Site-Selective Glycosylation Catalyzed by Bis-Thioureas

Citation

Li, Qiuhan. 2021. Stereo- and Site-Selective Glycosylation Catalyzed by Bis-Thioureas. Doctoral dissertation, Harvard University Graduate School of Arts and Sciences.

Link

https://nrs.harvard.edu/URN-3:HUL.INSTREPOS:37368297

Terms of use

This article was downloaded from Harvard University's DASH repository, and is made available under the terms and conditions applicable to Other Posted Material (LAA), as set forth at

https://harvardwiki.atlassian.net/wiki/external/NGY5NDE4ZjgzNTc5NDQzMGIzZWZhMGFlOWI2M2EwYTg

Accessibility

https://accessibility.huit.harvard.edu/digital-accessibility-policy

Share Your Story

The Harvard community has made this article openly available.
Please share how this access benefits you. Submit a story

HARVARD UNIVERSITY
Graduate School of Arts and Sciences

DISSERTATION ACCEPTANCE CERTIFICATE

The undersigned, appointed by the

Department of Chemistry & Chemical Biology

have examined a dissertation entitled:

Stereo- and Site-Selective Glycosylation Catalyzed by Bis-Thioureas

presented by: Qiuhan Li

candidate for the degree of Doctor of Philosophy and hereby certify that it is worthy of acceptance.

Signature _____
Typed name: Professor Eric N. Jacobsen

Signature _____
Typed name: Professor Christina Woo

Signature _____
Typed name: Professor Theodore A. Betley

Date: 5 May 2021

Stereo- and Site-Selective Glycosylation Catalyzed by Bis-Thioureas

A dissertation presented by

Qiuhan Li

to

The Department of Chemistry and Chemical Biology

in partial fulfillment of the requirements

for the degree of

Doctor of Philosophy

in the subject of

Chemistry

Harvard University

Cambridge, Massachusetts

May 2021

© 2021 Qiuhan Li
All rights reserved.

Dissertation Advisor: Eric N. Jacobsen *Qiuhan Li*

Stereo- and Site-Selective Glycosylation Catalyzed by Bis-Thioureas

Abstract

Carbohydrates play numerous important roles in biological systems such as energy storage, structural support, and cellular recognition and signaling. Glycosylation of small molecules, peptides, and protein pharmaceuticals has shown significant potential for enhancing biodistribution by affecting molecular structure, hydrophilicity, stability, and bioavailability. With the goal of understanding the biological function of oligosaccharides, chemical glycosylation strategies have been developed to control the stereochemical outcome of sugar couplings. Glycosylation involves coupling partners that are stereochemically complex and densely functionalized, and the reactivity and stereoselectivity of glycosylation strongly depend on the identity of sugar coupling partners. Therefore, the development of a unified strategy for stereo- and site-control in the construction of glycosidic linkages presents a fundamental challenge. The dissertation presented herein describes the development of bis-thiourea-catalyzed stereo- and site-selective glycosylation of carbohydrates and complex pharmaceuticals under mild conditions.

In Chapter 1, we describe the current methods for the construction of β-1,2-*cis* glycosidic linkages and their limitations. Although high stereoselectivity can be achieved with current strategies, they employ coupling partners that require multi-step syntheses and highly Lewis acidic activation conditions. We also review the state-of-the-art strategies for catalyst-controlled site-selective glycosylation. Although *cis*-diols can be easily distinguished by current methods and

undergo stereoselective glycosylation with excellent site-control, site-selective glycosylation of *trans*-diols still presents a fundamental challenge.

In Chapter 2, we describe the development of highly β-selective, bis-thiourea-catalyzed 1,2-*cis*-*O*-pyranosylations employing easily accessible acetonide-protected donors to address the limitations of current methodologies. A wide variety of alcohol nucleophiles, including complex natural products, glycosides, and amino acids were β-mannosylated and rhamnosylated successfully using an operationally simple protocol under mild and neutral conditions. Less nucleophilic acceptors such as phenols were also glycosylated efficiently in excellent yields and with high β-selectivities. Computational analysis supports our proposal that the enhancement in β-selectivity observed with acetonide protection is achieved by the acceleration of a stereospecific S_N2-type pathway promoted by the bis-thiourea catalyst.

In Chapter 3, we describe catalyst-controlled, highly stereo- and site-selective glycosylations for the construction of β-1,2-*trans* and β-1,2-*cis* glycosidic linkages. The development of catalysts that effectively engage in CH/π interactions with glycosidic nucleophiles was critical for controlling site-selectivity. Kinetic and computational studies provided evidence that catalyst-controlled site-selectivity is achieved by stabilizing the rate-limiting transition state through attractive noncovalent interactions.

Table of Contents

Title ... i

Copyright ... ii

Abstract ... iii

Acknowledgement ... vii

List of Abbreviations ... xi

Chapter 1 Current Methodologies for Stereo- and Site-Selective Synthesis of β-1,2-*cis*-Glycosidic Linkages ... 1

1.1 Introduction ... 1

1.2 General Strategy for β-1,2-*trans* Glycosylation ... 2

1.3 Prevalence of β-1,2-*cis* Glycosidic linkages and the Challenges of Their Synthesis ... 5

1.4 Current Methodologies for β-1,2-*cis* Glycosylation and Their Limitations ... 8

1.5 Summary for β-1,2-*cis* Glycosylation Methods and Outlook ... 33

1.6 Current Methodologies for Site-Selective Glycosylation and Their Limitations ... 40

1.7 Summary for Site-Selective Glycosylation Methods and Outlook ... 50

Chapter 2 Highly Selective β-Mannosylations and β-Rhamnosylations Catalyzed by Bis-thioureas ... 53

2.1 Introduction ... 53

2.2 Our Approach ... 55

2.3 Catalyst and Reaction Optimization ... 58

2.4 Computational Analysis ... 64

2.5 Acceptor Scope of β-Mannsoylation and Hammett Study ... 67

2.6 Acceptor Scope of β-Rhamnosylation ... 73

2.7 Deprotection and One-pot Mannosylation and Deprotection ... 75

2.8 Conclusion and Outlook ... 76

2.9 Progress toward Chromatography-Free Synthesis of Bis-thioureas ... 77

2.10 Experimental Information ... 80

2.10.1 General Experiment Procedures, Materials, and Instrumentation ... 80

2.10.2 Additional Substrates for β-Mannosylations and β-Rhamnosylations ... 82

2.10.3 Synthesis and Characterization of Glycosyl Phosphates ... 83

2.10.4 Synthesis and Characterization of Acceptors ... 86

2.10.5 Synthesis and Characterization of Catalysts ... 90

2.10.6 Anomeric Configuration Assignment ... 90

2.10.7 Synthesis and Characterization of Products 93
2.10.8 X-Ray Crystallographic Structure Data 130
2.10.9 Computational Analysis 146
Chapter 3 Catalyst-Controlled Stereo- and Site-Selective Glycosylation Catalyzed by Bis-Thioureas 167
3.1 Introduction 167
3.2 Catalyst Optimization 171
3.3 Acceptor Scope 179
3.4 Mechanistic Studies 183
3.5 Iterative Glycosylation 193
3.6 Initial Attempt to Develop Site Selective Benzylation 194
3.7 Conclusion and Outlook 196
3.8 Experimental Information 196
3.8.1 General Experiment Procedures, Materials, and Instrumentation 196
3.8.2 Additional Catalyst Optimization Data 198
3.8.3 Reaction Condition Optimization 199
3.8.4 Additional Substrates for Site-selective Galactosylation and Mannosylation 199
3.8.5 Synthesis and Characterization of Catalysts 200
3.8.6 Synthesis and Characterization of Acceptors 227
3.8.7 Synthesis and Characterization of Glycosyl Phosphates 245
3.8.8 Anomeric Configuration and Connectivity Assignment 246
3.8.9 Synthesis and Characterization of Products 247
3.8.10 Michaelis-Menten Kinetics 280
3.8.11 Initial Rate Comparison between Polyols and Mono-protected Analogs 290
3.8.12 Interaction Energy Calculation 290
3.8.13 Transition State Calculation 306

Acknowledgement

I would like to begin by thanking my research advisor, Professor Eric Jacobsen, for his continued support and mentorship during graduate school. I appreciated Eric for convincing me to join the glycosylation subgroup. It has been a great journey to work on such interesting, challenging, and rewarding projects. The way Eric approaches research projects and scientific problems has profound influence on me, from which I will forever benefit throughout my scientific career. I have learned how to become a better scientist from his ability to articulate difficult concepts, his remarkable communication skills, and his high level of professionalism. Eric has brought in a group of brilliant scientists and fostered a collaborative and constructive environment where people have the freedom to explore innovative ideas and learn from each other. It has been a great privilege to have the opportunity to learn from him and the entire Jacobsen group.

I am very grateful to have Professor Christina Woo and Ted Betley on my committee. During each of my GAC meetings, they provided with me their thoughtful feedback and offered their new perspectives on the research I presented. Their comments encouraged me to think more broadly on the future directions of my projects and make them as impactful as possible. Their encouragement and support have been very valuable throughout my time in graduate school.

I would like to extend my gratitude to Professor Corinna Schindler, my undergraduate research advisor at University of Michigan. I am very thankful that Corinna was willing to take me in her lab when I was an inexperienced sophomore without any previous laboratory experiences or any organic chemistry knowledge. I learned organic laboratory techniques directly from her, and working with her, side by side, has been an invaluable experience to me. She was extremely patient, caring, approachable, and supportive. I was very grateful to have Corinna as my mentor when I was first introduced to organic chemistry. I could not ask for a better mentor. The positive

experience working in her lab was the reason why I decided to pursue my graduate study in catalysis.

I want to thank the entire Jacobsen group for their support during the last five years. They have created a congenial environment. It has been a great pleasure to get to know them and working with and learning from them. Thanks, Nicole Minotti, for tirelessly keeping the lab running smoothly. I cannot think what the lab would look like without her. She was always available and happy to answer any questions. Thank you for your support.

I have been fortunate to have great mentors during my time in graduate school. Dr. Samuel Levi has been a great mentor for my first three years in the Jacobsen group. He introduced me to glycosylation, and I learned so much about the field from him. He was extremely passionate, enthusiastic, and knowledgeable. He has given my invaluable feedback on my research, and his excitement about chemistry has inspired me to work hard. The way he tackled research problems has significant influence on how I approach scientific problems. I enjoyed talking to him in lab every day, and I always learned something, whether it is about chemistry or random facts, after each conversion. Dr. Shauna Paradine was my first mentor from the Jacobsen group. She took me under her wing as a summer rotator. She made me feel welcome when I first got to know the Jacobsen group. Her amazing work ethics, strong emphasis on lab safety, and dedication motivated me to become a better scientist. I cannot wait to see the achievements coming out from her independent research group.

I have also had the great pleasure to get to know many talented and fabulous graduate students and postdocs. Dr. Andrew Bendelsmith has been a great friend. Andrew reached out to me and encouraged me to do another rotation with the Jacobsen group, for which I will always be grateful. Whenever I had questions about chemistry, Andrew was always there to help. He is one

of the most friendly, kind, and thoughtful people I have met. I enjoyed talking about random things with him and teaching him Chinese. Working with him in the same bay has been one of the best memories of my time in the lab. Both Drs. Prithvi Vangal and Moriana Haj have been great officemates. I am so glad that we shared the same office for the past four years. I always enjoyed our conversions in the office. They are both fantastic chemists and wonderful, kind, supportive, and empathetic people. Thank you, Prithvi, for helping me navigate OPT applications, revising my paper manuscripts, and discussing any research problems I had. Thank you, Moriana, for all your support and all the fun conversions about red line, politics, and many other topics. I know both of you will be successful no matter what you choose to do in the future. Dr. Diego Diaz is a great officemate and a wonderful friend. Diego joined the lab in January 2020, and we quickly became good friends, but then pandemic forced us to quarantine at home. I wished we could spend more time together. “Monthly chat” with Diego has kept me sane through the pandemic. I enjoyed bouncing around project ideas with him. He is a very knowledgeable, talented, and thoughtful person. I wish him a wonderful rest of his postdoc, and good luck to his job applications. He has accomplished a lot so far, and I am sure that the future holds great things for him! Dr. Katrina Mennie is an amazing scientist. I always admire her work ethics and determination. Talking to Katrina, Sam, and Andrew in the front office has been one of my best times in the lab. Thank you, Dr. Elias Picazo, for being a genuine and thoughtful labmate. I enjoyed our conversions about NIO, and sorry that I was not able to bring “inside information” to you. Good luck to your independent career at USC. Corin has been a wonderful collaborator on the site selective glycosylation. He is very talented and extremely knowledgeable about computations. I am sure he will have a successful PhD. Thank you, Dennis Kutateladze and Hayden Sharma, for being wonderful classmates. I have learned a lot from your enthusiasm about chemistry and scientific

thinking. Martin Reiterer has also been a great labmate. I will always remember all the fun conversations we have had.

I cannot thank enough for my parents for their unconditional support. They supported my dream to come to the US for education. Although it was hard for them to not miss me during holiday seasons when family members gather for celebration, they were understanding when I could not go back. They supported every decision I made and never wanted to put any pressure on me. Their confidence in me has encouraged me to do my best. I am extremely grateful to have such supportive parents. Yunjie Yang, my best friend for the past ten years, has always been there during my ups and downs. He was there when I had something to celebrate, and he was also there when I encountered problems. He always encouraged me to try my best and motivated me to pursue my goals through determination. I cannot thank him enough for his support!

List of Abbreviations

Å	Angstrom
Ac	acetyl
aq.	aqueous
alk	alkyl
Ar	aryl
Bn	benzyl
Bu	butyl
Bz	benzoyl
˚C	degree Celsius
c	centi
cis	on the same side
CPME	cyclopentyl methyl ether
δ	chemical shift in parts per million
d	day(s); doublet (spectral)
d.r.	diastereomeric ratio
DCM	dichloromethane
DFT	density functional theory
DMSO	dimethyl sulfoxide
DMTST	dimethyl(methylthio)sulfonium trifluoromethanesulfonate
DTBMP	2,6-di-*tert*-butyl-4-methylpyridine
Et	ethyl
EtOAc	ethyl acetate
ESI	electrospray ionization
eq.	equivalent

g	gram
gem	geminal
h	hour(s)
HPLC	high performance liquid chromatography
HRMS	high resolution mass spectrometry
Hz	hertz
i	iso
J	coupling constant
k_{cat}	catalytic rate constant
K_M	Michaelis constant
k_{obs}	observed rate constant
L	liter(s)
LG	leaving group
m	micro
m	meta
m	meter; milli; multiplet(spectral)
M	molar
Me	methyl
min	minute(s)
mol	mole
MS	mass spectrometry
MTBE	methyl *tert*-butyl ether
NMR	nuclear magnetic resonance
o	ortho
OPMP	*para*-methoxyphenoxyl

OTf	trifluoromethanesulfonate
p	para
Ph	phenyl
PMB	*para*-methoxybenzyl
PMP	1,2,2,6,6-pentamethylpiperidine
Pr	propyl
q	quartet (spectral)
R	rectus
r.r.	regioisomeric ratio
r.t.	room temperature
S	sinister
S_N1	unimolecular nucleophilic substitution
S_N2	bimolecular nucleophilic substitution
t	*tert*, tertiary
trans	on the opposite side
TBAF	tetrabutylammonium fluoride
TBDPS	*tert*-butyldiphenylsilyl
TBS	*tert*-butyldimethyl silyl
TfOH	*triflic acid*
THF	tetrahydrofuran
TMS	trimethylsilyl
TMSOTf	trimethylsilyl trifluoromethanesulfonate
Ts	tosyl
TTBP	2,4,6-tri-*tert*-butylpyrimidine

Chapter 1

Current Methodologies for Stereo- and Site-Selective Synthesis of β-1,2-*cis*-Glycosidic Linkages

1.1 Introduction

Carbohydrates play numerous important roles in biological systems such as energy storage, structural support, and cellular recognition and signaling.[1] Many naturally occurring small molecules are glycosylated, and the sugar moieties are often found to be critical to their biological

[1] Varki, A.; Cummings, R. D.; Esko, J. D.; Stanley, P.; Hart, G. W.; Aebi, M.; Darvill, A. G.; Kinoshita, T.; Packer, N. H.; Prestegard, J. H.; Schnaar, R. L.; Seeberger, P. H. *Essentials of Glycobiology*, 3rd ed.; Cold Spring Harbor Laboratory Press: New York, 2009.

activity.[2] Glycosylation of small molecules, peptides and protein pharmaceuticals has shown significant potential for enhancing biodistribution by affecting molecular structure, hydrophilicity, stability, and bioavailability.[3] In order to study the functions of oligosaccharides in biological processes, it is necessary to gain access to samples of structurally well-defined oligosaccharides. Therefore, significant efforts have been devoted to the development of stereo- and site selective chemical glycosylation methods. Section 1.2 describes the strategies for the synthesis of β-1,2-*trans* glycosidic linkages. Section 1.3 describes the importance of β-1,2-*cis* glycosides in nature and the unique challenges associated with the construction of β-1,2-*cis* glycosidic linkages. Section 1.4 describes the current methodologies available for β-1,2-*cis* glycosylations and their limitations. Section 1.5 summarizes the methods for β-1,2-*cis* glycosylations and describes how to address the limitations associated with current strategies. Section 1.6 and 1.7 describe reagent-controlled and catalyst-controlled approaches for site selective glycosylation and how a more general method could be developed by relying on attractive noncovalent interactions between catalysts and substrates.

1.2 General Strategy for β-1,2-*trans* Glycosylation

Typically, chemical glycosylation involves the use of stable glycosyl donors bearing a leaving group at the anomeric position for easy handling and long-term storage. The glycosyl donors can be activated under Lewis or Brønsted acidic conditions or using oxidizing reagents to generate highly reactive intermediates such as glycosyl triflates, which are labile toward substitution (Figure 1.1A). The intermediates can react with glycosyl acceptors to generate

[2] Kaplan, J.; Korty, B. D.; Axelsen, P. H.; Loll, P. J. The Role of Sugar Residues in Molecular Recognition by Vancomycin. *J. Med. Chem*. **2001**, *44*, 1837–1840.
[3] For a review, see: (a) Sola, R. J.; Griebenow, K. Effects of Glycosylation on the Stability of Protein Pharmaceuticals *J. Pharm. Sci*. **2009**, *98*, 1223–1245.

glycosidic linkages. One of the key challenges that need to be addressed by chemical glycosylation is how to control the stereoselectivity of the substitution event. The substitution event at the anomeric center can occur via a traditional S_N2 or S_N1 pathway, or somewhere along the continuum connecting the two limiting mechanisms (Figure 1.1B).[4] Although the displacement of leaving groups via an S_N2 or S_N2-like pathway is stereospecific, the addition of glycosyl acceptors to oxocarbenium intermediates can theoretically occur from both α- and β-face, giving rise to a mixture of α- and β-anomers. It has been a heavy focus in the field of chemical glycosylation to develop a general strategy to control the stereoselectivity of substitution.

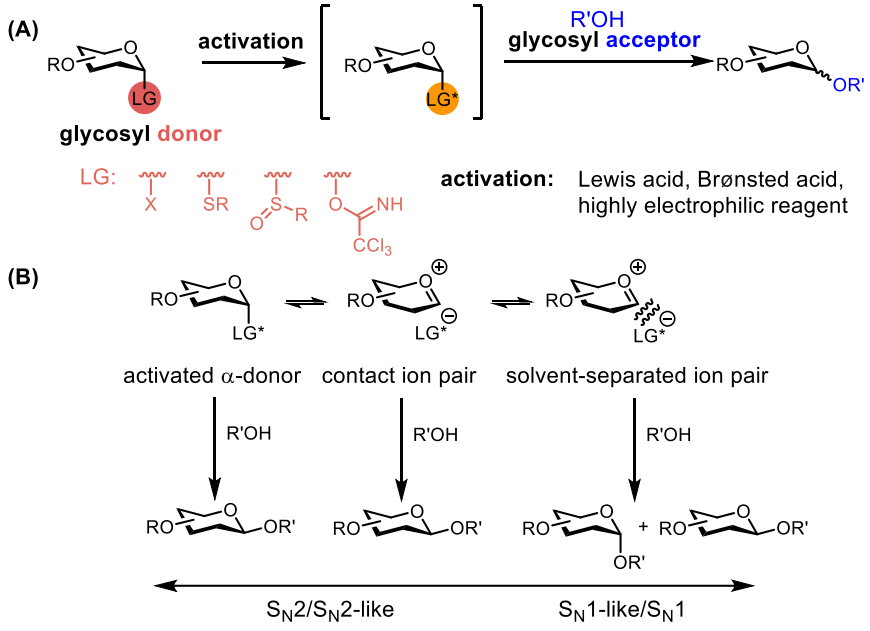


Figure 1.1 (A) Typical strategies for chemical glycosylation. (B) Glycosylation reactions occur along the SN1-SN2 continuum.

[4] Crich, D. En Route to the Transformation of Glycoscience: A Chemist's Perspective on Internal and External Crossroads in Glycochemistry. *J. Am. Chem. Soc.* **2021,** *143*, 17–34.

Over the past several decades, a large library of stable glycosyl donors has been utilized in chemical glycosylation including glycosyl halides[5], thioglycosides[6], glycosyl imidates[7], and glycosyl phosphates[8]. Although numerous chemical glycosylation methods utilizing a wide variety of glycosyl donors have been reported, these methods employ neighboring group participation as the common strategy to impart stereoselectivity in β-1,2-*trans* glycosylation (Figure 1.2).[9] The anchimeric assistance strategy involves the use of participating groups at the C2 position of glycosyl donors, and the canonical participating groups are ester-type protecting groups such as acetate, benzoate, and pivalate. These neighboring groups impart stereoselectivity by forming a *cis*-dioxolenium adduct at the anomeric center. Upon activation of glycosyl donors, participating groups can displace anomeric leaving groups via an S_N2-like pathway or attack the oxocarbenium intermediates via an S_N1-like pathway from the same face, resulting in *cis*-dioxolenium adducts. Glycosyl acceptors can react with the dioxolenium intermediates in a stereospecific invertive manner, resulting in the *trans*-relationship between glycosyl acceptors and the C2 position of glycosyl donors. When the C2 position of glycosyl donors is on the α-face, as in the case of galactose and glucose, invertive substitution of acceptors results in β-1,2-*trans* glycosidic linkages. However, when the C2 position resides on the β-face as seen in mannose and rhamnose, the neighboring group participation strategy will generate α-1,2-*trans* glycosides. The invertive nature of substitution at the dioxolenium intermediates precludes the application of such strategy to

[5] Toshima, K. Glycosyl Halides. In *Glycoscience: Chemistry and Chemical Biology*, Fraser-Reid, B. O.; Tatsuta, K.; Thiem, J., Eds. Springer Berlin Heidelberg: Berlin, Heidelberg, 2008; pp 429–449.
[6] Lian, G.; Zhang, X.; Yu, B. Thioglycosides in Carbohydrate research. *Carbohydr. Res.* **2015,** *403*, 13–22.
[7] Schmidt, R. R.; Michel, J. Facile Synthesis of α- and β-*O*-Glycosyl Imidates; Preparation of Glycosides and Disaccharides. *Angew. Chem. Int. Ed*. **1980**, *19*, 731–732.
[8] Oka, N.; Sato, K.; Wada, T. Recent Progress in the Synthesis of Glycosyl Phosphate Derivatives. *Trends Glycosci. Glycotechnol*. **2012**, *24*, 152–168.
[9] Guo, J.; Ye, X. S. Protecting groups in carbohydrate chemistry: influence on stereoselectivity of glycosylations. *Molecules* **2010,** *15*, 7235–7265.

enforce nucleophile delivery *cis* to the C2 position of glycosyl donors. Therefore, distinct stereocontrol strategies need to be developed for the construction of β-1,2-*cis* glycosidic linkages.

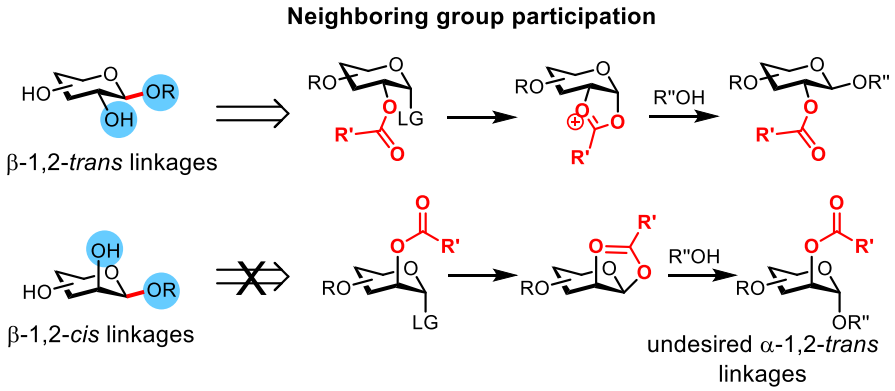


Figure 1.2 Stereochemical outcomes of glycosylation via neighboring group participation.

1.3 Prevalence of β-1,2-*cis* Glycosidic linkages and the Challenges of Their Synthesis

Pyranosides bearing β-1,2-*cis*-*O*-glycosidic linkages are found in many biologically important oligosaccharides that play crucial roles ranging from structural support to cellular recognition (Figure 1.3).[10] β-Mannosides are found at the branch-points of asparagine-linked glycopeptides, the structure of which is known to define unique antibody-effector function for a given isotype.[11] Similar to cellulose, a polymer of β-linked glucose, mannose can also form linear polymers when being β-linked through the C4 position, and the resulting β-mannans are the primary constituent of hard and soft woods.[12]

[10] Varki, A.; Cummings, R. D.; Esko, J. D.; Stanley, P.; Hart, G. W.; Aebi, M.; Darvill, A. G.; Kinoshita, T.; Packer, N. H.; Prestegard, J. H.; Schnaar, R. L.; Seeberger, P. H. *Essentials of Glycobiology*, 3rd ed.; Cold Spring Harbor Laboratory Press: New York, 2009.
[11] Moremen, K. W.; Tiemeyer, M.; Nairn, A. V. Vertebrate Protein Glycosylation: Diversity, Synthesis and Function. *Nat. Rev. Mol. Cell Biol*. **2012**, *13*, 448–462.
[12] Aspinall, G. O. *The Polysaccharides*; Academic Press: London, 1982; Vol. 1.

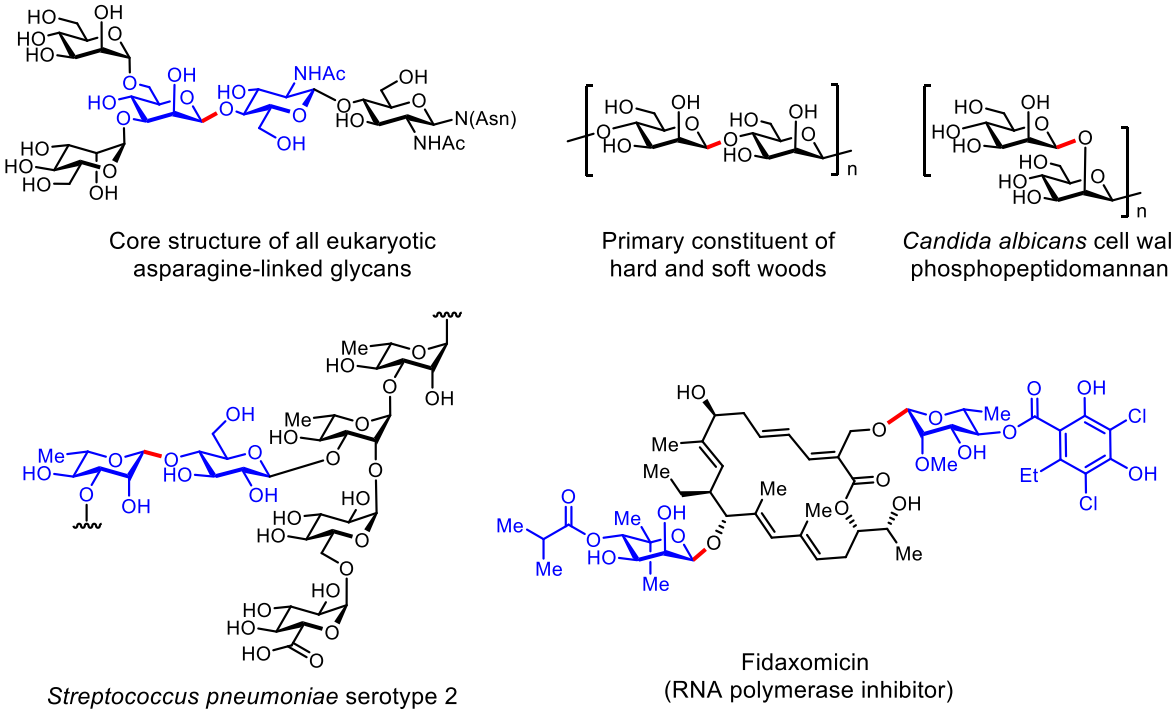


Figure 1.3 Examples of oligosaccharides and natural products containing β-1,2-*cis* glycosides.

β-1,2-*cis*-Linkages are also found in bacterial capsular polysaccharides and biologically active natural products, and improved understanding of their immunological or biological effects may be of value in the development of therapeutics. The β-(1→2)-mannans, the homopolymers of β-mannosides linked through the C2 position, are the critical components of the *Candida albicans* cell wall phosphopeptidomannan and have been shown to be able to elicit specific antibody response against *Candida albicans* in rodent models of systemic and vaginal candidosis.[13] β-Rhamnosides are found in several serotypes of *Streptococcus pneumoniae*, a Gram-positive encapsulated commensal bacterium that is responsible for invasive pneumococcal diseases like

[13] (a) Faille, C.; Michalski, J. C.; Strecker, G.; Mackenzie, D. W. R.; Camus, D.; Poulain, D. Immunoreactivity of neoglycolipids constructed from oligomannosidic residues of the Candida albicans cell wall. *Infect. Immun*. **1990**, *58*, 3537–3544. (b) De Bernardis, F.; Boccanera, M.; Adriani, D.; Spreghini, E.; Santoni, G.; Cassone, A. Protective role of antimannan and anti-aspartyl proteinase antibodies in an experimental model of Candida albicans vaginitis in rats. *Infect. Immun*. **1997**, *65*, 3399–3405.

pneumonia.[14] Significant efforts have been devoted to the development of glycoconjugate vaccines based on synthetic oligosaccharides. In order to conduct systematic structure-activity relationship studies, it is necessary to synthesize a library of synthetic oligosaccharides that resemble the repeating unit of *Streptococcus pneumoniae* capsular polysaccharide. Additionally, β-1,2-*cis* glycosidic linkages are present in many of the members in tiacumicin family of natural products.[15] Fidaxomicin (tiacumicin B), a glycosylated macrolide antibiotic, is an RNA synthesis inhibitor and currently being used in the clinic for the treatment of *Clostridium difficile* infections. Fidaxomicin has also been reported to be active against drug resistant strains of *Mycobacterium tuberculosis*.[16] The promising biological activity of fidaxomicin has attracted significant efforts to develop synthetic routes to access it and its derivatives for bioactivity studies.[17] One of the key challenges associated with the total synthesis of fidaxomicin is the selective construction of the two β-1,2-*cis* glycosidic linkages between the macrocycle and carbohydrate residues.

The challenges associated with the construction of β-1,2-*cis* glycosides have been well-recognized in the field of carbohydrate chemistry (Figure 1.4). β-Glycosides are intrinsically less stable than their α-diastereomers as a result of diminished anomeric stabilization.[18] The $\sigma^*_{C\text{-}O}$ has

[14] Emmadi, M.; Khan, N.; Lykke, L.; Reppe, K.; S, G. P.; Lisboa, M. P.; Wienhold, S. M.; Witzenrath, M.; Pereira, C. L.; Seeberger, P. H. A Streptococcus pneumoniae Type 2 Oligosaccharide Glycoconjugate Elicits Opsonic Antibodies and Is Protective in an Animal Model of Invasive Pneumococcal Disease. *J. Am. Chem. Soc*. **2017**, *139*, 14783–14791.
[15] For a review on the lipiarmycins/tiacumicins, see: Erb, W.; Zhu, J. From natural product to marketed drug: the tiacumicin odyssey. *Nat.Prod. Rep*. **2013**, *30*, 161–174.
[16] Kurabachew, M.; Lu, S. H. J.; Krastel, P.; Schmitt, E. K.; Suresh, B. L.; Goh, A.; Knox, J. E.; Ma, N. L.; Jiricek, J.; Beer, D.; Cynamon, M.; Petersen, F.; Dartois, V.; Keller, T.; Dick, T.; Sambandamurthy, V. K. *J. Antimicrob. Chemother*. **2008**, *62*, 713–719.
[17] (a) Kaufmann, E.; Hattori, H.; Miyatake-Ondozabal, H.; Gademann, K. Total Synthesis of the Glycosylated Macrolide Antibiotic Fidaxomicin. *Org. Lett.* **2015,** *17*, 3514–3517. (b) Hattori, H.; Kaufmann, E.; Miyatake-Ondozabal, H.; Berg, R.; Gademann, K. Total Synthesis of Tiacumicin A. Total Synthesis, Relay Synthesis, and Degradation Studies of Fidaxomicin (Tiacumicin B, Lipiarmycin A3). *J. Org. Chem.* **2018,** *83*, 7180–7205. (c) Norsikian, S.; Tresse, C.; Francois-Eude, M.; Jeanne-Julien, L.; Masson, G.; Servajean, V.; Genta-Jouve, G.; Beau, J. M.; Roulland, E. Total Synthesis of Tiacumicin B: Implementing H-bond-Directed Acceptor Delivery for Highly Selective beta-Glycosylations. *Angew. Chem. Int. Ed.* **2020**, *59*, 6612–6616.
[18] Kirby, A. J. The Anomeric Effect and Related Stereoelectronic Effects at Oxygen; Springer-Verlag: Berlin, 1983.

poor orbital overlap with the nonbonding orbital on the endocyclic oxygen (n_O); therefore, hyperconjugative stabilization from filled n_O orbital to empty $\sigma^*_{C\text{-}O}$ orbital is weak for β-glycosides. Additionally, due to the *cis* relationship between C2 position of glycosyl donors and incoming acceptors, there is significant steric congestion on the β-face of sugars, disfavoring nucleophilic attack from the β-face. The lack of anomeric stabilization and the steric hinderance on the β-face render β-1,2-*cis* glycosylation thermodynamically and kinetically disfavored. Therefore, it has been an important objective in synthetic carbohydrate chemistry to develop selective methods for β-1,2-*cis* glycosylation given the importance of β-1,2-*cis* glycosidic linkages in nature.

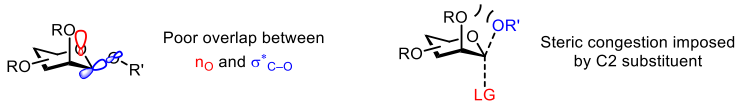


Figure 1.4 Challenges associated with β-1,2-*cis*-pyranosyl glycosidic bond construction.

1.4 Current Methodologies for β-1,2-*cis* Glycosylation and Their Limitations

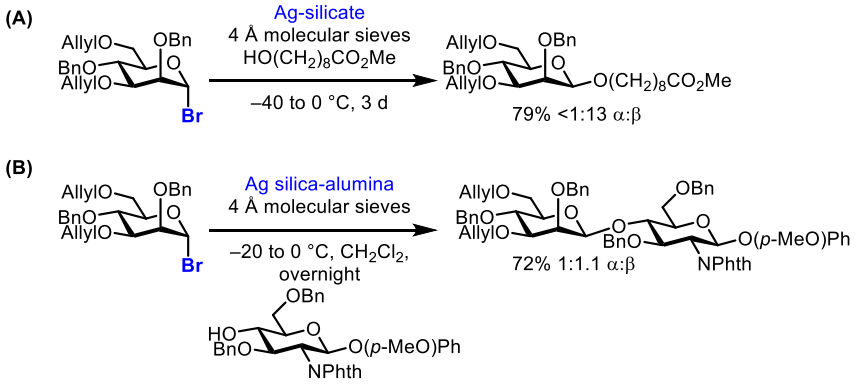


Figure 1.5 Examples of β-1,2-*cis* Glycosylation via Koenigs-Knorr coupling.

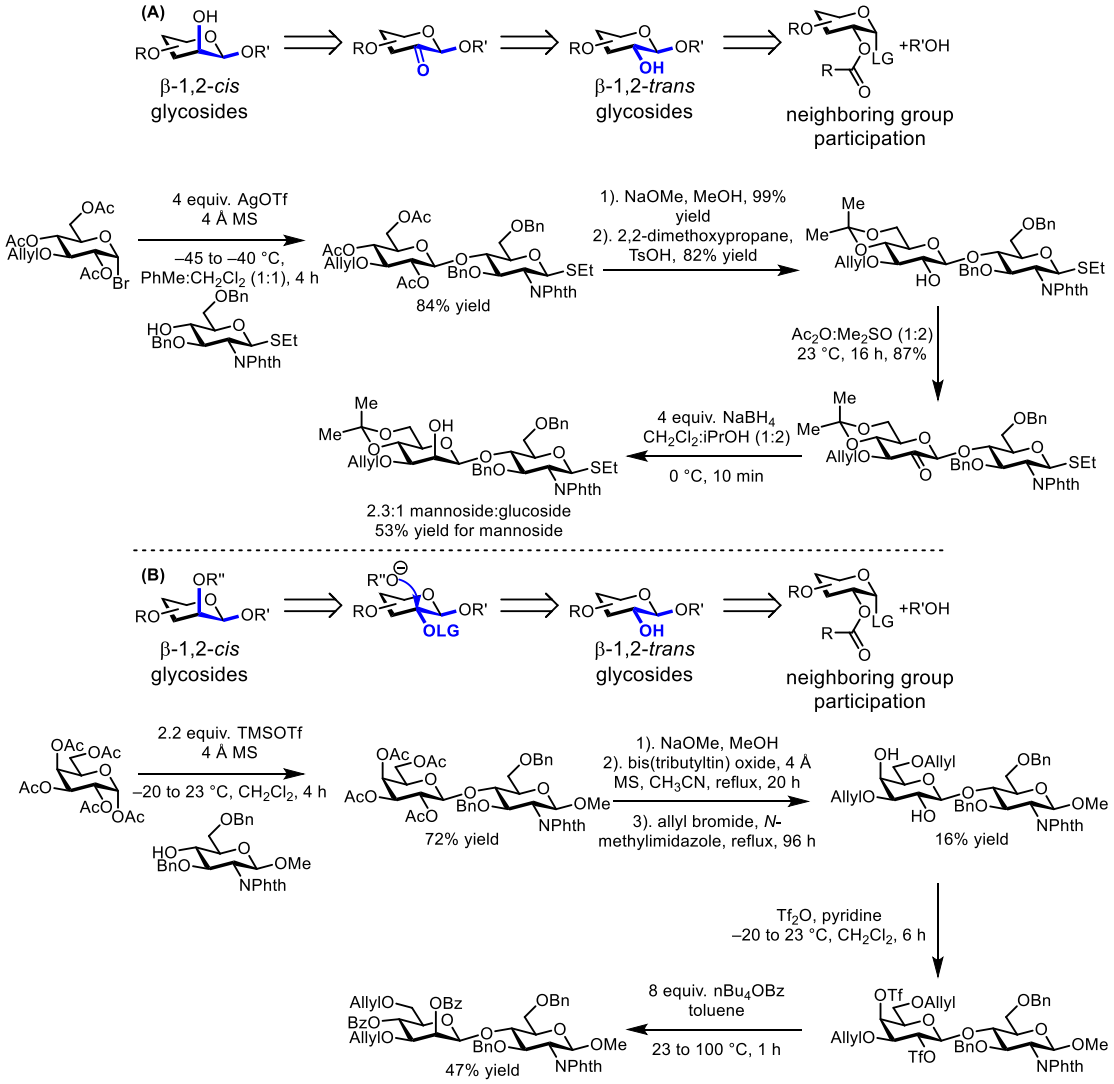
Koenigs-Knorr coupling. Koenigs-Knorr coupling reactions involve the use of insoluble silver salt promoters to activate glycosyl halides. This method has been applied to β-mannosylation. Ley

and coworkers reported the direct coupling of mannosyl bromide with a long chain alcohol using silver silicate, a heterogeneous promoter (Figure 1.5A).[19] The reaction was moderately selective (<1:13 α:β) but required long reaction time (3 d). The stereoselectivity is not well-understood due to the heterogeneous nature of the reaction medium. Mannosyl bromides were proposed to be activated on the surface of silver silicate, essentially blocking the α-face of mannose and resulting in nucleophilic attack from the β-face. Unfortunately, the Koenigs–Knorr coupling method was found to have highly limited scope in acceptors. Mannosylation of the less reactive C4 position of a glucosamine derivative was unselective (1:1.1 α:β) when mannosyl bromide was activated by silver silica-alumina (Figure 1.5B).[20] Therefore, due to the narrow acceptor scope and moderate β-selectivity, the application of silver salt-promoted Koenigs–Knorr coupling in the construction of β-1,2-*cis* glycosidic linkages has been limited.

Epimerization of β-Glucosides. This indirect method for β-1,2-*cis* glycosidic linkage synthesis takes advantage of neighboring group participation strategy that reliably generates β-1,2-*trans* glycosides. Since mannose is the C2-epimer of glucose, selective epimerization of the C2 position of β-glucosides will afford the desired β-mannosides. The anomeric configuration of resulting mannosides is determined in the initial β-1,2-*trans* glycosylation. After glucosylation of glycosyl acceptors via neighboring group participation, the C2 position of glucose can then be oxidize to the corresponding ketone, which can be selectively reduced using suitable hydride reagents (Figure 1.6A). Because hydrides preferentially attack C2-ketone from equatorial position over axial

[19] Grice, P.; Ley, S. V.; Pietruszka, J.; Osborn, H. M. I.; Priepke, H. W. M.; Warriner, S. L. A New Strategy for Oligosaccharide Assembly Exploiting Cyclohexane-1,2-diacetal Methodology: An Efficient Synthesis of a High Mannose Type Nonasaccharide. *Eur. J. Chem*. **1997**, *3*, 431–440.
[20] Matsuo, I.; Nakahara, Y.; Ito, Y.; Nukada, T.; Nakahara, Y.; Ogawa, T. Synthesis of a Glycopeptide Carrying a N-Linked Core Pentasaccharide. *Bioorg. Med. Chem*. **1995**, *3*, 1455–1463.

position, β-mannosides can be obtained as the major product. This three-step sequence for β-mannosylation has been explored by Kerékgyárto and co-workers.[21] The initial β-glucoside was synthesized using a 2-*O*-acetyl donor via neighboring group participation. Oxidation of C2 alcohol was achieved with Albright-Goldman oxidation (DMSO and Ac_2O). Reduction of the resulting C2 ketone with sodium borohydride gave rise to a mixture of β-mannoside and β-glucoside (2.3:1 mannoside:glucoside).



[21] Kerékgyárto, J.; van der Ven, J. G. M.; Kamerling, J. P.; Lipták, A.; Vliegenthart, J. F. G. Synthesis of a selectively protected trisaccharide building block that is part of xylose-containing carbohydrate chains from N-glycoproteins. *Carbohydr. Res*. **1993**, *238*, 135–145.

Figure 1.6 (A) Construction of β-mannosides via glucosylation/oxidation/reduction sequence. (B) Construction of β-mannosides visa glycosylation/S_N2 inversion.

Alternatively, instead of following oxidation-reduction sequence to epimerize the C2 position of β-glucosides, direct nucleophilic displacement of C2 position by an oxygen nucleophile via an S_N2 pathway can also afford β-mannosides (Figure 1.6B). Such epimerization process requires nucleophilic attack from the sterically hindered axial position, and the stereoelectronic interaction between the axially orientated lone pair of the ring oxygen and incoming negatively charged nucleophile further disfavors axial attack; as a result, elevated temperatures are often needed to overcome the high energetic barrier of axial nucleophilic attack. David and co-workers applied such protocol to β-mannosylation.[22] Displacement of C2-OTf by tetrabutylammonium benzoate was achieved at 100 °C with only modest yield (<50 %). Fürstner and co-workers have found that the efficiency of displacement of C2-OTf can be greatly improved by means of ultrasound.[23] Upon sonication, the displacement proceeded at ambient temperatures with good yields (>80 %). Although the anomeric selectivity of β-1,2-*trans* glycosylation is generally high, the three-step glucosylation-modification-reduction/displacement sequence renders the synthesis of β-1,2-*cis* glycosides highly inefficient. The epimerization protocol has become less appealing as direct glycosylation methods for β-1,2-*cis* glycosylation continue to be developed.

The Use of Electron-Withdrawing Protecting Group. As described in section 1.2, upon activation of glycosyl donors, several reactive intermediates could be generated. Although the displacement of a labile leaving group in α-configuration could proceed via a stereospecific

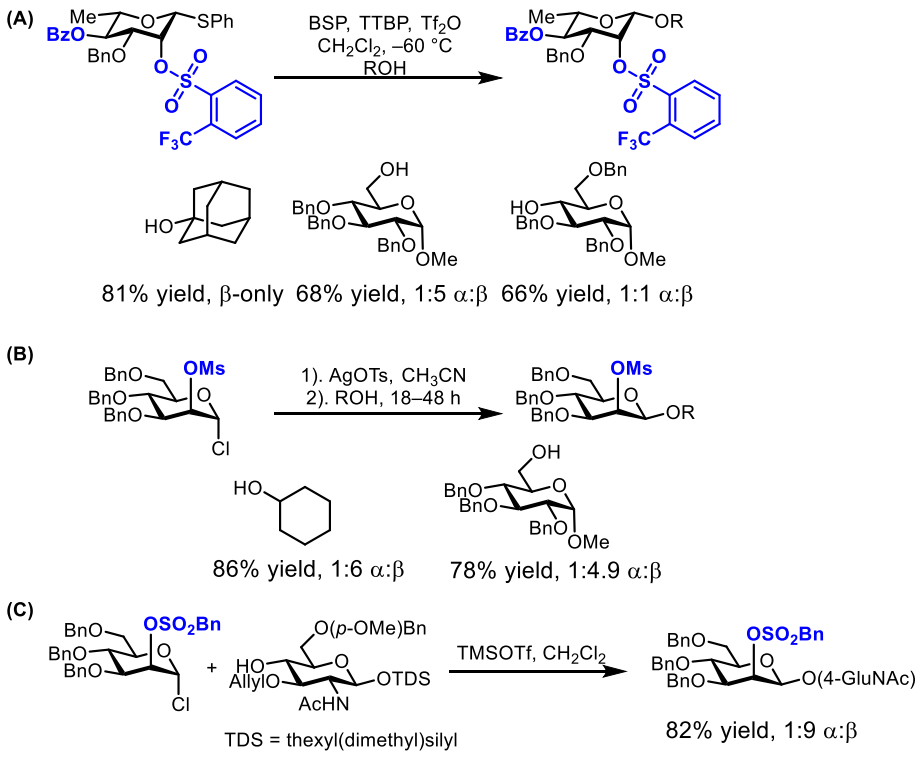
[22] Alais, J.; David, S. Preparation of disaccharides having a β-D-mannopyranosyl group from N-phthaloyllactosamine derivatives by double or triple S_N2 substitution. *Carbohydr. Res*. **1990**, *201*, 69–77.
[23] Fürstner, A.; Konetzki, I. A Practical Synthesis of β-D-Mannopyranosides. *Tetrahedron Lett*. **1998**, *39*, 5721–5724.

pathway to afford β-glycosides, nucleophilic addition to an oxocarbenium intermediate via an S_N1 pathway could generate both α- and β-anomers. The installment of electron-withdrawing protecting groups on glycosyl donors can destabilize oxocarbenium intermediates because of their cationic nature. The nucleophilic addition to an oxocarbenium intermediate is generally highly exergonic; therefore, the transition state of the nucleophilic addition will be more geometrically similar to the oxocarbenium ion and will likely have significant cationic character. As a result, electron-withdrawing protecting groups could destabilize the S_N1 pathway, thereby favoring the stereospecific pathway.

Crich and co-workers developed a rhamnosyl donor possessing two electron-withdrawing protecting groups for β-rhamnosylation.[24] Both the 2-*O*-trifluoromethylbenzenesulfonyl and the 4-*O*-benzoyl groups are necessary for achieving β-selectivity (Figure 1.7A). Although complete β-selectivity was obtained with simple alcohol (1-adamantanol), only modest β-selectivity was achieved with primary and secondary sugar acceptors (1:1–1:5 α:β). 2-*O*-Methylsulfonyl group has also been explored as a protecting group for mannosyl and rhamnosyl donors to stabilize α-mannosyl and α-rhamnosyl sulfonate esters and promote stereospecific displacement of α-sulfonates by Schuerch and co-workers,[25] although the acceptor scope was limited to simple alcohols such as methanol and cyclohexanol and a primary sugar nucleophile (Figure 1.7B). Mannosyl trichloroacetimidate bearing a 2-*O*-benzylsulfonyl group was found to undergo selective glycosylation with a poorly reactive 4-OH-glucosamine derivative (1:9 α:β) when promoted by

[24] Crich, D.; Picione, J. Direct Synthesis of the β-L-Rhamnopyranosides. *Org. Lett*. **2003**, *5*, 781–784.
[25] Srivastava, V. K.; Schuerch, C. Synthesis of β-D-Mannopyranosides and β-L-Rhamnopyranosides by Glycosidation at C-l. *J. Org. Chem*. **1981**, *46*, 1121–1126.

catalytic amounts of trimethylsilyl trifluoromethanesulfonate (TMSOTf),[26] demonstrating the possibility of achieving synthetically useful level of β-selectivity with less reactive but important sugar nucleophiles by applying electron-withdrawing group strategy (Figure 1.7C). Despite the promising progress, the difficulty with the deprotection of sulfonyl group impedes the utilization of this strategy. Typically, highly reducing conditions (Na in NH_3 or sodium amalgam in alcohol) or strongly basic reagents ($NaNH_2$) are needed for deprotection and could cause issues with functional group compatibility. To address such limitations, a carbonate protecting group has been developed as an alternative to sulfonyl group to protect diol in glycosyl donors while still being able to destabilize oxocarbenium intermediates through electron-withdrawing effects.



[26] Abdel-Rahman, A. A.-H.; Jonke, S.; El Ashry, E. S. H.; Schmidt, R. R. Stereoselective Synthesis of β-D-Mannopyranosides with Reactive Mannopyranosyl Donors Possessing a Neighboring Electron-Withdrawing Group. *Angew. Chem., Int. Ed*. **2002**, *41*, 2972–2974.

Figure 1.7 β-1,2-*cis* Glycosylations with donors possessing electron-withdrawing groups.

Crich and co-workers developed 3,4-*O*-carbonate protected rhamnosyl donors for β-rhamnosylation (Figure 1.8).[27] Moderate β-selectivity was obtained with 3β-cholestanol (1:6 α:β) and primary sugar acceptor (1:4.5 α:β) when rhamnosyl thioglycosides were activated with 1-benzenesulfinyl piperidine (BSP) and triflic anhydride (Tf_2O). However, unselective glycosylation was observed with secondary sugar nucleophiles. The carbonate protecting group could be cleaved under milder conditions (NaOMe in MeOH) than sulfonyl protecting groups; nevertheless, the low level of β-selectivity highly limits the application of electron-withdrawing protection strategy to oligosaccharide synthesis.

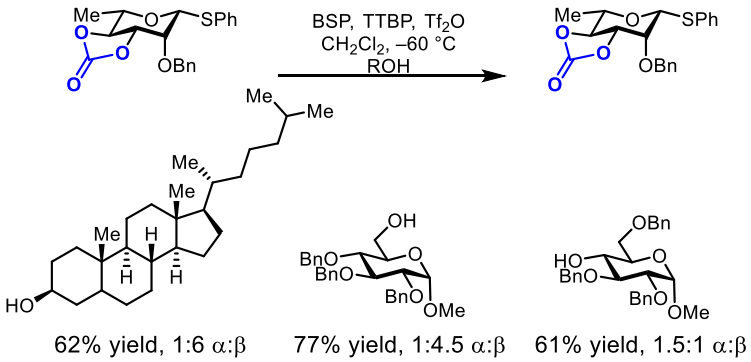


Figure 1.8 β-Rhamnosylation with a donor possessing a 3,4-O-carbonate protecting group.

Intramolecular Aglycone Delivery. The intramolecular aglycone delivery method involves the use of a temporary tether on the C2 position of glycosyl donors, which can link the acceptor with donor. With the acceptor covalently attached to the donor's β-face, the acceptor can react intramolecularly with the C1 position upon activation of glycosyl donors to generate desired β-

[27] Crich, D.; Vinod, A. U.; Picione, J. The 3,4-*O*-Carbonate Protecting Group as a β-Directing Group in Rhamnopyranosylation in Both Homogeneous and Heterogeneous Glycosylations As Compared to the Chameleon-like 2,3-*O*-Carbonates. *J. Org. Chem*. **2003**, *68*, 8453–8458.

1,2-*cis* glycosidic linkages. The temporary tether can be formed prior to glycosylation or *in situ* and can be subsequently removed easily. Typically, intramolecular aglycone delivery can be applied to glycosylation of both primary and secondary sugar acceptors with complete β-selectivity and good yields. Hindsgaul and co-workers found that 2-*O*-isopropenyl protected mannosyl donors could react with glycosyl acceptors with catalytic amount of triflic acid (TfOH) to form a donor-acceptor adduct tethered by a *gem*-dimethyl group (Figure 1.9A).[28] Upon treatment of *N*-iodosuccinimide (NIS), the donor-acceptor adduct underwent intramolecular rearrangement to the desire β-glycoside, and formation of α-anomer was not observed. The isopropenyl protecting group was cleaved *in situ* with the addition of water in the presence of excess NIS.

[28] Barresi, F.; Hindsgaul, O. Synthesis of β-Mannopyranosides by Intramolecular Aglycon Delivery. *J. Am. Chem. Soc*. **1991**, *113*, 9376–9377.

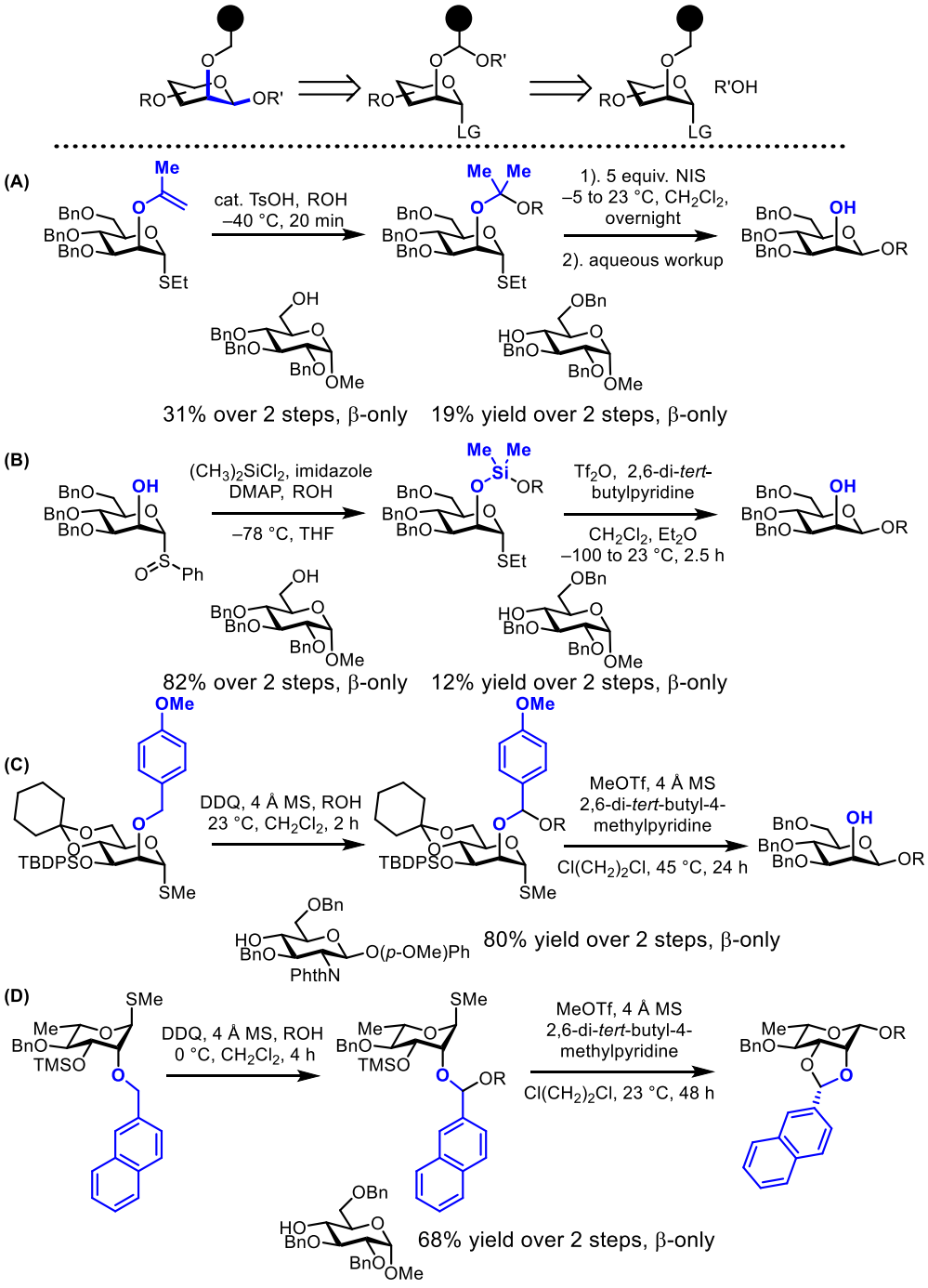


Figure 1.9 Construction of β-1,2-*cis* glycosides via intramolecular aglycone delivery.

Many different tethers have been developed since the initial report in 1991. Stork and co-workers developed dimethyl silyl linker to bridge the C2 position of mannosyl donors and

acceptors (Figure 1.9B).[29] The silyl tethers were efficiently constructed by treating equimolar mixture of donors and acceptors with dimethyldichlorosilane. Activation of the tethered mannosyl sulfoxides with Tf_2O afforded the desired β-mannosides with exclusive β-selectivity and generally high yields. The relatively low stability of isopropenyl ethers and dimethyl silyl ethers prompted Ogawa, Ito, and co-workers to develop a more stable *p*-methoxybenzyl (PMB) ether tether (Figure 1.9C).[30] PMB ether can be oxidized to a *para*-quinone methide-type intermediate using 2.3-dichloro-5.6-dicyano-*p*-benzo-quinone (DDQ), which can then react with acceptors to form mixed acetals. The mixed acetals without purification can be subjected to glycosylation and undergo intramolecular rearrangement to afford the β-mannosides. The intramolecular aglycone delivery strategy has also been extended to the construction of other β-1,2-*cis* glycosidic linkages such as β-rhamnosides (Figure 1.9D). Ito and co-workers relied on 2-naphthylmethyl protection at the C2 position of rhamnosyl donors.[31] Upon oxidation with DDQ, 2-naphthylmethyl ether can react with acceptors to form the mixed acetals presumably by a similar mechanism followed by PMB ether oxidation. A range of primary and secondary sugar acceptors underwent β-rhamnosylation with good yields and complete β-selectivity. Despite the excellent stereocontrol of intramolecular aglycone delivery strategy, the need for a specific protecting group at the C2 position of glycosyl donors, serving as the temporary tether, renders donor syntheses highly inefficient. Due to the similar reactivity of free hydroxyl groups on carbohydrates, it is highly challenging to selectively protect the C2 position of donors with the tether group in the presence of other unprotected

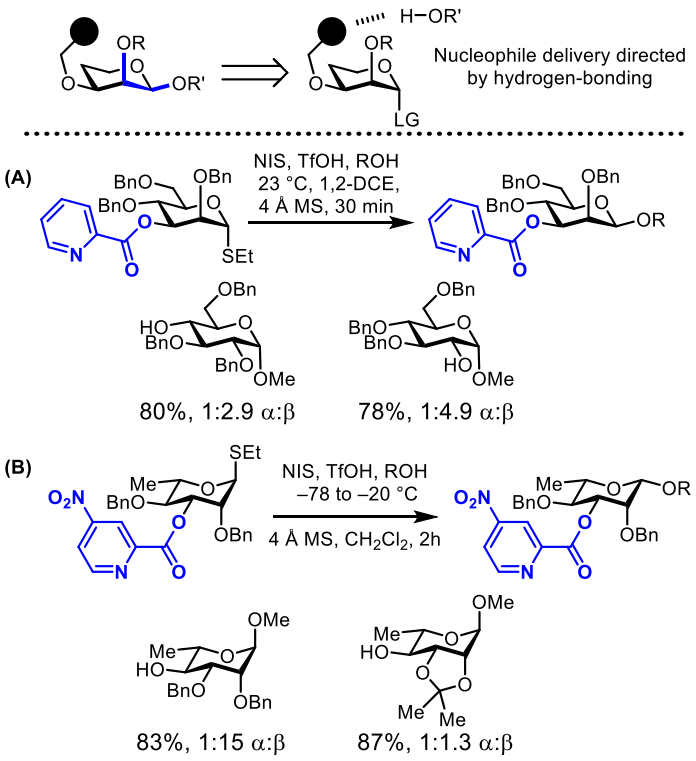
[29] (a) Stork, G.; La Clair, J. J. Stereoselective Synthesis of b-Mannopyranosides via the Temporary Silicon Connection Method. *J. Am. Chem. Soc*. **1996**, *118*, 247–248. (b) Stork, G.; Kim, G. Stereocontrolled Synthesis of Disaccharides via the Temporary Silicon Connection. *J. Am. Chem. Soc*. **1992**, *114*, 1087–1088.

[30] (a) Ito, Y.; Ogawa, T. A Novel Approach to the Stereoselective Synthesis of β-Mannosides. *Angew. Chem., Int. Ed*. **1994**, *33*, 1765–1767. (b) Ito, Y.; Ohnishi, Y.; Ogawa, T.; Nakahara, Y. Highly Optimized β-Mannosylation via *p*-Methoxybenzyl Assisted Intramolecular Aglycon Delivery. *Synlett* **1998**, 1102–1104.

[31] Lee, Y. J.; Ishiwata, A.; Ito, Y. Stereoselective Synthesis of β-L-Rhamnopyranosides. *J. Am. Chem. Soc*. **2008**, *130*, 6330–6331

hydroxyl groups. Therefore, a long, multi-step protecting group manipulation sequence is often needed for the installment of the temporary linkers. The inefficiency of donor syntheses has remained as the major drawback of the intramolecular aglycone delivery strategy.

Hydrogen-bond-mediated Aglycone Delivery. The hydrogen-bond-mediated aglycone delivery strategy relies on the use of picoloyl protecting groups on hydroxyl groups remote to the anomeric center. The picoloyl moiety acts as a hydrogen-bond acceptor for the incoming nucleophile; thereby directing acceptors to attack from the same face. Demchenko and co-workers found that glycosylation of primary and secondary sugar nucleophiles with 3-*O*-picoloyl protected mannosyl thioglycosides proceeded with moderate β-selectivity (1:2.9–1:10 α:β) (Figure 1.10A).[32]



[32] Pistorio, S. G.; Yasomanee, J. P.; Demchenko, A. V. Hydrogen-Bond-Mediated Aglycone Delivery: Focus on β-Mannosylation. *Org. Lett*. **2014**, *16*, 716–719.

Figure 1.10 Construction of β-1,2-*cis* glycosides via hydrogen-bond-mediated aglycone delivery.

Similarly, hydrogen-bond-mediated aglycone delivery strategy has also been applied to β-rhamnosylation. 4-Nitropicoloyl group was utilized to protect the C3 position of rhamnosyl thioglycosides, affording β-rhamnosides with moderate β-selectivity (1:1–1:15 α:β) when activated by NIS and TfOH (Figure 1.10B).[33] Despite the promising level of β-selectivity, the application of hydrogen-bond-mediated aglycone delivery strategy to oligosaccharide synthesis is limited because the stereoselectivity is highly sensitive to the protection scheme on acceptors. Although rhamnosylation of a 2,3-*O*-dibenzyl protected acceptor proceeded with high anomeric selectivity (1:15 α:β), unselective rhamnosylation was observed when the 2,3-*O*-dibenzyl protecting group was replaced by an isoproprylidene group. Similarly, replacement of 2-*O*-benzyl with 2-*O*-benzoyl group on a glucose acceptor resulted in significant decrease of β-selectivity from 1:15 to 1:1 α:β. The influence of acceptor protection scheme on the stereoselectivity of hydrogen-bond-mediated aglycone delivery has not been well-understood. Therefore, the generality of this strategy needs to be carefully examined. Additionally, the need for a specific protecting group on the C3 position of mannosyl and rhamnosyl donors results in lengthy synthesis of glycosyl donors, rendering the overall glycosylation highly inefficient.

Anomeric *O*-Alkylation. Hodosi and co-workers realized that the C1 and C2 position of mannose can form a *cis*-1,2-*O*-stannylene acetal when treated with dibutyltin oxide (Figure 1.11A).[34] *cis*-

[33] Lei, J.-C.; Ruan, Y.-X.; Luo, S.; Yang, J.-S. Stereodirecting Effect of C3-Ester Groups on the Glycosylation Stereochemistry of L-Rhamnopyranose Thioglycoside Donors: Stereoselective Synthesis of α- and β-L-Rhamnopyranosides. *Eur. J. Org. Chem*. **2019**, 6377–6382.
[34] Hodosi, G.; Kováč, P. A Fundamentally New, Simple, Stereospecific Synthesis of Oligosaccharides Containing the β-Mannopyranosyl and β-Rhamnopyranosyl Linkage. *J. Am. Chem. Soc*. **1997**, *119*, 2335–2336.

Stannylene acetals are formed because they are thermodynamically more stable than *trans*-stannylene acetals. The formation of a *cis*-1,2-*O*-stannylene acetal with mannosyl or rhamnosyl donors locks the anomeric position in β-configuration. Because the equatorial alkoxide (C1 position) is more nucleophilic than the axial alkoxide (C2 position) and the rest of unactivated hydroxyl groups on glycosyl donors, the anomeric alkoxide can preferentially react with electrophiles via an S_N2 pathway to generate β-1,2-*cis* glycosides with high stereochemical fidelity. Because the only *cis*-diol moiety in mannose and rhamnose is the C2-hydroxyl and the C1-hydroxyl in β-configuration, the stannylene acetal activation strategy allows for the use of partially protected donors for glycosylation, which greatly improves efficiency of glycosylation by eliminating synthetic steps for protecting group manipulation. Although the β-selectivity is generally high due to the strong preference for *cis*-stannylene acetals, long reaction times are often necessary to achieve good yields especially with secondary triflates of carbohydrates. Alternatively, metal salts can be used to deprotonate and chelate with C1 and C2 position of mannose and rhamnose, and chelation effects favor the formation of equatorial C1-alkoxide over the axial alkoxide. The equatorial C1-alkoxide is more nucleophilic because equatorial positions are less sterically hindered than axial positions, resulting in faster rate of substitution. Zhu and co-workers found that cesium carbonate was the suitable base for *O*-alkylation of mannosyl donor (Figure 1.11B).[35] β-Mannosides were obtained with good yields and complete β-selectivity after substitution at primary or secondary triflates of carbohydrates.

[35] Nguyen, H.; Zhu, D.; Li, X.; Zhu, J. Stereoselective Construction of β-Mannopyranosides by Anomeric *O*-Alkylation: Synthesis of the Trisaccharide Core of N-linked Glycans. *Angew. Chem. Int. Ed*. **2016**, *55*, 4767–4771.

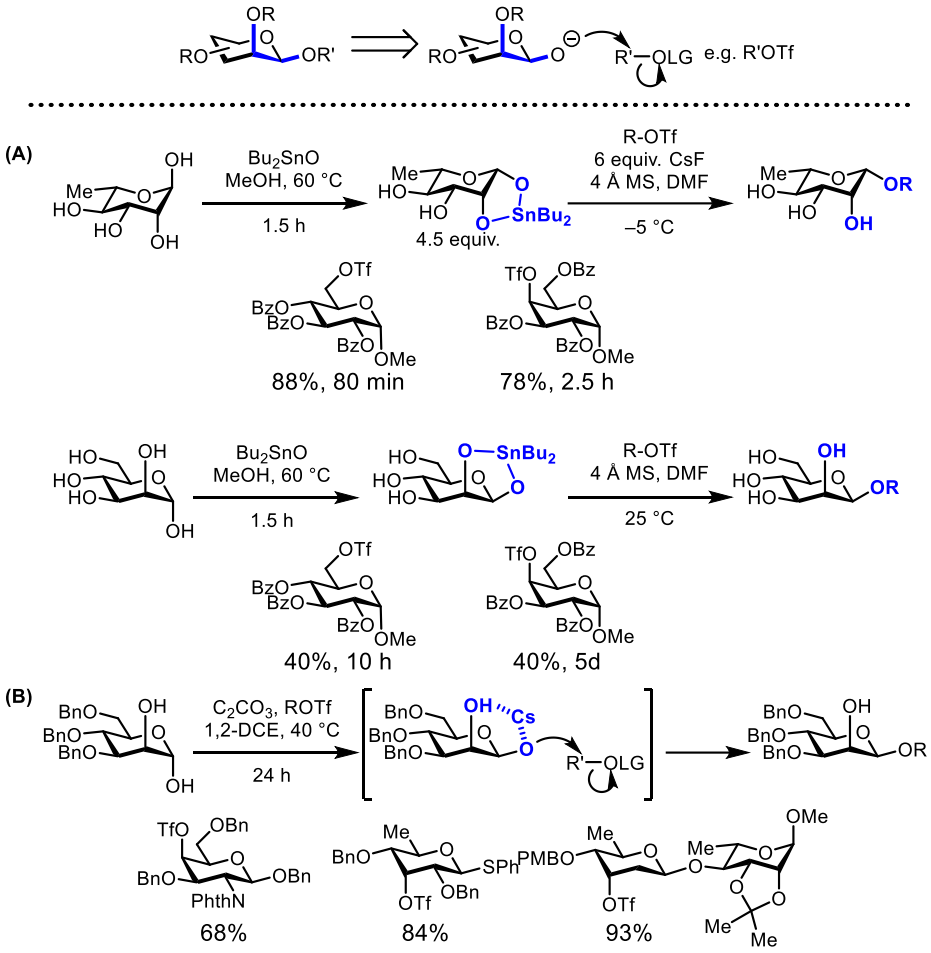


Figure 1.11 β-1,2-*cis* Glycosylations via anomeric *O*-alkylation.

One key limitation of anomeric *O*-alkylation is that C1-alkoxide can only react with axial triflates because in order to displace equatorial triflates, C1-alkoxide needs to attack from axial position, which is kinetically highly unfavorable (Figure 1.12A) due to 1,3-diaxial interactions. As a result, anomeric *O*-alkylation cannot be applied to synthesize β-1,2-*cis* glycosidic linkages with axial hydroxyl groups such as the C2 position of mannose and C4 position of galactose.

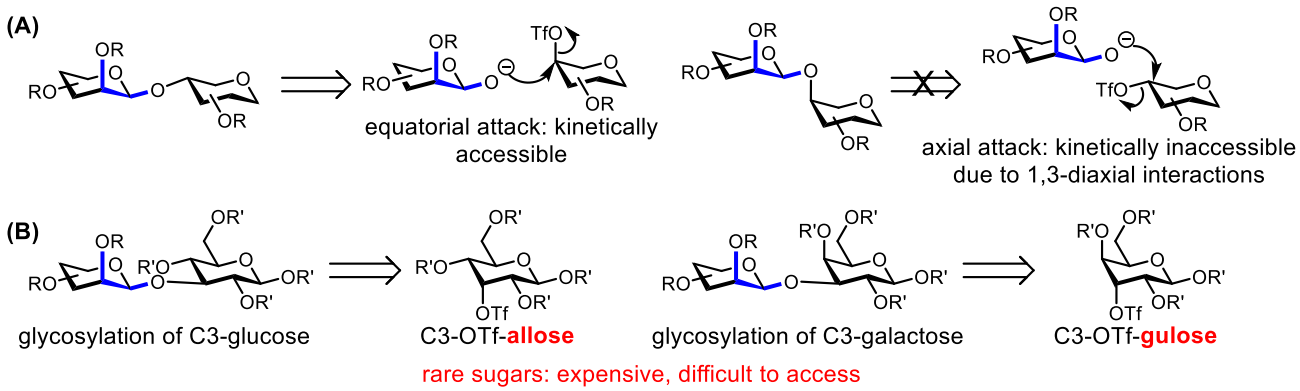
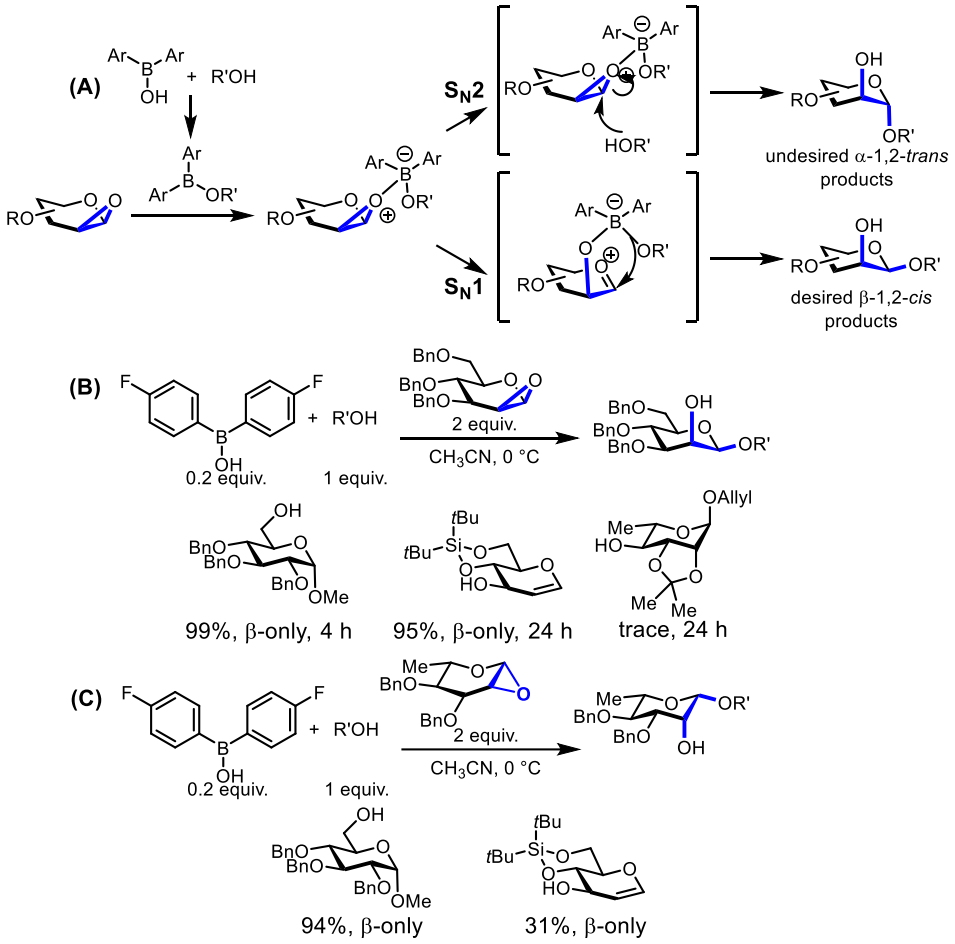


Figure 1.12 Limitations associated with anomeric *O*-alkylation.

Because nucleophilic substitution readily occurs at axial triflates with inversion of stereochemistry on sugar electrophiles, rare sugar electrophiles with axial triflates are often required (Figure 1.12B). For example, in order to construct β-1,2-*cis*-glycosidic linkages with glucose, the epimer of glucose has to be used as the electrophile. Nucleophilic attack at the C3 triflate of allose gives rise to C3-glycoslated glucose. Similarly, C3-triflate of gulose is required to synthesize glycosidic linkages with C3 position of galactose. Unlike glucose and galactose, it is much harder to access rare sugars such as allose and gulose because they are not broadly produced in nature and are highly expensive when they are commercially available. The need for rare sugars is unattractive and greatly limits the application of anomeric *O*-alkylation to oligosaccharide synthesis. Additionally, this strategy has limited electrophile scope because the displacement of equatorial triflate to form glycosidic linkages with axial position of acceptors is kinetically unfavorable.

The Use of 1,2-Anhydropyranosyl Donors (Glycal Epoxides). This strategy utilizes 1,2-anhydromannose as the donor, which can be activated by a borinic acid catalyst. Toshima and co-workers found that diaryl borinic acids can react with glycosyl acceptors to form acceptor-derived

borinic esters (Figure 1.13A).[36] The acceptor-derived borinic ester can coordinate to and activate 1,2-anhydromannose to afford the tetracoordinate borinate ester. Another equivalent of acceptor can react with the activated glycosyl donor via an S_N2 pathway to generate the undesired α-1,2-*trans* glycosides. Alternatively, upon the formation of the tetracoordinate borinate ester with 1,2-anhydromannose, epoxide ring opening can occur via an S_N1 pathway to form an oxocarbenium intermediate and a tetracoordinate borinate ester with C2 alkoxide of donors. The acceptor can then be delivered intramolecularly from the borinate ester to generate the desired β-1,2-*cis* glycosides.



[36] Tanaka, M.; Nashida, J.; Takahashi, D.; Toshima, K. Glycosyl-Acceptor-Derived Borinic Ester-Promoted Direct and β-Stereoselective Mannosylation with a 1,2-Anhydromannose Donor. *Org Lett*. **2016**, *18*, 2288–2291.

Figure 1.13 Boronic acid-catalyzed β-1,2-*cis* glycosylations utilizing 1,2-anhydropyranosyl donors.

Toshima and co-workers found that the Lewis acidity of borinic acids strongly influenced the stereoselectivity of glycosylation. β-Selectivity increased as the borinic acid catalyst became more Lewis acidic, suggesting that s more Lewis acidic catalyst was able to activate the epoxide toward an S_N1 pathway. Although complete β-selectivity was obtained with simple alcohols and some primary and secondary sugar nucleophiles, glycosylation with less reactive acceptors, such as 4-OH-rhamnose, proceeded with low yields (Figure 1.13B). The same strategy has also been applied to β-rhamnosylation by Toshima (Figure 1.13C).[37] The low reactivity with poorly reactive acceptors, such as 4-OH-glucose, was again observed, but complete β-selectivity and good yields were obtained with primary and more reactive secondary sugar acceptors. It is worth noting that this strategy can be applied to site selective synthesis of β-1,2-*cis* glycosides, which will be discussed in Section 1.6. Despite the excellent stereocontrol of borinic acid-catalyzed glycosylation, the major drawback of this strategy is the inefficient synthesis of 1,2-anhydromannose and 1,2-anhydrorhamnose, which prevents the wide application of this strategy to oligosaccharide synthesis. The reported procedure for the synthesis of 1,2-anhydro-3,4,6-tri-*O*-benzyl-β-D-mannose required 7 steps starting from D-mannose, while 8 steps were needed to prepare 1,2-anhydro-3,4-di-*O*-benzyl-β-L-rhamnose.

Protecting-group Control. **(a) 4,6-Benzylidene Acetal**. The state-of-the-art strategy for β-mannosylation is the use of 4,6-benzylidene acetal protection on mannosyl donors.[38] The

[37] Nishi, N.; Sueoka, K.; Iijima, K.; Sawa, R.; Takahashi, D.; Toshima, K. Stereospecific β-L-Rhamnopyranosylation through an S_Ni-Type Mechanism by Using Organoboron Reagents. *Angew. Chem. Int. Ed*. **2018**, *57*, 13858–13862.
[38] (a) Crich, D.; Sun, S. Direct Synthesis of β-Mannopyranosides by the Sulfoxide Method. *J. Org. Chem*. **1997**, *62*, 1198–1199. (b) Crich, D.; Sun, S. Direct Formation of β-Mannopyranosides and Other Hindered Glycosides from

mechanism of stereocontrol induced by 4,6-benzylidene acetal protection has been studied previously.[39] The primary ^{13}C KIE values for the α- and β-mannoside (1.005±0.002 for α-mannoside and 1.023±0.003 for β-mannoside) products are distinct, suggesting the formation of the two anomers is operating through different mechanisms (Figure 1.14A). The value for β-mannoside is close to the range (1.03–1.08) expected for a bimolecular (S_N2) reaction[40] and is in good agreement with the computed primary ^{13}C KIE (1.018) obtained with a loosely associative, concerted transition state displaying nucleophile attachment ahead of leaving group (triflate) departure. However, the ^{13}C KIE value for α-mannoside is consistent with the expected values (1.00–1.01) for a unimolecular (S_N1) reaction[31] and does not agree with the computed primary ^{13}C KIE (1.023) obtained with an associative, concerted (S_N2-like) transition state. Instead, the authors propose that the formation of α-mannosides with 4,6-benzylidene acetal protection proceeds through a dissociative mechanism in which discrete oxocarbenium intermediate is formed. The 4,6-benzylidene acetal protection of mannose destabilizes oxocarbenium intermediates and imparts stereoselectivity by favoring stereospecific glycosylation pathways via transient α-mannosyl triflate intermediates.

Thioglycosides. *J. Am. Chem. Soc*. **1998**, *120*, 435–436. (c) Crich, D.; Sun, S. Formation of β-Mannopyranosides of Primary Alcohols Using the Sulfoxide Method. *J. Org. Chem*. **1996**, *61*, 4506–4507. For reviews, see (d) Aubry, S.; Sasaki, K.; Sharma, I.; Crich, D. Influence of Protecting Groups on the Reactivity and Selectivity of Glycosylation: Chemistry of the 4,6-O-Benzylidene Protected Mannopyranosyl Donors and Related Species. In *Reactivity Tuning in Oligosaccharide Assembly*; Fraser-Reid, B., Cristóbal López, J., Eds.; Top. *Curr. Chem*. **2011**, *301*, 141–188. (e) Crich, D. Mechanism of a Chemical Glycosylation Reaction. *Acc. Chem. Res*. **2010**, *43*, 1144–1153.

[39] (a) Huang, M.; Garrett, G. E.; Birlirakis, N.; Bohe, L.; Pratt, D. A.; Crich, D. Dissecting the Mechanisms of a Class of Chemical Glycosylation Using Primary ^{13}C Kinetic Isotope Effects. *Nat. Chem*. **2012**, *4*, 663–667. (b) Crich, D.; Chandrasekera, N. S. Mechanism of 4,6-*O*-Benzylidene-Directed β-Mannosylation as Determined by α-Deuterium Kinetic Isotope Effects. *Angew. Chem. Int. Ed*. **2004**, *43*, 5386–5389.

[40] Berti, P. J.; Tanaka, K. S. E. Transition state analysis using multiple kinetic isotope effects: mechanisms of enzymatic and non-enzymatic glycoside hydrolysis and transfer. *Adv. Phys. Org. Chem*. **2002**, *37*, 239–313.

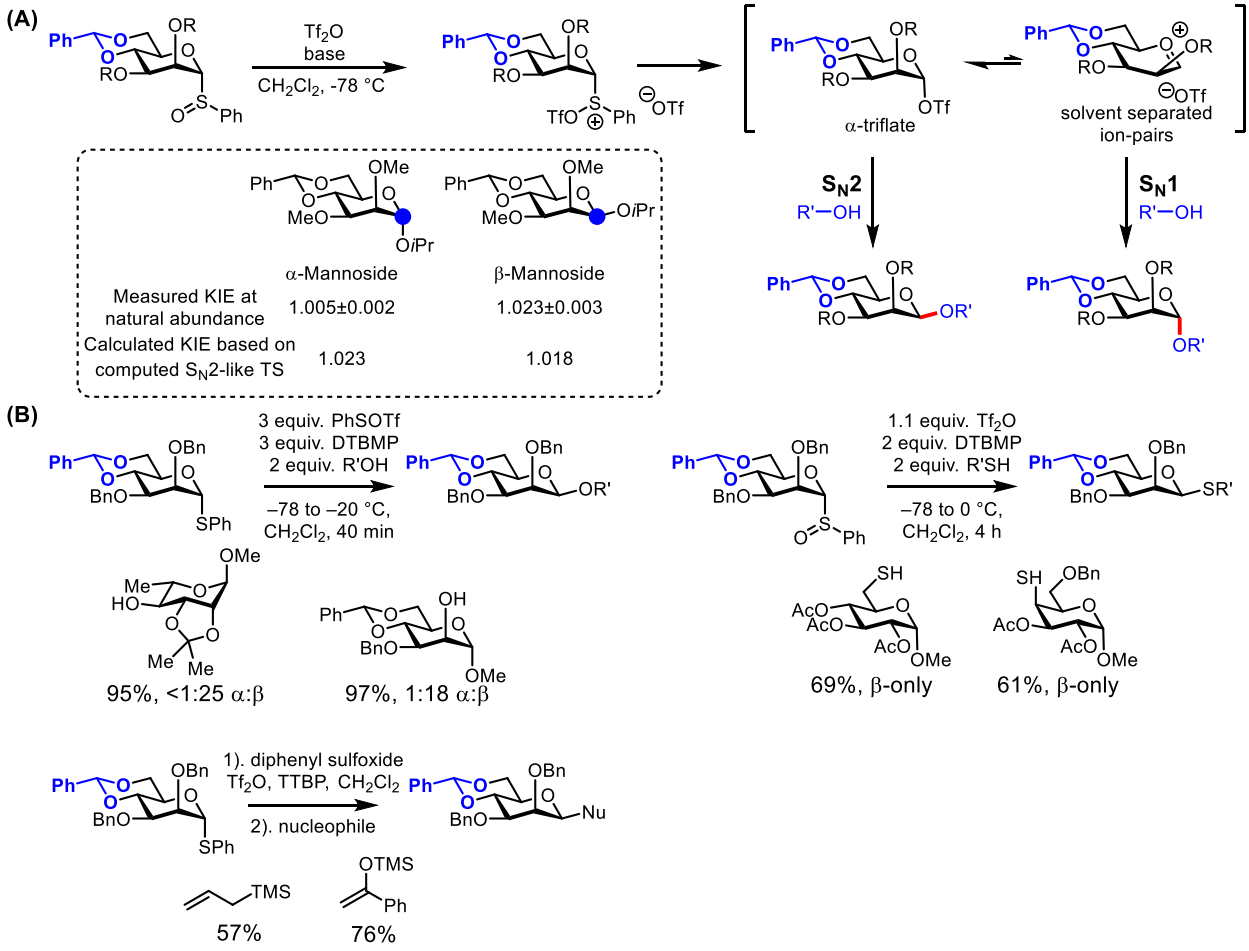


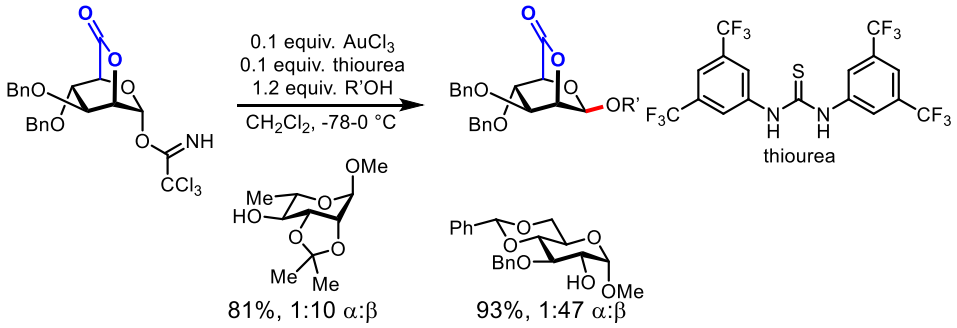
Figure 1.14 β-Mannosylations with 4,6-benzylidene acetal protected donors.

This protection strategy has been widely applied in oligosaccharide synthesis and has broad acceptor scope including primary and secondary alcohol nucleophiles,[41] thiol,[42] and carbon-based nucleophiles (Figure 1.14B)[43]. There are two limitations of 4,6-benzylidene acetal protection strategy. The specific protecting group requires multi-step syntheses from D-mannose (at least 6

[41] Crich, D.; Li, W.; Li, H. Direct Chemical Synthesis of the β-Mannans: Linear and Block Syntheses of the Alternating β-(1→3)-β-(1→4)-Mannan Common to *Rhodotorula glutinis*, *Rhodotorula mucilaginosa*, and *Leptospira biflexa*. *J. Am. Chem. Soc*. **2004**, *126*, 15081–15086.
[42] Crich, D.; Li, H. Direct Stereoselective Synthesis of β-Thiomannosides. *J. Org. Chem.* **2000**, *65*, 801–805.
[43] Moumé-Pymbock, M.; Crich, D. Stereoselective C-glycoside formation with 2-*O*-benzyl-4,6-*O*-benzylidene protected 3-deoxy gluco- and mannopyranoside donors: comparison with *O*-glycoside formation. *J. Org. Chem.* **2012,** *77*, 8905–8912.

steps), and this strategy cannot be applied to impart β-selectivity in the synthesis of β-1,2-*cis* glycosidic linkages with 6-deoxy-glycosyl donors such as rhamnose because of the lack C6-hydroxyl group.

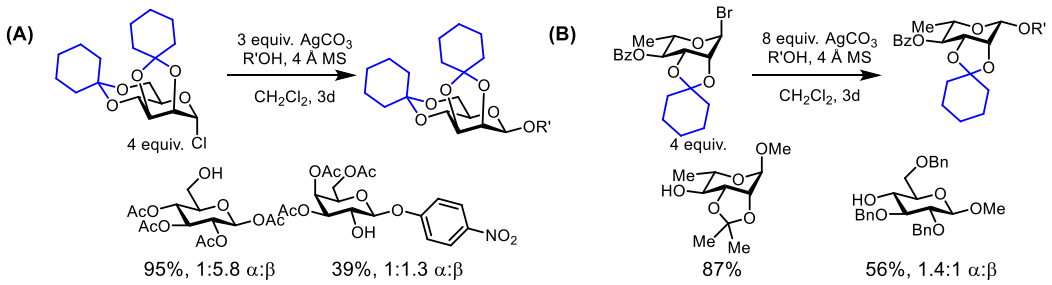
(b) 2,6-Lactone. Sasaki and co-workers developed a different protection strategy for β-mannosylation utilizing 2,6-lactone protection. When activated by $AuCl_3$ and bis[3,5-bis(trifluoromethyl)phenyl] thiourea, 2,6-lactone-protected mannosyl trichloroacetimidate underwent glycosylation with primary and secondary sugar nucleophiles with high β-selectivity (1:10–1:47 α:β) and good yields (Figure 1.15). The authors propose that 2,6-lactone protection plays two important roles in imparting β-selectivity. Acting as a strongly electron-withdrawing group, the 2,6-lactone protection can destabilize cationic oxocarbenium intermediate and favor stereospecific displacement of leaving group. Additionally, the authors propose that 2,6-lactone locks the oxocarbenium intermediate in a $^{2,5}B$ conformation, and nucleophilic attack preferentially occurs from the β-face to minimize steric clash with C4 position of donor.[44] Similar to the 4,6-benzylidene acetal protection strategy, the donor synthesis of 2,6-lactone is relatively lengthy as 6 steps are needed to convert D-mannose to 2,6-lactone protected mannosyl trichloroacetimidate.



[44] Sasaki, K.; Hashimoto, Y. 2,6-Lactones as a New Entry in Stereoselective Glycosylations. *Synlett* **2017**, *28*, 1121–1126.

Figure 1.15 β-Mannosylations with 2,6-lactone protected donors.

(c) 2,3-Acetal. Garegg and co-workers found that 2,3:4,6-di-*O*-cyclohexylidene protected mannosyl chloride underwent β-selective mannosylation when activated by heterogeneous silver-based promoters such as silver carbonate (Figure 1.16A).[45] Although good β-selectivity (1:4.2–5.8 α:β) was obtained with simple primary sugar nucleophiles, diminished level of β-selectivity (1:1.3–1.6 α:β) was observed when this method was applied to mannosylate secondary sugar nucleophiles. The use of 2,3-cyclohexylidene acetal was also attempted on rhamnosyl donors. Iversen and co-workers developed a very similar strategy, where silver carbonate was used to activate 2,3-*O*-cyclohexylidene protected rhamnosyl bromides and promote rhamnosylation (Figure 1.16B).[46] Good yields of β-rhamnosides were reported without commenting on the α:β selectivity. Unselective rhamnosylation was observed (1.4:1 α:β) with a relatively unreactive 4-OH-glucose nucleophile. Due to the limited acceptor scope and less than ideal level of β-selectivity, the 2,3-protection strategy has not been adopted by other groups.



[45] Garegg, P. J.; Iversen, T.; Johansson, R. Synthesis of Disaccharides Containing β-D-Mannopyranosyl Groups. *Acta Chem. Scand*. **1980**, *B34*, 505–508.
[46] Iversen, T.; Bundle, D. R. A New and Efficient Synthesis of β-L-Rhamnopyranosides. *Carbohydr. Res*. **1980**, *84*, C13–C15.

Figure 1.16 β-1,2-*cis* Glycosylations with 2,3-acetal protected donors.

At a first glance, it seems that the 2,3-acetal protection imparts β-selectivity by constraining the conformation of glycosyl donors, to which nucleophile addition selectively occurs from the β-face. However, Crich and co-workers conducted a comparison study and concluded that the heterogeneous nature of the silver promoters was crucial for achieving β-selectivity.[18] When rhamnosyl bromides were activated with silver triflate, a soluble promoter, where rhamnosyl triflates form *in situ*, α-selective rhamnosylation was universally observed even with 2,3-carbonate protection. However, when 2,3-carbonate protected rhamnosyl bromides were activated with insoluble silver(I) oxide, β-selective rhamnosylation was achieved. This comparison is consistent with the proposal that insoluble silver promoters induce β-selectivity by blocking the α-face when glycosyl donors are activated on the surface of promoters.The phenomenon that 2,3-acetal protected mannosyl or rhamnosyl donors undergo α-selective glycosylation in homogeneous system was observed by other research groups. Cloninger and co-workers found that bis-acetonide-protected mannosyl trichloroacetimidate underwent α-selective glycosylation when activated by indium(III) triflate.[47] Nguyen and co-workers found that the same transformation can be promoted using cationic $Pd(CH_3CN)_4(BF_4)_2$ with excellent α-selectivity.[48] Unselective mannosylation (1:1 α:β) was observed by Crich and co-workers when bis-acetonide-protected mannosyl sulfoxide was activated with Tf_2O.[49] All of the reported α-selective examples of glycosylation with 2,3-acetal-protected donors under homogeneous activation conditions suggest that 2,3-acetal-protected

[47] Mattson, A. L.; Michel, A. K.; Cloninger, M. J. Using In(III) as a Promoter for Glycosylation. *Carbohydr. Res*. **2012**, *347*, 142–146.
[48] Yang, J.; Cooper-Vanosdell, C.; Mensah, E. A.; Nguyen, H. M. Cationic Palladium(II)-Catalyzed Stereoselective Glycosylation with Glycosyl Trichloroacetimidates. *J. Org. Chem*. **2008**, *73*, 794–800.
[49] Crich, D.; Sun, S. Direct Chemical Synthesis of β-Mannopyranosides and Other Glycosides via Glycosyl Triflates. *Tetrahedron* **1998**, *54*, 8321–8348.

donors are inherently α-selective, and the β-selectivity observed with silver-based promoters is likely due to the heterogeneity nature of the activation conditions.

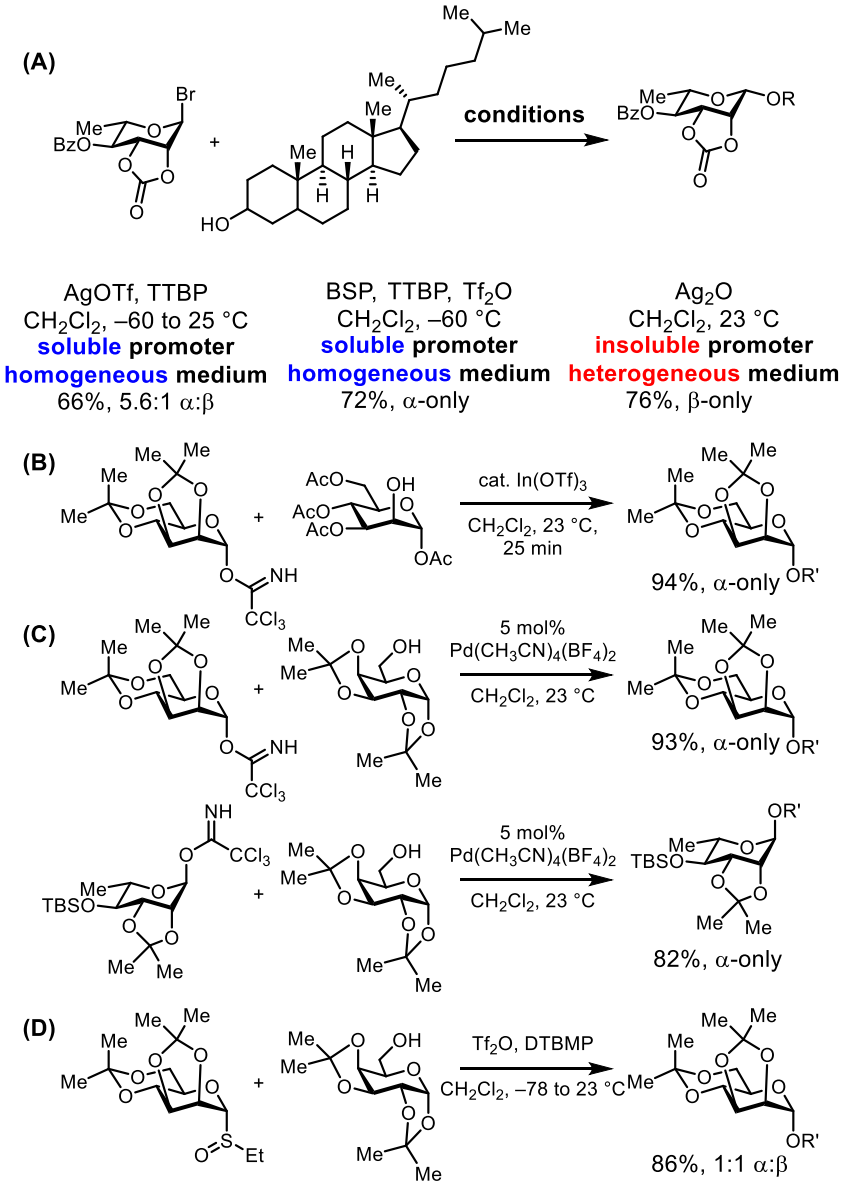


Figure 1.17 α-Glycosylations with 2,3-acetal protected glycosyl donors under homogeneous activation conditions.

Enzymatic Glycosylation. Enzymatic glycosylation has its unique advantages in stereo- and regiocontrol when compared to chemical glycosylation. Due to its high substrate specificity,

glycotransferases or glycosidases can catalyze glycosylation of unprotected substrates, affording structurally homogeneous saccharides. Grout and co-workers found that a β-mannosidase purified from *Aspergillus oryzae* catalyzed the transfer of a β-mannosyl unit from *p*-nitrophenyl-β-D-mannopyranoside to a disaccharide, specifically to the 4-OH of the non-reducing unit, to give the desired trisaccharide with complete stereo- and site control, although the yields were relatively low (26%) (Figure 1.18A).[50] Large excess of disaccharide (5.5-fold excess) was needed in this protocol. The use of excess nucleophiles is not ideal because nucleophiles, especially polysaccharide nucleophiles, are often the more precious coupling partner in glycosylations.

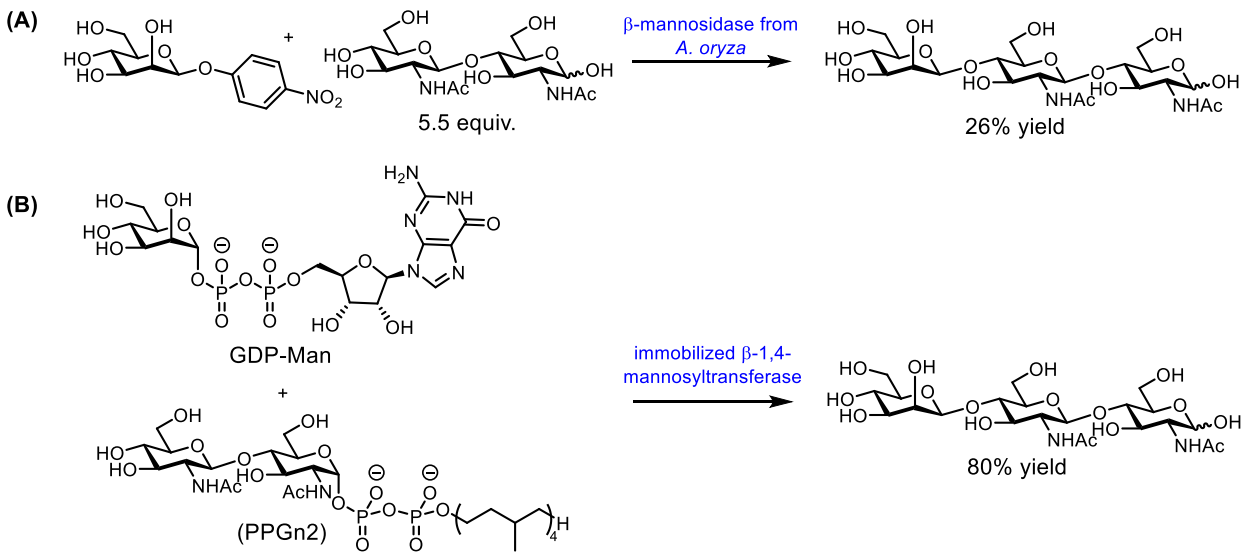


Figure 1.18 Enzymatic β-mannosylations.

Flitsch and co-workers performed over production of full-length and transmembrane-deleted yeast β-1,4-mannosyltransferases in *Escherichia coli*.[51] The functionally pure recombinant

[50] Sing, S.; Scigelova, M.; Crout, D. H. G. Glycosidase-catalysed synthesis of oligosaccharides: a two-step synthesis of the core trisaccharide of *N*-linked glycoproteins using the β-*N*-acetylhexosaminidase and the β-mannosidase from *Aspergillus oryzae*. *Chem. Commun*.**1996**, 993–994.

[51] Watt, G. M.; Revers, L.; Webberley, M. C.; Wilson, I. B. H.; Flitsch, S. L. Efficient Enzymatic Synthesis of the Core Trisaccharide of *N*-Glycans with a Recombinant β-Mannosyltransferase. *Angew. Chem. Int. Ed*. **1997**, *36*, 2354–2356.

enzyme was immobilized on an affinity column charged with nickel(II) ions. Although immobilization improved the stability of enzymes, the transferases still had limited shelf-life and were only stable for a few days at 4 °C. The β-1,4-mannosyltransferase catalyzed the transfer of a β-mannosyl unit from guanosine diphosphate mannose (GDP-mannose) to phytanyl-pyrophosphoryl-α-*N*,*N*-diacetylchitobioside (PPGn2) (Figure 1.18B). Upon acidic hydrolysis of the pyrophosphoryl residual, the desired trisaccharide was obtained with 80% yield. Despite the excellent stereocontrol of enzymatic glycosylation, the application of mannosyltransferases or mannosidases to β-mannosylation still remain impractical due to the low expression level of enzymes and their limited availability and shelf-life. Due to the high specificity of enzymes, the extension of enzymatic mannosylation beyond its natural substrate is not straightforward and potentially requires protein engineering. Not all classes of β-1,2-*cis*-glycosides can be synthesized enzymatically. Although several α-rhamnosyltransferases have been reported,[52] no β-rhamnosyltransferases have been structurally characterized.

[52] Wagstaff, B. A.; Zorzoli, A.; Dorfmueller, H. C. NDP-rhamnose biosynthesis and rhamnosyltransferases: building diverse glycoconjugates in nature. *Biochem. J.* **2021**, *478*, 685–701.

1.5 Summary for β-1,2-*cis* Glycosylation Methods and Outlook

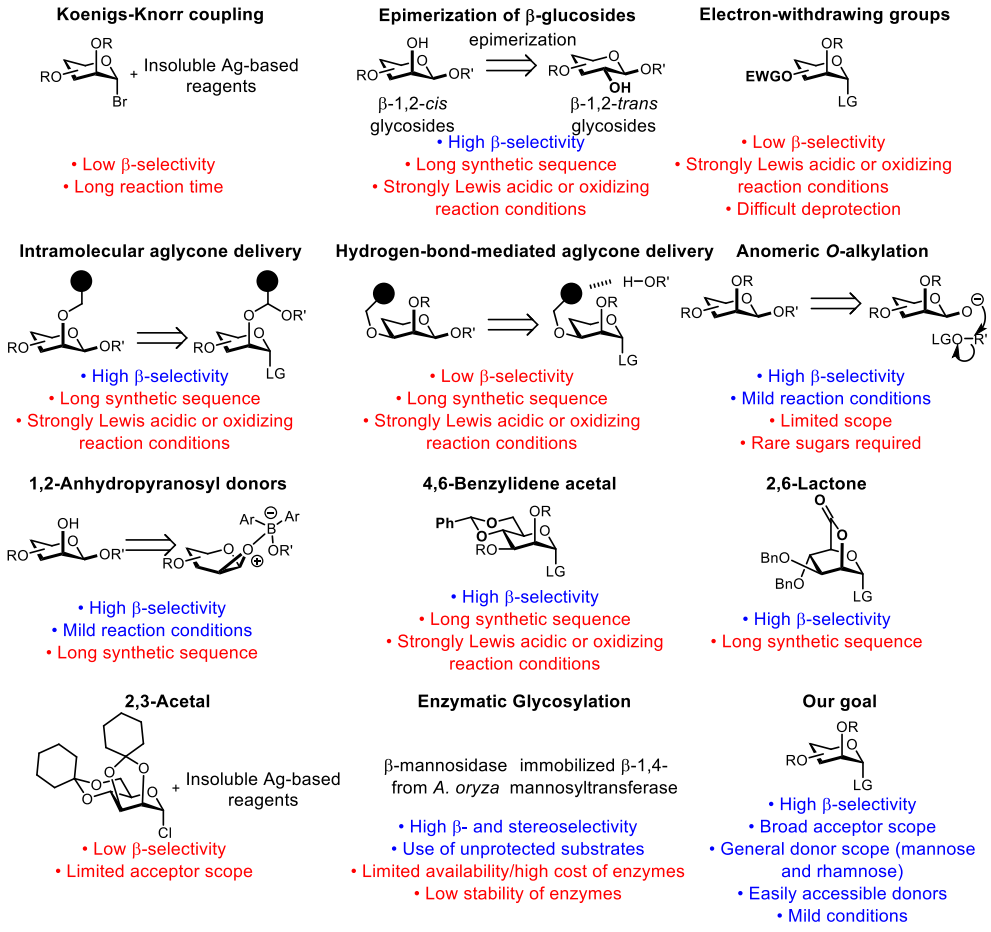


Figure 1.19 Summary of advantages and limitations associated with current methods for β-1,2-*cis* glycosylations.

Over the last several decades, many β-1,2-*cis* glycosylation methods have been developed (Figure 1.19). Several methods (Koenigs-Knorr coupling, the use of electron-withdrawing protecting groups, hydrogen-bond-mediated aglycone delivery) suffer from low level of β-selectivity. Methods relying on the epimerization of β-glucosides, intramolecular aglycone delivery, and the use of 1,2-anhydropyranosyl donors offer excellent stereocontrol; however, they are not widely utilized in oligosaccharide synthesis due to the long synthetic sequence.

Epimerization of β-glucosides requires deprotection, oxidation, and reduction sequence after glucosylation, while multi-step syntheses (often >6 steps) are needed to install specialized protecting groups for intramolecular aglycone delivery or to synthesize specialized glycosyl donors such as 1,2-anhydropyranosyl donors. The long synthetic sequence reduces the overall efficiency and yields of glycosylation. Despite the high β-selectivity, anomeric *O*-alkylation has limited substrate scope. *O*-Alkylation of secondary sugar electrophiles is very challenging when the leaving group is at equatorial position because of the unfavorable steric interactions during axial attack. While enzymatic glycosylation is appealing due to its excellent stereo- and site control, it is difficult to gain access to β-mannosyltransferases or β-rhamnosyltransferases, which are not commercially available due to their relatively low stability and availability. Enzymatic mannosylation and rhamnosylation require GDP-mannose and GDP-rhamnose, which are very expensive from commercial sources. The uridine diphosphate (UDP) byproduct from enzymatic glycosylation could inhibit the glycotransferases and may need to be removed through coupled processes.

The use of 4,6-benzylidene acetal protection has remained as the most popular method for β-mannosylation because the strategy offers high β-selectivity, although the number of synthetic steps required for donor synthesis is still higher than ideal. Activation of 4,6-benzylidene acetal protected donors is typically under strongly Lewis acidic or oxidizing reaction conditions. This limitation is shared by many other methods such as intramolecular aglycone delivery because these methods generally employ stable glycosyl donors such as glycosyl sulfoxides or glycosyl trichloroacetimidates that require relatively forcing activation conditions. Although the activation conditions are generally compatible with carbohydrate substrates as the 4,6-benzylidene acetal protection strategy has been widely utilized in oligosaccharide synthesis. The harsh conditions

display poor tolerance toward a wide variety of common functional groups and therefore have limited utility for the glycosylation of complex acceptors. Chen and co-workers evaluated different mannosyl donors in *N*-glycosylation of cyclic guanidine.[53] They found that *N*-mannosylation with mannosyl trichloroacetimidate donor and ethyl sulfide donor under various Lewis acid-promoted conditions (e.g., with TMSOTf, BF_3OEt_2, and NIS) failed to give any *N*-mannosylated product due to the poor compatibility of Lewis basic functional groups under Lewis acidic conditions (Figure 1.20).

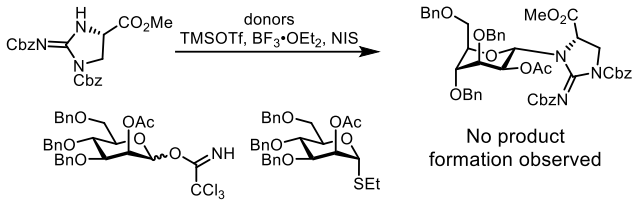


Figure 1.20 Incompatibility between Lewis basic acceptors and Lewis acidic conditions used to activate glycosyl donors.

Although 4,6-benzylidene acetal protection strategy has been the state-of-the-art strategy in oligosaccharide synthesis, there is still no unified strategy for the construction of β-1,2-*cis* glycosidic linkages in glycosylated natural products. Nagamitsu and co-workers found that intramolecular aglycone strategy did not provide the desired β-mannoside in their synthesis of simpotentin, a potentiator of amphotericin B.[54] Instead, they opted to perform β-glycosylation with ulosyl bromide followed by reduction to afford the desired β-mannoside (Figure 1.21A). The β-selectivity achieved with ulosyl bromide has been ascribed to the electron-withdrawing nature of

[53] Wang, B.; Liu, Y.; Jiao, R.; Feng, Y.; Li, Q.; Chen, C.; Liu, L.; He, G.; Chen, G. Total Synthesis of Mannopeptimycins α and β. *J. Am. Chem. Soc.* **2016**, *138*, 3926–3932.
[54] Ohtawa, M.; Shimizu, E.; Saito, A.; Sakamoto, S.; Waki, A.; Kondo, A.; Yagi, A.; Uchida, R.; Tomoda, H.; Nagamitsu, T. Total Synthesis and Absolute Configuration of Simpotentin, a Potentiator of Amphotericin B Activity. *Org. Lett.* **2019**, *21*, 5596–5599.

ketone and the use of heterogeneous promoters.[55] Electron-withdrawing ketone functionality destabilizes α-selective pathways that proceed via S_N1 addition to oxocarbenium intermediates, while surface activation of glycosyl donors by insoluble silver activators blocks α-face from nucleophilic attack. Williams and co-workers selected a similar strategy to synthesize the β-mannosyl linkage. They performed β-glucosylation, and the C2 position was epimerized through an oxidation/reduction process via the ulosyl sugar (Figure 1.21B).[56] They cited the minimization of the number of protecting groups and the high diastereoselectivity in both the glycosylation and reduction steps as the reasons for selecting the stepwise glucosylation/inversion sequence over direct β-mannosylation strategies. The low β-selectivity of direct β-mannosylation also prompted Schobert and co-workers to utilize glucosylation/inversion strategy in their synthesis of epicoccamide D (Figure 1.21C).[57] Therefore, we aim to develop a β-1,2-*cis* glycosylation method that is broadly applicable to acceptors beyond carbohydrates. The development of glycosylation methods has traditionally focused on optimizing around carbohydrate acceptors during reaction development, as a result, the methods are highly optimized for sugar substrates but may not be translatable to other classes of substrates. By testing structurally and functional-group diverse set of acceptors during method development, we seek to develop efficient and selective glycosylations of both carbohydrate and complex molecules.

[55] For a recent review, see: Kaji, E.; Lichtenthaler, F. W. 2-Oxo- and 2-Oximinoglycosyl Halides Versatile Glycosyl Donors for the Construction of β-D-Mannose and β-D-Mannosamine-containing Oligosaccharides. *Trends Glycosci. Glycotechnol*. **1993**, *5*, 121–142.

[56] van der Peet, P. L.; Gunawan, C.; Watanabe, M.; Yamasaki, S.; Williams, S. J. Synthetic β-1,2-Mannosyloxymannitol Glycolipid from the Fungus *Malassezia pachydermatis* Signals through Human Mincle. *J. Org. Chem.* **2019**, 84, 6788–6797.

[57] Loscher, S.; Schobert, R. Total Synthesis and Absolute Configuration of Epicoccamide D, a Naturally Occurring Mannosylated 3-Acyltetramic Acid. *Chem. Eur. J*. **2013**, *19*, 10619–10624.

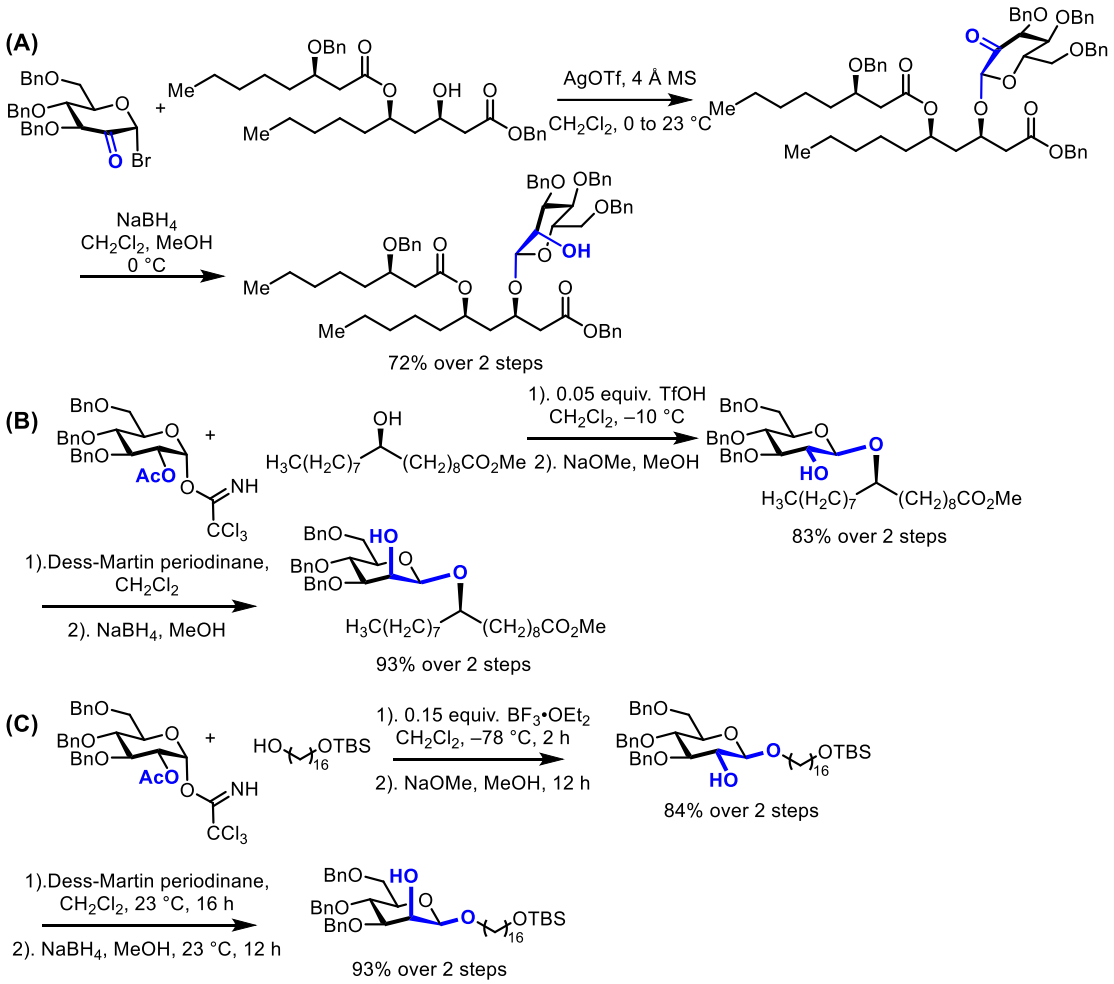


Figure 1.21 β-1,2-*cis* Glycosylation methods utilized in the construction of β-mannosyl linkages in natural product synthesis.

Due to the lack of C6-hydroxyl group in many bacterial saccharides such as rhamnose and noviose, syntheses of β-1,2-*cis*-glycosides containing such sugar residuals have to rely on different strategies. Fidaxomicin contains one β-rhamnosyl and one β-noviosyl linkage. Gademann and co-workers applied 2,3-carbonate strategy to construct the β-noviosyl linkage with low level of β-

selectivity (1:3 α:β) (Figure 1.22).[58] After extensive optimization, they were able to obtain modest β-selectivity (1:4 α:β) in rhamnosylation.

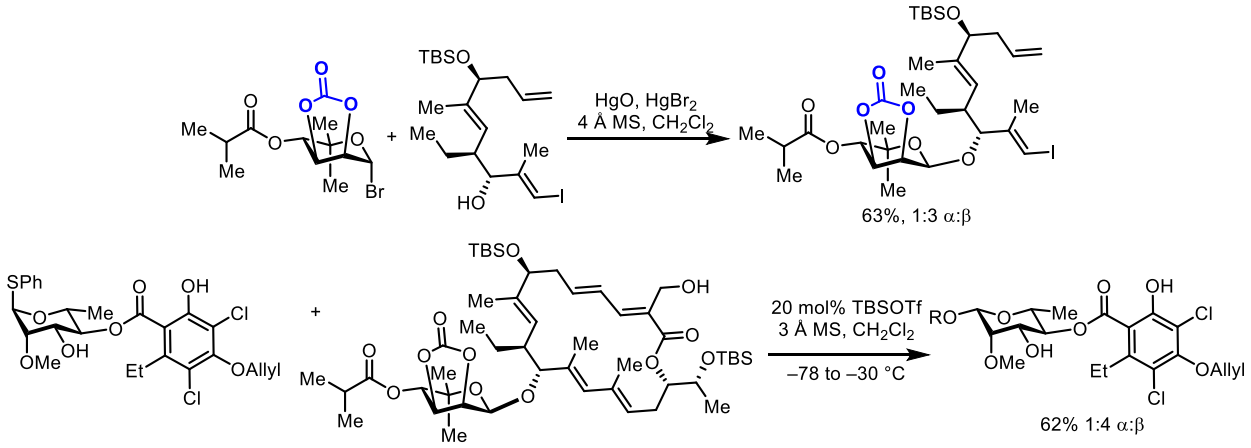


Figure 1.22 Synthesis of β-1,2-*cis* glycosides containing sugar residuals lacking C6-hydroxyl.

The lack of highly β-selective methods for glycosylation of carbohydrates lacking C6-hydroxyl groups prompted us to develop a general method for β-mannosylation and β-rhamnosylation (Figure 1.19). We would like to employ mannosyl and rhamnosyl donors that can be easily synthesized from D-mannose and L-rhamnose efficiently and in short synthetic sequence because the inefficient synthesis of glycosyl donors is one of the reasons why strategies such as intramolecular aglycone delivery and the use of 1,2-anhydropyranosyl donor have not been widely used. Additionally, the glycosylation conditions need to be mild and compatible with sensitive functional groups. Glycosylation of small molecules, peptides and protein pharmaceuticals has shown significant potential for enhancing the biological stability and activity.[2] Sugiyama and co-workers found that both the identify and the anomeric configuration of carbohydrate residuals have

[58] Kaufmann, E.; Hattori, H.; Miyatake-Ondozabal, H.; Gademann, K. Total Synthesis of the Glycosylated Macrolide Antibiotic Fidaxomicin. *Org. Lett*. **2015**, *17*, 3514-3517.

significant impact on the binding profile of glycosylated vasopressin (Figure 1.23A).[59] Davis and co-workers found that glucosylation of leu-enkephalin improved the blood-brain barrier permeability and metabolic half-life in mouse serum (Figure 1.23B).[60] To explore the full potential of clinical relevance of glycosylation pharmaceuticals and natural products, it is necessary to have access to a library of glycosylated compounds. However, pharmaceuticals and natural products often possess sensitive functional groups; therefore, glycosylation must be performed under mild conditions. The development of a mild, general, β-selective methods for β-1,2-*cis*-glycosylation will be discussed in Chapter 2.

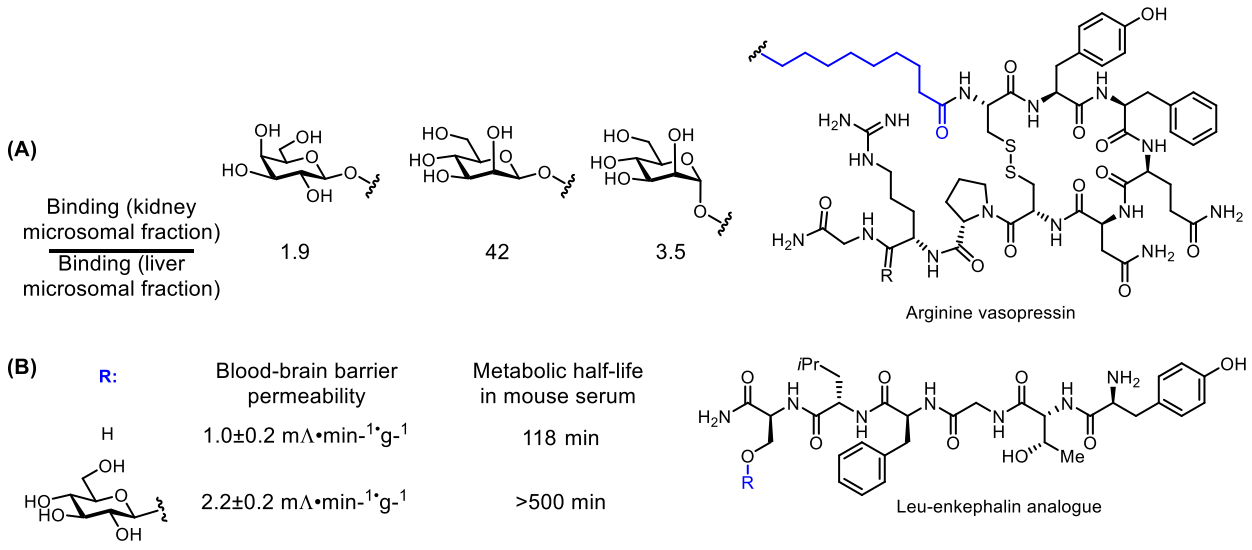


Figure 1.23 Effects of glycosylation on properties of pharmaceuticals.

[59] Suzuki, K.; Susaki, H.; Okuno, S.; Yamada, H.; Watanabe, H. K.; Sugiyama, Y. Specific Renal Delivery of Sugar-Modified Low-Molecular-Weight Peptides *J. Pharmacol. Exp. Ther*. **1999**, *288*, 888–897.
[60] Egleton, R. D.; Mitchell, S. A.; Huber, J. D.; Palian, M. M.; Polt, R.; Davis, T. P. Improved Blood-Brain Barrier Penetration and Enhanced Analgesia of an Opioid Peptide by Glycosylation. *J. Pharmacol. Exp. Ther*. **2001**, *299*, 967–972.

1.6 Current Methodologies for Site-Selective Glycosylation and Their Limitations

Due to the presence of multiple similarly reactive hydroxyl groups, glycosylation of unprotected nucleophiles often leads to a mixture of regioisomers. Therefore, controlling stereo- and site selectivity of glycosylation has been a long-standing challenge in synthetic carbohydrate chemistry. Protecting groups have been routinely applied to mask undesired functionalization sites and induce anomeric and site selectivity. Despite its wide use in chemical glycosylation, several limitations remain to be addressed. Protecting groups can deactivate unprotected hydroxyl groups by increasing steric congestion and reducing their nucleophilicity via electronic perturbation, decreasing the rate of glycosylation. Thus, careful optimization of protecting groups is often necessary to achieve high reactivity and selectivity, and the choice of protecting groups can be substrate dependent. Moreover, the installment of specific protecting groups requires multi-step syntheses from unfunctionalized monomers, rendering the overall glycosylation inefficient.

Stannylene acetal. Approaches based on complexation-induced activation have been used to achieve site selectivity via reagent-controlled glycosylations. Glycosyl acceptor activation by stannylene acetal formation has proved to be a broadly useful approach, enabling selective couplings with a range of unprotected pyranoside substrates. Stannane reagents such as dibutyltin oxide can form stannylene acetal adducts with *cis*-1,2-diol and 1,3-diol moieties in nucleophiles and activate them toward glycosylation by increasing the nucleophilicity through complexation (Figure 1.24A). Typically, one hydroxyl group in a *cis*-diol moiety in sugar nucleophiles is at equatorial position, and the other one is at axial position. Selective coupling with the equatorial hydroxyl group in stannylene acetal is often observed because of the unfavorable steric interactions between glycosyl donors and axial hydroxyl group. The stannylene acetal strategy typically

employs a two-step procedure—formation of stannylene acetal by refluxing glycosyl acceptors with dibutyltin oxide followed by glycosylation.

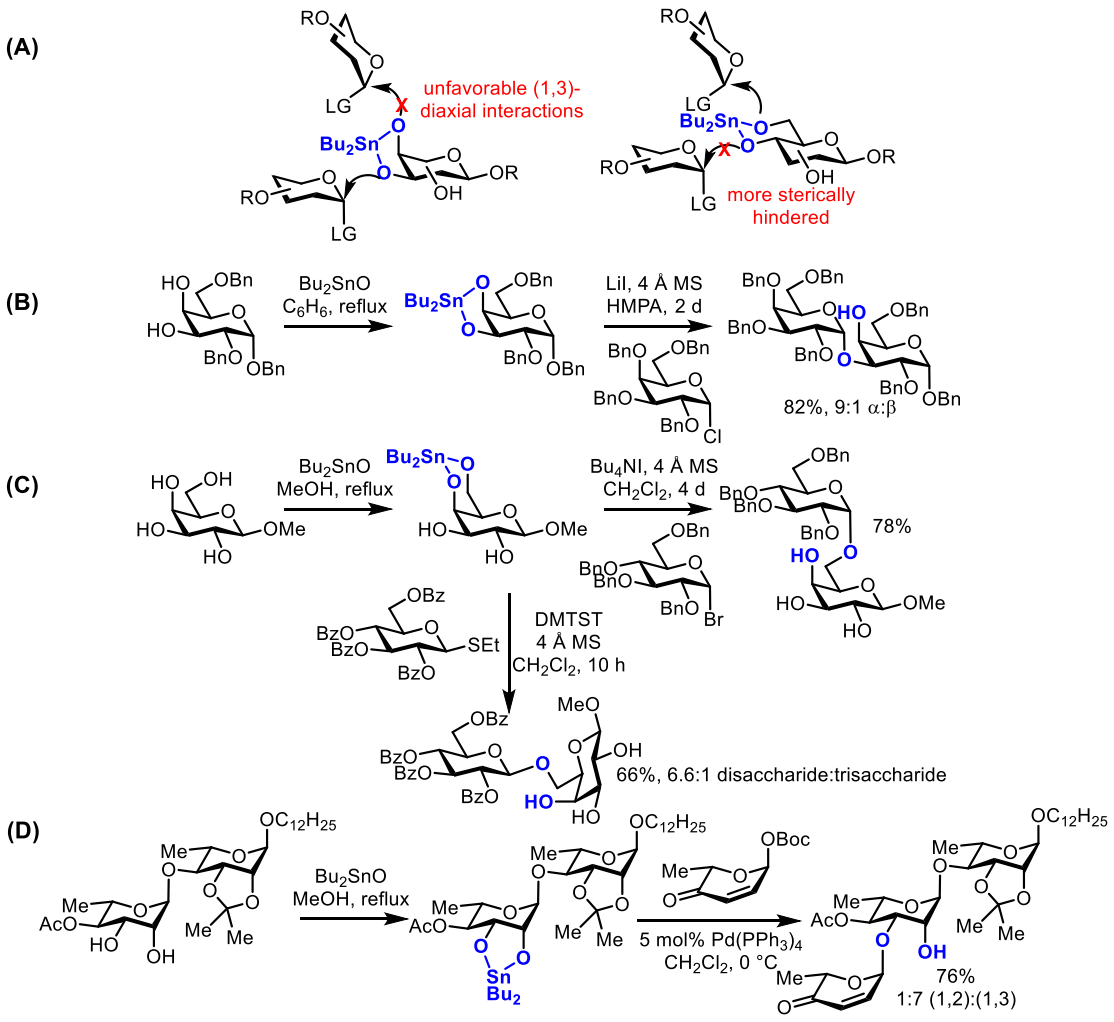


Figure 1.24 Site selective glycosylation promoted by stoichiometric tin-based reagents.

Augé and Veyrières showed that the equatorial hydroxyl group of the dibutylstannylene derivative of a galactose-derived C3,C4-*cis*-diol was glycosylation with good yield (82%) and stereoselectivity (9:1 α:β) (Figure 1.24B).[61] Garegg and co-workers applied the stannylene acetal

[61] Augé, C.; Veyrières, A. Stannylene derivatives in glycoside synthesis. Application to the synthesis of the blood-group B antigenic determinant. *J. Chem. Soc., Perkin Trans. 1* **1979**, 1825−1832.

activation strategy to functionalize fully unprotected methyl β-D-galactopyranoside (Figure 1.24C).[62] Glucosylation at the C6 position was observed as the only disaccharide product with no formation of trisaccharides observed when benzylated glucosyl bromide was used as the glycosyl donor. When benzoylated glucosyl thioglycosides were employed as the glycosyl donor, formation of trisaccharides was observed (6.6:1 disaccharide:trisaccharide) with C6-glucosylation was the only disaccharide product. O'Doherty and co-workers applied the stannylene acetal activation to achieve the site selective, palladium-catalyzed coupling of allylic carbonate with a rhamnopyranoside-derived diol (1:7 (1,2):(1,3)) (Figure 1.24D).[63] Direct coupling of the rhamnosyl diol provided the (1,2)-coupling product as the major regioisomer (4:1 (1,2):(1,3)).

Catalytic activation of minimally protected glycosyl acceptors with stannylene acetals has been realized by Muramatsu and co-workers using diphenyltin dichloride (Figure 1.25).[64] The C3-position of mannosyl, galactosyl, and rhamnosyl acceptors underwent glycosylation with glycosyl bromides when activated by silver(I) oxide. The formation of stannylene acetals selectively occurs with *cis*-diol moieties because *cis*-adducts are thermodynamically more stable than the *trans*-adducts. Nucleophilic attack by equatorial hydroxyl groups is more facile than that by axial hydroxyl groups due to the unfavorable steric interactions between electrophiles and axial substituents during axial attack.

---

[62] Garegg, P. J.; Maloisel, J.-L.; Oscarson, S. Stannylene activation in glycoside synthesis: regioselective glycosylations at the primary position of galactopyranosides unprotected in the 2-, 3-, 4-, and 6-positions. *Synthesis* **1995**, *1995*, 409−414.

[63] Wu, B.; Li, M.; O'Doherty, G. A. Synthesis of several cleistriolide and cleistetroside natural products via a divergent *de novo* asymmetric approach. *Org. Lett*. **2010**, *12*, 5466−5469.

[64] Muramatsu, W.; Yoshimatsu, H. Regio- and stereochemical controlled Koenigs−Knorr-type monoglycosylation of secondary hydroxy groups in carbohydrates utilizing the high site recognition ability of organotin catalysts. *Adv. Synth. Catal*. **2013**, *355*, 2518−2524.

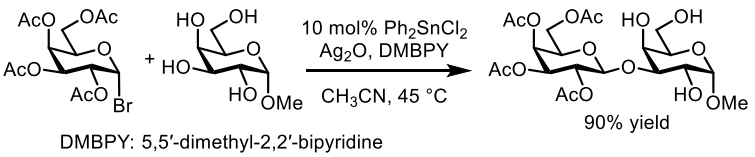


Figure 1.25 Site selective glycosylation catalyzed by diphenyltin dichloride.

Boronic Ester as Transient Protecting Groups. Condensation of boronic acids with diols under mild conditions can afford cyclic boronic esters, which prevent the same diol moieties from undergoing glycosylation, thus serving as transient protecting groups. The formation of boronic esters typically occurs under mild conditions by heating boronic acid and diols or employing drying agents such as molecular sieves to sequester water and drive the equilibrium toward boronic esters. The cleavage of boronic esters can occur by acidic hydrolysis,[65] transesterification of pinacol,[66] or liquid-liquid extraction with a basic aqueous sorbitol solution[67]. Madsen and co-workers showed that phenyl boronic acid selectively reacted with the *cis*-diol moiety in unprotected rhamnosyl acceptor to form *C2*,*C3*-boronic ester in the presence of molecular sieves (Figure 1.26).[64] The unprotected C4-position underwent glycosylation with galactosyl bromide when activated by silver(I) triflate. The boronic ester was cleaved under acidic conditions (MeOH and acidic resins).

[65] Fenger, T. H.; Madsen, R. Regioselective glycosylation of unprotected phenyl 1-thioglycopyranosides with phenylboronic acid as a transient masking group. *Eur. J. Org. Chem*. **2013**, *2013*, 5923−5933.
[66] Fukuhara, K.; Shimada, N.; Nishino, T.; Kaji, E.; Makino, K. Regioselective, tin-free sulfation of unprotected hexopyranosides by using phenylboronic acid. *Eur. J. Org. Chem*. **2016**, *2016*, 902−905.
[67] Mothana, S.; Grassot, J.-M.; Hall, D. G. Multistep phase-switch synthesis by using liquid-liquid partitioning of boronic acids: productive tags with an expanded repertoire of compatible reactions. *Angew. Chem. Int. Ed*. **2010**, *49*, 2883−2887.

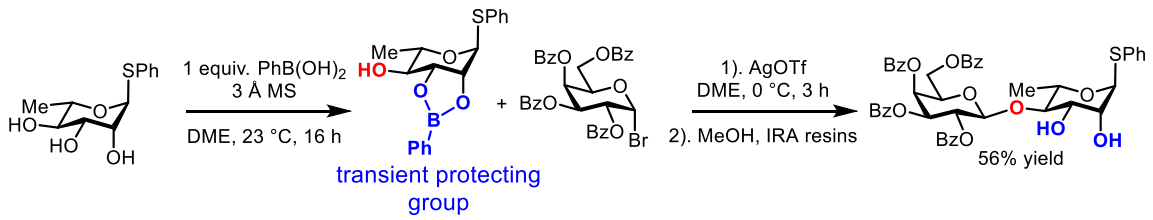
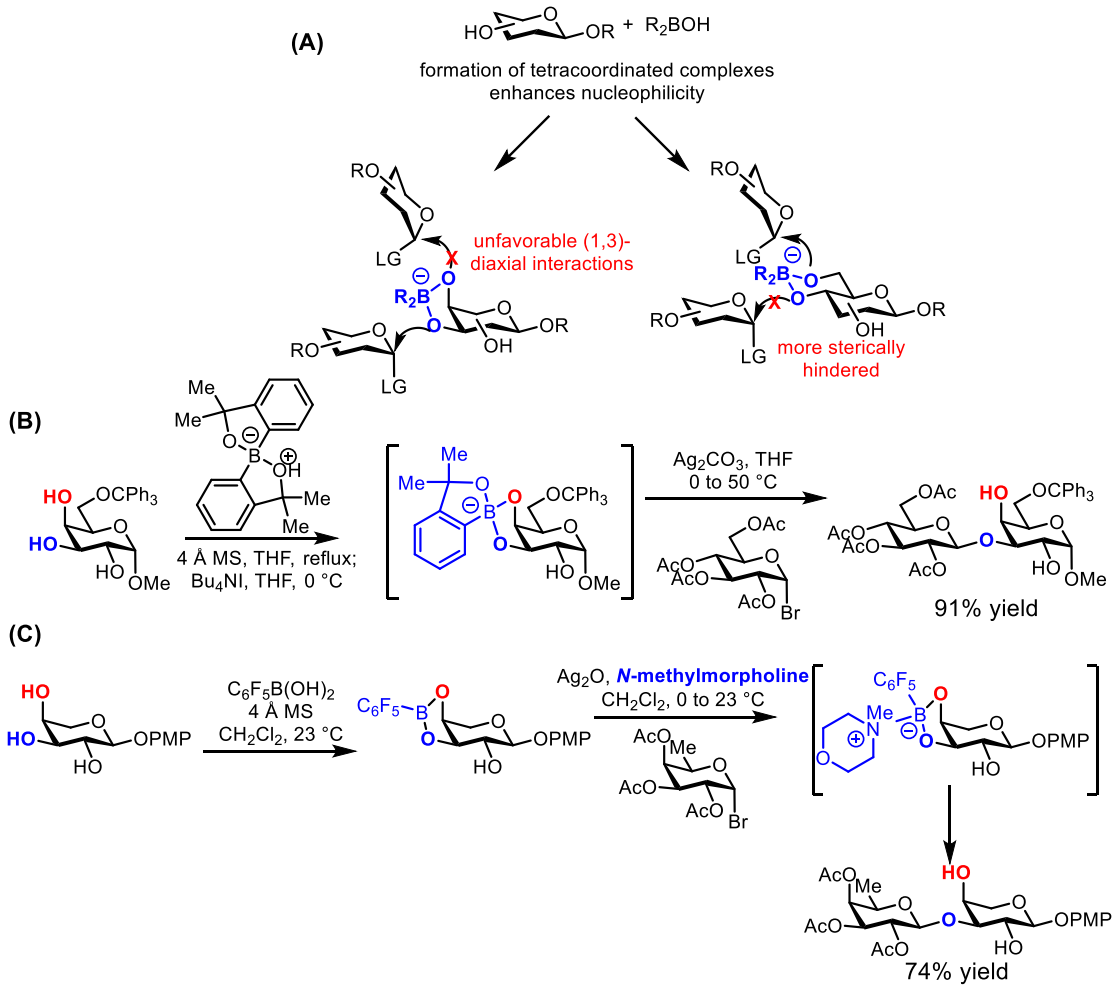


Figure 1.26 Site selective glycosylation using boronic acids as transient protecting groups.

Tetracoordinate Organoboron Complexes. The nucleophilic nature of tetracoordinate borinic acid−diol or boronic acid-diol complexes enhances rather than attenuates the nucleophilicity of complexed hydroxyl groups relative to free hydroxyl groups (Figure 1.27A). Similar to the formation of boronic esters, the site of tetracoordinate boronate formation in carbohydrate substrates is a *cis*-vicinal diol moiety or a 1,3-diol involving an exocyclic C6-OH. Generally, glycosylation occurs at the less hindered B–O moiety (i.e., primary > secondary and equatorial > axial) in the resulting boronate. Aoyama and co-workers showed that a diarylboronic acid derivative formed a tetracoordinate organoboron complex with C3,C4-diol present in a galactose acceptor (Figure 1.27B).[68] The intramolecular B–O coordination was proposed to be crucial to the function of the organoboron promoter. The less hindered C3-position in the organoboron complex reacted with glucosyl bromide upon activation by silver(I) carbonate to afford the (1,3)-product with 91% yield. Taylor and co-workers found that tertiary amines could coordinate with boronic esters, forming tetracoordinate organoboron complexes and activating them toward glycosylation (Figure 1.27C).[69] Pentafluorophenylboronic acid reacted with C3,C4-diol in arabinopyranoside to

[68] Oshima, K.; Aoyama, Y. Regiospecific glycosidation of unprotected sugars via arylboronic activation. *J. Am. Chem. Soc*. **1999**, *121*, 2315−2316.
[69] Mancini, R. S.; McClary, C. A.; Anthonipillai, S.; Taylor, M. S. Organoboron-promoted regioselective glycosylations in the synthesis of a saponin-derived pentasaccharide from *Spergularia ramosa*. *J. Org. Chem*. **2015**, *80*, 8501−8510.

form a boronic ester. The addition of *N*-methylmorpholine promoted glycosylation of the C3-position by coordinating to the boronic ester.



Although the two examples discussed previously employ stoichiometric amount of boronic acids, catalytic amount of boronic or borinic acids can be used to generate tetracoordinate organoboron complexes *in situ*, which undergo glycosylation with glycosyl donors in a one-pot procedure. Diarylborinic acid catalysis has been used to achieve selective monoglycosylation of 1,3- or *cis*-1,2-diol moieties in minimally protected glycosyl acceptor substrates. Taylor and co-

workers designed a diphenylborinic acid catalyst with a pendant amine.[70] The catalyst selectively formed a covalent adduct with the *cis*-diol moiety in minimally protected galactose by replacing the amino alcohol ligand with the diol functionality. The more reactive equatorial position (C3-position of galactose) underwent glycosylation with glucosyl bromide to afford the (1,3)-product with 74% yield. More recently, Taylor and co-workers found that the tetracoordinate organoboron complexes, formed catalytically from glycosyl acceptors and an oxaboraanthracene-derived borinic acid catalyst, could react with glycosyl methanesulfonates (mesylates), generated *in situ* from the corresponding hemiacetals.[71] Mechanistic studies provided evidence that the glycosylation proceeded via an S_N2 displacement of α-glycosyl mesylates, affording the β-products with 75% yield and synthetically useful level of β-selectivity (1:10 α:β). Similar to the reactivity trend observed in reactions employing stoichiometric boronic acids, glycosylation occurs at the less hindered B–O moiety.

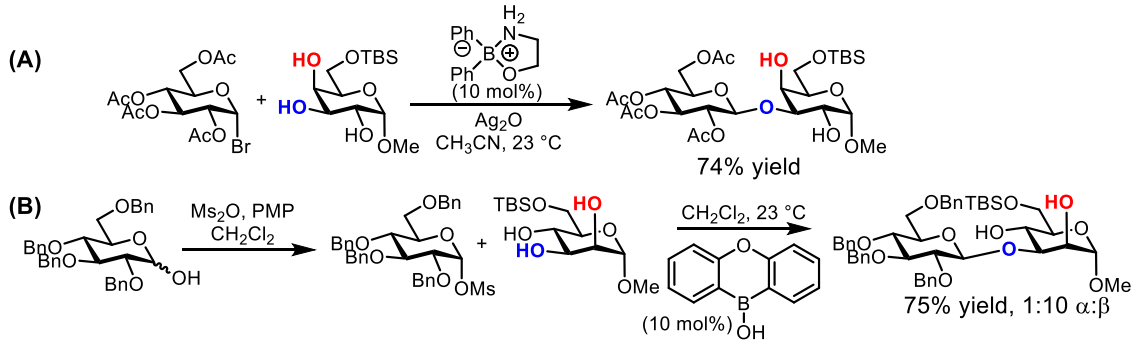


Figure 1.28 Site selective glycosylation catalyzed by borinic acids.

[70] Gouliaras, C.; Lee, D.; Chan, L.; Taylor, M. S. Regioselective activation of glycosyl acceptors by a diarylborinic acid-derived catalyst. *J. Am. Chem. Soc*. **2011**, *133*, 13926−13929.
[71] D'Angelo, K. A.; Taylor, M. S. Borinic acid catalyzed stereo- and regioselective couplings of glycosyl methanesulfonates. *J. Am. Chem. Soc*. **2016**, *138*, 11058−11066.

Site selective construction of 1,2-*cis*-glycosidic linkages has been achieved using boronic acid catalysts in combination with glycal epoxide electrophiles (1,2-anhydropyranosyl donors) by Toshima and co-workers. The key tetracoordinate organoboron complex is proposed to arise from an interaction of the glycosyl acceptor-derived boronic ester with the glycal epoxide (Figure 1.29). Such interaction subsequently activates the glycal epoxide and promotes intramolecular aglycone delivery. Site selective mannosylation of the C3-position of galactosyl and mannosyl acceptors was catalyzed by 4-nitrophenylboronic acid with high yields (75% and 71% respectively) and site selectivity ((1,3)-only and 3.4:1 (1,3):(1,4) respectively).[72] This methodology has been successfully extended to site selective rhamnosylation.[73]

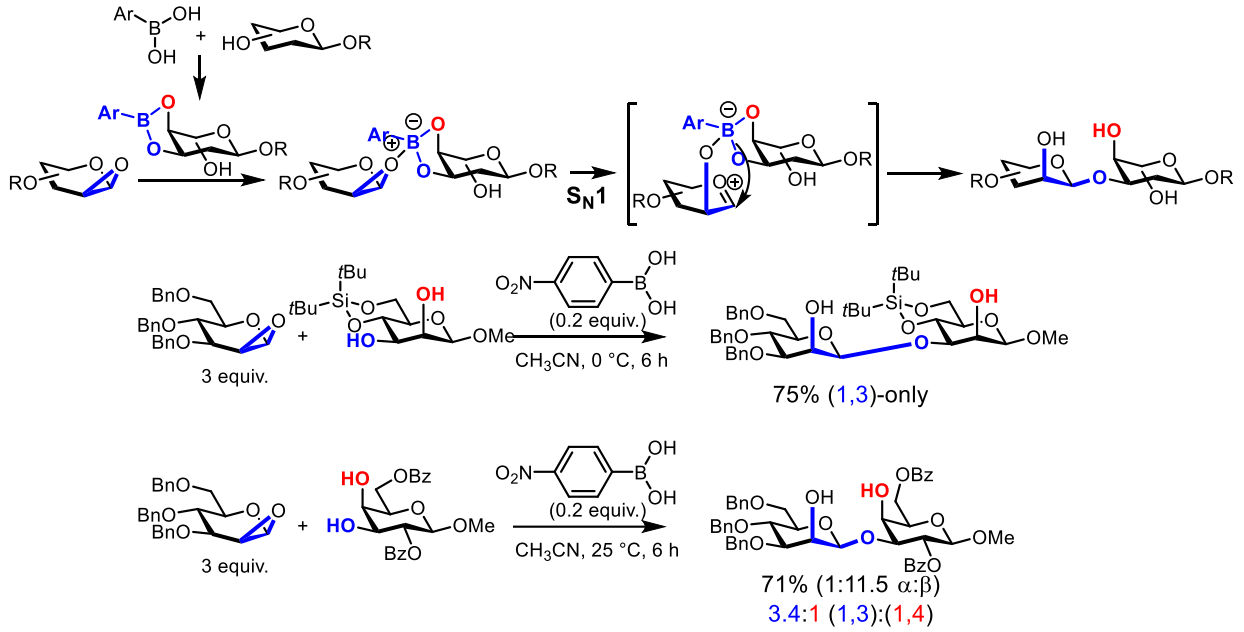


Figure 1.29 Site selective mannosylation catalyzed by boronic acids.

[72] Nishi, N.; Nashida, J.; Kaji, E.; Takahashi, D.; Toshima, K. Regio- and stereoselective beta-mannosylation using a boronic acid catalyst and its application in the synthesis of a tetrasaccharide repeating unit of lipopolysaccharide derived from *E. coli O75*. *Chem. Commun.* **2017**, *53*, 3018–3021.

[73] Nishi, N.; Sueoka, K.; Iijima, K.; Sawa, R.; Takahashi, D.; Toshima, K. Stereospecific β-L-Rhamnopyranosylation through an S_Ni-Type Mechanism by Using Organoboron Reagents. *Angew. Chem. Int. Ed*. **2018**, *57*, 13858–13862.

Calcium(II)-promoted Glycosylation. Miller and co-workers demonstrated that site selective glycosylation of the C3'-position of sucrose could be achieved using glycosyl fluoride donors in the presence of calcium(II) salts and trimethylamine with completely unprotected glycosyl donors and sucrose (Figure 1.30).[74] The origin of site selectivity is not well-understood, but preliminary mechanistic studies suggested that intramolecular hydrogen-bonding interactions play important roles in chelation with calcium cation, thus influencing the reactivity of hydroxyl groups on sucrose.

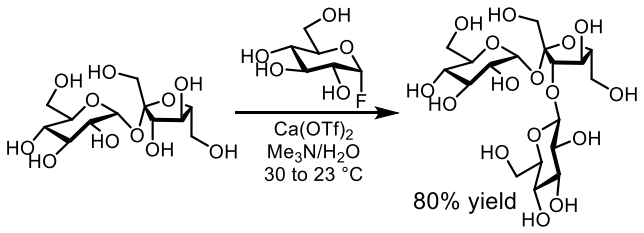


Figure 1.30 Aqueous-phase glucosylation of sucrose promoted by $Ca(OTf)_2$ and trimethylamine.

Chiral Phosphoric Acid-catalyzed Glycosylation. Nagorny and co-workers applied chiral phosphoric acid catalysis to site selective acetalization of partially protected glucose derivatives (Figure 1.31A). The chirality of catalysts was found to have influence on the site selectivity. While (*R*)-CPA1 catalyzed acetalization of a glucose derivative with 10:1 C2:C3, (*S*)-CPA1 promoted the reaction with 1.6:1 C2:C3.[75] Due to the pseudo-homotopic relationship between C2- and C3-hydroxyl groups, complete reversal of site selectivity is not expected with the enantiomer of catalyst. Nagorny and co-workers also applied the same strategy to site selective glycosylation of

[74] Pelletier, G.; Zwicker, A.; Allen, C. L.; Schepartz, A.; Miller, S. J. Aqueous glycosylation of unprotected sucrose employing glycosyl fluorides in the presence of calcium ion and trimethylamine. *J. Am. Chem. Soc*. **2016**, *138*, 3175−3182.

[75] Mensah, E.; Camasso, N.; Kaplan, W.; Nagorny, P. Chiral phosphoric acid directed regioselective acetalization of carbohydrate-derived 1,2-diols. *Angew. Chem, Int. Ed*. **2013**, *52*, 12932−12936.

protected 2-deoxystreptamine and macrolide aglycone. However, this strategy has not been extended to site selective glycosylation of carbohydrates. α-Mannosylation of a 2-deoxystreptamine derivative with mannosyl trichloroacetimidate was achieved using chiral phosphoric acid catalysis (Figure 1.31B).[76] Due to the homotopic nature of the hydroxyl groups, reversal of diastereoselectivity was observed with the enantiomer of catalyst. While anomeric selectivity was high, moderate diastereoselectivity was achieved (2:1 d.r. with (*R*)-CPA2 and 1:6.1 d.r. with (*S*)-CPA2). Chiral phosphoric acid derivatives were used to enforce stereo- and site selectivity of glycosylation of 6-deoxy-erythronolide B (6-dEB) (Figure 1.31C).[77] The level of stereo- and site-control varied significantly depending on the site of glycosylation. Glycosylation of C3-position of 6-dEB with 6-deoxy-gluocosyl trichloroacetimidate proceeded with low site selectivity (2.7:1 C3:C5) but high stereoselectivity (>99:1 α:β). However, glycosylation of C5-position of 6-dEB with the same glycosyl donor proceeded with high site selectivity (1:99 C3:C5) and high stereoselectivity (>99:1 α:β). The identify of glycosyl donors also influenced stereo- and site selectivity of glycosylation. Much lower stereoselectivity (1.7:1 α:β) was observed with 6-deoxy-galactosyl trichloroacetimidate in glycosylation of C5-position of 6-dEB.

[76] Lee, J.; Borovika, A.; Khomutnyk, Y.; Nagorny, P. Chiral phosphoric acid-catalyzed desymmetrizative glycosylation of 2-deoxystreptamine and its application to aminoglycoside synthesis. *Chem. Commun*. **2017**, *53*, 8976−8979.

[77] Tay, J.-H.; Argüelles, A. J.; DeMars, M. D., II; Zimmerman, P. M.; Sherman, D. H.; Nagorny, P. Regiodivergent glycosylations of 6-deoxy-erythronolide B and oleandomycin-derived macrolactones enabled by chiral acid catalysis. *J. Am. Chem. Soc*. **2017**, *139*, 8570−8578.

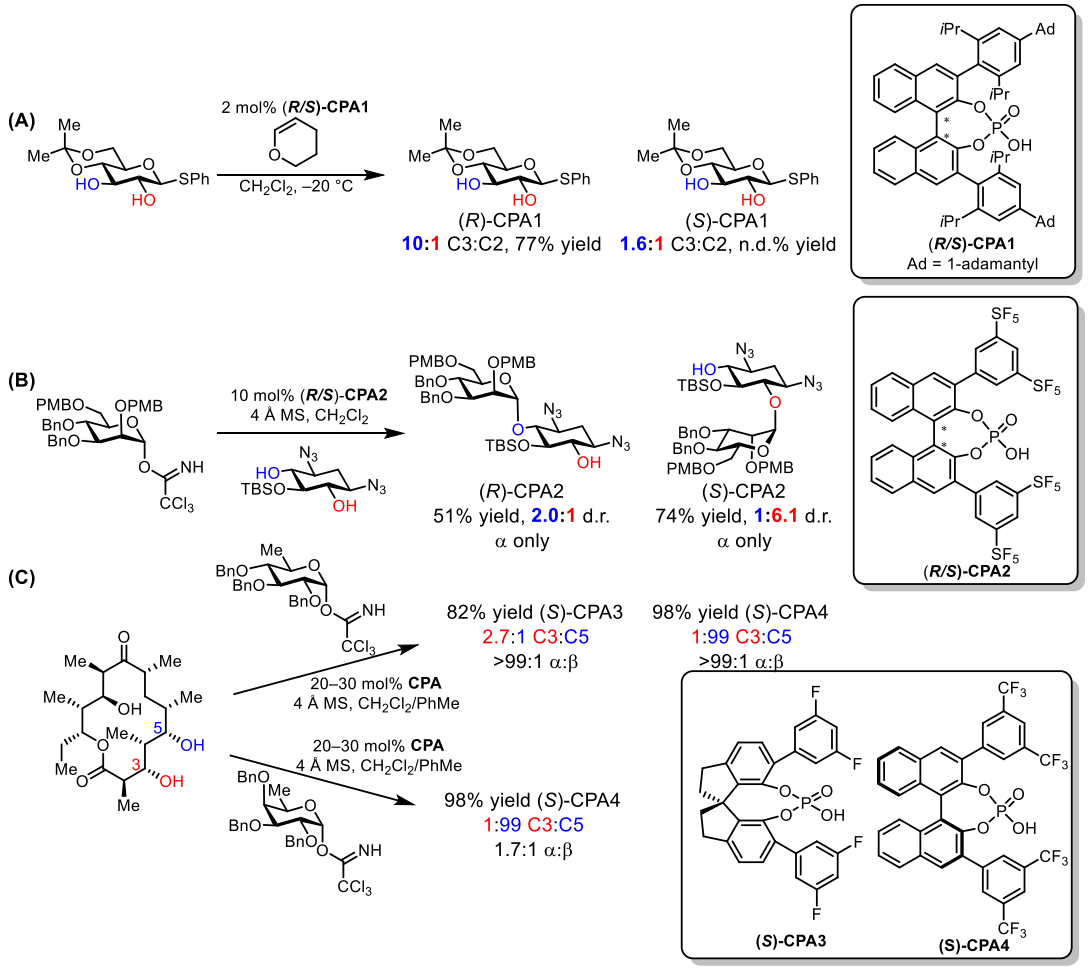


Figure 1.31 Chiral phosphoric acids-catalyzed site selective functionalization of alcohols.

1.7 Summary for Site-Selective Glycosylation Methods and Outlook

The majority of site selective glycosylation methods employ stoichiometric reagents or catalysts that can selectively form covalent adducts with diol moieties in minimally protected glycosyl acceptors (Figure 1.32A). Due to the greater thermodynamic stability of six-membered and *cis*-five-membered cyclic adducts, organoboron and organotin reagents or catalysts selectively activate 1,3-diols and *cis*-1,2-diol moieties rather than *trans*-1,2-diols. More recently, Toshima and co-workers designed a diboron catalyst for site selective glycosylation of *trans*-1,2-diols, but the site selectivity was controlled by the size of protecting groups on glycosyl acceptors rather than

the catalyst.[78] Therefore, a general method for site selective glycosylation of carbohydrate substrates containing *trans*-1,2-diols is still lacking.

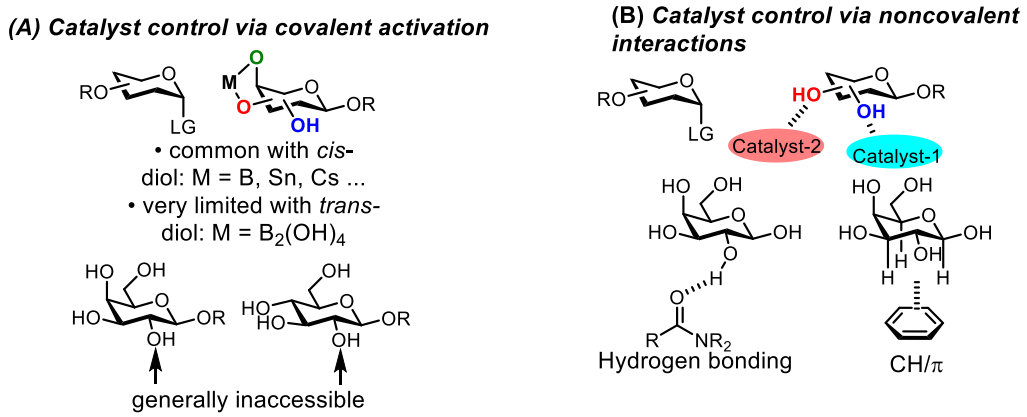


Figure 1.32 Two distinct strategies for catalyst-controlled site selective glycosylations.

Chiral phosphoric acid catalysis, on the other hand, induces site selectivity via noncovalent interactions (Figure 1.32B). There is no covalent adduct formed between glycosyl acceptors and catalysts. The site selectivity is controlled by attractive noncovalent interactions such as π-π or CH-π interactions and repulsive interactions such as steric interactions. Because in principle there are no constrains on the stereochemical relationship of hydroxyls on glycosyl acceptors, organocatalytic site selective glycosylation relying on noncovalent interactions can be theoretically applied to functionalize both *cis*- and *trans*-diols. However, current methods suffer from low stereo- and site selectivity. Although chiral phosphoric acid catalysis has been utilized to functionalize complex alcoholic acceptors, it has not been applied to modulate stereo- and site selectivity of sugar-sugar coupling reactions. We envision that there is an opportunity to develop

[78] Tomita, S.; Tanaka, M.; Inoue, M.; Inaba, K.; Takahashi, D.; Toshima, K. Diboron-Catalyzed Regio- and 1,2-*cis*-α-Stereoselective Glycosylation of *trans*-1,2-Diols. *J. Org. Chem.* **2020,** *85*, 16254–16262.

a highly β-selective and site selective method for glycosylation of carbohydrates containing *trans*-diol moieties. The details of this study will be described in Chapter 3.

Chapter 2

Highly Selective β-Mannosylations and β-Rhamnosylations Catalyzed by Bis-thioureas

2.1 Introduction[1]

Due to the prevalence of pyranosides bearing β-1,2-*cis*-*O*-glycosidic linkages in many biologically important oligosaccharides, the construction of well-defined β-1,2-*cis*-glycosidic linkages is therefore an important objective in synthetic chemistry, but one that presents fundamental challenges as describe in Chapter 1. β-1,2-*cis*-*O*-Glycosides are intrinsically less stable than their α-diastereomers as a result of diminished anomeric stabilization and increased

[1] Portions of this chapter have been reproduced or adapted from: Li, Q.; Levi, S. M.; Jacobsen, E. N. Highly Selective β-Mannosylations and β-Rhamnosylations Catalyzed by Bis-thiourea. *J. Am. Chem. Soc.* **2020**, *142*, 11865–11872.

steric congestion. These effects are also manifested in glycosylation pathways, resulting in a strong kinetic preference for α-products in typical mannosylation and rhamnosylation reactions.

Significant efforts have been devoted to overcoming the inherent α-selectivity and developing β-1,2-*cis* glycosylation methods as described in Chapter 1. Each of the successful strategies employs donors with specific protecting group schemes requiring multi-step syntheses. The strongly Lewis acidic or oxidizing reaction conditions required for these couplings display poor tolerance toward a wide variety of common functional groups and therefore have limited utility for the glycosylation of complex acceptors.[2] Finally, no general methods for 1,2-*cis* glycosylation of less reactive nucleophiles such as neutral phenols have been identified to date. In particular, electron-rich *O*-aryl glycosides are difficult to access as they are prone to Fries-type rearrangement pathways to afford *C*-glycosides under Lewis acidic conditions.[3]

[2] Levi, S. M.; Jacobsen, E. N. Catalyst-Controlled Glycosylations. *Org. React*. **2019**, *100*, 801−852.
[3] (a) Mahling, J.-A.; Schmidt, R. R. Aryl C-Glycosides from O-Glycosyl Trichloroacetimidates and Phenol Derivatives with Trimethylsilyl Trifluoromethanesulfonate (TMSOTf) as the Catalyst. *Synthesis* **1993**, 325−328. For reviews, see (b) Suzuki, K. Lessons from Total Synthesis of Hybrid Natural Products. *Chem. Rec*. **2010**, *10*, 291–307. (c) dos Santos, R. G.; Jesus, A. R.; Caio, J. M.; Rauter, A. P. Fries-type Reactions for the *C*-Glycosylation of Phenols. *Curr. Org. Chem*. **2011**, *15*, 128−148.

2.2 Our Approach

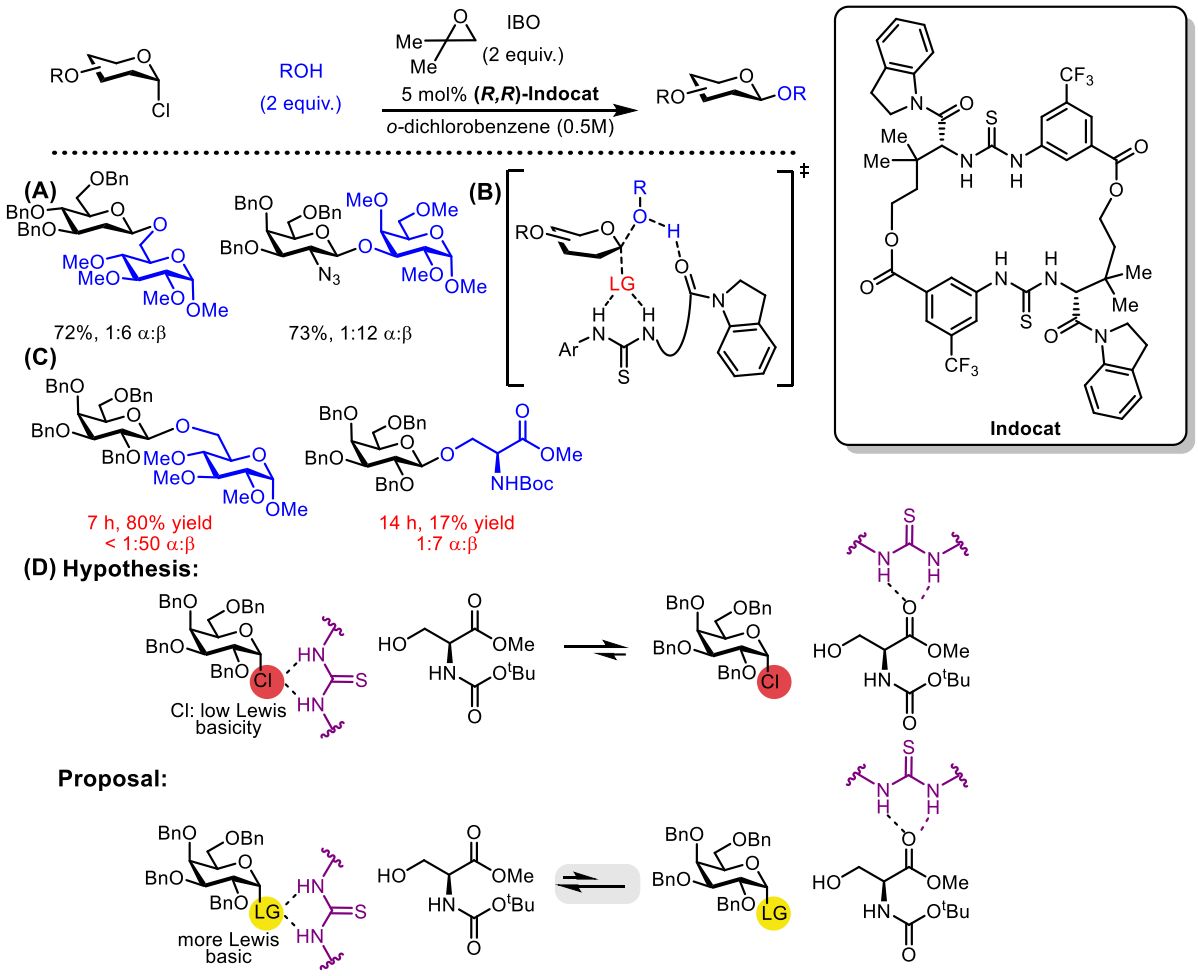


Figure 2.1 Stereospecific glycosylations catalyzed by a macrocyclic bis-thiourea and the limitations of chloride-activation strategy.

We aim to develop a broadly applicable method for β-mannosylations and β-rhamnosylations that employs easily synthesized glycosyl donors and mild activation conditions. In 2017, we reported that macrocyclic bis-thiourea derivatives catalyzed stereospecific glycosylation reactions.[4] A variety of glycosyl donors can be activated by (*R,R*)-Indocat, and high β-selectivities were generally obtained with simply sugar acceptors (Figure 2.1A). We proposed that the bis-thiourea derivatives catalyze stereospecific glycosylations via a dual activation mode

[4] Park, Y.; Harper, K. C.; Kuhl, N.; Kwan, E. E.; Liu, R. Y.; Jacobsen, E. N. Macrocyclic Bis-thioureas Catalyze Stereospecific Glycosylation Reactions. *Science* **2017**, *355*, 162−166.

(Figure 2.1B). The two thiourea moieties engage in 4H-binding to chloride leaving group and activate glycosyl chlorides toward substitution, while the indoline-amides function as the general base for the activation of nucleophiles. Although (*R,R*)-Indocat promoted galactosylation of a simple primary sugar nucleophile with high yield (80%) and high β-selectivity (<1:50 α:β), much lower yield (17%) and β-selectivity (1:7 α:β) were observed in the glycosylation of nucleophiles possessing multiple Lewis basic functional groups such as esters and carbamates (Figure 2.1C). We hypothesized that the low reactivity observed with Lewis basic nucleophiles could arise from the unproductive binding of catalysts to Lewis basic sites on nucleophiles rather than glycosyl chlorides, due to the low Lewis basicity of glycosyl chlorides (Figure 2.1D). We proposed that increasing the Lewis basicity of leaving groups could result in higher affinity toward the thiourea moiety, thus improving the catalytic efficiency and enabling superior functional group compatibility.

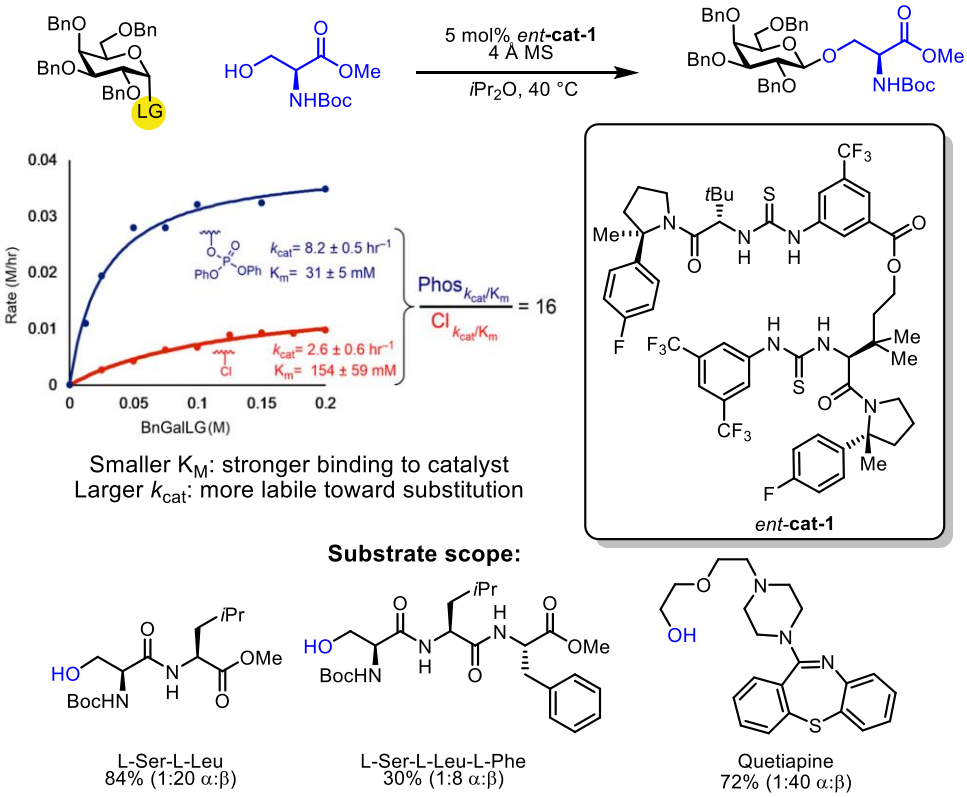


Figure 2.2 Improved catalytic efficiency of glycosylations achieved by employing phosphate leaving group.

We hypothesized that our synthetic hydrogen-bond-donor catalysts would be well suited to bind an organic phosphate leaving group due to its high Lewis basicity. Michaelis-Menten kinetic analyses of reactions with galactosyl chloride and galactosyl phosphate showed that galactosyl phosphates bind more strongly to catalysts and the phosphate-catalyst complexes are more labile toward substitution, resulting in a 16-fold increase in catalytic efficiency (Figure 2.2).[5] The improved binding and reactivity of glycosyl phosphate donors prompted us to investigate the nucleophile scope of glycosylation. Nucleophiles containing multiple Lewis basic functionality and basic nitrogens underwent galactosylation catalyzed by *ent*-**cat-1** with high β-selectivity (1:8–40, α:β). We proposed that the phosphate activation strategy could be applied to β-mannosylations and rhamnosylations. While the construction of β-1,2-*trans*-*O*-pyranosyl linkages and β-1,2-*cis*-*O*-furanosyl linkages[6] has been demonstrated using the appropriate α-glycosylphosphate donors with linked bis-thiourea catalysts such as **cat-1**, very limited success has been achieved as yet in the application of this strategy to β-1,2-*cis*-*O*-pyranosyl linkages.

[5] Levi, S. M.; Li, Q.; Rötheli, A. R.; Jacobsen, E. N. Catalytic Activation of Glycosyl Phosphates for Stereoselective Coupling Reactions. *Proc. Natl. Acad. Sci. U. S. A*. **2019**, *116*, 35−39.
[6] Mayfield, A. B.; Metternich, J. B.; Trotta, A. H.; Jacobsen, E. N. Stereospecific Furanosylations Catalyzed by Bis-thiourea Hydrogen-Bond Donors. *J. Am. Chem. Soc*. **2020**, *142*, 4061−4069.

2.3 Catalyst and Reaction Optimization

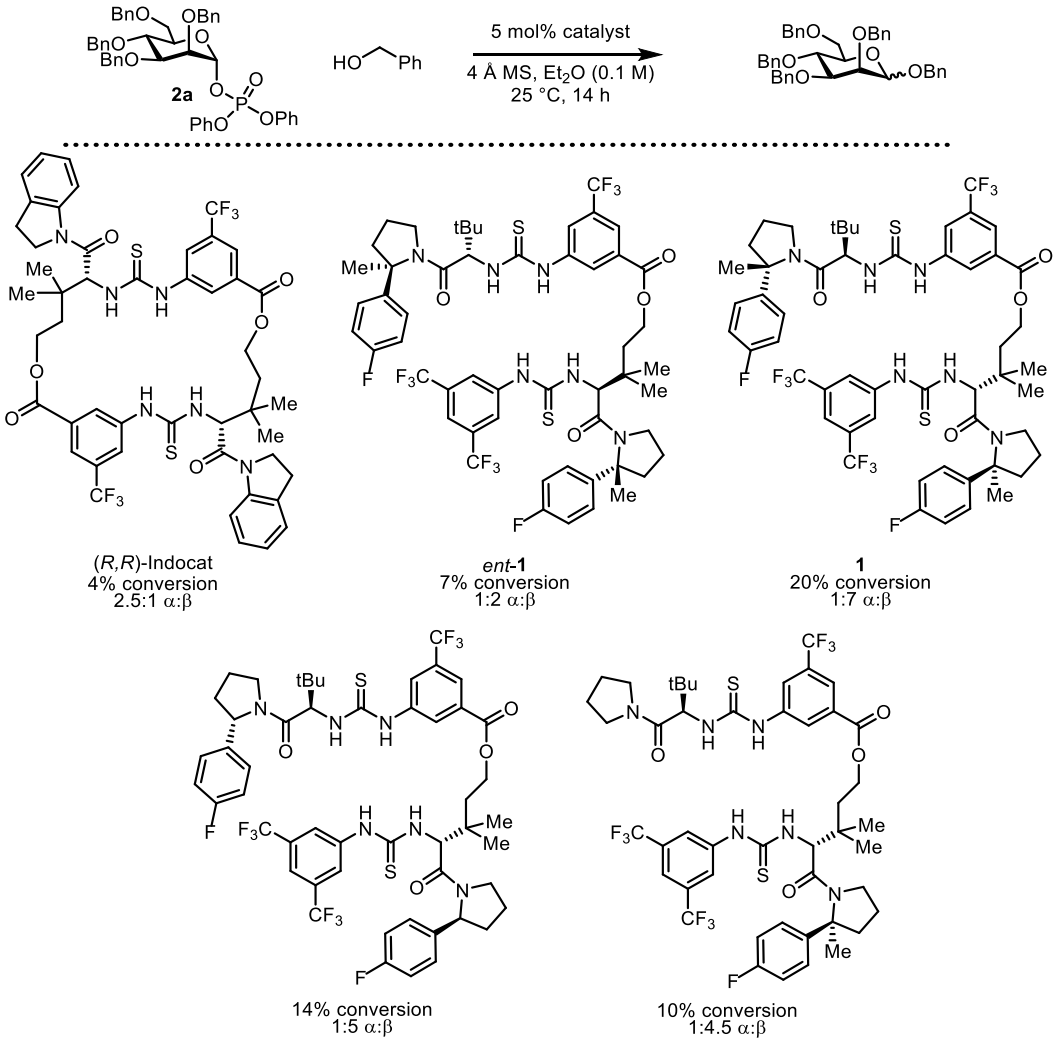


Figure 2.3 Catalyst evaluation for mannsoylation of benzyl alcohol with **2a**.

We began our investigation by evaluating different bis-thiourea derivatives in mannosylation of benzyl alcohol with perbenzyl protected mannosyl phosphate **2a** (Figure 2.3). (*R,R*)-Indocat, the optimal catalyst for promoting stereospecific glycosylation with glycosyl chlorides, promoted α-selective mannosylation with very low reactivity. Macrocyclic bis-thioureas were originally optimized to activate chloride leaving group. We proposed that the rigid structure of the macrocycle confines the size of binding pocket so that it may not be able to

accommodate a significantly larger phosphate leaving group, resulting in poor reactivity and selectivity in promoting mannosylation with **2a**. Catalyst **1** promoted mannosylation with higher β-selectivity (1:7 vs 1:2 α:β) and reactivity (20% vs 7% conversion) than *ent*-**1**. Such stereochemical matching between catalyst and glycosyl donor points to the precise catalyst-substrate interactions in the catalytic glycosylation event. Further decreasing catalyst rigidity by removing methyl substitution on aryl pyrrolidine moieties in catalyst led to diminished β-selectivity. The aryl substituent on "northern" aryl pyrrolidine amide was also found to be important for β-selectivity.

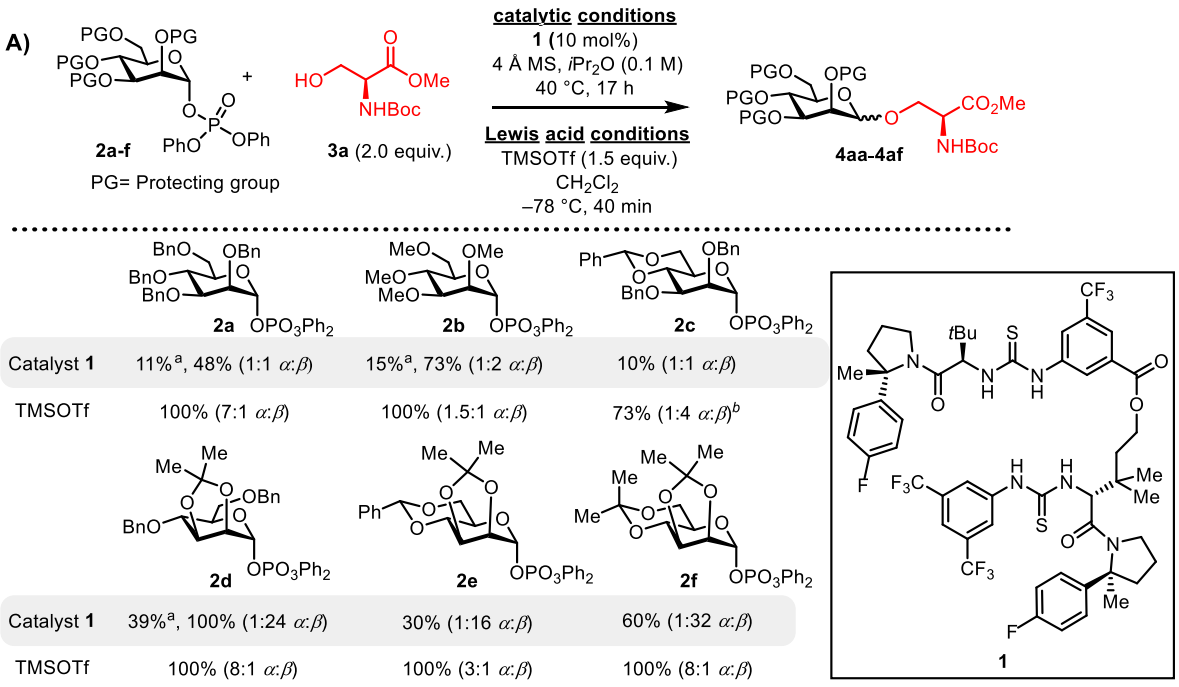


Figure 2.4 Protecting-group effects on bis-thiourea-catalyzed and TMSOTf-promoted mannosylations of primary alcohol **3a** and secondary alcohol nucleophile **3b**. Conversions were determined by ^{1}H NMR analysis of crude product mixtures with mesitylene as an internal standard. Selectivities were determined by ^{1}H NMR analysis of crude product mixtures. [a]Conversions after 3 h. Selectivies remained constant over time. [b]Reaction run at –40 °C.

Catalyst **1** was selected as the optimal catalyst and was evaluated in the mannosylation of a more challenging model acceptor **3a** containing Lewis basic functional groups (Figure 2.4A). Simple alkyl protecting schemes such as perbenzyl (**2a**) or permethyl (**2b**) resulted in largely unselective coupling reactions (1:1 to 1:2 α:β). Variation of the protecting groups on the mannosyl diphenylphospate donor resulted in pronounced effects on anomeric selectivity. Incorporation of the 4,6-benzylidene acetal protecting group (as in **2c**) pioneered by Crich for β-selective mannosylations under strong Lewis acid conditions again led to an unselective reaction in the presence of catalyst **1**. However, a dramatic increase in β-selectivity was observed under catalytic conditions when the C2 and C3 substituents were bridged by an acetonide protecting group. Thus, coupling reactions with donors **2d-f** all afforded high β-selectivity (1:16–32 α:β) with the relatively unhindered acceptor **3a**.[7] Mannosylation of the more sterically congested secondary nucleophile **3b** was found to be substantially more β-selective with **2f** than with **2d** (1:24 vs 1:10 α:β Figure 2.4B). The bis-acetonide-protected mannose derivative **2f** also offers important practical advantages, being prepared in a simple two-step sequence from D-mannose, and affording

[7] Higher reactivity of **2f** was achieved by increasing reaction temperature to 50 °C, albeit with slightly lower β-selectivity (85% conversion, 1:19 α:β).

glycosylation products that may be selectively or fully deprotected under mild conditions (*vide infra*).[8]

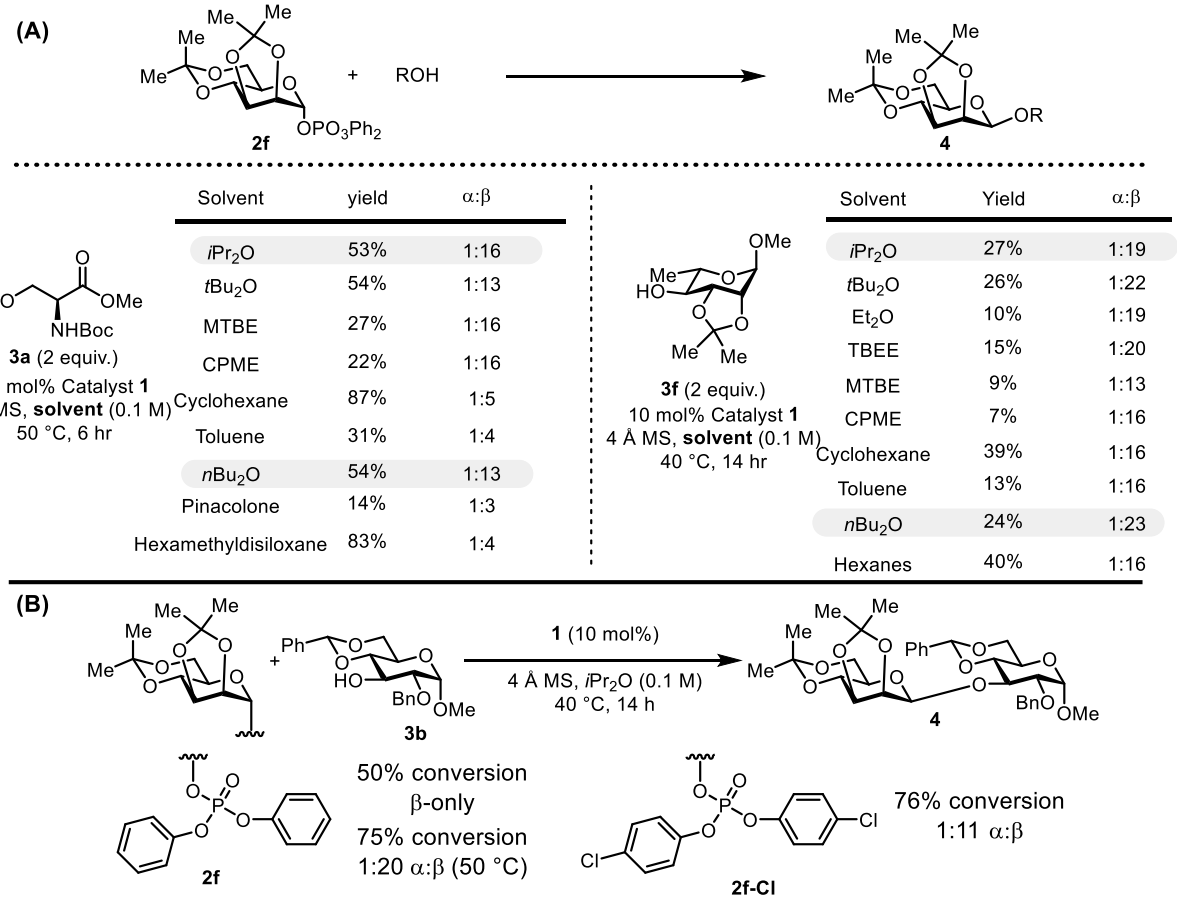
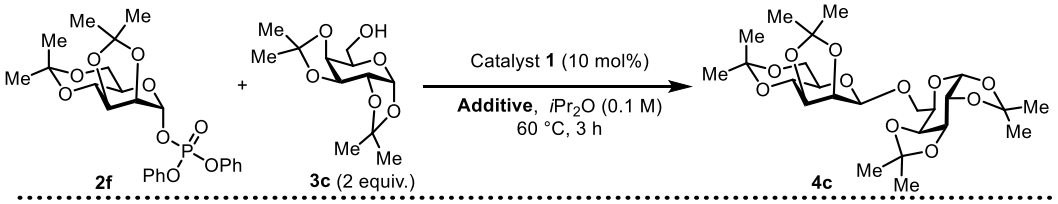


Figure 2.5 Effects of solvents and phosphate leaving group on the β-selectivity and reactivity of mannosylations. Yields and conversions were determined by ^{1}H NMR analysis of crude product mixtures with mesitylene as an internal standard. Selectivities were determined by ^{1}H NMR analysis of crude product mixtures.

[8] For selective hydrolysis of 4,6-acetonides, see (a) Combemale, S.; Assam-Evoung, J.-N.; Houaidji, S.; Bibi, R.; Barragan-Montero, V. Gold Nanoparticles Decorated with Mannose-6-phosphate Analogues. *Molecules* **2014**, *19*, 1120–1149. (b) Neogi, A.; Majhi, T. P.; Achari, B.; Chattopadhyay, P. Palladium-Catalyzed Intramolecular C–O Bond Formation: An Approach to the Synthesis of Chiral Benzodioxocines. *Eur. J. Org. Chem*. **2008**, *2008*, 330–336. For deprotection of bis-acetonide, see (c) Cocinero, E. J.; Stanca-Kaposta, E. C.; Scanlan, E. M.; Gamblin, D. P.; Davis, B. G.; Simons, J. P. Conformational Choice and Selectivity in Singly and Multiply Hydrated Monosaccharides in the Gas Phase. *Chem. Eur. J*. **2008**, *14*, 8947–8955.

Effects of different reaction parameters on bis-thiourea-catalyzed mannosylation were investigated. Different solvents were evaluated in mannosylation of amino acid acceptor **3a** and secondary sugar acceptor **3f** (Figure 2.5A). Mannosylation of **3a** afforded products with higher β-selectivies in ethereal solvents (1:13–16 α:β) than that in nonpolar solvents such as cyclohexane and toluene (1:3–5 α:β), although the effects of solvent polarity on β-selectivity were less pronounced in mannosylation of **3f**. Among different ethereal solvents, mannosylation in diisopropyl ether, di-*n*-butyl ether, and di-*tert*-butyl ether proceeded to higher conversions than that in other ethereal solvents with shorter alkyl chains. Diisopropyl ether was selected because of its greater ability to solubilize acceptors. A screen of phosphate leaving groups revealed the diphenyl derivatives as optimal (Figure 2.5B). The more electron-withdrawing bis-(4-cholorophenyl) phosphates were found to be more reactive but less β-selective in the presence of **1**.



(A) **Additive screening**
Catalyst **1** (10 mol%)
Additive, iPr$_2$O (0.1 M)
60 °C, 3 h

Additive	Conversion	Yield	α:β
4Å MS	74%	69%	1:13
$TMSCHN_2$	63%	61%	1:9
Isobutylene oxide	72%	43%	1:4
K_2CO_3	46%	28%	1:6
$NaHCO_3$	100%	40%	1:1
Na_2HPO_4	100%	30%	1:1
Basic alumina	100%	13%	1:2.3

(B) **Catalyst loading**
Catalyst **1** (**X** mol%)
4 Å MS, iPr$_2$O (0.1 M)
60 °C, 3 h

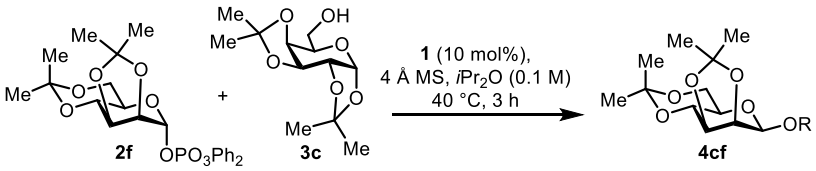
Mol%	Conversion	α:β
0	3%	1.5:1
1	12%	1:7
2.5	26%	1:9
5	49%	1:12
10	74%	1:13
20	96%	1:13

(C) **Temperature**
Catalyst **1** (10 mol%)
4 Å MS, iPr$_2$O (0.1 M)
Temperature, 3 h

Temp. (°C)	Conversion	α:β
40	30%	1:19
50	51%	1:16
60	74%	1:13

Figure 2.6 Effects of additive, catalyst loading, and reaction temperature on the β-selectivity and reactivity of mannosylations. Conversions and yields were determined by ^{1}H NMR analysis of crude product mixtures with mesitylene as an internal standard. Selectivities were determined by ^{1}H NMR analysis of crude product mixtures.

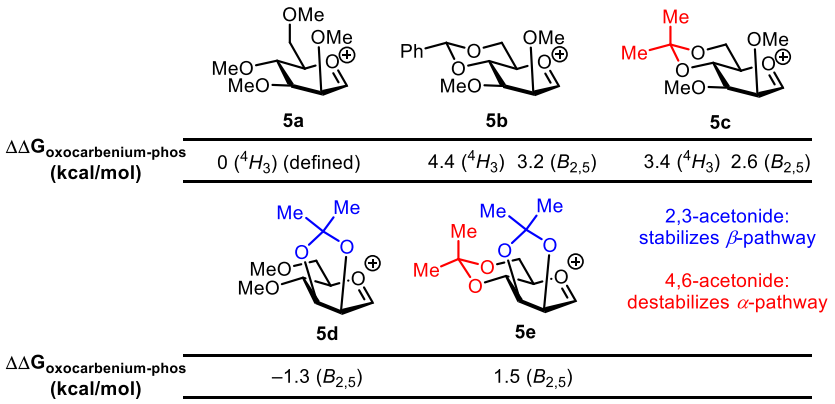
As observed previously in related bis-thiourea-catalyzed glycosylations of glycosyl phosphates, the inclusion of 4 Å molecular sieves is crucial for minimizing undesired hydrolysis of donors and sequestering the phosphoric acid by-product, which has been shown to promote glycosyations unselectively (Figure 2.6A).[5,6] Catalyst loading had influence on both the conversion and β-selectivity of mannosylation (Figure 2.6B). β-selectivity increased as the catalyst loading was increased to 5 mol%, and no further increase in β-selectivity was observed when the loading was above 5 mol%, suggesting that the catalytic reactions outcompete with the unselective background reactions at 5 mol% catalyst loading. 10 mol% was selected as the optimal catalyst loading to achieve high conversions after 24 hours. As reaction temperature increased, higher conversion and lower β-selectivity were observed (Figure 2.6C). We selected 50 °C as the optimal reaction temperature because it offered a good balance between conversion and β-selectivity. Effects of varying the stoichiometry of donor **2f** and acceptor **3c** were also investigated (Figure 2.7). While slightly higher conversions were obtained when the stoichiometry of either **2f** or **3c** was increased, those improvements were offset by observable decreases in β-selectivity. Accordingly, subsequent scope studies were carried out with 2 equivalents of acceptor in the case of simple nucleophiles or equimolar ratios of donor and acceptor in the case of complex nucleophiles.



Entry	equiv 2f	equiv 3c	conversion	α:β
1	1	1	24%	1:19
2	2	1	36%	1:15
3	3	1	31%	1:14
4	4	1	29%	1:12
5	1	2	30%	1:19
6	1	3	28%	1:16
7	1	4	32%	1:12

Figure 2.7 Stoichiometry optimization. Conversions were determined by ^{1}H NMR analysis of crude product mixtures with mesitylene as an internal standard. Selectivities were determined by ^{1}H NMR analysis of crude product mixtures.

2.4 Computational Analysis



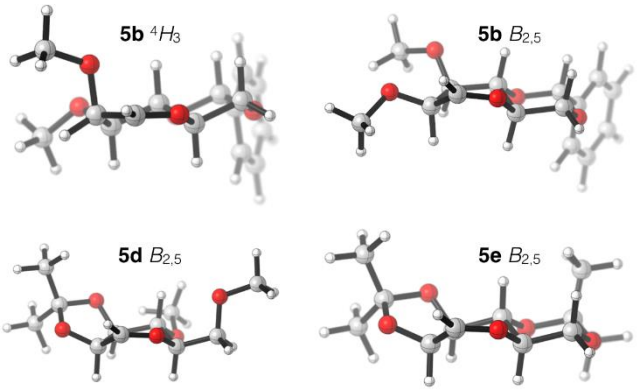


Figure 2.8 Computed energies of oxocarbenium ion intermediates relative to the corresponding α-mannosyl diphenyl phosphates. Calculations were performed at B3LYP/6-311+G(d,p)//B3LYP/6-31G(d) with D3BJ dispersion corrections and PCM (H_2O). Free energy corrections were determined at the B3LYP/6-31G(d) level of theory at 298.15 K using Grimme's quasi-harmonic free energy correction. Similar trends were observed in ether solvation model and other levels of theory (see experimental for full details).

We sought to elucidate the origin of the remarkably beneficial effect of the 2,3-acetonide protecting group on β-selective mannosylations with catalyst **1** through density functional theory computations (Figure 2.8).[9] B3LYP/6-311+G(d,p)//B3LYP/6-31G(d) were selected because they have been previously applied to compute the transition states of glycosylation reactions and geometries and energies of oxocarbenium ion intermediates.[10] Oxocarbenium ion intermediates were computed in isolation due to the observation of undesired ion-pair collapse into glycosyl phosphates when computations were performed in the presence of diphenyl phosphate anions. Crich has proposed that 4,6-benzylidene acetal protection of mannose serves to destabilize the corresponding oxocarbenium ion species relative to acyclic protection schemes (e.g. **5b** vs **5a**), thereby favoring stereospecific glycosylation pathways via transient α-mannosyl triflate intermediates.[11] Computational modeling of the oxocarbenium ions **5a** and **5b** fully supports that

[9] As described in Chapter 1 Section 1.4, mannosylations with bis-acetonide donors under homogeneous Lewis acidic conditions were generally α-selective or unselective.

[10] (a) Whitfield, D. M. Computational Studies of the Role of Glycopyranosyl Oxacarbenium Ions in Glycobiology and Glycochemistry. *Adv. Carbohydr. Chem. Biochem*. **2009**, *62*, 83–159. (b) Ionescu, A. R.; Whitfield, D. M.; Zgierski, M. Z.; Nukada, T. Investigations into the Role of Oxacarbenium Ions in Glycosylation Reactions by *ab initio* Molecular Dynamics. *Carbohydr. Res*. **2006**, *341*, 2912–2920. (c) Barnett, C. B.; Wilkinson, K. A.; Naidoo, K. J. Molecular Details from Computational Reaction Dynamics for the Cellobiohydrolase I Glycosylation Reaction. *J. Am. Chem. Soc*. **2011**, *133*, 19474–19482.

[11] (a) Huang, M.; Garrett, G. E.; Birlirakis, N.; Bohe, L.; Pratt, D. A.; Crich, D. Dissecting the Mechanisms of a Class of Chemical Glycosylation Using Primary ^{13}C Kinetic Isotope Effects. *Nat. Chem*. **2012**, *4*, 663–667. (b) Crich, D.; Chandrasekera, N. S. Mechanism of 4,6-*O*-Benzylidene-Directed β-Mannosylation as Determined by α-Deuterium Kinetic Isotope Effects. *Angew. Chem. Int. Ed*. **2004**, *43*, 5386–5389.

hypothesis, with the 4,6-benzylidene-protected derivative **5b** calculated to be destabilized by 4.4 and 3.2 kcal/mol ($^4H_3$ and $B_{2,5}$ conformation respectively) relative to the unbridged analog **5a**. The oxocarbenium ion **5c** derived from 4,6-acetonide-protected donor is conformationally similar to **5b** and displays a similar destabilizing effect. However, a similar analysis of 2,3-acetonide-protected oxocarbenium ion **5d** revealed that it was instead stabilized by 1.3 kcal/mol relative to the unbridged analog **5a**. Thus, the dramatic increases in β-selectivity resulting from 2,3-acetonide protection cannot be ascribed to destabilization of an α-selective S_N1-type pathway.

Recently, high β-selectivity has been demonstrated in mannosylations utilizing 4,6-benzylidene acetal-protected donors in systems in which the formation of transient α-mannosyl triflates is not possible.[12] In those cases, the stereoselectivity has been ascribed to preferential axial attack of nucleophiles on the energetically accessible $B_{2,5}$ conformation of the oxocarbenium ion intermediates,[12b,13] a similar conformation to that calculated for **5d** and **5e**. However, if this mode of stereoselectivity were operative in reactions catalyzed by bis-thiourea **1**, comparable levels of β-selectivity might be expected with **2c** and **2f** because of the similarity in the conformations of **5b**_$B_{2,5}$ and **5e**. In fact, dramatically higher β-selectivity is observed with donor **2f** (α:β =1:32 vs 1:1 for **2c**, Figure 2.4A). Furthermore, the divergent selectivities observed with **2d–f** in **1**-catalyzed and trimethylsilyl triflate (TMSOTf)-promoted reactions (1:16–32 vs 3–8:1 α:β, Figure 2.4A)

[12] (a) Sun, P.; Wang, P.; Zhang, Y.; Zhang, X.; Wang, C.; Liu, S.; Lu, J.; Li, M. Construction of β-Mannosidic Bonds via Gold(I)-Catalyzed Glycosylations with Mannopyranosyl *ortho*-Hexynylbenzoates and Its Application in Synthesis of Acremomannolipin A. *J. Org. Chem*. **2015**, *80*, 4164–4175. (b) Heuckendorff, M.; Bendix, J.; Pedersen, C. M.; Bols, M. β-Selective Mannosylation with a 4,6-Silylene-tethered Thiomannosyl Donor. *Org. Lett*. **2014**, *16*, 1116–1119.

[13] (a) Moume-Pymbock, M.; Crich, D. Stereoselective *C*-Glycoside Formation with 2-*O*-Benzyl-4,6-*O*-benzylidene Protected 3-Deoxy Gluco- and Mannopyranoside Donors: Comparison with *O*-Glycoside Formation. *J. Org. Chem*. **2012**, *77*, 8905–8912. (b) Nukada, T.; Bérces, A.; Whitfield, D. M. Can the Stereochemical Outcome of Glycosylation Reactions Be Controlled by the Conformational Preferences of the Glycosyl Donor? *Carbohydr. Res*. **2002**, *337*, 765–774.

appear to be inconsistent with stereoselective S_N1 addition to $B_{2,5}$ oxocarbenium ion intermediates in both pathways. We propose instead that the enhancement in β-selectivity is achieved by acceleration of a stereospecific S_N2-type pathway promoted by the bis-thiourea catalyst **1**, consistent with the observation that increased reactivity is observed with 2,3-acetonide protection **2d** relative to unbridged analogs **2a**–**b** (39% vs 11%, 15% conversion respectively). However, the basis for the acceleration effect resulting from the interplay between protecting group and catalyst remains to be determined, and the possibility that reactions proceed through a catalyst-promoted β-selective S_N1 pathway cannot be strictly ruled out. Further examination of the mechanism of substitutions catalyzed by **1** and related bis-thioureas is the focus of continuing investigation.[14]

2.5 Acceptor Scope of β-Mannsoylation and Hammett Study

The scope of catalytic, β-selective mannosylation reactions with the bis-acetonide donor **2f** was explored, with particular attention to cases where the mild and neutral conditions could provide a unique advantage over traditional Lewis acid-promoted glycosylation protocols (Figure 2.9). Sugar derivatives were found to be excellent substrates for the methodology, with both primary (6-OH-galactose **3c** and 6-OH-glucose **3d**) and secondary glycosyl acceptors (2-OH-galactose **3e** and 4-OH-rhamnose **3f**) undergoing mannosylation with high β-selectivity.[15] The β-mannoside of C4-linked *N*-acetylglucosamine derivative **3g** is of particular interest as it is a conserved branch-point on all *N*-glycans.[16] A wide variety of other alcohols containing Lewis basic

[14] The bis-acetonide-protected oxocarbenium intermediate **5e** was found to be destabilized by 2.8 kcal/mol relative to **5d**, suggesting that the high β-selectivities obtained with donor **2f** even with relatively unreactive, hindered nucleophiles result from a combination of acceleration of β-selective and deceleration of α-selective pathways arising from **5e**.

[15] Chromatographic separation of **4b** from **3b** was challenging, so accurate isolated yield could not be determined. Thus, **3b** was not included in Figure 2.9.

[16] Moremen, K. W.; Tiemeyer, M.; Nairn, A. V. Vertebrate Protein Glycosylation: Diversity, Synthesis and Function. *Nat. Rev. Mol. Cell Biol*. **2012**, *13*, 448–462

functional groups including esters, carbamates, and tertiary amines (**3a**, **3h**–**i**, and **S3f**) were also found to undergo β-mannosylations selectively and cleanly, with no decomposition of nucleophiles observed. Substrates bearing multiple hydroxyl groups such as deoxycholic acid octyl ester (**S3g**), pleuromutilin (**3j**) and FK-506 (**3k**) were found to undergo glycosylation at the least hindered position with high site-selectivity.[17,18]

Phenolic acceptors were found to display excellent reactivity toward **2f** under catalysis by bis-thiourea **1** to afford β-mannosylation products (Figure 2.9). A wide assortment of phenol derivatives, including sterically hindered substrates such as clofoctol (**3l**) and α-tocopherol (**3m**) were mannosylated with high β-selectivity. Excellent functional group tolerance was again demonstrated, such as in the glycosylation of the β-lactam-containing amoxicillin derivative **3n**. Fries-type rearrangement of *O*-aryl glycosides to *C*-glycosides, which is common with electron-rich phenol derivatives (e.g. **3o** and **3q**) under Lewis acidic conditions,[3] was not observed in any reactions promoted by **1**.

[17] The more accessible C32 position of FK-506 has been selectively functionalized previously. For examples, see (a) Chamni, S.; He, Q.-L.; Dang, Y.; Bhat, S.; Liu, J. O.; Romo, D. Diazo Reagents with Small Steric Footprints for Simultaneous Arming/SAR Studies of Alcohol-Containing Natural Products *via* O–H Insertion. *ACS Chem. Biol*. **2011**, *6*, 1175–1181. (b) McPherson, M.; Yang, Y.; Hammond, P. W.; Kreider, B. L. Drug Receptor Identification from Multiple Tissues Using Cellular-Derived mRNA Display Libraries. *Chem. Biol*. **2002**, *9*, 691–698.

[18] The anomeric configuration of **4k** was assigned based on $^{1}J_{C1\text{-}H1}$ (158.2 Hz) of deprotected compound **8b**. No other glycosylated FK-506 derivatives were detectable in the crude NMR spectra or isolated upon chromatographic purification.

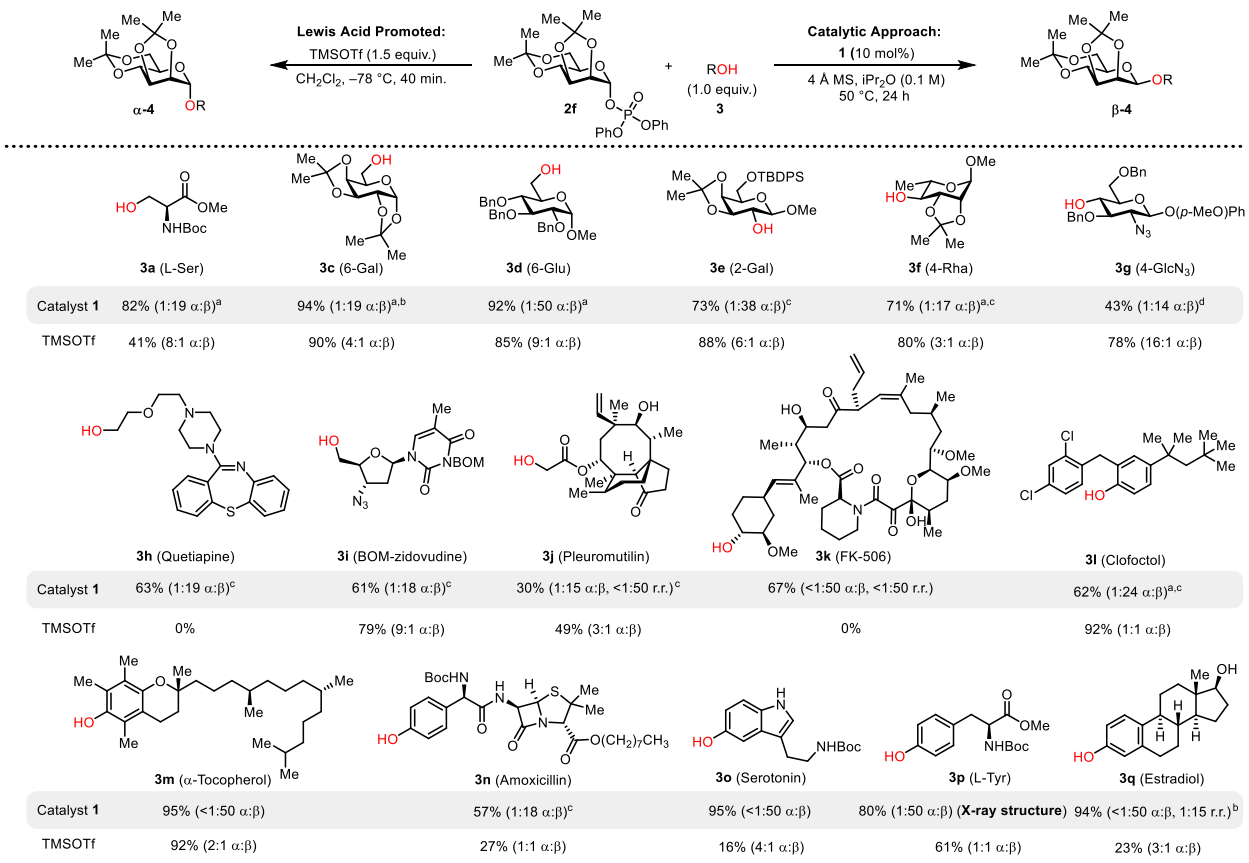
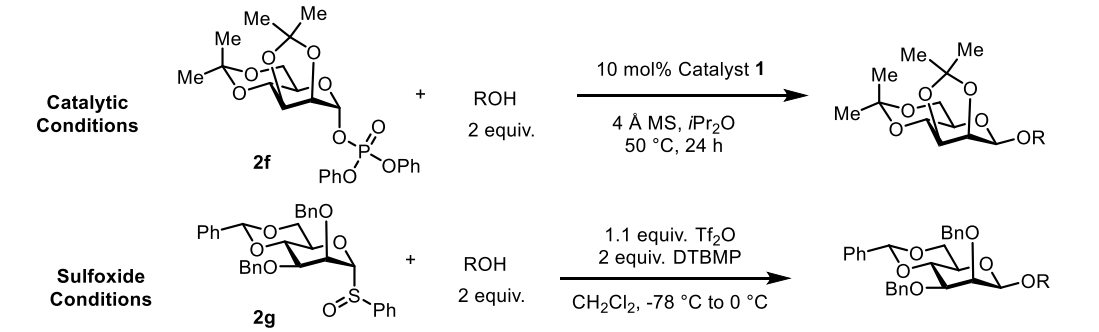


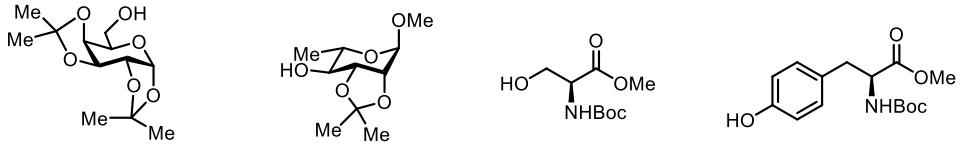
Figure 2.9 Acceptor scope of β-mannosylations. Yields of reactions catalyzed by **1** reflect isolated yields of pure β-products. Yields of TMSOTf reactions reflect combined yield of the α- and β-products and were determined by ^{1}H NMR analysis of crude product mixtures with mesitylene as an internal standard. Selectivities were determined by ^{1}H NMR analysis of crude product mixtures. [a]2.0 equiv. nucleophilic coupling partners were used. [b]Reaction was run at 40 °C. [c]48 h reaction time. [d]63 h reaction time.

Mannosylations with donor **2f** using catalyst **1** were compared to reactions promoted by the Lewis acid TMSOTf.[19] In all the examples illustrated in Figure 4, the reactions catalyzed by **1**

[19] The TMSOTf-promoted glycosylation reactions were carried out using the procedures reported by Seeberger and Hashimoto: (a) Plante, O. J.; Palmacci, E. R.; Andrade, R. B.; Seeberger, P. H. Oligosaccharide Synthesis with Glycosyl Phosphate and Dithiophosphate Triesters as Glycosylating Agents. *J. Am. Chem. Soc*. **2001**, *123*, 9545−9554. (b) Tsuda, T.; Nakamura, S.; Hashimoto, S. A Highly Stereoselective Construction of 1,2-*trans*-*β*-Glycosidic Linkages

afforded the mannosylation products cleanly and with high β-selectivity. In contrast, TMSOTf-promoted reactions yielded α-anomers as the major glycosylation products in almost all cases, consistent with the expected intrinsic preference for α-product in mannosylations proceeding via oxocarbenium ion intermediates. Functionally complex acceptors such as FK-506 (**3k**) were unstable to the Lewis acid activation conditions, while substrates possessing Lewis basic functionality such as quetiapine (**3h**) afforded none of the desired glycosylation products. Other sensitive substrates such as amoxicillin (**3n**) and serotonin (**3o**) underwent mannosylation in low yield and anomeric selectivity under TMSOTf conditions, with formation of multiple side products.





	3c (6-Gal)	3f (4-Rha)	3a (L-Ser)	3p (L-Tyr)
Catalyst 1	94% (1:19 α:β)	71% (1:19 α:β)	82% (1:19 α:β)	80% (1:50 α:β)
Sulfoxide	91% (1:6 α:β)	88% (1:32 α:β)	69% (1:12 α:β)	42% (1:3 α:β)
Literature (by Crich)	86% (1:6 α:β)	90% (<1:24 α:β)		

Capitalizing on 2-azido-2-deoxy-D-Glycosyl Diphenylphosphates as Glycosyl Donors. *Tetrahedron* **2004**, *60* 10711–10737.

Figure 2.10 Comparison of the hydrogen-bond-donor-catalyzed method to Crich's 4,6-benzylidene acetal protection strategy. The sulfoxide yields reflect NMR yield relative to internal standard. The yields obtained with Catalyst **1** reflected isolated yields.

The bis-thiourea-catalyzed β-mannosylation method was compared to the state-of-the-art method for β-mannosylation developed by Crich (Figure 2.10).[20] As describes in Chapter 1, the 4,6-benzylidene acetal protection strategy has remained as the most general means of forming β-mannosides. We successfully reproduced Crich's procedure on previously reported acceptors **3c** and **3f**. We then applied the method to other unreported acceptors, including **3a** and **3p**. The improved yield and selectivity with the hydrogen-bond-donor-catalyzed approach serve to illustrate cases where one method may be preferentially used. Higher yields (82% vs 69%) and β-selectivity (1:19 α:β vs 1:12 α:β) were obtained with mannosylation of **3a** catalyzed by **1**. Formation of a small amount of unidentified side product (<15%) was observed in mannosylation with **3a**. When less nucleophilic coupling partners such as phenols were tested in the comparison study, the bis-thiourea-catalyzed method had clear advantages and provided products with high yields and β-selectivity. L-Tyr **3p** was cleanly mannosylated with excellent anomeric selectivity (1:50 α:β) and yield (80%) when catalyzed by **1**, but formation of several side products (42% yield) and much lower β-selectivity (1:3 α:β) were observed when Crich's method was applied to mannosylate **3p**.

[20] Crich, D.; Sun, S. Direct Chemical Synthesis of β-Mannopyranosides and Other Glycosides via Glycosyl Triflates. *Tetrahedron* **1998**, *54*, 8321–8348.

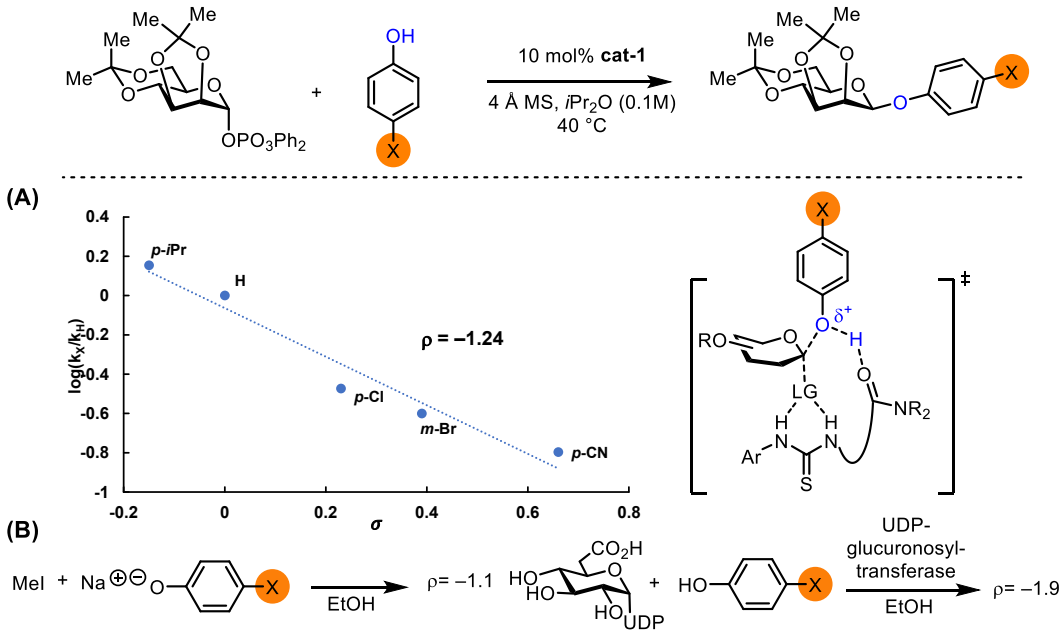


Figure 2.11 Hammett study with differently substituted phenols in mannosylation.

The ability of catalyst **1** to promote highly efficient and β-selective mannosylations of phenolic nucleophiles allowed us to utilize differently substituted phenols to perform a Hammett study (Figure 2.11A). A negative ρ-value (–1.24) indicates that there is more partial positive charge built up in the transition state than in the ground state. The magnitude of ρ-value is similar to the value reported for S_N2 displacement of phenolate (–1.1) with methyl iodide (Figure 2.11B),[21] suggesting that mannosylation of phenols proceeded via a similar S_N2 pathway. A similar Hammett study has been conducted in the context of enzymatic glucuronidation (Figure 2.11B).[22] The UDP-glucuronosyltransferase is proposed to catalyze glucuronidation of phenols via a dual general acid/general base activation mechanism and promote a stereospecific displacement of α-UDP. The similarity in ρ-values obtained in the enzymatic glucuronidation reactions and in bis-thiourea-

[21] Lewis, E. S.; Vanderpool, S. Relative Reactivities of Phenoxides with Methylating Agents. *J. Am. Chem. Soc.* **1977**, *99*, 1946–1949.
[22] Yin, H.; Bennett, G.; Jones, J. P. Mechanistic studies of uridine diphosphate glucuronosyltransferase. *Chem.-Biol. Interact*. **1994**, *90*, 47–58.

catalyzed mannosylation supports our proposal that catalyst **1** promotes β-selective mannosylation by promoting stereospecific S_N2 displacement of α-phosphates.

2.6 Acceptor Scope of β-Rhamnosylation

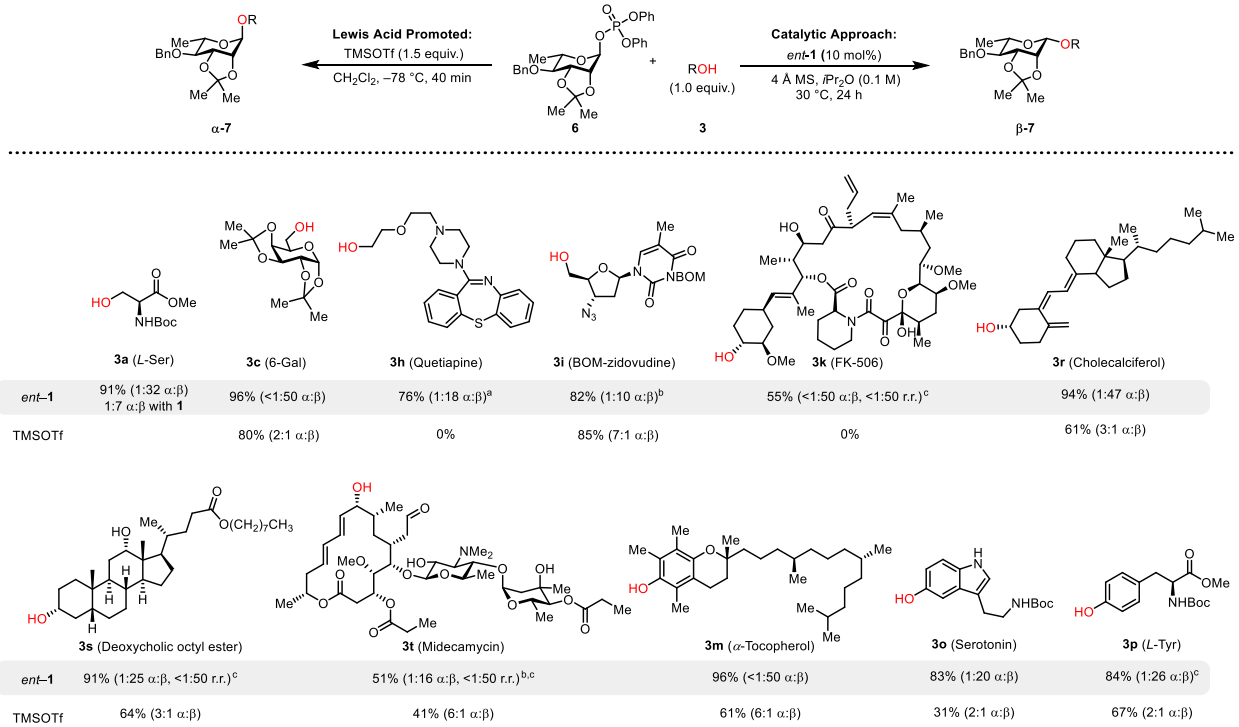


Figure 2.12 Acceptor scope of β-rhamnosylations. Yields of reactions catalyzed by *ent*-**1** reflect isolated yields of pure β-products. Yields of TMSOTf reactions reflect combined yield of the α- and β-products and were determined by ^{1}H NMR analysis of crude product mixtures with mesitylene as an internal standard. Selectivities were determined by ^{1}H NMR analysis of crude product mixtures. [a]Reaction was run at 50 °C for 48 h. [b]48 h reaction time. [c]Reaction was run at 40 °C.

We sought to explore whether the 2,3-acetonide protection strategy applied successfully in β-1,2-*cis* mannosylations catalyzed by **1** might be extended to other interesting glycosyl donors. Rhamnose is the C6-deoxy analogue of mannose, and it presents another long-standing challenge

as a coupling partner in β-1,2-*cis* glycosylation reactions. Because the C6 hydroxyl of mannose is lacking, the 4,6-benzylidene acetal protecting group strategy pioneered by Crich for β-mannosylations is not applicable. As described in Chapter 1, alternative strategies for β-rhamnoside synthesis have been identified, but the reported successful examples have been limited to simple alcohols as nucleophilic coupling partners. The 2,3-acetonide-protected L-rhamnose phosphate donor **6** was evaluated with **3a** as a model acceptor (Figure 2.12). L-Rhamnose is pseudoenantiomeric with D-mannose, and we observed that a large improvement in β-selectivity was achieved by using the enantiomer of catalyst **1** (1:7 α:β with catalyst **1** vs 1:32 α:β with *ent*-catalyst **1**, Figure 2.12). Such stereochemical matching points to precise catalyst-substrate interactions in the catalytic glycosylation event and is consistent with observations we have made previously in less challenging glycosylation reactions.[5,6] The nucleophile scope in β-rhamnosylations catalyzed by *ent*-**1** was examined and proved to be similarly broad to that documented above in β-mannosylations (Figure 2.12). Thus, excellent functional group compatibility was demonstrated with substrates bearing Lewis basic groups such as tertiary amines (**3h**), imide (**3i**), and carbamates (**3o–p**), as well as with complex natural products (e.g. **3k** and **3t**).[23] Excellent β-selectivity and reactivity were observed in the rhamnosylation of phenols as well. Reactions promoted by TMSOTf displayed limited functional group tolerance and generally favored the α-rhamnosylation products in cases where glycosylation product was obtained.

[23] The anomeric configuration of **7k** was assigned based on $^{1}J_{C1\text{-}H1}$ (158.2 Hz). We did not isolate any other glycosylated FK-506 derivatives after chromatographic purification, and no discernible peaks corresponding to other glycosylated FK-506 derivatives were present in the crude NMR. We therefore reported the selectivity as <1:50 α:β.

2.7 Deprotection and One-pot Mannosylation and Deprotection

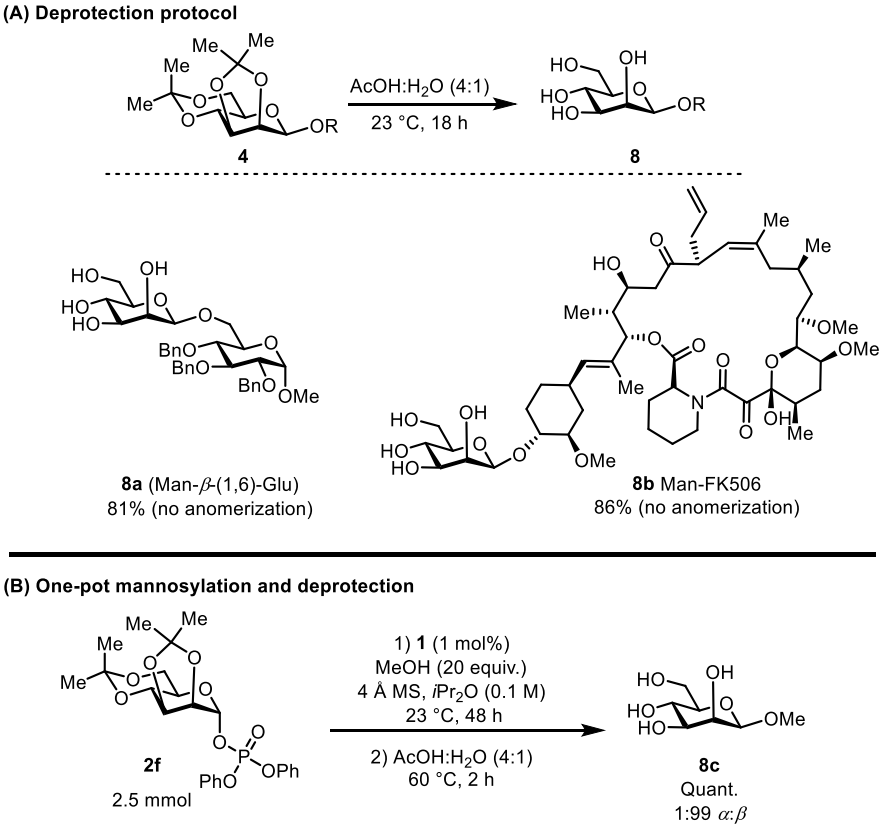


Figure 2.13 (A) Protocol for bis-acetonide deprotection under mildly acidic hydrolytic conditions. (B) Multi-millimole-scale synthesis of methyl β-D-mannopyranoside. Yields reflect isolated yields of pure β-products. Selectivities were determined by ^{1}H NMR analysis of crude product mixtures.

The acetonide-protected glycosylation products are readily unmasked under mild conditions.[8c] Thus, both acetonides on disaccharide **4d** were hydrolyzed in a 4:1 acetic acid:water mixture at room temperature, with the β-mannoside product isolated in 81% yield with no erosion of anomeric purity (Figure 2.13A). Similarly, mannosylated FK-506 (**4k**) was also deprotected in 86% yield with no detectable anomerization, demonstrating how even highly sensitive functional groups are tolerant to the mildly acidic hydrolytic conditions. The potential practicality of the

mannosylation procedure was demonstrated in a multi-millimole-scale synthesis of methyl β-D-mannopyranoside **8c**. The shortest prior reported stereoselective synthesis of **8c** required 7 steps from D-mannose.[24] Using the approach outline herein and in Figure 2.13B, **8c** was prepared in 2 steps from **2f** and isolated in >95% purity without column chromatography (4 steps from D-mannose). The glycosylation step was performed on 2.5 mmol scale using 1 mol% catalyst **1** to provide the acetonide protected-mannoside quantitatively,[25] and that material was subjected to the deprotection protocol directly to afford the fully deprotected β-mannoside **8c** in 1:99 α:β selectivity.

2.8 Conclusion and Outlook

We have demonstrated that β-mannosides and β-rhamnosides can be mildly and selectively accessed under catalyst control using readily accessible 2,3-acetonide-protected glycosyl phosphate donors. The catalytic protocol is compatible with extensive functional group complexity on the nucleophilic coupling partner, so we anticipate this method may enable exploration of the effect of specific *O*-glycosylation on a wide range chemical matter, although the application of the current methodology to highly sterically congested nucleophiles is still limited. Superior reactivity and β-selectivity are observed in bis-thiourea-catalyzed glycosylation with less nucleophilic coupling partners such as neutral phenols when the catalytic protocol is compared to the 4,6-benzylidene protection strategy, the state-of-the-art method for β-mannosylation. Work is currently underway to elucidate the origins of selectivity imparted by the 2,3-acetonide protecting

[24] The stereoselective synthesis utilized 4,6-benzylidene acetal strategy for β-mannosylations. Crich, D.; Banerjee, A.; Yao, Q. Direct Chemical Synthesis of the β-D-Mannans: The β-(1→2) and β-(1→4) Series. *J. Am. Chem. Soc*. **2004**, *126*, 14930–14934.
[25] The reaction proceeded to 94% conversion after 22 h.

group in connection with the bis-thiourea catalyst, and to further illuminate the scope of potential coupling partners in these catalytic glycosylation reactions.

2.9 Progress toward Chromatography-Free Synthesis of Bis-thioureas

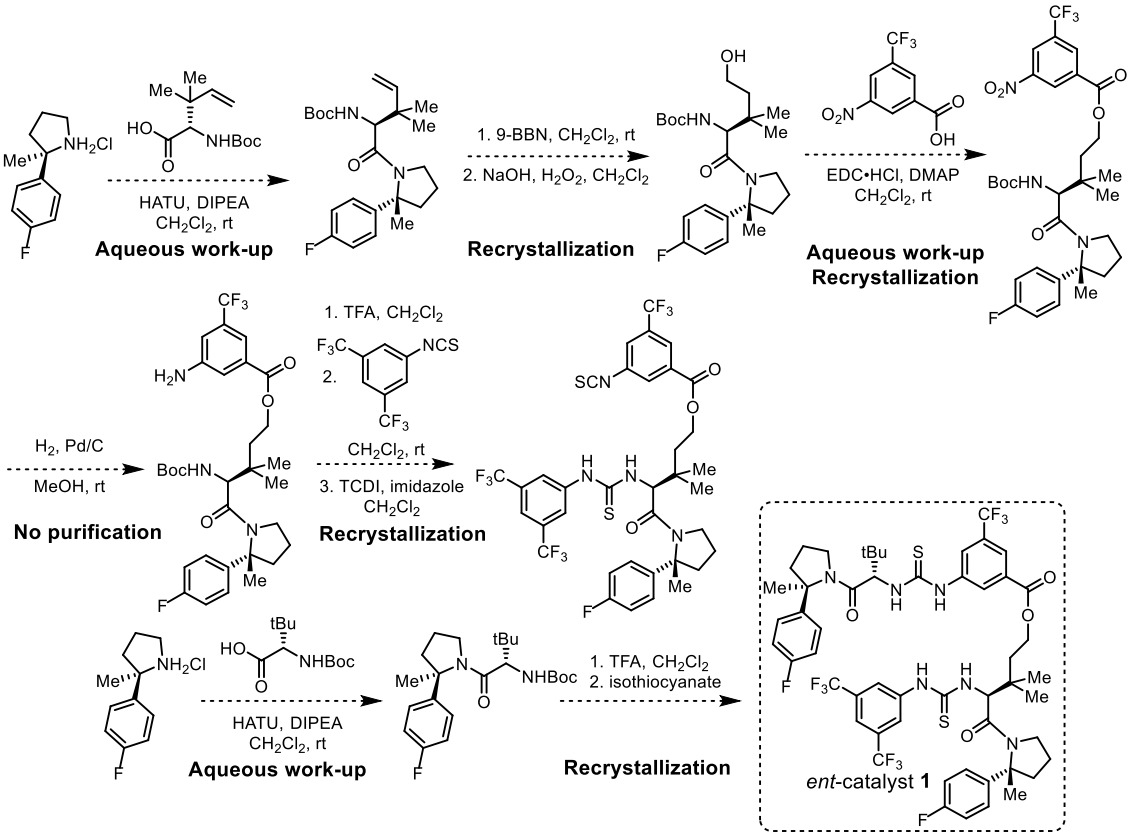


Figure 2.14 Synthetic route of chromatography-free synthesis of *ent*-catalyst **1**.

Bis-thiourea derivatives such as catalyst **1** have been shown to catalyze stereospecific pyranosylation and furanosylation to construct β-1,2-*trans* and β-1,2-cis glycosidic linkages under mild conditions with broad scope in acceptors. We envisioned that the catalytic protocols described herein and previously could be ideally suitable for complex molecule diversification. One major hurdle that could limit the adoption of bis-thiourea-catalyzed glycosylation methods is the access to bis-thiourea catalysts. The longest linear sequence of the synthesis of bis-thioureas is 10 steps. Although each synthetic step is high yielding, the need for chromatographic purification renders it

difficult to scale up the catalyst synthesis to produce bis-thioureas on decagrams scale. Therefore, we aimed to develop a chromatography-free synthesis of bis-thioureas. Our proposed synthetic route is shown in Figure 2.14. We proposed that products from each step in the synthetic route could be purified via either aqueous work-up or recrystallization.

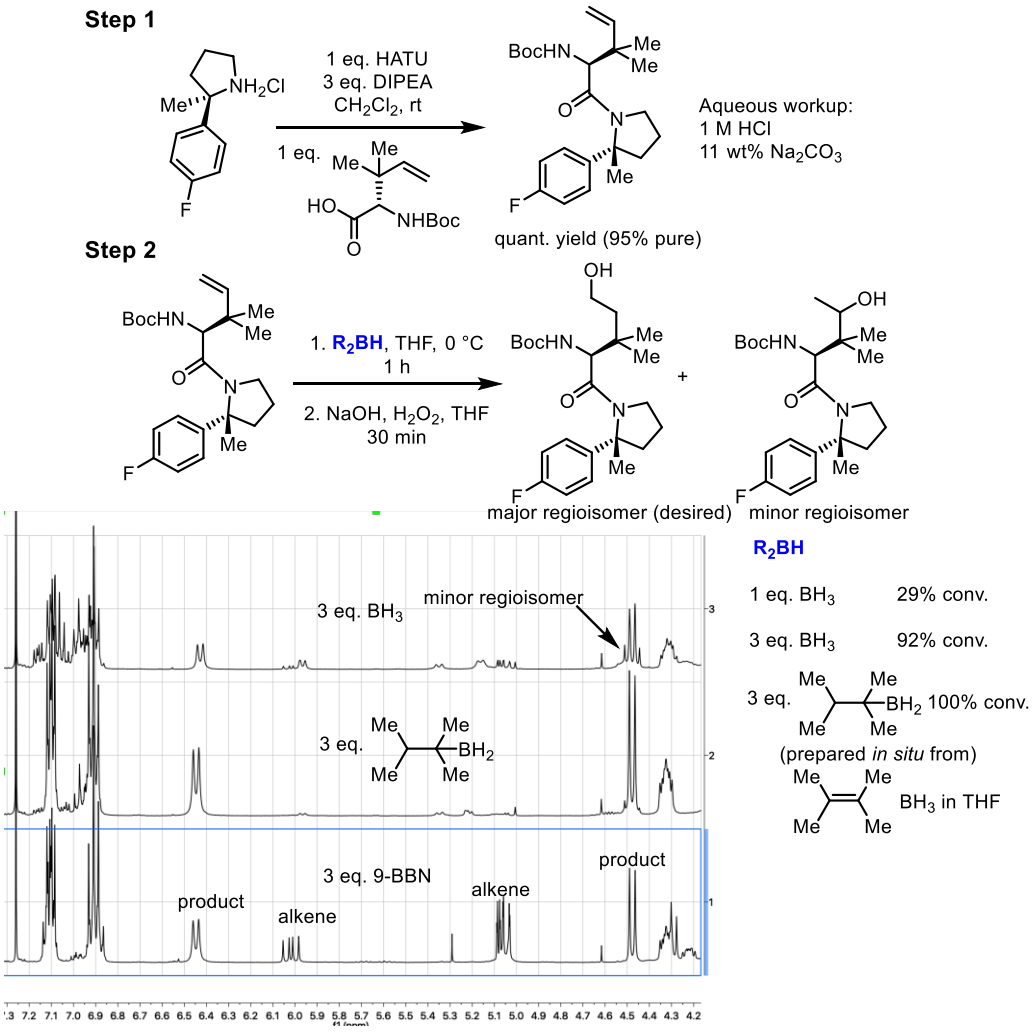


Figure 2.15 Chromatography-free amide coupling and hydroboration/oxidation.

We focused on the first amide coupling and the second hydroboration/oxidation step. When equimolecular amine and carboxylic acid are treated with HATU, Fei and co-workers found that the stoichiometric byproducts, tetramethyl urea and 1-hydroxy-7-azabenzotriazole (HOAt), can be

removed via aqueous wash.[26] Excess *N,N*-diisopropylethylamine (DIPEA) and amines can be removed through wash with aqueous hydrochloric acid solution, and HOAt can be removed via aqueous wash with aqueous sodium carbonate solution. We performed the amide coupling with 1.1 equivalent of secondary amine, 1 equivalent of carboxylic acid, and 1 equivalent of HATU to ensure complete conversion (Figure 2.15 Step 1). Upon aqueous wash with 1 M HCl (aq.) and 11 wt% Na_2CO_3 (aq), the product was obtained with quantitative yield and 95% purity as determined by ^{1}H NMR. Excess amines, HOAt, and tetramethyl urea were successfully removed and were not observed by ^{1}H NMR, and no chromatographic purification was needed after the first step. We then turned our focus to optimize the second hydroboration/oxidation step (Figure 2.15 Step 2). The oxidation byproduct derived from 9-borabicyclo(3.3.1)nonane (9-BBN) is *cis*-1,5-cyclooctanediol, which is crystalline and is difficult to be removed via recrystallization. Therefore, we investigated different borane reagents and compared their reactivity and regioselectivity. Hydroboration with 1 equivalent of borane in tetrahydrofuran (BH_3 in THF) proceeded with low conversion (29%) after 1 hour at 0 °C. Higher conversion was achieved by increasing the amount of borane to 3 equivalents. However, the formation of minor regioisomer was observed. Although clean formation of the desired major regioisomer was observed in reaction with 9-BBN, conversion of alkene was incomplete after 1 hour. We found that the optimal borane reagent for hydroboration is thexylborane generated *in situ* from tetramethyl ethylene and BH_3 in THF. Complete conversion of alkene was observed after 1 hour with 3 equivalents of thexylborane with high regioselectivity (>15:1 major:minor). More importantly, 2,3-dimethyl-2-butanol, the oxidation byproduct derived from thexylborane, has a relatively low boiling point (120 °C) at atmospheric pressure; therefore, it can be removed easily under vacuum. The

[26] Fei, Z.; Kong, W.; Wang, H.; Peng, J.; Sun, F.; Yin, Y.; Bajwa, J.; Jiang, X. A Scalable Synthesis of a Hydroxamic Acid LpxC Inhibitor. *Org. Process Res. Dev.* **2012**, *16*, 1436–1441.

hydroboration/oxidation step was rendered chromatography-free by using thexylborane as the reagent to cleanly convert the alkene to the desired primary alcohol. Future work is needed to complete the synthesis.

2.10 Experimental Information

2.10.1 General Experiment Procedures, Materials, and Instrumentation

Unless otherwise described, all reactions for the preparation of substrates were performed in standard, oven- or flame-dried glassware equipped with PTFE-coated magnetic stir bars and fitted with rubber septa under an inert atmosphere of nitrogen. All catalytic experiments were performed in a flame-dried round bottom flask sealed with a yellow polyethylene cap under an atmosphere of air. Stainless steel syringes or Hamilton gas-tight glass syringes fitted with stainless-steel needles were used to transfer air- and moisture-sensitive liquids. Reported concentrations refer to solution volumes at room temperature. Concentration of organic solutions under reduced pressure was performed on a Büchi rotary evaporator using house vacuum (~ 40 mm Hg). Reactions were monitored by thin-layer chromatography (TLC) on Silica Gel 60 F254 plates (EMD). Plates were visualized by exposure to UV light (λ = 254 nm) and/or by staining with *p*-anisaldehyde, ninhydrin, or ceric ammonium molybdate (CAM) stain, which developed upon heating. Column chromatography (using a Biotage® Isolera Four™) was performed using reusable cartridges filled with SiliaFlash P60 (230–400 mesh, SiliCycle).

All commercially available reagents were purchased from Sigma–Aldrich, Alfa Aesar, Strem, Oakwood, Matrix Scientific, Ark Pharm Inc., Toronto Research Chemicals, Chem-Impex Int'l. Inc., or TCI and used without purification, unless otherwise indicated. Deuterated NMR solvents were purchased from Cambridge Isotope Laboratories. Anhydrous solvents (*tert*-butyl methyl ether, dichloromethane, *N,N*-dimethylformamide, ethyl ether, methanol, tetrahydrofuran, toluene)

were prepared by passing the solvent through an activated alumina column. Triethylamine, *N,N*-diisopropylethylamine, and pyridine were distilled from CaH_2 at atmospheric pressure.

NOTE: Diisopropyl ether is known to form peroxides and should be handled with appropriate care. Anhydrous diisopropyl ether containing either BHT or hydroquinone as stabilizer was purchased in from Sigma-Aldrich and used without purification.

Proton nuclear magnetic resonance (^{1}H NMR) spectra and proton-decoupled carbon nuclear magnetic resonance (^{13}C NMR) spectra were recorded at 25 °C (unless stated otherwise) on Varian Unity/Inova 500 (500 MHz) or Varian Unity/Inova 600 (600 MHz) spectrometers at the Harvard University nuclear magnetic resonance facility. Chemical shifts for protons are reported in parts per million downfield from tetramethylsilane and are referenced to residual proton resonances of the NMR solvent. Chemical shifts for carbon are reported in parts per million downfield from tetramethylsilane and are referenced to the carbon resonances of the NMR solvent. The solvent peak was referenced to 7.26 ppm for ^{1}H and 77.16 ppm for ^{13}C for $CDCl_3$. Data are represented as follows: chemical shift, integration, multiplicity (br = broad, s = singlet, d = doublet, t = triplet, q = quartet, qn = quintet, sp = septet, m = multiplet), coupling constants (J) in Hertz (Hz).

High-resolution mass spectrometric data were obtained on an Agilent 6210 time-of-flight HPLC/MS spectrometer (ESI-TOF)

X-ray crystallographic data was collected at the Harvard X-ray Laboratory. The structural refinement details for the X-ray crystallographic data are described in the individual CIFs. X-ray crystallographic data for **S8** and **4p** have been deposited at the Cambridge Crystallographic Data Centre (CCDC), 12 Union Road, Cambridge CB21EZ, UK; fax: (+44)122-333-6033. These data

can be obtained free of charge via the Internet at www.ccdc.cam.ac.uk/data_request/cif using the CCDC numbers given above.

2.10.2 Additional Substrates for β-Mannosylations and β-Rhamnosylations

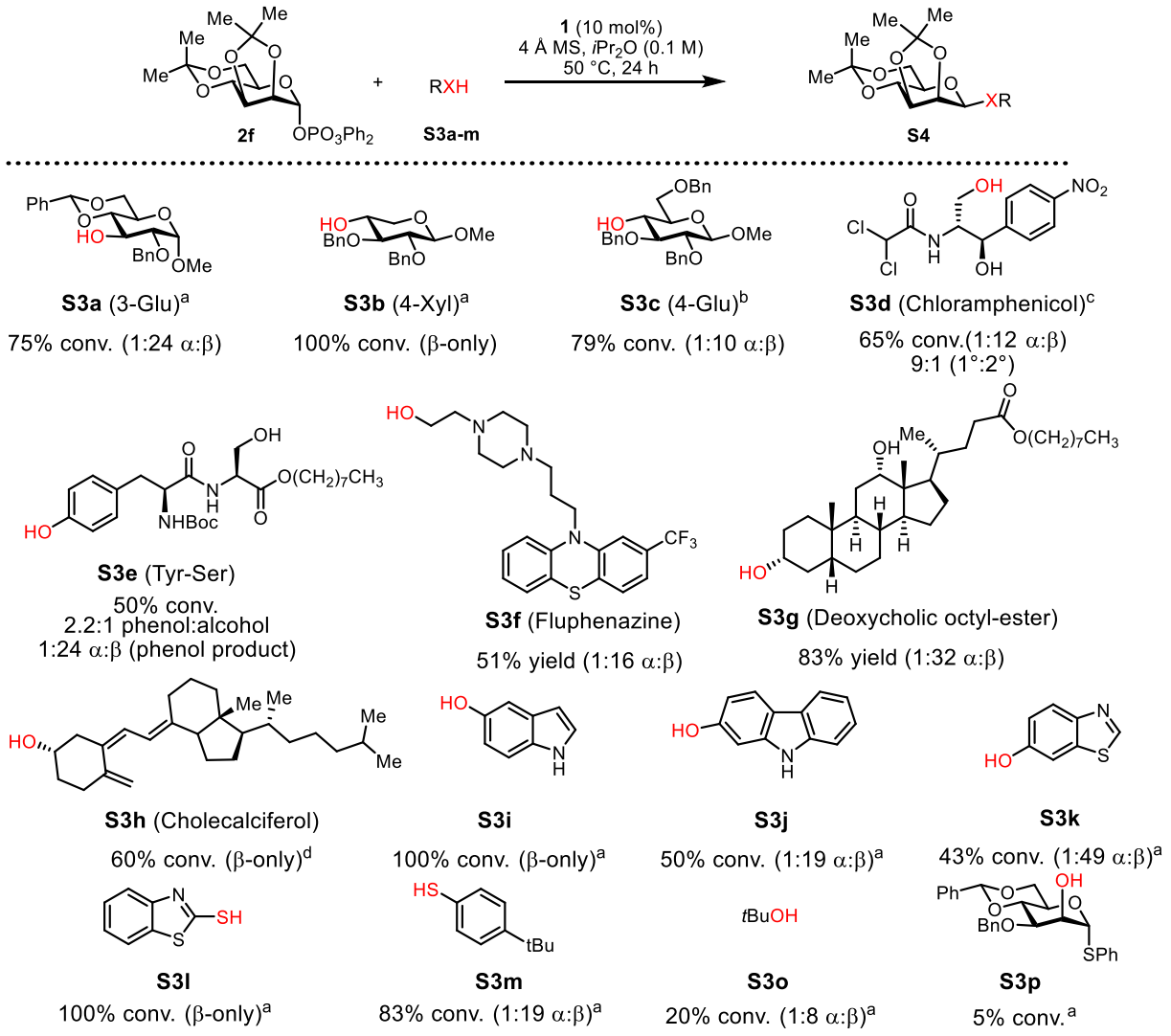


Figure 2.16 Additional substrates for mannosylation reaction with bis-acetonide mannosyl phosphate, **2f.** Conversion was determined by ^{1}H NMR relative to an internal standard. Yields were isolated product yields. Selectivity was determined by ^{1}H NMR analysis of the crude reaction mixture. [a]Reactions were performed at 40 °C. [b]Reactions were run in cyclohexane at 50

°C for 48 hours. [c]Reactions were run at 0.05 M at 50 °C for 48 hours. [d]Reactions were performed at 25 °C. Tertiary alcohols and hindered secondary alcohols were poorly reactive.

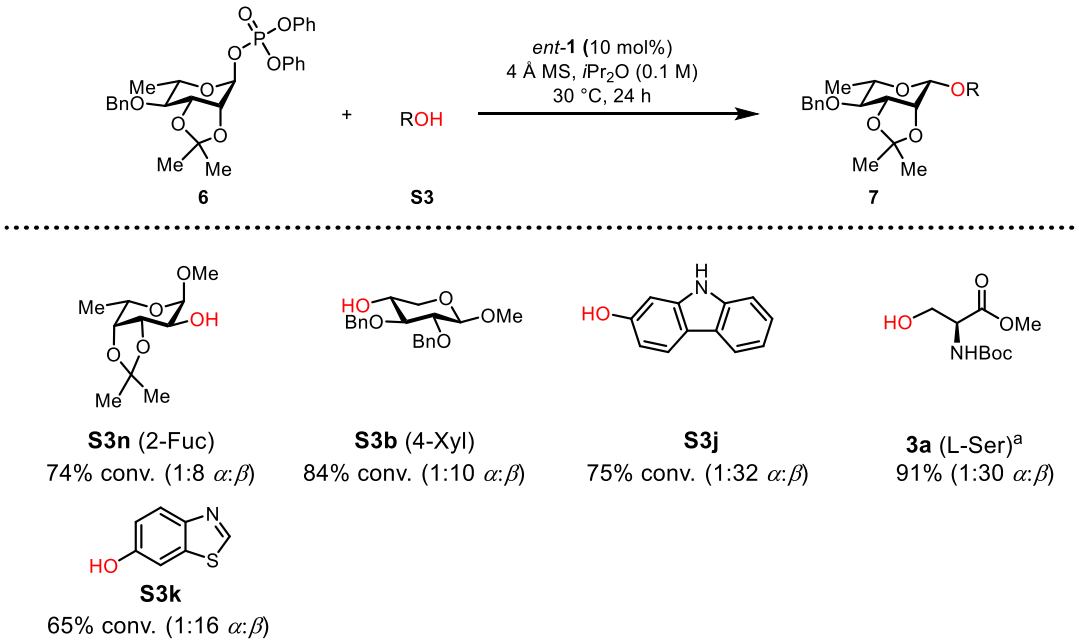


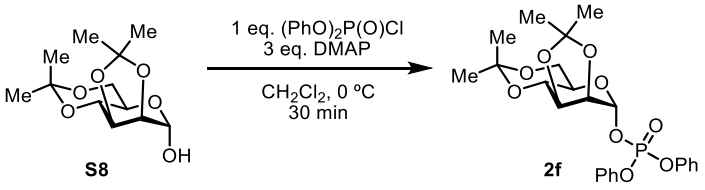
Figure 2.17 Additional substrates for rhamnosylation reaction with 2,3-acetonide protected rhamnosyl phosphate, **6.** Conversion was determined by ^{1}H NMR relative to an internal standard. Yields were isolated product yields. Selectivity was determined by ^{1}H NMR analysis of the crude reaction mixture. [a]Reactions were performed at 40 °C. Tertiary alcohols were poorly reactive (< 15% conversion). Rhamnosylation of highly hindered secondary alcohols was only moderately β-selective (*ca*. 1:5 α:β).

2.10.3 Synthesis and Characterization of Glycosyl Phosphates

2a-f were prepared by following the procedure for the preparation of **2f**. Characterization of **2a** and **2c** was consistent with previously reported data.[27]

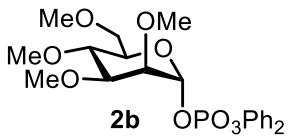
[27] Tsuda, T.; Arihara, R.; Sato, S.; Koshiba, M.; Nakamura, S.; Hashimoto, S. Direct and Stereoselective Synthesis of β-D-Mannosides using 4,6-*O*-Benzylidene-protected Mannosyl Diethyl Phosphite as a Donor. *Tetrahedron* **2005**, *61*, 10719–10733.

2,3:4,6-di-*O*-isopropylidene-*α*-d-mannopyranosyl diphenylphosphate (2f)



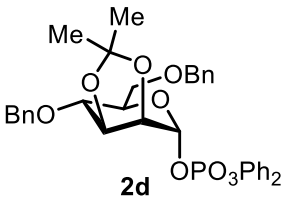
2,3:4,6-di-*O*-isopropylidene-*α*-d-mannopyranose **S8** was prepared as previously reported.[8c] To a flame-dried 100 mL round bottom flask equipped with a stir bar was added 2,3:4,6-di-*O*-isopropylidene-α-d-mannopyranose **S8** (1.40 g, 5.38 mmol, 1 equiv) and 4-dimethylaminopyridine (DMAP, 1.97 g, 16.1 mmol, 3 equiv). The reaction flask was evacuated and backfilled with N_2 three times. To the reaction flask was added 54 mL dry CH_2Cl_2, and the reaction was cooled to 0 °C. To the cooled solution was added diphenyl phosphoryl chloride (1.1 mL, 5.38 mmol, 1 equiv) dropwise. The reaction was stirred at 0 °C for 30 minutes and then concentrated under reduced pressure (note: the temperature of rotary evaporator water bath should be around 10 °C). The crude mixture was purified by column chromatography (0% Et_2O/hexanes to 6% Et_2O/hexanes) on 50 g silanized silica gel to give the product, **2f**, in 47% yield (1.24 g, 2.52 mmol) as a colorless, viscous oil. ^{1}H NMR (500 MHz, $CDCl_3$) δ 7.39 – 7.32 (m, 4H), 7.26 – 7.19 (m, 6H), 6.09 (d, J = 6.5 Hz, 1H, H-1), 4.19 – 4.13 (m, 2H), 3.78 – 3.71 (m, 1H), 3.68 – 3.57 (m, 3H), 1.53 (s, 3H), 1.48 (s, 3H), 1.41 (s, 3H), 1.32 (s, 3H). ^{13}C NMR (126 MHz, $CDCl_3$) δ 150.5 (d, J = 5.3 Hz), 150.4 (d, J = 5.3 Hz), 130.0, 130.0, 125.8, 125.7, 120.2 (d, J = 5.1 Hz), 120.1 (d, J = 4.9 Hz), 110.3, 99.9, 97.5 (d, J = 5.5 Hz), 75.8 (d, J = 12.5 Hz), 74.5, 71.9, 63.7, 61.5, 29.0, 28.2, 26.3, 18.8. ^{31}P NMR (162 MHz, $CDCl_3$) δ -14.06. HRMS (ESI) m/z calculated for $C_{24}H_{29}O_9P$ $[M+Na]^+$: 515.1441; found: 515.1443.

Note: the mannosyl donor is best stored as a solution in ethereal solvents over a small amount of 4 Å molecular sieves.



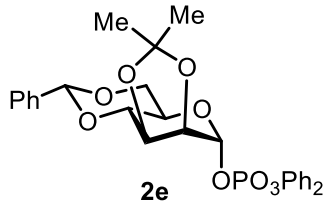
2b

Characterization of **2b**: ^{1}H NMR (500 MHz, $CDCl_3$) δ 7.38 – 7.32 (m, 4H), 7.25 – 7.18 (m, 6H), 5.98 (dd, J = 6.4, 2.0 Hz, 1H, H-1), 3.66 (ddd, J = 9.8, 4.0, 1.7 Hz, 1H), 3.58 – 3.52 (m, 3H), 3.51 (s, 3H), 3.46 (s, 3H), 3.45 – 3.39 (m, 5H), 3.35 (s, 3H).



2d

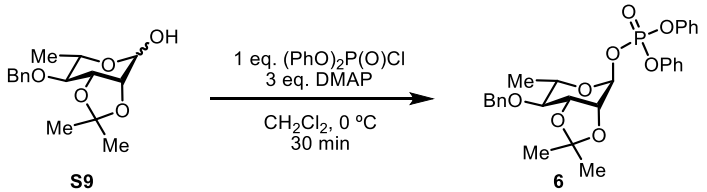
Characterization of **2d**: ^{1}H NMR (600 MHz, $CDCl_3$) δ 7.35 – 7.25 (m, 12H), 7.27 – 7.13 (m, 8H), 6.17 (d, J = 6.5 Hz, 1H, H-1), 4.84 (d, J = 11.3 Hz, 1H), 4.58 (d, J = 12.2 Hz, 1H), 4.55 (d, J = 11.3 Hz, 1H), 4.46 (d, J = 12.2 Hz, 1H), 4.32 (dd, J = 7.1, 5.7 Hz, 1H), 4.13 (d, J = 5.6 Hz, 1H), 3.84 (ddd, J = 10.2, 3.7, 2.0 Hz, 1H), 3.72 (dd, J = 10.2, 7.1 Hz, 1H), 3.67 (dd, J = 11.1, 3.6 Hz, 1H), 3.47 – 3.44 (dd, 1H) overlaps with Et_2O peak, 1.49 (s, 3H), 1.33 (s, 3H).



2e

Characterization of **2e**: ^{1}H NMR (600 MHz, $CDCl_3$) δ 7.49 – 7.46 (m, 2H), 7.39 – 7.31 (m, 7H), 7.25 – 7.18 (m, 4H), 6.13 (d, J = 6.4 Hz, 1H, H-1), 5.53 (s, 1H), 4.35 (dd, J = 8.0, 5.7 Hz, 1H), 4.21 (d, J = 5.8 Hz, 1H), 4.00 (dd, J = 10.3, 5.2 Hz, 1H), 3.82 (dd, J = 10.0, 5.2 Hz, 1H), 3.70 (dd, J = 10.0, 8.1 Hz, 1H), 3.66 (t, J = 10.2 Hz, 1H), 1.57 (s, 3H), 1.34 (s, 3H).

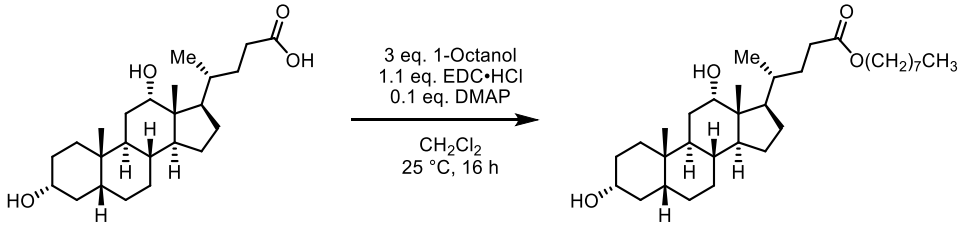
2,3-*O*-isopropylidene-4-*O*-benzyl-α-L--rhamnopyranosyl diphenylphosphate (6)



2,3-*O*-isopropylidene-4-*O*-benzyl-*α*-l-rhamnopyranose **S9** was prepared as previously reported.[28] To a flame-dried 100 mL round bottom flask equipped with a stir bar was added 2,3-*O*-isopropylidene-4-*O*-benzyl-*α*-l-rhamnopyranose, **S9** (0.734 g, 2.49 mmol, 1 equiv) and 4-dimethylaminopyridine (DMAP, 0.914 g, 7.48 mmol, 3 equiv). The reaction flask was evacuated and backfilled with N_2 three times. To the reaction flask was added 25 mL dry CH_2Cl_2, and the reaction was cooled to 0 °C. To the cooled solution was added diphenyl phosphoryl chloride (0.52 mL, 2.49 mmol, 1 equiv) dropwise. The reaction was stirred at 0 °C for 30 minutes and then concentrated under reduced pressure (note: the temperature of rotary evaporator water bath should be around 10 °C). Hexanes (50 mL) were added to the crude mixture, and the suspension was filtered by vacuum filtration. The filtrate was diluted with Et_2O (50 mL) and transferred to a separatory funnel. The organic layer was washed with 1 M HCl(aq) (2 x12 mL), sat. NaHCO3(aq) (20 mL) and brine (20 mL), dried over Na_2SO_4 and concentrated under reduced pressure to give the product, **6**, in 92% yield (1.204 g, 2.29 mmol) as a colorless, viscous oil. Characterization of this compound was consistent with previously reported data.[5]

Note: the rhamnosyl donor is best stored as a solution in ethereal solvents over a small amount of 4 Å molecular sieves.

2.10.4 Synthesis and Characterization of Acceptors

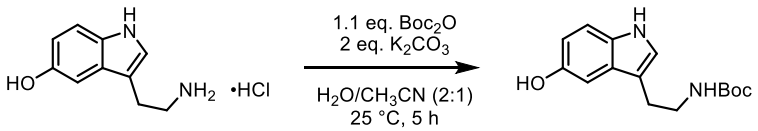


S10 Deoxycholic acid

3s (Deoxycholic octyl-ester)

[28] Nguyen, H. M.; Poole, J. L.; Gin, D. Y. Chemoselective Iterative Dehydrative Glycosylation. *Angew. Chem. Int. Ed*. **2001**, *40*, 414–417.

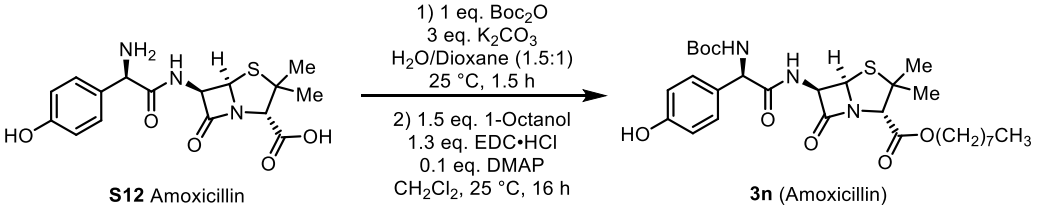
To a flame-dried 25 mL round bottom flask equipped with a stir bar was added deoxycholic acid **S10** (0.2 g, 0.51 mmol, 1 equiv), 1-octanol (0.199 g, 1.53 mmol, 3 equiv.) and 5 mL dry CH_2Cl_2. The solution was cooled to 0 °C. To the cooled reaction mixture was added EDC•HCl (0.107 g, 0.56 mmol, 1.1 equiv) and 4-dimethylaminopyridine (DMAP, 6 mg, 0.05 mmol, 0.1 equiv). at 0 °C. After the reaction was stirred at room temperature overnight, the reaction was concentrated under reduced pressure and purified by column chromatography (5% EtOAc/hexanes to 70% EtOAc/hexanes) to give deoxycholic acid octyl ester, **3s**, in 80% yield (0.206 g, 0.41 mmol) as a colorless, viscous oil. ^{1}H NMR (600 MHz, $CDCl_3$) δ 4.04 (t, *J* = 6.7 Hz, 2H), 3.97 (t, *J* = 3.0 Hz, 1H), 3.60 (tt, *J* = 11.0, 4.6 Hz, 1H), 2.35 (ddd, *J* = 15.1, 9.9, 5.0 Hz, 1H), 2.21 (ddd, *J* = 15.7, 9.4, 6.8 Hz, 1H), 1.89 – 1.48 (m, 18H), 1.44 – 1.20 (m, 19H), 1.16 – 1.01 (m, 2H), 1.01 – 0.92 (m, 4H), 0.90 (s, 3H), 0.87 (t, *J* = 7.0 Hz, 3H), 0.66 (s, 3H). ^{13}C NMR (126 MHz, $CDCl_3$) δ 174.5, 73.2, 71.8, 64.5, 48.3, 47.4, 46.6, 42.2, 36.5, 36.1, 35.4, 35.3, 34.2, 33.7, 31.9, 31.5, 31.0, 30.5, 29.3, 29.3, 28.8, 27.6, 27.3, 26.2, 26.0, 23.8, 23.2, 22.7, 17.3, 14.2, 12.8. HRMS (ESI) m/z calculated for $C_{32}H_{56}O_4$ [M+H]+: 505.4251; found: 505.4253.



S11 Serotonin •HCl **3o**

To a 50 mL round bottom flask containing 4 mL H_2O and 2 mL CH_3CN was added serotonin•HCl **S11** (0.3 g, 1.41 mmol, 1 equiv), K_2CO_3 (0.390 g, 2.82 mmol, 2 equiv.) and di-*tert*-butyl dicarbonate (Boc_2O, 0.339 g, 1.55 mmol, 1.1 equiv.). After the reaction was stirred at room temperature for 5 hours, the reaction mixture was diluted with H_2O and extracted with Et_2O (2 x 25 mL). The organic layer was washed with sat. NaCl(aq), dried over Na_2SO_4 and concentrated to give Boc-Serotonin, **3o**, in 92% yield (0.360 g, 1.30 mmol) as a light brown foamy solid. ^{1}H NMR

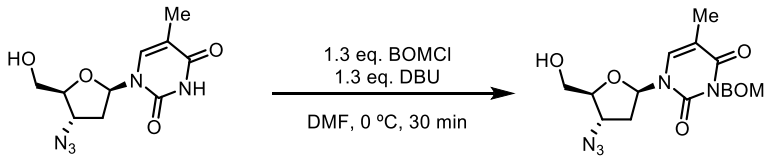
(600 MHz, $CDCl_3$) δ 8.06 (s, 1H), 7.18 (d, *J* = 8.6 Hz, 1H), 7.00 (d, *J* = 2.4 Hz, 1H), 6.94 (s, 1H), 6.80 (dd, *J* = 8.6, 2.4 Hz, 1H), 5.99 (s, 1H), 4.72 (s, 1H), 3.41 (q, *J* = 6.7 Hz, 2H), 2.84 (t, *J* = 7.0 Hz, 2H), 1.44 (s, 9H). ^{13}C NMR (126 MHz, $CDCl_3$) δ 156.5, 149.8, 131.6, 128.0, 123.3, 112.2, 112.1, 112.0, 103.4, 79.7, 40.8, 28.6, 25.8. HRMS (ESI) m/z calculated for $C_{15}H_{20}N_2O_3$ $[M+H]^+$: 277.1547; found: 277.1546.



To a 100 mL round bottom flask containing 24 mL H_2O and 14 mL dioxane was added amoxicillin trihydrate **S12** (0.4 g, 1.09 mmol, 1 equiv). The suspension was cooled to 0 °C. K_2CO_3 (0.454 g, 3.28 mmol, 3 equiv) and a solution of di-*tert*-butyl dicarbonate (Boc_2O, 0.239 g, 1.09 mmol, 1 equiv) in 2 mL dioxane were added to the cooled solution. After the reaction was stirred at room temperature for 1.5 hours, a solution of 1M HCl was added to the reaction mixture until pH=1. The reaction mixture was extracted with EtOAc (2 x 30 mL). The combined organic layers were washed with brine (15 mL), dried over Na_2SO_4 and concentrated under reduced pressure to give the protected Amoxicillin derivative in quantitative yield, which was directly used in the next step without purification.

To a flame-dried 50 mL round bottom flask equipped with a stir bar was added Boc-Amx-OH (0.510 g, 1.09 mmol, 1 equiv), 1-octanol (0.214 g, 1.64 mmol, 1.5 equiv) and 11 mL dry CH_2Cl_2. The solution was cooled to 0 °C. To the cooled solution was added EDC•HCl (0.273 g, 1.42 mmol, 1.3 equiv) and 4-dimethylaminopyridine (DMAP, 13 mg, 0.11 mmol, 0.1 equiv) at 0 °C. The reaction was allowed to warm to room temperature overnight. The reaction was then concentrated

under reduced pressure and purified by column chromatography (5% EtOAc/hexanes to 35% EtOAc/hexanes) to give **3n** in 33% yield (0.206 g, 0.36 mmol) as a white foamy solid. ^{1}H NMR (600 MHz, $CDCl_3$) δ 7.22 (s, 1H), 7.05 (d, *J* = 8.6 Hz, 2H), 6.90 (d, *J* = 9.2 Hz, 1H), 6.57 (d, *J* = 8.0 Hz, 2H), 5.70 – 5.57 (m, 2H), 5.48 (d, *J* = 4.2 Hz, 1H), 5.08 (s, 1H), 4.39 (s, 1H), 4.17 – 4.10 (m, 2H), 1.67 – 1.61 (m, 2H), 1.56 (s, 3H), 1.45 – 1.42 (m, 12H), 1.36 – 1.20 (m, 10H), 0.87 (t, *J* = 7.0 Hz, 3H). ^{13}C NMR (126 MHz, $CDCl_3$) δ 173.4, 170.8, 167.8, 156.9, 155.4, 128.7, 128.3, 116.2, 80.8, 70.7, 68.0, 66.1, 64.8, 58.7, 31.8, 29.2, 29.2, 28.5, 28.5, 27.0, 26.0, 22.7, 14.2. HRMS (ESI) m/z calculated for $C_{29}H_{44}N_3O_7S_1$ $[M+H]^+$: 578.2894; found: 578.2897.



S13 Zidovudine **3i**

To an oven-dried 20 mL vial equipped with a stir bar was added zidovudine **S13** (0.350 g, 1.31 mmol, 1 equiv) and 2.7 mL dry DMF. The solution was cooled to 0 °C. To the cooled solution was added 1,8-diazabicyclo(5.4.0)undec-7-ene (DBU, 0.25 mL, 1.70 mmol, 1.3 equiv) and benzyl chloromethyl ether (BOMCl, 0.24 mL, 1.70 mmol, 1.3 equiv). The reaction was stirred at 0 °C for 30 minutes and then diluted with H_2O. The solution was extracted with Et_2O twice. The combined organic layers were washed with H_2O (2 x 15 mL) and brine (10 mL), dried over Na_2SO_4 and concentrated under reduced pressure. The resulted oil was purified by column chromatography (30% EtOAc/hexanes to 60% EtOAc/hexanes) to give BOM-zidovudine, **3i**, in 85% yield (0.431 g, 1.11 mmol) as a colorless, viscous oil. ^{1}H NMR (600 MHz, $CDCl_3$) δ 7.43 (s, 1H), 7.35 (d, *J* = 7.0 Hz, 2H), 7.31 (t, *J* = 7.6 Hz, 2H), 7.25 (t, *J* = 6.7 Hz, 1H), 6.07 (t, *J* = 6.4 Hz, 1H), 5.47 (s, 2H), 4.69 (s, 2H), 4.34 (dt, *J* = 7.4, 5.1 Hz, 1H), 3.97 – 3.92 (m, 2H), 3.82 – 3.75 (m, 1H), 2.82 – 2.75 (m, 1H), 2.43 (ddd, *J* = 13.6, 7.4, 6.1 Hz, 1H), 2.37 (ddd, *J* = 13.9, 6.7, 5.3 Hz, 1H), 1.90 (t,

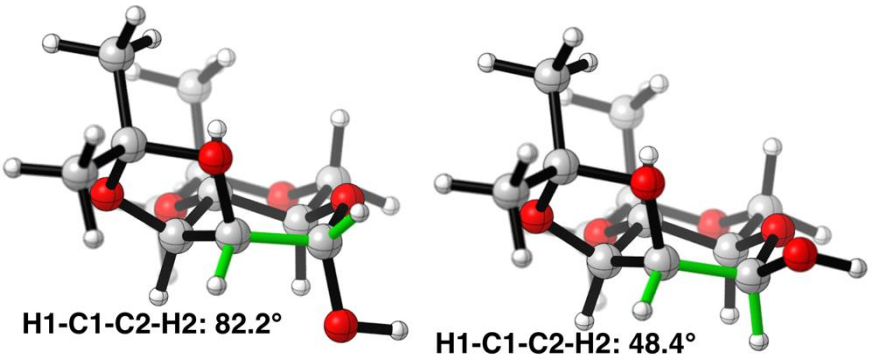
J = 0.8 Hz, 3H). ^{13}C NMR (126 MHz, $CDCl_3$) δ 163.5, 151.0, 137.9, 135.4, 128.4, 127.8, 127.7, 110.5, 87.0, 84.6, 72.4, 70.7, 61.9, 59.9, 37.6, 13.3. HRMS (ESI) m/z calculated for $C_{18}H_{21}N_5O_5$ $[M+H]^+$: 388.1615; found: 388.1616.M+H]$^+$: 578.2894; found: 578.2897.

2.10.5 Synthesis and Characterization of Catalysts

Catalyst **1** and *ent*-catalyst **1** were synthesized as described previously.[29]

2.10.6 Anomeric Configuration Assignment

The assignment of anomeric configuration of mannosyl and rhamnosyl linkages was conducted by utilizing $^3J_{H1\text{-}H2}$, $^1J_{C1\text{-}H1}$, and the chemical shift of the H-5 proton data.



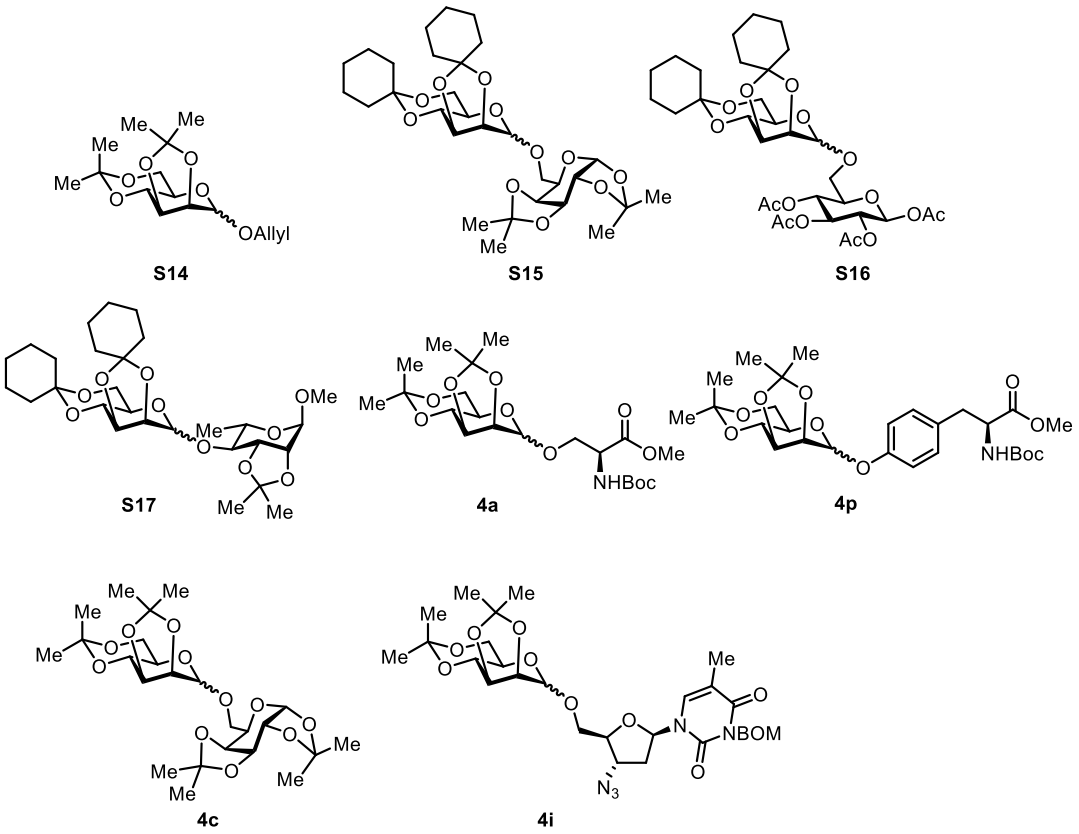
The conformation of acetonide-protected mannosides and rhamnosides deviates from chair conformation due to the presence of 2,3-acetonide. As a result, the dihedral angle of H1-C1-C2-H2 in α-configuration is very different from that in β-configuration. The structures shown above were optimized at B3LYP/6-31G(d), and the dihedral angles of interest were highlighted in green. Because the coupling constant of vicinal proton-proton coupling depends on dihedral angle, we could use Karplus equation to predict the relative magnitude of coupling constant.[30] In the α-

[29] Kennedy, C. R.; Lehnherr, D.; Rajapaksa, N. S.; Ford, D. D.; Park, Y.; Jacobsen, E. N. Mechanism-Guided Development of a Highly Active Bis-Thiourea Catalyst for Anion-Abstraction Catalysis. *J. Am. Chem. Soc*. **2016**, *138*, 13525–13528.
[30] Karplus, M. Contact Electron-Spin Coupling of Nuclear Magnetic Moments. *J. Chem. Phys*. **1959**, *30*, 11–15.

configuration, the H1-C1-C2-H2 dihedral angle (82.2°) is very close to 90°, and Karplus equation predicts a coupling constant close to 0 Hz. As the dihedral angle decreases to 0°, the coupling constant increases. Since the dihedral angle in β-configuration (48.4°) is much close to 0° than that in α-configuration, a large $^{3}J_{H1\text{-}H2}$ coupling constant is expected for β-anomers. This is indeed what we observed. $^{3}J_{H1\text{-}H2}$ for α-products is 0 Hz, and that for β-products is 2.5–3.0 Hz. The difference in coupling constant for acetonide-protected and related cyclohexylidene-protected α- and β-mannosides has been observed previously.[31] Several examples from the literature and this work have been tabulated below.

Compound	$^{3}J_{H1\text{-}H2}$ for α-anomer (Hz)	$^{3}J_{H1\text{-}H2}$ for β-anomer (Hz)	Reference
S14	0	2.4	Ref. 30a
S15	0	2.4	Ref. 30b
S16	0	2.4	Ref. 30b
S17	0	2.4	Ref. 30b
4a	0	3.1	This work
4p	0	3.1	This work

[31] (a) Kunig, J.; Lonnecke, P.; Hey-Hawkins, E. Enantiomerically Pure 3-Hydroxypropyl Diisopropylidene Mannose Derivatives. *Carbohydr. Res.* **2011**, *346*, 1154–1160. (b) Garegg, P. J.; Iversen, T.; Johansson, R. Synthesis of Disaccharides Containing β-D-Mannopyranosyl Groups. *Acta Chem. Scand*. **1980**, *B34*, 505–508.



$^{1}J_{C1\text{-}H1}$ coupling constants were also useful for the assignment of anomeric configuration in mannosyl and rhamnosyl linkages. In a study by Bock and Pedersen,[32] the $^{1}J_{C1\text{-}H1}$ coupling constants for a number of carbohydrate derivatives (*O*-glycosides) have been measured. The $^{1}J_{C1\text{-}H1}$ of α-anomers ranges from 170 to 177 Hz with an average of 171.8±2.4 Hz, while that of β-anomers ranges from 160 to 165 Hz with an average of 161.8±1.5 Hz. Because of the 10 Hz difference in coupling constant between α- and β-anomers, $^{1}J_{C1\text{-}H1}$ coupling constants have been used by Crich to assign anomeric configuration of mannosyl linkages.[33]

Additionally, Crich and coworkers noted that the chemical shift of H-5 proton resonance could be utilized to distinguish anomeric configuration in the 4,6-benzylidene-protected mannosides.[20]

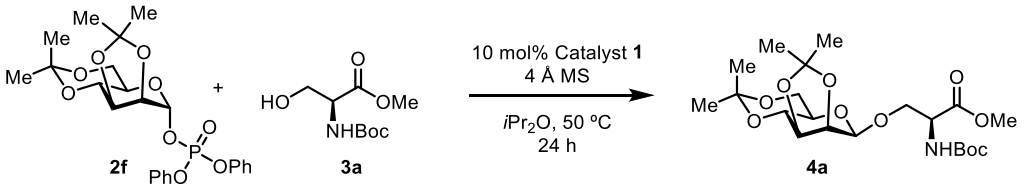
[32] Block, K.; Pederson, C. A Study of ^{13}CH Coupling Constants in Hexopyranoses. *J. Chem. Soc., Perkin Trans*. **1974**, 3877–3882.
[33] Crich, D.; Smith, M. Solid-Phase Synthesis of *β*-Mannosides. *J. Am. Chem. Soc*. **2002**, *124*, 8867–8869

They observed that H-5 proton resonance in β-mannosides typically appears in the 3.3–3.4 ppm region, while in α-mannosides, the resonance is shifted downfield and appears in the 3.6–3.9 ppm region. We have observed a similar trend in bis-acetonide-protected mannosides presumably because 4,6-benzylidene acetal and 4,6-acetonide induce similar chair conformation with C-4, C-5, and C-6 position. Three examples from this work are shown below.

Compound	δ H-5 for α-anomer (ppm)	δ H-5 for β-anomer (ppm)
4a	3.50	3.34
4c	3.60	3.30
4i	3.49	3.26

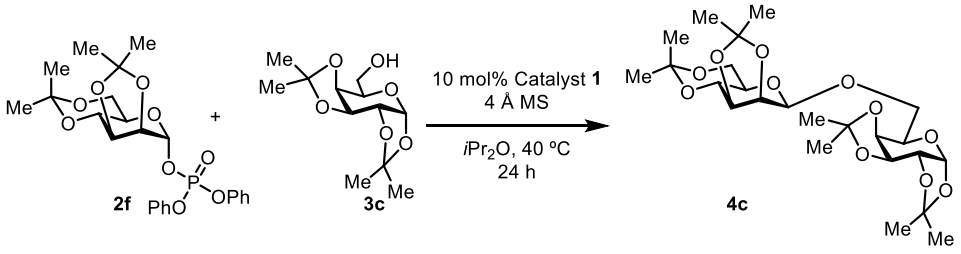
Selectvities were assigned using anomeric proton peaks in the crude mixture. In *O*-alkyl glycosides, anomeric proton peaks typically appear around 5 ppm. The anomeric proton peaks are shifted downfield in *O*-aryl glycosides and often appear around 5.4 ppm. In most cases, the region between 5–6 ppm is relatively clean, so accurate integration can be obtained. Peaks used in assignment will be noted in the characterization data of each compound.

2.10.7 Synthesis and Characterization of Products



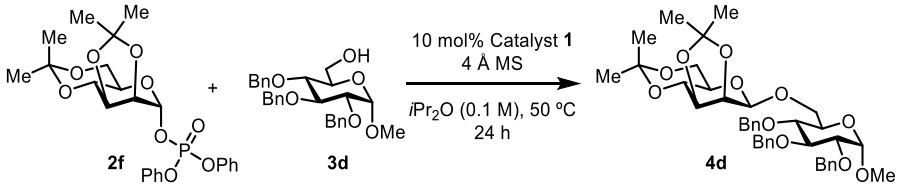
To a flame-dried 10 mL round bottom flask equipped with a stir bar was added Boc-Ser-OMe **3a** (0.088 g, 0.40 mmol, 2 equiv), catalyst (22.3 mg, 0.02 mmol, 0.1 equiv) and activated 4 Å molecular sieves (0.2 g). To the reaction mixture was added a solution of mannosyl phosphate (0.098 g, 0.20 mmol, 1 equiv) in 2 mL anhydrous diisopropyl ether. The flask was sealed with a yellow polyethylene cap under an atmosphere of air and parafilm was used to seal the cap tightly.

The mixture was then heated with efficient stirring at 50 ˚C in an oil bath for 24 hours over which time the mixture thickened. The mixture was cooled to room temperature, and 100 μL aliquot was diluted with diethyl ether and filtered to remove the molecular sieves. This solution was concentrated and ^{1}H NMR analysis on the crude mixture was used to determine the anomeric selectivity (1:19 α:β). The mixture was then purified by column chromatography (20% Et_2O/hexanes to 60% Et_2O/hexanes) to give the desired product **4a** in 82% yield (0.075 g, 0.163 mmol) as a colorless oil. ^{1}H NMR (600 MHz, $CDCl_3$) δ 5.40 (d, *J* = 8.9 Hz, 1H), 4.82 (d, *J* = 3.1 Hz, 1H, H-1, β-anomer), 4.49 (dt, *J* = 9.0, 3.4 Hz, 1H), 4.26 (dd, *J* = 7.3, 3.2 Hz, 1H), 4.24 – 4.17 (m, 2H), 4.14 (dd, *J* = 10.6, 7.2 Hz, 1H), 3.90 (dd, *J* = 10.8, 5.3 Hz, 1H), 3.76 (s, 3H), 3.72 – 3.63 (m, 2H), 3.34 (td, *J* = 10.6, 5.3 Hz, 1H, H-5, β-anomer), 1.53 (s, 6H), 1.43 (s, 9H), 1.40 (s, 3H), 1.35 (s, 3H). ^{13}C NMR (126 MHz, $CDCl_3$) δ 171.0, 155.6, 111.4, 99.8, 98.2, 80.2, 75.9, 73.7, 71.4, 69.3, 66.0, 63.3, 53.9, 52.7, 29.1, 28.4, 26.7, 25.6, 19.1. HRMS (ESI) m/z calculated for $C_{21}H_{35}NO_{10}$ $[M+Na]^+$: 484.2153; found: 484.2152. α-Anomer: ^{1}H NMR (600 MHz, $CDCl_3$) 4.97 ppm (s, 1H) 3.50 (td, *J* = 10.2, 5.7 Hz, 1H, H-5)



To a flame-dried 5 mL round bottom flask equipped with a stir bar was added 1,2:3,4-di-*O*-isopropylidene-d-galactopyranose **3c** (0.104 g, 0.40 mmol, 2 equiv), Catalyst **1** (22.3 mg, 0.02 mmol, 0.1 equiv.) and activated 4 Å molecular sieves (0.2 g). To the reaction mixture was added a solution of mannosyl phosphate (0.098 g, 0.20 mmol, 1 equiv) in 2 mL anhydrous diisopropyl ether. The flask was sealed with a yellow polyethylene cap under an atmosphere of air and parafilm

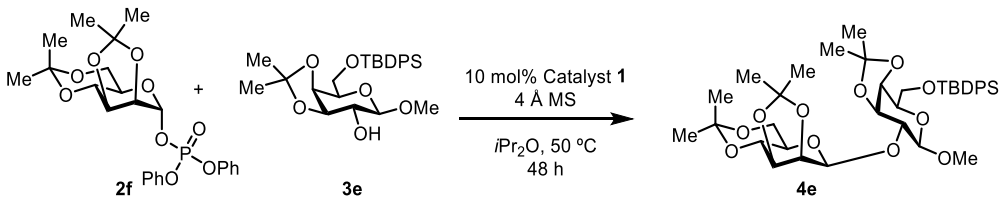
was used to seal the cap tightly. The mixture was then heated with efficient stirring at 40 ˚C in an oil bath for 24 hours over which time the mixture thickened. The mixture was cooled to room temperature, and 100 μL aliquot was diluted with diethyl ether and filtered to remove the molecular sieves. This solution was concentrated and ^{1}H NMR analysis on the crude mixture was used to determine the anomeric selectivity (1:19 α:β). The mixture was then purified by column chromatography (Et_2O/hexanes) to give the desired product **4c** in 94% yield (0.094 g, 0.188 mmol) as a colorless oil. ^{1}H NMR (500 MHz, $CDCl_3$) δ 5.53 (d, *J* = 5.0 Hz, 1H), 4.95 (d, *J* = 2.7 Hz, 1H, H-1, β-anomer), 4.61 (dd, *J* = 7.9, 2.4 Hz, 1H), 4.34 – 4.28 (m, 2H), 4.25 (d, *J* = 7.9 Hz, 1H), 4.18 (t, *J* = 6.8 Hz, 1H), 4.13 (dd, *J* = 10.3, 7.3 Hz, 1H), 4.07 – 4.01 (m, 2H), 3.93 (dd, *J* = 10.8, 5.4 Hz, 1H), 3.80 (t, *J* = 10.5 Hz, 1H), 3.67 (td, *J* = 9.0, 5.5 Hz, 1H), 3.30 (td, *J* = 10.2, 5.4 Hz, 1H, H-5, β-anomer), 1.54 (s, 3H), 1.53 (s, 4H), 1.52 (s, 3H), 1.45 (s, 3H), 1.42 (s, 3H), 1.37 (s, 3H), 1.32 (d, *J* = 3.0 Hz, 6H). ^{13}C NMR (126 MHz, $CDCl_3$) δ 111.2, 109.5, 108.8, 99.7, 98.7 ($^1J_{C\text{-}H}$ = 163.7 Hz, C-1), 96.5, 76.4, 74.4, 72.1, 71.4, 70.8, 70.6, 67.9, 67.8, 66.0, 62.9, 29.2, 27.6, 26.2, 26.2, 26.1, 25.1, 24.7, 19.2. HRMS (ESI) m/z calculated for $C_{24}H_{38}O_{11}$ $[M+Na]^+$: 525.2306; found: 525.2305. α-Anomer: ^{1}H NMR (600 MHz, $CDCl_3$) 5.06 ppm (s, 1H, H-1), 3.60 (td, *J* = 10.2, 5.6 Hz, 1H, H-5)



Methyl 2,3,4-tri-*O*-benzyl-α-D-glucopyranoside **3d** was prepared as previously reported.[34] To a flame-dried 5 mL round bottom flask equipped with a stir bar was added methyl 2,3,4-tri-*O*-

[34] Kotammagari, T. K.; Gonnade, R. G.; Bhattacharya, A. K. Biomimetic Total Synthesis of Angiopterlactone B and Other Potential Natural Products. *Org. Lett*. **2017**, *19*, 3564–3567.

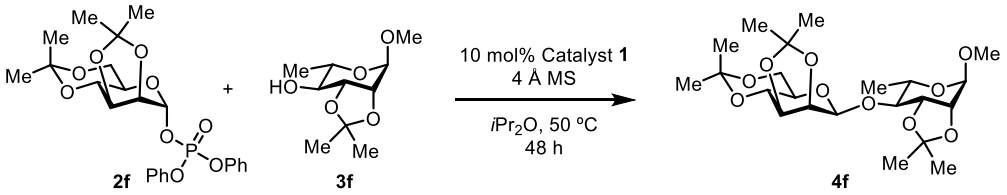
benzyl-α-D-glucopyranoside **3c** (0.186 g, 0.40 mmol, 2 equiv), Catalyst **1** (22.3 mg, 0.02 mmol, 0.1 equiv) and activated 4 Å molecular sieves (0.2 g). To the reaction mixture was added a solution of mannosyl phosphate (0.098 g, 0.20 mmol, 1 equiv) in 2 mL anhydrous diisopropyl ether. The flask was sealed with a yellow polyethylene cap under an atmosphere of air and parafilm was used to seal the cap tightly. The mixture was then heated with efficient stirring at 50 ˚C in an oil bath for 24 hours over which time the mixture thickened. The mixture was cooled to room temperature, and 100 μL aliquot was diluted with diethyl ether and filtered to remove the molecular sieves. This solution was concentrated and ^{1}H NMR analysis on the crude mixture was used to determine the anomeric selectivity (1:50 α:β). The mixture was then purified by column chromatography (Et_2O/hexanes) to give the desired product **4d** in 92% yield (0.130 g, 0.184 mmol). ^{1}H NMR (600 MHz, $CDCl_3$) δ 7.37 – 7.23 (m, 15H), 4.98 (d, *J* = 10.8 Hz, 1H), 4.87 (d, *J* = 11.0 Hz, 1H), 4.84 – 4.76 (m, 3H), 4.63 (t, *J* = 11.6 Hz, 2H), 4.55 (d, *J* = 2.4 Hz, 1H, H-1, β-anomer), 4.25 – 4.19 (m, 2H), 4.15 (t, *J* = 6.8 Hz, 1H), 4.04 (d, *J* = 11.0 Hz, 1H), 3.99 (t, *J* = 9.3 Hz, 1H), 3.87 (dd, *J* = 10.4, 5.0 Hz, 1H), 3.80 (dd, *J* = 10.1, 5.1 Hz, 1H), 3.76 (t, *J* = 10.4 Hz, 1H), 3.66 (dd, *J* = 10.6, 4.7 Hz, 1H), 3.55 – 3.46 (m, 2H), 3.37 (s, 3H), 3.27 (td, *J* = 9.6, 4.6 Hz, 1H, H-5, β-anomer), 1.55 (s, 3H), 1.43 (s, 3H), 1.41 (s, 3H), 1.34 (s, 3H). ^{13}C NMR (126 MHz, $CDCl_3$) δ 138.8, 138.4, 138.2, 128.5, 128.5, 128.5, 128.1, 128.0, 128.0, 127.8, 127.8, 127.7, 111.0, 99.7, 98.2, 98.1, 82., 80.03, 78.0, 76.0, 75.8, 75.1, 74.1, 73.5, 71.5, 70.2, 67.2, 66.1, 62.9, 55.2, 29.1, 27.4, 25.6, 18.9. HRMS (ESI) m/z calculated for $C_{40}H_{50}O_{11}$ $[M+Na]^+$: 729.3245; found: 729.3244. α-Anomer: ^{1}H NMR (600 MHz, $CDCl_3$) 5.08 ppm (s, 1H)



6-*O*-(*tert*-butyldiphenylsilyl)-3,4-*O*-isopropylidene-β-D-galactopyranoside **3e** was prepared as previously reported.[35] To a flame-dried 10 mL round bottom flask equipped with a stir bar was added methyl 6-*O*-(*tert*-butyldiphenylsilyl)-3,4-*O*-isopropylidene-β-D-galactopyranoside **3e** (0.095 g, 0.20 mmol, 1 equiv), catalyst (22.3 mg, 0.02 mmol, 0.1 equiv) and activated 4 Å molecular sieves (0.2 g). To the reaction mixture was added a solution of mannosyl phosphate (0.098 g, 0.20 mmol, 1 equiv) in 2 mL anhydrous diisopropyl ether. The flask was sealed with a yellow polyethylene cap under an atmosphere of air and parafilm was used to seal the cap tightly. The mixture was then heated with efficient stirring at 50 ˚C in an oil bath for 48 hours over which time the mixture thickened. The mixture was cooled to room temperature, and 100 μL aliquot was diluted with diethyl ether and filtered to remove the molecular sieves. This solution was concentrated and ^{1}H NMR analysis on the crude mixture was used to determine the anomeric selectivity (1:35 α:β). The mixture was then purified by column chromatography (hexanes to 20% EtOAc/hexanes) to give the desired product **4e** in 73% yield (0.103 g, 0.146 mmol) as a white foamy solid. ^{1}H NMR (600 MHz, $CDCl_3$) δ 7.72 – 7.68 (m, 4H), 7.46 – 7.33 (m, 6H), 5.38 (d, *J* = 3.1 Hz, 1H, H-1, β-anomer), 4.56 (dd, *J* = 10.7, 6.9 Hz, 1H), 4.32 (dd, *J* = 7.5, 3.1 Hz, 1H), 4.28 – 4.23 (m, 2H), 4.21 – 4.17 (m, 2H), 3.99 – 3.92 (m, 2H), 3.90 – 3.82 (m, 3H), 3.79 (dd, *J* = 8.1, 6.8 Hz, 1H), 3.52 (s, 3H), 3.39 (ddd, *J* = 10.7, 9.2, 6.4 Hz, 1H), 1.56 (s, 3H), 1.53 (s, 3H), 1.49 (s, 3H), 1.42 (s, 3H), 1.37 (s, 3H), 1.32 (s, 3H), 1.06 (s, 9H). ^{13}C NMR (126 MHz, $CDCl_3$) δ 135.7, 135.7, 133.5, 133.4, 129.8, 127.8, 127.7, 111.4, 110.2, 102.3, 99.6, 95.5, 80.0, 76.2, 76.1, 74.0, 73.4, 73.4, 71.1, 65.9, 63.2, 62.8, 56.8, 29.2, 28.0, 26.9, 26.8, 26.4, 25.9, 19.3, 19.2. HRMS (ESI)

[35] Dubey, R.; Reynolds, D.; Abbas, S. A.; Matta, K. L. Synthesis of *O*-α-L-fucopyranosyl-(1→3)-*O*-β-D-galactopyranosyl-(1→4)-2-acetamido-2-deoxy-D-glucopyranose (*N*-acetyl-3′-*O*-α-L-fucopyranosyllactosamine). *Carbohydr. Res*. **1988**, *183*, 155–162.

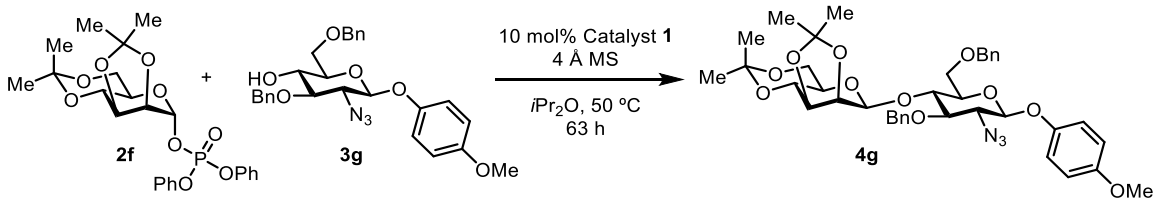
m/z calculated for $C_{38}H_{54}O_{11}Si$ $[M+Na]^+$: 737.3328; found: 737.3325. α-Anomer: ^1H NMR (600 MHz, $CDCl_3$) 5.39 ppm (s, 1H, H-1)



2,3-*O*-isopropylidene-α-L-rhamnopyranoside was prepared as previously reported.[36] To a flame-dried 25 mL round bottom flask equipped with a stir bar was added methyl 2,3-*O*-isopropylidene-α-L-rhamnopyranoside **3f** (0.087 g, 0.40 mmol, 2 equiv), Catalyst **1** (22.3 mg, 0.02 mmol, 0.1 equiv) and activated 4 Å molecular sieves (0.4 g). To the reaction mixture was added a solution of mannosyl phosphate, **2f** (0.098 g, 0.20 mmol, 1 equiv) in 4 mL anhydrous cyclohexane. The flask was sealed with a yellow polyethylene cap under an atmosphere of air and parafilm was used to seal the cap tightly. The mixture was then heated with efficient stirring at 50 ˚C in an oil bath for 48 hours over which time the mixture thickened. The mixture was cooled to room temperature, and 100 μL aliquot was diluted with diethyl ether and filtered to remove the molecular sieves. This solution was concentrated and ^1H NMR analysis on the crude mixture was used to determine the anomeric selectivity (1:17 α:β). The mixture was then purified by column chromatography (5% Et_2O/hexanes to 35% Et_2O/hexanes) to give the desired product **4f** in 71% yield (0.065 g, 0.141 mmol) as a colorless oil. ^1H NMR (600 MHz, $CDCl_3$) δ 5.32 (d, J = 2.7 Hz, 1H, H-1, β-anomer), 4.83 (s, 1H), 4.30 (dd, J = 6.4, 2.7 Hz, 1H), 4.21 (dd, J = 7.4, 5.6 Hz, 1H), 4.16 (t, J = 6.8 Hz, 1H), 4.07 (d, J = 5.6 Hz, 1H), 4.02 (dd, J = 10.5, 7.3 Hz, 1H), 3.90 (dd, J = 10.9, 5.4 Hz, 1H), 3.74 (t, J = 10.6 Hz, 1H), 3.69 (dq, J = 9.9, 6.2 Hz, 1H), 3.58 (dd, J = 9.9, 7.4 Hz, 1H), 3.34 (s, 3H), 3.25

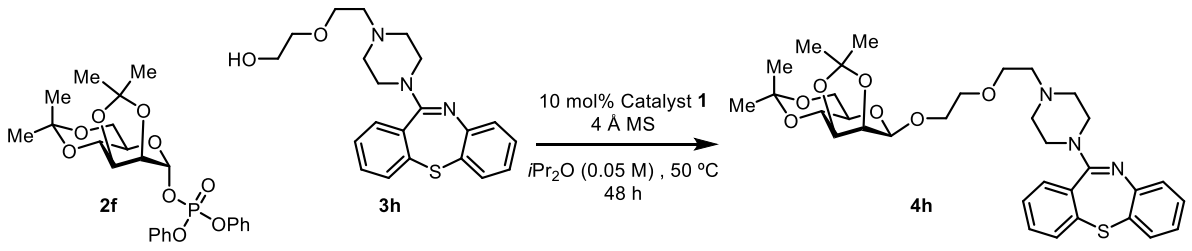
[36] Sun, X.; Lee, H.; Lee, S.; Tan, K. L. Catalyst Recognition of *cis*-1,2-Diols Enables Site-Selective Functionalization of Complex Molecules. *Nat. Chem*. **2013**, *5*, 790–795.

(td, J = 10.3, 5.4 Hz, 1H, H-5, β-anomer), 1.52 (s, 3H), 1.51 – 1.48 (m, 6H), 1.40 (s, 3H), 1.35 (s, 3H), 1.34 – 1.30 (m, 6H). ^{13}C NMR (126 MHz, $CDCl_3$) δ 111.3, 109.4, 99.7, 98.0, 97.3 ($^1J_{C\text{-}H}$ = 163.5 Hz, C-1), 79.1, 78.4, 76.4, 76.1, 74.3, 72.2, 66.0, 63.9, 62.8, 54.9, 29.1, 28.0, 27.6, 26.4, 26.1, 19.2, 18.1. HRMS (ESI) m/z calculated for $C_{22}H_{36}O_{10}$ $[M+Na]^+$: 483.2201; found: 483.2200. α-Anomer: ^{1}H NMR (600 MHz, $CDCl_3$) 5.10 ppm (s, 1H, H-1)



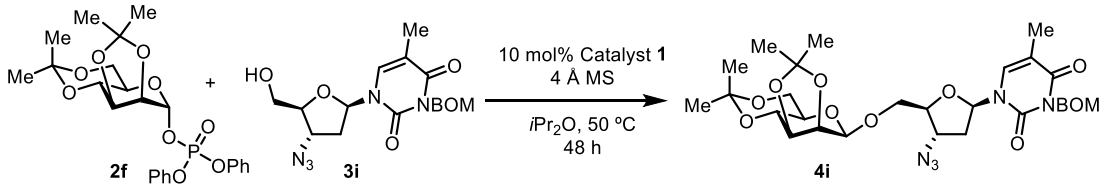
To a flame-dried 10 mL round bottom flask equipped with a stir bar was added 4-methoxyphenyl 2-azido-3,6-di-*O*-benzyl-2-deoxy-β-D-glucopyranoside **3g** (0.098 g, 0.20 mmol, 1 equiv), Catalyst **1** (22.3 mg, 0.02 mmol, 0.1 equiv) and activated 4 Å molecular sieves (0.20 g). To the reaction mixture was added a solution of mannosyl phosphate (0.098 g, 0.20 mmol, 1 equiv) in 2.0 mL anhydrous diisopropyl ether. The flask was sealed with a yellow polyethylene cap under an atmosphere of air and parafilm was used to seal the cap tightly. The mixture was then heated with efficient stirring at 50 ˚C in an oil bath for 63 hours over which time the mixture thickened. The mixture was cooled to room temperature, and 100 μL aliquot was diluted with diethyl ether and filtered to remove the molecular sieves. This solution was concentrated and ^{1}H NMR analysis on the crude mixture was used to determine the anomeric selectivity (1:14 α:β). The mixture was then purified by column chromatography (5% EtOAc/hexanes to 20% EtOAc/hexanes followed by 0% MeOH/CH_2Cl_2 to 1% MeOH/CH_2Cl_2) to give the desired product **4g** in 43% yield (0.063 g, 0.086 mmol) as a white foamy solid. ^{1}H NMR (500 MHz, $CDCl_3$) δ 7.46 – 7.41 (m, 2H), 7.40 – 7.27 (m, 8H), 7.07 – 7.02 (m, 2H), 6.86 – 6.81 (m, 2H), 5.05 (d, J = 10.6 Hz, 1H), 4.81 (d, J = 10.9 Hz,

1H), 4.80 (d, J = 2.0 Hz, 1H, H-1, β-anomer), 4.73 (d, J = 12.0 Hz, 1H), 4.68 (d, J = 8.1 Hz, 1H), 4.48 (d, J = 12.0 Hz, 1H), 4.09 (t, J = 9.5 Hz, 1H), 3.96 – 3.90 (m, 2H), 3.83 – 3.73 (m, 5H), 3.72 – 3.61 (m, 3H), 3.61 – 3.55 (m, 2H), 3.38 (t, J = 10.5 Hz, 1H), 2.92 (td, J = 10.2, 5.5 Hz, 1H, H-5, β-anomer), 1.56 (s, 3H), 1.44 (s, 3H), 1.40 (s, 3H), 1.34 (s, 3H). ^{13}C NMR (126 MHz, $CDCl_3$) δ 155.8, 151.2, 138.6, 137.7, 128.7, 128.3, 128.2, 127.8, 127.7, 118.9, 114.7, 110.7, 101.8, 99.7, 99.6 ($^1J_{C\text{-}H}$ = 159.4 Hz, C-1), 81.0, 77.6, 76.8, 75.0, 74.8, 74.6, 73.8, 72.5, 68.0, 66.2, 65.7, 61.8, 55.8, 29.1, 28.4, 26.4, 18.8. HRMS (ESI) m/z calculated for $C_{39}H_{47}N_3O_{11}$ $[M+Na]^+$: 756.3103; found: 756.3105. α-Anomer: ^{1}H NMR (600 MHz, $CDCl_3$) 5.55 ppm (s, 1H, H-1)



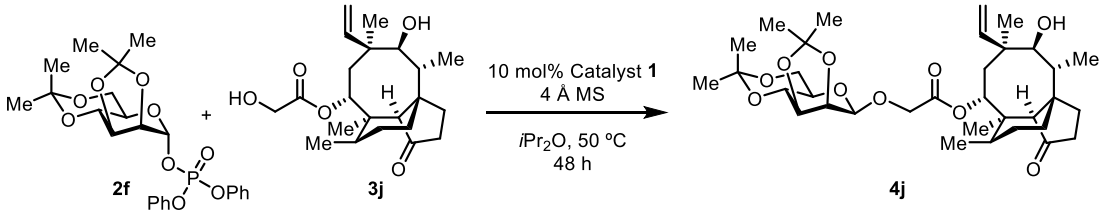
To a flame-dried 25 mL round bottom flask equipped with a stir bar was added quetiapine **3h** (0.077 g, 0.20 mmol, 1 equiv), Catalyst **1** (22.3 mg, 0.02 mmol, 0.1 equiv) and activated 4 Å molecular sieves (0.4 g). To the reaction mixture was added a solution of mannosyl phosphate, **2f** (0.098 g, 0.20 mmol, 1 equiv) in 4 mL anhydrous diisopropyl ether. The flask was sealed with a yellow polyethylene cap under an atmosphere of air and parafilm was used to seal the cap tightly. The mixture was then heated with efficient stirring at 50 ˚C in an oil bath for 44 hours over which time the mixture thickened. The mixture was cooled to room temperature, and 100 μL aliquot was diluted with diethyl ether and filtered to remove the molecular sieves. This solution was concentrated and ^{1}H NMR analysis on the crude mixture was used to determine the anomeric selectivity (1:19 α:β). The mixture was then purified by column chromatography (50% EtOAc/hexanes to 100% EtOAc/hexanes) to give the desired product **4h** in 63% yield (0.079 g,

0.126 mmol) as a light-yellow oil. ^{1}H NMR (600 MHz, $CDCl_3$) δ 7.50 (d, *J* = 7.9 Hz, 1H), 7.38 (dd, *J* = 7.7, 1.6 Hz, 1H), 7.33 – 7.26 (m, 3H), 7.19 – 7.13 (m, 1H), 7.06 (dd, *J* = 8.0, 1.4 Hz, 1H), 6.89 – 6.84 (m, 1H), 4.87 – 4.86 (m, 1H, H-1, β-anomer), 4.28 (ddd, *J* = 6.1, 2.6, 1.1 Hz, 1H), 4.13 (ddd, *J* = 13.4, 7.6, 6.0 Hz, 1H), 4.06 – 4.01 (m, 1H), 4.01 – 3.96 (m, 1H), 3.91 (ddd, *J* = 10.8, 5.5, 1.5 Hz, 1H), 3.82 – 3.72 (m, 2H), 3.73 – 3.60 (m, 5H), 3.60 – 3.27 (m, 3H), 3.23 (qd, *J* = 10.3, 5.5 Hz, 1H, H-5, β-Anomer), 2.77 – 2.48 (m, 6H), 1.55 (d, *J* = 4.2 Hz, 3H), 1.51 (d, *J* = 3.5 Hz, 3H), 1.42 (s, 3H), 1.35 (d, *J* = 3.1 Hz, 3H). ^{13}C NMR (126 MHz, $CDCl_3$) δ 160.8, 149.0, 140.0, 134.2, 132.2, 130.8, 129.2, 129.1, 128.3, 128.0, 125.4, 122.9, 111.1, 99.8, 99.0 ($^1J_{C\text{-}H}$ = 160.6 Hz, C-1), 76.5, 74.5, 72.2, 70.3, 69.2, 68.8, 68.7, 66.0, 62.6, 58.0, 53.5, 29.1, 27.8, 26.2, 19.1. HRMS (ESI) m/z calculated for $C_{33}H_{44}N_3O_7S$ $[M+H]^+$: 626.2894; found: 626.2897. α-Anomer: ^{1}H NMR (600 MHz, $CDCl_3$) 5.00 ppm (s, 1H, H-1)



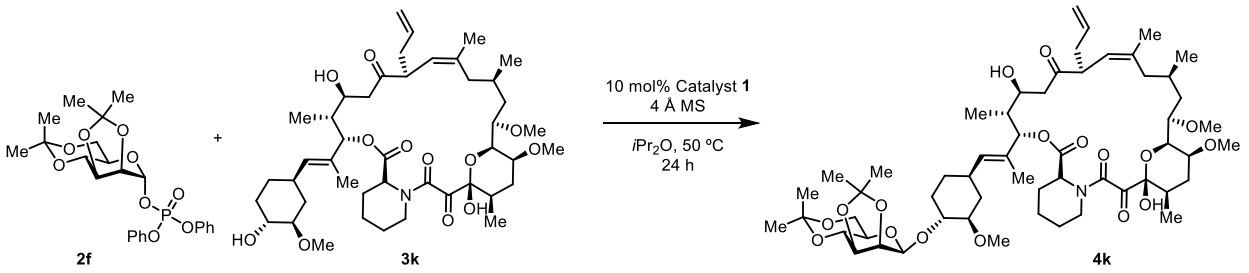
To a flame-dried 10 mL round bottom flask equipped with a stir bar was added BOM-zidovudine **3i** (0.058 g, 0.15 mmol, 1 equiv), catalyst (16.7 mg, 0.015 mmol, 0.1 equiv) and activated 4 Å molecular sieves (0.15 g). To the reaction mixture was added a solution of mannosyl phosphate (0.062 g, 0.15 mmol, 1 equiv) in 1.5 mL anhydrous diisopropyl ether. The flask was sealed with a yellow polyethylene cap under an atmosphere of air and parafilm was used to seal the cap tightly. The mixture was then heated with efficient stirring at 50 ˚C in an oil bath for 48 hours over which time the mixture thickened. The mixture was cooled to room temperature, and 100 µL aliquot was diluted with diethyl ether and filtered to remove the molecular sieves. This solution was concentrated and ^{1}H NMR analysis on the crude mixture was used to determine the anomeric

selectivity (1:18 α:β). The mixture was then purified by column chromatography (5% EtOAc/hexanes to 30% EtOAc/hexanes) to give the desired product **4i** in 61% yield (0.057 g, 0.091 mmol) as a colorless oil. ^{1}H NMR (600 MHz, $CDCl_3$) δ 7.46 (d, *J* = 1.4 Hz, 1H), 7.38 – 7.34 (m, 2H), 7.31 (t, *J* = 7.6 Hz, 2H), 7.26 – 7.22 (m, 1H), 6.28 (t, *J* = 6.7 Hz, 1H), 5.47 (s, 2H), 4.85 (d, *J* = 2.5 Hz, 1H, H-1, β-anomer), 4.68 (s, 2H), 4.30 (dt, *J* = 7.6, 4.0 Hz, 1H), 4.28 (dd, *J* = 6.0, 2.6 Hz, 1H), 4.20 (dd, *J* = 11.0, 2.5 Hz, 1H), 4.16 (dd, *J* = 7.7, 6.0 Hz, 1H), 4.06 (q, *J* = 3.2 Hz, 1H), 3.99 (dd, *J* = 10.3, 7.7 Hz, 1H), 3.93 (dd, *J* = 10.9, 5.5 Hz, 1H), 3.74 (t, *J* = 10.6 Hz, 1H), 3.69 (dd, *J* = 11.0, 3.2 Hz, 1H), 3.26 (td, *J* = 10.3, 5.5 Hz, 1H, H-5, β-anomer), 2.39 (ddd, *J* = 13.8, 6.3, 3.9 Hz, 1H), 2.30 (dt, *J* = 14.0, 7.2 Hz, 1H), 1.98 (d, *J* = 1.2 Hz, 3H), 1.51 (s, 3H), 1.44 (s, 3H), 1.40 (s, 3H), 1.35 (s, 3H). ^{13}C NMR (126 MHz, $CDCl_3$) δ 163.5, 151.0, 138.0, 134.6, 128.3, 127.7, 127.7, 110.9, 110.7, 99.8, 98.9 ($^{1}J_{C\text{-}H}$ = 161.1 Hz, C-1), 85.4, 82.6, 76.4, 74.2, 72.3, 71.9, 70.6, 68.9, 66.4, 62.4, 61.0, 37.5, 29.0, 27.8, 25.9, 18.8, 13.4. HRMS (ESI) m/z calculated for $C_{30}H_{39}N_5O_{10}$ $[M+Na]^+$: 652.2589; found: 652.2592. α-Anomer: ^{1}H NMR (600 MHz, $CDCl_3$) 5.10 ppm (s, 1H, H-1), 3.49 (td, *J* = 10.2, 5.6 Hz, 1H, H-5).



To a flame-dried 10 mL round bottom flask equipped with a stir bar was added pleuromutilin **3j** (0.076 g, 0.20 mmol, 1 equiv), Catalyst **1** (22.3 mg, 0.02 mmol, 0.1 equiv) and activated 4 Å molecular sieves (0.20 g). To the reaction mixture was added a solution of mannosyl phosphate (0.098 g, 0.20 mmol, 1 equiv) in 2.0 mL anhydrous diisopropyl ether. The flask was sealed with a yellow polyethylene cap under an atmosphere of air and parafilm was used to seal the cap tightly.

The mixture was then heated with efficient stirring at 50 ˚C in an oil bath for 48 hours over which time the mixture thickened. The mixture was cooled to room temperature, and 100 μL aliquot was diluted with diethyl ether and filtered to remove the molecular sieves. This solution was concentrated and ^{1}H NMR analysis on the crude mixture was used to determine the anomeric selectivity (1:15 α:β, <1:50 r.r.). The mixture was then purified by column chromatography (10% EtOAc/hexanes to 65% EtOAc/hexanes). Fractions containing the desired product and unreacted pleuromutilin were combined and concentrated under reduced pressure. The resulted mixture was further purified by preparative HPLC using IBN (Diacel) column (5% *i*PrOH/hexanes) to give the desired product **4j** in 30% yield (0.037 g, 0.060 mmol) as a white solid. ^{1}H NMR (600 MHz, $CDCl_3$) δ 6.48 (dd, *J* = 17.4, 11.0 Hz, 1H), 5.82 (d, *J* = 8.5 Hz, 1H), 5.34 (d, *J* = 11.7 Hz, 1H), 5.21 (d, *J* = 17.3 Hz, 1H), 4.92 (d, *J* = 2.5 Hz, 1H, H-1, β-anomer), 4.39 (dd, *J* = 6.0, 2.6 Hz, 1H), 4.29 – 4.20 (m, 2H), 4.19 – 4.13 (m, 1H), 4.06 (dd, *J* = 10.3, 7.6 Hz, 1H), 3.84 (dd, *J* = 10.9, 5.5 Hz, 1H), 3.78 (t, *J* = 10.5 Hz, 1H), 3.35 (dd, *J* = 10.7, 6.5 Hz, 1H), 3.19 (td, *J* = 10.2, 5.5 Hz, 1H, H-5, β-anomer), 2.33 (p, *J* = 7.0 Hz, 1H), 2.29 – 2.15 (m, 2H), 2.12 – 2.03 (m, 2H), 1.79 – 1.74 (m, 1H), 1.71 – 1.61 (m, 3H), 1.55 (d, *J* = 20.7 Hz, 7H), 1.49 – 1.44 (m, 2H), 1.44 – 1.34 (m, 10H), 1.29 (d, *J* = 16.1 Hz, 1H), 1.20 – 1.08 (m, 4H), 0.87 (d, *J* = 7.0 Hz, 3H), 0.70 (d, *J* = 7.1 Hz, 3H). ^{13}C NMR (126 MHz, $CDCl_3$) δ 217.0, 168.8, 138.9, 117.6, 111.3, 99.9, 98.3 ($^{1}J_{C\text{-}H}$ = 160.3 Hz, C-1), 76.5, 74.7, 74.3, 72.0, 69.1, 66.3, 66.1, 62.4, 58.2, 45.6, 44.9, 44.1, 41.9, 36.7, 36.2, 34.6, 30.5, 29.1, 27.8, 27.0, 26.5, 26.2, 25.0, 19.1, 16.7, 15.0, 11.6. HRMS (ESI) m/z calculated for $C_{34}H_{52}O_{10}$ $[M+Na]^{+}$: 643.3453; found: 643.3455. α-Anomer: ^{1}H NMR (600 MHz, $CDCl_3$) 5.08 ppm (s, 1H, H-1)



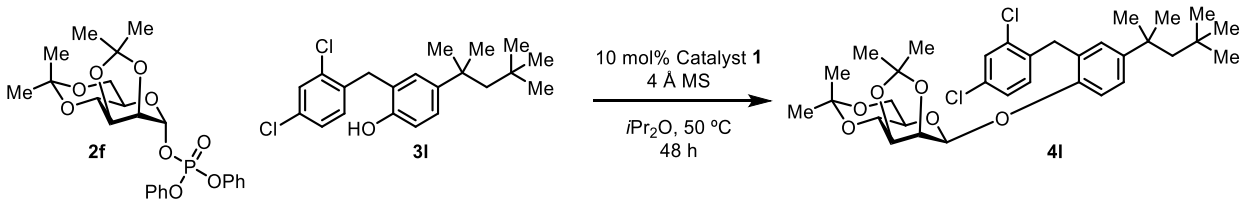
2f 3k 4k

To a flame-dried 5 mL round bottom flask equipped with a stir bar was added FK-506, **3i** (0.150 g, 0.19 mmol, 1.0 equiv.), Catalyst **1** (20 mg, 0.02 mmol, 0.1 equiv) and activated 4 Å molecular sieves (0.2 g). To the reaction mixture was added a solution of mannosyl phosphate (0.093 g, 0.19 mmol, 1 equiv) in 1.9 mL anhydrous diisopropyl ether. The flask was sealed with a yellow polyethylene cap under an atmosphere of air and parafilm was used to seal the cap tightly. The mixture was then heated with efficient stirring at 50 ˚C in an oil bath for 24 hours over which time the mixture thickened. The mixture was cooled to room temperature, and 100 μL aliquot was diluted with diethyl ether and filtered to remove the molecular sieves. This solution was concentrated and ^{1}H NMR analysis on the crude mixture was used to determine the anomeric selectivity. (<1:50 α:β, <1:50 r.r.). The mixture was then purified by column chromatography (EtOAc/hexanes) to give the desired product **4k** in 67% yield (0.133 g, 0.127 mmol) as a white foamy solid. ^{1}H NMR (500 MHz, CD_3CN, as 4:1 rotamers) δ 5.80 - 5.68 (m, 1H), 5.18 (d, *J* = 4.4 Hz, 1H), 5.14 (t, *J* = 10.0 Hz, 1H), 5.03 (q, *J* = 1.6 Hz, 0.8H), 5.00 (q, *J* = 1.6 Hz, 0.5H), 4.98 – 4.91 (m, 3H, H-1), 4.61 – 4.54 (m, 1H), 4.42 (d, *J* = 1.2 Hz, 0.8H), 4.30 (d, *J* = 13.6 Hz, 0.8H), 4.27 – 4.20 (m, 2H), 4.09 (t, *J* = 7.0 Hz, 1H), 3.94 (dq, *J* = 8.2, 4.1 Hz, 0.2H), 3.90 (dq, *J* = 8.5, 4.5 Hz, 0.8H), 3.80 (dd, *J* = 10.6, 5.6 Hz, 1H), 3.75 (t, *J* = 10.3 Hz, 1H), 3.68 (dd, *J* = 9.7, 2.6 Hz, 0.2H), 3.60 (dd, *J* = 9.7, 1.4 Hz, 0.8H), 3.58 – 3.42 (m, 4H), 3.41 – 3.37 (m, 1H), 3.34 (d, *J* = 1.6 Hz, 6H), 3.32 (s, 1H), 3.29 (s, 2H), 3.26 (s, 1H), 3.23 (dt, *J* = 10.3, 5.2 Hz, 1H), 3.18 – 3.09 (m, 1H), 2.97 (d, *J* = 4.5 Hz, 0.8H), 2.89 (td, *J* = 12.9, 2.8 Hz, 0.8H), 2.78 – 2.67 (m, 1H), 2.45 – 2.38

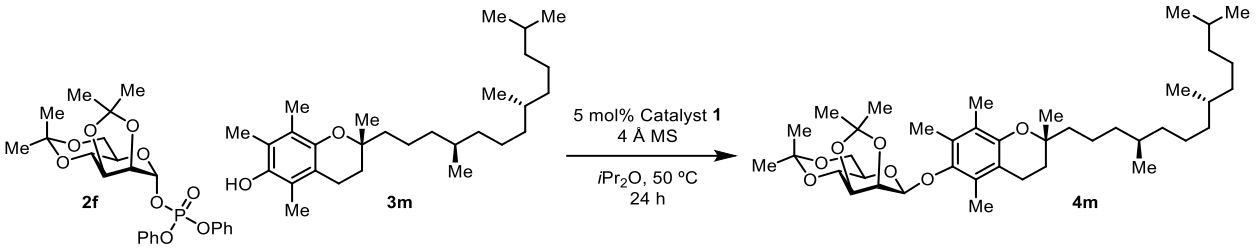
(m, 1H), 2.37 – 2.30 (m, 1H), 2.26 (d, J = 13.7 Hz, 0.6H), 2.22 – 2.15 (m, 2H), 2.09 – 1.99 (m, 4H), 1.90 – 1.84 (m, 1H), 1.80 – 1.69 (m, 4H), 1.64 (dd, J = 14.9, 1.3 Hz, 2H), 1.60 (dd, J = 18.1, 1.3 Hz, 5H), 1.48 (d, J = 7.7 Hz, 7H), 1.41 – 1.26 (m, 12H), 1.24 – 1.12 (m, 2H), 1.10 – 0.94 (m, 2H), 0.92 – 0.80 (m, 10H). ^{13}C NMR (126 MHz, $CDCl_3$, as a mixture of rotamers) δ 212.7, 212.6, 196.2, 192.7, 169.0, 168.7, 165.8, 164.7, 139.8, 139.0, 135.6, 135.4, 132.5, 131.9, 129.5, 129.5, 122.7, 122.5, 116.7, 111.4, 99.5, 98.7, 97.0, 93.9, 93.8, 81.8, 77.7, 77.2, 77.0, 76.6, 76.1, 75.2, 74.0, 73.7, 73.6, 72.8, 72.2, 71.1, 70.1, 69.1, 65.9, 65.8, 63.4, 57.7, 57.7, 57.6, 57.0, 56.6, 56.4, 56.1, 52.9, 52.8, 52.7, 48.6, 48.4, 43.9, 43.8, 43.2, 40.3, 39.7, 39.3, 36.7, 36.6, 36.4, 35.6, 35.5, 35.2, 34.7, 34.7, 34.6, 33.7, 32.9, 32.7, 32.6, 30.4, 29.7, 29.1, 28.5, 27.7, 26.8, 26.3, 26.1, 25.9, 24.6, 24.6, 21.2, 20.9, 20.5, 19.5, 19.2, 16.3, 16.1, 16.0, 15.9, 15.3, 14.4, 14.2, 14.2, 14.2, 9.8, 9.4. HRMS (ESI) m/z calculated for $C_{56}H_{87}NO_{17}$ $[M+Na]^+$: 1068.5866; found: 1068.5878.

FK-506 derivatives have been reported to exist as a mixture of rotamers in a number of NMR solvents.[37] The rotameric ratio of **4k** (3.3:1 major:minor rotamer) matched with the ratio reported in the literature.[36] The anomeric configuration of **4k** was assigned based on $^1J_{C1\text{-}H1}$ (158.2 Hz) of deprotected compound **8b**. The coupling constant falls in the range of β-*O*-glycosides. We did not isolate any other glycosylated FK-506 derivatives, and no discernible peaks corresponding to other glycosylated FK-506 derivatives were present in the crude NMR. Therefore, we reported the selectivity as <1:50 α:β.

[37] a) Chamni, S.; He, Q.-L.; Dang, Y.; Bhat, S.; Liu, J. O.; Romo, D. Diazo Reagents with Small Steric Footprints for Simultaneous Arming/SAR Studies of Alcohol-Containing Natural Products *via* O–H Insertion. *ACS Chem. Biol*. **2011**, *6*, 1175–1181. (b) Peddibhotla, S.; Dang, Y.; Liu, J. O.; Romo, D. Simultaneous Arming and Structure/Activity Studies of Natural Products Employing O-H Insertions: An Expedient and Versatile Strategy for Natural Products-Based Chemical Genetics. *J. Am. Chem. Soc*. **2007**, *129*, 12222–12231.

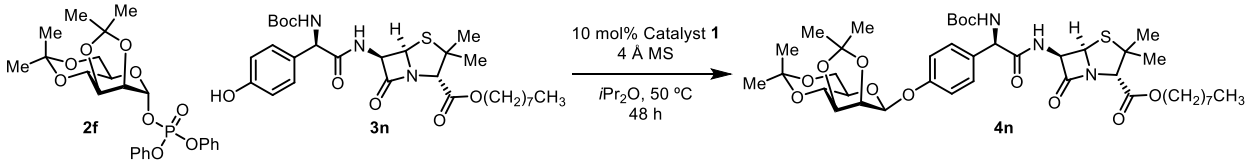


To a flame-dried 10 mL round bottom flask equipped with a stir bar was added clofoctol, **3n** (0.146 g, 0.40 mmol, 2 equiv), Catalyst **1** (22.3 mg, 0.02 mmol, 0.1 equiv) and activated 4 Å molecular sieves (0.2 g). To the reaction mixture was added a solution of mannosyl phosphate, **2f** (0.098 g, 0.20 mmol, 1 equiv) in 2 mL anhydrous diisopropyl ether. The flask was sealed with a yellow polyethylene cap under an atmosphere of air and parafilm was used to seal the cap tightly. The mixture was then heated with efficient stirring at 50 ˚C in an oil bath for 48 hours over which time the mixture thickened. The mixture was cooled to room temperature, and 100 μL aliquot was diluted with diethyl ether and filtered to remove the molecular sieves. This solution was concentrated and ^{1}H NMR analysis on the crude mixture was used to determine the anomeric selectivity (1:24 α:β). The mixture was then purified by column chromatography (hexanes to 15% Et_2O/hexanes) to give the desired product **4l** in 62% yield (0.075 g, 0.124 mmol) as a white foamy solid. ^{1}H NMR (600 MHz, $CDCl_3$) δ 7.37 (d, J = 2.1 Hz, 1H), 7.19 (dd, J = 8.6, 2.5 Hz, 1H), 7.10 – 7.07 (m, 2H), 7.03 – 6.96 (m, 2H), 5.42 (d, J = 3.0 Hz, 1H, H-1, β-anomer), 4.33 (dd, J = 6.5, 3.0 Hz, 1H), 4.29 – 4.20 (m, 2H), 4.13 (d, J = 16.1 Hz, 1H), 4.07 (d, J = 16.0 Hz, 1H), 3.90 (dd, J = 10.9, 5.3 Hz, 1H), 3.62 (t, J = 10.6 Hz, 1H), 3.41 (td, J = 10.1, 5.3 Hz, 1H, H-5, β-anomer), 1.65 (s, 2H), 1.51 (s, 3H), 1.42 – 1.40 (m, 6H), 1.39 (s, 3H), 1.30 (s, 6H), 0.67 (s, 9H). ^{13}C NMR (126 MHz, $CDCl_3$) δ 153.3, 144.5, 137.5, 135.0, 132.3, 131.5, 129.1, 129.0, 127.1, 126.9, 125.7, 115.0 ($^{1}J_{C\text{-}H}$ = 158.5 Hz, C-1), 111.3, 99.8, 97.3, 76.1, 73.8, 71.4, 66.3, 63.1, 57.1, 38.1, 33.7, 32.4, 31.9, 31.7, 29.1, 27.0, 25.5, 19.0. HRMS (ESI) m/z calculated for $C_{33}H_{44}Cl_2O_6$ $[M+Na]^+$: 629.2407; found: 629.2410. α-Anomer: ^{1}H NMR (600 MHz, $CDCl_3$) 5.66 ppm (s, 1H, H-1)



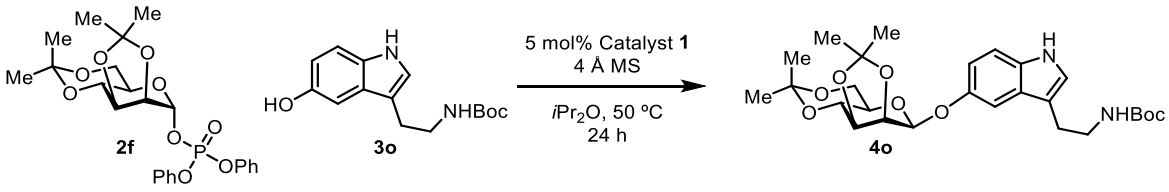
To a flame-dried 5 mL round bottom flask equipped with a stir bar was added α-tocopherol **3m** (0.086 g, 0.20 mmol, 1.0 equiv), Catalyst **1** (11 mg, 0.01 mmol, 0.05 equiv) and activated 4 Å molecular sieves (0.2 g). To the reaction mixture was added a solution of mannosyl phosphate, **2f** (0.098 g, 0.20 mmol, 1 equiv) in 2 mL anhydrous diisopropyl ether. The flask was sealed with a yellow polyethylene cap under an atmosphere of air and parafilm was used to seal the cap tightly. The mixture was then heated with efficient stirring at 50 ˚C in an oil bath for 24 hours over which time the mixture thickened. The mixture was cooled to room temperature, and 100 μL aliquot was diluted with diethyl ether and filtered to remove the molecular sieves. This solution was concentrated and ^{1}H NMR analysis on the crude mixture was used to determine the anomeric selectivity (<1:50 α:β). The mixture was then purified by column chromatography (Et_2O/hexanes) to give the desired product **4m** in 95% yield (0.128 g, 0.190 mmol) as a light-yellow oil. ^{1}H NMR (500 MHz, $CDCl_3$) δ 4.93 (d, *J* = 2.5 Hz, 1H, H-1, β-anomer), 4.53 (dd, *J* = 5.7, 2.5 Hz, 1H), 4.18 (dd, *J* = 7.6, 5.7 Hz, 1H), 4.04 (dd, *J* = 10.3, 7.6 Hz, 1H), 3.88 – 3.79 (m, 2H), 3.12 (td, *J* = 9.9, 6.0 Hz, 1H, H-5, β-anomer), 2.61 – 2.52 (m, 2H), 2.22 (s, 3H), 2.17 (s, 3H), 2.08 (s, 3H), 1.89 – 1.70 (m, 2H), 1.65 (s, 3H), 1.58 – 1.49 (m, 10H), 1.46 (s, 3H), 1.43 (s, 3H), 1.41 – 1.33 (m, 3H), 1.32 – 1.24 (m, 6H), 1.23 (s, 3H), 1.20 – 1.10 (m, 3H), 1.10 – 1.00 (m, 3H), 0.89 – 0.82 (m, 12H). ^{13}C NMR (126 MHz, $CDCl_3$) δ 148.4, 147.3, 128.0, 126.3, 122.9, 117.5, 111.2, 101.7, 99.7, 76.9, 74.9, 74.6, 72.2, 66.1, 62.1, 40.4, 39.5, 37.6, 37.5, 37.5, 37.4, 32.9, 32.8, 31.3, 29.1, 28.1, 26.3, 24.9, 24.5, 23.9, 22.8, 22.7, 21.1, 20.8, 19.9, 19.8, 19.1, 14.0, 13.1, 12.0.HRMS (ESI) m/z

calculated for $C_{41}H_{68}O_7$ [M+Na]$^+$: 695.4857; found: 695.4855. α-Anomer: ^{1}H NMR (600 MHz, $CDCl_3$) 5.14 ppm (s, 1H, H-1)



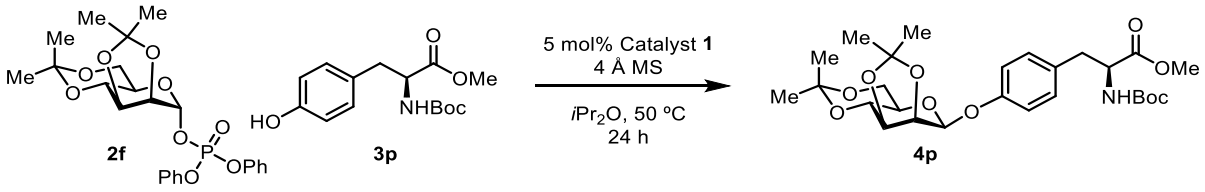
To a flame-dried 10 mL round bottom flask equipped with a stir bar was added amoxicillin **3n** (0.116 g, 0.20 mmol, 1 equiv), catalyst (22.3 mg, 0.02 mmol, 0.1 equiv) and activated 4 Å molecular sieves (0.2 g). To the reaction mixture was added a solution of mannosyl phosphate, **2f** (0.098 g, 0.20 mmol, 1 equiv) in 2 mL anhydrous diisopropyl ether. The flask was sealed with a yellow polyethylene cap under an atmosphere of air and parafilm was used to seal the cap tightly. The mixture was then heated with efficient stirring at 50 ˚C in an oil bath for 48 hours over which time the mixture thickened. The mixture was cooled to room temperature, and 100 μL aliquot was diluted with diethyl ether and filtered to remove the molecular sieves. This solution was concentrated and ^{1}H NMR analysis on the crude mixture was used to determine the anomeric selectivity (1:18 α:β). The mixture was then purified by column chromatography (5% Et_2O/hexanes to 60% Et_2O/hexanes) to give the desired product **4n** in 57% yield (0.093 g, 0.113 mmol) as a white foamy solid. ^{1}H NMR (600 MHz, $CDCl_3$) δ 7.27 (d, J = 8.7 Hz, 2H), 7.02 (d, J = 8.7 Hz, 2H), 6.67 (d, J = 9.3 Hz, 1H), 5.62 (dd, J = 9.2, 4.2 Hz, 1H), 5.59 (br, 1H), 5.47 (d, J = 4.3 Hz, 1H), 5.43 (d, J = 2.9 Hz, 1H, H-1, β-anomer), 5.15 (br, 1H), 4.44 – 4.39 (m, 1H), 4.38 (s, 1H), 4.36 – 4.31 (m, 2H), 4.19 – 4.08 (m, 2H), 3.90 (dd, J = 10.9, 5.3 Hz, 1H), 3.64 (t, J = 10.6 Hz, 1H), 3.49 – 3.42 (m, 1H, H-1, α-anomer), 1.63 (h, J = 6.5 Hz, 2H), 1.59 (s, 3H), 1.55 (s, 3H), 1.49 (s, 3H), 1.44 (s, 3H), 1.43 – 1.37 (m, 14H), 1.36 – 1.20 (m, 11H), 0.86 (t, J = 7.0 Hz, 3H). ^{13}C NMR (126 MHz, $CDCl_3$) δ 173.3, 170.0, 167.7, 157.3, 155.1, 131.6, 128.8, 117.5, 111.8, 99.8,

96.5, 80.5, 76.2, 73.7, 71.5, 70.7, 68.1, 66.2, 66.0, 64.8, 63.2, 58.7, 31.8, 29.2, 29.2, 29.1, 28.5, 28.4, 27.1, 27.1, 26.0, 25.9, 22.7, 19.1, 14.2. HRMS (ESI) m/z calculated for $C_{41}H_{62}N_3O_{12}S_1$ $[M+H]^+$: 820.4049; found: 820.4044 α-Anomer: ^{1}H NMR (600 MHz, $CDCl_3$) 5.74 ppm (s, 1H, H-1)



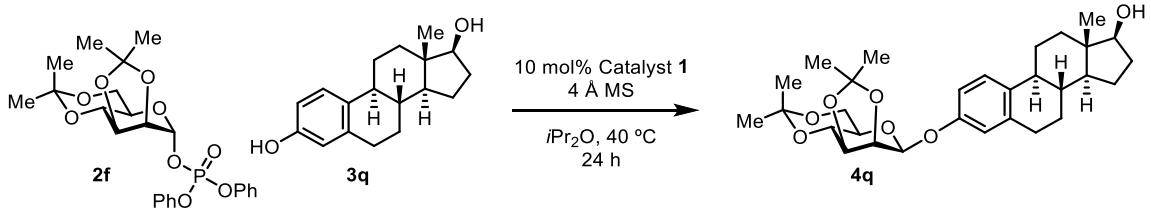
To a flame-dried 10 mL round bottom flask equipped with a stir bar was added Boc-Serotonin **3o** (0.055 g, 0.20 mmol, 1 equiv), Catalyst **1** (11.2 mg, 0.01 mmol, 0.05 equiv) and activated 4 Å molecular sieves (0.2 g). To the reaction mixture was added a solution of mannosyl phosphate, **2f** (0.098 g, 0.20 mmol, 1 equiv) in 2 mL anhydrous diisopropyl ether. The flask was sealed with a yellow polyethylene cap under an atmosphere of air and parafilm was used to seal the cap tightly. The mixture was then heated with efficient stirring at 50 ˚C in an oil bath for 24 hours over which time the mixture thickened. The mixture was cooled to room temperature, and 100 μL aliquot was diluted with diethyl ether and filtered to remove the molecular sieves. This solution was concentrated and ^{1}H NMR analysis on the crude mixture was used to determine the anomeric selectivity (<1:50 α:β). The mixture was then purified by column chromatography (5% EtOAc/hexanes to 30% EtOAc/hexanes) to give the desired product **4o** in 95% yield (0.099 g, 0.190 mmol) as a light yellow foamy solid. ^{1}H NMR (600 MHz, $CDCl_3$) δ 8.16 (s, 1H), 7.30 – 7.23 (m, 2H), 7.03 – 6.96 (m, 2H), 5.43 (d, *J* = 2.8 Hz, 1H, H-1, β-anomer), 4.63 (br, 1H), 4.48 (dd, *J* = 6.4, 2.9 Hz, 1H), 4.40 – 4.29 (m, 2H), 3.96 (dd, *J* = 10.9, 5.4 Hz, 1H), 3.78 (t, *J* = 10.6 Hz, 1H), 3.47 – 3.38 (m, 3H), 2.89 (t, *J* = 7.0 Hz, 2H), 1.66 (s, 3H), 1.53 (s, 3H), 1.45 – 1.42 (m, 15H). ^{13}C NMR (126 MHz, $CDCl_3$) δ 156.1, 151.5, 133.0, 127.9, 123.3, 114.4, 113.2, 111.8, 111.6,

106.6 ($^1J_{C\text{-}H}$ = 158.4 Hz, C-1), 99.8, 98.6, 79.3, 76.5, 74.3, 71.8, 66.2, 63.1, 40.7, 29.2, 28.6, 27.5, 26.1, 25.9, 19.2. HRMS (ESI) m/z calculated for $C_{27}H_{38}N_2O_8$ $[M+Na]^+$: 541.2520; found: 541.2521. α-Anomer: ^{1}H NMR (600 MHz, $CDCl_3$) 5.75 ppm (s, 1H, H-1)



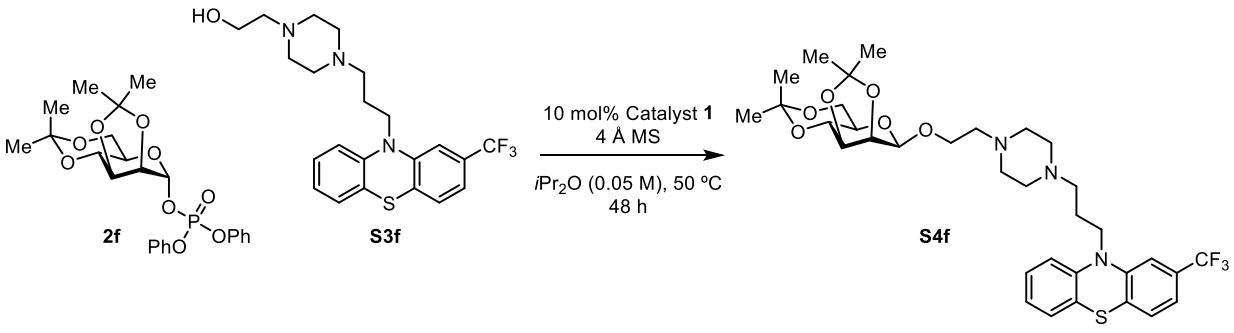
To a flame-dried 10 mL round bottom flask equipped with a stir bar was added Boc-Tyr-OMe **3p** (0.059 g, 0.20 mmol, 1 equiv), Catalyst **1** (11.2 mg, 0.01 mmol, 0.05 equiv) and activated 4 Å molecular sieves (0.22 g). To the reaction mixture was added a solution of mannosyl phosphate (0.108 g, 0.22 mmol, 1.1 equiv) in 2.2 mL anhydrous diisopropyl ether. The flask was sealed with a yellow polyethylene cap under an atmosphere of air and parafilm was used to seal the cap tightly. The mixture was then heated with efficient stirring at 50 ˚C in an oil bath for 24 hours over which time the mixture thickened. The mixture was cooled to room temperature, and 100 μL aliquot was diluted with diethyl ether and filtered to remove the molecular sieves. This solution was concentrated and ^{1}H NMR analysis on the crude mixture was used to determine the anomeric selectivity (1:50 α:β). The mixture was then purified by column chromatography (hexanes to 25% EtOAc/hexanes). Fractions containing the desired product and unreacted Boc-Tyr-OMe were combined and concentrated under reduced pressure. The organic mixture was diluted with Et_2O and washed with 1M NaOH(aq) to remove unreacted **3p**. The organic layer was dried over Na_2SO_4 and concentrated under reduced pressure to give the desired product **4p** in 80% yield (0.086 g, 0.159 mmol) as a white foamy solid. ^{1}H NMR (600 MHz, $CDCl_3$) δ 7.02 (d, J = 8.2 Hz, 2H), 6.95 (d, J = 8.2 Hz, 2H), 5.41 (d, J = 3.1 Hz, 1H, H-1, β-anomer), 4.97 (d, J = 8.3 Hz, 1H), 4.53 (q, J = 6.6 Hz, 1H), 4.41 (dd, J = 6.1, 2.8 Hz, 1H), 4.37 – 4.30 (m, 2H), 3.91 (dd, J = 10.9, 5.3 Hz, 1H),

3.72 – 3.61 (m, 4H), 3.45 (td, J = 10.0, 9.6, 5.5 Hz, 1H, H-5, β-anomer), 3.09 – 2.93 (m, 2H), 1.60 (s, 3H), 1.50 (s, 3H), 1.44 – 1.33 (m, 15H). ^{13}C NMR (126 MHz, $CDCl_3$) δ 172.4, 156.3, 155.1, 130.4, 130.1, 117.0 ($^1J_{C\text{-}H}$ = 160.7 Hz, C-1), 111.8, 99.8, 96.6, 80.0, 76.2, 73.7, 71.5, 66.1, 63.2, 54.4, 52.3, 37.6, 29.1, 28.4, 27.1, 25.9, 19.1. HRMS (ESI) m/z calculated for $C_{27}H_{39}NO_{10}$ $[M+Na]^+$: 560.2466; found: 560.2468. α-Anomer: ^{1}H NMR (600 MHz, $CDCl_3$) 5.73 ppm (s, 1H, H-1)



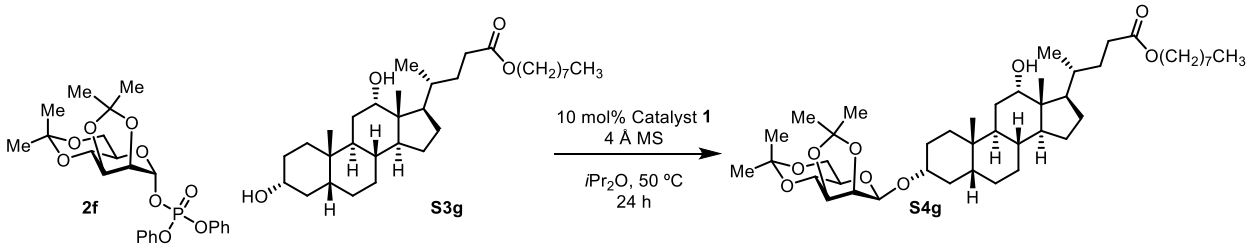
To a flame-dried 5 mL round bottom flask equipped with a stir bar was added estradiol **3q** (0.054 g, 0.20 mmol, 1.0 equiv), Catalyst **1** (22.3 mg, 0.01 mmol, 0.10 equiv) and activated 4 Å molecular sieves (0.2 g). To the reaction mixture was added a solution of mannosyl phosphate, **2f** (0.098 g, 0.20 mmol, 1 equiv) in 2 mL anhydrous diisopropyl ether. The flask was sealed with a yellow polyethylene cap under an atmosphere of air and parafilm was used to seal the cap tightly. The mixture was then heated with efficient stirring at 40 ˚C in an oil bath for 24 hours over which time the mixture thickened. The mixture was cooled to room temperature, and 100 μL aliquot was diluted with diethyl ether and filtered to remove the molecular sieves. This solution was concentrated and ^{1}H NMR analysis on the crude mixture was used to determine the anomeric selectivity (<1:50 α:β, 1:15 r.r.). The mixture was then purified by column chromatography (Et_2O/hexanes) to give the desired product **4q** in 94% yield (0.097 g, 0.188 mmol) as a white foamy solid. ^{1}H NMR (600 MHz, $CDCl_3$) δ 7.20 (d, J = 8.6 Hz, 1H), 6.84 (dd, J = 8.6, 2.7 Hz, 1H), 6.77 (d, J = 2.6 Hz, 1H), 5.41 (d, J = 2.9 Hz, 1H, H-1, β-anomer), 4.42 (dd, J = 6.8, 3.0 Hz,

1H), 4.40 – 4.30 (m, 2H), 3.93 (dd, *J* = 10.9, 5.3 Hz, 1H), 3.75 – 3.66 (m, 2H), 3.45 (td, *J* = 10.3, 5.3 Hz, 1H, H-5, β-anomer), 2.88 – 2.79 (m, 2H), 2.31 (dq, *J* = 13.3, 3.9 Hz, 1H), 2.18 (td, *J* = 11.3, 4.3 Hz, 1H), 2.15 – 2.06 (m, 1H), 1.94 (dt, *J* = 12.6, 3.3 Hz, 1H), 1.91 – 1.84 (m, 1H), 1.73 – 1.65 (m, 1H), 1.62 (s, 3H), 1.54 – 1.44 (m, 5H), 1.42 (d, *J* = 9.0 Hz, 7H), 1.40 – 1.23 (m, 4H), 1.22 – 1.15 (m, 1H), 0.77 (s, 3H). ^{13}C NMR (126 MHz, $CDCl_3$) δ 155.1, 138.2, 134.8, 126.5, 117.0, 114.4 ($^1J_{C\text{-}H}$ = 160.7 Hz, C-1), 111.8, 99.8, 96.9, 82.0, 76.3, 73.9, 71.6, 66.1, 63.3, 50.2, 44.1, 43.4, 38.8, 36.8, 30.7, 29.9, 29.1, 27.3, 27.2, 26.4, 26.0, 23.2, 19.2, 11.2. HRMS (ESI) m/z calculated for $C_{44}H_{74}O_9$ $[M+Na]^+$: 769.5225; found: 769.5225. α-Anomer: ^{1}H NMR (600 MHz, $CDCl_3$) 5.72 ppm (s, 1H, H-1).



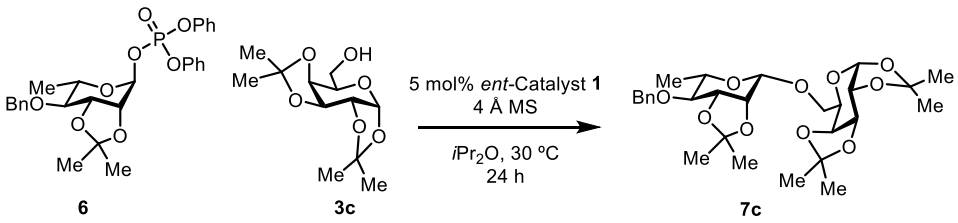
To a flame-dried 25 mL round bottom flask equipped with a stir bar was added fluphenazine **S3f** (0.088 g, 0.20 mmol, 1 equiv), Catalyst **1** (22.3 mg, 0.02 mmol, 0.1 equiv) and activated 4 Å molecular sieves (0.4 g). To the reaction mixture was added a solution of mannosyl phosphate, **2f** (0.098 g, 0.20 mmol, 1 equiv) in 4 mL anhydrous diisopropyl ether. The flask was sealed with a yellow polyethylene cap under an atmosphere of air and parafilm was used to seal the cap tightly. The mixture was then heated with efficient stirring at 50 ˚C in an oil bath for 48 hours over which time the mixture thickened. The mixture was cooled to room temperature, and 100 μL aliquot was diluted with diethyl ether and filtered to remove the molecular sieves. This solution was concentrated and ^{1}H NMR analysis on the crude mixture was used to determine the anomeric

selectivity (1:16 α:β). The mixture was then purified by column chromatography (50% EtOAc/hexanes to 100% EtOAc/hexanes followed by 0% MeOH/CH_2Cl_2 to 4% MeOH/CH_2Cl_2) to give the desired product **S4f** in 51% yield (0.069 g, 0.102 mmol) as a light-yellow oil. ^{1}H NMR (600 MHz, $CDCl_3$) δ 7.19 – 7.07 (m, 4fH), 7.02 (d, *J* = 1.7 Hz, 1H), 6.95 – 6.86 (m, 2H), 4.85 (d, *J* = 2.6 Hz, 1H, H-1, β-anomer), 4.27 (dd, *J* = 6.1, 2.6 Hz, 1H), 4.14 (dd, *J* = 7.6, 6.1 Hz, 1H), 4.03 (dd, *J* = 10.4, 7.6 Hz, 1H), 3.99 – 3.87 (m, 4H), 3.76 (t, *J* = 10.5 Hz, 1H), 3.73 – 3.66 (m, 1H), 3.23 (td, *J* = 10.3, 5.5 Hz, 1H, H-5, β-anomer), 2.72 – 2.10 (m, 12H), 1.92 (p, *J* = 6.9 Hz, 2H), 1.55 (s, 3H), 1.50 (s, 3H), 1.42 (s, 3H), 1.36 (s, 3H).^{19}F NMR (376 MHz, $CDCl_3$) δ -62.47. ^{13}C NMR (126 MHz, $CDCl_3$) δ 145.8, 144.4, 130.0, 129.5 (q, *J* = 32.0 Hz), 127.7, 127.6, 127.5, 125.4, 124.2, 123.2, 119.1, 119.1, 116.0, 112.0, 112.0, 111.1, 99.8, 98.9, 76.4, 74.5, 72.1, 67.2, 66.0, 62.7, 57.7, 55.4, 53.7, 53.3, 45.4, 29.1, 27.7, 26.1, 24.2, 19.1. HRMS (ESI) m/z calculated for $C_{34}H_{44}F_3N_3O_6S$ $[M+H]^+$: 680.2976; found: 680.2979. α-Anomer: ^{1}H NMR (600 MHz, $CDCl_3$) 5.01 ppm (s, 1H, H-1)



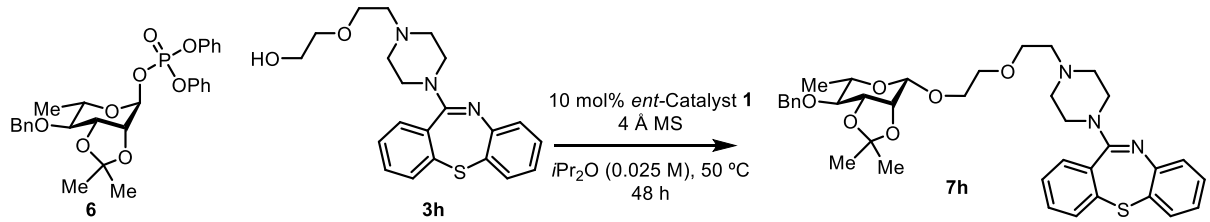
To a flame-dried 10 mL round bottom flask equipped with a stir bar was added deoxycholic acid octyl-ester **S3g** (0.101 g, 0.20 mmol, 1 equiv), Catalyst **1** (22.3 mg, 0.02 mmol, 0.1 equiv) and activated 4 Å molecular sieves (0.2 g). To the reaction mixture was added a solution of mannosyl phosphate, **2f** (0.098 g, 0.20 mmol, 1 equiv) in 2 mL anhydrous diisopropyl ether. The flask was sealed with a yellow polyethylene cap under an atmosphere of air and parafilm was used to seal the cap tightly. The mixture was then heated with efficient stirring at 50 ˚C in an oil bath for 24

hours over which time the mixture thickened. The mixture was cooled to room temperature, and 100 μL aliquot was diluted with diethyl ether and filtered to remove the molecular sieves. This solution was concentrated and ^{1}H NMR analysis on the crude mixture was used to determine the anomeric selectivity (1:32 α:β, <1:50 r.r.). The mixture was then purified by column chromatography (10% Et_2O/hexanes to 60% Et_2O/hexanes) to give the desired product **S4g** in 83% yield (0.124 g, 0.167 mmol) as a colorless oil. ^{1}H NMR (600 MHz, $CDCl_3$) δ 4.87 (d, *J* = 2.4 Hz, 1H, H-1, β-anomer), 4.22 (dd, *J* = 5.7, 2.4 Hz, 1H), 4.09 (dd, *J* = 7.7, 5.7 Hz, 1H), 4.03 (t, *J* = 6.7 Hz, 2H), 3.98 – 3.88 (m, 3H), 3.79 (t, *J* = 10.6 Hz, 1H), 3.69 – 3.61 (m, 1H), 3.18 (td, *J* = 10.2, 5.5 Hz, 1H, H-5, β-anomer), 2.34 (ddd, *J* = 15.0, 9.8, 5.0 Hz, 1H), 2.21 (ddd, *J* = 15.5, 9.2, 6.8 Hz, 1H), 1.98 (q, *J* = 12.6 Hz, 1H), 1.89 – 1.67 (m, 7H), 1.66 – 1.53 (m, 8H), 1.52 – 1.44 (m, 7H), 1.44 – 1.18 (m, 26H), 1.15 – 0.99 (m, 2H), 0.95 (d, *J* = 6.3 Hz, 3H), 0.93 – 0.82 (m, 7H), 0.65 (s, 3H). ^{13}C NMR (126 MHz, $CDCl_3$) δ 174.4, 111.1, 99.7, 97.7 ($^1J_{C\text{-}H}$ = 158.6 Hz, C-1), 80.0, 76.7, 75.3, 73.2, 72.4, 66.1, 64.5, 62.5, 48.3, 47.5, 46.6, 42.4, 36.1, 35.2, 35.2, 34.4, 33.7, 31.9, 31.5, 31.0, 29.3, 29.3, 29.1, 28.8, 28.7, 28.1, 27.5, 27.2, 26.9, 26.3, 26.2, 26.1, 23.7, 23.2, 22.7, 19.1, 17.4, 14.2, 12.9. HRMS (ESI) m/z calculated for $C_{44}H_{74}O_9$ $[M+Na]^+$: 769.5225; found: 769.5225. α-Anomer: ^{1}H NMR (600 MHz, $CDCl_3$) 5.17 ppm (s, 1H, H-1)



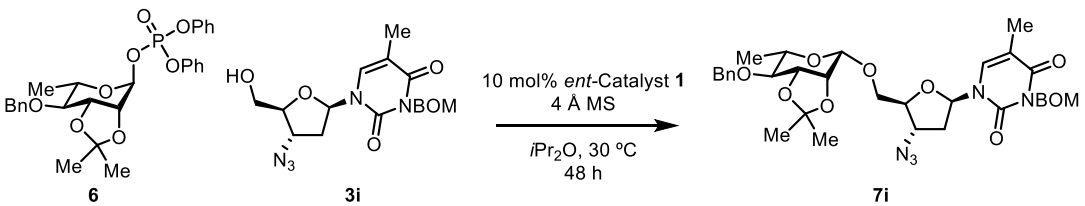
To a flame-dried 10 mL round bottom flask equipped with a stir bar was added 1,2:3,4-di-*O*-isopropylidene-α-D-galactopyranose **3c** (0.039 g, 0.15 mmol, 1 equiv), *ent*-Catalyst **1** (8.4 mg, 0.0075 mmol, 0.05 equiv) and activated 4 Å molecular sieves (0.15 g). To the reaction mixture

was added a solution of rhamnosyl phosphate **6** (0.079 g, 0.15 mmol, 1 equiv) in 1.5 mL anhydrous diisopropyl ether. The flask was sealed with a yellow polyethylene cap under an atmosphere of air and parafilm was used to seal the cap tightly. The mixture was then heated with efficient stirring at 30 ˚C in an oil bath for 24 hours over which time the mixture thickened. The mixture was cooled to room temperature, and 100 μL aliquot was diluted with diethyl ether and filtered to remove the molecular sieves. This solution was concentrated and ^{1}H NMR analysis on the crude mixture was used to determine the anomeric selectivity (1:52 α:β). The mixture was then purified by column chromatography (3% EtOAc/hexanes to 25% EtOAc/hexanes) to give the desired product **7c** in 96% yield (0.077 g, 0.144 mmol) as a colorless oil. ^{1}H NMR (600 MHz, $CDCl_3$) δ 7.36 – 7.30 (m, 4H), 7.29 – 7.25 (m, 1H), 5.49 (d, *J* = 5.0 Hz, 1H), 4.87 (d, *J* = 11.5 Hz, 1H), 4.78 (d, *J* = 2.0 Hz, 1H, H-1, β-anomer), 4.63 – 4.58 (m, 2H), 4.34 (dd, *J* = 8.0, 1.8 Hz, 1H), 4.29 (dd, *J* = 5.0, 2.3 Hz, 1H), 4.27 – 4.21 (m, 2H), 4.06 (ddd, *J* = 8.0, 5.7, 1.8 Hz, 1H), 4.00 (dd, *J* = 10.0, 5.9 Hz, 1H), 3.78 (dd, *J* = 10.0, 8.3 Hz, 1H), 3.42 – 3.35 (m, 2H), 1.54 (s, 3H), 1.51 (s, 3H), 1.43 (s, 3H), 1.39 (s, 3H), 1.34 – 1.30 (m, 9H). ^{13}C NMR (126 MHz, $CDCl_3$) δ 138.3, 128.4, 128.1, 127.8, 110.7, 109.2, 108.6, 98.8, 96.4, 81.1, 80.1, 74.7, 72.9, 70.8, 70.8, 70.7, 67.8, 65.7, 27.9, 26.4, 26.2, 26.1, 25.0, 24.6, 18.7. HRMS (ESI) m/z calculated for $C_{28}H_{40}O_{10}$ $[M+Na]^+$: 559.2514; found: 559.2510. α-Anomer: ^{1}H NMR (600 MHz, $CDCl_3$) 4.98 ppm (s, 1H, H-1)

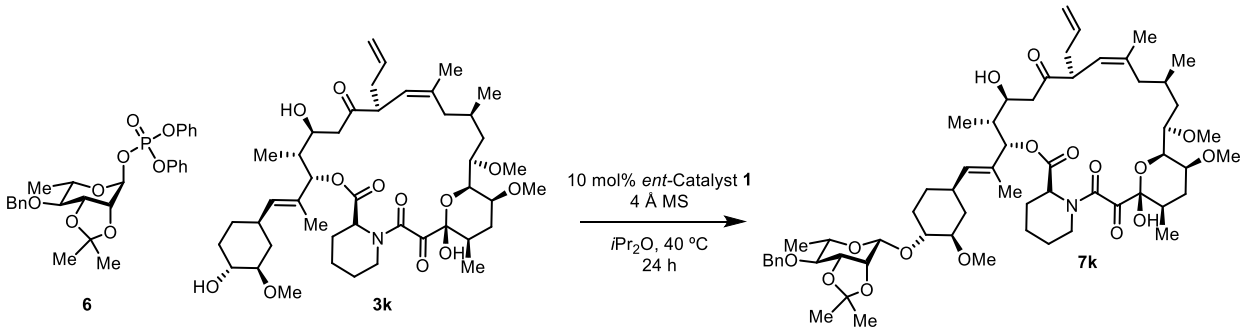


To a flame-dried 10 mL round bottom flask equipped with a stir bar was added quetiapine **3h** (0.058 g, 0.15 mmol, 1 equiv), *ent*-Catalyst **1** (16.7 mg, 0.015 mmol, 0.1 equiv) and activated 4 Å

molecular sieves (0.6 g). To the reaction mixture was added a solution of rhamnosyl phosphate **6** (0.079 g, 0.15 mmol, 1 equiv) in 6 mL anhydrous diisopropyl ether. The flask was sealed with a yellow polyethylene cap under an atmosphere of air and parafilm was used to seal the cap tightly. The mixture was then heated with efficient stirring at 50 ˚C in an oil bath for 48 hours over which time the mixture thickened. The mixture was cooled to room temperature, and 100 μL aliquot was diluted with diethyl ether and filtered to remove the molecular sieves. This solution was concentrated and ^{1}H NMR analysis on the crude mixture was used to determine the anomeric selectivity (1:18 α:β). The mixture was then purified by column chromatography (50% EtOAc/hexanes to 100% EtOAc/hexanes) to give the desired product **7h** in 76% yield (0.075 g, 0.114 mmol) as a white foamy solid. ^{1}H NMR (600 MHz, $CDCl_3$) δ 7.49 (d, J = 7.7 Hz, 1H), 7.43 – 7.24 (m, 9H), 7.16 (t, J = 7.6 Hz, 1H), 7.07 (d, J = 7.9 Hz, 1H), 6.87 (t, J = 7.5 Hz, 1H), 4.88 (dd, J = 11.5, 3.3 Hz, 1H), 4.80 (s, 1H, H-1, β-anomer), 4.61 (d, J = 11.5 Hz, 1H), 4.28 – 4.17 (m, 2H), 4.01 (dt, J = 11.3, 4.4 Hz, 1H), 3.84 – 3.76 (m, 1H), 3.75 – 3.68 (m, 1H), 3.68 – 3.41 (m, 6H), 3.40 – 3.21 (m, 3H), 2.73 – 2.45 (m, 6H), 1.54 (s, 3H), 1.38 (s, 3H), 1.32 (d, J = 5.7 Hz, 3H). ^{13}C NMR (126 MHz, $CDCl_3$) δ 160.7, 149.0, 139.9, 138.2, 134.2, 132.2, 132.1, 130.8, 129.1, 129.0, 128.3, 128.3, 128.0, 128.0, 127.7, 125.3, 122.8, 110.6, 98.8 ($^{1}J_{C\text{-}H}$ = 157.2 Hz, C-1), 81.1, 80.1, 74.7, 72.8, 70.7, 70.3, 69.1, 68.7, 68.7, 57.9, 53.4, 27.9, 26.4, 18.5. HRMS (ESI) m/z calculated for $C_{37}H_{45}N_3O_6S$ $[M+H]^+$: 660.3102; found: 660.3102. α-Anomer: ^{1}H NMR (600 MHz, $CDCl_3$) 4.99 ppm (s, 1H, H-1)



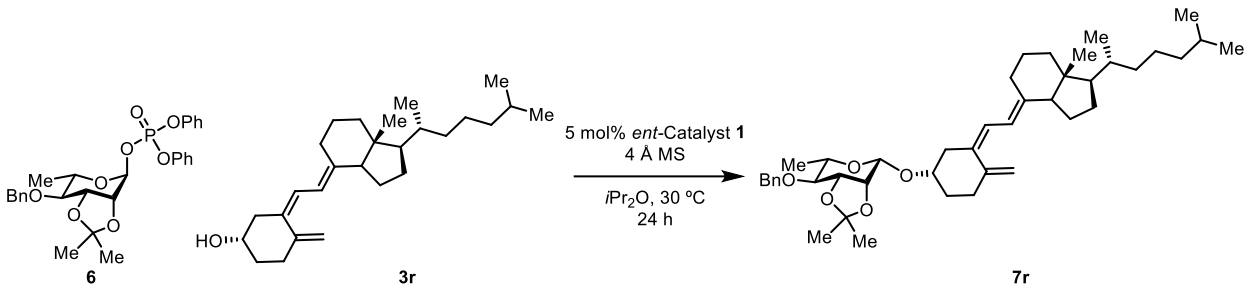
To a flame-dried 10 mL round bottom flask equipped with a stir bar was added BOM-zidovudine **3i** (0.039 g, 0.10 mmol, 1 equiv), *ent*-Catalyst **1** (11.2 mg, 0.01 mmol, 0.1 equiv) and activated 4 Å molecular sieves (0.1 g). To the reaction mixture was added a solution of rhamnosyl phosphate, **6** (0.052 g, 0.10 mmol, 1 equiv) in 1 mL anhydrous diisopropyl ether. The flask was sealed with a yellow polyethylene cap under an atmosphere of air and parafilm was used to seal the cap tightly. The mixture was then heated with efficient stirring at 30 ˚C in an oil bath for 48 hours over which time the mixture thickened. The mixture was cooled to room temperature, and 100 μL aliquot was diluted with diethyl ether and filtered to remove the molecular sieves. This solution was concentrated and ^{1}H NMR analysis on the crude mixture was used to determine the anomeric selectivity (1:10 α:β). The mixture was then purified by column chromatography (5% EtOAc/hexanes to 35% EtOAc/hexanes) to give the desired product, **7b**, in 82% yield (0.054 g, 0.082 mmol) as a light yellow foamy solid. ^{1}H NMR (600 MHz, $CDCl_3$) δ 7.53 (t, *J* = 1.2 Hz, 1H), 7.40 – 7.23 (m, 10H), 6.33 (t, *J* = 6.8 Hz, 1H), 5.49 (s, 2H), 4.84 (d, *J* = 11.6 Hz, 1H), 4.79 (d, *J* = 2.1 Hz, 1H, H-1, β-anomer), 4.70 (s, 2H), 4.63 (d, *J* = 11.7 Hz, 1H), 4.38 (dt, *J* = 6.7, 3.4 Hz, 1H), 4.30 (t, *J* = 6.4 Hz, 1H), 4.27 (dd, *J* = 6.0, 1.6 Hz, 1H), 4.04 (q, *J* = 2.7 Hz, 1H), 4.00 (dd, *J* = 11.4, 2.1 Hz, 1H), 3.91 (dd, *J* = 11.2, 2.0 Hz, 1H), 3.49 (dq, *J* = 8.8, 6.4 Hz, 1H), 3.36 (dd, *J* = 8.5, 6.4 Hz, 1H), 2.40 – 2.29 (m, 2H), 1.93 (s, 3H), 1.49 (s, 3H), 1.35 (s, 3H), 1.33 (d, *J* = 6.2 Hz, 3H). ^{13}C NMR (126 MHz, $CDCl_3$) δ 163.5, 151.2, 138.1, 138.0, 134.8, 128.5, 128.4, 128.2, 128.0, 127.8, 127.7, 110.7, 110.4, 98.2 ($^{1}J_{C\text{-}H}$ = 158.6 Hz, C-1), 85.3, 83.4, 80.0, 79.5, 74.3, 72.7, 72.3, 71.6, 70.6, 68.5, 61.7, 37.4, 27.7, 26.2, 19.0, 13.5. HRMS (ESI) m/z calculated for $C_{34}H_{41}N_5O_9$ $[M+Na]^+$: 686.2796; found: 686.2797. α-Anomer: ^{1}H NMR (600 MHz, $CDCl_3$) 5.01 ppm (s, 1H, H-1)



To a flame-dried 10 mL round bottom flask equipped with a stir bar was added FK-506 **3k** (0.080 g, 0.1 mmol, 1 equiv), *ent*-Catalyst **1** (11.2 mg, 0.01 mmol, 0.1 equiv) and activated 4 Å molecular sieves (0.1 g). To the reaction mixture was added a solution of rhamnosyl phosphate, **6** (0.053 g, 0.1 mmol, 1 equiv) in 1.0 mL anhydrous diisopropyl ether. The flask was sealed with a yellow polyethylene cap under an atmosphere of air and parafilm was used to seal the cap tightly. The mixture was then heated with efficient stirring at 40 ˚C in an oil bath for 24 hours over which time the mixture thickened. The mixture was cooled to room temperature, and 100 μL aliquot was diluted with diethyl ether and filtered to remove the molecular sieves. This solution was concentrated and ^{1}H NMR analysis on the crude mixture was used to determine the anomeric selectivity (<1:50 α:β, <1:50 r.r.). The mixture was then purified by column chromatography (5% EtOAc/hexanes to 40% EtOAc/hexanes) to give the desired product **7k** in 55% yield (0.059 g, 0.055 mmol) as a white foamy solid. ^{1}H NMR (600 MHz, CD_3CN, as a mixture of rotamers) δ 7.37 - 7.32 (m, 4H), 7.29 (dq, *J* = 7.9, 2.7 Hz, 1H), 5.80 – 5.67 (m, 1H), 5.17 (d, *J* = 4.5 Hz, 1H), 5.15 – 5.10 (m, 1H), 5.04 – 5.02 (m, 0.8H), 5.01 – 4.98 (m, 1.5H), 4.97 – 4.91 (m, 2H), 4.80 (d, *J* = 11.6 Hz, 1H), 4.62 – 4.55 (m, 2H), 4.43 (s, 0.7H), 4.30 (d, *J* = 13.6 Hz, 0.7H), 4.21 (dd, *J* = 5.6, 1.0 Hz, 1H), 4.17 (t, *J* = 6.2 Hz, 1H), 3.93 (dq, *J* = 8.6, 4.4 Hz, 0.3H), 3.89 (dq, *J* = 8.4, 4.4 Hz, 0.7H), 3.67 (dd, *J* = 9.6, 2.5 Hz, 0.3H), 3.60 (d, *J* = 9.7 Hz, 0.7H), 3.56 (dd, *J* = 11.1, 3.8 Hz, 0.7H), 3.47 (ddt, *J* = 24.1, 9.0, 5.8 Hz, 3H), 3.38 (td, *J* = 10.4, 4.5 Hz, 1H), 3.34 (dd, *J* = 5.1, 0.9

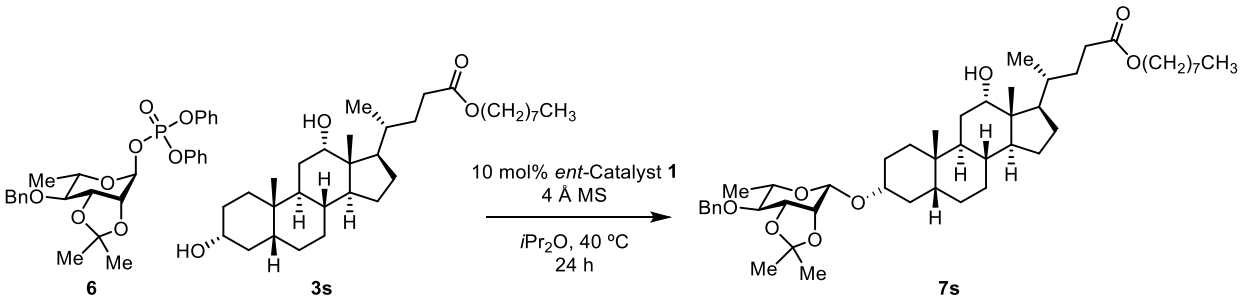
Hz, 6H), 3.31 (d, *J* = 0.9 Hz, 1H), 3.30 – 3.27 (m, 3H), 3.26 (s, 0.7H), 3.25 – 3.20 (m, 1H), 3.16 – 3.07 (m, 1H), 2.96 (d, *J* = 4.4 Hz, 0.7H), 2.93 – 2.85 (m, 0.7H), 2.75 (dd, *J* = 14.8, 5.0 Hz, 0.7H), 2.70 (dd, *J* = 17.0, 4.1 Hz, 0.3H), 2.46 – 2.36 (m, 1H), 2.34 – 2.23 (m, 2H), 2.19 – 2.15 (m, 1H), 2.09 – 2.02 (m, 2H), 1.88 (dd, *J* = 14.3, 9.8 Hz, 1H), 1.78 – 1.69 (m, 2H), 1.70 – 1.63 (m, 2H), 1.61 (s, 2H), 1.59 – 1.50 (m, 3H), 1.48 (s, 3H), 1.42 – 1.20 (m, 16H), 1.19 – 1.03 (m, 2H), 1.01 – 0.92 (m, 2H), 0.91 – 0.80 (m, 11H). ^{13}C NMR (126 MHz, $CDCl_3$, as a mixture of rotamers) δ 212.8, 212.7, 196.2, 192.8, 169.0, 168.8, 165.9, 164.7, 139.9, 139.0, 138.3, 135.6, 135.4, 132.4, 131.9, 129.9, 129.7, 128.4, 128.2, 127.8, 122.8, 122.5, 116.8, 110.7, 110.7, 100.5 ($^1J_{C\text{-}H}$ = 156.9 Hz), 98.7, 97.1, 83.4, 83.0, 82.9, 81.1, 80.4, 78.0, 77.4, 76.7, 75.3, 75.2, 73.7, 72.9, 72.9, 72.3, 70.7, 70.1, 69.1, 57.6, 57.6, 57.1, 56.7, 56.4, 56.2, 53.0, 52.9, 52.8, 48.7, 48.5, 44.0, 43.4, 40.5, 39.9, 39.3, 36.7, 36.7, 36.5, 35.7, 35.5, 35.3, 34.7, 34.7, 33.7, 33.0, 32.8, 32.6, 31.7, 31.1, 30.4, 29.8, 28.1, 27.8, 26.5, 26.3, 26.1, 24.8, 24.7, 24.6, 21.2, 21.0, 20.5, 19.6, 18.5, 18.5, 16.3, 16.1, 16.1, 15.9, 14.4, 14.2, 9.9, 9.6. HRMS (ESI) m/z calculated for $C_{60}H_{89}NO_{16}$ $[M+Na]^+$: 1102.6074; found: 1102.6083.

As seen in **4k**, FK-506 derivative **7k** also exists as a mixture of rotamers. The rotameric ratio of **7k** (3.1:1 major:minor rotamer) matched with the ratio reported in the literature.[36] The anomeric configuration of **7k** was assigned based on $^1J_{C1\text{-}H1}$ (156.9 Hz) of **7k**. The coupling constant falls in the range of β-*O*-glycosides. In addition, 1D ROESY experiment showed cross peaks between H-1 and H-3 and H-5 resonance when H-1 was radiated, suggesting that H-1, H-3, and H-5 reside on the same face of the ring, which is only possible when H1 is in β-configuration. We did not isolate any other glycosylated FK-506 derivatives, and no discernible peaks corresponding to other glycosylated FK-506 derivatives were present in the crude NMR. Therefore, we reported the selectivity as only <1:50 α:β.



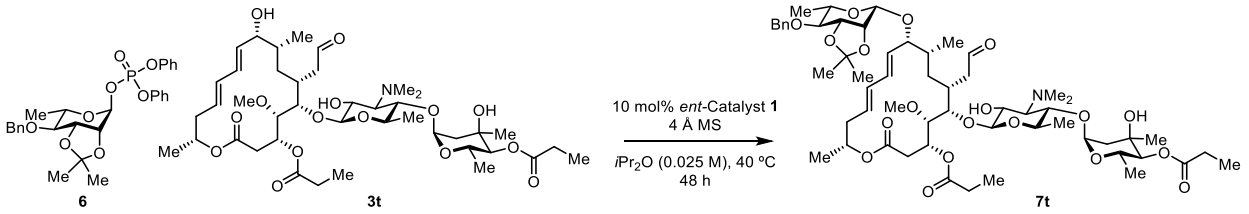
To a flame-dried 10 mL round bottom flask equipped with a stir bar was added cholecalciferol **3r** (0.058 g, 0.15 mmol, 1 equiv), *ent*-Catalyst **1** (8.4 mg, 0.0075 mmol, 0.05 equiv) and activated 4 Å molecular sieves (0.15 g). To the reaction mixture was added a solution of rhamnosyl phosphate, **6** (0.079 g, 0.15 mmol, 1 equiv) in 1.5 mL anhydrous diisopropyl ether. The flask was sealed with a yellow polyethylene cap under an atmosphere of air and parafilm was used to seal the cap tightly. Aluminum foil was used to cover the flask to keep the reaction in the dark. The reaction mixture was stirred at 30 °C for 24 hours over which time the mixture thickened, and 100 μL aliquot was diluted with diethyl ether and filtered to remove the molecular sieves. This solution was concentrated and ^{1}H NMR analysis on the crude mixture was used to determine the anomeric selectivity (β-only). The mixture was then purified by column chromatography (100% hexanes to 15% Et_2O/hexanes) to give the desired product **7r** in 94% yield (0.093 g, 0.141 mmol) as a colorless oil. ^{1}H NMR (600 MHz, $CDCl_3$) δ 7.39 - 7.31 (m, 4H), 7.30 - 7.26 (m, 1H), 6.21 (d, *J* = 11.2 Hz, 1H), 6.01 (d, *J* = 11.2 Hz, 1H), 5.03 (s, 1H, H-1, β-anomer), 4.88 (d, *J* = 11.6 Hz, 1H), 4.84 – 4.78 (m, 2H), 4.63 (d, *J* = 11.5 Hz, 1H), 4.26 – 4.18 (m, 2H), 3.91 – 3.82 (m, 1H), 3.46 – 3.37 (m, 2H), 2.85 – 2.78 (m, 1H), 2.70 (dd, *J* = 12.9, 3.0 Hz, 1H), 2.48 – 2.35 (m, 2H), 2.15 – 2.04 (m, 2H), 2.03 – 1.93 (m, 2H), 1.92 – 1.82 (m, 1H), 1.73 – 1.59 (m, 3H), 1.58 – 1.43 (m, 7H), 1.40 (s, 3H), 1.39 – 1.21 (m, 9H), 1.18 – 1.07 (m, 3H), 1.05 – 0.96 (m, 1H), 0.92 (d, *J* = 6.4 Hz, 3H), 0.87 (dd, *J* = 6.7, 2.9 Hz, 6H), 0.54 (s, 3H) ^{13}C NMR (126 MHz, $CDCl_3$) δ 144.9, 142.1,

138.4, 135.7, 128.4, 128.2, 127.8, 122.0, 117.8, 112.7, 110.9, 97.0 ($^1J_{C\text{-}H}$ = 158.1 Hz, C-1), 81.0, 80.1, 77.3, 75.2, 72.9, 70.7, 56.7, 56.4, 45.9, 44.5, 40.7, 39.6, 36.3, 32.9, 32.5, 29.1, 28.1, 27.9, 27.8, 26.5, 24.0, 23.6, 23.0, 22.7, 22.4, 19.0, 18.9, 12.2. HRMS (ESI) m/z calculated for $C_{43}H_{64}O_5$ $[M+Na]^+$: 683.4646; found: 683.4647. α-Anomer: ^{1}H NMR (600 MHz, $CDCl_3$) 5.12 ppm (s, 1H, H-1)



To a flame-dried 10 mL round bottom flask equipped with a stir bar was added deoxycholic octyl-ester **3s** (0.049 g, 0.097 mmol, 1 equiv), *ent*-Catalyst **1** (10.8 mg, 0.01 mmol, 0.1 equiv) and activated 4 Å molecular sieves (0.1 g). To the reaction mixture was added a solution of rhamnosyl phosphate, **6** (0.051 g, 0.097 mmol, 1 equiv) in 1.0 mL anhydrous diisopropyl ether. The flask was sealed with a yellow polyethylene cap under an atmosphere of air and parafilm was used to seal the cap tightly. The mixture was then heated with efficient stirring at 40 ˚C in an oil bath for 20 hours over which time the mixture thickened. The mixture was cooled to room temperature, and 100 µL aliquot was diluted with diethyl ether and filtered to remove the molecular sieves. This solution was concentrated and ^{1}H NMR analysis on the crude mixture was used to determine the anomeric selectivity (1:25 α:β, <1:50 r.r.). The mixture was then purified by column chromatography (2% EtOAc/hexanes to 20% EtOAc/hexanes) to give the desired product **7s** in 91% yield (0.069 g, 0.088 mmol) as a colorless oil. ^{1}H NMR (600 MHz, $CDCl_3$) δ 7.36 – 7.30 (m, 4H), 7.28 – 7.24 (m, 1H), 4.87 (d, J = 11.5 Hz, 1H), 4.78 (d, J = 1.4 Hz, 1H, H-1, β-anomer), 4.61

(d, J = 11.5 Hz, 1H), 4.21 – 4.18 (m, 2H), 4.04 (t, J = 6.7 Hz, 2H), 3.96 – 3.91 (m, 1H), 3.65 (td, J = 11.3, 5.6 Hz, 1H), 3.36 – 3.28 (m, 2H), 2.35 (ddd, J = 14.9, 9.8, 4.9 Hz, 1H), 2.21 (ddd, J = 15.6, 9.2, 6.8 Hz, 1H), 1.92 – 1.76 (m, 6H), 1.73 (dt, J = 14.3, 3.4 Hz, 1H), 1.68 (q, J = 9.6 Hz, 1H), 1.63 – 1.57 (m, 4H), 1.56 – 1.52 (m, 5H), 1.52 – 1.45 (m, 3H), 1.43 – 1.22 (m, 25H), 1.14 – 1.00 (m, 2H), 0.99 – 0.92 (m, 4H), 0.91 – 0.85 (m, 6H), 0.65 (s, 3H). ^{13}C NMR (126 MHz, $CDCl_3$) δ 174.4, 138.3, 128.4, 128.2, 127.8, 110.8, 97.4 ($^1J_{C\text{-}H}$ = 154.8 Hz, C-1), 81.2, 80.3, 79.9, 75.5, 73.1, 72.9, 70.7, 64.5, 48.2, 47.3, 46.6, 42.2, 36.2, 35.5, 35.2, 34.4, 33.7, 32.9, 31.9, 31.4, 31.0, 29.3, 29.3, 28.8, 28.8, 28.3, 28.1, 27.5, 27.4, 26.5, 26.2, 26.0, 23.8, 23.2, 22.7, 18.5, 17.4, 14.2, 12.8. HRMS (ESI) m/z calculated for $C_{48}H_{76}O_8$ $[M+Na]^+$: 803.5432; found: 803.5428. α-Anomer: ^{1}H NMR (600 MHz, $CDCl_3$) 5.12 ppm (s, 1H, H-1)

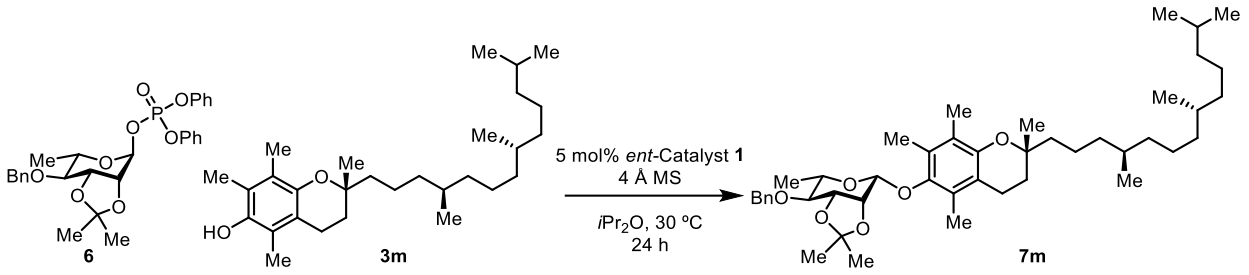


To a flame-dried 10 mL round bottom flask equipped with a stir bar was added midecamycin **3t** (0.081 g, 0.1 mmol, 1 equiv), catalyst (11.2 mg, 0.01 mmol, 0.1 equiv) and activated 4 Å molecular sieves (0.4 g). To the reaction mixture was added a solution of rhamnosyl phosphate, **6** (0.068 g, 0.13 mmol, 1.3 equiv) in 4 mL anhydrous diisopropyl ether. The flask was sealed with a yellow polyethylene cap under an atmosphere of air and parafilm was used to seal the cap tightly. The mixture was then heated with efficient stirring at 40 ˚C in an oil bath for 48 hours over which time the mixture thickened. The mixture was cooled to room temperature, and 100 μL aliquot was diluted with diethyl ether and filtered to remove the molecular sieves. This solution was concentrated and ^{1}H NMR analysis on the crude mixture was used to determine the anomeric

selectivity (1:16 α:β, <1:50 r.r.). The mixture was then purified by column chromatography (50% EtOAc/hexanes to 75% EtOAc/hexanes) to give the desired product **7t** as a mixture of anomers in 51% yield (0.056 g, 0.051 mmol) as a white solid. ^{1}H NMR (600 MHz, $CDCl_3$) δ 9.57 (s, 1H), 7.34 – 7.29 (m, 4H), 7.27 – 7.23 (m, 1H), 6.60 (dd, *J* = 15.3, 10.6 Hz, 1H), 6.10 (dd, *J* = 14.9, 10.7 Hz, 1H), 5.80 (ddd, *J* = 15.0, 11.2, 3.7 Hz, 1H), 5.45 (dd, *J* = 15.3, 10.0 Hz, 1H), 5.10 (d, *J* = 11.1 Hz, 1H), 5.05 (d, *J* = 3.8 Hz, 1H, H-1, β-anomer), 5.02 – 4.94 (m, 1H), 4.84 (d, *J* = 11.7 Hz, 1H), 4.67 (d, *J* = 2.2 Hz, 1H), 4.59 (dd, *J* = 12.2, 10.9 Hz, 2H), 4.47 – 4.41 (m, 1H), 4.38 (d, *J* = 7.5 Hz, 1H), 4.16 (t, *J* = 6.2 Hz, 1H), 4.09 (dd, *J* = 5.9, 2.2 Hz, 1H), 4.06 (dd, *J* = 10.1, 4.3 Hz, 1H), 3.86 (d, *J* = 9.2 Hz, 1H), 3.53 – 3.48 (m, 4H), 3.37 – 3.28 (m, 2H), 3.28 – 3.24 (m, 2H), 3.22 (dd, *J* = 9.3, 1.9 Hz, 1H), 2.81 – 2.66 (m, 2H), 2.65 – 2.55 (m, 1H), 2.50 (s, 7H), 2.47 – 2.38 (m, 5H), 2.34 (dd, *J* = 18.8, 2.6 Hz, 1H), 2.25 (d, *J* = 13.0 Hz, 1H), 2.18 – 2.06 (m, 2H), 2.04 – 1.96 (m, 2H), 1.83 (dd, *J* = 14.3, 4.0 Hz, 1H), 1.52 (s, 3H), 1.43 (td, *J* = 13.6, 3.7 Hz, 1H), 1.35 (s, 3H), 1.24 (d, *J* = 6.1 Hz, 6H), 1.2 – 1.14 (m, 9H), 1.14 – 1.08 (m, 6H), 0.99 (d, *J* = 6.6 Hz, 3H), 0.96 – 0.88 (m, 1H). ^{13}C NMR (126 MHz, $CDCl_3$) δ 201.1, 174.5, 173.9, 170.0, 138.3, 138.0, 133.3, 131.8, 128.4, 128.3, 128.2, 127.7, 124.2, 110.5, 103.9, 97.1, 95.0 ($^{1}J_{C\text{-}H}$ = 157.6 Hz, C-1), 84.9, 81.0, 80.1, 78.6, 77.6, 77.2, 76.0, 75.2, 73.1, 72.7, 71.7, 70.5, 69.5, 69.2, 68.8, 68.8, 63.6, 62.5, 42.4, 42.1, 41.8, 41.1, 37.4, 33.0, 30.5, 28.7, 27.9, 27.7, 27.7, 26.3, 25.4, 20.5, 18.9, 18.9, 17.9, 15.4, 9.4, 9.0. HRMS (ESI) m/z calculated for $C_{57}H_{87}NO_{19}$ $[M+H]^+$: 1090.5945; found: 1090.5958. α-Anomer: ^{1}H NMR (600 MHz, $CDCl_3$) 9.6 ppm (s, 1H), 5.54 (dd, *J* = 15.2, 9.7 Hz, 1H).

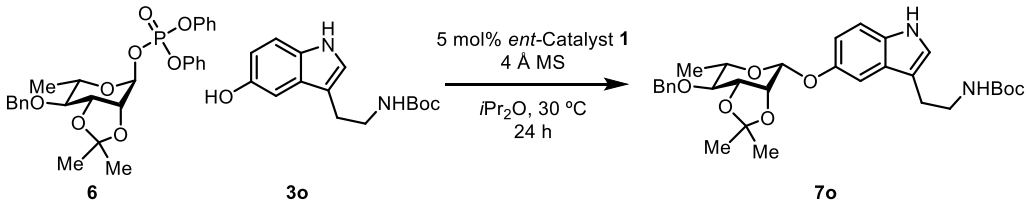
The anomeric proton for α-anomer overlaps with other resonance. Instead, the above two proton resonance was used to determine selectivity. In addition to the diagnostic $^{1}J_{C\text{-}H}$ coupling constant (157.6 Hz), the assignment of β-configuration was further supported by 1-D ROESY experiment. 1D ROESY experiment showed cross peaks between H-1 and H-3 and H-5 resonance when H-1

was radiated, suggesting that H-1, H-3, and H-5 reside on the same face of the ring, which is only possible when H-1 is in β-configuration.



To a flame-dried 10 mL round bottom flask equipped with a stir bar was added α-tocopherol **3m** (0.065 g, 0.15 mmol, 1 equiv), *ent*-Catalyst **1** (8.4 mg, 0.0075 mmol, 0.05 equiv) and activated 4 Å molecular sieves (0.15 g). To the reaction mixture was added a solution of rhamnosyl phosphate, **6** (0.079 g, 0.15 mmol, 1 equiv) in 1.5 mL anhydrous diisopropyl ether. The flask was sealed with a yellow polyethylene cap under an atmosphere of air and parafilm was used to seal the cap tightly. The mixture was then heated with efficient stirring at 30 ˚C in an oil bath for 24 hours over which time the mixture thickened. The mixture was cooled to room temperature, and 100 μL aliquot was diluted with diethyl ether and filtered to remove the molecular sieves. This solution was concentrated and ^{1}H NMR analysis on the crude mixture was used to determine the anomeric selectivity (<1:50 α:β). The mixture was then purified by column chromatography (hexanes to 10% Et_2O/hexanes) to give the desired product **7m** in 96% yield (0.102 g, 0.144 mmol) as a colorless oil. ^{1}H NMR (600 MHz, $CDCl_3$) δ 7.38 – 7.32 (m, 4H), 7.30 – 7.27 (m, 1H), 4.88 (d, *J* = 11.5 Hz, 1H), 4.80 (d, *J* = 1.9 Hz, 1H, H-1, β-anomer), 4.64 (d, *J* = 11.6 Hz, 1H), 4.51 (dd, *J* = 5.6, 2.0 Hz, 1H), 4.27 (t, *J* = 6.1 Hz, 1H), 3.36 (dd, *J* = 9.3, 6.6 Hz, 1H), 3.24 (dq, *J* = 9.2, 6.1 Hz, 1H), 2.62 – 2.52 (m, 2H), 2.21 (s, 3H), 2.17 (s, 3H), 2.08 (s, 3H), 1.84 – 1.79 (m, 1H), 1.77 – 1.72 (m, 1H), 1.63 (s, 3H), 1.58 (s, 1H), 1.57 – 1.50 (m, 3H), 1.48 (s, 3H), 1.46 – 1.01 (m, 26H), 0.90

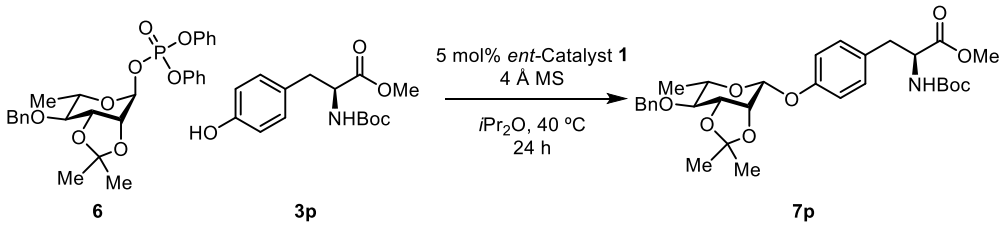
– 0.82 (m, 13H). ^{13}C NMR (126 MHz, $CDCl_3$) δ 148.3, 147.5, 138.3, 128.4, 128.4, 128.2, 127.8, 126.8, 122.7, 117.4, 110.8, 101.6, 80.8, 80.4, 75.0, 74.9, 72.9, 71.2, 40.4, 39.5, 37.6, 37.6, 37.6, 37.4, 32.9, 32.8, 31.3, 28.1, 26.6, 24.9, 24.6, 24.1, 22.9, 22.8, 21.2, 20.8, 19.9, 19.8, 18.4, 13.9, 13.1, 12.0. HRMS (ESI) m/z calculated for $C_{45}H_{70}O_6$ $[M+Na]^+$: 729.5065; found: 729.5065. α-Anomer: ^{1}H NMR (600 MHz, $CDCl_3$) 5.10 ppm (s, 1H, H-1)



6 3o 7o

To a flame-dried 10 mL round bottom flask equipped with a stir bar was added Boc-Serotonin **3o** (0.041 g, 0.15 mmol, 1 equiv), *ent*-Catalyst **1** (8.4 mg, 0.0075 mmol, 0.05 equiv) and activated 4 Å molecular sieves (0.15 g). To the reaction mixture was added a solution of rhamnosyl phosphate, **6** (0.079 g, 0.15 mmol, 1 equiv) in 1.5 mL anhydrous diisopropyl ether. The flask was sealed with a yellow polyethylene cap under an atmosphere of air and parafilm was used to seal the cap tightly. The mixture was then heated with efficient stirring at 30 ˚C in an oil bath for 24 hours over which time the mixture thickened. The mixture was cooled to room temperature, and 100 μL aliquot was diluted with diethyl ether and filtered to remove the molecular sieves. This solution was concentrated and ^{1}H NMR analysis on the crude mixture was used to determine the anomeric selectivity (1:20 α:β). The mixture was then purified by column chromatography (5% EtOAc/hexanes to 35% EtOAc/hexanes) to give the desired product **7o** in 83% yield (0.069 g, 0.125 mmol) as a light yellow foamy solid. ^{1}H NMR (600 MHz, $CDCl_3$) δ 8.27 (s, 1H), 7.41 – 7.33 (m, 4H), 7.33 – 7.27 (m, 2H), 7.23 (d, J = 8.7 Hz, 1H), 7.03 (dd, J = 8.8, 2.3 Hz, 1H), 6.97 (s, 1H), 5.31 (d, J = 2.4 Hz, 1H, H-1, β-anomer), 4.93 (d, J = 11.5 Hz, 1H), 4.71 – 4.59 (m, 2H),

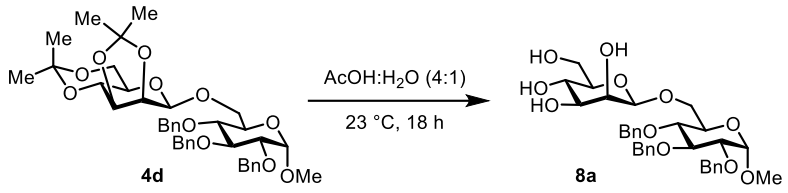
4.46 (dd, J = 6.3, 2.4 Hz, 1H), 4.36 (t, J = 6.1 Hz, 1H), 3.63 – 3.53 (m, 2H), 3.49 – 3.28 (m, 2H), 2.93 – 2.76 (m, 2H), 1.64 (s, 3H), 1.48 (s, 3H), 1.44 (s, 9H), 1.37 (d, J = 5.6 Hz, 3H). ^{13}C NMR (126 MHz, $CDCl_3$) δ 156.1, 151.7, 138.3, 133.0, 128.4, 128.1, 127.8, 127.7, 123.3, 114.3 ($^1J_{C\text{-}H}$ = 159.6 Hz, C-1), 112.9, 111.6, 111.0, 106.9, 98.8, 80.9, 80.0, 79.3, 74.8, 72.9, 70.9, 40.7, 28.5, 27.8, 26.4, 25.9, 19.1. HRMS (ESI) m/z calculated for $C_{31}H_{40}N_2O_7$ $[M+Na]^+$: 575.2728; found: 575.2726. α-Anomer: ^{1}H NMR (600 MHz, $CDCl_3$) 5.68 ppm (s, 1H, H-1)



6 **3p** **7p**

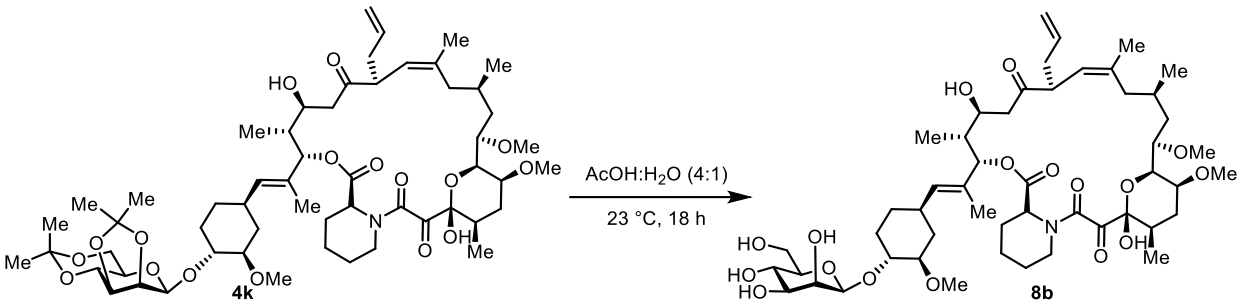
To a flame-dried 10 mL round bottom flask equipped with a stir bar was added Boc-Tyr-OMe **3p** (0.044 g, 0.15 mmol, 1 equiv), *ent*-Catalyst **1** (8.4 mg, 0.0075 mmol, 0.05 equiv) and activated 4 Å molecular sieves (0.15 g). To the reaction mixture was added a solution of rhamnosyl phosphate, **6** (0.079 g, 0.15 mmol, 1 equiv) in 1.5 mL anhydrous diisopropyl ether. The flask was sealed with a yellow polyethylene cap under an atmosphere of air and parafilm was used to seal the cap tightly. The mixture was then heated with efficient stirring at 40 ˚C in an oil bath for 24 hours over which time the mixture thickened. The mixture was cooled to room temperature, and 100 μL aliquot was diluted with diethyl ether and filtered to remove the molecular sieves. This solution was concentrated and ^{1}H NMR analysis on the crude mixture was used to determine the anomeric selectivity (1:26 α:β). The mixture was then purified by column chromatography (10% Et_2O/hexanes to 50% Et_2O/hexanes) to give the desired product **7p** in 84% yield (0.072 g, 0.126 mmol) as a white foamy solid. ^{1}H NMR (600 MHz, $CDCl_3$) δ 7.39 – 7.32 (m, 4H), 7.31 – 7.27 (m, 1H), 7.03 (d, J = 8.4 Hz, 2H), 7.00 (d, J = 8.6 Hz, 2H), 5.32 (d, J = 2.4 Hz, 1H, H-1, β-anomer),

4.97 (d, J = 8.3 Hz, 1H), 4.90 (d, J = 11.5 Hz, 1H), 4.64 (d, J = 11.5 Hz, 1H), 4.58 – 4.51 (m, 1H), 4.40 (dd, J = 6.5, 2.3 Hz, 1H), 4.37 (t, J = 6.1 Hz, 1H), 3.69 (s, 3H), 3.65 – 3.54 (m, 2H), 3.09 – 2.95 (m, 2H), 1.61 (s, 3H), 1.45 (s, 3H), 1.42 (s, 9H), 1.33 (d, J = 5.5 Hz, 3H). ^{13}C NMR (126 MHz, CDCl3$_3$) δ 172.5, 156.6, 155.2, 138.2, 130.3, 130.0, 128.4, 128.1, 127.8, 117.0 ($^1J_{C\text{-}H}$ = 161.5 Hz, C-1), 111.1, 96.7, 80.6, 80.0, 79.6, 74.4, 72.8, 71.0, 54.6, 52.3, 37.6, 28.4, 27.5, 26.2, 19.3. HRMS (ESI) m/z calculated for $C_{31}H_{41}NO_9$ $[M+Na]^+$: 594.2674; found: 594.2672. α-Anomer: ^{1}H NMR (600 MHz, $CDCl_3$) 5.66 ppm (s, 1H, H-1)



To a 20 mL vial equipped with a stir bar was added **4d** (65 mg, 0.092 mmol, 1 equiv), 1.4 mL acetic acid and 0.35 mL water. The reaction was stirred at room temperature for 18 hours. The reaction was diluted with toluene and concentrated at reduced pressure. The organic residual was purified by column chromatography (3% MeOH/DCM) to give the desired product **8a** in 81% yield (46.5 mg, 0.074 mmol) as a white solid. ^{1}H NMR (500 MHz, $CDCl_3$) δ 7.38 – 7.27 (m, 15H), 4.99 (d, J = 10.8 Hz, 1H), 4.88 (d, J = 11.6 Hz, 1H), 4.80 (d, J = 10.8 Hz, 1H), 4.76 (d, J = 12.1 Hz, 1H), 4.65 (d, J = 12.1 Hz, 1H), 4.62 (d, J = 3.5 Hz, 1H), 4.55 (d, J = 11.6 Hz, 1H), 4.12 (s, 1H), 4.03 – 3.94 (m, 2H), 3.87 – 3.68 (m, 6H), 3.65 – 3.55 (m, 2H), 3.53 – 3.47 (m, 3H), 3.41 – 3.31 (m, 4H), 3.27 (br, 1H), 3.08 (dt, J = 9.6, 3.1 Hz, 1H). ^{13}C NMR (126 MHz, $CDCl_3$) δ 138.7, 138.3, 138.2, 128.6, 128.6, 128.5, 128.2, 128.1, 128.0, 128.0, 128.0, 127.7, 100.7 ($^1J_{C\text{-}H}$ = 157.2 Hz, C-1), 98.0, 82.1, 79.8, 76.2, 75.8, 74.9, 74.0, 73.3, 71.2, 70.0, 68.0, 66.1, 61.0, 55.5. HRMS (ESI) m/z calculated for $C_{34}H_{42}O_{11}$ $[M+Na]^+$: 649.2619; found: 649.2623.

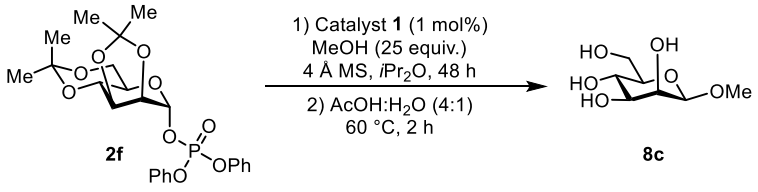
The $^{3}J_{H1\text{-}H2}$ coupling constant cannot be used to distinguish α- and β-configuration anymore once the 2,3-acetonide is removed. However, the $^{1}J_{C1\text{-}H1}$ coupling constant of anomeric carbon can still be used to assign anomeric configuration. A coupling constant of 157.2 Hz indicates β-configuration.



To a 20 mL vial equipped with a stir bar was added **4k** (30 mg, 0.029 mmol, 1 equiv), 0.45 mL acetic acid and 0.11 mL water. The reaction was stirred at room temperature for 18 hours. The reaction was diluted with toluene and concentrated at reduced pressure. The organic residual was purified by column chromatography (3% MeOH/DCM) to give the desired product **8b** in 86% yield (23.7 mg, 0.023 mmol) as a white solid. ^{1}H NMR (600 MHz, $CDCl_3$, as mixtures of rotamers) δ 5.77 – 5.62 (m, 1H), 5.29 (s, 0.6H), 5.18 (s, 0.4H), 5.07 (d, J = 8.8 Hz, 0.6H), 5.05 – 4.95 (m, 4H), 4.93 – 4.69 (m, 3H), 4.66 (s, 1H), 4.60 (d, J = 4.2 Hz, 1H), 4.42 (d, J = 14.1 Hz, 1H), 4.22 (s, 0.7H), 4.02 – 3.91 (m, 3H), 3.92 – 3.84 (m, 1H), 3.81 (d, J = 11.5 Hz, 1H), 3.75 – 3.64 (m, 2H), 3.61 – 3.52 (m, 2H), 3.50 – 3.42 (m, 1H), 3.42 – 3.35 (m, 7H), 3.33 (s, 2H), 3.30 – 3.22 (m, 3H), 3.19 (d, J = 8.0 Hz, 1H), 3.12 (s, 0.7H), 2.99 (td, J = 13.5, 3.1 Hz, 0.7H), 2.77 (dd, J = 15.9, 3.1 Hz, 0.7H), 2.71 (dd, J = 17.5, 2.5 Hz, 0.4H), 2.51 – 2.39 (m, 1H), 2.36 – 2.20 (m, 3H), 2.20 – 2.12 (m, 3H), 2.10 – 1.98 (m, 4H), 1.98 – 1.90 (m, 1H), 1.90 – 1.84 (m, 1H), 1.84 – 1.71 (m, 3H), 1.62 (dd, J = 19.8, 11.8 Hz, 8H), 1.57 – 1.41 (m, 3H), 1.41 – 1.30 (m, 1H), 1.30 – 1.21 (m, 2H), 1.12 – 1.03 (m, 2H), 1.02 – 0.80 (m, 10H). ^{13}C NMR (126 MHz, $CDCl_3$, as mixtures of rotamers) δ 212.8,

196.3, 192.7, 169.1, 168.8, 165.9, 164.8, 140.0, 139.1, 135.7, 135.5, 132.8, 132.3, 129.6, 122.8, 122.6, 116.8, 98.8, 97.2, 96.7 ($^{1}J_{C\text{-}H}$ = 158.2 Hz, C-1), 81.2, 78.0, 76.7, 76.5, 75.3, 74.3, 73.8, 73.0, 72.3, 71.5, 70.1, 69.0, 66.4, 61.1, 57.7, 57.2, 56.7, 56.5, 56.3, 56.2, 53.1, 52.9, 52.9, 48.7, 48.5, 44.0, 43.9, 43.5, 40.5, 40.0, 39.4, 35.9, 35.7, 35.6, 35.3, 34.7, 33.8, 33.1, 32.8, 32.7, 30.5, 29.1, 27.8, 26.3, 26.2, 24.7, 24.6, 21.3, 21.0, 20.5, 19.6, 16.4, 16.2, 16.1, 15.9, 14.4, 14.2, 10.0, 9.7. HRMS (ESI) m/z calculated for $C_{50}H_{79}NO_{17}$ $[M+Na]^{+}$: 988.5240; found: 988.5247.

The $^{3}J_{H1\text{-}H2}$ coupling constant cannot be used to distinguish α- and β-configuration anymore once the 2,3-acetonide is removed. However, the $^{1}J_{C1\text{-}H1}$ coupling constant of anomeric carbon can still be used to assign anomeric configuration. A coupling constant of 158.2 Hz indicates β-configuration.

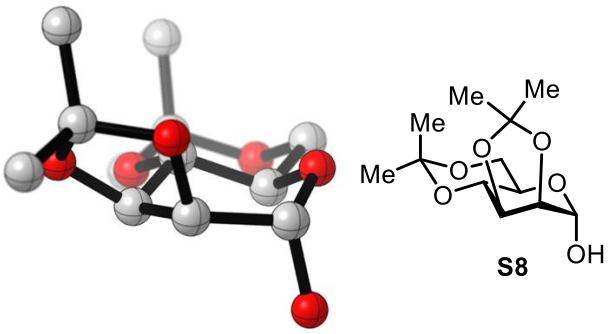


To a flame-dried 100 mL round bottom flask equipped with a stir bar was added Catalyst **1** (28 mg, 0.025 mmol, 0.01 equiv) and activated 4 Å molecular sieves (2.50 g). To the reaction mixture was added a solution of mannosyl phosphate, **2f** (1.23 g, 2.50 mmol, 1.0 equiv.) in 25.0 mL anhydrous diisopropyl ether and 1.01 mL (25.0 mmol, 25 equiv.) anhydrous methanol. The flask was sealed with a yellow polyethylene cap under an atmosphere of air and parafilm was used to seal the cap tightly. The mixture was then stirred at room temperature 23 ˚C for 22 hours over which time the mixture thickened. A 100 μL aliquot was diluted with diethyl ether and filtered to remove the molecular sieves. This solution was concentrated and ^{1}H NMR analysis on the crude mixture was used to determine the anomeric selectivity (99:1 β:α) and conversion (94%). The

mixture stirred an additional 26 hours to ensure complete conversion of starting material to product. The mixture was diluted with diethyl ether and filtered through a pad of Celite. The mixture was concentrated to provide the desired product quantitatively as a viscous oil. This material was carried through to the next step directly. To a 250 mL round-bottom flask was charged the glycosylated product, 12 mL acetic acid, and 3 mL deionized water. This mixture was stirred under nitrogen at 60 ˚C for 2 hours at which point TLC analysis indicated complete consumption of the bis-acetonide-protected mannoside. The mixture was directly concentrated in the flask and azeotroped with toluene (x2) to quantitatively afford the deprotected **8c** (485 mg, 2.5 mmol, 99:1 β:α) without further purification. Spectral data of **8c** matched its previously reported values.[38]

2.10.8 X-Ray Crystallographic Structure Data

2,3:4,6-di-*O*-isopropylidene-*α*-D-mannopyranose S8



S8

X-ray Crystallography: A crystal mounted on a diffractometer was collected data at 100 K. The intensities of the reflections were collected by means of a Bruker APEX DUO CCD diffractometer ($Cu_{K\alpha}$ radiation, λ=1.54178 Å), and equipped with an Oxford Cryosystems nitrogen flow apparatus. The collection method involved 1.0° scans in ω at -30°, -55°, -80°, 30°, 55°, 80° and

[38] Tanaka, T.; Kikuta, N.; Kimura, Y.; Shoda, S.-I. Metal-Catalyzed Stereoselective and Protecting-Group-Free Synthesis of 1,2-*cis*-Glycosides Using 4,6-Dimethoxy-1,3,5-triazin-2-yl Glycosides as Glycosyl Donors. *Chem. Lett.* **2015**, *44*, 846–848.

115° in 2θ. Data integration down to 0.84 Å resolution was carried out using SAINT V8.37 A (Bruker diffractometer, 2015) with reflection spot size optimization. Absorption corrections were made with the program SADABS (Bruker diffractometer, 2015). The structure was solved by the Intrinsic Phasing methods and refined by least-squares methods again F^2 using SHELXT-2014 (Sheldrick, 2015) and SHELXL-2014 (Sheldrick, 2015) with OLEX 2 interface (Dolomanov, et al., 2009). Non-hydrogen atoms were refined anisotropically, and hydrogen atoms were allowed to ride on the respective atoms. Crystal data as well as details of data collection and refinement are summarized in Table 2.1, geometric parameters are shown in Table 2.2 and Hydrogen-bond parameters are listed in Table 2.3. The Ortep plots produced with SHELXL-2014 program, and the other drawings were produced with Accelrys DS Visualizer 2.0 (Accelrys, 2007).[39]

Table 2.1 Experimental details

	QL-II-3
Crystal data	
Chemical formula	$C_{12}H_{20}O_6$
M_r	260.28
Crystal system, space group	Monoclinic, $P2_1$
Temperature (K)	100
a, b, c (Å)	6.4201 (2), 10.7569 (3), 19.4267 (6)
β (°)	93.2719 (16)
V (Å^3)	1339.43 (7)
Z	4
Radiation type	Cu $K\alpha$
μ (mm^{-1})	0.87
Crystal size (mm)	0.16 × 0.12 × 0.08
Data collection	

[39] (a) Bruker AXS APEX3, Bruker AXS, Madison, Wisconsin, 2015. (b) O. V. Dolomanov, L. J. Bourhis, R. J. Gildea, J. A. K. Howard and H. Puschmann J. Appl. Cryst. 2009, 42, 339-341. (c) G. M. Sheldrick, *Acta Cryst*. 2015. A**71**, 3-8. (d) G. M. Sheldrick, *Acta Cryst*. 2015, C**71**, 3-8. (e) Accelrys DS Visualizer v2.0.1, Accelrys Software. Inc., 2007. (f) A. L. Spek *PLATON, A Multipurpose Crystallographic Tool*, Utrecht University, Utrecht, The Netherlands, 2010.

Diffractometer	Bruker D8 goniometer with CCD area detector
Absorption correction	Multi-scan twinabs
T_{min}, T_{max}	0.598, 0.753
No. of measured, independent and observed [$I > 2\sigma(I)$] reflections	7980, 7980, 7768
R_{int}	0.0456
$(\sin \theta/\lambda)_{max}$ (Å^{-1})	0.595
Refinement	
$R[F^2 > 2\sigma(F^2)]$, $wR(F^2)$, S	0.032, 0.086, 1.05
No. of reflections	7980
No. of parameters	342
No. of restraints	1
H-atom treatment	H atoms treated by a mixture of independent and constrained refinement
$\Delta\rho_{max}$, $\Delta\rho_{min}$ (e Å^{-3})	0.13, -0.20
Absolute structure	Flack x determined using 2068 quotients [(I+)-(I-)]/[(I+)+(I-)] (Parsons, Flack and Wagner, Acta Cryst. B69 (2013) 249-259).
Absolute structure parameter	0.01 (6)

Computer programs: *SAINT* 8.37A (Bruker-AXS, 2015), *SHELXT2014* (Sheldrick, 2015), *SHELXL2014* (Sheldrick, 2015), Bruker *SHELXTL* (Sheldrick, 2015).

Table 2.2 Geometric parameters (Å, º)

O1—C1	1.422 (4)	O11—C21	1.423 (4)
O1—C8	1.429 (4)	O11—C28	1.433 (4)
O2—C1	1.402 (4)	O12—C21	1.404 (4)
O2—H2	0.87 (5)	O12—H12	0.80 (4)
O3—C3	1.426 (4)	O13—C22	1.424 (4)
O3—C2	1.433 (4)	O13—C23	1.436 (4)
O4—C4	1.436 (4)	O14—C24	1.432 (4)
O4—C3	1.448 (4)	O14—C23	1.450 (3)
O5—C5	1.436 (4)	O15—C25	1.443 (4)
O5—C6	1.453 (3)	O15—C26	1.450 (4)
O6—C6	1.421 (4)	O16—C26	1.421 (4)
O6—C7	1.434 (4)	O16—C27	1.439 (4)
C1—C2	1.528 (5)	C21—C22	1.528 (5)

C1—H1	1.0000	C21—H21	1.0000
C2—C4	1.534 (4)	C22—C24	1.524 (4)
C2—H2A	1.0000	C22—H22	1.0000
C3—C10	1.502 (5)	C23—C30	1.496 (5)
C3—C9	1.518 (4)	C23—C29	1.512 (4)
C4—C5	1.513 (4)	C24—C25	1.518 (4)
C4—H4	1.0000	C24—H24	1.0000
C5—C8	1.512 (5)	C25—C28	1.510 (5)
C5—H5	1.0000	C25—H25	1.0000
C6—C12	1.512 (5)	C26—C32	1.514 (5)
C6—C11	1.514 (4)	C26—C31	1.515 (4)
C7—C8	1.511 (4)	C27—C28	1.508 (4)
C7—H7A	0.9900	C27—H27A	0.9900
C7—H7B	0.9900	C27—H27B	0.9900
C8—H8	1.0000	C28—H28	1.0000
C9—H9A	0.9800	C29—H29A	0.9800
C9—H9B	0.9800	C29—H29B	0.9800
C9—H9C	0.9800	C29—H29C	0.9800
C10—H10A	0.9800	C30—H30A	0.9800
C10—H10B	0.9800	C30—H30B	0.9800
C10—H10C	0.9800	C30—H30C	0.9800
C11—H11A	0.9800	C31—H31A	0.9800
C11—H11B	0.9800	C31—H31B	0.9800
C11—H11C	0.9800	C31—H31C	0.9800
C12—H12A	0.9800	C32—H32A	0.9800
C12—H12B	0.9800	C32—H32B	0.9800
C12—H12C	0.9800	C32—H32C	0.9800
C1—O1—C8	111.7 (2)	C21—O11—C28	111.6 (2)
C1—O2—H2	109 (3)	C21—O12—H12	107 (3)
C3—O3—C2	105.9 (2)	C22—O13—C23	106.0 (2)
C4—O4—C3	108.7 (2)	C24—O14—C23	108.7 (2)
C5—O5—C6	114.5 (2)	C25—O15—C26	114.2 (2)
C6—O6—C7	114.1 (2)	C26—O16—C27	114.4 (2)
O2—C1—O1	111.9 (2)	O12—C21—O11	112.1 (2)
O2—C1—C2	105.9 (3)	O12—C21—C22	105.9 (3)
O1—C1—C2	113.0 (3)	O11—C21—C22	112.9 (3)

O2—C1—H1	108.6	O12—C21—H21	108.6
O1—C1—H1	108.6	O11—C21—H21	108.6
C2—C1—H1	108.6	C22—C21—H21	108.6
O3—C2—C1	109.3 (3)	O13—C22—C24	102.1 (2)
O3—C2—C4	101.6 (2)	O13—C22—C21	108.8 (3)
C1—C2—C4	117.1 (3)	C24—C22—C21	117.3 (2)
O3—C2—H2A	109.5	O13—C22—H22	109.4
C1—C2—H2A	109.5	C24—C22—H22	109.4
C4—C2—H2A	109.5	C21—C22—H22	109.4
O3—C3—O4	105.7 (2)	O13—C23—O14	105.3 (2)
O3—C3—C10	107.9 (3)	O13—C23—C30	107.9 (3)
O4—C3—C10	110.4 (3)	O14—C23—C30	111.0 (3)
O3—C3—C9	111.5 (3)	O13—C23—C29	110.8 (3)
O4—C3—C9	108.7 (3)	O14—C23—C29	108.8 (3)
C10—C3—C9	112.5 (3)	C30—C23—C29	112.9 (3)
O4—C4—C5	112.2 (3)	O14—C24—C25	112.0 (3)
O4—C4—C2	102.9 (2)	O14—C24—C22	103.2 (2)
C5—C4—C2	112.3 (3)	C25—C24—C22	112.2 (3)
O4—C4—H4	109.7	O14—C24—H24	109.8
C5—C4—H4	109.7	C25—C24—H24	109.8
C2—C4—H4	109.7	C22—C24—H24	109.8
O5—C5—C8	108.9 (2)	O15—C25—C28	109.0 (2)
O5—C5—C4	109.0 (3)	O15—C25—C24	108.4 (3)
C8—C5—C4	109.4 (3)	C28—C25—C24	109.8 (3)
O5—C5—H5	109.8	O15—C25—H25	109.9
C8—C5—H5	109.8	C28—C25—H25	109.9
C4—C5—H5	109.8	C24—C25—H25	109.9
O6—C6—O5	109.9 (2)	O16—C26—O15	110.0 (2)
O6—C6—C12	112.9 (3)	O16—C26—C32	112.6 (3)
O5—C6—C12	110.8 (3)	O15—C26—C32	110.9 (3)
O6—C6—C11	105.5 (3)	O16—C26—C31	105.8 (3)
O5—C6—C11	105.0 (3)	O15—C26—C31	105.0 (3)
C12—C6—C11	112.4 (3)	C32—C26—C31	112.2 (3)
O6—C7—C8	107.7 (3)	O16—C27—C28	107.2 (3)
O6—C7—H7A	110.2	O16—C27—H27A	110.3
C8—C7—H7A	110.2	C28—C27—H27A	110.3
O6—C7—H7B	110.2	O16—C27—H27B	110.3

C8—C7—H7B	110.2	C28—C27—H27B	110.3
H7A—C7—H7B	108.5	H27A—C27—H27B	108.5
O1—C8—C7	109.4 (3)	O11—C28—C27	109.5 (3)
O1—C8—C5	108.7 (2)	O11—C28—C25	108.4 (2)
C7—C8—C5	109.1 (3)	C27—C28—C25	109.0 (3)
O1—C8—H8	109.9	O11—C28—H28	109.9
C7—C8—H8	109.9	C27—C28—H28	109.9
C5—C8—H8	109.9	C25—C28—H28	109.9
C3—C9—H9A	109.5	C23—C29—H29A	109.5
C3—C9—H9B	109.5	C23—C29—H29B	109.5
H9A—C9—H9B	109.5	H29A—C29—H29B	109.5
C3—C9—H9C	109.5	C23—C29—H29C	109.5
H9A—C9—H9C	109.5	H29A—C29—H29C	109.5
H9B—C9—H9C	109.5	H29B—C29—H29C	109.5
C3—C10—H10A	109.5	C23—C30—H30A	109.5
C3—C10—H10B	109.5	C23—C30—H30B	109.5
H10A—C10—H10B	109.5	H30A—C30—H30B	109.5
C3—C10—H10C	109.5	C23—C30—H30C	109.5
H10A—C10—H10C	109.5	H30A—C30—H30C	109.5
H10B—C10—H10C	109.5	H30B—C30—H30C	109.5
C6—C11—H11A	109.5	C26—C31—H31A	109.5
C6—C11—H11B	109.5	C26—C31—H31B	109.5
H11A—C11—H11B	109.5	H31A—C31—H31B	109.5
C6—C11—H11C	109.5	C26—C31—H31C	109.5
H11A—C11—H11C	109.5	H31A—C31—H31C	109.5
H11B—C11—H11C	109.5	H31B—C31—H31C	109.5
C6—C12—H12A	109.5	C26—C32—H32A	109.5
C6—C12—H12B	109.5	C26—C32—H32B	109.5
H12A—C12—H12B	109.5	H32A—C32—H32B	109.5
C6—C12—H12C	109.5	C26—C32—H32C	109.5
H12A—C12—H12C	109.5	H32A—C32—H32C	109.5
H12B—C12—H12C	109.5	H32B—C32—H32C	109.5
C8—O1—C1—O2	66.7 (3)	C28—O11—C21—O12	66.5 (3)
C8—O1—C1—C2	-52.7 (3)	C28—O11—C21—C22	-53.1 (3)
C3—O3—C2—C1	163.5 (2)	C23—O13—C22—C24	38.6 (3)
C3—O3—C2—C4	39.1 (3)	C23—O13—C22—C21	163.3 (2)

O2—C1—C2—O3	156.5 (2)	O12—C21—C22—O13	156.3 (2)
O1—C1—C2—O3	-80.7 (3)	O11—C21—C22—O13	-80.7 (3)
O2—C1—C2—C4	-88.8 (3)	O12—C21—C22—C24	-88.6 (3)
O1—C1—C2—C4	34.1 (4)	O11—C21—C22—C24	34.5 (4)
C2—O3—C3—O4	-29.9 (3)	C22—O13—C23—O14	-29.2 (3)
C2—O3—C3—C10	-148.0 (2)	C22—O13—C23—C30	-147.8 (2)
C2—O3—C3—C9	88.0 (3)	C22—O13—C23—C29	88.2 (3)
C4—O4—C3—O3	7.3 (3)	C24—O14—C23—O13	6.8 (3)
C4—O4—C3—C10	123.7 (3)	C24—O14—C23—C30	123.3 (3)
C4—O4—C3—C9	-112.6 (3)	C24—O14—C23—C29	-111.9 (3)
C3—O4—C4—C5	-104.7 (3)	C23—O14—C24—C25	-104.6 (3)
C3—O4—C4—C2	16.3 (3)	C23—O14—C24—C22	16.3 (3)
O3—C2—C4—O4	-33.5 (3)	O13—C22—C24—O14	-33.4 (3)
C1—C2—C4—O4	-152.5 (3)	C21—C22—C24—O14	-152.2 (3)
O3—C2—C4—C5	87.4 (3)	O13—C22—C24—C25	87.3 (3)
C1—C2—C4—C5	-31.6 (4)	C21—C22—C24—C25	-31.5 (4)
C6—O5—C5—C8	-55.0 (3)	C26—O15—C25—C28	-55.0 (3)
C6—O5—C5—C4	-174.3 (2)	C26—O15—C25—C24	-174.5 (2)
O4—C4—C5—O5	-80.0 (3)	O14—C24—C25—O15	-80.1 (3)
C2—C4—C5—O5	164.6 (2)	C22—C24—C25—O15	164.3 (2)
O4—C4—C5—C8	161.0 (2)	O14—C24—C25—C28	161.0 (2)
C2—C4—C5—C8	45.6 (3)	C22—C24—C25—C28	45.4 (3)
C7—O6—C6—O5	-56.5 (3)	C27—O16—C26—O15	-56.3 (3)
C7—O6—C6—C12	67.8 (3)	C27—O16—C26—C32	67.9 (3)
C7—O6—C6—C11	-169.1 (3)	C27—O16—C26—C31	-169.2 (3)
C5—O5—C6—O6	53.9 (3)	C25—O15—C26—O16	53.3 (3)
C5—O5—C6—C12	-71.6 (3)	C25—O15—C26—C32	-71.9 (3)
C5—O5—C6—C11	166.8 (3)	C25—O15—C26—C31	166.7 (3)
C6—O6—C7—C8	60.0 (3)	C26—O16—C27—C28	60.2 (3)
C1—O1—C8—C7	-171.4 (3)	C21—O11—C28—C27	-171.6 (3)
C1—O1—C8—C5	69.6 (3)	C21—O11—C28—C25	69.5 (3)
O6—C7—C8—O1	-177.4 (2)	O16—C27—C28—O11	-177.6 (2)
O6—C7—C8—C5	-58.6 (3)	O16—C27—C28—C25	-59.2 (3)
O5—C5—C8—O1	175.9 (2)	O15—C25—C28—O11	176.7 (2)
C4—C5—C8—O1	-65.0 (3)	C24—C25—C28—O11	-64.7 (3)
O5—C5—C8—C7	56.7 (3)	O15—C25—C28—C27	57.5 (3)
C4—C5—C8—C7	175.8 (3)	C24—C25—C28—C27	176.1 (2)

Table 2.3 Hydrogen-bond parameters

D—H···*A*	*D*—H (Å)	H···*A* (Å)	*D*···*A* (Å)	*D*—H···*A* (°)
O2—H2···O5^{i}	0.87 (5)	1.91 (5)	2.780 (3)	172 (4)
O12—H12···O15^{ii}	0.80 (4)	1.99 (4)	2.786 (3)	175 (4)

Symmetry code(s): (i) -*x*+1, *y*-1/2, -*z*+1; (ii) -*x*+1, *y*+1/2, -*z*.

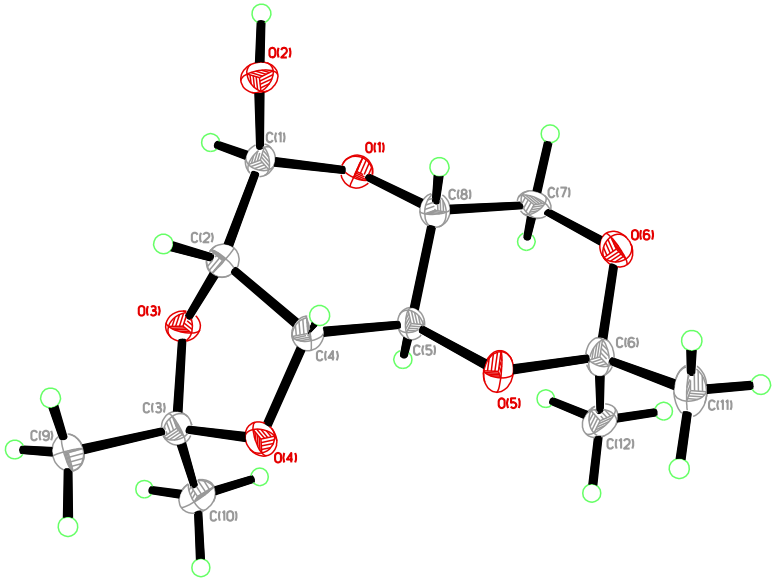


Figure 2.18. Perspective views showing 50% probability displacement.

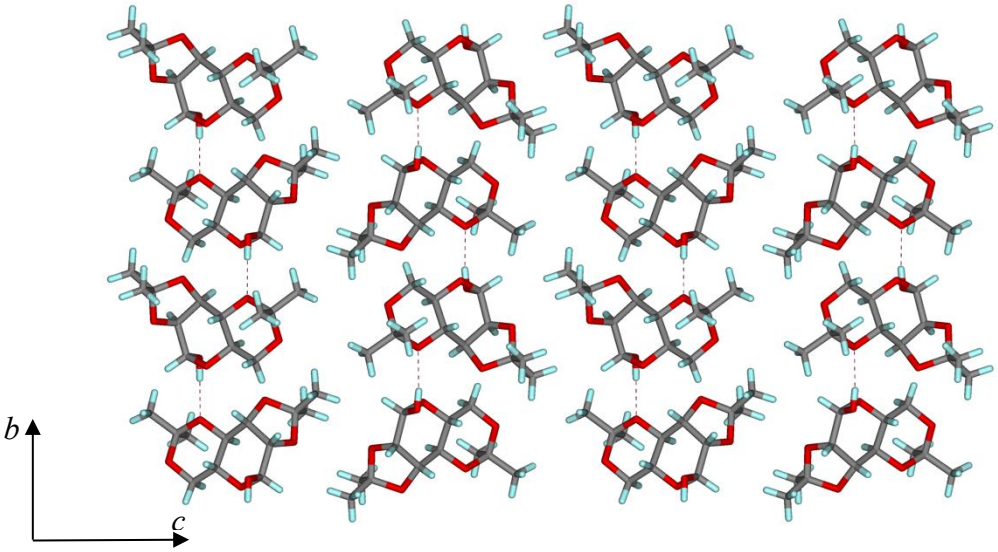
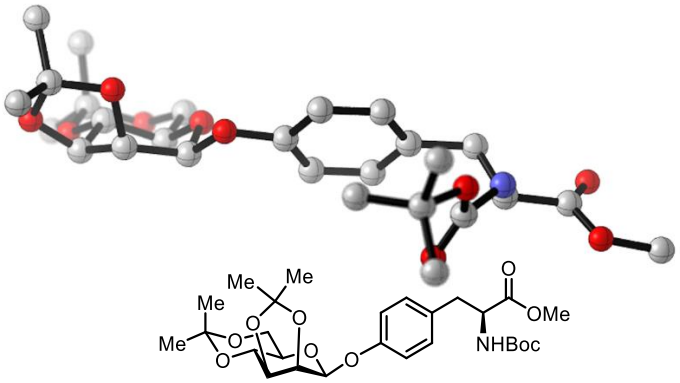


Figure 2.19 Three-dimensional supramolecular architecture viewed along the *a*-axis direction.



4p

X-ray Crystallography: A crystal mounted on a diffractometer was collected data at 100 K. The intensities of the reflections were collected by means of a Bruker APEX DUO CCD diffractometer ($Cu_{K\alpha}$ radiation, λ=1.54178 Å), and equipped with an Oxford Cryosystems nitrogen flow apparatus. The collection method involved 1.0° scans in ω at -30°, -55°, -80°, 30°, 55°, 80° and 115° in 2θ. Data integration down to 0.84 Å resolution was carried out using SAINT V8.37 A (Bruker diffractometer, 2015) with reflection spot size optimization. Absorption corrections were made with the program SADABS (Bruker diffractometer, 2015). The structure was solved by the Intrinsic Phasing methods and refined by least-squares methods again F^2 using SHELXT-2014 (Sheldrick, 2015) and SHELXL-2014 (Sheldrick, 2015) with OLEX 2 interface (Dolomanov, et al., 2009). Non-hydrogen atoms were refined anisotropically, and hydrogen atoms were allowed to ride on the respective atoms. Crystal data as well as details of data collection and refinement are summarized in Table 2.4, geometric parameters are shown in Table 2.5, and hydrogen-bond parameters are listed in Table 2.6. The Ortep plots produced with SHELXL-2014 program, and the other drawings were produced with Accelrys DS Visualizer 2.0 (Accelrys, 2007).[38]

Table 2.4. Experimental details

	QL-III-Tyr

Crystal data	
Chemical formula	$C_{31}H_{48.67}NO_{10.33}$
M_r	600.73
Crystal system, space group	Monoclinic, $P2_1$
Temperature (K)	100
a, b, c (Å)	5.1612 (3), 30.938 (2), 9.7231 (6)
β (°)	91.905 (3)
V (Å^3)	1551.72 (17)
Z	2
Radiation type	Cu $K\alpha$
μ (mm^{-1})	0.79
Crystal size (mm)	0.18 × 0.14 × 0.10
Data collection	
Diffractometer	Bruker D8 goniometer with CCD area detector
Absorption correction	Multi-scan *SADABS*
T_{min}, T_{max}	0.757, 0.806
No. of measured, independent and observed [$I > 2\sigma(I)$] reflections	41074, 5409, 5349
R_{int}	0.032
$(\sin \theta/\lambda)_{max}$ (Å^{-1})	0.597
Refinement	
$R[F^2 > 2\sigma(F^2)]$, $wR(F^2)$, S	0.033, 0.090, 1.09
No. of reflections	5409
No. of parameters	450
No. of restraints	80
H-atom treatment	H atoms treated by a mixture of independent and constrained refinement
$\Delta\rho_{max}$, $\Delta\rho_{min}$ (e Å^{-3})	0.22, -0.28
Absolute structure	Flack x determined using 2517 quotients [(I+)-(I-)]/[(I+)+(I-)] (Parsons, Flack and Wagner, Acta Cryst. B69 (2013) 249-259).
Absolute structure parameter	-0.03 (5)

Computer programs: *SAINT* 8.37A (Bruker-AXS, 2015), *SHELXT2014* (Sheldrick, 2015), *SHELXL2014* (Sheldrick, 2015), Bruker *SHELXTL* (Sheldrick, 2015).

Table 2.5 Geometric parameters (Å, º)

O1—C13	1.386 (3)	C16—C17	1.387 (4)
O1—C1	1.397 (3)	C16—C19	1.508 (4)
O2—C2	1.420 (3)	C17—C18	1.393 (4)
O2—C3	1.434 (3)	C17—H17	0.9500
O3—C4	1.425 (3)	C18—H18	0.9500
O3—C3	1.443 (3)	C19—C20	1.535 (4)
O4—C5	1.422 (3)	C19—H19A	0.9900
O4—C6	1.442 (3)	C19—H19B	0.9900
O5—C6	1.430 (3)	C20—C21	1.524 (4)
O5—C7	1.431 (3)	C20—H20	1.0000
O6—C1	1.428 (3)	C22—H22A	0.9800
O6—C8	1.428 (3)	C22—H22B	0.9800
O7—C21	1.327 (3)	C22—H22C	0.9800
O7—C22	1.450 (3)	C24—C27	1.505 (5)
O8—C21	1.196 (3)	C24—C25	1.508 (5)
O9—C23	1.345 (3)	C24—C26	1.534 (4)
O9—C24	1.479 (3)	C25—H25A	0.9800
O10—C23	1.211 (3)	C25—H25B	0.9800
N1—C23	1.353 (3)	C25—H25C	0.9800
N1—C20	1.451 (3)	C26—H26A	0.9800
N1—H1	0.84 (3)	C26—H26B	0.9800
C1—C2	1.528 (4)	C26—H26C	0.9800
C1—H1A	1.0000	C27—H27A	0.9800
C2—C4	1.532 (4)	C27—H27B	0.9800
C2—H2	1.0000	C27—H27C	0.9800
C3—C10	1.511 (4)	C1S—C2S	1.688 (16)
C3—C9	1.518 (4)	C1S—H1SA	0.9800
C4—C5	1.521 (4)	C1S—H1SB	0.9800
C4—H4	1.0000	C1S—H1SC	0.9800
C5—C8	1.517 (4)	C2S—C3S	1.451 (12)
C5—H5	1.0000	C2S—H2SA	0.9900
C6—C11	1.502 (4)	C2S—H2SB	0.9900
C6—C12	1.513 (4)	C3S—C4S	1.631 (15)
C7—C8	1.517 (4)	C3S—H3SA	0.9900
C7—H7A	0.9900	C3S—H3SB	0.9900
C7—H7B	0.9900	C4S—C5S	1.560 (15)
C8—H8	1.0000	C4S—H4SA	0.9900

C9—H9A	0.9800	C4S—H4SB	0.9900
C9—H9B	0.9800	C5S—C6S	1.549 (14)
C9—H9C	0.9800	C5S—H5SA	0.9900
C10—H10A	0.9800	C5S—H5SB	0.9900
C10—H10B	0.9800	C6S—H6SA	0.9800
C10—H10C	0.9800	C6S—H6SB	0.9800
C11—H11A	0.9800	C6S—H6SC	0.9800
C11—H11B	0.9800	O1S—C12S	1.42 (2)
C11—H11C	0.9800	O1S—H1S	0.8400
C12—H12A	0.9800	C11S—C12S	1.363 (18)
C12—H12B	0.9800	C11S—H11D	0.9800
C12—H12C	0.9800	C11S—H11E	0.9800
C13—C14	1.384 (4)	C11S—H11F	0.9800
C13—C18	1.386 (4)	C12S—C13S	1.35 (2)
C14—C15	1.392 (4)	C12S—H12S	1.0000
C14—H14	0.9500	C13S—H13A	0.9800
C15—C16	1.391 (4)	C13S—H13B	0.9800
C15—H15	0.9500	C13S—H13C	0.9800
C13—O1—C1	117.8 (2)	C16—C19—H19A	108.9
C2—O2—C3	105.85 (19)	C20—C19—H19A	108.9
C4—O3—C3	108.6 (2)	C16—C19—H19B	108.9
C5—O4—C6	112.72 (19)	C20—C19—H19B	108.9
C6—O5—C7	115.25 (19)	H19A—C19—H19B	107.7
C1—O6—C8	110.48 (19)	N1—C20—C21	110.9 (2)
C21—O7—C22	115.1 (2)	N1—C20—C19	111.6 (2)
C23—O9—C24	121.2 (2)	C21—C20—C19	109.6 (2)
C23—N1—C20	122.5 (2)	N1—C20—H20	108.2
C23—N1—H1	117 (2)	C21—C20—H20	108.2
C20—N1—H1	119 (2)	C19—C20—H20	108.2
O1—C1—O6	107.5 (2)	O8—C21—O7	123.6 (3)
O1—C1—C2	107.8 (2)	O8—C21—C20	124.3 (2)
O6—C1—C2	113.2 (2)	O7—C21—C20	112.0 (2)
O1—C1—H1A	109.4	O7—C22—H22A	109.5
O6—C1—H1A	109.4	O7—C22—H22B	109.5
C2—C1—H1A	109.4	H22A—C22—H22B	109.5
O2—C2—C1	112.2 (2)	O7—C22—H22C	109.5

O2—C2—C4	101.9 (2)	H22A—C22—H22C	109.5
C1—C2—C4	114.5 (2)	H22B—C22—H22C	109.5
O2—C2—H2	109.3	O10—C23—O9	126.1 (2)
C1—C2—H2	109.3	O10—C23—N1	125.3 (2)
C4—C2—H2	109.3	O9—C23—N1	108.5 (2)
O2—C3—O3	106.0 (2)	O9—C24—C27	110.5 (3)
O2—C3—C10	108.4 (2)	O9—C24—C25	110.2 (3)
O3—C3—C10	110.1 (2)	C27—C24—C25	113.3 (2)
O2—C3—C9	111.3 (2)	O9—C24—C26	101.8 (2)
O3—C3—C9	108.0 (2)	C27—C24—C26	108.9 (3)
C10—C3—C9	112.8 (2)	C25—C24—C26	111.5 (3)
O3—C4—C5	110.9 (2)	C24—C25—H25A	109.5
O3—C4—C2	102.5 (2)	C24—C25—H25B	109.5
C5—C4—C2	111.0 (2)	H25A—C25—H25B	109.5
O3—C4—H4	110.7	C24—C25—H25C	109.5
C5—C4—H4	110.7	H25A—C25—H25C	109.5
C2—C4—H4	110.7	H25B—C25—H25C	109.5
O4—C5—C8	109.4 (2)	C24—C26—H26A	109.5
O4—C5—C4	109.5 (2)	C24—C26—H26B	109.5
C8—C5—C4	110.4 (2)	H26A—C26—H26B	109.5
O4—C5—H5	109.2	C24—C26—H26C	109.5
C8—C5—H5	109.2	H26A—C26—H26C	109.5
C4—C5—H5	109.2	H26B—C26—H26C	109.5
O5—C6—O4	109.3 (2)	C24—C27—H27A	109.5
O5—C6—C11	106.0 (2)	C24—C27—H27B	109.5
O4—C6—C11	106.0 (2)	H27A—C27—H27B	109.5
O5—C6—C12	112.7 (2)	C24—C27—H27C	109.5
O4—C6—C12	111.0 (2)	H27A—C27—H27C	109.5
C11—C6—C12	111.4 (2)	H27B—C27—H27C	109.5
O5—C7—C8	108.9 (2)	C2S—C1S—H1SA	109.5
O5—C7—H7A	109.9	C2S—C1S—H1SB	109.5
C8—C7—H7A	109.9	H1SA—C1S—H1SB	109.5
O5—C7—H7B	109.9	C2S—C1S—H1SC	109.5
C8—C7—H7B	109.9	H1SA—C1S—H1SC	109.5
H7A—C7—H7B	108.3	H1SB—C1S—H1SC	109.5
O6—C8—C5	108.0 (2)	C3S—C2S—C1S	109.7 (11)
O6—C8—C7	108.9 (2)	C3S—C2S—H2SA	109.7

C5—C8—C7	109.0 (2)	C1S—C2S—H2SA	109.7
O6—C8—H8	110.3	C3S—C2S—H2SB	109.7
C5—C8—H8	110.3	C1S—C2S—H2SB	109.7
C7—C8—H8	110.3	H2SA—C2S—H2SB	108.2
C3—C9—H9A	109.5	C2S—C3S—C4S	121.1 (11)
C3—C9—H9B	109.5	C2S—C3S—H3SA	107.1
H9A—C9—H9B	109.5	C4S—C3S—H3SA	107.1
C3—C9—H9C	109.5	C2S—C3S—H3SB	107.1
H9A—C9—H9C	109.5	C4S—C3S—H3SB	107.1
H9B—C9—H9C	109.5	H3SA—C3S—H3SB	106.8
C3—C10—H10A	109.5	C5S—C4S—C3S	148.9 (14)
C3—C10—H10B	109.5	C5S—C4S—H4SA	99.5
H10A—C10—H10B	109.5	C3S—C4S—H4SA	99.5
C3—C10—H10C	109.5	C5S—C4S—H4SB	99.5
H10A—C10—H10C	109.5	C3S—C4S—H4SB	99.5
H10B—C10—H10C	109.5	H4SA—C4S—H4SB	104.1
C6—C11—H11A	109.5	C6S—C5S—C4S	150.1 (14)
C6—C11—H11B	109.5	C6S—C5S—H5SA	99.1
H11A—C11—H11B	109.5	C4S—C5S—H5SA	99.1
C6—C11—H11C	109.5	C6S—C5S—H5SB	99.1
H11A—C11—H11C	109.5	C4S—C5S—H5SB	99.1
H11B—C11—H11C	109.5	H5SA—C5S—H5SB	104.0
C6—C12—H12A	109.5	C5S—C6S—H6SA	109.5
C6—C12—H12B	109.5	C5S—C6S—H6SB	109.5
H12A—C12—H12B	109.5	H6SA—C6S—H6SB	109.5
C6—C12—H12C	109.5	C5S—C6S—H6SC	109.5
H12A—C12—H12C	109.5	H6SA—C6S—H6SC	109.5
H12B—C12—H12C	109.5	H6SB—C6S—H6SC	109.5
C14—C13—C18	119.8 (3)	C12S—O1S—H1S	109.5
C14—C13—O1	115.2 (2)	C12S—C11S—H11D	109.5
C18—C13—O1	124.9 (2)	C12S—C11S—H11E	109.5
C13—C14—C15	120.3 (3)	H11D—C11S—H11E	109.5
C13—C14—H14	119.9	C12S—C11S—H11F	109.5
C15—C14—H14	119.9	H11D—C11S—H11F	109.5
C16—C15—C14	121.0 (3)	H11E—C11S—H11F	109.5
C16—C15—H15	119.5	C13S—C12S—C11S	110 (2)
C14—C15—H15	119.5	C13S—C12S—O1S	107.3 (15)

C17—C16—C15	117.6 (3)	C11S—C12S—O1S	134.8 (17)
C17—C16—C19	120.2 (3)	C13S—C12S—H12S	98.9
C15—C16—C19	122.2 (3)	C11S—C12S—H12S	98.9
C16—C17—C18	122.2 (3)	O1S—C12S—H12S	98.9
C16—C17—H17	118.9	C12S—C13S—H13A	109.5
C18—C17—H17	118.9	C12S—C13S—H13B	109.5
C13—C18—C17	119.0 (3)	H13A—C13S—H13B	109.5
C13—C18—H18	120.5	C12S—C13S—H13C	109.5
C17—C18—H18	120.5	H13A—C13S—H13C	109.5
C16—C19—C20	113.5 (2)	H13B—C13S—H13C	109.5
C13—O1—C1—O6	-63.9 (3)	O4—C5—C8—C7	56.8 (3)
C13—O1—C1—C2	173.8 (2)	C4—C5—C8—C7	177.4 (2)
C8—O6—C1—O1	-176.68 (19)	O5—C7—C8—O6	-171.44 (19)
C8—O6—C1—C2	-57.8 (3)	O5—C7—C8—C5	-53.9 (3)
C3—O2—C2—C1	161.0 (2)	C1—O1—C13—C14	173.7 (2)
C3—O2—C2—C4	38.1 (2)	C1—O1—C13—C18	-5.6 (4)
O1—C1—C2—O2	45.8 (3)	C18—C13—C14—C15	1.8 (4)
O6—C1—C2—O2	-72.9 (3)	O1—C13—C14—C15	-177.5 (2)
O1—C1—C2—C4	161.4 (2)	C13—C14—C15—C16	-1.2 (4)
O6—C1—C2—C4	42.7 (3)	C14—C15—C16—C17	-0.6 (4)
C2—O2—C3—O3	-26.5 (3)	C14—C15—C16—C19	179.6 (3)
C2—O2—C3—C10	-144.6 (2)	C15—C16—C17—C18	1.9 (4)
C2—O2—C3—C9	90.7 (3)	C19—C16—C17—C18	-178.3 (3)
C4—O3—C3—O2	2.6 (3)	C14—C13—C18—C17	-0.5 (4)
C4—O3—C3—C10	119.6 (2)	O1—C13—C18—C17	178.7 (3)
C4—O3—C3—C9	-116.8 (2)	C16—C17—C18—C13	-1.3 (4)
C3—O3—C4—C5	-98.5 (2)	C17—C16—C19—C20	-93.9 (3)
C3—O3—C4—C2	20.1 (3)	C15—C16—C19—C20	85.9 (3)
O2—C2—C4—O3	-35.6 (2)	C23—N1—C20—C21	-133.9 (3)
C1—C2—C4—O3	-157.0 (2)	C23—N1—C20—C19	103.6 (3)
O2—C2—C4—C5	83.0 (2)	C16—C19—C20—N1	-68.0 (3)
C1—C2—C4—C5	-38.5 (3)	C16—C19—C20—C21	168.8 (2)
C6—O4—C5—C8	-59.6 (3)	C22—O7—C21—O8	-0.5 (4)
C6—O4—C5—C4	179.3 (2)	C22—O7—C21—C20	177.0 (2)
O3—C4—C5—O4	-77.1 (3)	N1—C20—C21—O8	-137.2 (3)
C2—C4—C5—O4	169.6 (2)	C19—C20—C21—O8	-13.6 (4)

O3—C4—C5—C8	162.4 (2)	N1—C20—C21—O7	45.3 (3)
C2—C4—C5—C8	49.1 (3)	C19—C20—C21—O7	169.0 (2)
C7—O5—C6—O4	-56.4 (3)	C24—O9—C23—O10	-8.7 (5)
C7—O5—C6—C11	-170.3 (2)	C24—O9—C23—N1	173.2 (3)
C7—O5—C6—C12	67.6 (3)	C20—N1—C23—O10	10.8 (4)
C5—O4—C6—O5	57.7 (3)	C20—N1—C23—O9	-171.1 (2)
C5—O4—C6—C11	171.6 (2)	C23—O9—C24—C27	68.3 (4)
C5—O4—C6—C12	-67.3 (3)	C23—O9—C24—C25	-57.7 (4)
C6—O5—C7—C8	55.7 (3)	C23—O9—C24—C26	-176.2 (3)
C1—O6—C8—C5	68.6 (2)	C1S—C2S—C3S—C4S	178.5 (10)
C1—O6—C8—C7	-173.2 (2)	C2S—C3S—C4S—C5S	-142 (2)
O4—C5—C8—O6	174.97 (19)	C3S—C4S—C5S—C6S	157 (2)
C4—C5—C8—O6	-64.5 (2)		

Table 2.6 Hydrogen-bond parameters

D—H···*A*	*D*—H (Å)	H···*A* (Å)	*D*···*A* (Å)	*D*—H···*A* (°)
N1—H1···O10^{i}	0.84 (3)	2.17 (3)	2.938 (3)	152 (3)

Symmetry code(s): (i) *x*-1, *y*, *z*.

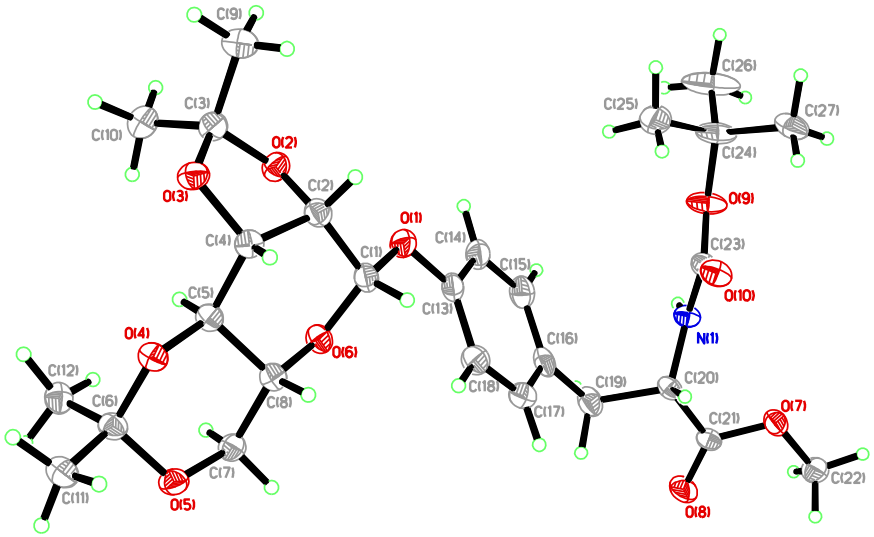


Figure 2.20 Perspective views showing 50% probability displacement.

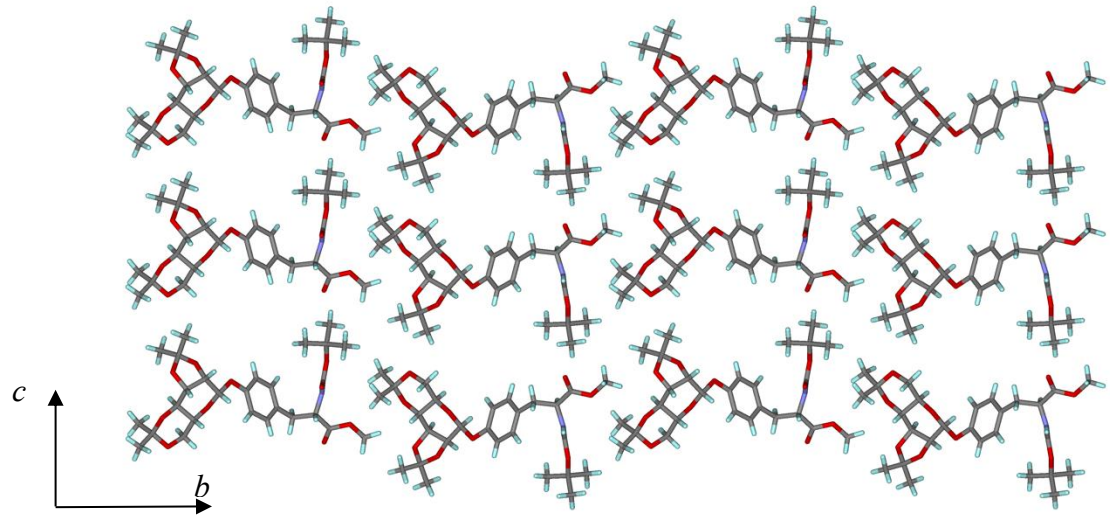


Figure 2.21 Three-dimensional supramolecular architecture viewed along the *a*-axis direction. Disordered solvents have been omitted.

2.10.9 Computational Analysis

Computational Method

Calculations were performed using the Gaussian 16 program[40] on the Odyssey cluster supported by Harvard University's Faculty of Arts and Sciences Research Computing group. The geometries of all ground-state structures were fully optimized at the B3LYP/6-31G(d) level of theory[41] with

[40] Gaussian 16, Revision A.03, M. J. Frisch, G. W. Trucks, H. B. Schlegel, G. E. Scuseria, M. A. Robb, J. R. Cheeseman, G. Scalmani, V. Barone, G. A. Petersson, H. Nakatsuji, X. Li, M. Caricato, A. V. Marenich, J. Bloino, B. G. Janesko, R. Gomperts, B. Mennucci, H. P. Hratchian, J. V. Ortiz, A. F. Izmaylov, J. L. Sonnenberg, D. Williams-Young, F. Ding, F. Lipparini, F. Egidi, J. Goings, B. Peng, A. Petrone, T. Henderson, D. Ranasinghe, V. G. Zakrzewski, J. Gao, N. Rega, G. Zheng, W. Liang, M. Hada, M. Ehara, K. Toyota, R. Fukuda, J. Hasegawa, M. Ishida, T. Nakajima, Y. Honda, O. Kitao, H. Nakai, T. Vreven, K. Throssell, J. A. Montgomery, Jr., J. E. Peralta, F. Ogliaro, M. J. Bearpark, J. J. Heyd, E. N. Brothers, K. N. Kudin, V. N. Staroverov, T. A. Keith, R. Kobayashi, J. Normand, K. Raghavachari, A. P. Rendell, J. C. Burant, S. S. Iyengar, J. Tomasi, M. Cossi, J. M. Millam, M. Klene, C. Adamo, R. Cammi, J. W. Ochterski, R. L. Martin, K. Morokuma, O. Farkas, J. B. Foresman, and D. J. Fox, Gaussian, Inc., Wallingford CT, 2016.

[41]) (a) Becke, A. D. Density-Functional Exchange-Energy Approximation with Correct Asymptotic Behavior. *Phys. Rev. A* **1988**, *38*, 3098–3100. (b) Lee, C.; Yang, W.; Parr, R. G. Development of the Colle-Salvetti Correlation-Energy Formula into a Functional of the Electron Density. *Phys. Rev. B* **1988**, *37*, 785–789. (c) Becke, A. D. Density-Functional Thermochemistry. III. The Role of Exact Exchange. *J. Chem. Phys*. **1993**, *98*, 5648–5652. (d) Stephens, P. J.; Devlin, F. J.; Chabalowski, C. F.; Frisch, M. J. Ab Initio Calculation of Vibrational Absorption and Circular Dichroism Spectra Using Density Functional Force Fields *J. Phys. Chem*. **1994**, *98*, 11623–11627.

empirical dispersion correction (D3BJ)[42] and solvent correction. Single point energies were computed at the B3LYP/6-311+G(d,p) level of theory[40] with empirical dispersion correction (D3BJ)[41] and solvent correction. A polarization continuum model was used with either diethyl ether or water as the solvent.[43] Single point energies of oxocarbenium ion intermediates and glycosyl phosphates were compared within the same solvation model. Default geometric and SCF convergence criteria were used. Stationary points were verified by harmonic frequency calculations. Free energy corrections were determined at the B3LYP/6-31G(d) level of theory at 298.15 K using Grimme's quasi-harmonic free energy correction.[44] All molecular structures were rendered in CYLView.[45]

B3LYP level of theory was selected because it has been previously applied to efficiently and accurately compute the transition states of glycosylation and the geometries and energies of oxocarbenium ion intermediates.[46] 6-31G(d) basis set was selected for the initial geometrical optimization because it allowed for efficient geometrical and energy calculations of relatively large systems. Larger basis set 6-311+G(d,p) was chosen to compute the single point energies of optimized structures to minimize basis set superposition error and obtain more accurate energies.

Procedure for Geometric Optimization of Glycosyl Phosphates

---

[42] (a) Grimme, S.; Antony, J.; Ehrlich, S.; Krieg, H. A Consistent and Accurate Ab Initio Parametrization of Density Functional Dispersion Correction (DFT-D) for the 94 elements H-Pu. *J. Chem. Phys*. **2010**, *132*, 154104–154119. (b) Grimme, S.; Ehrlich, S.; Goerigk, L. Effect of the Damping Function in Dispersion Corrected Density Functional Theory. *J. Comp. Chem*. **2010**, *32*, 1456–1465.

[43] Scalmani, G.; Frisch, M. J. Continuous Surface Charge Polarizable Continuum Models of Solvation. I. General Formalism. *J. Chem. Phys*. **2010**, *132*, 114110–114115.

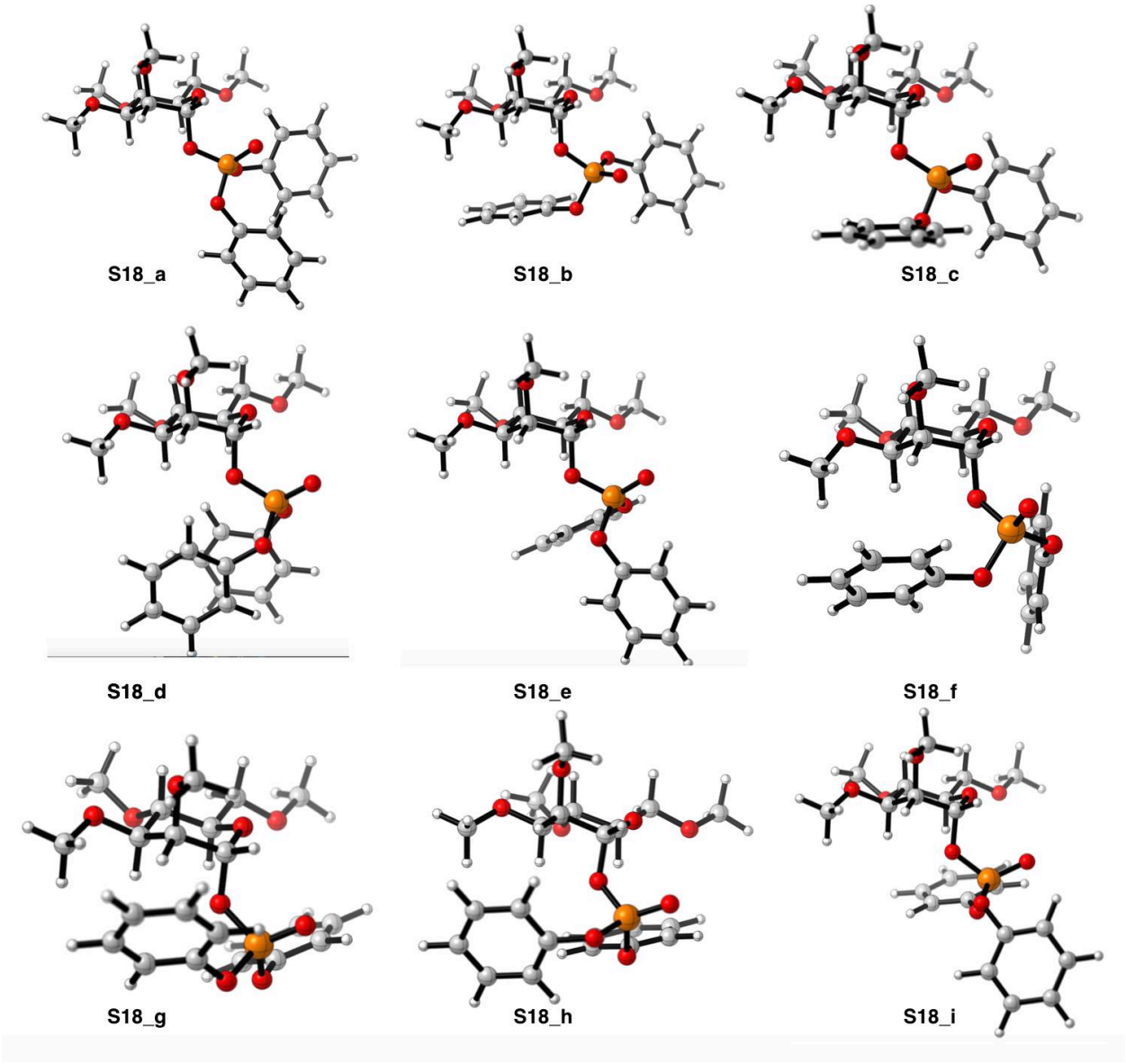
[44] Grimme, S. Supramolecular Binding Thermodynamics by Dispersion-Corrected Density Functional Theory. *Chem. Eur. J*. **2012**, *18*, 9955–9964.

[45] C. Y. Legault, CYLview, 1.0b; Université de Sherbrooke, 2009 (http://www.cylview.org)

[46] (a) Whitfield, D. M. Computational Studies of the Role of Glycopyranosyl Oxacarbenium Ions in Glycobiology and Glycochemistry. *Adv. Carbohydr. Chem. Biochem*. **2009**, *62*, 83–159. (b) Ionescu, A. R.; Whitfield, D. M.; Zgierski, M. Z.; Nukada, T. Investigations into the Role of Oxacarbenium Ions in Glycosylation Reactions by *ab initio* Molecular Dynamics. *Carbohydr. Res*. **2006**, *341*, 2912–2920. (c) Barnett, C. B.; Wilkinson, K. A.; Naidoo, K. J. Molecular Details from Computational Reaction Dynamics for the Cellobiohydrolase I Glycosylation Reaction. *J. Am. Chem. Soc*. **2011**, *133*, 19474–19482.

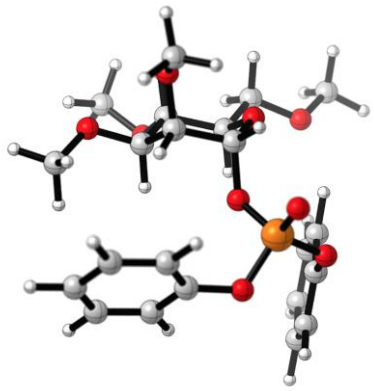
We recognized that the diphenyl phosphate group can adopt several different conformations due to the free bond rotation of phenyl groups. A large number of input structures with different phosphate conformations were optimized at the B3LYP/6-31G(d) level of theory. Each optimized structure with zero imaginary frequency indicated a local minimum. By comparing the energy of each local minimum, we selected the structure with the lowest energy as the global minimum. This procedure was followed for geometric optimization of all glycosyl phosphates. We included the conformational space of 2,3,4,6-tetra-*O*-methyl-α-D-mannopyranosyl diphenylphosphate **S18** as an example to illustrate this process.

Conformation	$G(B3LYP)_{phosphate}$ (hartree)
S18_a	-1873.892539
S18_b	-1873.891287
S18_c	-1873.891963
S18_d	-1873.887981
S18_e	-1873.890462
S18_f	-1873.896629 (lowest energy conformation)
S18_g	-1873.892657
S18_h	-1873.892486
S18_i	-1873.889130



Optimized Structures of Glycosyl Phosphates and Oxocarbenium Ion Intermediates

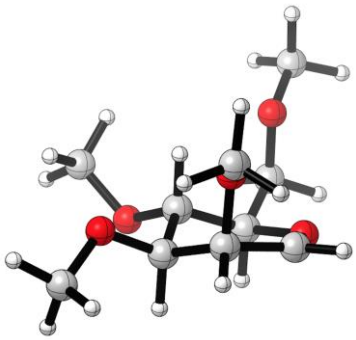
Optimized Structure of 2,3,4,6-Tetra-*O*-methyl-α-D-mannopyranosyl diphenylphosphate **S18_f**



C	0.79520600	2.53107300	-0.56895700
C	1.70954700	1.48130100	0.08375500
C	-0.05490100	0.69841300	1.49541100
C	-1.05956900	1.69870800	0.91108300
C	-0.65798900	2.05707200	-0.52733200
H	1.71139300	0.58556400	-0.54706800
H	0.87759400	3.48365300	-0.02938300
H	-0.24811600	0.50384400	2.55031400
H	-2.05479400	1.23538200	0.92375300
H	-0.73509500	1.14738300	-1.14089100
C	3.13087900	1.98561700	0.23145200
H	3.44536800	2.43821300	-0.71881100
H	3.16380200	2.76158300	1.01262800
O	1.25765700	1.12372800	1.40549500
O	3.97416700	0.89968600	0.57221700
O	1.24554800	2.66933400	-1.90911200
O	-1.47326200	3.07747900	-1.07211300
O	-1.04713000	2.88446700	1.68386300
O	-0.23019000	-0.54094100	0.74817300
P	-0.57601600	-1.93267000	1.45769900
O	-1.08950200	-1.85032100	2.84203900
O	-1.53043100	-2.61596000	0.34746100
O	0.73123200	-2.85999200	1.35523400
C	-2.55389700	-1.87925500	-0.26823300
C	-3.57058200	-1.30264200	0.48945500
C	-2.52137600	-1.77816600	-1.65511800
C	-4.58044300	-0.59870200	-0.17065400
H	-3.56645100	-1.40447600	1.56938300
C	-3.54413200	-1.08247300	-2.30216300
H	-1.70531900	-2.23632100	-2.20365600
C	-4.57212800	-0.49113100	-1.56310100
H	-5.37660700	-0.14090800	0.40817100
H	-3.53165600	-0.99855000	-3.38445500
H	-5.36157700	0.05433700	-2.07042800
C	1.52541900	-2.87102400	0.19020000
C	1.26802700	-3.81662100	-0.79664700

C	2.55900800	-1.94776900	0.08225200
C	2.08229600	-3.83361200	-1.93168000
H	0.44720900	-4.51438800	-0.67470200
C	3.35895400	-1.97072400	-1.06123600
H	2.72238000	-1.21139900	0.85958100
C	3.12452700	-2.91247000	-2.06633000
H	1.89594000	-4.56581400	-2.71141700
H	4.15228600	-1.23682400	-1.15722100
H	3.74912600	-2.92721000	-2.95434000
C	-1.91289300	2.84455600	2.81066900
H	-1.62078300	2.07120300	3.53388900
H	-1.84478400	3.82156800	3.29373000
H	-2.95191400	2.66280500	2.50262200
C	-2.75719900	2.62795200	-1.48020500
H	-2.67989700	1.79548800	-2.19255700
H	-3.37109800	2.29768600	-0.63214800
H	-3.24826200	3.47569700	-1.96327000
C	1.16832600	3.99363500	-2.42519900
H	1.57823900	3.95651700	-3.43764900
H	0.13375800	4.34834100	-2.45864800
H	1.76977900	4.68853600	-1.82183300
C	5.32050600	1.30156900	0.75307000
H	5.89357600	0.40436700	0.99745800
H	5.73030500	1.75465700	-0.16197100
H	5.41559900	2.02741900	1.57442400

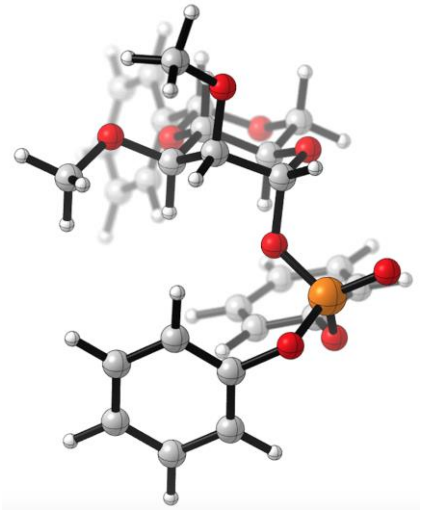
Optimized Structure of 2,3,4,6-Tetra-*O*-methyl-D-mannopyranosyl oxocarbenium ion **5a**



C	0.19870000	0.74766000	-0.20265700
C	1.13006400	-0.02074600	-1.14739500
C	-0.46446500	-1.85546000	-1.08751000
C	-1.53647500	-1.01423000	-0.48128100
C	-1.26588400	0.49260000	-0.54751700
H	1.05868900	0.37184800	-2.16332700
H	0.38636200	0.42502300	0.82568500
H	-0.61875400	-2.92046600	-1.25030800
H	-2.52269100	-1.28344400	-0.86642700

H	-1.45731200	0.84275000	-1.57221000
C	2.57152500	-0.06282800	-0.69555900
H	3.15633700	-0.69225100	-1.38186500
H	2.96130300	0.96353300	-0.75804100
O	0.71321100	-1.46238100	-1.29381400
O	2.60754600	-0.55902700	0.62212000
O	0.53948900	2.10338500	-0.39097800
O	-2.06945300	1.17437500	0.38407700
O	-1.31842700	-1.50136100	0.84595600
C	-2.40425900	-2.26055300	1.40696500
H	-2.63814400	-3.13622400	0.79413200
H	-2.06210800	-2.58024100	2.39117500
H	-3.28709100	-1.62038600	1.49976200
C	-3.33504000	1.58871700	-0.12936600
H	-3.20741000	2.27188200	-0.97860700
H	-3.94867100	0.73511300	-0.44418400
H	-3.84145700	2.10910800	0.68502600
C	0.71050600	2.83273500	0.82612100
H	0.98637500	3.84877000	0.53781100
H	-0.21966400	2.85117800	1.40292900
H	1.51298600	2.39582200	1.43403300
C	3.92456200	-0.58593000	1.15573900
H	3.84599700	-0.97599000	2.17215400
H	4.57993000	-1.24000500	0.56392200
H	4.36100300	0.42225000	1.18422300

Optimized Structure of 2,3-Di-*O*-methyl-4,6-*O*-benzylidene-α-D-mannopyranosyl diphenylphosphate **S19**

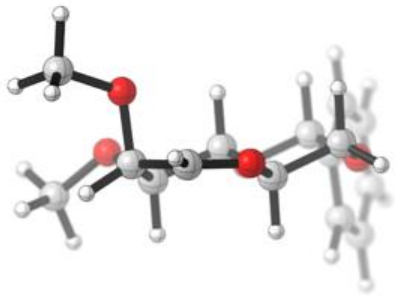


C	1.36140400	1.60733300	-1.41378900
C	-0.80603100	0.68491900	-1.43820800
C	-1.27812200	1.61521800	-0.31655600

C	-0.11648000	1.92495200	0.60799200
C	0.99601000	2.55442100	-0.26262000
H	2.09100000	2.05890500	-2.08468500
H	0.25833100	0.98392400	1.03673600
H	-0.48846300	-0.25685300	-0.98744000
O	0.27276100	1.24632300	-2.19507300
O	1.94108800	0.44230800	-0.76874400
O	-0.55299200	2.78567900	1.64410300
C	-1.98490900	0.40908700	-2.35728200
H	-2.31709400	1.34013800	-2.84167100
H	-1.73038400	-0.32375700	-3.12464000
O	-3.03227600	-0.15927200	-1.57191900
O	3.63525200	0.02525800	-2.72728000
C	0.28691200	2.76429700	2.78714500
H	-0.19946700	3.37855500	3.54792200
H	0.40939800	1.74084100	3.16964000
H	1.28270700	3.18219800	2.58045600
O	-2.32386400	0.94400700	0.38022700
C	-3.41523600	0.66958700	-0.48258900
H	-3.79681900	1.62426500	-0.88331900
H	-1.65513400	2.55604700	-0.74169300
O	0.57781500	3.75428200	-0.88558900
C	0.77779100	4.93282600	-0.11285200
H	1.82167100	5.00769100	0.22517900
H	0.55805400	5.77517400	-0.77295400
H	0.11307600	4.96089800	0.75512000
H	1.90023200	2.72767500	0.33613300
P	3.13299700	-0.41484900	-1.41289200
O	4.29059100	-0.39055300	-0.28506200
O	2.59752300	-1.93438200	-1.30705700
C	3.98315800	-0.71362400	1.04630300
C	3.55554500	0.29450300	1.90606700
C	4.12820600	-2.02945700	1.47529800
C	3.25475500	-0.02959000	3.22939800
H	3.46343300	1.30890600	1.53613500
C	3.82649200	-2.34116200	2.80280400
H	4.45772100	-2.78731900	0.77373000
C	3.38527700	-1.34623100	3.67830600
H	2.91914700	0.74888400	3.90788800
H	3.93353600	-3.36470400	3.14866700
H	3.14834100	-1.59487100	4.70813900
C	1.24800900	-2.27973500	-1.14793900
C	0.72569700	-2.38794400	0.13793500
C	0.48089300	-2.54220000	-2.27813600
C	-0.61290800	-2.75423100	0.28778400
H	1.35613900	-2.17681500	0.99435100

C	-0.85632400	-2.90956000	-2.11176600
H	0.92738000	-2.44959700	-3.26233600
C	-1.40722100	-3.00813000	-0.83279000
H	-1.03409700	-2.83446900	1.28544700
H	-1.46926600	-3.10772600	-2.98553600
H	-2.45330000	-3.26740000	-0.71031900
C	-4.46885800	-0.06602800	0.29814700
C	-4.10121700	-1.14811100	1.10535800
C	-5.81233100	0.29450000	0.19269500
C	-5.07389000	-1.86283000	1.80082000
H	-3.05248900	-1.41068100	1.18637000
C	-6.78854100	-0.42217800	0.88854700
H	-6.09671600	1.13563500	-0.43427800
C	-6.42029200	-1.50163800	1.69221200
H	-4.78459900	-2.70078100	2.42888700
H	-7.83287500	-0.13592900	0.80394300
H	-7.17833400	-2.05924400	2.23496900

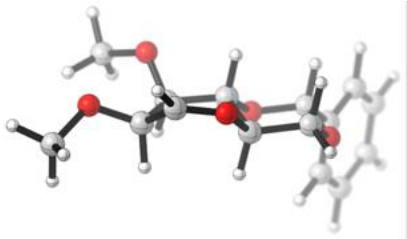
Optimized Structure of 2,3-Di-*O*-methyl-4,6-*O*-benzylidene-D-mannopyranosyl oxocarbenium ion **5b_$^4H_3$**



C	-3.28427600	-1.29767800	-0.57221800
C	-0.91485000	-1.53126300	-0.60029700
C	-0.81636800	-0.15981300	0.06905500
C	-1.79465100	0.80158500	-0.58408500
C	-3.20095100	0.18735000	-0.43879700
H	-4.25143900	-1.79501100	-0.57150700
H	-1.55521400	0.88664100	-1.65337300
H	-0.70783600	-1.45820700	-1.66906300
O	-2.29250800	-2.08065800	-0.50986500
O	-1.73762600	2.04590500	0.05823800
C	0.05218700	-2.49796300	0.07001100
H	-0.21892100	-2.63901700	1.12546000
H	0.07541700	-3.46523200	-0.43329300
O	1.34722300	-1.91928600	-0.06065700
C	-2.08040700	3.15133800	-0.77885500
H	-1.97330300	4.04551300	-0.16309500
H	-1.40204500	3.21421000	-1.63903300

H	-3.11440200	3.08765700	-1.14014800
O	0.51981500	0.27235000	-0.10292300
C	1.43730500	-0.62738300	0.52548800
H	1.18128100	-0.69671400	1.59341400
H	-1.05636400	-0.24856200	1.13854200
O	-3.56514100	0.12717500	0.94541800
C	-4.87259400	0.64383400	1.26489800
H	-5.65437100	0.12256700	0.70499900
H	-5.00326500	0.47026900	2.33249100
H	-4.90082400	1.71450700	1.04279100
H	-3.94854000	0.69918300	-1.04814300
C	2.82738900	-0.10490800	0.31370200
C	3.31877400	0.04614900	-0.98829700
C	3.62968600	0.23056000	1.40532900
C	4.60860700	0.53117800	-1.19276600
H	2.68754900	-0.21721600	-1.83089600
C	4.92299200	0.71622500	1.19963000
H	3.24519100	0.11257600	2.41473100
C	5.41244800	0.86661100	-0.09846500
H	4.98873800	0.64807800	-2.20332700
H	5.54454200	0.97567200	2.05134700
H	6.41796200	1.24426700	-0.25958900

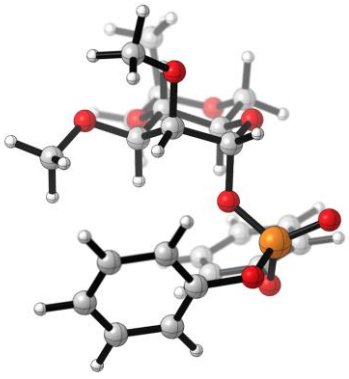
Optimized Structure of 2,3-Di-*O*-methyl-4,6-*O*-benzylidene-D-mannopyranosyl oxocarbenium ion **5b_*B*$_{2,5}$**



C	-3.15062900	1.35445700	-0.20268400
C	-0.84867900	1.60105900	0.12887300
C	-0.67938800	0.20845300	-0.48501800
C	-1.75955500	-0.77642600	-0.04466800
C	-3.04234300	0.03505400	0.45824700
H	-4.08551600	1.72632400	-0.62116600
H	-1.40285000	-1.34948900	0.81772000
H	-0.88416100	1.57250900	1.21979000
O	-2.15659400	2.12572800	-0.33630600
O	-2.07199600	-1.60187600	-1.12148500
C	0.26201300	2.51735000	-0.36597400
H	0.18507800	2.64996200	-1.45385300
H	0.23564500	3.49180600	0.12248700

O	1.48809900	1.89164400	-0.00433300
C	-2.41691500	-2.94687800	-0.77068900
H	-2.57043900	-3.47295700	-1.71421200
H	-1.59662400	-3.42034300	-0.21718400
H	-3.33342400	-2.97692900	-0.17643100
O	0.59830900	-0.27077900	-0.11662500
C	1.63810800	0.60030200	-0.57619600
H	1.56834300	0.67785500	-1.67146200
H	-0.75563100	0.31190600	-1.57830900
O	-4.19811700	-0.71612400	0.28068500
C	-5.15846000	-0.58136500	1.33755900
H	-5.53861100	0.44513200	1.40339400
H	-5.97644500	-1.25733600	1.08903500
H	-4.71604100	-0.86919500	2.29871900
H	-2.83630600	0.25914500	1.52214000
C	2.95366200	0.03161100	-0.13440300
C	3.21432900	-0.12909300	1.23155000
C	3.91523200	-0.33652300	-1.07659300
C	4.43451500	-0.65601100	1.64884800
H	2.46062800	0.16025600	1.95678400
C	5.13831700	-0.86472400	-0.65731100
H	3.70962400	-0.21017300	-2.13601400
C	5.39806100	-1.02441400	0.70440600
H	4.63609000	-0.77993100	2.70873500
H	5.88448500	-1.14960000	-1.39288200
H	6.34894800	-1.43480400	1.03154600

Optimized Structure of 2,3-Di-*O*-methyl-4,6-*O*-acetonide-α-D-mannopyranosyl diphenylphosphate **S20**

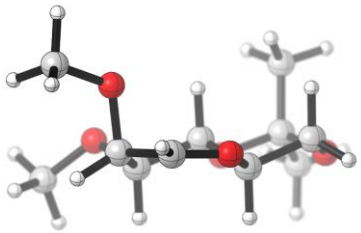


C	0.37321100	0.52860500	-1.74542800
C	-1.73801100	-0.05001400	-0.87854300
C	-1.87341600	1.29233700	-0.15642600
C	-0.49757000	1.77644500	0.26574500
C	0.36126800	1.87809200	-1.01643600
H	0.90885300	0.59229300	-2.69220300

H	-0.04777000	1.03009800	0.93647900
H	-1.31958700	-0.77549800	-0.17831800
O	-0.89503100	0.04221500	-2.03612700
O	1.06472800	-0.36520300	-0.83676300
O	-0.61423600	3.01758500	0.93844800
C	-3.12198800	-0.51910800	-1.29342000
H	-3.54713500	0.16147100	-2.04434200
H	-3.08641800	-1.52618600	-1.71412800
O	-3.93564000	-0.60217200	-0.12572100
O	1.87674900	-2.04910900	-2.68674800
C	0.50698500	3.31622400	1.76035300
H	0.27840700	4.25014400	2.27820200
H	0.67800100	2.52095700	2.49951800
H	1.42739800	3.44953200	1.17660100
O	-2.70130300	1.08179900	0.98164900
C	-4.00902700	0.58780600	0.66620800
H	-2.30884600	2.03945900	-0.83033400
O	-0.17070800	2.80826200	-1.94351800
C	0.32673600	4.13573700	-1.80260300
H	1.42547400	4.14837700	-1.83016100
H	-0.05710100	4.70214500	-2.65438300
H	-0.01730400	4.59492800	-0.87131500
H	1.39726400	2.13234900	-0.76279200
P	1.98665300	-1.59052200	-1.28697900
O	3.48983400	-1.14776500	-0.90382700
O	1.66731200	-2.66925000	-0.12569100
C	3.70950800	-0.29457900	0.19517800
C	3.92516200	1.05656800	-0.05822800
C	3.71206500	-0.81139600	1.48680800
C	4.13510300	1.91854200	1.01970100
H	3.92058900	1.41701200	-1.08145500
C	3.91950200	0.06272400	2.55678500
H	3.54581800	-1.87059200	1.64495400
C	4.12541400	1.42495000	2.32708100
H	4.30181700	2.97522700	0.83490900
H	3.91864000	-0.32611400	3.57037000
H	4.28256800	2.09924600	3.16303900
C	0.34923200	-2.84443500	0.33141300
C	0.02441600	-2.34579600	1.58937000
C	-0.58231000	-3.50262100	-0.46512900
C	-1.28041700	-2.50768800	2.05826600
H	0.77873300	-1.82587300	2.16999600
C	-1.88524300	-3.65440800	0.01576400
H	-0.29121900	-3.87567600	-1.44117800
C	-2.23659400	-3.15500500	1.27143600
H	-1.55074100	-2.11468700	3.03342300

H	-2.62506800	-4.15900800	-0.59776800
H	-3.25383000	-3.26207700	1.63231700
C	-4.60655600	0.15362400	1.99455700
H	-4.69405300	1.01165300	2.66631500
H	-5.59847600	-0.27781100	1.83714000
H	-3.95717000	-0.59696500	2.45249500
C	-4.85833800	1.65890700	-0.02491200
H	-5.87300100	1.27895800	-0.17299700
H	-4.90329100	2.55372300	0.60225200
H	-4.46078600	1.94677900	-1.00082800

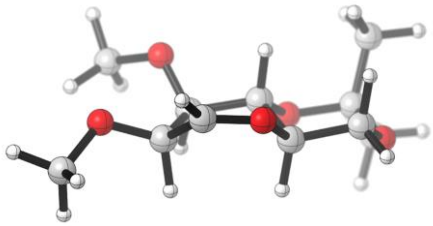
Optimized Structure of 2,3-Di-*O*-methyl-4,6-*O*-acetonide-D-mannopyranosyl oxocarbenium ion **5c_$^4H_3$**



C	-1.78652200	-1.73916900	-0.64547000
C	0.53530000	-1.22361700	-0.74461700
C	0.23028400	0.08878100	-0.02422700
C	-1.02000900	0.71772200	-0.61825000
C	-2.16356900	-0.30566000	-0.46600500
H	-2.55208000	-2.51169800	-0.63612600
H	-0.85423600	0.90583400	-1.68849000
H	0.66358900	-1.06009700	-1.81604200
O	-0.60017600	-2.17735200	-0.63329100
O	-1.32823600	1.89968500	0.06939000
C	1.78033600	-1.85956300	-0.14445500
H	1.60446400	-2.12821500	0.90459600
H	2.08146400	-2.75306600	-0.69335000
O	2.82734100	-0.91002300	-0.29835500
C	-2.04305200	2.85882600	-0.71044600
H	-2.19440300	3.72581100	-0.06569600
H	-1.46261000	3.15460900	-1.59353500
H	-3.02049100	2.47938100	-1.03407000
O	1.35088900	0.92377600	-0.22380100
C	2.58776100	0.37986900	0.27941900
H	0.05306800	-0.10216000	1.04137700
O	-2.45268000	-0.50882700	0.92268900
C	-3.84878300	-0.46182900	1.27794000
H	-4.42311100	-1.22100300	0.73884400
H	-3.88493200	-0.66255000	2.34820700
H	-4.24469100	0.53428900	1.05970600

H	-3.05011300	-0.03574200	-1.04345500
C	3.67569600	1.28313500	-0.27225400
H	3.54573000	2.29916700	0.10843400
H	4.65718800	0.91157200	0.03210100
H	3.61838800	1.29698000	-1.36348200
C	2.59560300	0.32619200	1.80713400
H	3.57573100	-0.01533100	2.14985300
H	2.40884900	1.32612800	2.20729500
H	1.84282300	-0.35010300	2.21817200

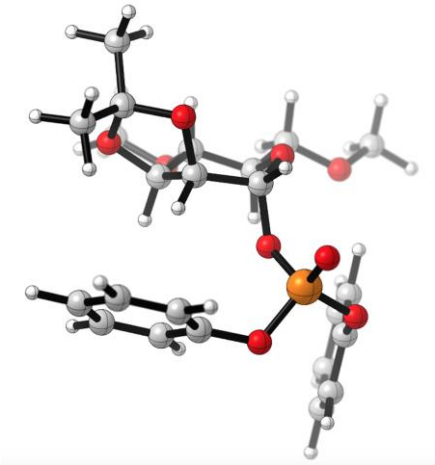
Optimized Structure of 2,3-Di-*O*-methyl-4,6-*O*-acetonide-D-mannopyranosyl oxocarbenium ion **5c_*B*$_{2,5}$**



C	-1.68170300	-1.61916200	0.55418800
C	0.52472400	-1.34440500	-0.17603600
C	0.38736600	0.13509500	0.19018800
C	-0.97349100	0.71945900	-0.18309800
C	-2.04476100	-0.46241700	-0.29494700
H	-2.40351300	-2.12595500	1.19399500
H	-0.91594800	1.17682600	-1.17618200
H	0.32393900	-1.53326900	-1.23293400
O	-0.50525600	-2.08173400	0.59972600
O	-1.33841400	1.64408200	0.79204200
C	1.90427000	-1.84630400	0.22373400
H	2.01877700	-1.81283500	1.31403700
H	2.07709900	-2.86728300	-0.11894900
O	2.84309400	-1.02038000	-0.45111800
C	-2.09173000	2.76294700	0.31171100
H	-2.24458800	3.41412300	1.17386500
H	-1.52718500	3.30282300	-0.45865000
H	-3.05787700	2.44590800	-0.08843700
O	1.40745100	0.84330600	-0.47734600
C	2.74357600	0.38228800	-0.18191000
H	0.47770200	0.22095000	1.28139400
O	-3.32081400	0.00212300	0.00291700
C	-4.36195400	-0.58299800	-0.79105400
H	-4.44141400	-1.66203000	-0.61209300
H	-5.28631000	-0.09407400	-0.48389800
H	-4.18094600	-0.40240500	-1.85751500
H	-1.95468700	-0.82766800	-1.33548200

C	3.14325200	0.72027600	1.25394900
H	4.17515200	0.40271600	1.42455000
H	3.07545600	1.80077500	1.40415700
H	2.51374200	0.23479300	2.00307700
C	3.63500000	1.06059200	-1.20573900
H	3.57968400	2.14544400	-1.08715500
H	4.67026400	0.73949100	-1.06767200
H	3.30485200	0.79027700	-2.21178500

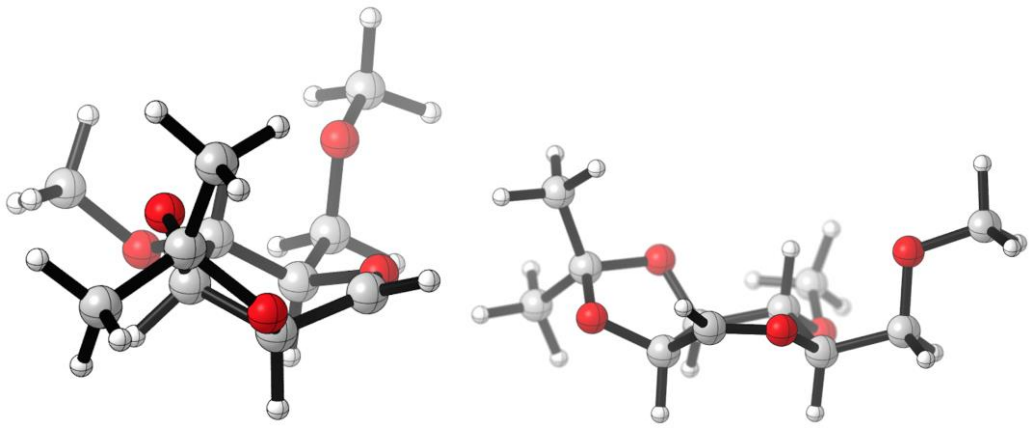
Optimized Structure of 2,3-*O*-Isopropylidene-4,6-di-*O*-methyl-α-D-mannopyranosyl diphenylphosphate **S21**



C	0.41425700	0.23787700	-1.41266500
C	-0.18391700	2.14371200	-0.12941400
C	1.18789200	2.23617700	0.54828200
C	1.84671400	0.84811300	0.64128400
C	1.71463400	0.02975700	-0.64493000
H	0.51078600	-0.08946800	-2.44827300
H	1.44148800	0.32279700	1.51016900
H	-0.85758900	1.52775500	0.47573500
O	-0.03273000	1.54415100	-1.43326900
O	-0.57229800	-0.58653500	-0.73315600
O	3.26457700	0.94604500	0.78847700
C	-0.81252000	3.50611000	-0.33939700
H	-0.77669900	4.06033900	0.60778700
H	-0.23003500	4.06591100	-1.08860200
O	-0.82733300	-2.23600700	-2.74601800
H	1.83094200	2.89345900	-0.05429900
O	2.80348900	0.52013400	-1.41805000
C	3.88347700	0.72261600	-0.49922500
H	1.83435300	-1.03864500	-0.43683700
P	-1.28751300	-1.85487800	-1.39401100
O	-1.13384300	-2.96261900	-0.22173200

O	-2.86337900	-1.55595600	-1.33920900
C	0.11559100	-3.09132700	0.40970600
C	1.15186200	-3.75848600	-0.23625300
C	0.27569800	-2.52263500	1.66996200
C	2.39215500	-3.84670600	0.40186200
H	0.98874200	-4.18348100	-1.22060000
C	1.51845000	-2.61963600	2.29710900
H	-0.55711900	-2.00131700	2.12931000
C	2.57816000	-3.27520200	1.66292000
H	3.21194800	-4.35881600	-0.09203900
H	1.65975900	-2.17465000	3.27710700
H	3.54524400	-3.34135400	2.15115700
C	-3.44023400	-0.92196200	-0.21848000
C	-3.42953100	0.46716100	-0.15738200
C	-4.01818700	-1.70495000	0.77451600
C	-4.01611600	1.09115400	0.94432100
H	-2.95285100	1.05103500	-0.93507800
C	-4.61060000	-1.06606700	1.86670000
H	-3.99664100	-2.78576500	0.69006300
C	-4.60873000	0.32851600	1.95412900
H	-3.99142600	2.17427700	1.00534100
H	-5.06783900	-1.66232600	2.65042500
H	-5.06465700	0.81823400	2.80923800
C	4.65501600	1.95765600	-0.93329700
H	5.45245900	2.16993200	-0.21563100
H	5.10540900	1.79569700	-1.91715700
H	3.98594400	2.82020700	-0.98672800
C	4.75202100	-0.52704100	-0.39936300
H	5.23922800	-0.72767000	-1.35830600
H	5.52351000	-0.38510900	0.36345600
H	4.14518300	-1.39244200	-0.11875500
O	-2.14924100	3.33405100	-0.77355800
O	0.97389600	2.79946800	1.83132300
C	2.14626900	3.32295900	2.44682100
H	1.81820400	3.83056800	3.35684400
H	2.86062300	2.53340000	2.70349700
H	2.64599400	4.04643900	1.78722400
C	-2.80229300	4.56953600	-1.00688700
H	-2.29995100	5.14545500	-1.79831700
H	-3.82234000	4.33861800	-1.32188000
H	-2.83549100	5.18425100	-0.09508400

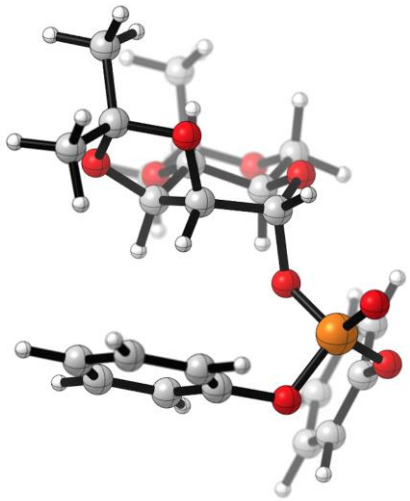
Optimized Structure of 2,3-*O*-Isopropylidene-4,6-di-*O*-methyl-D-mannopyranosyl oxocarbenium ion **5d_*B*$_{2,5}$**



C	-0.23652900	-1.98752500	-0.42871200
C	1.53411700	-0.45962500	-0.93645100
C	0.68456000	0.63776300	-0.28018400
C	-0.80969100	0.46163600	-0.59026200
C	-1.21946000	-0.99854000	-0.94187900
H	-0.54828800	-2.94442800	-0.00948000
H	-1.08555100	1.12209700	-1.41907300
H	1.42567700	-0.47054500	-2.02264500
O	1.00216600	-1.78810300	-0.46017600
O	-1.58148900	0.69733600	0.57065300
C	2.99074800	-0.44150600	-0.54079400
H	3.49641700	-1.32364700	-0.96031300
H	3.43677900	0.45594600	-0.99239200
O	3.06369600	-0.41798600	0.86393900
C	4.40195400	-0.35006600	1.33856300
H	4.34945500	-0.33271800	2.42860100
H	4.98280900	-1.22495700	1.01526300
H	4.90261400	0.56087000	0.98222800
O	1.20071300	1.84416700	-0.78194300
C	0.85390900	2.97742800	0.01750700
H	1.31826900	3.84180200	-0.45869200
H	-0.23248100	3.12162400	0.05783400
H	1.24060700	2.86393200	1.03815800
H	0.81977500	0.56300700	0.80622100
O	-2.47066800	-1.20243300	-0.35036600
H	-1.25180600	-1.14215900	-2.03553200
C	-2.80645700	-0.02545800	0.45044900
C	-3.23072900	-0.48197800	1.83040800
H	-3.44487800	0.38642400	2.45935400
H	-4.13354900	-1.09395700	1.75942300
H	-2.43055300	-1.06932100	2.28803200
C	-3.86029100	0.78128800	-0.29328000
H	-4.75879800	0.17575900	-0.43913900

H	-4.12348300	1.67025600	0.28674500
H	-3.49114900	1.09565600	-1.27362700

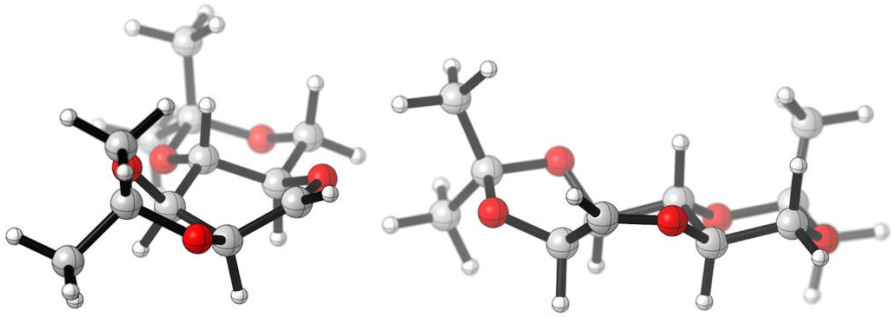
Optimized Structure of 2,3:4,6-di-*O*-Isopropylidene-α-D-mannopyranosyl diphenylphosphate **2f**



C	0.13529000	0.54392500	-1.55499600
C	-1.50085100	-0.94469500	-0.78582900
C	-2.27872500	0.13921300	-0.04856900
C	-1.33335600	1.21388200	0.47936900
C	-0.34169100	1.64795800	-0.60888000
H	0.55551100	0.95958700	-2.47112800
H	-0.83665000	0.86165600	1.38713700
H	-0.76583400	-1.39837700	-0.11387300
O	-0.83770300	-0.37314400	-1.92345600
O	1.16827900	-0.15029900	-0.81196700
O	-2.01813900	2.42948400	0.77009200
C	-2.47230900	-2.01716200	-1.24809400
H	-3.15636000	-1.60926100	-2.00446000
H	-1.95148000	-2.87352700	-1.68234800
O	-3.16671500	-2.50669700	-0.10328300
O	3.06776800	0.31803800	-2.55458100
O	-2.97787600	-0.45152800	1.03996200
C	-3.86167100	-1.51597800	0.66213300
H	-2.97217800	0.60756800	-0.75728600
O	-1.10952500	2.60070300	-1.33299400
C	-1.86685400	3.32617400	-0.35526500
H	0.54082100	2.11635200	-0.16088200
P	2.67855800	-0.34624100	-1.29363600
O	3.49649500	0.07250300	0.04057500
O	2.91122600	-1.93755000	-1.32791600
C	3.04764300	1.17737300	0.78637600
C	3.33458700	2.46719800	0.35172500
C	2.30761200	0.93342000	1.93989000

C	2.85320500	3.54747500	1.09667900
H	3.91005200	2.61551600	-0.55566000
C	1.83470500	2.02053400	2.67557000
H	2.09588500	-0.08955600	2.23193400
C	2.10195900	3.32662800	2.25344300
H	3.06371700	4.56003300	0.76707600
H	1.25008500	1.84571700	3.57334000
H	1.72625900	4.16914300	2.82534400
C	2.26010000	-2.76530700	-0.39098100
C	1.05462300	-3.35393400	-0.75956700
C	2.83481300	-2.97622900	0.85763100
C	0.39847200	-4.17383800	0.15986900
H	0.64115600	-3.15214700	-1.74172900
C	2.16878500	-3.80109500	1.76764600
H	3.77430600	-2.49687400	1.10753700
C	0.95232300	-4.39516800	1.42361400
H	-0.55021700	-4.62839500	-0.10847000
H	2.60307800	-3.97403500	2.74742100
H	0.43715500	-5.02972500	2.13789200
C	-5.08373100	-0.98234000	-0.09059000
H	-5.60400500	-0.24916800	0.53192200
H	-4.82277300	-0.49966700	-1.03508400
H	-5.76596100	-1.80818500	-0.31023000
C	-4.24728600	-2.20390900	1.96096100
H	-4.76663400	-1.50140500	2.61793200
H	-4.90550200	-3.05198200	1.75524900
H	-3.34444900	-2.56345500	2.46166900
C	-3.22509800	3.65463300	-0.95210400
H	-3.84337800	4.16797500	-0.21032600
H	-3.10740900	4.30924000	-1.82080900
H	-3.73238300	2.73812500	-1.26397600
C	-1.10189000	4.55838400	0.11608000
H	-0.97582200	5.26510100	-0.70962800
H	-1.65306200	5.05362700	0.92111900
H	-0.11670800	4.27479800	0.49676600

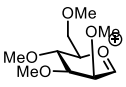
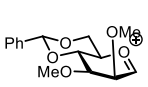
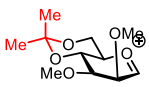
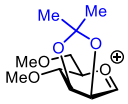
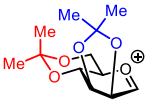
Optimized Structure of 2,3:4,6-di-*O*-Isopropylidene- D-mannopyranosyl oxocarbenium ion **5e_*B*$_{2,5}$**



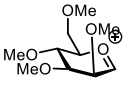
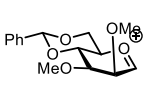
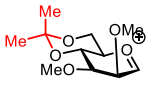
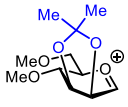
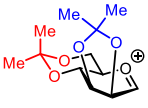
C	1.10387900	2.15103600	0.10805600
C	-1.06356500	1.34844100	-0.34972300
C	-0.54923700	-0.04032400	0.04752400
C	0.82748700	-0.29547000	-0.54755800
C	1.64825500	1.02933800	-0.70350000
H	1.75380800	2.86365600	0.61520600
H	0.72724500	-0.78189200	-1.52307300
H	-1.05065200	1.49515900	-1.43082500
O	-0.13225000	2.35930400	0.22958900
O	1.63029700	-1.02916800	0.34859000
C	-2.45230500	1.57355400	0.22808100
H	-2.40966300	1.59367700	1.32380400
H	-2.89032600	2.50712300	-0.12701000
O	-3.26525400	0.52036000	-0.27067300
O	-1.46984000	-0.99147400	-0.43336600
C	-2.82380100	-0.80579300	0.03679400
H	-0.45067900	-0.07454900	1.14056900
O	2.95100500	0.72609700	-0.30101400
C	2.99510200	-0.66873900	0.13349300
H	1.60476900	1.38093900	-1.75017300
C	-2.94117400	-1.11914800	1.52767000
H	-2.61328700	-2.14582100	1.70921300
H	-2.34285000	-0.45662300	2.15723300
H	-3.98574100	-1.02127300	1.83412700
C	-3.67177600	-1.72880200	-0.81853300
H	-3.36408600	-2.76603200	-0.66565000
H	-4.72436200	-1.62516600	-0.54429900
H	-3.54612100	-1.46637500	-1.87184800
C	3.72059400	-0.73635000	1.46043000
H	3.73428800	-1.76736100	1.82408300
H	4.75145900	-0.39379900	1.34006600
H	3.21051300	-0.10308000	2.19046300
C	3.62687900	-1.50458100	-0.96979500
H	4.64887100	-1.16360600	-1.15546400
H	3.65404200	-2.55535600	-0.66816000
H	3.05907500	-1.41954000	-1.90090600

Table of $\Delta\Delta G_{oxocarbenium–phosphate}$ in Different PCM Solvation Models at Different Levels of Theory

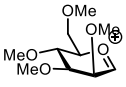
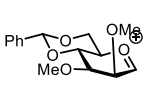
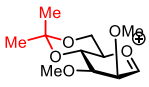
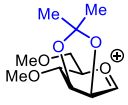
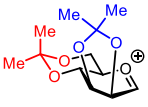
B3LYP/6-311+G(d,p), PCM(water)

	 **5a**	 **5b**	 **5c**	 **5d**	 **5e**
$\Delta\Delta G_{oxocarbenium-phos}$ **(kcal/mol)**	0 ($^4H_3$) (defined)	4.4 ($^4H_3$) 3.2 ($B_{2,5}$)	3.4 ($^4H_3$) 2.6 ($B_{2,5}$)	–1.3 ($B_{2,5}$)	1.5 ($B_{2,5}$)

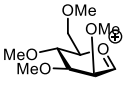
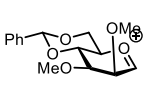
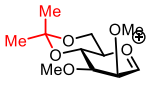
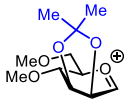
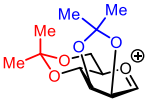
B3LYP/6-311+G(d,p), PCM(ether)

	 **5a**	 **5b**	 **5c**	 **5d**	 **5e**
$\Delta\Delta G_{oxocarbenium-phos}$ **(kcal/mol)**	0 ($^4H_3$) (defined)	4.5 ($^4H_3$) 3.4 ($B_{2,5}$)	3.3 ($^4H_3$) 2.3 ($B_{2,5}$)	–1.3 ($B_{2,5}$)	2.1 ($B_{2,5}$)

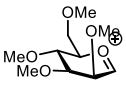
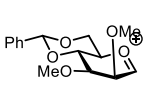
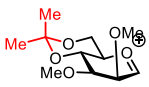
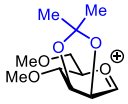
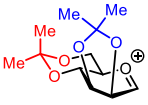
M062X/6-311+G(d,p), PCM(water)

	 **5a**	 **5b**	 **5c**	 **5d**	 **5e**
$\Delta\Delta G_{oxocarbenium-phos}$ **(kcal/mol)**	0 ($^4H_3$) (defined)	5.0 ($^4H_3$) 2.5 ($B_{2,5}$)	4.1 ($^4H_3$) 2.0 ($B_{2,5}$)	–2.7 ($B_{2,5}$)	0 ($B_{2,5}$)

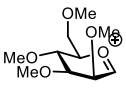
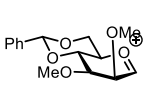
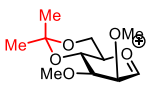
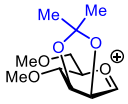
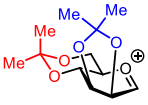
M062X/6-311+G(d,p), PCM(ether)

	 **5a**	 **5b**	 **5c**	 **5d**	 **5e**
$\Delta\Delta G_{oxocarbenium-phos}$ **(kcal/mol)**	0 ($^4H_3$) (defined)	4.8 ($^4H_3$) 2.5 ($B_{2,5}$)	3.8 ($^4H_3$) 1.6 ($B_{2,5}$)	–2.9 ($B_{2,5}$)	0.4 ($B_{2,5}$)

ωB97-xD/6-311+G(d,p), PCM(water)

	 **5a**	 **5b**	 **5c**	 **5d**	 **5e**
$\Delta\Delta G_{oxocarbenium-phos}$ **(kcal/mol)**	0 ($^4H_3$) (defined)	5.0 ($^4H_3$) 3.2 ($B_{2,5}$)	4.1 ($^4H_3$) 2.8 ($B_{2,5}$)	–1.8 ($B_{2,5}$)	1.1 ($B_{2,5}$)

ωB97-xD/6-311+G(d,p), PCM(ether)

	 **5a**	 **5b**	 **5c**	 **5d**	 **5e**
$\Delta\Delta G_{oxocarbenium-phos}$ **(kcal/mol)**	0 ($^4H_3$) (defined)	5.0 ($^4H_3$) 3.5 ($B_{2,5}$)	3.8 ($^4H_3$) 2.4 ($B_{2,5}$)	–1.9 ($B_{2,5}$)	1.7 ($B_{2,5}$)

Chapter 3

Catalyst-Controlled Stereo- and Site-Selective Glycosylation Catalyzed by Bis-Thioureas

3.1 Introduction

Protecting groups have been long used to distinguish otherwise identical functional groups in organic synthesis.[1] While their installment is operationally simple and reliable, the practice of protecting group manipulation is inelegant as it requires multi-step protection-deprotection sequence. Therefore, protecting-group free synthesis remains a long-sought goal in the field of

[1] (a) Schelhaas, M.; Waldmann, H. Protecting Group Strategies in Organic Synthesis. *Angew. Chem. Int. Ed*. **1996**, *35*, 2056–2083. (b) Kocienski, P. J. Protecting Groups, 3 ed.; Georg Thieme Verlag: New York, 2005. (c) Wutz, P. G. M. Greene's Protective Groups in Organic Synthesis, 5 ed.; John Wiley & Sons, Inc.: Hoboken, NJ, 2014.

organic chemistry.[2] Synthetic carbohydrate chemistry epitomizes the challenges and advantages of developing a protecting-group free synthetic approach. The difficulty of controlling the reactivity of multiple similarly reactive hydroxyl groups is rendered more challenging by the need to control the stereoselectivity of addition into the anomeric center of a second saccharide.

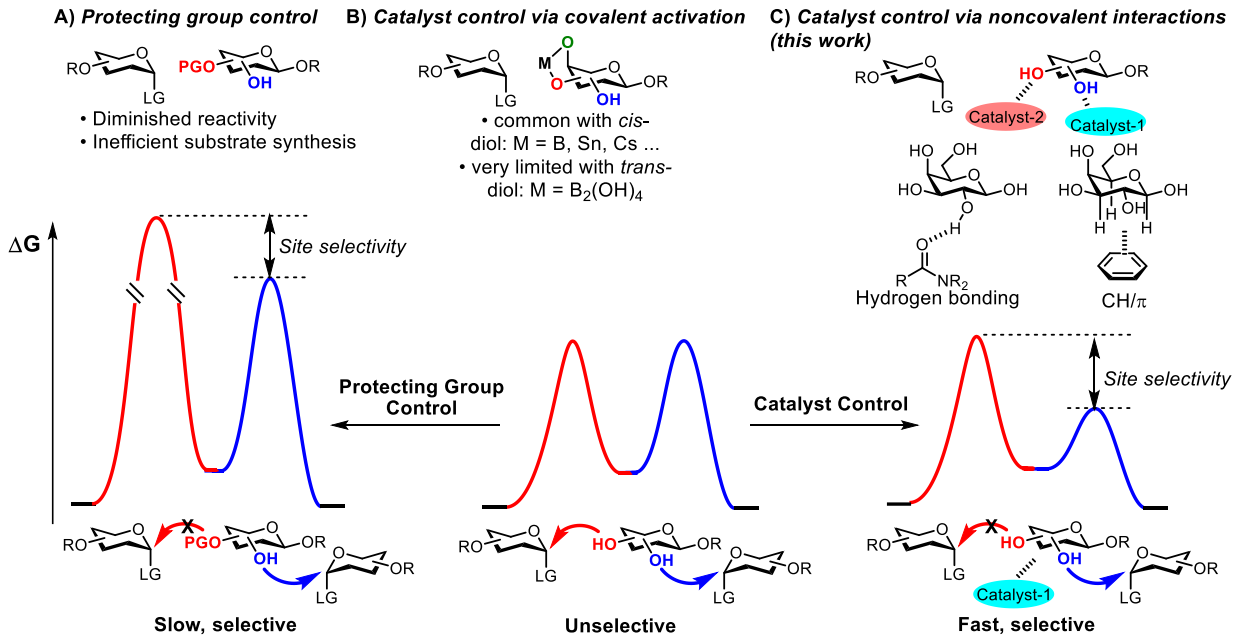


Figure 3.1 Three distinct strategies to control site selectivity of glycosylations and their implications for the rate of glycosylation.

The challenge associated with the stereo- and site-control in chemical glycosylation has traditionally been tackled using specialized protecting group (Figure 3.1A). Despite its broad use in chemical oligosaccharides synthesis, several limitations remain to be addressed. Protecting groups can deactivate unprotected hydroxyl groups by increasing steric congestion and reducing

[2] (a) Fernandes, R. A. Protecting-Group-Free Organic Synthesis: Improving Economy and Efficiency; John Wiley & Sons, Inc.: Hoboken, NJ, 2018. (b) Young, I. S.; Baran, P. S. Protecting-group-free synthesis as an opportunity for invention. *Nat. Chem.* **2009**, *1*, 193–205. (c) Hoffmann, R. W. Protecting-Group-Free Synthesis. *Synthesis* **2006**, *21*, 3531–3541.

their nucleophilicity via electronic perturbation, decreasing the rate of glycosylation.[3] Thus, careful optimization of protecting groups is often necessary to achieve high reactivity and selectivity, and the choice of protecting groups can be substrate-dependent.[4] Moreover, the installment of specific protecting groups requires multi-step syntheses from unfunctionalized monomers, rendering the overall glycosylation inefficient. An alternative approach that can potentially address these limitations relies on the use of small molecule catalysts to control both the stereo- and site selectivity of glycosylation with minimally protected substrates, obviating the need for specifically protected reaction partners.

As described in Chapter 1, current catalyst-controlled site selective approaches employ reagents that can form covalent cyclic adducts with hydroxyl groups and activate them toward glycosylation (Figure 3.1B).[5] Catalytically formed cyclic adducts have commonly been applied to functionalize *cis*-diols due to the formation of more thermodynamically stable *cis*-adducts. Although glycosylation of *trans*-diols was recently realized using a diboron catalyst for the synthesis of α-glycosides, the site selectivity was controlled by the size of protecting groups on

[3] (a) van der Vorm, S.; van Hengst, J. M. A.; Bakker, M.; Overkleeft, H. S.; van der Marel, G. A.; Codée, J. D. C. Mapping the Relationship between Glycosyl Acceptor Reactivity and Glycosylation Stereoselectivity. *Angew. Chem. Int. Ed.* **2018**, *57*, 8240–8244. (b) van der Vorm, S.; Hansen, T.; Overkleeft, H. S.; van der Marel, G. A.; Codée, J. D. C. The influence of acceptor nucleophilicity on the glycosylation reaction mechanism. *Chem. Sci.* **2017**, *8*, 1867–1875. For reviews, see: (c) van der Vorm, S.; Hansen, T.; van Hengst, J. M. A.; Overkleeft, H. S.; van der Marel, G. A.; Codée, J. D. C. Acceptor reactivity in glycosylation reactions. *Chem. Soc. Rev.* **2019**, *48*, 4688–4706. (d) Green, L. G.; Ley, S. V. Protecting Groups: Effects on Reactivity, Glycosylation Stereoselectivity, and Coupling Efficiency. In *Carbohydrates in Chemistry and Biology*, Ernst, B.; Hart, G. W.; Sinaý, P., Eds.; Wiley-VCH.: Weinheim, Germany, 2000.

[4] (a) Guo, J.; Ye, X. S. Protecting groups in carbohydrate chemistry: influence on stereoselectivity of glycosylations. *Molecules* **2010,** *15*, 7235–7265. (b) Volbeda, A. G.; van der Marel, G. A.; Codée, J. D. C. Protecting Group Strategies in Carbohydrate Chemistry. In *Protecting Groups Strategies and Applications in Carbohydrate Chemistry*, Vidal, S., Eds.; Wiley-VCH.: Weinheim, Germany, 2019.

[5] For reviews, see: (a) Bati, G.; He, J. X.; Pal, K. B.; Liu, X. W. Stereo- and regioselective glycosylation with protection-less sugar derivatives: an alluring strategy to access glycans and natural products. *Chem. Soc. Rev.* **2019**, *48*, 4006–4018. (b) Ding, Y.; Vara Prasad, C. V. N. S.; Wang, B. Glycosylation on Unprotected or Partially Protected Acceptors. *Eur. J. Org. Chem*. **2020**, 1784–1801.

the nucleophiles rather than the catalyst.[6] Therefore, a general method for catalyst-controlled glycosylation of *trans*-diols to generate β-glycosides is still lacking.

We proposed that a more general and fundamentally different catalyst-controlled approach, which is not constrained by the inherent stereochemical relationship of substrates, would take advantage of noncovalent interactions to selectively stabilize the pathway to major product (Figure 3.1C). Carbohydrates can engage in multiple noncovalent interactions, such as hydrogen-bonding and CH/π interactions. CH/π interactions between carbohydrates and electron-rich aromatic protein side chains have been evidenced in noncovalently bound carbohydrate-protein complexes.[7] Such interactions are pivotal to saccharide recognition and have been exploited to design synthetic receptors for carbohydrate binding.[8] Careful design of catalysts capable of harnessing such interactions could enable site selective glycosylation at hydroxyl groups previously inaccessible by strategies that rely on the catalytic formation of cyclic adducts. Although attractive noncovalent interactions have been utilized in site selective protection of carbohydrates,[9] examples of catalyst-

[6] Tomita, S.; Tanaka, M.; Inoue, M.; Inaba, K.; Takahashi, D.; Toshima, K. Diboron-Catalyzed Regio- and 1,2-*cis*-α-Stereoselective Glycosylation of *trans*-1,2-Diols. *J. Org. Chem.* **2020**, *85*, 16254–16262.

[7] (a) Hudson, K. L.; Bartlett, G. J.; Diehl, R. C.; Agirre, J.; Gallagher, T.; Kiessling, L. L.; Woolfson, D. N. Carbohydrate-Aromatic Interactions in Proteins. *J. Am. Chem. Soc.* **2015**, *137*, 15152–15160. (b) Asensio, J. L.; Arda, A.; Canada, F. J.; Jimenez-Barbero, J. Carbohydrate-Aromatic Interactions. *Acc. Chem. Res*. **2013**, *46*, 946–954. (c) Screen, J.; Stanca-Kaposta, E. C.; Gamblin, D. P.; Liu, B.; Macleod, N. A.; Snoek, L. C.; Davis, B. G.; Simons, J. P. IR-spectral signatures of aromatic-sugar complexes: probing carbohydrate-protein interactions. *Angew. Chem. Int. Ed.* **2007**, *46*, 3644–3648.

[8] (a) Ferrand, Y.; Crump, M. P.; Davis, A. P. A Synthetic Lectin Analog for Biomimetic Disaccharide Recognition. *Science* **2007**, *318*, 619–622. (b) Ke, C.; Destecroix, H.; Crump, M. P.; Davis, A. P. A simple and accessible synthetic lectin for glucose recognition and sensing. *Nat. Chem*. **2012**, *4*, 718–723. (c) Barwell, N. P.; Davis, A. P. Substituent Effects in Synthetic Lectins - Exploring the Role of CH−π Interactions in Carbohydrate Recognition. *J. Org. Chem*. **2011**, *76*, 6548–6557.

[9] (a) Xiao, G.; Cintron-Rosado, G. A.; Glazier, D. A.; Xi, B. M.; Liu, C.; Liu, P.; Tang, W. Catalytic Site-Selective Acylation of Carbohydrates Directed by Cation-n Interaction. *J. Am. Chem. Soc.* **2017**, *139*, 4346–4349. (b) Kawabata, T.; Muramatsu, W.; Nishio, T.; Shibata, T.; Schedel, H. A Catalytic One-Step Process for the Chemo- and Regioselective Acylation of Monosaccharides. *J. Am. Chem. Soc*. **2007**, *129*, 12890–12895. For a review, see: (c) Dimakos, V.; Taylor, M. S. Site-Selective Functionalization of Hydroxyl Groups in Carbohydrate Derivatives. *Chem. Rev.* **2018**, *118*, 11457–11517.

controlled glycosylation, where both stereo- and site selectivity are controlled by noncovalent interactions, remain scarce and suffer from low levels of stereo- and site selectivity.[10]

3.2 Catalyst Optimization

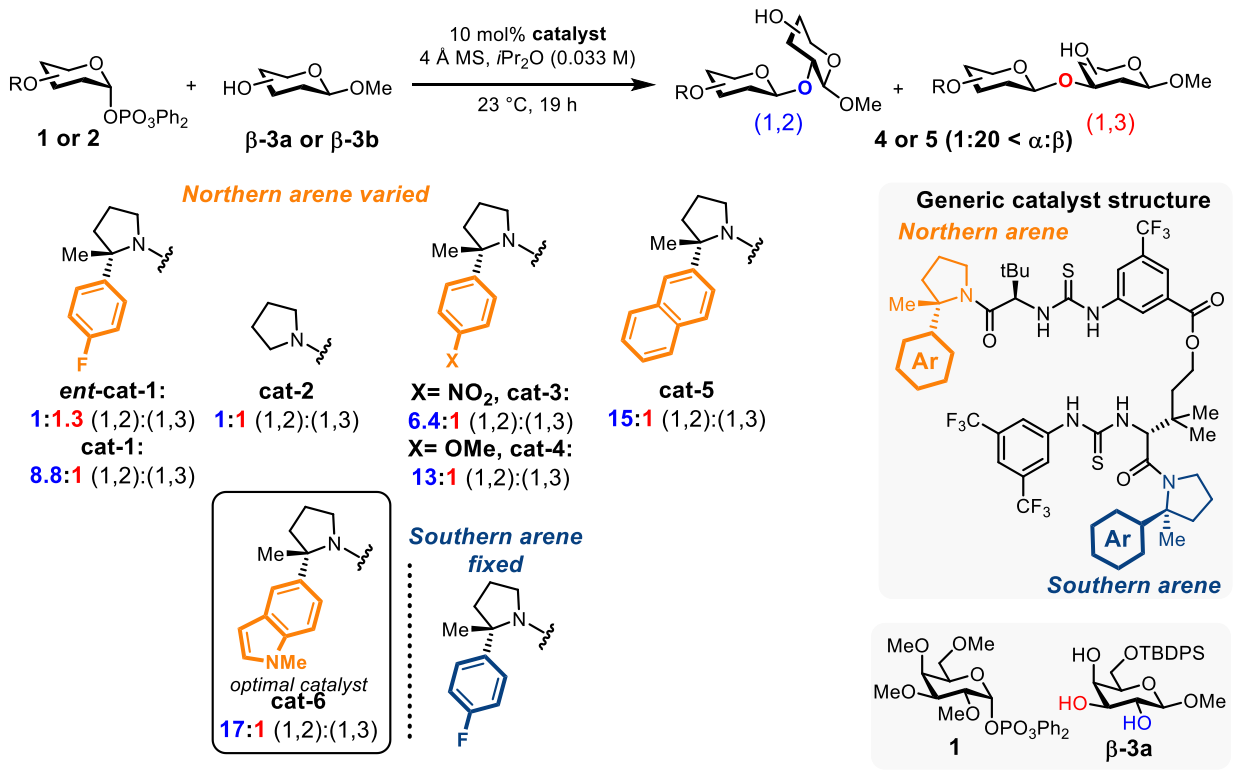


Figure 3.2 Effects of the electronic nature of "northern" arenes on site selectivity in galactosylation.

With the goal of developing a catalyst-controlled stereo- and site selective method for β-1,2-*trans* and β-1,2-*cis* glycosylations, we hypothesized that our recently reported stereospecific β-glycosylation approach catalyzed by precisely designed bis-thiourea derivatives could be applied to selectively functionalize minimally protected nucleophiles containing *trans*-diols. Bis-thiourea derivatives ***ent*-cat-1** and **cat-1** have been shown to catalyze highly β-selective

[10] (a) Lee, J.; Borovika, A.; Khomutnyk, Y.; Nagorny, P. Chiral phosphoric acid-catalyzed desymmetrizative glycosylation of 2-deoxystreptamine and its application to aminoglycoside synthesis. *Chem. Commun*. **2017**, *53*, 8976−8979. (b) Tay, J.-H.; Argüelles, A. J.; DeMars, M. D., II; Zimmerman, P. M.; Sherman, D. H.; Nagorny, P. Regiodivergent glycosylations of 6-deoxy-erythronolide B and oleandomycin-derived macrolactones enabled by chiral acid catalysis. *J. Am. Chem. Soc*. **2017**, *139*, 8570−8578.

glycosylation reactions with pyranosyl phosphates through a dual general base/general acid activation mode, which allows for stereospecific couplings with a variety of protic nucleophiles.[11] ***Ent*-cat-1** catalyzed galactosylation of **β-3a** with poor site selectivity (1:1.3 (1,2):(1,3)), slightly favoring the (1,3)-product; however, a switch in site preference and a dramatic increase in site selectivity (8.8:1 (1,2):(1,3)) were observed in galactosylation catalyzed by **cat-1** (Figure 3.2). The importance of catalyst stereochemistry points to precise catalyst-substrate interactions in the catalytic glycosylation event. The preference for (1,2)-glycosylation achieved with **cat-1** is in stark contrast to and complementary to the selectivity obtained with current cyclic adduct activation methods, where (1,3)-glycosylation is observed due to the formation of adduct between catalysts and the C3,C4-*cis*-diol.

The unique site selectivity prompted us to evaluate different bis-thiourea derivatives in order to identify highly (1,2)-selective catalysts. We hypothesized that altering the aryl-pyrrolidine and amide moieties of the catalyst might influence the site selectivity of a glycosylation reaction because the general bases are involved in nucleophile activation. While β-selectivity was high universally (<1:20 α:β), we observed that the site selectivity of galactosylation was highly responsive to changes made in the "northern" aryl pyrrolidine amides (Figure 3.2). The simple pyrrolidine catalyst without the “northern” arene (**cat-2**) promoted unselective galactosylation, indicating that the aryl substituent could serve as an important point of contact between catalyst and nucleophile in the selectivity-determining step. Therefore, different “northern” aryl substituents were assessed, revealing that site selectivity is sensitive to the electronic nature of

[11] (a) Levi, S. M.; Li, Q.; Rötheli, A. R.; Jacobsen, E. N. Catalytic Activation of Glycosyl Phosphates for Stereoselective Coupling Reactions. *Proc. Natl. Acad. Sci. U. S. A*. **2019**, *116*, 35−39. (b) : Li, Q.; Levi, S. M.; Jacobsen, E. N. Highly Selective β-Mannosylations and β-Rhamnosylations Catalyzed by Bis-thiourea. *J. Am. Chem. Soc.* **2020**, *142*, 11865–11872.

arenes (**cat-1,3–6**). Site selectivity improved with increasing electron density of arenes (6.1–17:1 (1,2):(1,3)), with the 5-*N*-methyl indole catalyst (**cat-6**) being optimal catalyst for site selective galactosylation. The positive correlation between site selectivity and the electron density of arenes suggests that attractive noncovalent interactions influenced by the electronic properties of the substituents may play a critical role in controlling site selectivity.

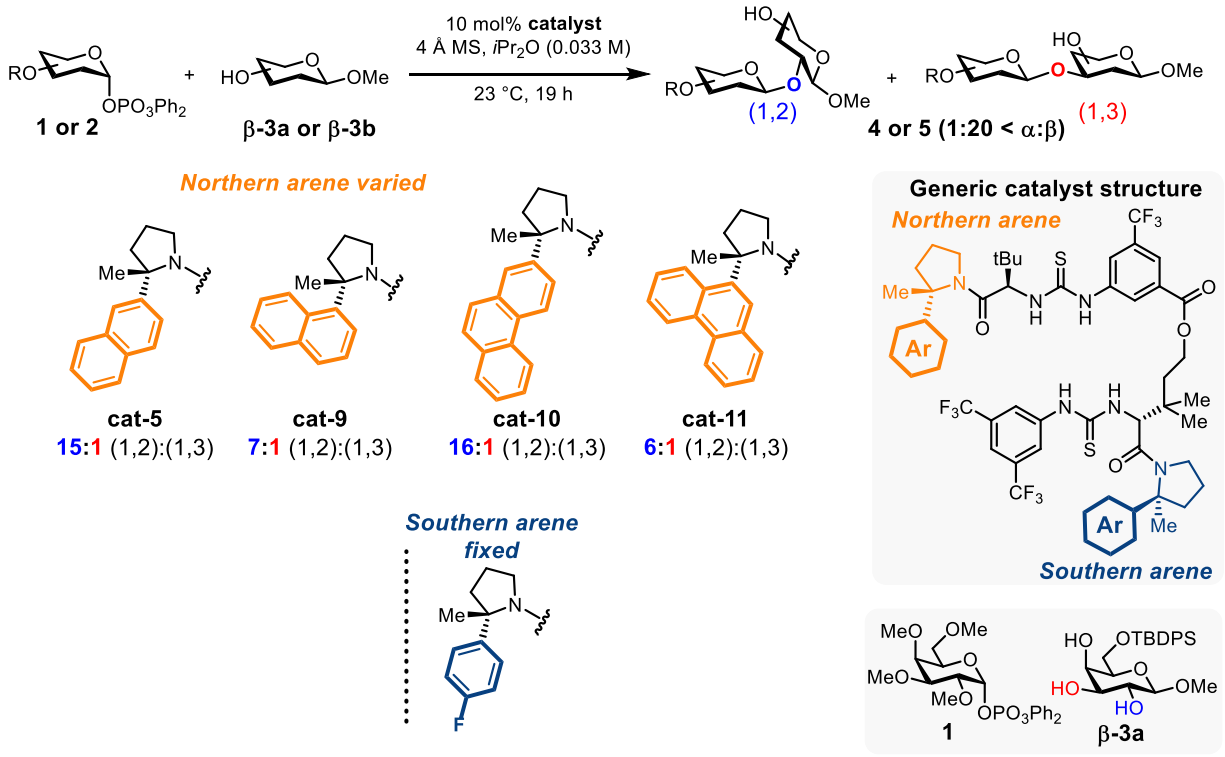


Figure 3.3 Effects of the disposition of "northern" arene on site selectivity in galactosylation.

The effects of the disposition of "northern" arene on site selectivity was also investigated (Figure 3.3). Catalysts bearing *ortho*-fused arenes (**cat-9** and **cat-11**) promoted galactosylation with lower site selectivity than catalysts bearing arene without *ortho*-substitution (**cat-5** and **cat-10**). The sensitivity to the spatial disposition of the aryl group is consistent with a highly ordered network of attractive non-covalent interactions in the selectivity-determining transition state.

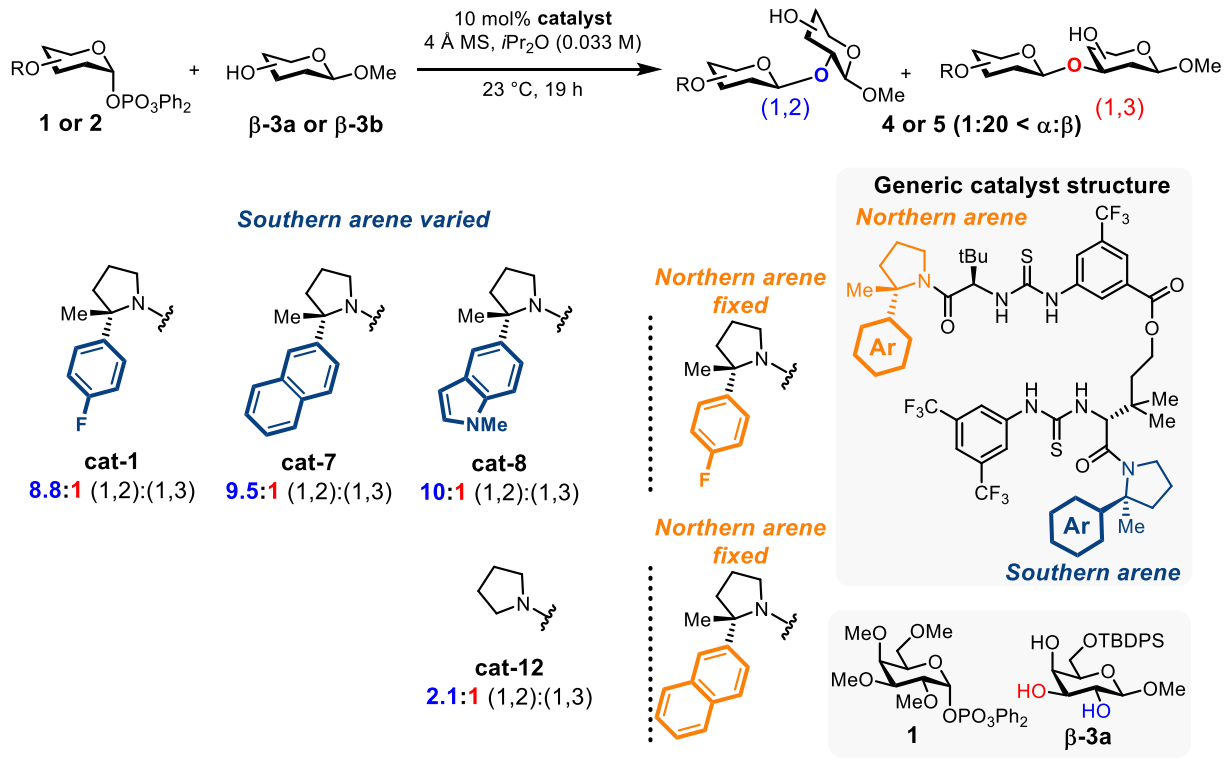


Figure 3.4 Effects of the electronic nature of "southern" arenes on site selectivity in galactosylation.

While site selective galactosylation was sensitive to changes in the "northern" arene, variation of "southern" arene (**cat-1,7–8**) had a much weaker influence on site selectivity (8.8–10:1 (1,2):(1,3)), indicating that only the "northern" aryl pyrrolidine amide is involved in nucleophile activation (Figure 3.4). Replacing the "southern" arene with pyrrolidine (**cat-12**) as an attempt to simplify catalyst synthesis, however, resulted in diminished site selectivity (2.1:1 (1,2):(1,3)) presumably because the fully substituted "southern" aryl pyrrolidine rigidifies the conformation of catalyst to the active conformation (Figure 3.4).

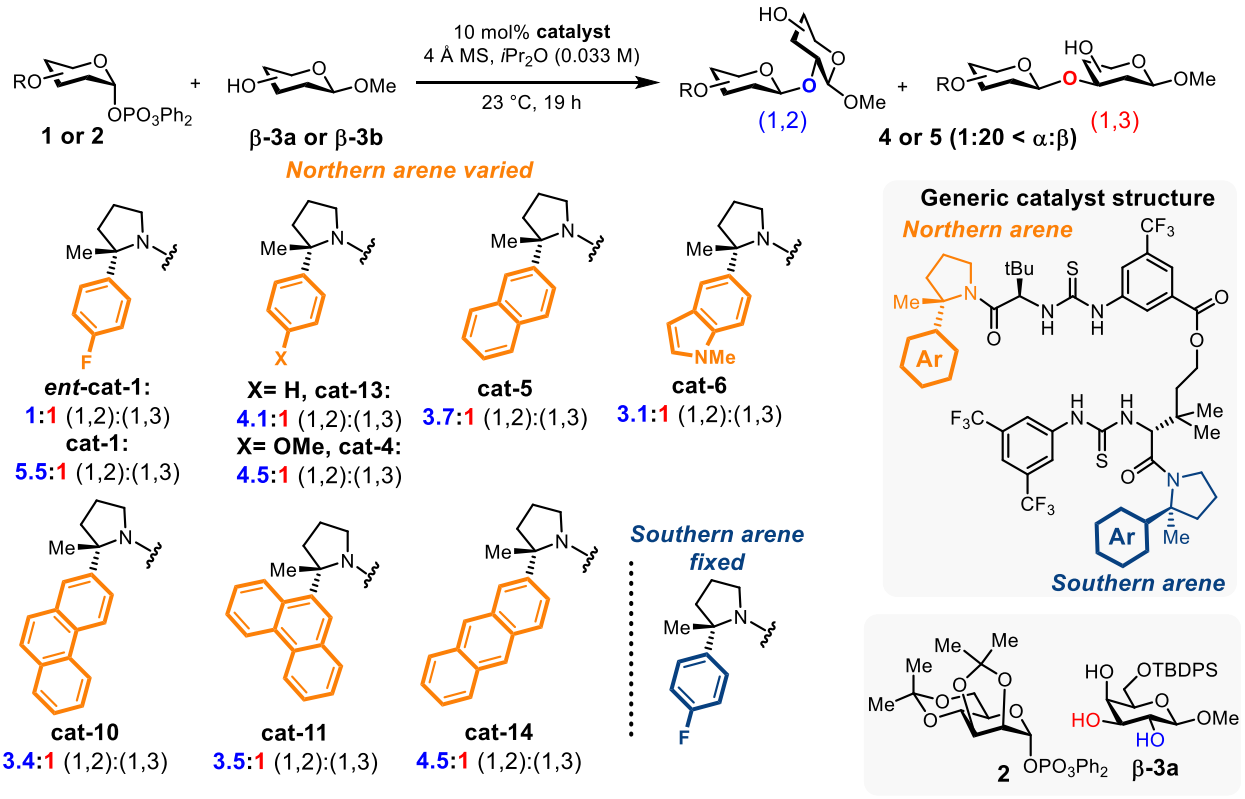


Figure 3.5 Effects of the electronic nature of "northern" arenes on site selectivity in mannosylation.

We then sought to identify a highly (1,2)-selective catalyst for site selective mannosylation, which exemplifies a structurally distinct class of β-glycosides that is inaccessible by current site selective glycosylation methods. While unselective mannosylation was observed (1:1 (1,2):(1,3)) with ***ent*-cat-1**, modest site selectivity (5.5:1 (1,2):(1,3)) was obtained with **cat-**1, again pointing to the specific catalyst-substrate matching in bis-thiourea-catalyzed glycosylations (Figure 3.5). In contrast to the trend observed in galactosylation, site selectivity was not responsive to the electronic change in "northern" arenes. Despite the large change in electronic nature of arenes going from 4-fluorophenyl to *N*-methylindole and expanded arenes such as phenanthrene and

anthracene, site selectivity in mannosylation remained relatively unperturbed (3.1–5.5:1 (1,2):(1,3)).

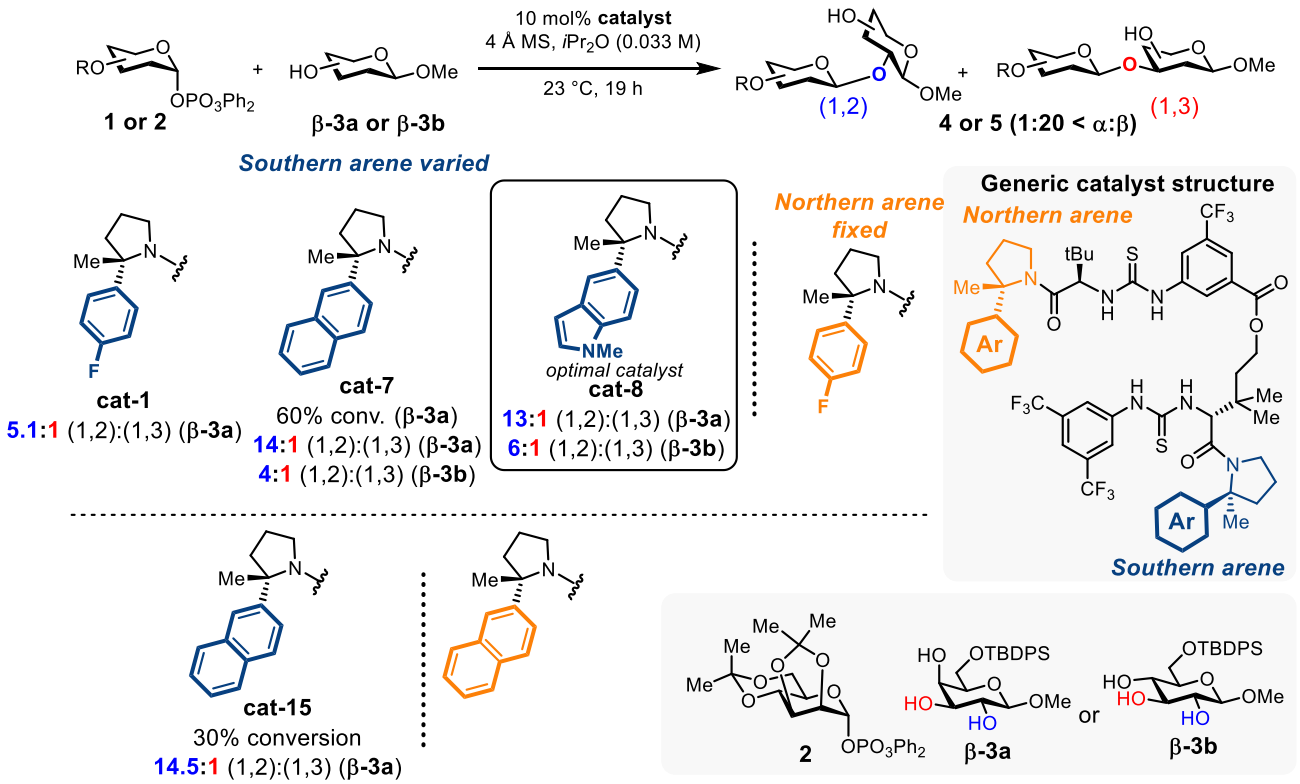


Figure 3.6 Effects of the electronic nature of "southern" arenes on site selectivity in mannosylation.

We then investigated the effects of "southern" arenes on the site selectivity of mannosylation (Figure 3.6). Contrary to the trend observed in galactosylation, site selectivity was highly responsive to alterations of the "southern" arene (5.5–14:1 (1,2):(1,3) with **cat-1,7–8**), suggesting that depending on the identity of the sugar, the catalyst is flexible enough to engage in productive glycosylation with either of the two amido arylpyrrolidines acting as general bases. A similar electronic effect on site selectivity was observed in mannosylation, where selectivity improved as the "southern" arene became more electron-rich. Because the correlation between

electronic nature of catalyst arene and site selectivity was observed in both galactosylation and mannosylation, we propose that catalyst arenes engage in specific interactions with nucleophiles rather than electrophiles. Incorporation of the electron-rich arene (2-naphthyl) on both "northern" and "southern" aryl pyrrolidines (**cat-15**), as an attempt to develop a universal catalyst for both galactosylation and mannosylation, resulted in similar site selectivity (14.5:1 (1,2):(1,3)) but lower reactivity (30% conversion) compared to **cat-7** (14:1 (1,2):(1,3), 60% conversion), likely due to the weaker binding of glycosyl phosphates to a highly sterically congested catalyst. Mannosylation of **β-3b** was found to be more (1,2)-selective with **cat-8** (6:1 (1,2):(1,3)) than with **cat-7** (4:1 (1,2):(1,3)). Therefore, **cat-6** and **cat-8** were selected as the optimal catalysts for galactosylation and mannosylation, respectively.

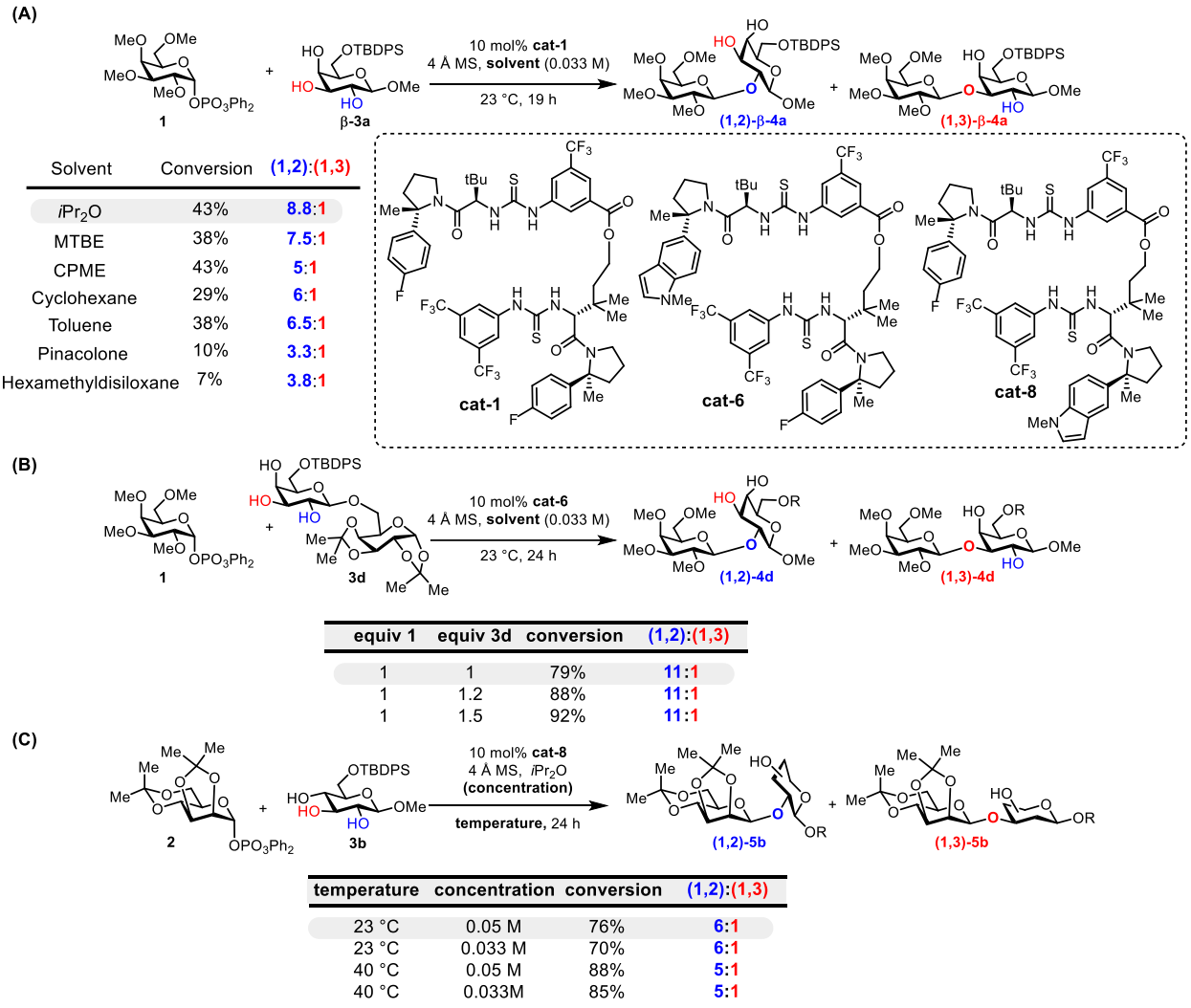


Figure 3.7. Effects of solvents, stoichiometry, temperature, and concentration on conversions and site selectivity. Conversions were determined by ^{1}H NMR relative to mesitylene as an internal standard. Selectivities were determined by ^{1}H NMR analysis of the crude unacylated reaction mixture.

Effects of different reaction parameters on reactivity and site selectivity were investigated (Figure 3.7A). Diisopropyl ether was selected as the optimal solvent for site selective glycosylation. Similar level of conversions was achieved with glycosylation in ethereal solvents

and toluene. Due to the polar nature of nucleophiles, the solubility of **β-3a** is highly limited in very nonpolar solvents such as hexamethyldisiloxane and pinacolone, resulting in very low reactivity.

The stoichiometry of nucleophiles was found to have no impact on site selectivity (Figure 3.7B). Slightly higher conversions were achieved by increasing the equivalence of **3d**. For simple monosaccharide nucleophiles (**β-3a–c**), 1.5 equivalents of nucleophiles were used to ensure high conversion of coupling partners. For other monosaccharide nucleophiles and all disaccharide nucleophiles, 1 equivalent of nucleophiles was used so that the more precious coupling partner will not be used in excess.

Temperature was found to influence both conversion and site selectivity (Figure 3.7C). Higher conversion but lower site selectivity were observed in mannosylation of **3b** when the temperature increased from 23 °C to 40 °C. Generally, many of the site selective galactosylations were run at 23 °C, while most of the site selective mannosylations were run at 50 °C to achieve the optimal balance between reactivity and site selectivity. Concentration did not have significant impact on conversion and site selectivity. We selected 0.033 M as the optimal concentration due to the relative low solubility of minimally unprotected nucleophiles in diisopropyl ether.

3.3 Acceptor Scope

The scope of β-selective and site selective galactosylation and mannosylation was explored (Figure 3.8). The size of the anomeric substituent had minimal impact on site selectivity despite the proximity of the anomeric position to the hydroxyl group undergoing glycosylation. β-Monosaccharides (**β-3a–c**) and minimally protected disaccharides containing a β-galactose or β-glucose motif (**3d–g**, **3l–m**) were glycosylated at the C-2 of galactose or glucose selectively and cleanly, with no over-glycosylation (<5 %) observed. β-Glucoside-containing pharmaceuticals and

natural products (**3h–i**, **3n**) underwent site selective glycosylation with synthetically useful level of (1,2)-selectivity (3.5–7 (1,2):(1,3)). The insensitivity of site selectivity to anomeric substituents indicates that they project away from the key interactions with the catalyst arene that are responsible for imparting site selectivity. However, the anomeric configuration of nucleophiles was found to have profound impact on site selectivity. α-Monosaccharides (**α-3a** and **α-3b**) displayed significantly lower site selectivity (2.1:1 and 1:1.7 (1,2):(1,3) respectively).

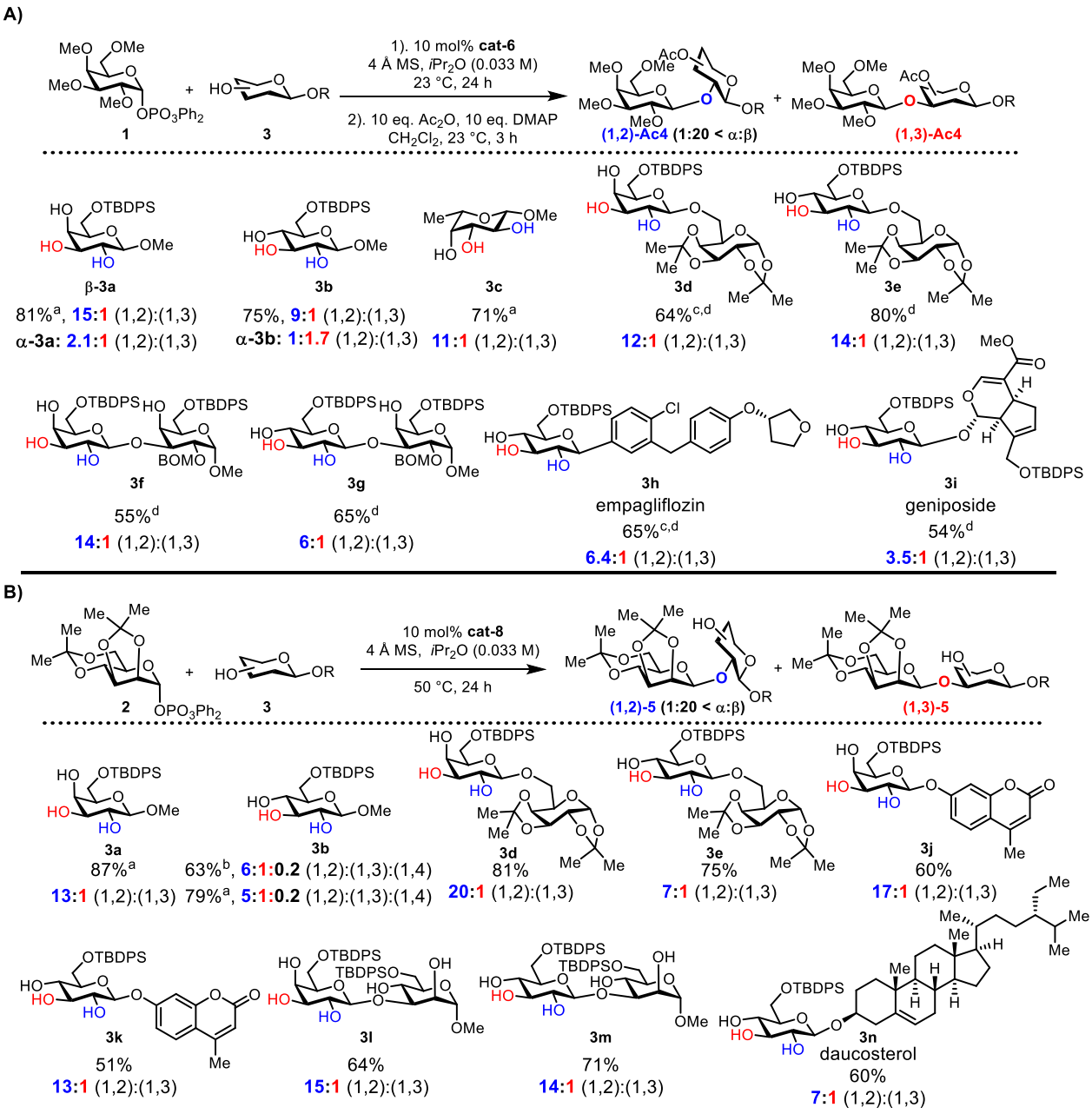
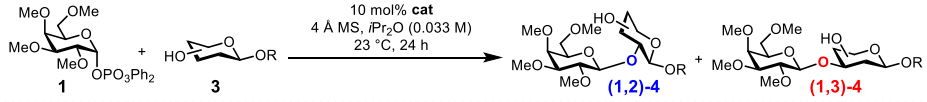
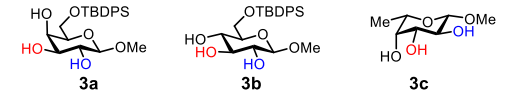
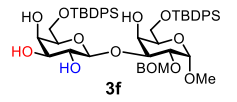


Figure 3.8 Nucleophile scope of site selective galactosylations and mannosylations. Selectivities were determined by ^{1}H NMR analysis of crude unacylated product mixtures. Yields of site selective galactosylations reflect isolated yields of acylated (1,2)-product after the two-step galactosylation/acylation sequence. Yields of site selective mannosylations reflect isolated yields of a mixture of unacylated (1,2)- and (1,3)-products. [a]Reaction performed at 40 °C. [b]Reaction performed at 23 °C. [c]Reaction performed at 4 °C. [d]48 h reaction time.

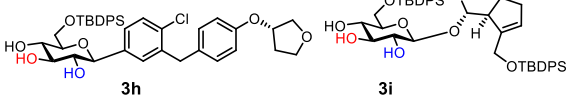




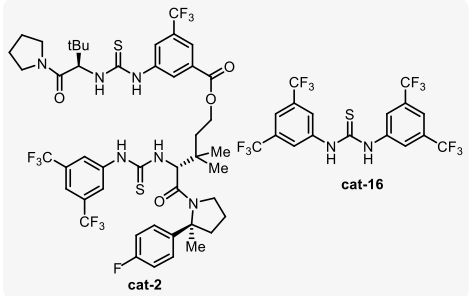
	3a	3b	3c	3d	3e
cat-2	1.7:1 (1,2):(1,3)	2:1 (1,2):(1,3)	2:1 (1,2):(1,3)	1:1 (1,2):(1,3)	3:1 (1,2):(1,3)
cat-16	1:1.1 (1,2):(1,3)	1:1 (1,2):(1,3)	1:1 (1,2):(1,3)	1:1 (1,2):(1,3)	2:1 (1,2):(1,3)

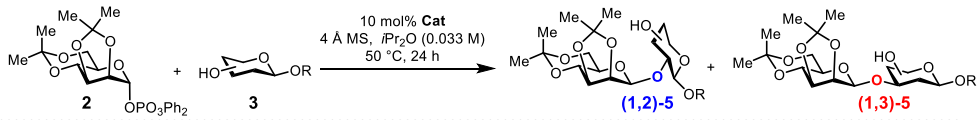


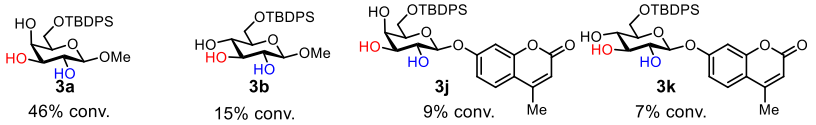
	3f	3g
cat-2	1:1.2 (1,2):(1,3)	1:1 (1,2):(1,3)
cat-16	complex mixture	complex mixture



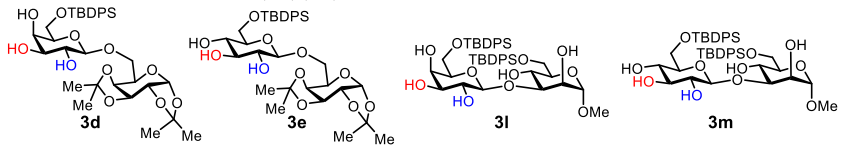
	3h	3i
cat-2	1:1.6 (1,2):(1,3)	1:2.4 (1,2):(1,3)
cat-16	1:1 (1,2):(1,3)	1:6 (1,2):(1,3)



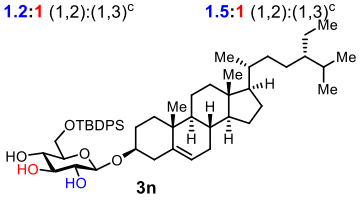




	3a	3b	3j	3k
cat-17	46% conv. 1:1 (1,2):(1,3)[b]	15% conv. 1.5:1 (1,2):(1,3)[b]	9% conv. 2:1 (1,2):(1,3)[b]	7% conv. 1:1 (1,2):(1,3)[b]
cat-16	15% conv. 2:1 (1,2):(1,3)[c]	6% conv. 2.2:1 (1,2):(1,3)[c]	no conversion	no conversion



	3d	3e	3l	3m
cat-17	35% conv. 1:2.1 (1,2):(1,3)[b]	28% conv. 1.4:1 (1,2):(1,3)[b]	20% conv. 3:1 (1,2):(1,3)[b]	25% conv. 1.2:1 (1,2):(1,3)[b]
cat-16	7% conv. 1.2:1 (1,2):(1,3)[c]	7% conv. 1.5:1 (1,2):(1,3)[c]	8% conv. 1.1:1 (1,2):(1,3)[c]	15% conv. 1.5:1 (1,2):(1,3)[c]



	3n
cat-17	40% conv. 1:1.2 (1,2):(1,3)[b]
cat-16	19% conv. 1:1 (1,2):(1,3)[b]

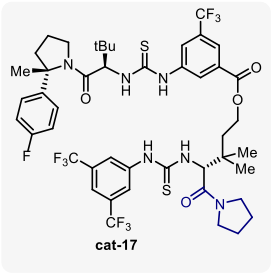


Figure 3.9 Inherent site selectivities of galactosylations and mannosylations. Conversions were determined by ^{1}H NMR relative to mesitylene as an internal standard. Selectivities were determined by ^{1}H NMR analysis of the crude unacylated reaction mixture.

The inherent site preference of nucleophiles was assessed by activating glycosyl phosphates with an achiral hydrogen-bond-donor, **cat-16** (Figure 3.9). Low site-selectivities obtained with **cat-16** demonstrated that none of the acceptors has strong inherent bias toward (1,2)-products. Unselective glycosylations were observed in site selective galactosylation and mannosylation promoted by **cat-2** and **cat-17** respectively, showcasing the importance of aryl substituents on catalysts in controlling site selectivity.

3.4 Mechanistic Studies

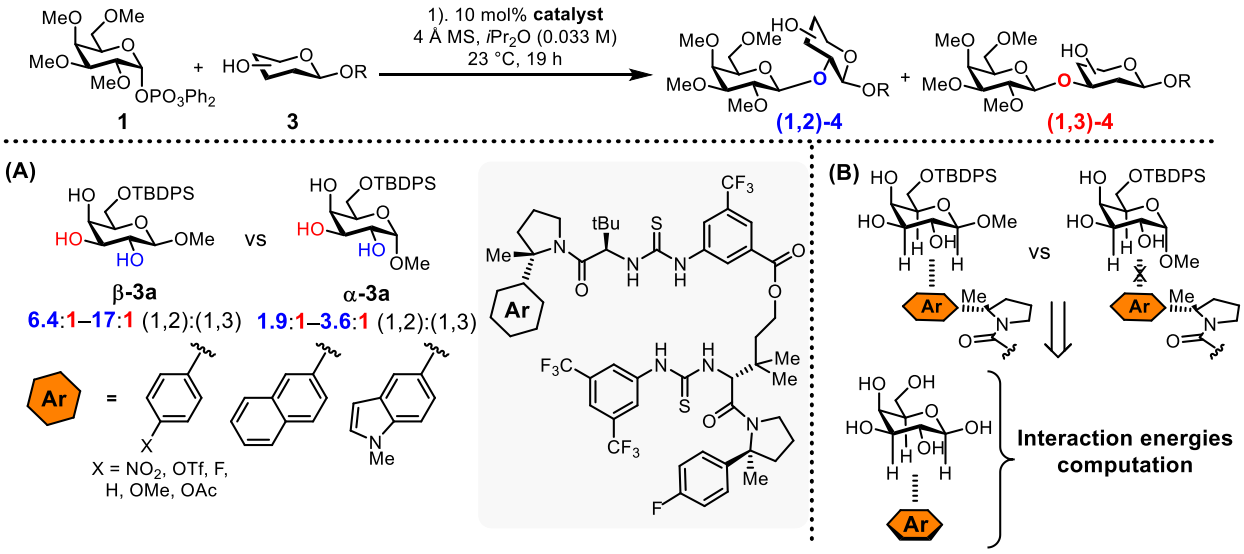


Figure 3.10 (A) Site selectivity in galactosylation of **β-** and **α-3a** promoted by different catalysts. (B) Model used for computed interaction energies

We sought to understand the diverging behavior of **α-** and **β-3a** and elucidate the origin of catalyst aryl substituent effects on site selectivity. A thorough catalyst evaluation revealed that site

selectivity for galactosylation of **α-** and **β-3a** responded differently to electronic perturbation of catalyst arenes (Fig. 3.10A). The site selectivity in galactosylation of **β-3a** (6.4–17:1 (1,2):(1,3)) increased as catalyst arenes became more electron-rich, while minimal changes in site selectivity (1.9–3.6:1 (1,2):(1,3)) were observed in galactosylation of **α-3a**. We hypothesized that the contrasting trend observed with **α-** and **β-3a** could result from their differing ability to effectively engage in CH/π interactions with catalyst arenes (Fig. 3.10B) in their transition states. The strength of such interactions strongly depends on the sugar configuration. Experimental and theoretical studies have shown that stacking preferentially occurs on the face presenting multiple axially oriented C-H bonds, and axial hydroxyl groups, on the other hand, disfavor such stacking interactions.[12]

To test the aforementioned hypothesis, we performed a linear free energy relationship (LFER) study by correlating the experimental $\Delta\Delta G^{\ddagger}$ derived from site selectivity with computed interaction energies of β-galactose and different arenes. Interaction energies were evaluated between β-galactose, serving as the model for nucleophiles, and substituted benzenes, naphthalene, and *N*-methylindole serving as truncated versions of the catalysts at B97D/TZV level of theory.[13] B97-D/TZV level of theory was selected because it has been previously applied to efficiently and accurately calculate interaction energies for prototypical CH/π interactions.[14] The B97-D energies

[12] (a) Tsuzuki, S.; Uchimaru, T.; Mikami, M. Magnitude and nature of carbohydrate-aromatic interactions in fucose-phenol and fucose-indole complexes: CCSD(T) level interaction energy calculations. *J. Phys. Chem. A* **2011**, *115*, 11256–11262. (b) Raju, R. K.; Ramraj, A.; Vincent, M. A.; Hillier, I. H.; Burton, N. A. Carbohydrate-protein recognition probed by density functional theory and *ab initio* calculations including dispersive interactions. *Phys. Chem. Chem. Phys*. **2008**, *10*, 6500–6508.

[13] (a) Grimme, S. Semiempirical GGA-type density functional constructed with a long-range dispersion correction. *J. Comput. Chem*. **2006**, *27*, 1787−1799. (b) Becke, A. Density-functional thermochemistry. V. Systematic optimization of exchange-correlation functionals. *J. Chem. Phys*. **1997**, *107*, 8554−8560.

[14] Bloom, J. W. G.; Raju, R. K.; Wheeler, S. E. Physical Nature of Substituent Effects in XH/π Interactions. *J. Chem. Theory Comput.* **2012**, *8*, 3167–3174.

were found to be in good agreement with the CCSD(T) data by Wheelers and coworkers. In order to further validate the predictability of B97-D/TZV level of theory in computing CH/π interactions between arenes and carbohydrates, we calculated interaction energies of carbohydrate-arene complexes that have been computed previously by Tsuzuki and co-workers, and the interaction energies at CCSD(T)/basis limit level of theory were reported by the authors.[13a] We then compared the energies obtained at B97-D/TZV level of theory to energies computed at CCSD(T)/basis limit (Figure 3.11). An excellent correlation ($R^2 = 0.99$) was observed, suggesting that B97-D/TZV correctly predicted the relative stability of carbohydrate-arene complexes although B97-D/TZV consistently overestimated the absolute energy.

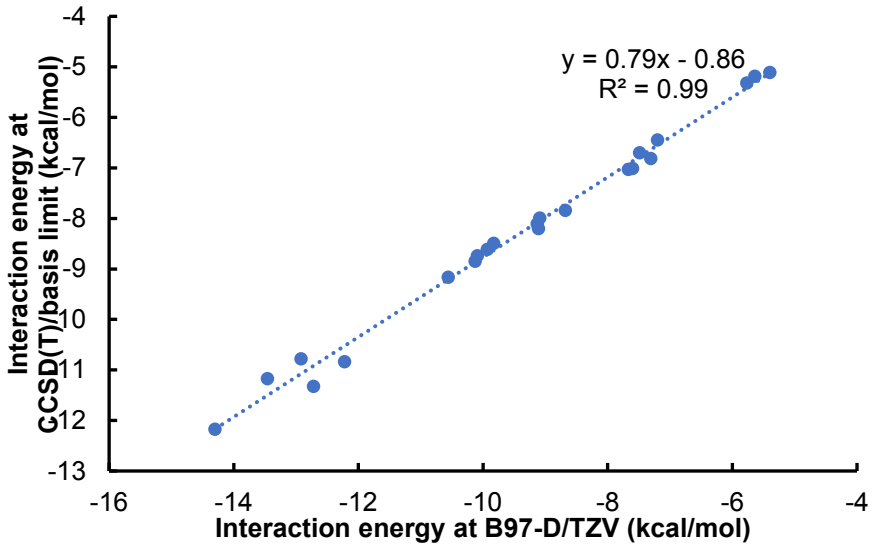


Figure 3.11 Correlation between energies calculated at B97-D/TZV and energies computed at CCSD(T)/basis limit.

Due to the excellent predictive power of B97-D/TZV level of theory, the geometries of galactose-arene complexes were optimized at B97-D/TZV level of theory with PCM (ether)[15] by

[15] Scalmani, G.; Frisch, M. J. Continuous Surface Charge Polarizable Continuum Models of Solvation. I. General Formalism. *J. Chem. Phys*. **2010**, *132*, 114110–114115.

fixing the coordinates of arenes. Galactose(H5)-arene complexes were selected for single point energy. Single point energy calculation with counterpoise corrections was performed to calculate the interaction energies of optimized galactose-arene complexes at B97-D/TZV level of theory (Figure 3.12). Shorter distance from C5-H to arene (3.30 Å vs 3.41 Å) is featured in the more stable carbohydrate-arene complex (–9.21 vs –6.53 kcal/mol).

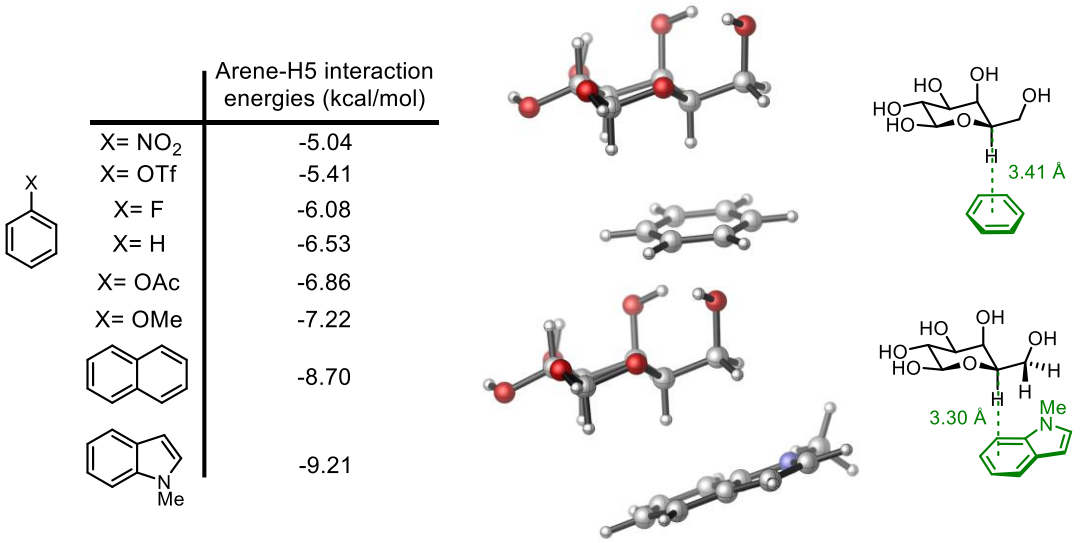


Figure 3.12 Table of interaction energies calculated at B97-D/TZV.

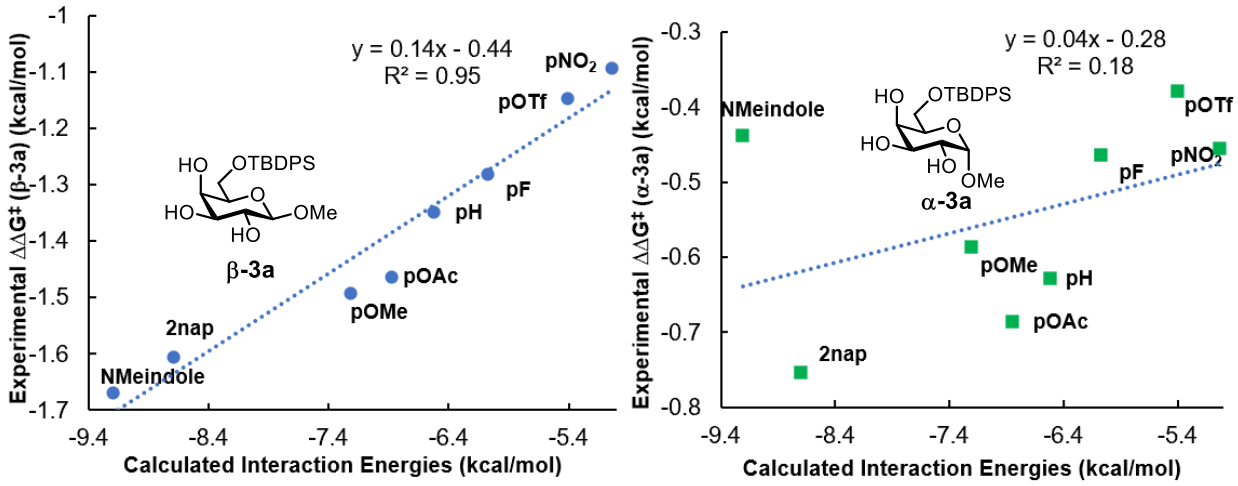


Figure 3.13 Correlation of experimental site selectivity ($\Delta\Delta G^{\ddagger} = -RT\ln(r.r.)$) with computed interaction energies between substituted catalyst arenes and galactose.

The experimental $\Delta\Delta G^{\ddagger}$ derived from site selectivity was correlated with computed interaction energies (Figure 3.13). A good correlation was observed in the case of **β-3a**, while no statistically significant correlation was seen with **α-3a**. This study supports our hypothesis that attractive CH/π interactions present in the selectivity-determining step are crucial for controlling site selectivities and corroborates the feasibility of exploiting carbohydrate-aromatic interactions to impart site selectivity in glycosylation reactions.

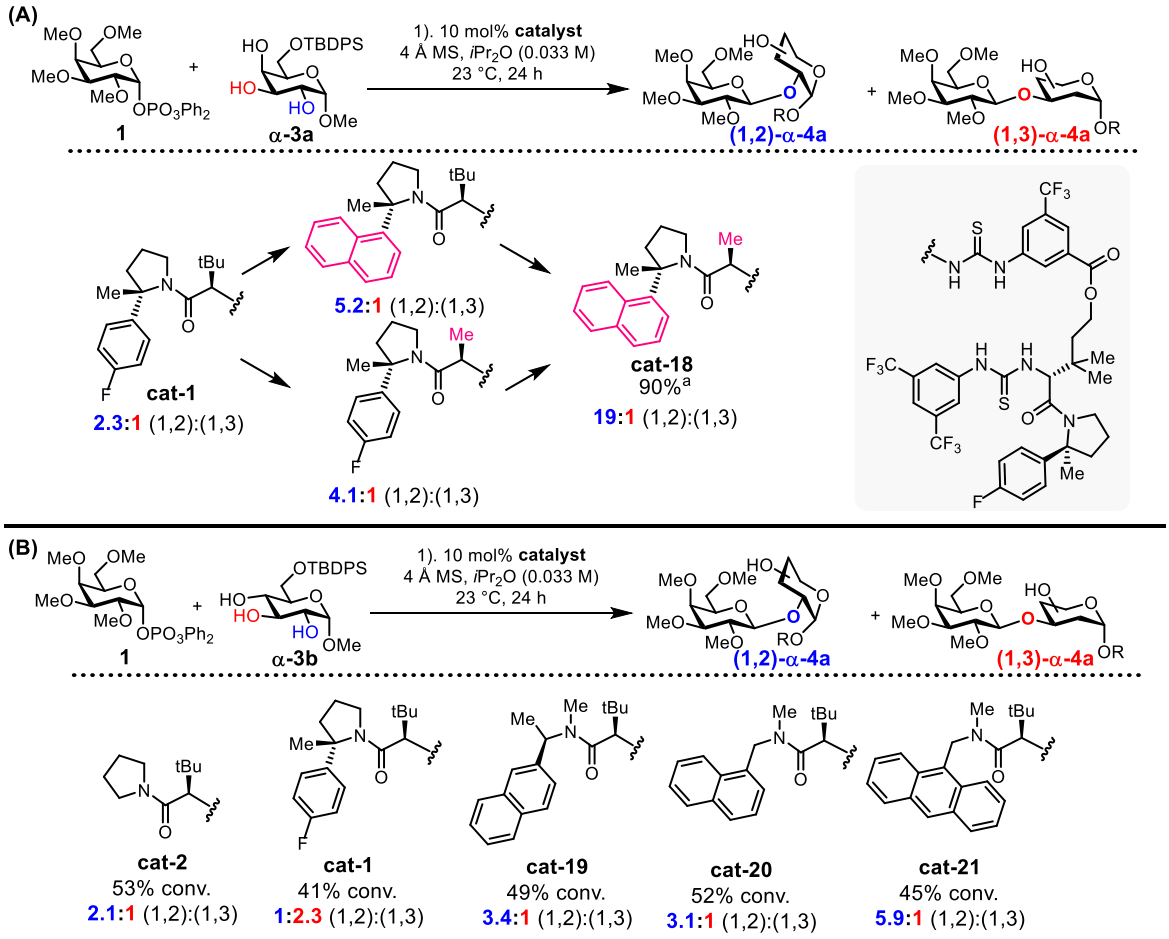


Figure 3.14 Catalyst optimization for galactosylation of **α-3a** and **α-3b**. Selectivities were determined by ^{1}H NMR analysis of crude unacylated product mixtures. [a] MTBE instead of isopropyl ether. Yield reflect isolated yields of acylated (1,2)-product after the two-step galactosylation/acylation sequence.

The poor ability of **α-3a** to engage in CH/π interaction with catalyst arene precludes the utilization of such interactions to influence site selectivity; however, we were intrigued by the possibility of exploiting other networks of noncovalent interactions to enforce site-control in the galactosylation of **α-3a**. Expansion of the catalyst 4-fluorophenyl to a 1-napthyl arene and replacement of the structurally rigid *tert*-leucine with a more flexible alanine resulted in a highly (1,2)-selective galactosylation catalyzed by **cat-18** (19:1 (1,2):(1,3)) (Figure 3.14A). Encouraged by the ability to design a highly selective catalyst for galactosylation of **α-3a**, we turned our focus to optimize catalyst for site selective galactosylation of **α-3b** (Figure 3.14B). Galactosylation of **α-3b** catalyzed by a catalyst bearing aryl pyrrolidine moiety (**cat-1**) afforded (1,3)-product as the major regioisomer (1:2.3 (1,2):(1,3)), in stark contrast to galactosylation of **β-3b**, where the (1,2)-product was obtained as the major product with catalysts bearing aryl pyrrolidine moieties. However, preference for (1,2)-product was observed with bis-thiourea derivatives bearing arylethyl amine fragments (**cat-19–21**). The differences in how site selectivity responds to changes in catalyst amide moiety indicate that **α-** and **β-3a** interact differently with catalysts in selectivity-determining step. Although the modes of site-control are likely distinct for site selective glycosylation of α-carbohydrates and β-carbohydrates, the promising initial results demonstrate the generality of a catalyst-controlled approach for achieving site selectivity and suggests that in addition to CH/π interactions, other networks of noncovalent interactions can be harnessed to impart site selectivity in glycosylation of different systems.

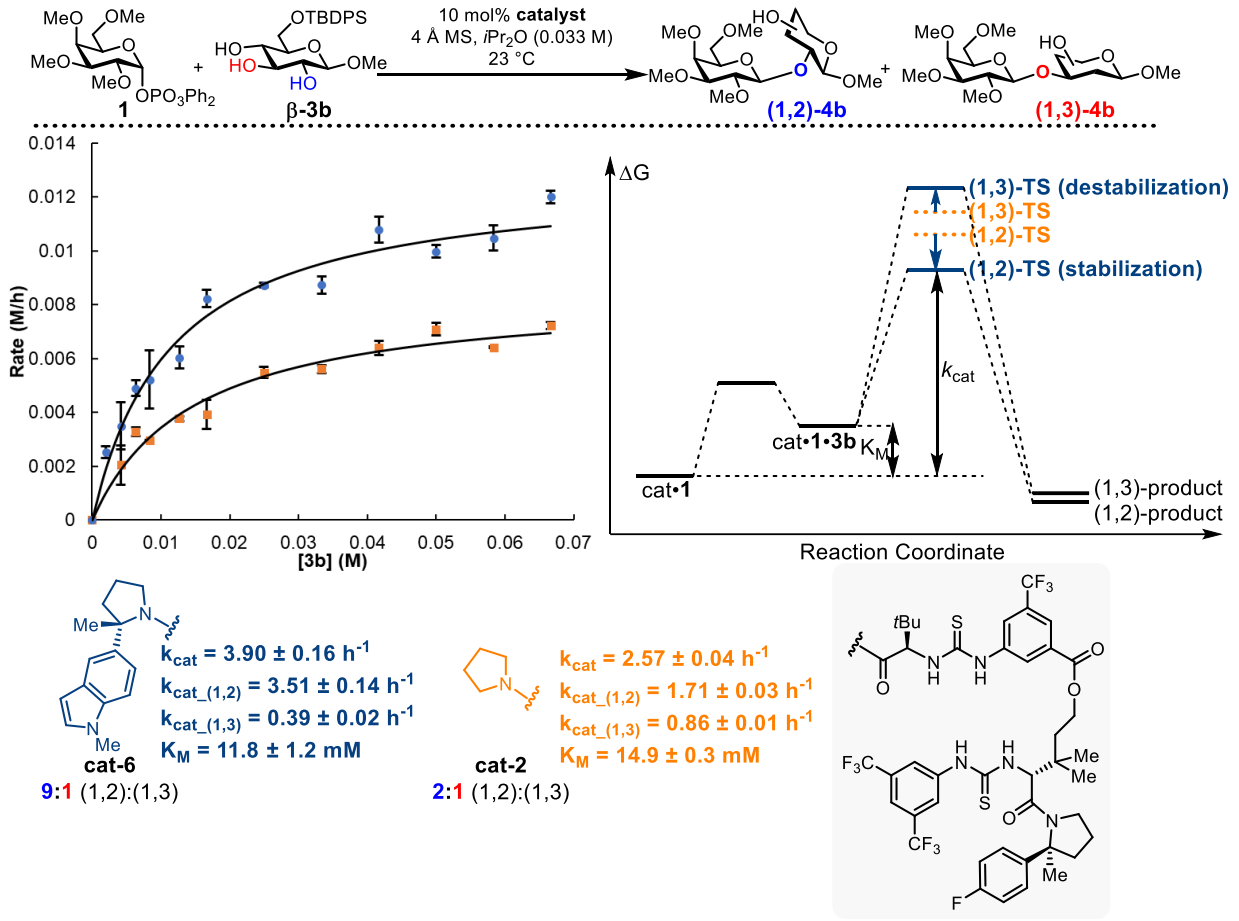


Figure 3.15 Michaelis-Menten kinetic analyses of reactions catalyzed by (1,2)-selective **cat-6** and unselective **cat-2**.

After establishing the importance of CH/π interactions in imparting site selectivity, we sought to understand how the presence of such interactions in the selectivity-determining step leads to enhanced site selectivities. Michaelis-Menten kinetic analyses of reactions catalyzed by selective 5-NMeindole-bisthiourea (**cat-6**) and unselective pyrrolidine-bisthiourea (**cat-2**) revealed similar Michaelis constant (K_M), suggesting that phosphate•cat complexes bind to nucleophiles with similar strength for **cat-6** and **cat-2** (Figure 3.15). Therefore, the enhanced site selectivity cannot be attributed to the ability of **cat-6** to form more stable phosphate•cat•nucleophile ternary complexes that preferentially undergo (1,2)-glycosylation.

Instead, a faster maximum rate (k_{cat}) for more selective **cat-6** indicated that rate acceleration observed with **cat-6** is mainly due to transition state stabilization presumably by attractive carbohydrate-aromatic interactions. Higher $k_{cat_(1,2)}$ and lower $k_{cat_(1,3)}$ for more selective **cat-6** relative to unselective **cat-2** indicate that higher site selectivity was achieved by stabilizing the major (1,2)-pathway and destabilizing the minor (1,3)-pathway. The observation that more site selective catalysts promote glycosylation with improved reactivity and that minimally protected nucleophiles displayed enhanced reactivity compared to the protected counterpart (up to 10 fold increase in initial rate, Figure 3.16) is in stark contrast to the scenario for protecting-group-controlled glycosylation, where site selectivity is typically achieved with diminished reactivity of nucleophiles due to steric congestion and electronic deactivation by neighboring protecting groups.

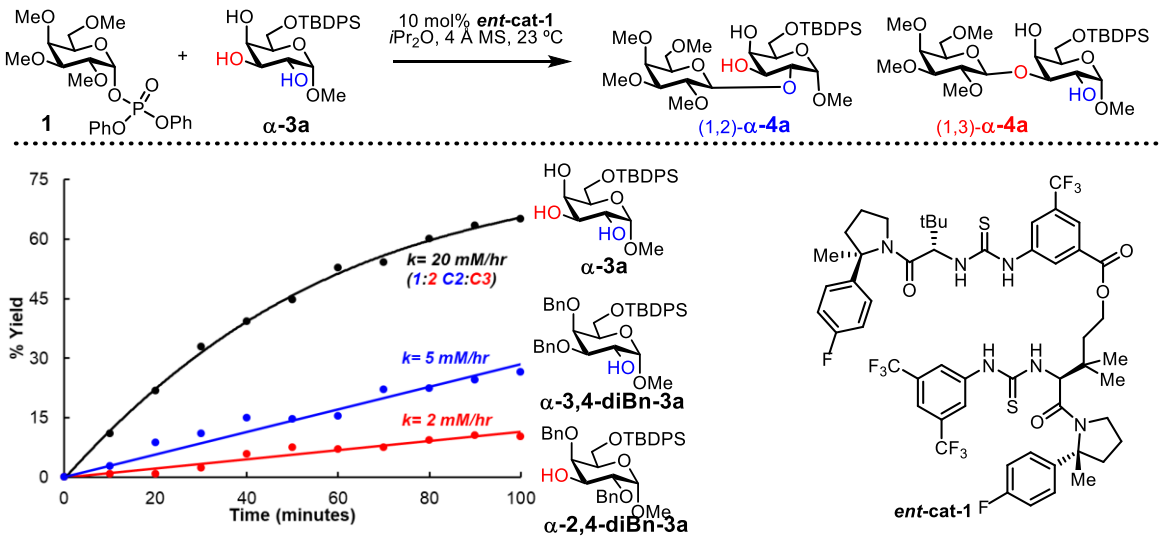


Figure 3.16 Kinetics for partially protected galactose derivatives, **a-3a**, **a-3,4-diBn-3a**, and **a-2,4-diBn-3a**.

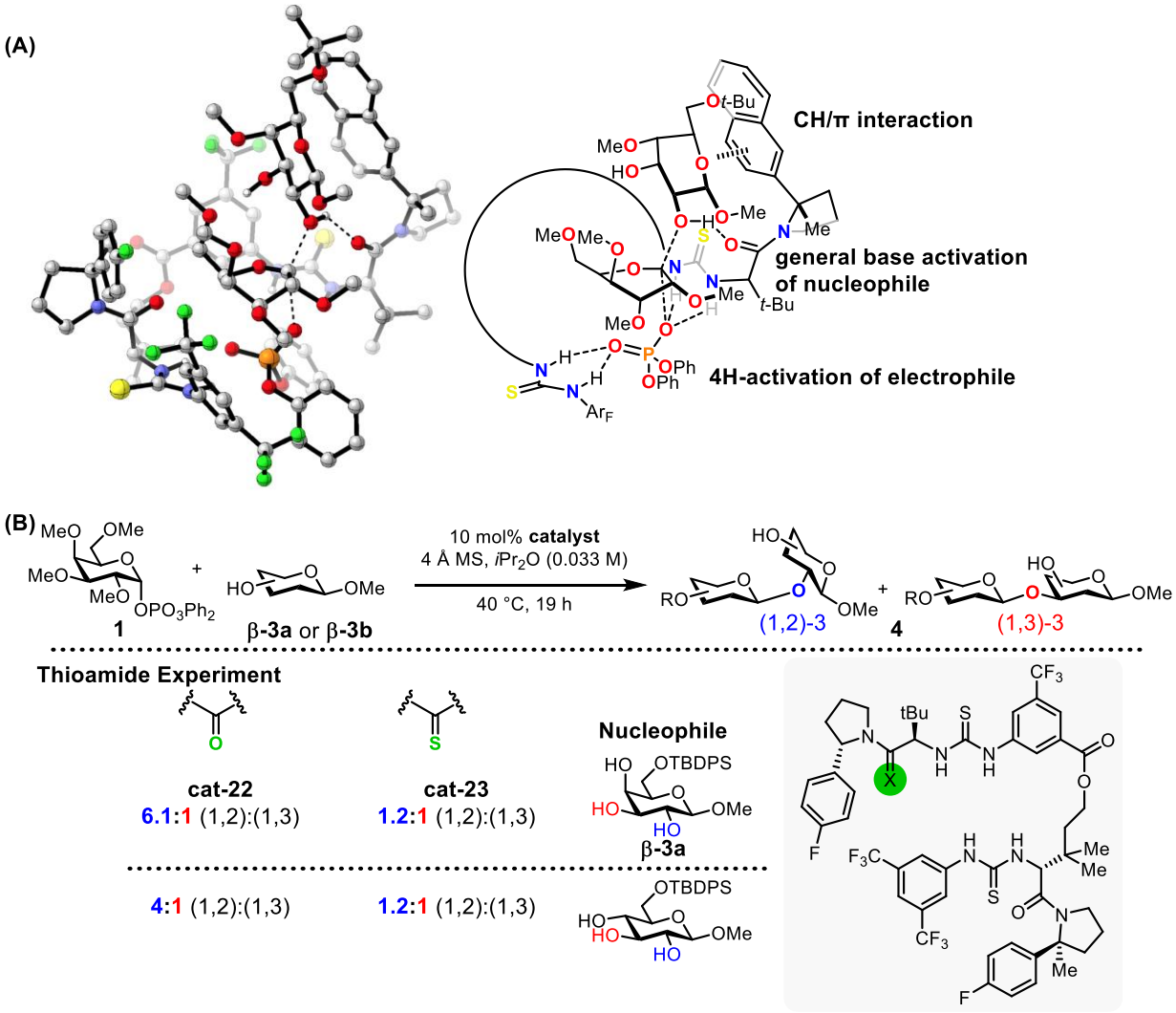


Figure 3.17 A) Computed (1,2)-transition state structure of galactosylation of β-galactose. (B) Site selectivity of galactosylation of **β-3a** and **β-3b** promoted by **cat-22** bearing a "northern" amide and **cat-23** bearing a "northern" thioamide.

Density functional theory calculations on the galactosylation of β-galactose were carried out to assess the viability of the proposed mechanism. Both (1,2) and (1,3) transition states predicted an asynchronous S_N2-like mechanism involving 4H-activation of the diphenylphosphate group and amide-mediated nucleophile activation (Figure 3.17A). The computed general base activation mechanism was consistent with the experimental observation that replacing the

"northern" amide with thioamide, a weaker hydrogen-bond acceptor,[16] resulted in diminished site selectivity (Figure 3.17B). However, the predicted sense of site selectivity was opposite of that observed experimentally. We hypothesized that this discrepancy might be caused by poor modelling of solvation: while unprotected sugars are likely to engage in explicit hydrogen-bonding interactions with the ethereal solvent, these interactions will not be accounted for by implicit solvent models. Indeed, QM/MM molecular dynamics simulations in explicit solvent suggest that the C4 hydroxyl on the nucleophile engages in hydrogen-bonding interactions with the solvent which were not accounted for in the implicit solvent calculations. Replacing the poorly modelled C4 hydroxyl with a methoxy resulted in a predicted selectivity favoring the (1,2)-product.

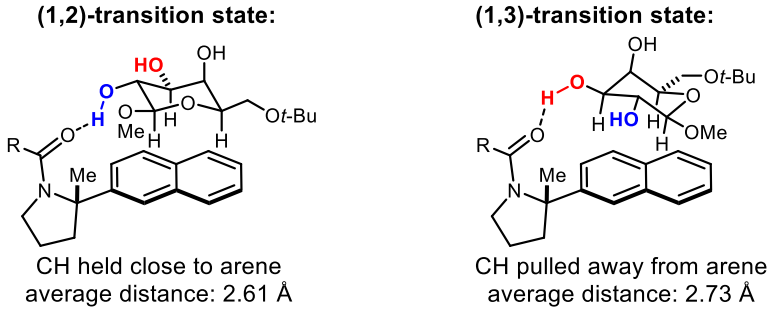


Figure 3.18 Differences in CH/π contacts between (1,2)- and (1,3)-transition states.

Analysis of the computed structures revealed that the (1,2) transition state contained markedly closer CH/π contacts than the (1,3) transition state (average nucleophile–arene distance of 2.61 Å and 2.73 Å, respectively), consistent with the increase in (1,2) selectivity induced by electron-rich aryl groups via CH/π interactions (Figure 3.18). Activation of the C3 hydroxyl group by the aryl pyrrolidine amide requires a close amide–hydroxyl contact, pulling the nucleophile farther from the aryl group and weakening the stabilizing CH/π interaction. Since the C2 methine

[16] Alemán, C. On the Ability of Modified Peptide Links to Form Hydrogen Bonds. *J. Phys. Chem. A* **2001**, *105*, 6717–6723.

is not oriented toward the aryl group, activation of the C2 hydroxyl is less deleterious to this interaction.

3.5 Iterative Glycosylation

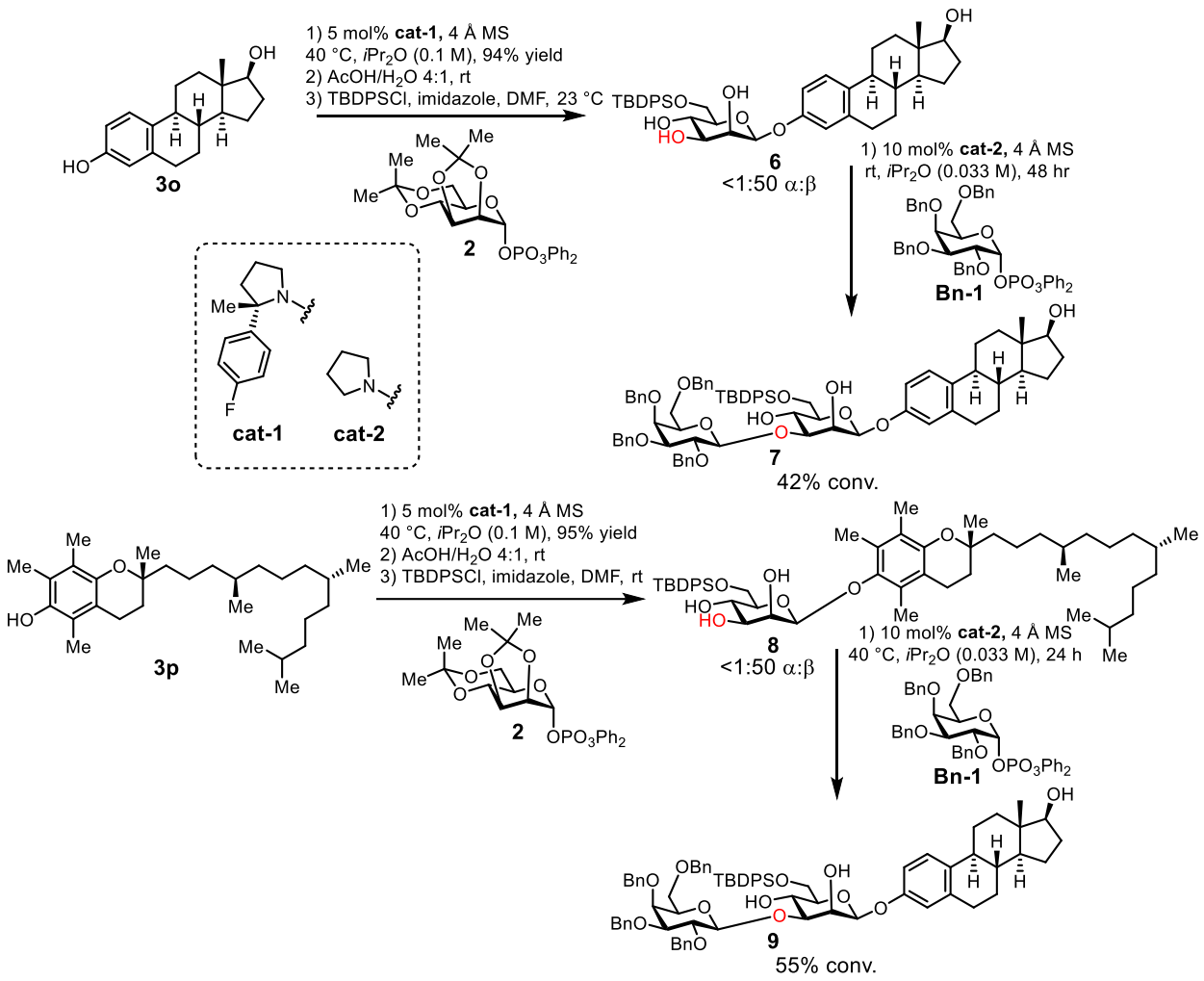


Figure 3.19 Iterative glycosylation of estradiol and α-tocopherol. Conversions were determined by ^{1}H NMR relative to mesitylene as an internal standard. Selectivities were determined by ^{1}H NMR analysis of the crude unacylated reaction mixture.

We sought to examine the possibility of applying bis-thiourea-catalyzed site selective glycosylations and bis-thiourea-catalyzed mannosylation to efficiently install disaccharide

moieties on complex molecules (Figure 3.19). We selected estradiol (**3o**) and α-tocopherol (**3p**) as our model acceptors because mannosylation of phenol nucleophiles cannot be achieved with high β-selectivity with traditional β-selective mannosylation strategies such as 4,6-benzylidene acetal protection strategy as demonstrated in Chapter 2 Section 2.4. Therefore, our previously reported bis-thiourea-catalyzed mannosylation has its unique advantage in promoting highly β-selective glycosylation of phenols. Mannosylation of **3o** catalyzed by **cat-1** proceeded with high yield (94%) and high β-selectivity (<1:50 α:β). Cleavage of acetonide protecting group can be conducted under acidic conditions, and no epimerization of the anomeric stereocenter was observed. The triol **6** after silyl protection was subject to site selective galactosylation catalyzed by **cat-2**. Site selective glycosylation of the most reactive C3 position of mannoside in **6** was observed as the only glycosylation product with moderate conversion (42%). Similarly, mannosylation of **3p** proceeded with high yield (95%) and high β-selectivity (<1:50 α:β). C3-glycosylation of triol **8** was observed as the sole regioisomer with 55% conversion.

3.6 Initial Attempt to Develop Site Selective Benzylation

We hypothesized that the ability of exploiting CH/π interactions to control site selectivity of glycosylation could allow us to apply this strategy to the general functionalization of carbohydrates. We selected benzylation as our model system to examine the possibility of relying on attractive noncovalent interactions to impart site selectivity in alkylation. No conversions were observed when **β-3a** was treated with benzyl phosphate derivatives and **cat-6**, the optimal catalyst for site selective galactosylation (Figure 3.20). We hypothesized that the installment of electron-donating substituents on benzyl substituent could increase the reactivity of benzyl phosphates by stabilizing the partial positive charge developed on benzylic carbon in the transition state. We then investigated diphenyl phosphate derivative of 4-methoxyl benzyl alcohol. Indeed, good reactivity

(70% conversion) was observed with 4-methoxy benzyl diphenylphosphate. However, three monobenzylation products were formed unselectively (1:1.5:1.5). The lack of site selectivity in benzylation was likely due to the drastically different stereochemical shape of galactosyl phosphate and benzyl phosphate, resulting in different geometries of transition states. Although **β-3b** and catalyst aryl substituent are in proximity to engage in CH/π interactions in the transition state of site selective glycosylation, such interactions may not be present in the transition state of site selective benzylation. Therefore, further catalyst optimization is needed to design a catalyst structure that allows for close contact between nucleophiles and catalyst arenes when the catalyst binds to benzyl phosphate derivatives.

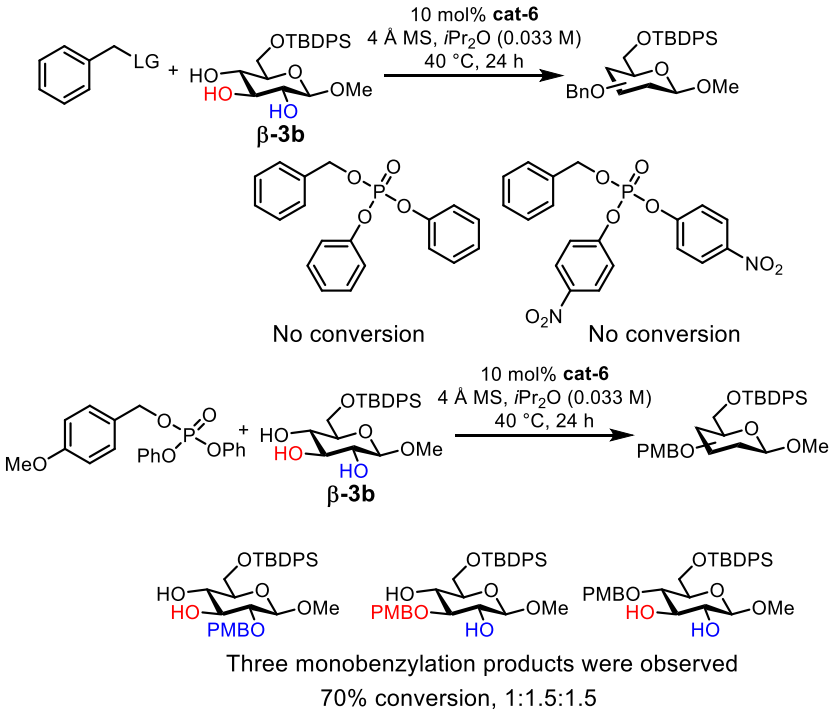


Figure 3.20 Preliminary results of site selective benzylation.

3.7 Conclusion and Outlook

We have developed highly (1,2)-selective galactosylations and mannosylations of β-carbohydrates using bis-thioureas bearing electron-rich arenes. Structure activity relationships and correlation studies demonstrate the importance of CH/π interactions between nucleophiles and catalyst arenes in controlling the site selectivity of glycosylation. Kinetic and computational studies suggested that carbohydrate-aromatic interactions stabilize the major (1,2)-pathway, resulting in catalytic glycosylations that are both faster and more site selective. The study reported herein showcases the feasibility of exploiting noncovalent interactions to achieve high stereo- and site control in catalytic glycosylations.

3.8 Experimental Information

3.8.1 General Experiment Procedures, Materials, and Instrumentation

Unless otherwise described, all reactions for the preparation of substrates were performed in standard, oven- or flame-dried glassware equipped with PTFE-coated magnetic stir bars and fitted with rubber septa under an inert atmosphere of nitrogen. All catalytic experiments were performed in a flame-dried round bottom flask sealed with a yellow polyethylene cap under an atmosphere of air. Stainless steel syringes or Hamilton gas-tight glass syringes fitted with stainless-steel needles were used to transfer air- and moisture-sensitive liquids. Reported concentrations refer to solution volumes at room temperature. Concentration of organic solutions under reduced pressure was performed on a Büchi rotary evaporator using house vacuum (~ 40 mm Hg). Reactions were monitored by thin-layer chromatography (TLC) on Silica Gel 60 F254 plates (EMD). Plates were visualized by exposure to UV light (λ = 254 nm) and/or by staining with *p*-anisaldehyde, ninhydrin, or ceric ammonium molybdate (CAM) stain, which developed upon heating. Column

chromatography (using a Biotage® Isolera Four™) was performed using reusable cartridges filled with SiliaFlash P60 (230–400 mesh, SiliCycle).

All commercially available reagents were purchased from Sigma–Aldrich, Alfa Aesar, Strem, Oakwood, Matrix Scientific, Ark Pharm Inc., Toronto Research Chemicals, Chem-Impex Int'l. Inc., or TCI and used without purification, unless otherwise indicated. Deuterated NMR solvents were purchased from Cambridge Isotope Laboratories. Anhydrous solvents (*tert*-butyl methyl ether, dichloromethane, *N,N*-dimethylformamide, ethyl ether, methanol, tetrahydrofuran, toluene) were prepared by passing the solvent through an activated alumina column. Triethylamine, *N,N*-diisopropylethylamine, and pyridine were distilled from CaH_2 at atmospheric pressure.

NOTE: Diisopropyl ether is known to form peroxides and should be handled with appropriate care. Anhydrous diisopropyl ether containing either BHT or hydroquinone as stabilizer was purchased in from Sigma-Aldrich and used without purification.

Proton nuclear magnetic resonance (^{1}H NMR) spectra and proton-decoupled carbon nuclear magnetic resonance (^{13}C NMR) spectra were recorded at 25 °C (unless stated otherwise) on Bruker AVANCE NEO 400 (400 MHz), Bruker AVANCE NEO 400B (400 MHz), Varian Unity/Inova 500 (500 MHz), or Agilent DD2 600 (600 MHz) spectrometers at the Harvard University nuclear magnetic resonance facility. Chemical shifts for protons are reported in parts per million downfield from tetramethylsilane and are referenced to residual proton resonances of the NMR solvent. Chemical shifts for carbon are reported in parts per million downfield from tetramethylsilane and are referenced to the carbon resonances of the NMR solvent. The solvent peak was referenced to 7.26 ppm for ^{1}H and 77.16 ppm for ^{13}C for $CDCl_3$. Data are represented as follows: chemical shift, integration, multiplicity (br = broad, s = singlet, d = doublet, t = triplet, q = quartet, qn = quintet, sp = septet, m = multiplet), coupling constants (J) in Hertz (Hz).

High-resolution mass spectrometric data were obtained on an Agilent 6210 time-of-flight HPLC/MS spectrometer (ESI-TOF).

3.8.2 Additional Catalyst Optimization Data

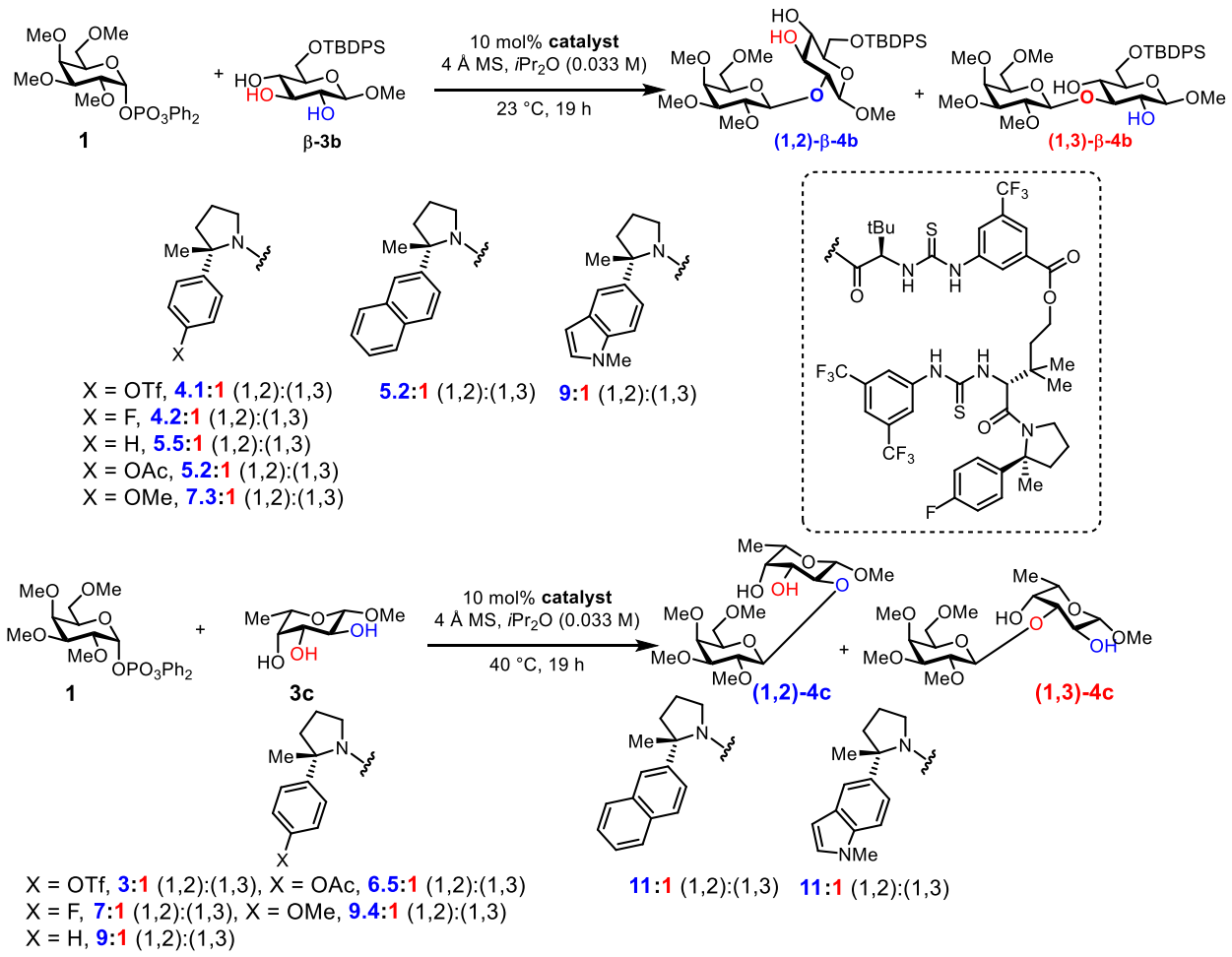


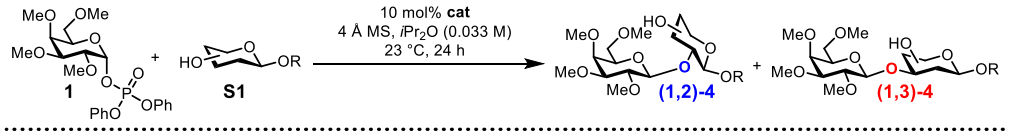
Figure 3.21 Effects of the electronic nature of "northern" arenes on site selectivity in galactosylation of **β-3b** and **3c**. Selectivities were determined by ^{1}H NMR analysis of the crude unacylated reaction mixture.

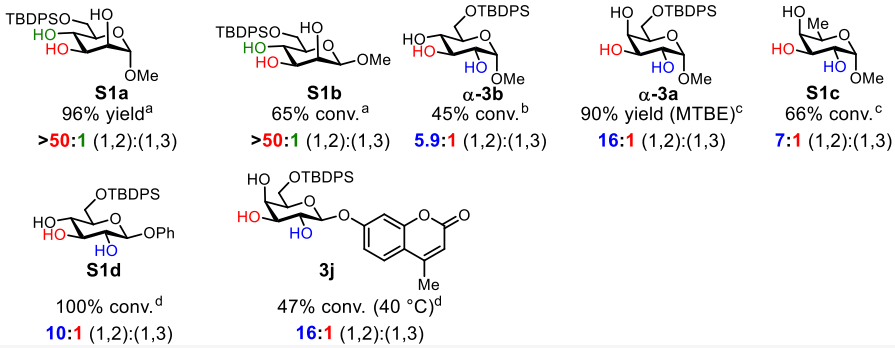
The electronic trend observed in galactosylation of **β-3b** and **3c** is similar to that observed with **β-3a**. Site-selectivity increased as the aryl substituent became more electron-rich, suggesting

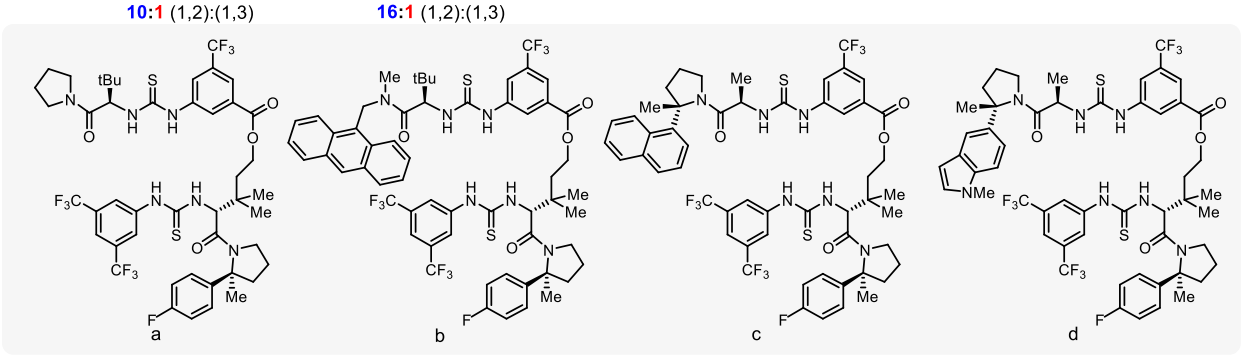
that the importance of CH/π interactions in controlling site selectivity is general across different β-carbohydrates.

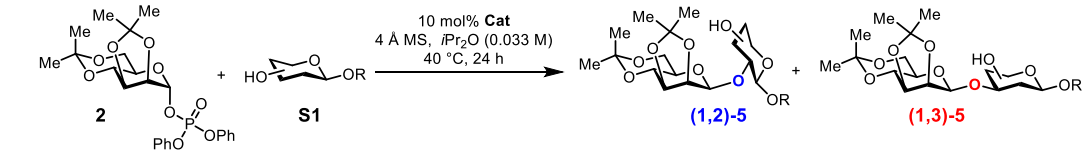
3.8.3 Reaction Condition Optimization

3.8.4 Additional Substrates for Site-selective Galactosylation and Mannosylation









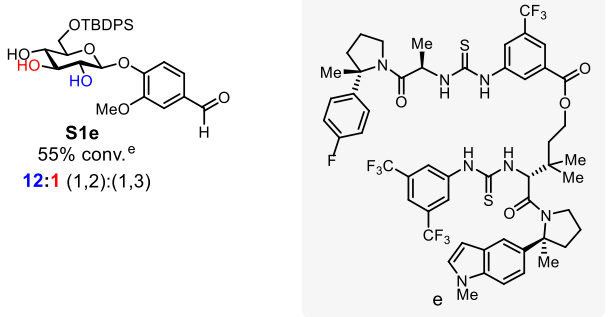
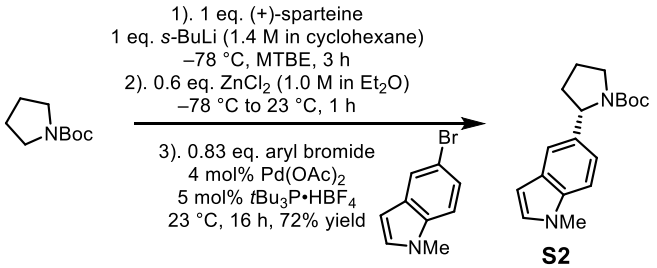


Figure 3.22 Additional substrates for site-selective galactosylations and mannosylations. Conversions were determined by ^{1}H NMR relative to mesitylene as an internal standard. Selectivities were determined by ^{1}H NMR analysis of the crude unacylated reaction mixture. Yields reflect isolated yields of pure (1,2)-products.

Substrates with large inherent reactivity differences, such as α-mannose and β-mannose were glycosylated with high site selectivity at the most reactive position with the simple pyrrolidine catalyst. Good site selectivities were obtained with α-acceptors through extensive catalyst optimization.

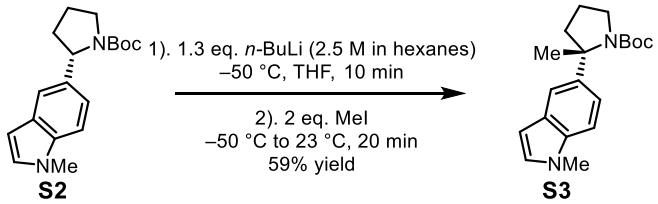
3.8.5 Synthesis and Characterization of Catalysts



***tert*-Butyl (S)-2-(1-methyl-1H-indol-5-yl)pyrrolidine-1-carboxylate (S2)**. **S2** was synthesized following a modified procedure.[17] To a flame-dried 100 mL round bottom flask equipped with a stir bar was added 21 mL anhydrous MTBE, *N*-Boc-pyrrolidine (1.81 mL, 10.3 mmol, 1 equiv.), and (+)-sparteine (2.37 mL, 10.3 mmol, 1 equiv.). The reaction mixture was cooled to –78 °C. To the cooled solution was added *sec*-BuLi (1.4 M in cyclohexane, 7.4 mL, 10.3 mmol, 1 equiv.) dropwise over 10 minutes. The reaction mixture was stirred at –78 °C for 3 hours. To the reaction mixture was then added 1.0 M $ZnCl_2$ in Et_2O (6.2 mL, 6.2 mmol, 0.6 equiv.). The reaction mixture

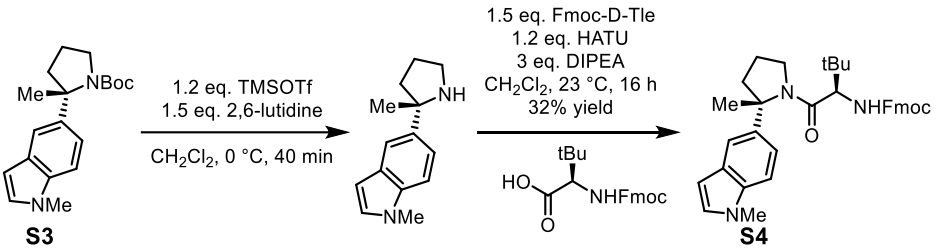
[17] Campos, K. R.; Klapars, A.; Waldman, J. H.; Dormer, P. G.; Chen, C.-Y. Enantioselective, Palladium-Catalyzed r-Arylation of N-Boc-pyrrolidine. *J. Am. Chem. Soc*. **2006**, *128*, 3538–3539.

was stirred at –78 °C for 30 minutes then warmed to 23 °C. The resulting pale white mixture was stirred for 30 minutes at 23 °C. To the reaction mixture was added 5-bromo-1-methylindole (1.8 g, 8.57 mmol, 0.83 equiv.) followed by $Pd(OAc)_2$ (0.093 g, 0.41 mmol, 0.04 equiv.) and tBu$_3$P•HBF$_4$ (0.15 g, 0.52 mmol, 0.05 equiv.) in one portion. The heterogeneous mixture was stirred overnight in a water bath at 23 °C. The light brown reaction mixture was quenched with 0.7 mL of NH_4OH, and the mixture was stirred for 30 minutes. The resulting slurry was filtered over Celite and washed with Et_2O. The filtrate was washed with 1 M HCl and then twice with deionized water. The organic layer was dried over sodium sulfate, filtered, and concentrated under reduced pressure. The crude mixture was purified by column chromatography (0% Et_2O/hexanes to 30% Et_2O/hexanes) on 100 g silica gel to give the product, **S2**, in 72% yield (1.85 g, 6.17 mmol) as a light yellow solid. ^{1}H NMR (400 MHz, $CDCl_3$) δ 7.39 (s, 1H), 7.24 (d, J = 7.8 Hz, 1H), 7.10 – 6.96 (m, 2H), 6.41 (dd, J = 3.1, 0.7 Hz, 1H), 5.07 (s, 0.3H, minor rotamer), 4.92 (s, 0.7H, major rotamer), 3.76 (s, 3H), 3.71 – 3.53 (m, 2H), 2.31 (br, 1H), 2.02 – 1.77 (m, 3H), 1.46 (s, 2.3H, minor rotamer), 1.17 (s, 5.9H, major rotamer). ^{13}C NMR (101 MHz, $CDCl_3$, major rotamer) δ 155.0, 136.1, 135.9, 129.0, 119.7, 117.6, 108.9, 100.8, 79.0, 61.6, 47.1, 36.4, 33.0, 28.3, 23.1. minor rotamer: δ 154.7, 135.3, 128.5, 109.1, 61.1, 47.5, 35.4, 28.7, 23.6. HRMS (ESI) m/z calculated for $C_{18}H_{24}N_2O_2$ $[M+Na]^+$: 323.1730; found: 323.1723.



***tert*-Butyl (S)-2-methyl-2-(1-methyl-1H-indol-5-yl)pyrrolidine-1-carboxylate (S3)**. **S3** was synthesized following a modified procedure.[18] To a flame-dried 100 mL round bottom flask equipped with a stir bar was added aryl pyrrolidine **S2** (1 g, 3.33 mmol, 1 equiv.) and 40 mL anhydrous THF. The reaction mixture was cooled to –50 °C. To the cooled solution was added *n*-BuLi (2.5 M in hexanes, 1.73 mL, 4.33 mmol, 1.3 equiv.) dropwise over 5 minutes. The resulting dark orange solution was stirred at –50 °C for 10 minutes. To the reaction mixture was then added methyl iodide (0.41 mL, 6.66 mmol, 2 equiv.). The light yellow solution was stirred at –50 °C for 10 minutes then warmed to 23 °C. The reaction mixture was stirred for another 10 minutes at 23 °C. The reaction mixture was quenched with sat. NH_4Cl (aq) and diluted with CH_2Cl_2. The organic layer was washed with sat. NaCl(aq.), dried over Na_2SO_4, and concentrated under reduced pressure. The crude mixture was purified by column chromatography (0% Et_2O/hexanes to 10% Et_2O/hexanes) on 50 g silica gel to give the product, **S3**, in 59% yield (0.62 g, 1.97 mmol) as a white solid. ^{1}H NMR (400 MHz, $CDCl_3$) δ 7.49 – 7.42 (m, 1H), 7.22 (d, J = 8.6 Hz, 1H), 7.10 (dd, J = 8.6, 1.7 Hz, 1H), 7.01 (d, J = 3.0 Hz, 1H), 6.42 (d, J = 2.6 Hz, 1H), 3.80 – 3.59 (m, 5H), 2.19 – 2.03 (m, 2H), 1.93 (s, 0.7H, minor rotamer), 1.88 – 1.78 (m, 4.4H, major rotamer), 1.46 (s, 2.3H, minor rotamer), 1.10 (s, 6.2H, major rotamer). ^{13}C NMR (101 MHz, $CDCl_3$, major rotamer) δ 154.8, 139.4, 135.4, 129.0, 128.1, 119.5, 117.2, 108.7, 100.9, 78.9, 65.4, 48.8, 46.3, 33.0, 28.3, 26.4, 22.0. minor rotamer: δ 153.7, 138.1, 135.6, 128.9, 128.4, 119.7, 117.1, 108.9, 101.1, 78.7, 66.0, 49.0, 45.3, 28.8, 26.6. HRMS (ESI) m/z calculated for $C_{19}H_{26}N_2O_2$ $[M+Na]^+$: 337.1886; found: 337.1880.

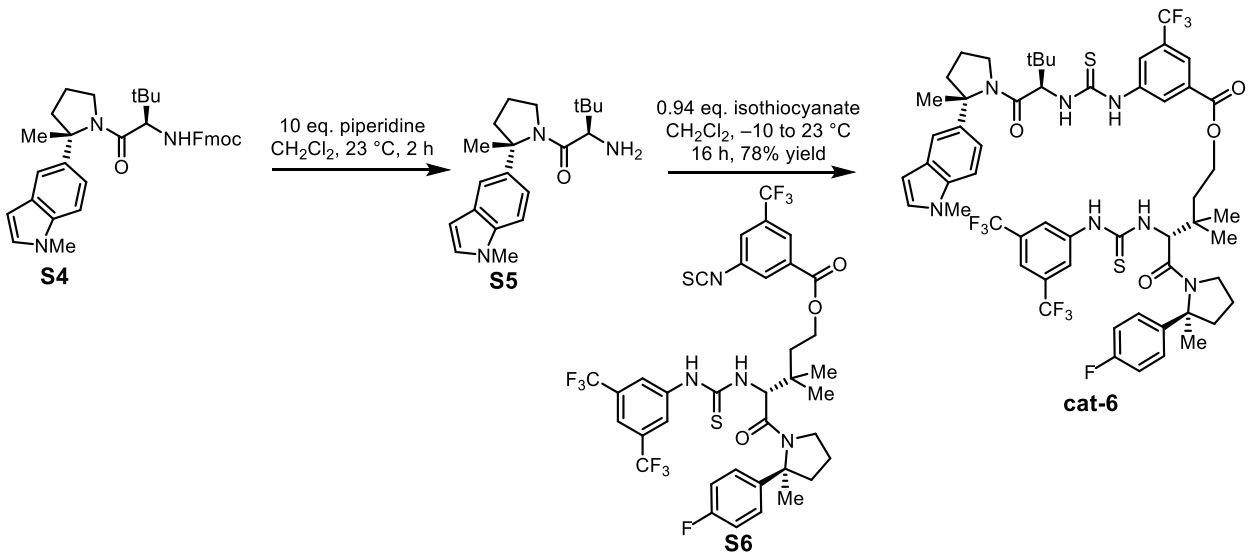
[18] Sheikh, N. S.; Leonori, D.; Barker, G.; Firth, J. D.; Campos, K. R.; Meijer, A. J. H. M.; O'Brien, P.; Coldham, I. An Experimental and in Situ IR Spectroscopic Study of the Lithiation−Substitution of N-Boc-2-phenylpyrrolidine and -piperidine: Controlling the Formation of Quaternary Stereocenters. *J. Am. Chem. Soc*. **2012**, *134*, 5300−5308.



(9H-fluoren-9-yl)methyl ((R)-3,3-dimethyl-1-((S)-2-methyl-2-(1-methyl-1H-indol-5-yl)pyrrolidin-1-yl)-1-oxobutan-2-yl)carbamate (S4). To a flame-dried 100 mL round bottom flask equipped with a stir bar was added aryl pyrrolidine **S3** (0.6 g, 1.91 mmol, 1 equiv.) and 22 mL anhydrous CH_2Cl_2. The reaction mixture was cooled to 0 °C. To the cooled solution was added 2,6-lutidine (0.34 mL, 2.86 mmol, 1.5 equiv.) and trimethylsilyl trifluoromethanesulfonate (TMSOTf, 0.41 mL, 2.29 mmol, 1.2 equiv.) dropwise. The pale pink solution was stirred at 0 °C for 40 minutes. The reaction mixture was quenched with sat. Na_2CO_3 (aq.) and then stirred at 23 °C for 10 minutes. The organic layer was separated, and the aqueous layer was extracted with CH_2Cl_2 (x2). The combined organic layers were washed with sat. NaCl (aq.), dried over Na_2SO_4, and concentrated under reduced pressure to afford the product, which was used directly in the next step without purification.

To a 20 mL scintillation vial containing aryl pyrrolidine (1.91 mmol, 1 equiv.) was added 10 mL anhydrous CH_2Cl_2, Fmoc-d-Tle (1.05 g, 2.87 mmol, 1.5 equiv.), HATU (0.871 g, 2.29 mmol, 1.2 equiv.), and *N*,*N*-Diisopropylethylamine (DIPEA, 1 mL, 5.73 mmol, 3 equiv.). The reaction mixture was stirred at 23 °C overnight. The reaction mixture was diluted CH_2Cl_2 and washed with 1 M HCl, sat. $NaHCO_3$ (aq.), and sat. NaCl (aq.). The organic layer was dried over Na_2SO_4 and concentrated under reduced pressure. The crude mixture was purified by column chromatography (10% Et_2O/hexanes to 50% Et_2O/hexanes) on 100 g silica gel to give the product, **S4**, in 32% yield (0.37 g, 0.67 mmol) as a foamy solid. ^{1}H NMR (600 MHz, $CDCl_3$) δ 7.81 – 7.77 (m, 2H), 7.66 (d,

J = 7.5 Hz, 1H), 7.62 (d, J = 7.5 Hz, 1H), 7.47 – 7.39 (m, 3H), 7.34 (t, J = 7.5 Hz, 1H), 7.29 (t, J = 7.3 Hz, 1H), 7.13 (d, J = 8.6 Hz, 1H), 7.03 (dd, J = 8.7, 1.9 Hz, 1H), 6.95 (d, J = 3.0 Hz, 1H), 6.35 (d, J = 3.0 Hz, 1H), 5.58 (d, J = 9.9 Hz, 1H), 4.58 – 4.48 (m, 2H), 4.38 – 4.27 (m, 2H), 4.22 – 4.15 (m, 1H), 3.94 – 3.85 (m, 1H), 3.65 (s, 3H), 2.16 – 2.04 (m, 2H), 2.00 (s, 3H), 1.97 – 1.82 (m, 2H), 1.09 (s, 9H). ^{13}C NMR (126 MHz, $CDCl_3$) δ 169.4, 156.9, 144.3, 143.9, 141.4, 141.3, 137.0, 135.5, 128.9, 128.4, 127.8, 127.7, 127.2, 125.6, 125.3, 120.1, 120.0, 118.8, 116.8, 109.0, 101.2, 67.8, 67.3, 59.5, 50.3, 47.5, 45.0, 35.5, 32.8, 26.6, 25.8, 22.6. HRMS (ESI) m/z calculated for $C_{35}H_{39}N_3O_3$ $[M+H]^+$: 550.3064; found: 550.3060.



Isothiocyanate **S6** was prepared as previously reported.[19]

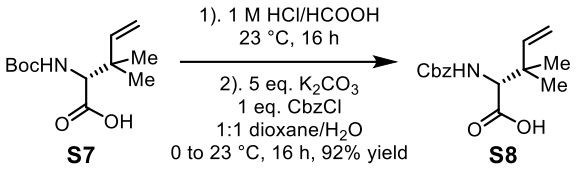
(R)-4-(3-(3,5-bis(trifluoromethyl)phenyl)thioureido)-5-((S)-2-(4-fluorophenyl)-2-methylpyrrolidin-1-yl)-3,3-dimethyl-5-oxopentyl 3-(3-((R)-3,3-dimethyl-1-((S)-2-methyl-2-(1-methyl-1H-indol-5-yl)pyrrolidin-1-yl)-1-oxobutan-2-yl)thioureido)-5-(trifluoromethyl)

[19] Kennedy, C. R.; Lehnherr, D.; Rajapaksa, N. S.; Ford, D. D.; Park, Y.; Jacobsen, E. N. Mechanism-Guided Development of a Highly Active Bis-Thiourea Catalyst for Anion-Abstraction Catalysis. *J. Am. Chem. Soc.* **2016**, *138,* 13525–13528.

benzoate (cat-6). To a 20 mL scintillation vial containing aryl pyrrolidine-d-Tle **S4** (0.2 g, 0.36 mmol, 1 equiv.) was added 3.2 mL anhydrous CH_2Cl_2 and piperidine (0.36 mL, 3.6 mmol, 10 equiv.). The reaction mixture was stirred at 23 °C for 2 hours. The reaction mixture was diluted with CH_2Cl_2 and washed with water (x2) and sat. NaCl (aq.). The organic layer was dried over Na_2SO_4 and concentrated. The deprotected product was co-evaporated with toluene (x3) under reduced pressure to remove piperidine. The product was used directly in the next step without purification.

To a 20 mL scintillation vial equipped with a stir bar was added isothiocyanate **S6** (0.28 g, 0.34 mmol, 1 equiv.) and 5 mL anhydrous CH_2Cl_2. The reaction mixture was cooled to –10 °C. To the cooled solution was added a precooled solution (–10 °C) of amine **S5** (0.119 g, 0.36 mmol, 1.06 equiv.) in 6 mL anhydrous CH_2Cl_2. The reaction mixture was allowed to warm to 23 °C overnight. The reaction mixture was then concentrated under reduced pressure. The crude mixture was purified by column chromatography (10% EtOAc/hexanes to 50% EtOAc/hexanes) on 50 g silica gel to give the product, **cat-3**, in 78% yield (0.298 g, 0.26 mmol) as a pale yellow solid. ^{1}H NMR (400 MHz, CD_3CN) δ 8.80 (s, 1H), 8.70 (s, 1H), 8.34 (s, 1H), 8.08 (s, 1H), 8.06 (s, 2H), 7.98 (s, 1H), 7.71 (s, 1H), 7.36 (d, *J* = 1.7 Hz, 1H), 7.22 (dd, *J* = 8.8, 5.4 Hz, 2H), 7.17 (dd, *J* = 14.1, 9.4 Hz, 2H), 7.09 (d, *J* = 8.7 Hz, 1H), 7.05 (dd, *J* = 8.7, 1.8 Hz, 1H), 6.98 (d, *J* = 3.1 Hz, 1H), 6.85 (t, *J* = 8.9 Hz, 2H), 6.16 (d, *J* = 3.0 Hz, 1H), 5.39 (d, *J* = 9.2 Hz, 1H), 5.38 (d, *J* = 9.4 Hz, 1H), 4.55 – 4.44 (m, 4H), 3.94 – 3.81 (m, 2H), 3.63 (s, 3H), 2.10 – 1.97 (m, 3H), 1.92 (s, 3H), 1.89 – 1.78 (m, 6H), 1.77 – 1.65 (m, 2H), 1.34 – 1.25 (m, 1H), 1.21 (s, 3H), 1.15 (s, 3H), 1.10 (s, 9H). (One proton signal overlaps with solvent peaks). ^{13}C NMR (101 MHz, CD_3CN) δ 182.7, 182.7, 170.4, 169.9, 165.5, 161.9 (d, *J* = 242.1 Hz), 143.5 (d, *J* = 3.0 Hz), 141.8, 141.4, 137.7, 136.1, 132.7, 132.0 (q, *J* = 33.3 Hz), 131.4 (q, *J* = 32.8 Hz), 130.2, 129.0, 128.5, 128.0 (d, *J* = 7.8 Hz), 124.9,

124.5, 124.8 (q, J = 3.4 Hz), 124.5 (q, J = 3.5 Hz), 124.6 (q, J = 271.9 Hz), 124.3 (q, J = 272.1 Hz), 122.6 (q, J = 3.6 Hz), 119.9, 118.8 (q, J = 3.7 Hz), 118.0, 115.1 (d, J = 21.2 Hz), 109.6, 101.2, 68.9, 68.2, 63.8, 63.4, 62.8, 51.1, 51.0, 45.6, 45.1, 38.5, 38.3, 36.2, 33.0, 27.1, 26.3, 25.6, 24.5, 24.2, 23.0. ^{19}F NMR (376 MHz, CD_3CN) δ -63.2, -63.4, -119.5. HRMS (ESI) m/z calculated for $C_{56}H_{61}F_{10}N_7O_4S_2$ $[M+H]^+$: 1150.4140; found: 1150.4098.

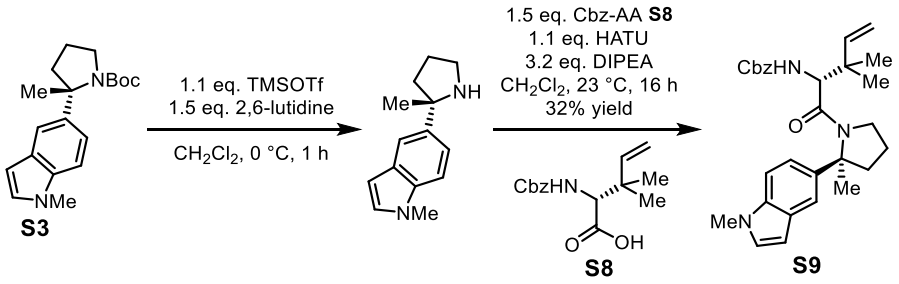


S7 was prepared as previously reported.[20]

(R)-2-(((benzyloxy)carbonyl)amino)-3,3-dimethylpent-4-enoic acid (S8). To a 50 mL round bottom flask equipped with a stir bar was added amino acid **S7** (1 g, 4.11 mmol, 1 equiv.), 1.62 mL of 1 M HCl, and 4.84 mL of formic acid. The reaction mixture was stirred at 23 °C overnight. The reaction mixture was then concentrated under reduced pressure. To a 50 mL round bottom flask containing deprotected amino acid was added 11 mL dioxane and 11 mL H_2O. The homogeneous solution was cooled to 0 °C. To the cooled solution was added K_2CO_3 (2.84 g, 20.6 mmol, 5 equiv.) and benzyl chloroformate (0.59 mL, 4.11 mmol, 1 equiv.). The reaction was warmed to 23 °C and then stirred at 23 °C overnight. Dioxane was removed under reduced pressure. The aqueous layer was diluted with H_2O and washed with hexanes (x2) to remove any remaining benzyl chloroformate. The aqueous layer was acidified with 3 M HCl until pH = 2. The aqueous layer was extracted with EtOAc (x3). The combined organic layers were washed with sat.

[20] Rossi, F.; Corcella, F.; Saverio, C.; Heidempergher, F.; Marchionni, C.; Auguadro, M.; Cattaneo, M.; Ceriani, L.; Visentin, G.; Ventrella, G.; Pinciroli, V.; Ramella, G.; Candiani, I.; Bedeschi, A.; Tomasi, A.; Kline, B. J.; Martinez, C. A.; Yazbeck, D.; Kucera, D. J. Process Research and Development and Scale-up of a 4,4-Difluoro-3,3-dimethylproline Derivative. *Org. Process Res. Dev*. **2008**, *12*, 322–328.

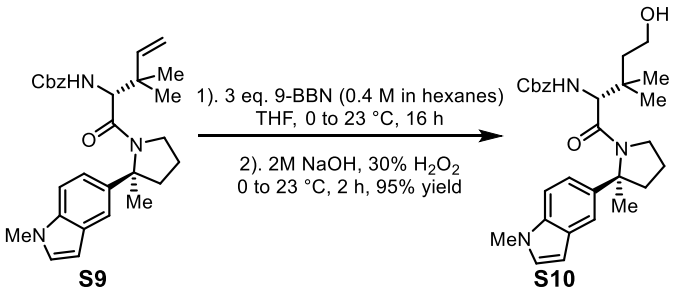
NaCl (aq.), dried over Na_2SO_4, and concentrated under reduced pressure to afford the desired product, **S8**, cleanly in 92% yield (1.05 g, 3.78 mmol) as a colorless oil. ^{1}H NMR (400 MHz, $CDCl_3$) δ 9.50 (br, 1H), 7.41 – 7.27 (m, 5H), 5.85 (dd, *J* = 17.3, 10.8 Hz, 1H), 5.28 (d, *J* = 9.1 Hz, 1H), 5.18 – 5.01 (m, 4H), 4.24 (d, *J* = 9.2 Hz, 1H), 1.15 (d, *J* = 5.7 Hz, 6H). ^{13}C NMR (101 MHz, $CDCl_3$) δ 176.0, 156.3, 142.6, 136.2, 128.7, 128.4, 128.3, 114.6, 67.4, 61.6, 40.3, 24.3, 23.8. HRMS (ESI) m/z calculated for $C_{15}H_{19}NO_4$ $[M+H]^+$: 278.1387; found: 278.1385.



Benzyl ((R)-3,3-dimethyl-1-((S)-2-methyl-2-(1-methyl-1H-indol-5-yl)pyrrolidin-1-yl)-1-oxopent-4-en-2-yl)carbamate (S9). To a flame-dried 100 mL round bottom flask equipped with a stir bar was added aryl pyrrolidine **S3** (0.95 g, 3.02 mmol, 1 equiv.) and 40 mL anhydrous CH_2Cl_2. The reaction mixture was cooled to 0 °C. To the cooled solution was added 2,6-lutidine (0.53 mL, 4.53 mmol, 1.5 equiv.) and trimethylsilyl trifluoromethanesulfonate (TMSOTf, 0.6 mL, 3.32 mmol, 1.1 equiv.) dropwise. The pale pink solution was stirred at 0 °C for 1 hour. The reaction mixture was quenched with sat. Na_2CO_3 (aq.) and then stirred at 23 °C for 10 minutes. The organic layer was separated, and the aqueous layer was extracted with CH_2Cl_2 (x2). The combined organic layers were washed with sat. NaCl (aq.), dried over Na_2SO_4, and concentrated under reduced pressure to afford the product, which was used directly in the next step without purification.

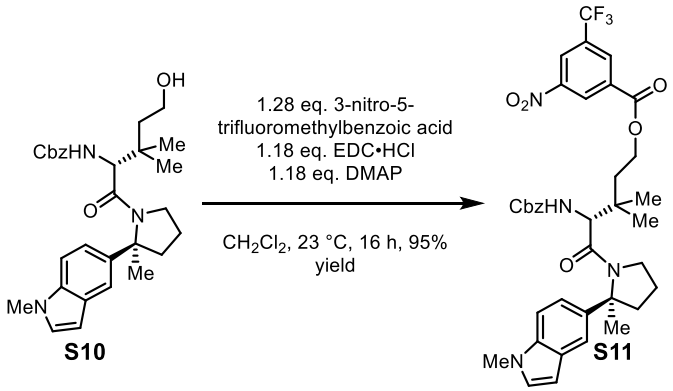
To a 20 mL scintillation vial containing aryl pyrrolidine (3.02 mmol, 1 equiv.) was added 13 mL anhydrous CH_2Cl_2, Cbz-amino acid **S8** (0.84 g, 3.02 mmol, 1.5 equiv.), HATU (1.263 g, 3.32

mmol, 1.1 equiv.), and *N*,*N*-Diisopropylethylamine (DIPEA, 1.7 mL, 9.66 mmol, 3.2 equiv.). The reaction mixture was stirred at 23 °C overnight. The reaction mixture was diluted CH_2Cl_2 and washed with 1 M HCl, sat. $NaHCO_3$ (aq.), and sat. NaCl (aq.). The organic layer was dried over Na_2SO_4 and concentrated under reduced pressure. The crude mixture was purified by column chromatography (10% Et_2O/hexanes to 50% Et_2O/hexanes) on 100 g silica gel to give the product, **S9**, in 32% yield (0.46 g, 0.97 mmol) as a foamy solid. ^{1}H NMR (600 MHz, $CDCl_3$) δ 7.43 (d, *J* = 1.8 Hz, 1H), 7.39 – 7.32 (m, 5H), 7.13 (d, *J* = 8.6 Hz, 1H), 7.02 (dd, *J* = 8.7, 1.9 Hz, 1H), 6.97 (d, *J* = 3.1 Hz, 1H), 6.36 (d, *J* = 3.0 Hz, 1H), 6.06 (dd, *J* = 17.3, 10.9 Hz, 1H), 5.39 (d, *J* = 9.8 Hz, 1H), 5.20 (d, *J* = 12.4 Hz, 1H), 5.16 (d, *J* = 12.3 Hz, 1H), 5.10 – 5.03 (m, 2H), 4.50 (d, *J* = 9.8 Hz, 1H), 4.19 (ddd, *J* = 9.8, 7.4, 5.2 Hz, 1H), 3.86 (dt, *J* = 9.9, 7.5 Hz, 1H), 3.72 (s, 3H), 2.11 (dt, *J* = 12.3, 6.1 Hz, 1H), 2.05 (ddd, *J* = 12.5, 8.4, 6.7 Hz, 1H), 1.96 (s, 3H), 1.94 – 1.85 (m, 2H), 1.16 (s, 3H), 1.14 (s, 3H). ^{13}C NMR (126 MHz, $CDCl_3$) δ 168.8, 156.8, 143.8, 137.1, 136.7, 135.5, 128.9, 128.6, 128.4, 128.1, 128.0, 118.9, 116.9, 113.6, 108.9, 101.2, 67.8, 66.9, 59.0, 50.2, 45.0, 40.8, 32.9, 25.6, 24.4, 23.1, 22.7. HRMS (ESI) m/z calculated for $C_{29}H_{35}N_3O_3$ $[M+H]^+$: 474.2751; found: 474.2744.

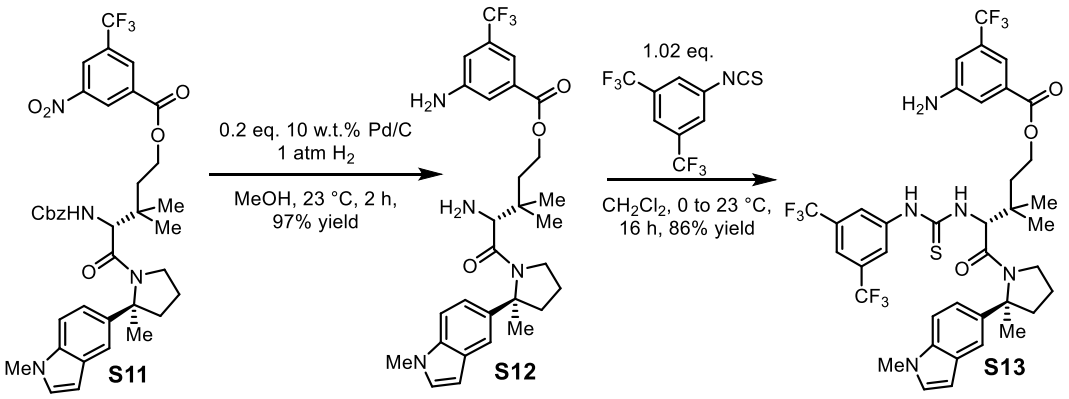


Benzyl ((R)-5-hydroxy-3,3-dimethyl-1-((S)-2-methyl-2-(1-methyl-1H-indol-5-yl)pyrrolidin-1-yl)-1-oxopentan-2-yl)carbamate (S10). To a flame-dried 100 mL round bottom flask equipped with a stir bar was added alkene **S9** (0.46 g, 0.97 mmol, 1 equiv.) and 9.7 mL anhydrous THF. The

reaction mixture was cooled to 0 °C. To the cooled solution was added 9-borabicyclo(3.3.1)nonane (0.4 M in hexanes, 7.3 mL, 2.91 mmol, 3 equiv.) slowly. The reaction mixture was then warmed to 23 °C and stirred at 23 °C overnight. At that time, the solution was cooled to 0 °C. To the reaction mixture was added 4.4 mL 2 M NaOH (aq.) dropwise and 3.9 mL 30% H_2O_2. The reaction mixture was then warmed to 23 °C and stirred at 23 °C for 2 hours. The mixture was diluted with EtOAc, and the organic layer was washed with water, 10% $Na_2S_2O_3$ (aq.) (x2), and sat. NaCl (aq.).The organic layer was dried over Na_2SO_4, and concentrated under reduced pressure. The crude mixture was purified by column chromatography (10% EtOAc/hexanes to 60% EtOAc/hexanes) on 50 g silica gel to give the product, **S10**, in 95% yield (0.451 g, 0.92 mmol) as a foamy solid. ^{1}H NMR (600 MHz, $CDCl_3$) δ 7.46 – 7.37 (m, 5H), 7.38 – 7.31 (m, 1H), 7.16 (d, *J* = 8.6 Hz, 1H), 7.05 – 6.98 (m, 3H), 6.38 (d, *J* = 3.0 Hz, 1H), 5.28 – 5.19 (m, 2H), 4.69 (d, *J* = 10.1 Hz, 1H), 4.38 – 4.33 (m, 2H), 3.89 (dd, *J* = 17.2, 8.8 Hz, 1H), 3.78 – 3.72 (m, 4H), 3.70 – 3.61 (m, 1H), 2.13 – 2.07 (m, 2H), 2.02 (s, 3H), 1.97 (ddd, *J* = 14.7, 10.3, 4.2 Hz, 1H), 1.93 – 1.83 (m, 2H), 1.39 (dt, *J* = 15.2, 3.9 Hz, 1H), 1.15 (s, 3H), 1.13 (s, 3H). ^{13}C NMR (126 MHz, $CDCl_3$) δ 170.6, 157.3, 136.8, 136.3, 135.5, 129.0, 128.5, 128.4, 128.0, 127.9, 118.7, 116.8, 109.0, 101.1, 68.2, 66.8, 59.1, 58.6, 50.4, 45.0, 41.5, 36.8, 32.8, 27.5, 26.2, 24.5, 22.2. HRMS (ESI) m/z calculated for $C_{29}H_{37}N_3O_4$ $[M+H]^+$: 492.2857; found: 492.2851.



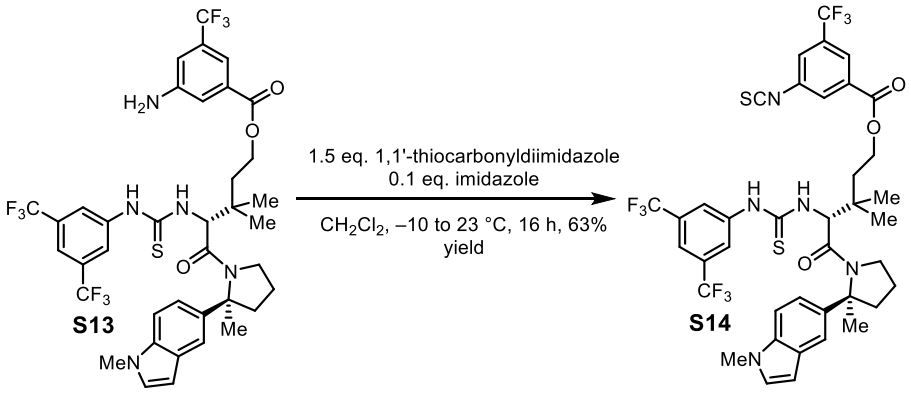
(R)-4-(((benzyloxy)carbonyl)amino)-3,3-dimethyl-5-((S)-2-methyl-2-(1-methyl-1H-indol-5-yl)pyrrolidin-1-yl)-5-oxopentyl 3-nitro-5-(trifluoromethyl)benzoate (S11). To a 20 mL scintillation vial containing alcohol **S10** (0.451 g, 0.92 mmol, 1 equiv.) was added 3.2 mL anhydrous CH_2Cl_2 and 3-nitro-5-trifluoromethylbenzoic acid (0.276 g, 1.17 mmol, 1.28 equiv.). The resulting mixture was stirred to homogeneity. To the mixture was added EDC•HCl (0.208 g, 1.08 mmol, 1.18 equiv) and 4-(dimethylamino)pyridine (DMAP, 0.132 g, 1.08 mmol, 1.18 equiv). The reaction mixture was stirred at 23 °C overnight. The crude reaction mixture was concentrated under reduced pressure and purified by column chromatography (0% EtOAc/hexanes to 30% EtOAc/hexanes) on 50 g silica gel to give the product, **S11**, in 95% yield (0.618 g, 0.87 mmol) as a pale yellow solid. ^{1}H NMR (500 MHz, $CDCl_3$) δ 9.02 (s, 1H), 8.68 (s, 1H), 8.62 (s, 1H), 7.44 – 7.31 (m, 6H), 7.13 (d, *J* = 8.6 Hz, 1H), 7.03 – 6.97 (m, 2H), 6.35 (d, *J* = 3.0 Hz, 1H), 5.52 (d, *J* = 10.0 Hz, 1H), 5.26 (d, *J* = 12.2 Hz, 1H), 5.18 (d, *J* = 12.4 Hz, 1H), 4.63 (d, *J* = 10.0 Hz, 1H), 4.57 (t, *J* = 7.4 Hz, 2H), 4.27 – 4.18 (m, 1H), 3.90 (q, *J* = 8.1 Hz, 1H), 3.73 (s, 3H), 2.16 – 2.08 (m, 2H), 2.07 – 1.89 (m, 7H), 1.19 (s, 3H), 1.16 (s, 3H). ^{13}C NMR (126 MHz, $CDCl_3$) δ 168.9, 163.2, 156.9, 148.5, 136.7, 136.5, 135.4, 133.5, 132.8 (q, J = 34.7 Hz), 131.9 (q, J = 3.3 Hz), 129.0, 128.6, 128.4, 128.2, 128.0, 127.5, 124.4 (q, J = 3.8 Hz), 122.5 (q, J = 273.3 Hz), 118.6, 116.7, 109.0, 101.1, 67.8, 67.1, 63.6, 58.9, 50.3, 44.9, 37.2, 36.9, 32.8, 25.7, 23.8, 23.2, 22.6. ^{19}F NMR (376 MHz, $CDCl_3$) δ -62.84. HRMS (ESI) m/z calculated for $C_{37}H_{39}F_3N_4O_7$ $[M+H]^+$: 709.2844; found: 709.2836.



(R)-4-(3-(3,5-bis(trifluoromethyl)phenyl)thioureido)-3,3-dimethyl-5-((S)-2-methyl-2-(1-methyl-1H-indol-5-yl)pyrrolidin-1-yl)-5-oxopentyl 3-amino-5-(trifluoromethyl)benzoate (S13). To a flame-dried 50 mL round bottom flask equipped with a stir bar was added 10 wt.% palladium on carbon (0.186 g, 0.17 mmol, 0.2 equiv.). The reaction flask was evacuated and backfilled with N_2. To the flask was added a solution of **S11** (0.618 g, 0.87 mmol, 1 equiv.) in 9 mL anhydrous methanol. The reaction flask was evacuated and backfilled with N_2 three times. The headspace was then evacuated until the solvent bubbled and backfilled with H_2 three times. The reaction mixture was stirred at 23 °C under H_2 pressure (1 atm via balloon) for 2 hours. The flask was then flushed with N_2 before the reaction mixture was diluted with EtOAc and filtered through a pad of Celite. The filtrate was washed with water, sat. Na_2CO_3 (aq.), and sat. NaCl (aq.). The organic layer was dried over Na_2SO_4 and concentrated under reduced pressure to afford the desired product, **S12**, in 97% yield, which was used directly in the next step without purification.

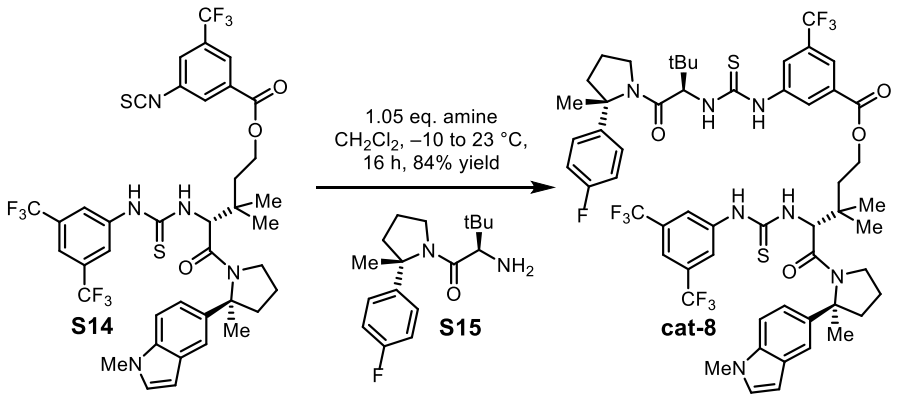
To a 20 mL scintillation vial containing amine **S12** (0.458 g, 0.84 mmol, 1 equiv.) was added 6.4 mL anhydrous CH_2Cl_2. The solution was cooled to 0 °C, and to the cooled solution was added 3,5-bis(trifluoromethyl)phenyl isothiocyanate (0.157 mL, 0.86 mmol, 1.02 equiv.) dropwise. The reaction mixture was allowed to warm to 23 °C overnight as the ice bath melted. At that time, the reaction mixture was concentrated under reduced pressure and purified by column chromatography

(0% EtOAc/hexanes to 35% EtOAc/hexanes) on 50 g silica gel to give the product, **S13**, in 86% yield (0.59 g, 0.72 mmol) as a white solid. ^{1}H NMR (600 MHz, $CDCl_3$) δ 7.65 (s, 2H), 7.61 (s, 1H), 7.45 (s, 2H), 7.29 (d, *J* = 1.8 Hz, 1H), 7.00 (s, 1H), 6.95 (dd, *J* = 8.6, 1.9 Hz, 1H), 6.81 (d, *J* = 3.3 Hz, 2H), 6.16 (d, *J* = 3.0 Hz, 1H), 5.57 (d, *J* = 9.5 Hz, 1H), 4.63 – 4.54 (m, 1H), 4.48 (td, *J* = 7.3, 2.3 Hz, 2H), 3.93 (s, 2H), 3.89 (dt, *J* = 10.2, 7.7 Hz, 1H), 3.49 (s, 3H), 2.08 – 2.02 (m, 2H), 1.99 – 1.93 (m, 5H), 1.86 (dt, *J* = 10.8, 6.5 Hz, 2H), 1.22 (d, *J* = 3.6 Hz, 6H). ^{13}C NMR (126 MHz, $CDCl_3$) δ 181.8, 169.9, 165.8, 147.3, 139.2, 136.2, 135.1, 132.1, 131.8 (q, *J* = 33.0 Hz), 129.1, 128.2, 124.6, 123.9 (q, *J* = 272.3 Hz), 123.1 (q, *J* = 272.9 Hz), 118.8, 118.7, 116.9, 116.0 (q, *J* = 5.5, 4.0 Hz), 115.3 (q, *J* = 3.4 Hz), 108.6, 100.9, 68.5, 63.2, 62.4, 50.7, 45.0, 37.8, 37.7, 32.5, 25.8, 24.5, 24.4, 22.6. ^{19}F NMR (376 MHz, $CDCl_3$) δ -62.81, -63.07. HRMS (ESI) m/z calculated for $C_{38}H_{38}F_9N_5O_3S$ $[M+H]^+$: 816.2624; found: 816.2617.



(R)-4-(3-(3,5-bis(trifluoromethyl)phenyl)thioureido)-3,3-dimethyl-5-((S)-2-methyl-2-(1-methyl-1H-indol-5-yl)pyrrolidin-1-yl)-5-oxopentyl 3-isothiocyanato-5-(trifluoromethyl) benzoate (S14). To a flame-dried 50 mL round bottom flask equipped with a stir bar was added 1,1′-thiocarbonyldiimidazole (0.193 g, 1.08 mmol, 1.5 equiv.), imidazole (5 mg, 0.07 mmol, 0.1 equiv.), and 5 mL anhydrous CH_2Cl_2. The yellow solution was cooled to –10 °C. To the cooled solution was added a precooled solution (–10 °C) of aniline **S13** (0.59 g, 0.72 mmol, 1 equiv.) in

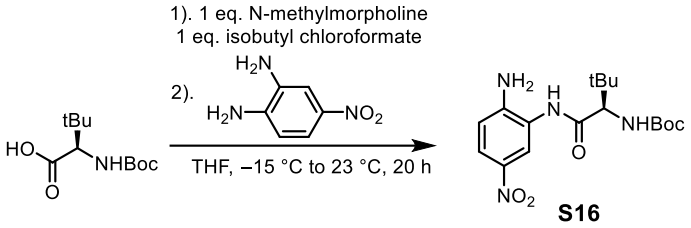
8 mL anhydrous CH_2Cl_2. The reaction mixture was stirred at –10 °C for 30 minutes and then warmed to 23 °C. The mixture was stirred at 23 °C overnight. At that time, the reaction mixture was concentrated under reduced pressure, and the crude mixture was purified by column chromatography (0% EtOAc/hexanes to 20% EtOAc/hexanes) on 100 g silica gel to give the product, **S14**, in 63% yield (0.39 g, 0.45 mmol) as a white solid. ^{1}H NMR (500 MHz, $CDCl_3$) δ 8.13 (s, 1H), 7.98 (s, 1H), 7.62 (s, 3H), 7.43 (s, 1H), 7.23 (s, 1H), 6.92 (d, J = 8.5 Hz, 1H), 6.81 (d, J = 3.0 Hz, 1H), 6.78 (d, J = 8.7 Hz, 1H), 6.15 (s, 1H), 5.60 (d, J = 9.6 Hz, 1H), 4.61 (dt, J = 10.9, 6.1 Hz, 1H), 4.53 (tt, J = 8.0, 3.9 Hz, 2H), 3.95 – 3.84 (m, 1H), 3.49 (s, 3H), 2.07 (t, J = 6.3 Hz, 2H), 2.01 – 1.93 (m, 5H), 1.88 (p, J = 6.9 Hz, 2H), 1.24 (s, 6H). ^{13}C NMR (126 MHz, $CDCl_3$) δ 181.9, 169.9, 164.0, 139.8, 139.0, 135.9, 135.1, 133.3, 133.1, 132.8 (q, J = 34.0 Hz), 131.5 (q, J = 33.3 Hz), 129.8, 129.1, 128.1, 126.4 (q, J = 3.4 Hz), 124.7 (d, J = 3.8 Hz), 124.5, 123.0 (q, J = 272.7 Hz), 122.9 (q, J = 273.0 Hz), 118.8, 118.7, 116.9, 108.5, 100.8, 68.6, 63.2, 63.0, 50.8, 45.1, 37.8, 37.7, 32.5, 25.9, 24.5, 24.4, 22.7. ^{19}F NMR (471 MHz, $CDCl_3$) δ -62.78, -63.01. HRMS (ESI) m/z calculated for $C_{39}H_{36}F_9N_5O_3S_2$ $[M+H]^+$: 858.2189; found: 858.2174.



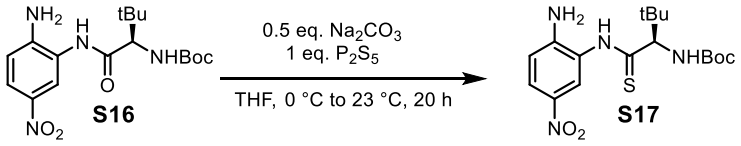
S15 was prepared as previously reported.[21]

[21] Lehnherr, D.; Ford, D. D.; Bendelsmith, A. J.; Kennedy, C. R.; Jacobsen, E. N. Conformational Control of Chiral Amido-Thiourea Catalysts Enables Improved Activity and Enantioselectivity. *Org. Lett.* **2016**, *18*, 3214–3217.

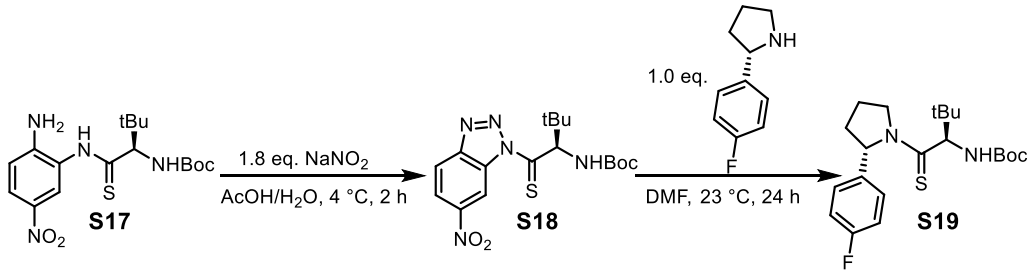
(R)-4-(3-(3,5-bis(trifluoromethyl)phenyl)thioureido)-3,3-dimethyl-5-((S)-2-methyl-2-(1-methyl-1H-indol-5-yl)pyrrolidin-1-yl)-5-oxopentyl 3-(3-((R)-1-((S)-2-(4-fluorophenyl)-2-methylpyrrolidin-1-yl)-3,3-dimethyl-1-oxobutan-2-yl)thioureido)-5-(trifluoromethyl) benzoate (cat-8). To a 20 mL scintillation vial equipped with a stir bar was added isothiocyanate **S14** (0.39 g, 0.45 mmol, 1 equiv.) and 5 mL anhydrous CH_2Cl_2. The reaction mixture was cooled to –10 °C. To the cooled solution was added a precooled solution (–10 °C) of amine **S15** (0.137 g, 0.47 mmol, 1.05 equiv.) in 5 mL anhydrous CH_2Cl_2. The reaction mixture was allowed to warm to 23 °C overnight. The reaction mixture was then concentrated under reduced pressure. The crude mixture was purified by column chromatography (0% EtOAc/hexanes to 30% EtOAc/hexanes) on 100 g silica gel to give the product, **cat-8**, in 84% yield (0.43 g, 0.38 mmol) as a pale yellow solid. ^{1}H NMR (400 MHz, CD_3CN) δ 8.65 (s, 1H), 8.57 (s, 1H), 8.25 (s, 1H), 8.02 (s, 2H), 7.97 (s, 1H), 7.94 (s, 1H), 7.66 (s, 1H), 7.33 (s, 1H), 7.29 (d, *J* = 9.4 Hz, 1H), 7.17 (dd, *J* = 8.7, 5.4 Hz, 2H), 7.03 (d, *J* = 9.1 Hz, 1H), 7.00 (s, 2H), 6.94 (d, *J* = 3.0 Hz, 1H), 6.78 (t, *J* = 8.9 Hz, 2H), 6.10 (d, *J* = 3.0 Hz, 1H), 5.47 (d, *J* = 9.4 Hz, 1H), 5.20 (d, *J* = 9.1 Hz, 1H), 4.52 – 4.37 (m, 4H), 3.88 (q, *J* = 8.3 Hz, 1H), 3.84 – 3.76 (m, 1H), 3.57 (s, 3H), 2.06 – 1.92 (m, 4H), 1.88 (s, 3H), 1.85 – 1.75 (m, 6H), 1.74 – 1.59 (m, 2H), 1.30 – 1.21 (m, 1H), 1.18 (s, 3H), 1.14 (s, 3H), 1.03 (s, 9H). ^{13}C NMR (101 MHz, CD_3CN) δ 182.8, 182.6, 170.3, 170.0, 165.5, 161.9 (d, *J* = 242.1 Hz), 143.4 (d, *J* = 3.0 Hz), 141.9, 141.2, 137.8, 136.1, 132.8, 131.9 (q, *J* = 33.3 Hz), 131.4 (q, *J* = 32.8 Hz), 130.2, 129.0, 128.6, 128.0 (d, *J* = 7.8 Hz), 125.0 (q, *J* = 4.0 Hz), 124.7 (q, *J* = 2.8 Hz), 124.6 (q, *J* = 272.0 Hz), 124.3 (q, *J* = 272.0 Hz), 122.7 (q, *J* = 3.5 Hz), 118.8 (q, *J* = 3.9 Hz), 119.9, 118.0, 115.1 (d, *J* = 21.2 Hz), 109.6, 101.1, 69.0, 68.2, 63.9, 63.5, 62.9, 51.2, 50.9, 45.5, 45.1, 38.5, 38.3, 36.2, 33.0, 27.1, 26.2, 25.6, 24.5, 24.3, 23.1, 23.0. ^{19}F NMR (376 MHz, CD_3CN) δ -63.3, -63.4, -119.4. HRMS (ESI) m/z calculated for $C_{56}H_{61}F_{10}N_7O_4S_2$ $[M+H]^+$: 1150.4140; found: 1150.4111.



***tert*-Butyl (R)-(1-((2-amino-5-nitrophenyl)amino)-3,3-dimethyl-1-oxobutan-2-yl)carbamate (S16)**. To a flame-dried 250 mL round bottom flask equipped with a stir bar was added Boc-D-Tle (3 g, 13 mmol, 1 equiv.) and 110 mL anhydrous THF. The solution was cooled to –15 °C. To the cooled solution was added *N*-methylmorpholine (2.9 mL, 26 mmol, 2 equiv.) and isobutyl chloroformate (1.68 mL, 13 mmol, 1 equiv.). The reaction mixture was stirred at –15 °C for 25 minutes. At that time, 1,2-diamino-4-nitrobenzene (2 g, 13 mmol, 1 equiv.) was added to the reaction mixture in one portion. The reaction mixture was allowed to warm to 23 °C overnight. The reaction mixture was then concentrated under reduced pressure. The crude mixture was dissolved in EtOAc. The organic layer was washed with sat. $NaHCO_3$ (aq.) (x2) and sat. NaCl (aq.). The organic layer was dried over Na_2SO_4 and concentrated under reduced pressure. The crude mixture was purified by column chromatography (10% EtOAc/hexanes to 40% EtOAc/hexanes) on 100 g silica gel to give the product, **S16**, in 55% yield (1.59 g, 7.15 mmol) as a yellow solid. ^{1}H NMR (400 MHz, $CDCl_3$) δ 8.52 (s, 1H), 7.94 (d, J = 2.5 Hz, 1H), 7.89 (dd, J = 9.0, 2.6 Hz, 1H), 6.61 (d, J = 8.9 Hz, 1H), 5.47 (d, J = 8.1 Hz, 1H), 4.85 (s, 2H), 4.06 (d, J = 8.1 Hz, 1H), 1.39 (s, 9H), 1.10 (s, 9H). ^{13}C NMR (101 MHz, $CDCl_3$) δ 171.0, 157.0, 149.0, 138.1, 124.4, 123.6, 121.0, 115.1, 81.0, 63.4, 34.0, 28.4, 26.9. HRMS (ESI) m/z calculated for $C_{17}H_{26}N_4O_5$ $[M+H]^+$: 367.1976; found: 367.1971.



***tert*-Butyl (R)-(1-((2-amino-5-nitrophenyl)amino)-3,3-dimethyl-1-thioxobutan-2-yl)carbamate (S17)**. To a flame-dried 200 mL round bottom flask equipped with a stir bar was added sodium carbonate (0.379 g, 3.56 mmol, 0.5 equiv.), phosphorus(V) sulfide (1.589 g, 7.15 mmol, 1 equiv.), and 100 mL anhydrous THF. The reaction mixture was stirred at 23 °C for 1 hour to yield a mostly homogeneous solution. The reaction mixture was cooled to 0 °C, and to the reaction mixture was added a solution of amide **S16** (2.62 g, 7.15 mmol, 1 equiv.) in 9 mL anhydrous THF. The reaction mixture was stirred at 0 °C for 30 minutes and then warmed to 23 °C. The mixture was stirred at 23 °C for 48 hours. At that time, the reaction mixture was concentrated under reduced pressure. The crude material was dissolved in EtOAc and washed with sat. $NaHCO_3$ (aq.). The aqueous layer was extracted with EtOAc (x2), and the combined organic layers were washed with sat. NaCl (aq.). The organic layer was dried over Na_2SO_4 and concentrated under reduced pressure. The crude mixture was purified by column chromatography (0% EtOAc/hexanes to 25% EtOAc/hexanes) on 200 g silica gel to give the product, **S17**, in 50% yield (1.37 g, 3.58 mmol) as a yellow solid. ^{1}H NMR (400 MHz, $CDCl_3$) δ 10.02 (br, 1H), 8.05 (dd, J = 9.0, 2.6 Hz, 1H), 8.00 (d, J = 2.5 Hz, 1H), 6.74 (d, J = 9.0 Hz, 1H), 5.63 (d, J = 9.0 Hz, 1H), 4.79 (br, 2H), 4.47 (d, J = 9.1 Hz, 1H), 1.33 (s, 9H), 1.17 (s, 9H). ^{13}C NMR (101 MHz, $CDCl_3$) δ 204.7, 157.5, 149.0, 138.4, 125.7, 124.9, 122.9, 115.4, 81.4, 68.7, 34.8, 28.4, 27.1. HRMS (ESI) m/z calculated for $C_{17}H_{26}N_4O_4S$ $[M+H]^+$: 383.1748; found: 383.1741.

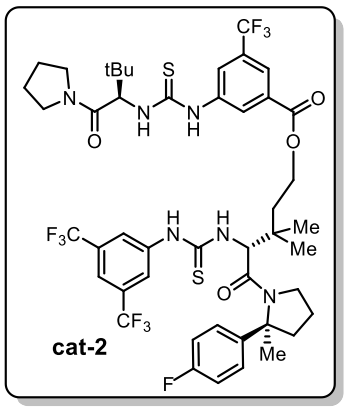


***tert*-Butyl ((R)-1-((S)-2-(4-fluorophenyl)pyrrolidin-1-yl)-3,3-dimethyl-1-thioxobutan-2-yl)carbamate (S19)**. To a 20 mL scintillation vial equipped with a stir bar was added amide **S17** (0.2 g, 0.52 mmol, 1 equiv.), 5.2 mL glacial acetic acid, and 0.28 mL H_2O. The solution was cooled in a water/ice bath carefully to avoid solvent freezing. To the cooled solution was added $NaNO_2$ (0.065 g, 0.94 mmol, 1.8 equiv.). The orange reaction mixture was stirred at 4 °C for 2 hours. At that time, the reaction mixture was diluted with EtOAc and hexanes. The organic layer was washed with H_2O (x2), sat. $NaHCO_3$ (aq.) (x2), and sat. NaCl (aq.). The organic layer was dried over Na_2SO_4 and concentrated under reduced pressure to afford the desired product **S18**, which was used directly in the next step without purification.

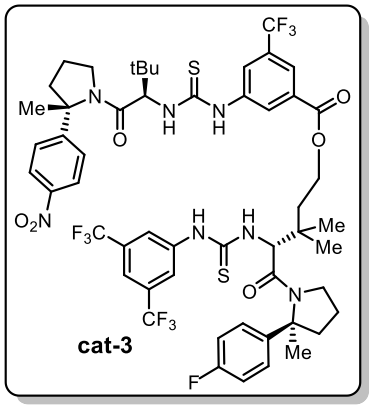
To a 20 mL scintillation vial containing benzotriazole **S18** (0.52 mmol, 1 equiv.) was added 3 mL anhydrous DMF and a solution of (S)-2-(4-fluorophenyl)pyrrolidine (0.086 g, 0.52 mmol, 1 equiv.) in 2 mL anhydrous DMF. The reaction mixture was stirred at 23 °C overnight. The reaction mixture was diluted with Et_2O and washed with H_2O, 10% LiCl (aq.) (x2), and sat. NaCl (aq.). The organic layer was dried over Na_2SO_4 and concentrated under reduced pressure. The crude mixture was purified by column chromatography (0% Et_2O/hexanes to 15% Et_2O/hexanes) on 25 g silica gel to give the product, **S19**, in 63% yield (0.13 g, 0.33 mmol) as a white solid. ^{1}H NMR (400 MHz, $CDCl_3$, * denotes minor rotamer) δ 7.28 – 7.23 (m, 0.6H*), 7.08 – 6.98 (m, 2H, 0.7H*), 6.92 (t, *J* = 8.7 Hz, 2H), 5.83 (d, *J* = 7.6 Hz, 1H), 5.78 (d, *J* = 8.0 Hz, 0.26H*), 5.40 (d, *J* = 10.4 Hz, 1H), 5.33 (d, *J* = 10.6 Hz, 0.27H*), 4.66 (d, *J* = 10.4 Hz, 1H), 4.60 (d, *J* = 10.6 Hz, 0.26H*), 4.49 – 4.40 (m, 1H), 4.18 – 4.06 (m, 0.32H*), 4.01 (dd, *J* = 14.4, 7.9 Hz, 0.29H*), 3.95 – 3.85 (m, 1H), 2.46 – 2.32 (m, 0.39H*), 2.32 – 2.15 (m, 1H, 0.4H*), 2.06 – 1.98 (m, 2H), 1.98 – 1.88 (m, 1H, 0.5H*), 1.46 (s, 9H), 1.45 (s, 2.3H*), 1.11 (s, 9H), 0.67 (s, 2.4H*). ^{13}C NMR (101 MHz, $CDCl_3$, major rotamer) ^{13}C NMR (101 MHz, $CDCl_3$) δ 202.0, 161.6 (d, *J* = 244.5 Hz), 156.9, 135.8

(d, J = 3.2 Hz), 127.3 (d, J = 7.9 Hz), 115.30 (d, J = 21.4 Hz), 79.9, 66.6, 63.1, 52.2, 35.3, 33.9, 28.5, 27.2, 23.0. Minor rotamer: δ 202.7, 162.39 (d, J = 247.0 Hz), 138.6 (d, J = 3.3 Hz), 128.6 (d, J = 8.1 Hz), 115.9 (d, J = 21.4 Hz), 155.7, 79.8, 65.3, 61.8, 54.7, 35.8, 35.5, 28.5, 26.8, 21.4. HRMS (ESI) m/z calculated for $C_{21}H_{31}FN_2O_2S$ $[M+H]^+$: 395.2163; found: 395.2158.

The catalysts shown below were synthesized by following a previously reported procedure.[20]

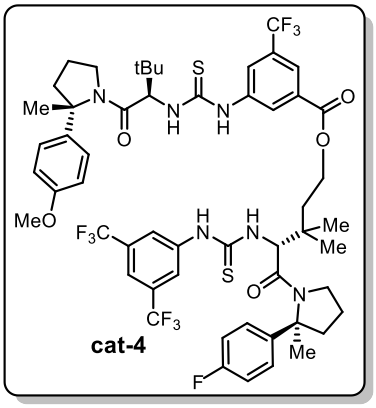


(R)-4-(3-(3,5-bis(trifluoromethyl)phenyl)thioureido)-5-((S)-2-(4-fluorophenyl)-2-methylpyrrolidin-1-yl)-3,3-dimethyl-5-oxopentyl 3-(3-((R)-3,3-dimethyl-1-oxo-1-(pyrrolidin-1-yl)butan-2-yl)thioureido)-5-(trifluoromethyl)benzoate (cat-2). ^{1}H NMR (500 MHz, CD_3CN) δ 9.21 (s, 2H), 8.37 (s, 2H), 8.21 (s, 2H), 7.97 (s, 1H), 7.72 (s, 1H), 7.36 – 7.19 (m, 4H), 6.92 (t, J = 8.9 Hz, 2H), 5.36 (d, J = 9.9 Hz, 1H), 5.17 (d, J = 8.8 Hz, 1H), 4.56 – 4.43 (m, 3H), 4.05 – 3.97 (m, 1H), 3.93 – 3.84 (m, 1H), 3.60 – 3.51 (m, 1H), 3.44 – 3.35 (m, 1H), 3.35 – 3.28 (m, 1H), 1.90 – 1.88 (m, 2H), 1.87 – 1.85 (m, 4H), 1.82 – 1.78 (m, 2H), 1.20 (s, 3H), 1.17 (s, 3H), 1.05 (s, 9H). ^{19}F NMR (376 MHz, CD_3CN) δ -63.4, -63.5, -119.7. ^{13}C NMR (101 MHz, CD_3CN) δ 182.7, 182.5, 177.3, 170.8, 169.8, 165.5, 162.0 (d, J = 241.8 Hz), 143.5 (d, J = 3.0 Hz), 142.2, 141.7, 132.8, 132.0 (q, J = 33.3 Hz), 131.3 (d, J = 32.5 Hz), 128.1 (d, J = 7.9 Hz), 124.7 (q, J = 271.9 Hz), 124.5, 124.4 (q, J = 272.0 Hz), 124.2, 122.3 (q, J = 3.4 Hz), 115.1 (d, J = 21.1 Hz), 80.1, 70.4, 68.2, 63.4, 63.3, 62.7, 51.0, 48.6, 46.7, 45.1, 38.5, 38.3, 36.3, 27.0, 25.6, 24.8, 24.4, 23.9, 23.0. HRMS (ESI) m/z calculated for $C_{46}H_{52}F_{10}N_6O_4S_2$ $[M+H]^+$: 1007.3405; found: 1007.3362.



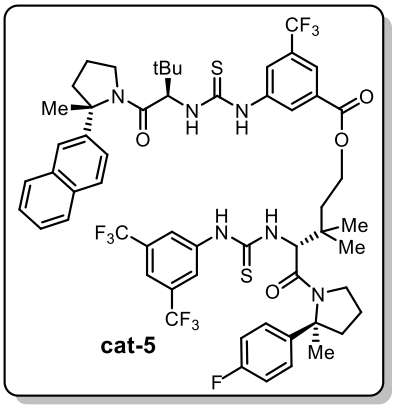
(R)-4-(3-(3,5-bis(trifluoromethyl)phenyl)thioureido)-5-((S)-2-(4-fluorophenyl)-2-methylpyrrolidin-1-yl)-3,3-dimethyl-5-oxopentyl 3-(3-((R)-3,3-dimethyl-1-((S)-2-methyl-2-(4-nitrophenyl)pyrrolidin-1-yl)-1-oxobutan-2-yl)thioureido)-5-(trifluoromethyl)benzoate (cat-3).

^{1}H NMR (400 MHz, CD_3CN) δ 8.77 (s, 1H), 8.72 (s, 1H), 8.39 (s, 1H), 8.10 (s, 2H), 8.07 (s, 1H), 8.02 – 7.95 (m, 3H), 7.72 (s, 1H), 7.48 (d, *J* = 8.9 Hz, 2H), 7.23 (dd, *J* = 8.8, 5.4 Hz, 2H), 7.14 (d, *J* = 9.2 Hz, 1H), 7.00 (d, *J* = 9.1 Hz, 1H), 6.87 (t, *J* = 8.9 Hz, 2H), 5.40 (d, *J* = 9.2 Hz, 1H), 5.21 (d, *J* = 9.0 Hz, 1H), 4.59 – 4.42 (m, 4H), 3.96 – 3.80 (m, 2H), 2.13 – 1.99 (m, 2H), 1.91 – 1.81 (m, 9H), 1.81 – 1.68 (m, 2H), 1.21 (s, 3H), 1.16 (s, 3H), 1.08 (s, 9H). (Proton signals overlaps with solvent peaks). ^{19}F NMR (376 MHz, CD_3CN) δ -63.3, -63.5, -119.6. ^{13}C NMR (101 MHz, CD_3CN) δ 182.7, 170.3, 169.8, 165.5, 161.9 (d, *J* = 242.2 Hz), 155.5, 147.1, 143.5 (d, *J* = 3.0 Hz), 142.0, 141.4, 132.9, 132.1 (q, *J* = 33.3 Hz), 131.6 (q, *J* = 32.9 Hz), 128.3, 128.0 (d, *J* = 7.8 Hz), 127.4, 124.7 (q, *J* = 3.6 Hz), 124.6 (q, *J* = 271.9 Hz), 124.4 (q, *J* = 3.2 Hz), 124.3 (q, *J* = 272.1 Hz), 123.8, 122.7 (q, *J* = 3.4 Hz), 118.8 (q, *J* = 3.4 Hz), 115.1 (d, *J* = 21.2 Hz), 68.3, 68.2, 63.8, 63.5, 62.7, 51.0, 50.9, 45.1, 44.7, 38.4, 38.2, 36.0, 27.0, 25.6, 25.0, 24.4, 24.1, 23.3, 23.0. HRMS (ESI) m/z calculated for $C_{53}H_{57}F_{10}N_7O_6S_2$ $[M+H]^+$: 1142.3725; found: 1142.3705.



(R)-4-(3-(3,5-bis(trifluoromethyl)phenyl)thioureido)-5-((S)-2-(4-fluorophenyl)-2-methylpyrrolidin-1-yl)-3,3-dimethyl-5-oxopentyl 3-(3-((R)-1-((S)-2-(4-methoxyphenyl)-2-methylpyrrolidin-1-yl)-3,3-dimethyl-1-oxobutan-2-yl)thioureido)-5-(trifluoromethyl)benzoate (cat-4).

^{1}H NMR (400 MHz, CD_3CN + 5 drops of DMSO-d6) δ 10.09 (s, 1H), 9.97 (s, 1H), 8.51 (s, 1H), 8.33 (s, 1H), 8.29 (s, 2H), 7.96 (d, *J* = 8.6 Hz, 2H), 7.75 (d, *J* = 9.2 Hz, 1H), 7.70 (s, 1H), 7.24 (dd, *J* = 8.8, 5.4 Hz, 2H), 7.15 (d, *J* = 8.9 Hz, 2H), 6.91 (t, *J* = 8.9 Hz, 2H), 6.72 (d, *J* = 8.8 Hz, 2H), 5.41 (d, *J* = 9.3 Hz, 1H), 5.30 (d, *J* = 9.3 Hz, 1H), 4.56 – 4.46 (m, 4H), 3.93 – 3.80 (m, 2H), 3.68 (s, 3H), 2.10 – 1.98 (m, 2H), 1.91 – 1.79 (m, 10H), 1.80 – 1.66 (m, 2H), 1.21 (s, 3H), 1.17 (s, 3H), 1.07 (s, 9H). (Proton signals overlaps with solvent peaks). ^{19}F NMR (376 MHz, CD_3CN) δ -63.2, -63.4, -119.7. ^{13}C NMR (101 MHz, CD_3CN) δ 182.5, 182.5, 170.1, 169.8, 165.7, 161.9 (d, *J* = 242.0 Hz), 158.7, 143.7 (d, *J* = 3.0 Hz), 142.8, 142.4, 139.7, 132.6, 131.8 (q, *J* = 33.1 Hz), 131.2 (q, *J* = 32.7 Hz), 128.0 (d, *J* = 7.9 Hz), 127.5, 127.3, 124.7 (q, *J* = 272.0 Hz), 124.4 (q, *J* = 272.0 Hz), 123.8 (q, *J* = 3.3 Hz), 123.3 (q, *J* = 3.5 Hz), 121.7 (q, *J* = 3.7 Hz), 115.1 (d, *J* = 21.2 Hz), 113.9, 68.0, 67.9, 63.5, 63.1, 62.2, 55.7, 51.0, 50.9, 45.3, 45.1, 38.3, 38.2, 36.1, 27.1, 25.6, 25.4, 24.4, 24.1, 23.1, 23.0. HRMS (ESI) m/z calculated for $C_{54}H_{60}F_{10}N_6O_5S_2$ $[M+H]^+$: 1127.3980; found: 1127.3959.

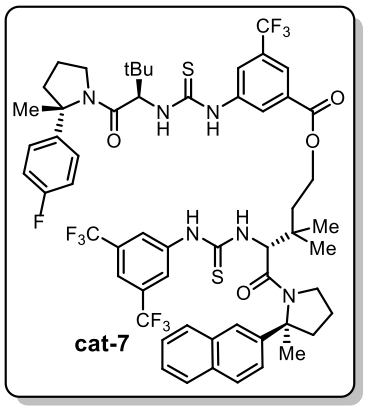


cat-5

(R)-4-(3-(3,5-bis(trifluoromethyl)phenyl)thioureido)-5-((S)-2-(4-fluorophenyl)-2-methylpyrrolidin-1-yl)-3,3-dimethyl-5-oxopentyl 3-(3-((R)-3,3-dimethyl-1-((S)-2-methyl-2-(naphthalen-2-yl)pyrrolidin-1-yl)-1-oxobutan-2-yl)thioureido)-5-(trifluoromethyl)benzoate (cat-5).

^{1}H NMR (400 MHz, CD_3CN) δ 8.98 (s, 1H), 8.78 (s, 1H), 8.33 (s, 1H), 8.14 (s, 1H), 8.03 (s, 2H), 7.99 (s, 1H), 7.72 – 7.59 (m, 5H), 7.41 – 7.30 (m, 2H), 7.29 – 7.09 (m, 5H), 6.85 (t, *J* = 8.9 Hz, 2H), 5.37 (d, *J* = 9.1 Hz, 1H), 5.34 (d, *J* = 9.2 Hz, 1H), 4.65 – 4.57 (m, 1H), 4.53 – 4.43 (m, 3H), 3.95 – 3.79 (m, 2H), 2.14 – 2.05 (m, 1H), 2.04 – 1.98 (m, 2H), 1.95 (s, 3H), 1.91 – 1.77 (m, 7H), 1.76 – 1.65 (m, 2H), 1.20 (s, 3H), 1.13 (s, 3H), 1.11 (s, 9H).

(Proton signals overlaps with solvent peaks). ^{13}C NMR (101 MHz, CD_3CN) δ 182.8, 182.7, 170.5, 169.8, 165.4, 161.91 (d, *J* = 242.2 Hz), 144.2, 143.4 (d, *J* = 3.0 Hz), 141.8, 141.4, 133.9, 132.8, 132.6, 132.0 (q, *J* = 33.3 Hz), 131.5 (q, *J* = 33.0 Hz), 128.6, 128.4, 128.2, 128.0, 128.0 (d, *J* = 8.0 Hz), 126.7, 126.3, 124.9, 124.8, 124.7 (q, *J* = 3.1 Hz), 124.6 (q, *J* = 271.8 Hz), 124.4 (q, *J* = 3.2 Hz), 124.3 (q, *J* = 272.1 Hz), 122.6 (q, *J* = 3.3 Hz), 118.9 (q, *J* = 4.4 Hz), 115.1 (d, *J* = 21.1 Hz), 68.9, 68.2, 63.9, 63.4, 62.8, 51.1, 51.0, 45.1, 44.8, 38.5, 38.2, 35.9, 27.1, 25.7, 25.6, 24.4, 24.2, 23.0, 23.0. ^{19}F NMR (376 MHz, CD_3CN) δ -63.2, -63.4, -119.6. HRMS (ESI) m/z calculated for $C_{57}H_{60}F_{10}N_6O_4S_2$ $[M+H]^+$: 1147.4031; found: 1147.4005.

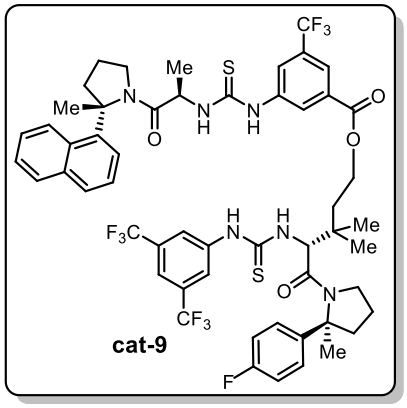


cat-7

(R)-4-(3-(3,5-bis(trifluoromethyl)phenyl)thioureido)-3,3-dimethyl-5-((S)-2-methyl-2-(naphthalen-2-yl)pyrrolidin-1-yl)-5-oxopentyl 3-(3-((R)-1-((S)-2-(4-fluorophenyl)-2-methylpyrrolidin-1-yl)-3,3-dimethyl-1-oxobutan-2-yl)thioureido)-5-(trifluoromethyl)benzoate (cat-7).

^{1}H NMR (400 MHz, CD_3CN) δ 8.88 (s, 1H), 8.84 (s, 1H), 8.31 (s, 1H), 8.13 (s, 2H), 8.08 (s, 1H), 7.98 (s, 1H), 7.75 – 7.60 (m, 4H), 7.44 – 7.33 (m, 2H), 7.31 – 7.18 (m, 2H), 7.07 (d, *J* = 9.1 Hz, 1H), 6.85 (t, *J* = 8.8 Hz, 2H), 5.47 (d, *J* = 9.2 Hz, 1H), 5.24 (d, *J* = 9.1 Hz, 1H), 4.67 – 4.58 (m, 1H), 4.56 – 4.40 (m, 3H), 3.93 (q, *J* = 8.3 Hz, 1H), 3.89 – 3.75 (m, 1H), 1.24 (s, 3H), 1.17 (s, 3H), 1.07 (s, 9H) (Proton signals overlaps with solvent peaks). ^{19}F NMR (376 MHz, CD_3CN) δ -63.3, -63.4, -119.4. ^{13}C NMR (101 MHz, CD_3CN) δ 182.7, 182.6, 170.3, 170.0, 165.5, 161.9 (d, *J* = 242.1 Hz), 144.4, 143.4 (d, *J* = 3.0 Hz), 142.0, 141.4, 134.0, 132.8, 132.7, 132.0 (q, *J* = 33.5 Hz), 131.4 (q, *J* = 32.9 Hz), 128.6, 128.5, 128.4, 128.1, 128.0 (d, *J* = 7.8 Hz), 126.7, 126.4, 124.9, 124.7, 124.6 (d, *J* = 271.9 Hz), 124.3, 124.3 (q, *J* = 272.2 Hz), 122.6 (q, *J* = 4.0, 3.4 Hz), 115.1 (d, *J* = 21.3 Hz), 68.9, 68.2, 63.8, 63.4, 62.9, 51.2, 50.9, 45.1, 44.8, 38.5,

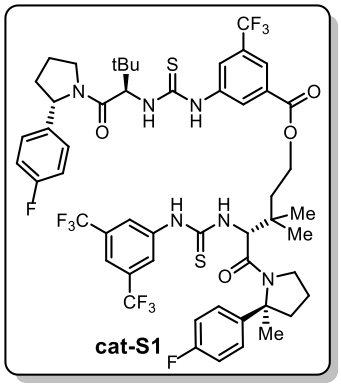
38.1, 36.1, 27.1, 25.6, 25.6, 24.5, 24.1, 23.1, 23.0. HRMS (ESI) m/z calculated for $C_{57}H_{60}F_{10}N_6O_4S_2$ $[M+H]^+$: 1147.4031; found: 1147.3994.



cat-9

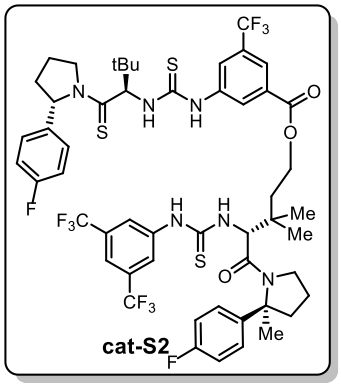
((R)-4-(3-(3,5-bis(trifluoromethyl)phenyl)thioureido)-5-((S)-2-(4-fluorophenyl)-2-methylpyrrolidin-1-yl)-3,3-dimethyl-5-oxopentyl 3-(3-((R)-1-((S)-2-methyl-2-(naphthalen-1-yl)pyrrolidin-1-yl)-1-oxopropan-2-yl)thioureido)-5-(trifluoromethyl)benzoate (cat-9).

^{1}H NMR (400 MHz, CD_3CN + 2 drops of DMSO-d6, *denotes the minor rotamer) δ 9.41 (s, 1H), 8.50 (s, 1H), 8.35 (s, 1H), 8.17 – 8.02 (m, 5H), 7.90 (s, 1H), 7.84 (s, 1H), 7.66 (s, 1H), 7.55 (t, *J* = 8.5 Hz, 2H), 7.36 (t, *J* = 8.0 Hz, 2H), 7.27 – 7.16 (m, 3H), 7.06 – 6.94 (m, 1H), 6.77 (t, *J* = 8.8 Hz, 2H), 5.38 (d, *J* = 9.2 Hz, 1H), 5.19 (t, *J* = 7.1 Hz, 1H), 4.56 – 4.42 (m, 2H), 4.42 – 4.30 (m, 1H), 4.27 – 4.19 (m, 1H), 3.92 – 3.79 (m, 2H), 3.73 – 3.64 (m, 0.6H), 3.63 – 3.57 (m, 0.2H*), 3.55 – 3.49 (m, 0.2H*), 2.67 – 2.53 (m, 1H), 2.31 – 2.15 (m, 1H), 2.13 – 1.98 (m, 6H), 1.91 – 1.78 (m, 6H), 1.41 (d, *J* = 7.0 Hz, 3H), 1.17 (d, *J* = 16.2 Hz, 6H). (Proton signals overlaps with solvent peaks). ^{19}F NMR (376 MHz, CD_3CN + 2 drops of DMSO-d6) δ -63.1, -63.3, -119.5. ^{13}C NMR (101 MHz, CD_3CN + 2 drops of DMSO-d6) δ 182.3, 182.1, 170.0, 165.1, 161.4 (d, *J* = 242.1 Hz), 143.1 (d, *J* = 3.0 Hz), 141.9, 140.7, 135.2, 131.7, 131.3 (q, *J* = 33.2 Hz), 130.3 (q, *J* = 32.9 Hz), 129.9, 129.7, 129.6, 128.2, 127.5 (d, *J* = 7.9 Hz), 126.0, 125.9, 125.6, 125.4, 125.4, 125.0, 124.2 (q, *J* = 272.2 Hz), 124.0, 124.0 (q, *J* = 272.1 Hz), 122.3, 114.8 (d, *J* = 21.2 Hz), 67.8, 62.9, 62.4, 53.3, 50.7, 48.1, 44.7, 41.2, 38.0, 37.8, 25.1, 24.1, 24.0, 23.4, 22.6, 16.5. HRMS (ESI) m/z calculated for $C_{54}H_{54}F_{10}N_6O_4S_2$ $[M+H]^+$: 1105.3561; found: 1105.3537.



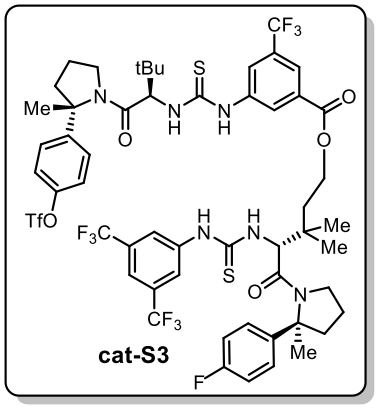
(R)-4-(3-(3,5-bis(trifluoromethyl)phenyl)thioureido)-5-((S)-2-(4-fluorophenyl)-2-methylpyrrolidin-1-yl)-3,3-dimethyl-5-oxopentyl 3-(3-((R)-1-((S)-2-(4-fluorophenyl)pyrrolidin-1-yl)-3,3-dimethyl-1-oxobutan-2-yl)thioureido)-5-(trifluoromethyl)benzoate (cat-S1).

^{1}H NMR (400 MHz, CD_3CN, a mixture of rotamers) δ 8.71 (s, 1.3H), 8.67 (s, 1H), 8.34 (s, 1H), 8.10 (s, 2H), 8.06 (s, 1H), 7.99 (s, 1H), 7.72 (s, 1H), 7.38 (dd, *J* = 8.6, 5.5 Hz, 0.5H), 7.23 (dd, *J* = 8.8, 5.3 Hz, 2H), 7.16 (dd, *J* = 8.6, 5.5 Hz, 3H), 7.07 (dd, *J* = 9.1, 3.7 Hz, 2H), 6.87 (q, *J* = 8.7 Hz, 4H), 5.86 (d, *J* = 8.0 Hz, 0.2H), 5.41 (d, *J* = 9.3 Hz, 1.2H), 5.32 (d, *J* = 9.2 Hz, 1H), 5.09 (d, *J* = 6.3 Hz, 1.2H), 4.54 – 4.42 (m, 3H), 4.37 (ddd, *J* = 10.8, 7.9, 3.8 Hz, 1H), 3.88 (q, *J* = 8.8 Hz, 1H), 3.81 (q, *J* = 9.1 Hz, 1H), 3.67 – 3.62 (m, 0.2H), 3.61 – 3.54 (m, 0.2H), 2.31 – 2.20 (m, 1H), 2.09 – 2.00 (m, 1H), 1.91 – 1.81 (m, 8H), 1.77 – 1.68 (m, 2H), 1.21 (s, 3.6H), 1.16 (s, 3.6H), 1.08 (s, 9H), 0.67 (s, 1.7H). (Proton signals overlaps with solvent peaks). ^{19}F NMR (376 MHz, CD_3CN, *denotes minor rotamer) δ -63.3*, -63.3, -63.5, -117.1*, -118.4, -119.5. ^{13}C NMR (101 MHz, CD_3CN, only major rotamer reported) δ 182.7, 182.6, 170.5, 169.9, 165.5, 163.3 (d, *J* = 29.6 Hz), 160.9 (d, *J* = 29.4 Hz), 143.5 (d, *J* = 2.9 Hz), 142.0, 141.5, 140.5 (d, *J* = 2.9 Hz), 132.8, 132.0 (q, *J* = 33.3 Hz), 131.4 (d, *J* = 32.7 Hz), 128.4, 128.3 (d, *J* = 8.1 Hz), 128.0 (d, *J* = 7.9 Hz), 124.8 (q, *J* = 3.5 Hz), 124.6 (q, *J* = 272.0 Hz), 124.4 (q, *J* = 3.1 Hz), 124.3 (q, *J* = 272.1 Hz), 122.6 (q, *J* = 3.8 Hz), 118.8 (q, *J* = 3.5 Hz), 115.5 (d, *J* = 21.5 Hz), 115.2 (d, *J* = 21.2 Hz), 68.2, 63.4, 63.3, 62.8, 61.4, 51.0, 49.2, 45.1, 38.4, 38.3, 36.0, 35.0, 27.0, 25.6, 24.4, 24.1, 23.8, 23.0. HRMS (ESI) m/z calculated for $C_{52}H_{55}F_{11}N_6O_4S_2$ $[M+H]^+$: 1101.3623; found: 1101.3604.



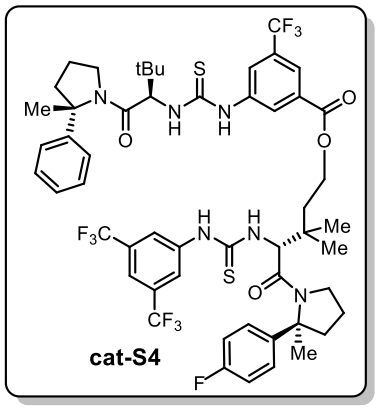
(R)-4-(3-(3,5-bis(trifluoromethyl)phenyl)thioureido)-5-((S)-2-(4-fluorophenyl)-2-methylpyrrolidin-1-yl)-3,3-dimethyl-5-oxopentyl 3-(3-((R)-1-((S)-2-(4-fluorophenyl)pyrrolidin-1-yl)-3,3-dimethyl-1-thioxobutan-2-yl)thioureido)-5-(trifluoromethyl)benzoate (cat-S2).

^{1}H NMR (400 MHz, CD_3CN, a mixture of rotamers) δ 8.85 (d, *J* = 15.3 Hz, 1H), 8.70 (s, 1H), 8.35 (s, 1H), 8.11 (d, *J* = 12.0 Hz, 3H), 8.02 (s, 1H), 7.73 (s, 1H), 7.40 (dd, *J* = 8.6, 5.4 Hz, 0.4H), 7.25 – 7.19 (m, 3H), 7.17 – 7.11 (m, 3H), 6.95 (t, *J* = 8.8 Hz, 2H), 6.84 (t, *J* = 8.9 Hz, 2H), 6.35 (d, *J* = 8.0 Hz, 0.2H), 5.72 (d, *J* = 7.6 Hz, 1H), 5.69 (d, *J* = 9.5 Hz, 1H), 5.62 (d, *J* = 9.8 Hz, 0.2H), 5.42 (d, *J* = 9.3 Hz, 1H), 4.72 (t, *J* = 9.4 Hz, 1H), 4.57 – 4.41 (m, 4H), 4.14 – 4.01 (m, 1H), 4.01 – 3.94 (m, 0.3H), 3.93 – 3.82 (m, 1H), 2.39 – 2.27 (m, 1H), 2.25 – 2.16 (m, 1H), 2.10 – 1.99 (m, 3H), 1.90 – 1.81 (m, 7H), 1.77 – 1.67 (m, 2H), 1.26 (s, 1H), 1.21 (s, 4H), 1.17 (s, 3H), 1.13 (s, 9H), 0.67 (s, 1.7H). (Proton signals overlaps with solvent peaks). ^{19}F NMR (376 MHz, CD_3CN, *denotes minor rotamer) δ -63.3*, -63.3, -63.4, -116.1*, -118.2, -119.5*, -119.5. ^{13}C NMR (101 MHz, CD_3CN, only major rotamer reported) δ 200.6, 182.8, 182.1, 170.0, 165.5, 163.3 (d, *J* = 38.4 Hz), 160.9 (d, *J* = 38.0 Hz), 143.4 (d, *J* = 3.0 Hz), 142.0, 141.1, 137.9 (d, *J* = 3.1 Hz), 133.0, 132.0 (q, *J* = 33.3 Hz), 131.6 (q, *J* = 32.9 Hz), 128.7 (d, *J* = 8.0 Hz), 128.4, 127.9 (d, *J* = 7.9 Hz), 124.9 (q, *J* = 3.9 Hz), 124.6 (q, *J* = 272.0 Hz), 124.4 (q, *J* = 3.5 Hz), 124.3 (q, *J* = 272.0 Hz), 122.9 (q, *J* = 3.8 Hz), 118.8 (q, *J* = 3.5 Hz), 115.6 (d, *J* = 21.5 Hz), 115.2 (d, *J* = 21.3 Hz), 68.2, 68.0, 67.2, 63.5, 62.8, 53.8, 51.1, 45.1, 38.4, 38.3, 37.0, 34.5, 27.4, 25.6, 24.4, 24.2, 23.5, 23.0. HRMS (ESI) m/z calculated for $C_{52}H_{55}F_{11}N_6O_3S_3$ $[M+H]^+$: 1117.3395; found: 1117.3368.



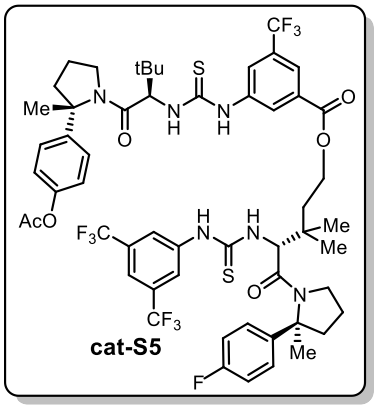
cat-S3

(R)-4-(3-(3,5-bis(trifluoromethyl)phenyl)thioureido)-5-((S)-2-(4-fluorophenyl)-2-methylpyrrolidin-1-yl)-3,3-dimethyl-5-oxopentyl 3-(3-((R)-3,3-dimethyl-1-((S)-2-methyl-2-(4-(((trifluoromethyl)sulfonyl)oxy)phenyl)pyrrolidin-1-yl)-1-oxobutan-2-yl)thioureido)-5-(trifluoromethyl)benzoate (cat-S3). ^{1}H NMR (400 MHz, CD_3CN) δ 8.75 (s, 1H), 8.72 (s, 1H), 8.39 (s, 1H), 8.11 (s, 3H), 8.01 (s, 1H), 7.73 (s, 1H), 7.40 (d, *J* = 8.9 Hz, 2H), 7.24 (dd, *J* = 8.8, 5.3 Hz, 2H), 7.15 (d, *J* = 8.9 Hz, 3H), 7.01 (d, *J* = 9.0 Hz, 1H), 6.87 (t, *J* = 8.9 Hz, 2H), 5.41 (d, *J* = 9.2 Hz, 1H), 5.22 (d, *J* = 9.1 Hz, 1H), 4.54 – 4.45 (m, 4H), 3.92 – 3.81 (m, 2H), 2.13 – 2.00 (m, 2H), 1.91 – 1.82 (m, 10H), 1.79 – 1.67 (m, 2H), 1.21 (s, 3H), 1.16 (s, 3H), 1.08 (s, 9H). (Proton signals overlaps with solvent peaks). ^{13}C NMR (101 MHz, CD_3CN) δ 182.8, 182.7, 170.3, 169.8, 165.5, 161.9 (d, *J* = 242.2 Hz), 148.6, 148.6, 143.5 (d, *J* = 3.0 Hz), 142.0, 141.5, 132.9, 132.1 (q, *J* = 33.4 Hz), 131.5 (q, *J* = 33.0 Hz), 128.4, 128.3, 128.0 (d, *J* = 7.8 Hz), 124.7 (q, *J* = 3.3 Hz), 124.6 (q, *J* = 272.0 Hz), 124.4 (q, *J* = 3.1 Hz), 124.3 (q, *J* = 272.0 Hz), 122.6 (q, *J* = 3.7 Hz), 121.5, 118.8 (q, *J* = 3.9 Hz), 115.16 (d, *J* = 21.3 Hz), 68.2, 68.1, 63.8, 63.4, 62.7, 51.0, 50.9, 45.1, 45.0, 38.4, 38.3, 36.0, 27.0, 25.6, 25.4, 24.4, 24.1, 23.1, 23.0. ^{19}F NMR (376 MHz, CD_3CN) δ -63.4, -63.5, -74.1, -119.6. HRMS (ESI) m/z calculated for $C_{54}H_{57}F_{13}N_6O_7S_3$ $[M+H]^+$: 1245.3316; found: 1245.3280.



(R)-4-(3-(3,5-bis(trifluoromethyl)phenyl)thioureido)-5-((S)-2-(4-fluorophenyl)-2-methylpyrrolidin-1-yl)-3,3-dimethyl-5-oxopentyl 3-(3-((R)-3,3-dimethyl-1-((S)-2-methyl-2-phenylpyrrolidin-1-yl)-1-oxobutan-2-yl)thioureido)-5-(trifluoromethyl)benzoate (cat-S4).

^{1}H NMR (400 MHz, CD_3CN) δ 8.69 (s, 2H), 8.37 (s, 1H), 8.10 (s, 3H), 8.00 (s, 1H), 7.73 (s, 1H), 7.27 – 7.19 (m, 4H), 7.19 – 7.12 (m, 3H), 7.10 – 7.02 (m, 2H), 6.86 (t, *J* = 8.9 Hz, 2H), 5.41 (d, *J* = 9.2 Hz, 1H), 5.32 (d, *J* = 9.2 Hz, 1H), 4.54 – 4.43 (m, 4H), 3.93 – 3.80 (m, 2H), 2.09 – 1.99 (m, 2H), 1.91 – 1.79 (m, 10H), 1.77 – 1.66 (m, 2H), 1.22 (s, 3H), 1.16 (s, 3H), 1.08 (s, 9H). (Proton signals overlaps with solvent peaks). ^{13}C NMR (101 MHz, CD_3CN) δ 182.7, 182.7, 170.2, 169.9, 165.5, 161.9 (d, *J* = 242.2 Hz), 147.4, 143.5 (d, *J* = 2.9 Hz), 141.9, 141.5, 132.9, 132.1 (q, *J* = 33.4 Hz), 131.5 (q, *J* = 33.0 Hz), 128.7, 128.5, 128.0 (d, *J* = 7.9 Hz), 126.7, 126.1, 124.9 (q, *J* = 3.6 Hz), 124.6 (q, *J* = 271.9 Hz), 124.5 (q, *J* = 2.8 Hz), 124.3 (q, *J* = 271.8 Hz), 122.6 (q, *J* = 3.6 Hz), 118.9 (q, *J* = 4.0 Hz), 115.2 (d, *J* = 21.3 Hz), 68.5, 68.2, 63.7, 63.4, 62.8, 51.0, 51.0, 45.2, 45.1, 38.5, 38.3, 36.2, 27.1, 25.6, 25.6, 24.5, 24.2, 23.0, 23.0. ^{19}F NMR (376 MHz, CD_3CN) δ -63.3, -63.4, -119.5. HRMS (ESI) m/z calculated for $C_{53}H_{58}F_{10}N_6O_4S_2$ $[M+H]^+$: 1097.3874; found: 1097.3848.

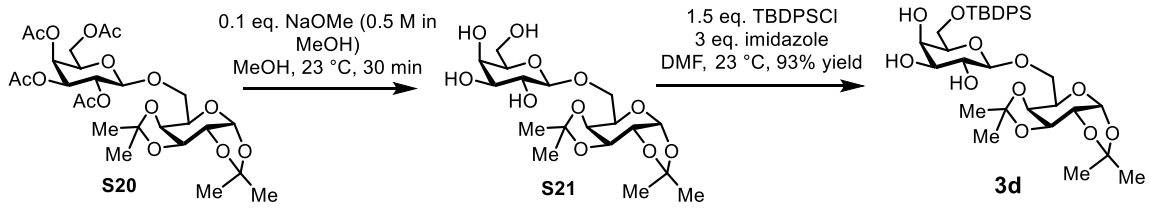


(R)-4-(3-(3,5-bis(trifluoromethyl)phenyl)thioureido)-5-((S)-2-(4-fluorophenyl)-2-methylpyrrolidin-1-yl)-3,3-dimethyl-5-oxopentyl 3-(3-((R)-1-((S)-2-(4-acetoxyphenyl)-2-methylpyrrolidin-1-yl)-3,3-dimethyl-1-oxobutan-2-yl)thioureido)-5-(trifluoromethyl)benzoate (cat-S5).

^{1}H NMR (400 MHz, CD_3CN) δ 8.69 (d, *J* = 2.3 Hz, 2H), 8.38 (s, 1H), 8.10 (s, 2H), 8.09 (s, 1H), 8.00 (s, 1H), 7.73 (s, 1H), 7.27 – 7.20 (m, 4H), 7.16 (d, *J* = 9.2 Hz, 1H), 7.08 (d, *J* = 9.2 Hz, 1H), 6.86 (t, *J* = 9.1 Hz, 4H), 5.40 (d, *J* = 9.2 Hz, 1H), 5.29 (d, *J* = 9.2 Hz, 1H), 4.55 – 4.43 (m, 4H), 3.94 – 3.81 (m, 2H), 2.17 (s, 3H), 2.10 – 2.00 (m, 2H), 1.91 – 1.80 (m, 10H), 1.78 – 1.66 (m, 2H), 1.21 (s, 3H), 1.16 (s, 3H), 1.08 (s, 9H). (Proton signals overlaps with solvent peaks). ^{13}C NMR (101 MHz, CD_3CN) δ 182.7, 170.6, 170.3, 169.9, 165.5, 161.9 (d, *J* = 242.1 Hz), 149.9, 145.0, 143.5 (d, *J* = 3.0 Hz), 141.9, 141.6, 132.8, 132.0 (q, *J* = 33.4 Hz), 131.4 (q, *J* = 32.7 Hz), 128.5, 128.0 (d, *J* = 7.9 Hz), 127.2, 124.8 (q, *J* = 3.8 Hz), 124.6 (q, *J* = 271.8 Hz), 124.5 (q, *J* = 3.7 Hz), 124.3 (q, *J* = 272.0 Hz), 122.6 (q, *J* = 3.7 Hz), 121.9, 118.8 (q, *J* = 3.9 Hz), 115.2 (d, *J* = 21.2 Hz), 68.2, 68.2, 63.7, 63.4, 62.8, 51.0, 50.9, 45.1, 45.1, 38.4, 38.3, 36.2, 27.1, 25.6, 25.6, 24.4, 24.2, 23.0, 21.2. ^{19}F NMR (376 MHz, CD_3CN) δ -63.3, -63.4, -119.5. HRMS (ESI) m/z calculated for $C_{55}H_{60}F_{10}N_6O_6S_2$ $[M+H]^+$: 1155.3929; found: 1155.3903.

3.8.6 Synthesis and Characterization of Acceptors

β-3a[22] and **3b**[23] were prepared as previously reported.



S20 were prepared as previously reported.[24]

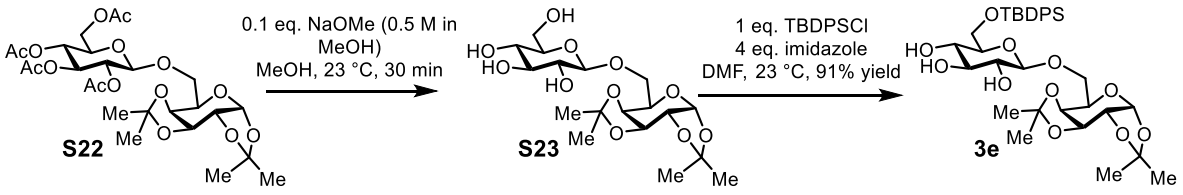
[22] Dubey, R.; Reynolds, D.; Abbas, S. A.; Matta, K. L. Synthetic studies in carbohydrates. Part LVI. Synthesis of *O*-α-L-fucopyranosyl-(1→3)-*O*-β-d-galactopyranosyl-(1→4)-2-acetamido-2-deoxy-D-glucopyranose (*N*-acetyl-3'-*O*-α-L-fucopyranosyllactosamine). *Carbohydr. Res*. **1998**, *183*, 155–162.

[23] Roën, A.; Padrón, J. I.; Vázquez, J. T. Hydroxymethyl Rotamer Populations in Disaccharides. *J. Org. Chem*. **2003**, *68*, 4615–4630.

[24] Galan, M. C.; Brunet, C.; Fuensanta, M. [bmim][OTf]: a versatile room temperature glycosylation promoter. *Tetrahedron Lett*. **2009**, *50*, 442–445.

1,2:3,4-di-*O*-Isopropylidene-6-*O*-(6′-*O*-*tert*-butyldiphenylsilyl-β-D-galactopyranosyl)-α-D-galactopyranoside (3d). To a 20 mL scintillation vial equipped with a stir bar was added disaccharide **S20** (0.304 g, 0.51 mmol, 1 equiv.), 2 mL anhydrous methanol, and sodium methoxide (0.5 M in methanol, 0.1 mL, 0.05 mmol, 0.1 equiv.). The reaction mixture was stirred at 23 °C for 30 minutes and then neutralized with methanol-washed Amberlite IRC120 H. The resin was filtered off, and the filtrate was concentrated under reduced pressure to afford the deprotected disaccharide **S21**, which was used directly in the next step without purification.

To a 20 mL scintillation vial containing deprotected disaccharide **S21** (0.51 mmol, 1 equiv.) was added 2 mL anhydrous DMF, imidazole (0.104 g, 1.53 mmol, 3 equiv.), and *tert*-butyl(chloro)diphenylsilane (TBDPSCl, 0.2 mL, 0.77 mmol, 1.5 equiv.). The reaction mixture was stirred at 23 °C until complete conversion of disaccharide. The reaction mixture was diluted with EtOAc and washed with water (x3) and sat. NaCl (aq.). The organic layer was dried over Na_2SO_4 and concentrated under reduced pressure. The crude mixture was purified by column chromatography (50% EtOAc/hexanes to 100% EtOAc/hexanes) on 25 g silica gel to give the product, **3d**, in 93% yield (0.313 g, 0.47 mmol) as a white solid. ^{1}H NMR (600 MHz, $CDCl_3$) δ 7.72 – 7.64 (m, 4H), 7.45 – 7.35 (m, 6H), 5.55 (d, J = 5.0 Hz, 1H), 4.58 (dd, J = 7.9, 2.4 Hz, 1H), 4.33 – 4.28 (m, 2H), 4.19 (dd, J = 7.9, 1.8 Hz, 1H), 4.08 (d, J = 2.9 Hz, 1H), 4.03 (dd, J = 11.0, 3.4 Hz, 1H), 4.01 – 3.98 (m, 1H), 3.95 (dd, J = 10.3, 6.9 Hz, 1H), 3.86 (dd, J = 10.3, 5.4 Hz, 1H), 3.73 – 3.66 (m, 2H), 3.60 (dd, J = 9.5, 3.3 Hz, 1H), 3.53 (t, J = 6.0 Hz, 1H), 3.13 (br, 1H), 2.71 (br, 1H), 1.51 (s, 3H), 1.43 (s, 3H), 1.31 (d, J = 3.4 Hz, 6H), 1.06 (s, 9H). ^{13}C NMR (126 MHz, $CDCl_3$) δ 135.7, 135.7, 133.4, 133.2, 129.9, 127.9, 127.9, 109.6, 109.0, 104.0, 96.4, 74.7, 73.8, 71.9, 71.3, 70.8, 70.5, 69.0, 68.5, 68.1, 62.7, 26.9, 26.1, 26.1, 25.0, 24.5, 19.3. HRMS (ESI) m/z calculated for $C_{34}H_{48}O_{11}Si$ $[M+NH_4]^+$: 678.3304; found: 678.3297.



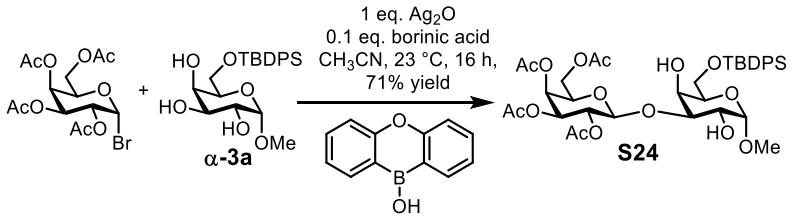
S29 were prepared as previously reported.[25]

1,2:3,4-di-*O*-Isopropylidene-6-*O*-(6′-*O*-*tert*-butyldiphenylsilyl-β-d-glucopyranosyl)-α-D-galactopyranoside (3e). To a 20 mL scintillation vial equipped with a stir bar was added disaccharide **S22** (0.123 g, 0.21 mmol, 1 equiv.), 1 mL anhydrous methanol, and sodium methoxide (0.5 M in methanol, 0.04 mL, 0.02 mmol, 0.1 equiv.). The reaction mixture was stirred at 23 °C for 30 minutes and then neutralized with methanol-washed Amberlite IRC120 H. The resin was filtered off, and the filtrate was concentrated under reduced pressure to afford the deprotected disaccharide **S23**, which was used directly in the next step without purification.

To a 20 mL scintillation vial containing deprotected disaccharide **S23** (0.21 mmol, 1 equiv.) was added 1.5 mL anhydrous DMF, imidazole (0.057 g, 0.84 mmol, 4 equiv.), and *tert*-butyl(chloro)diphenylsilane (TBDPSCl, 0.055 mL, 0.21 mmol, 1 equiv.). The reaction mixture was stirred at 23 °C until complete conversion of disaccharide. The reaction mixture was diluted with EtOAc and washed with water (x3) and sat. NaCl (aq.). The organic layer was dried over Na_2SO_4 and concentrated under reduced pressure. The crude mixture was purified by column chromatography (50% EtOAc/hexanes to 100% EtOAc/hexanes) on 25 g silica gel to give the product, **3e**, in 91% yield (0.126 g, 0.19 mmol) as a white solid. ^{1}H NMR (600 MHz, $CDCl_3$) δ

[25] Mukherjee, D.; Ray, P. K.; Chowdhury, U. S. Synthesis of glycosides via indium(III) chloride mediated activation of glycosyl halide in neutral condition. *Tetrahedron* **2001**, *57*, 7701–7704.

7.72 – 7.66 (m, 4H), 7.45 – 7.34 (m, 6H), 5.54 (d, J = 5.0 Hz, 1H), 4.59 (dd, J = 7.9, 2.4 Hz, 1H), 4.37 (d, J = 7.8 Hz, 1H), 4.31 (dd, J = 5.0, 2.4 Hz, 1H), 4.20 (dd, J = 7.9, 1.5 Hz, 1H), 4.04 – 3.98 (m, 2H), 3.95 – 3.89 (m, 2H), 3.74 – 3.69 (m, 1H), 3.63 – 3.56 (m, 2H), 3.46 – 3.14 (m, 5H), 1.52 (s, 3H), 1.43 (s, 3H), 1.31 (s, 6H), 1.06 (s, 9H). ^{13}C NMR (126 MHz, $CDCl_3$) δ 135.8, 135.7, 133.2, 133.2, 129.9, 127.9, 127.9, 109.6, 109.0, 103.4, 96.3, 76.5, 75.1, 73.5, 71.8, 71.3, 70.8, 70.5, 68.9, 68.1, 64.8, 26.9, 26.1, 26.1, 25.0, 24.5, 19.4. HRMS (ESI) m/z calculated for $C_{34}H_{48}O_{11}Si$ $[M+NH_4]^+$: 678.3304; found: 678.3298.

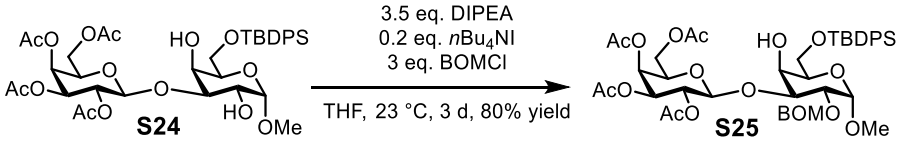


α-3a was prepared as previously reported.[26] **S24** and 10H-Dibenzo[b,e][1,4]oxaborinin-10-ol were synthesized following a modified procedure.[27]

Methyl 6-*O*-*tert*-butyldiphenylsilyl-3-*O*-(2',3',4',6'-tetra-*O*-acetyl-β-D-galactopyranosyl)-α-D-galactopyranoside (S24). To a flame-dried 20 mL scintillation vial equipped with a stir bar was added 2,3,4,6-tetra-*O*-acetyl-α-D-galactopyranosyl bromide (0.4 g, 0.97 mmol, 1 equiv.), methyl 6-*O*-(*tert*-butyldiphenylsilyl)-α-D-galactopyranoside **α-3a** (0.463 g, 1.07 mmol, 1.1 equiv.), silver(I) oxide (0.225 g, 0.97 mmol, 1 equiv.), and 10H-dibenzo[b,e][1,4]oxaborinin-10-ol (19 mg, 0.097 mmol, 0.1 equiv.). The scintillation vial was evacuated and backfilled with N_2. To the vial was added 7.5 mL anhydrous CH_3CN. The reaction mixture was stirred at 23 °C overnight. The

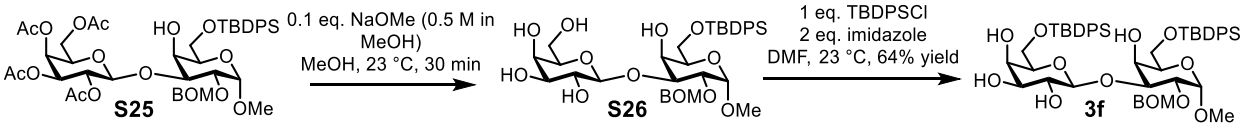
[26] Iynkkaran, I.; Bundle, D. R. Synthesis of a trisaccharide repeat of the zwitterionic Sp1 capsularpolysaccharide utilizing 2-azido-4-benzylamino-4N,3-O-carbonyl-2,4,6-trideoxy-D-galactopyranosyl trichloroacetimidate. *Carbohydr. Res*. **2013**, *378*, 26–34.
[27] Dimitrijević, E.; Taylor, M. S. 9-Hetero-10-boraanthracene-derived Borinic Acid Catalysts for Regioselective Activation of Polyols. *Chem. Sci*. **2013**, *4*, 3298–3303.

reaction was quenched with a small amount of methanol and filtered through a plug of Celite. The filtrate was concentrated under reduced pressure and purified by column chromatography (30% EtOAc/hexanes to 70% EtOAc/hexanes) on 50 g silica gel to give the product, **S24**, in 71% yield (0.53 g, 0.69 mmol) as a white solid. ^{1}H NMR (600 MHz, $CDCl_3$) δ 7.69 – 7.64 (m, 4H), 7.44 – 7.34 (m, 6H), 5.39 (d, *J* = 2.8 Hz, 1H), 5.22 (dd, *J* = 10.6, 7.9 Hz, 1H), 5.04 (dd, *J* = 10.5, 3.5 Hz, 1H), 4.79 (d, *J* = 4.0 Hz, 1H), 4.74 (d, *J* = 7.9 Hz, 1H), 4.14 – 4.05 (m, 3H), 4.00 – 3.95 (m, 1H), 3.92 (t, *J* = 6.8 Hz, 1H), 3.90 – 3.83 (m, 2H), 3.81 (t, *J* = 6.0 Hz, 1H), 3.77 (dd, *J* = 9.6, 3.2 Hz, 1H), 3.38 (s, 3H), 2.56 (s, 1H), 2.15 (s, 3H), 2.06 (s, 3H), 1.98 (s, 3H), 1.94 (s, 3H), 1.05 (s, 9H). ^{13}C NMR (126 MHz, $CDCl_3$) δ 170.4, 170.3, 170.2, 170.2, 135.6, 133.4, 129.8, 127.8, 102.2, 99.3, 81.3, 70.9, 70.6, 70.2, 69.1, 68.6, 68.1, 66.9, 63.2, 61.2, 55.2, 26.9, 20.9, 20.7, 20.7, 20.6, 19.3. HRMS (ESI) m/z calculated for $C_{37}H_{50}O_{15}Si$ $[M+NH_4]^+$: 780.3257; found: 780.3248.



Methyl 2-*O*-(benzyloxy)methyl-6-*O*-*tert*-butyldiphenylsilyl-3-*O*-(2',3',4',6'-tetra-*O*-acetyl-β-D-galactopyranosyl)-α-D-galactopyranoside (S25). To a 20 mL scintillation vial equipped with a stir bar was added disaccharide **S24** (0.53 g, 0.69 mmol, 1 equiv.) and 5 mL anhydrous THF. To the solution was added *N*,*N*-Diisopropylethylamine (DIPEA, 0.42 mL, 2.43 mmol, 3.5 equiv.), tetrabutylammonium iodide (0.052 g, 0.14 mmol, 0.2 equiv.), and benzyl chloromethyl ether (0.29 mL, 2.08 mmol, 3 equiv.). The reaction mixture was stirred at 23 °C for 3 days. The reaction mixture was quenched with methanol and concentrated under reduced pressure. The crude mixture was purified by column chromatography (10% EtOAc/hexanes to 50% EtOAc/hexanes) on 50 g silica gel to give the product, **S25**, in 80% yield (0.49 g, 0.55 mmol) as a white solid. ^{1}H NMR

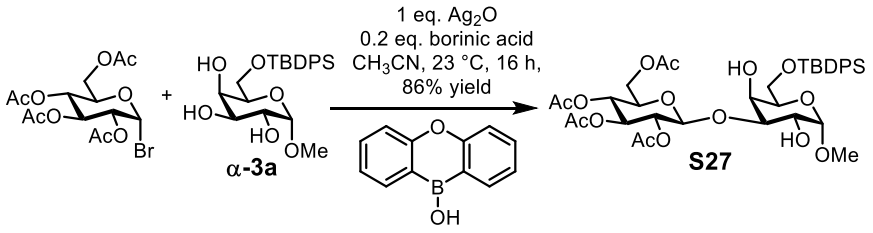
(400 MHz, $CDCl_3$) δ 7.70 – 7.65 (m, 4H), 7.46 – 7.26 (m, 11H), 5.38 (dd, *J* = 3.5, 1.1 Hz, 1H), 5.25 (dd, *J* = 10.5, 8.0 Hz, 1H), 5.00 (dd, *J* = 10.5, 3.5 Hz, 1H), 4.84 – 4.78 (m, 3H), 4.74 (d, *J* = 12.1 Hz, 1H), 4.69 (d, *J* = 8.0 Hz, 1H), 4.53 (d, *J* = 12.0 Hz, 1H), 4.11 – 4.06 (m, 3H), 4.01 (dd, *J* = 9.9, 3.6 Hz, 1H), 3.96 (dd, *J* = 9.9, 3.1 Hz, 1H), 3.93 – 3.85 (m, 3H), 3.85 – 3.80 (m, 1H), 3.35 (s, 3H), 2.56 (t, *J* = 1.7 Hz, 1H), 2.16 (s, 3H), 2.01 (s, 3H), 1.98 (s, 3H), 1.93 (s, 3H), 1.06 (s, 9H). ^{13}C NMR (101 MHz, $CDCl_3$) δ 170.4, 170.3, 170.2, 169.4, 137.8, 135.7, 133.5, 133.4, 129.8, 128.6, 127.8, 127.5, 101.9, 99.3, 96.4, 79.4, 75.0, 71.0, 70.8, 69.8, 69.7, 68.9, 68.7, 67.0, 63.4, 61.3, 55.2, 26.9, 20.9, 20.8, 20.7, 20.6, 19.3. HRMS (ESI) m/z calculated for $C_{45}H_{58}O_{16}Si$ $[M+NH_4]^+$: 900.3832; found: 900.3818.



Methyl 2-*O*-(benzyloxy)methyl-6-*O*-*tert*-butyldiphenylsilyl-3-*O*-(6′-*O*-*tert*-butyldiphenylsilyl -β-D-galactopyranosyl)-α-D-galactopyranoside (3f). To a 20 mL scintillation vial equipped with a stir bar was added disaccharide **S25** (0.49 g, 0.55 mmol, 1 equiv.), 2 mL anhydrous methanol, and sodium methoxide (0.5 M in methanol, 0.11 mL, 0.055 mmol, 0.1 equiv.). The reaction mixture was stirred at 23 °C for 30 minutes and then neutralized with methanol-washed Amberlite IRC120 H. The resin was filtered off, and the filtrate was concentrated under reduced pressure to afford the deprotected disaccharide **S26**, which was used directly in the next step without purification.

To a 20 mL scintillation vial containing deprotected disaccharide **S26** (0.55 mmol, 1 equiv.) was added 2 mL anhydrous DMF, imidazole (0.075 g, 1.1 mmol, 2 equiv.), and *tert*-butyl(chloro)diphenylsilane (TBDPSCl, 0.14 mL, 0.55 mmol, 1 equiv.). The reaction mixture was

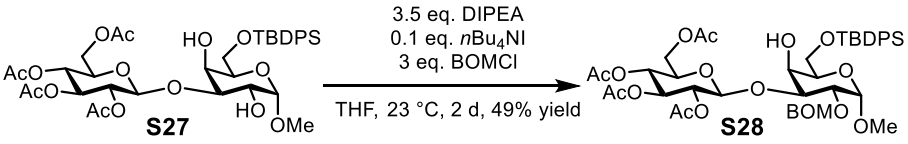
stirred at 23 °C until complete conversion of disaccharide. The reaction mixture was diluted with EtOAc and washed with water (x3) and sat. NaCl (aq.). The organic layer was dried over Na_2SO_4 and concentrated under reduced pressure. The crude mixture was purified by column chromatography (50% EtOAc/hexanes to 100% EtOAc/hexanes) on 25 g silica gel to give the product, **3f**, in 64% yield (0.33 g, 0.35 mmol) as a white solid. ^{1}H NMR (600 MHz, $CDCl_3$) δ 7.69 – 7.61 (m, 8H), 7.41 – 7.24 (m, 17H), 4.95 (d, *J* = 6.9 Hz, 1H), 4.85 – 4.82 (m, 2H), 4.72 (d, *J* = 12.0 Hz, 1H), 4.56 (d, *J* = 12.1 Hz, 1H), 4.48 (d, *J* = 7.7 Hz, 1H), 4.11 – 4.06 (m, 2H), 4.00 (dd, *J* = 10.3, 3.2 Hz, 2H), 3.89 – 3.76 (m, 5H), 3.69 (dd, *J* = 9.5, 7.7 Hz, 1H), 3.56 – 3.49 (m, 2H), 3.34 (s, 3H), 3.22 (br, 1H), 2.89 (br, 1H), 1.02 (s, 9H), 0.98 (s, 9H). ^{13}C NMR (126 MHz, $CDCl_3$) δ 137.6, 135.7, 135.6, 135.6, 133.4, 133.3, 133.1, 133.1, 130.0, 129.8, 128.6, 127.9, 127.8, 127.8, 104.3, 99.1, 96.2, 78.1, 75.6, 74.9, 73.6, 72.0, 70.1, 70.0, 69.9, 68.5, 63.8, 62.6, 55.1, 26.9, 26.8, 19.2, 19.2. HRMS (ESI) m/z calculated for $C_{53}H_{68}O_{12}Si_2$ $[M+NH_4]^+$: 970.4588; found: 970.4566.



S27 was synthesized following a modified procedure.[28]

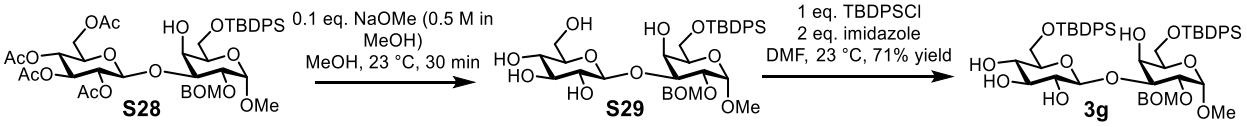
Methyl 6-*O*-*tert*-butyldiphenylsilyl-3-*O*-(2',3',4',6'-tetra-*O*-acetyl-β-D-glucopyranosyl)-α-D-galactopyranoside (S27). To a flame-dried 20 mL scintillation vial equipped with a stir bar was added 2,3,4,6-tetra-*O*-acetyl-α-D-glucopyranosyl bromide (0.4 g, 0.97 mmol, 1 equiv.), methyl 6-*O*-(*tert*-butyldiphenylsilyl)-α-D-galactopyranoside **α-3a** (0.463 g, 1.07 mmol, 1.1 equiv.), silver(I) oxide (0.225 g, 0.97 mmol, 1 equiv.), and 10H-dibenzo[b,e][1,4]oxaborinin-10-ol (38 mg, 0.19 mmol, 0.2 equiv.). The scintillation vial was evacuated and backfilled with N_2. To the vial was

added 7.5 mL anhydrous CH_3CN. The reaction mixture was stirred at 23 °C overnight. The reaction was quenched with a small amount of methanol and filtered through a plug of Celite. The filtrate was concentrated under reduced pressure and purified by column chromatography (30% EtOAc/hexanes to 70% EtOAc/hexanes) on 50 g silica gel to give the product, **S27**, in 86% yield (0.63 g, 0.83 mmol) as a white solid. ^{1}H NMR (500 MHz, $CDCl_3$) δ 7.70 – 7.64 (m, 4H), 7.45 – 7.34 (m, 6H), 5.24 (t, *J* = 9.6 Hz, 1H), 5.11 – 4.99 (m, 2H), 4.82 – 4.75 (m, 2H), 4.22 (dd, *J* = 12.3, 4.9 Hz, 1H), 4.11 – 4.05 (m, 2H), 3.98 (d, *J* = 6.2 Hz, 1H), 3.92 – 3.84 (m, 2H), 3.84 – 3.75 (m, 2H), 3.71 (ddd, *J* = 10.1, 5.0, 2.4 Hz, 1H), 3.39 (s, 3H), 2.05 (s, 3H), 2.03 (s, 3H), 2.01 (s, 3H), 1.99 (s, 3H), 1.05 (s, 9H). ^{13}C NMR (126 MHz, $CDCl_3$) δ 170.7, 170.3, 170.0, 169.5, 135.7, 133.4, 129.9, 127.8, 101.6, 99.3, 81.2, 72.5, 72.1, 71.6, 70.3, 68.5, 68.4, 68.2, 63.2, 61.9, 55.3, 26.9, 20.9, 20.7, 20.7, 19.3. HRMS (ESI) m/z calculated for $C_{37}H_{50}O_{15}Si$ $[M+NH_4]^+$: 780.3257; found: 780.3250.



Methyl 2-*O*-(benzyloxy)methyl-6-*O*-*tert*-butyldiphenylsilyl-3-*O*-(2',3',4',6'-tetra-*O*-acetyl-β-D-glucopyranosyl)-α-D-galactopyranoside (S28). To a 20 mL scintillation vial equipped with a stir bar was added disaccharide **S27** (0.547 g, 0.72 mmol, 1 equiv.) and 5 mL anhydrous THF. To the solution was added *N*,*N*-Diisopropylethylamine (DIPEA, 0.44 mL, 2.51 mmol, 3.5 equiv.), tetrabutylammonium iodide (0.026 g, 0.07 mmol, 0.1 equiv.), and benzyl chloromethyl ether (0.3 mL, 2.15 mmol, 3 equiv.). The reaction mixture was stirred at 23 °C for 2 days. The reaction mixture was quenched with methanol and concentrated under reduced pressure. The crude mixture was purified by column chromatography (10% EtOAc/hexanes to 50% EtOAc/hexanes) on 50 g

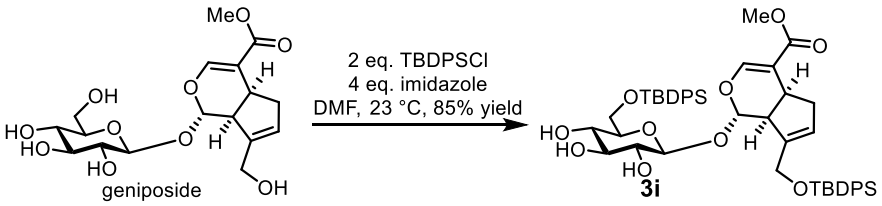
silica gel to give the product, **S28**, in 49% yield (0.31 g, 0.35 mmol) as a white solid. ^{1}H NMR (600 MHz, $CDCl_3$) δ 7.70 – 7.65 (m, 4H), 7.44 – 7.40 (m, 2H), 7.39 – 7.31 (m, 8H), 7.30 – 7.27 (m, 1H), 5.19 (t, *J* = 9.5 Hz, 1H), 5.09 – 5.02 (m, 2H), 4.84 – 4.80 (m, 2H), 4.78 (d, *J* = 6.9 Hz, 1H), 4.76 – 4.71 (m, 2H), 4.53 (d, *J* = 12.0 Hz, 1H), 4.21 (dd, *J* = 12.4, 5.1 Hz, 1H), 4.10 (d, *J* = 2.2 Hz, 1H), 4.06 (dd, *J* = 12.3, 2.4 Hz, 1H), 4.01 (dd, *J* = 9.9, 3.7 Hz, 1H), 3.96 (dd, *J* = 9.9, 3.1 Hz, 1H), 3.92 – 3.80 (m, 3H), 3.69 (ddd, *J* = 10.1, 5.0, 2.4 Hz, 1H), 3.34 (s, 3H), 2.56 (br, 1H), 2.02 (s, 3H), 2.00 (s, 3H), 1.99 (s, 3H), 1.98 (s, 3H), 1.05 (s, 9H). ^{13}C NMR (126 MHz, $CDCl_3$) δ 170.6, 170.3, 169.4, 169.3, 137.7, 135.7, 133.4, 133.4, 129.8, 128.6, 127.8, 127.5, 101.3, 99.3, 96.3, 79.1, 75.0, 72.7, 72.0, 71.2, 69.8, 69.7, 68.8, 68.4, 63.2, 61.8, 55.2, 26.9, 20.8, 20.7, 20.7, 19.3. HRMS (ESI) m/z calculated for $C_{45}H_{58}O_{16}Si$ $[M+NH_4]^+$: 900.3832; found: 900.3822.



Methyl 2-*O*-(benzyloxy)methyl-6-*O*-*tert*-butyldiphenylsilyl-3-*O*-(6′-*O*-*tert*-butyldiphenylsilyl -β-D-glucopyranosyl)-α-D-galactopyranoside (3g). To a 20 mL scintillation vial equipped with a stir bar was added disaccharide **S28** (0.31 g, 0.35 mmol, 1 equiv.), 2 mL anhydrous methanol, and sodium methoxide (0.5 M in methanol, 0.07 mL, 0.035 mmol, 0.1 equiv.). The reaction mixture was stirred at 23 °C for 30 minutes and then neutralized with methanol-washed Amberlite IRC120 H. The resin was filtered off, and the filtrate was concentrated under reduced pressure to afford the deprotected disaccharide **S29**, which was used directly in the next step without purification.

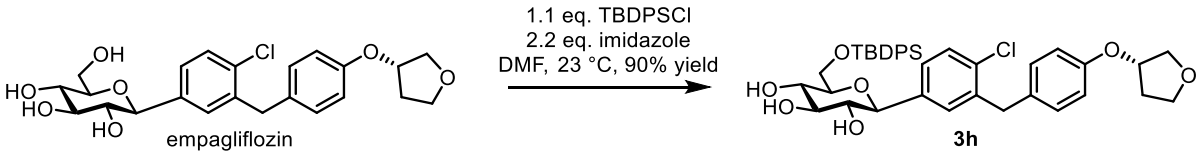
To a 20 mL scintillation vial containing deprotected disaccharide **S29** (0.35 mmol, 1 equiv.) was added 1.5 mL anhydrous DMF, imidazole (0.048 g, 0.7 mmol, 2 equiv.), and *tert*-

butyl(chloro)diphenylsilane (TBDPSCl, 0.09 mL, 0.35 mmol, 1 equiv.). The reaction mixture was stirred at 23 °C until complete conversion of disaccharide. The reaction mixture was diluted with EtOAc and washed with water (x3) and sat. NaCl (aq.). The organic layer was dried over Na_2SO_4 and concentrated under reduced pressure. The crude mixture was purified by column chromatography (50% EtOAc/hexanes to 100% EtOAc/hexanes) on 25 g silica gel to give the product, **3g**, in 71% yield (0.24 g, 0.25 mmol) as a white solid. ^{1}H NMR (600 MHz, $CDCl_3$) δ 7.67 – 7.62 (m, 8H), 7.41 – 7.27 (m, 17H), 4.93 (d, *J* = 6.8 Hz, 1H), 4.88 (d, *J* = 3.7 Hz, 1H), 4.86 (d, *J* = 6.8 Hz, 1H), 4.73 (d, *J* = 12.1 Hz, 1H), 4.60 (d, *J* = 12.1 Hz, 1H), 4.53 (d, *J* = 7.7 Hz, 1H), 4.11 – 4.06 (m, 2H), 3.99 (dd, *J* = 10.0, 3.2 Hz, 1H), 3.89 – 3.79 (m, 4H), 3.77 (t, *J* = 5.4 Hz, 1H), 3.61 (t, *J* = 9.1 Hz, 1H), 3.54 (t, *J* = 9.1 Hz, 1H), 3.46 – 3.42 (m, 1H), 3.40 (dd, *J* = 9.2, 7.7 Hz, 1H), 3.35 (s, 3H), 3.11 (br, 2H), 2.96 (br, 1H), 1.01 (s, 9H), 0.99 (s, 9H). ^{13}C NMR (126 MHz, $CDCl_3$) δ 137.6, 135.7, 135.7, 135.6, 133.3, 133.2, 132.9, 132.8, 130.1, 129.8, 128.6, 128.0, 128.0, 127.9, 127.8, 127.8, 127.8, 103.8, 99.1, 96.1, 78.4, 76.4, 75.7, 75.0, 73.8, 71.8, 70.1, 70.0, 69.9, 64.7, 64.1, 55.1, 26.8, 19.3, 19.2. HRMS (ESI) m/z calculated for $C_{53}H_{68}O_{12}Si_2$ $[M+NH_4]^+$: 970.4588; found: 970.4568.



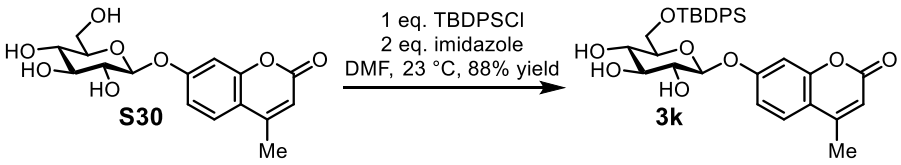
6-*O*-*tert*-Butyldiphenylsilyl-geniposide (3i). To a 20 mL scintillation vial equipped with a stir bar was added geniposide (0.196 g, 0. 5 mmol, 1 equiv.), 1.5 mL anhydrous DMF, imidazole (0.137 g, 2.02 mmol, 4 equiv.), and *tert*-butyl(chloro)diphenylsilane (TBDPSCl, 0.26 mL, 1 mmol, 2 equiv.). The reaction mixture was stirred at 23 °C until complete conversion. The reaction mixture was diluted with EtOAc and washed with water (x3) and sat. NaCl (aq.). The organic layer was

dried over Na_2SO_4 and concentrated under reduced pressure. The crude mixture was purified by column chromatography (30% EtOAc/hexanes to 90% EtOAc/hexanes) on 25 g silica gel to give the product, **3i**, in 85% yield (0.37 g, 0.42 mmol) as a white solid. ^{1}H NMR (500 MHz, $CDCl_3$) δ 7.65 – 7.60 (m, 8H), 7.45 (d, *J* = 1.3 Hz, 1H), 7.42 – 7.29 (m, 12H), 5.77 (s, 1H), 5.00 (d, *J* = 7.2 Hz, 1H), 4.66 (d, *J* = 7.8 Hz, 1H), 4.34 (d, *J* = 14.0 Hz, 1H), 4.27 (dd, *J* = 14.0, 2.3 Hz, 1H), 3.86 – 3.78 (m, 2H), 3.73 (s, 3H), 3.62 – 3.53 (m, 2H), 3.42 (dt, *J* = 8.7, 5.4 Hz, 1H), 3.28 (s, 1H), 3.24 – 3.17 (m, 2H), 2.96 (s, 1H), 2.82 (dd, *J* = 16.3, 8.5 Hz, 1H), 2.73 (t, *J* = 7.7 Hz, 1H), 2.48 (d, *J* = 1.8 Hz, 1H), 2.05 (ddt, *J* = 16.5, 7.4, 2.3 Hz, 1H), 1.00 (d, *J* = 1.3 Hz, 18H). ^{13}C NMR (126 MHz, $CDCl_3$) δ 167.8, 151.5, 142.2, 135.6, 135.6, 133.8, 133.8, 132.7, 130.1, 130.1, 129.8, 129.8, 128.0, 128.0, 127.8, 112.0, 98.4, 96.8, 76.3, 74.8, 73.4, 72.5, 65.0, 62.5, 51.4, 46.0, 38.6, 35.1, 26.9, 26.8, 19.4, 19.3. HRMS (ESI) m/z calculated for $C_{49}H_{60}O_{10}Si_2$ $[M+NH_4]^+$: 882.4063; found: 882.4048.



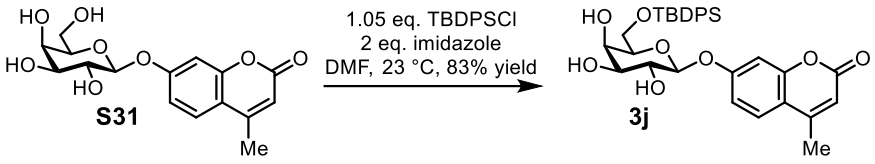
6-*O*-*tert*-Butyldiphenylsilyl-empagliflozin. To a 20 mL scintillation vial equipped with a stir bar was added empagliflozin (0.4 g, 0.89 mmol, 1 equiv.), 2 mL anhydrous DMF, imidazole (0.133 g, 1.95 mmol, 2.2 equiv.), and *tert*-butyl(chloro)diphenylsilane (TBDPSCl, 0.25 mL, 0.98 mmol, 1.1 equiv.). The reaction mixture was stirred at 23 °C until complete conversion. The reaction mixture was diluted with EtOAc and washed with water (x3) and sat. NaCl (aq.). The organic layer was dried over Na_2SO_4 and concentrated under reduced pressure. The crude mixture was purified by column chromatography (40% EtOAc/hexanes to 100% EtOAc/hexanes) on 25 g silica gel to give the product, **3h**, in 90% yield (0.55 g, 0.80 mmol) as a white solid. ^{1}H NMR (600 MHz, $CDCl_3$) δ 7.69 – 7.64 (m, 4H), 7.43 – 7.38 (m, 2H), 7.37 – 7.31 (m, 5H), 7.20 (d, *J* = 2.1 Hz, 1H), 7.16 (dd,

J = 8.2, 2.1 Hz, 1H), 7.06 (d, J = 8.6 Hz, 2H), 6.73 (d, J = 8.6 Hz, 2H), 4.83 (ddt, J = 6.2, 4.5, 2.4 Hz, 1H), 4.09 (d, J = 9.3 Hz, 1H), 4.04 (d, J = 15.2 Hz, 1H), 3.99 – 3.92 (m, 5H), 3.89 (dd, J = 10.8, 5.1 Hz, 1H), 3.86 (td, J = 8.2, 4.5 Hz, 1H), 3.81 (t, J = 9.1 Hz, 1H), 3.65 (t, J = 8.9 Hz, 1H), 3.50 (dt, J = 9.3, 4.7 Hz, 1H), 3.42 (t, J = 9.2 Hz, 1H), 2.18 – 2.06 (m, 2H), 1.05 (s, 9H). ^{13}C NMR (126 MHz, $CDCl_3$) δ 155.9, 139.0, 137.4, 135.7, 135.7, 134.2, 132.9, 132.8, 131.9, 130.3, 130.0, 130.0, 130.0, 129.8, 127.9, 127.9, 126.6, 115.5, 81.0, 78.4, 78.2, 77.3, 75.0, 73.2, 72.5, 67.3, 65.0, 38.5, 33.1, 26.9, 19.4. HRMS (ESI) m/z calculated for $C_{39}H_{45}ClO_7Si$ $[M+NH_4]^+$: 706.2961; found: 706.2955.

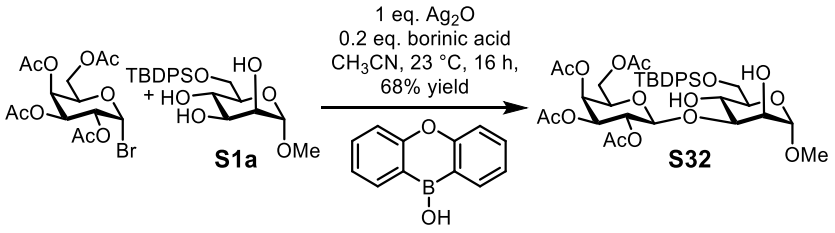


4-Methylumbelliferyl 6-*O*-*tert*-butyldiphenylsilyl-β-D-glucopyranoside (3k). To a 20 mL scintillation vial equipped with a stir bar was added 4-methylumbelliferyl-β-D-glucopyranoside **S30** (0.5 g, 1.48 mmol, 1 equiv.), 6 mL anhydrous DMF, imidazole (0.201 g, 2.96 mmol, 2 equiv.), and *tert*-butyl(chloro)diphenylsilane (TBDPSCl, 0.38 mL, 1.48 mmol, 1 equiv.). The reaction mixture was stirred at 23 °C until complete conversion. The reaction mixture was diluted with EtOAc and washed with water (x3) and sat. NaCl (aq.). The organic layer was dried over Na_2SO_4 and concentrated under reduced pressure. The crude mixture was purified by column chromatography (40% EtOAc/hexanes to 100% EtOAc/hexanes) on 50 g silica gel to give the product, **3k**, in 88% yield (0.75 g, 1.30 mmol) as a white solid. ^{1}H NMR (400 MHz, $CDCl_3$) δ 7.63 – 7.58 (m, 4H), 7.36 – 7.18 (m, 7H), 6.96 (dd, J = 8.8, 2.4 Hz, 1H), 6.92 (d, J = 2.3 Hz, 1H), 6.09 (d, J = 1.3 Hz, 1H), 5.01 – 4.89 (m, 1H), 4.58 (br, 1H), 4.31 (br, 1H), 3.96 (dd, J = 11.0, 3.2 Hz, 1H), 3.83 (dd, J = 11.0, 5.4 Hz, 2H), 3.78 – 3.72 (m, 2H), 3.69 – 3.61 (m, 1H), 3.61 – 3.53 (m,

1H), 2.27 (d, J = 1.2 Hz, 3H), 0.99 (s, 9H). ^{13}C NMR (101 MHz, $CDCl_3$) δ 161.4, 159.9, 154.6, 152.7, 135.7, 135.6, 133.1, 132.9, 129.9, 129.9, 127.8, 125.8, 115.1, 113.5, 112.7, 104.7, 100.2, 76.6, 76.2, 73.3, 71.1, 64.1, 26.9, 19.3, 18.8. HRMS (ESI) m/z calculated for $C_{32}H_{36}O_8Si$ $[M+H]^+$: 577.2252; found: 577.2248.



4-Methylumbelliferyl 6-*O*-*tert*-butyldiphenylsilyl-β-D-galactopyranoside (3j). To a 20 mL scintillation vial equipped with a stir bar was added 4-methylumbelliferyl-β-D-galactopyranoside **S31** (0.15 g, 0.44 mmol, 1 equiv.), 3 mL anhydrous DMF, imidazole (0.06 g, 0.89 mmol, 2 equiv.), and *tert*-butyl(chloro)diphenylsilane (TBDPSCl, 0.12 mL, 0.47 mmol, 1.05 equiv.). The reaction mixture was stirred at 23 °C until complete conversion. The reaction mixture was diluted with EtOAc and washed with water (x3) and sat. NaCl (aq.). The organic layer was dried over Na_2SO_4 and concentrated under reduced pressure. The crude mixture was purified by column chromatography (40% EtOAc/hexanes to 100% EtOAc/hexanes) on 25 g silica gel to give the product, **3j**, in 83% yield (0.21 g, 0.37 mmol) as a white solid. ^{1}H NMR (400 MHz, $CDCl_3$) δ 7.60 – 7.53 (m, 4H), 7.34 – 7.16 (m, 7H), 6.89 (dd, J = 8.8, 2.4 Hz, 1H), 6.78 (d, J = 2.3 Hz, 1H), 6.04 (d, J = 1.3 Hz, 1H), 4.85 (d, J = 7.6 Hz, 1H), 4.05 (d, J = 3.2 Hz, 1H), 4.04 – 3.95 (m, 1H), 3.85 (d, J = 5.4 Hz, 4H), 3.67 (dd, J = 9.4, 3.2 Hz, 1H), 3.60 (t, J = 5.5 Hz, 1H), 3.36 (br, 1H), 2.25 (d, J = 1.2 Hz, 3H), 0.97 (s, 9H). ^{13}C NMR (101 MHz, $CDCl_3$) δ 161.1, 159.8, 154.7, 152.6, 135.7, 135.6, 132.9, 132.7, 130.0, 127.9, 127.9, 125.7, 115.1, 113.7, 112.8, 104.4, 100.7, 75.1, 73.8, 71.4, 69.2, 63.4, 26.9, 19.2, 18.7. HRMS (ESI) m/z calculated for $C_{32}H_{36}O_8Si$ $[M+H]^+$: 577.2252; found: 577.2249.

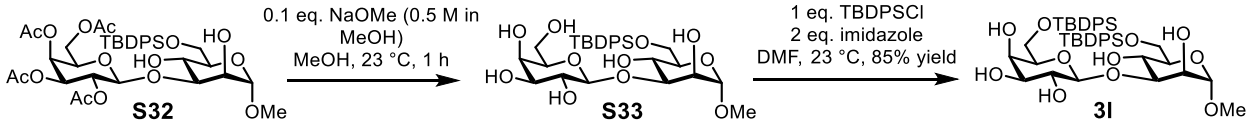


S1a was prepared as previously reported.[28] **S32** was synthesized following a modified procedure.[28]

Methyl 6-*O*-*tert*-butyldiphenylsilyl-3-*O*-(2',3',4',6'-tetra-*O*-acetyl-β-D-galactopyranosyl)-α-D-mannopyranoside (S32). To a flame-dried 20 mL scintillation vial equipped with a stir bar was added 2,3,4,6-tetra-*O*-acetyl-α-D-galactopyranosyl bromide (0.4 g, 0.97 mmol, 1 equiv.), methyl 6-*O*-(*tert*-butyldiphenylsilyl)-α-D-mannopyranoside **S1a** (0.463 g, 1.07 mmol, 1.1 equiv.), silver(I) oxide (0.225 g, 0.97 mmol, 1 equiv.), and 10H-dibenzo[b,e][1,4]oxaborinin-10-ol (38 mg, 0.19 mmol, 0.2 equiv.). The scintillation vial was evacuated and backfilled with N_2. To the vial was added 7.5 mL anhydrous CH_3CN. The reaction mixture was stirred at 23 °C overnight. The reaction was quenched with a small amount of methanol and filtered through a plug of Celite. The filtrate was concentrated under reduced pressure and purified by column chromatography (25% EtOAc/hexanes to 65% EtOAc/hexanes) on 50 g silica gel to give the product, **S32**, in 68% yield (0.495 g, 0.66 mmol) as a white solid. ^{1}H NMR (400 MHz, $CDCl_3$) δ 7.74 – 7.66 (m, 4H), 7.44 – 7.32 (m, 6H), 5.40 (d, *J* = 3.0 Hz, 1H), 5.24 (dd, *J* = 10.5, 7.9 Hz, 1H), 5.03 (dd, *J* = 10.5, 3.4 Hz, 1H), 4.77 (d, *J* = 1.5 Hz, 1H), 4.56 (d, *J* = 7.9 Hz, 1H), 4.18 – 4.07 (m, 2H), 4.03 – 3.96 (m, 2H), 3.89 (dd, *J* = 10.9, 6.1 Hz, 1H), 3.85 – 3.78 (m, 2H), 3.72 (dd, *J* = 8.9, 3.4 Hz, 1H), 3.69 – 3.61 (m, 1H), 3.42 (br, 1H), 3.40 (s, 3H), 2.27 (br, 1H), 2.15 (s, 3H), 2.08 (s, 3H), 1.99 (s, 3H), 1.98 (s, 3H), 1.05 (s, 9H). ^{13}C NMR (101 MHz, $CDCl_3$) δ 170.5, 170.2, 170.1, 169.9, 135.8, 135.7, 133.7,

[28] Nakagawa, Y.; Doi, T.; Taketani, T.; Takegoshi, K.; Igarashi, Y.; Ito, Y. Mannose-Binding Geometry of Pradimicin A. *Chem. Eur. J.* **2013***, 19,* 10516–10525.

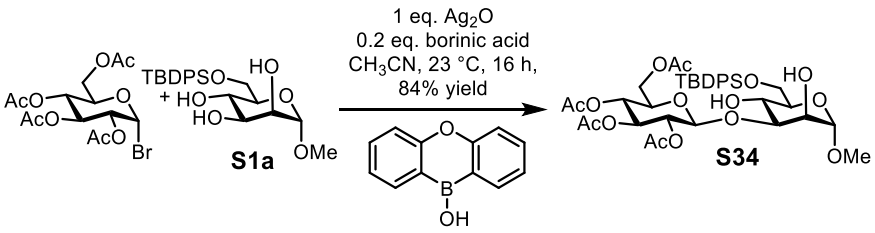
133.7, 129.7, 127.7, 127.7, 102.2, 100.1, 84.8, 72.6, 71.4, 70.6, 70.2, 69.2, 66.9, 66.1, 63.8, 61.7, 54.7, 26.9, 20.9, 20.7, 20.7, 20.6, 19.4. HRMS (ESI) m/z calculated for $C_{37}H_{50}O_{15}Si$ $[M+NH_4]^+$: 780.3257; found: 780.3250.



Methyl 6-*O*-*tert*-butyldiphenylsilyl-3-*O*-(6′-*O*-*tert*-butyldiphenylsilyl-β-D-galactopyranosyl)-α-D-mannopyranoside (3l). To a 20 mL scintillation vial equipped with a stir bar was added disaccharide **S32** (0.206 g, 0.27 mmol, 1 equiv.), 2 mL anhydrous methanol, and sodium methoxide (0.5 M in methanol, 0.05 mL, 0.027 mmol, 0.1 equiv.). The reaction mixture was stirred at 23 °C for 1 hour and then neutralized with methanol-washed Amberlite IRC120 H. The resin was filtered off, and the filtrate was concentrated under reduced pressure to afford the deprotected disaccharide **S33**, which was used directly in the next step without purification.

To a 20 mL scintillation vial containing deprotected disaccharide **S33** (0.27 mmol, 1 equiv.) was added 1.5 mL anhydrous DMF, imidazole (0.037 g, 0.54 mmol, 2 equiv.), and *tert*-butyl(chloro)diphenylsilane (TBDPSCl, 0.07 mL, 0.27 mmol, 1 equiv.). The reaction mixture was stirred at 23 °C until complete conversion of disaccharide. The reaction mixture was diluted with EtOAc and washed with water (x3), 10 wt.% LiCl (aq.), and sat. NaCl (aq.). The organic layer was dried over Na_2SO_4 and concentrated under reduced pressure. The crude mixture was purified by column chromatography (1% MeOH/CH_2Cl_2 to 8% MeOH/CH_2Cl_2) on 25 g silica gel to give the product, **3l**, in 85% yield (0.19 g, 0.23 mmol) as a white solid. ^{1}H NMR (400 MHz, $CDCl_3$) δ 7.74 – 7.61 (m, 8H), 7.39 – 7.26 (m, 12H), 5.13 (br, 1H), 4.67 (s, 1H), 4.47 (br, 1H), 4.19 (d, J = 7.7 Hz, 1H), 4.11 (br, 1H), 4.04 (d, J = 10.5 Hz, 1H), 3.98 (s, 1H), 3.88 – 3.70 (m, 7H), 3.69 – 3.64

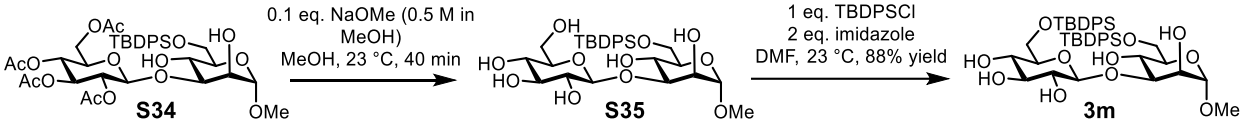
(m, 2H), 3.58 (br, 1H), 3.45 – 3.37 (m, 2H), 3.29 (s, 3H), 1.03 (s, 9H), 1.00 (s, 9H). ^{13}C NMR (101 MHz, $CDCl_3$) δ 135.8, 135.7, 135.7, 133.8, 133.8, 133.1, 133.0, 130.0, 129.6, 128.0, 127.9, 127.7, 102.1, 100.5, 81.2, 75.4, 73.6, 73.4, 71.3, 69.1, 68.9, 66.0, 64.3, 62.9, 54.5, 26.9, 26.9, 19.4, 19.2. HRMS (ESI) m/z calculated for $C_{45}H_{60}O_{11}Si_2$ $[M+NH_4]^+$: 850.4012; found: 850.4001.



S34 was synthesized following a modified procedure.[28]

Methyl 6-*O*-*tert*-butyldiphenylsilyl-3-*O*-(2',3',4',6'-tetra-*O*-acetyl-β-D-glucopyranosyl)-α-D-mannopyranoside (S34). To a flame-dried 20 mL scintillation vial equipped with a stir bar was added 2,3,4,6-tetra-*O*-acetyl-α-D-glucopyranosyl bromide (0.4 g, 0.97 mmol, 1 equiv.), methyl 6-*O*-(*tert*-butyldiphenylsilyl)-α-D-mannopyranoside **S1a** (0.463 g, 1.07 mmol, 1.1 equiv.), silver(I) oxide (0.225 g, 0.97 mmol, 1 equiv.), and 10H-dibenzo[b,e][1,4]oxaborinin-10-ol (38 mg, 0.19 mmol, 0.2 equiv.). The scintillation vial was evacuated and backfilled with N_2. To the vial was added 7.5 mL anhydrous CH_3CN. The reaction mixture was stirred at 23 °C overnight. The reaction was quenched with a small amount of methanol and filtered through a plug of Celite. The filtrate was concentrated under reduced pressure and purified by column chromatography (25% EtOAc/hexanes to 65% EtOAc/hexanes) on 50 g silica gel to give the product, **S34**, in 84% yield (0.62 g, 0.81 mmol) as a white solid. ^{1}H NMR (400 MHz, $CDCl_3$) δ 7.73 – 7.66 (m, 4H), 7.42 – 7.33 (m, 6H), 5.23 (t, J = 9.6 Hz, 1H), 5.07 – 4.98 (m, 2H), 4.76 (d, J = 1.5 Hz, 1H), 4.62 (d, J = 8.0 Hz, 1H), 4.20 (dd, J = 12.2, 2.7 Hz, 1H), 4.13 (dd, J = 12.2, 6.4 Hz, 1H), 4.00 (dd, J = 10.9, 2.4 Hz, 1H), 3.88 (dd, J = 10.9, 6.1 Hz, 1H), 3.85 – 3.82 (m, 1H), 3.81 – 3.75 (m, 2H), 3.72 (dd, J

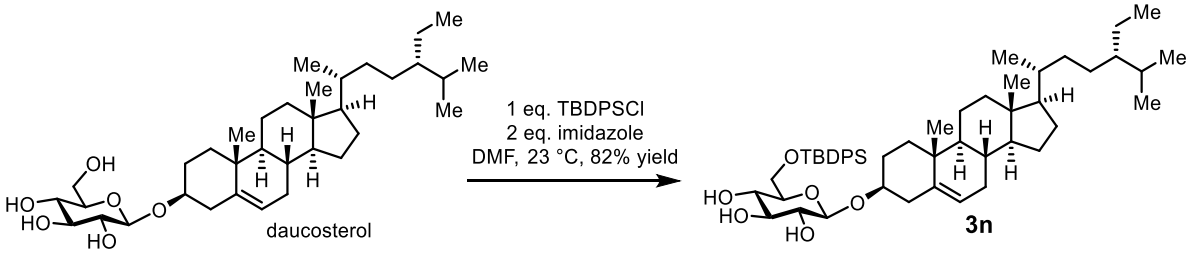
= 8.9, 3.3 Hz, 1H), 3.69 – 3.62 (m, 1H), 3.39 (s, 3H), 3.34 (br, 1H), 2.22 (br, 1H), 2.06 (s, 3H), 2.03 (s, 3H), 2.01 (s, 3H), 2.01 (s, 3H), 1.05 (s, 9H). ^{13}C NMR (101 MHz, $CDCl_3$) δ 170.6, 170.2, 169.7, 169.5, 135.8, 135.8, 133.7, 133.7, 129.7, 127.7, 127.7, 101.5, 100.1, 84.5, 72.6, 72.3, 72.2, 71.5, 70.0, 68.6, 66.2, 63.9, 62.1, 54.7, 26.9, 20.8, 20.7, 20.7, 19.4. HRMS (ESI) m/z calculated for $C_{37}H_{50}O_{15}Si$ $[M+NH_4]^+$: 780.3257; found: 780.3248.



Methyl 6-*O*-*tert*-butyldiphenylsilyl-3-*O*-(6′-*O*-*tert*-butyldiphenylsilyl-β-D-glucopyranosyl)-α-D-mannopyranoside (3m). To a 20 mL scintillation vial equipped with a stir bar was added disaccharide **S34** (0.2 g, 0.26 mmol, 1 equiv.), 2 mL anhydrous methanol, and sodium methoxide (0.5 M in methanol, 0.05 mL, 0.026 mmol, 0.1 equiv.). The reaction mixture was stirred at 23 °C for 40 minutes and then neutralized with methanol-washed Amberlite IRC120 H. The resin was filtered off, and the filtrate was concentrated under reduced pressure to afford the deprotected disaccharide **S35**, which was used directly in the next step without purification.

To a 20 mL scintillation vial containing deprotected disaccharide **S35** (0.26 mmol, 1 equiv.) was added 1.5 mL anhydrous DMF, imidazole (0.035 g, 0.52 mmol, 2 equiv.), and *tert*-butyl(chloro)diphenylsilane (TBDPSCl, 0.07 mL, 0.26 mmol, 1 equiv.). The reaction mixture was stirred at 23 °C until complete conversion of disaccharide. The reaction mixture was diluted with EtOAc and washed with water (x3), 10 wt.% LiCl (aq.), and sat. NaCl (aq.). The organic layer was dried over Na_2SO_4 and concentrated under reduced pressure. The crude mixture was purified by column chromatography (1% MeOH/CH_2Cl_2 to 6.5% MeOH/CH_2Cl_2) on 25 g silica gel to give the product, **3m**, in 88% yield (0.19 g, 0.23 mmol) as a white solid. ^{1}H NMR (400 MHz, $CDCl_3$)

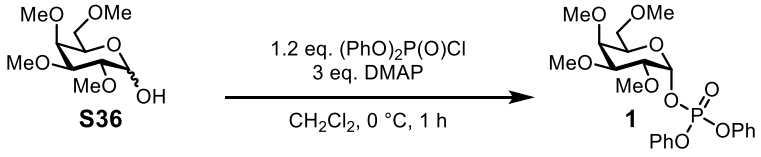
δ 7.77 – 7.60 (m, 8H), 7.40 – 7.27 (m, 12H), 5.54 (br, 1H), 5.01 (br, 1H), 4.63 (s, 1H), 4.32 (d, *J* = 7.2 Hz, 1H), 4.07 (d, *J* = 10.5 Hz, 1H), 3.97 (s, 1H), 3.90 – 3.82 (m, 3H), 3.81 – 3.64 (m, 6H), 3.52 – 3.36 (m, 4H), 3.29 (s, 3H), 1.06 (s, 9H), 1.00 (s, 9H). ^{13}C NMR (101 MHz, $CDCl_3$) δ 135.8, 135.7, 135.7, 133.8, 133.7, 133.0, 133.0, 129.9, 129.7, 127.9, 127.9, 127.8, 102.1, 100.5, 81.5, 76.3, 76.1, 73.3, 73.0, 71.1, 69.5, 66.0, 64.2, 64.0, 54.5, 26.9, 26.9, 19.4, 19.2. HRMS (ESI) m/z calculated for $C_{45}H_{60}O_{11}Si_2$ $[M+NH_4]^+$: 850.4012; found: 850.4004.



6-*O-tert*-Butyldiphenylsilyl-daucosterol (3n). To a 20 mL scintillation vial equipped with a stir bar was added daucosterol (0.25 g, 0.43 mmol, 1 equiv.) was added 7 mL anhydrous DMF, imidazole (0.059 g, 0.86 mmol, 2 equiv.), and *tert*-butyl(chloro)diphenylsilane (TBDPSCl, 0.11 mL, 0.43 mmol, 1 equiv.). The reaction mixture was stirred at 23 °C until complete conversion of disaccharide. The reaction mixture was diluted with EtOAc and washed with water (x3), 10 wt.% LiCl (aq.), and sat. NaCl (aq.). The organic layer was dried over Na_2SO_4 and concentrated under reduced pressure. The crude mixture was purified by column chromatography (40% EtOAc/hexanes to 90% EtOAc/hexanes) on 25 g silica gel to give the product, **3n**, in 82% yield (0.29 g, 0.35 mmol) as a white solid. Impurities from commercial daucosterol could not be removed and did not interfere with catalytic glycosylation. ^{1}H NMR (400 MHz, $CDCl_3$) δ 7.77 – 7.60 (m, 8H), 7.40 – 7.27 (m, 12H), 5.54 (br, 1H), 5.01 (br, 1H), 4.63 (s, 1H), 4.32 (d, *J* = 7.2 Hz, 1H), 4.07 (d, *J* = 10.5 Hz, 1H), 3.97 (s, 1H), 3.90 – 3.82 (m, 3H), 3.81 – 3.64 (m, 6H), 3.52 – 3.36 (m, 4H), 3.29 (s, 3H), 1.06 (s, 9H), 1.00 (s, 9H). ^{1}H NMR (400 MHz, CDCl3) δ 7.71 – 7.65 (m,

4H), 7.46 – 7.33 (m, 6H), 5.35 (d, J = 5.0 Hz, 1H), 4.38 (d, J = 7.7 Hz, 1H), 3.90 (qd, J = 10.7, 5.2 Hz, 2H), 3.62 – 3.49 (m, 3H), 3.49 – 3.30 (m, 4H), 2.87 (s, 1H), 2.36 (dd, J = 13.2, 2.8 Hz, 1H), 2.25 (t, J = 12.1 Hz, 1H), 2.05 – 1.89 (m, 3H), 1.87 – 1.76 (m, 2H), 1.71 – 1.09 (m, 10H), 1.05 (s, 9H), 0.99 (s, 4H), 0.96 – 0.89 (m, 4H), 0.89 – 0.75 (m, 8H), 0.69 (d, J = 7.3 Hz, 3H). ^{13}C NMR (101 MHz, $CDCl_3$) δ 140.4, 135.7, 135.7, 133.1, 133.0, 130.0, 127.9, 127.9, 122.2, 101.0, 79.1, 76.5, 74.9, 73.7, 72.3, 65.0, 56.9, 56.2, 50.3, 46.0, 42.5, 39.9, 39.0, 37.4, 36.8, 36.3, 34.1, 32.1, 32.0, 29.9, 29.3, 28.4, 26.9, 26.2, 24.4, 23.2, 21.2, 20.0, 19.5, 19.3, 19.2, 18.9, 12.1, 12.0. HRMS (ESI) m/z calculated for $C_{51}H_{78}O_6Si$ $[M+NH_4]^+$: 832.5906; found: 832.5893.

3.8.7 Synthesis and Characterization of Glycosyl Phosphates



S36 was prepared as previously reported.[29]

2,3,4,6-tetra-*O*-methyl-α-D-galactopyranosyl diphenylphosphate (1). To a flame-dried 200 mL round bottom flask equipped with a stir bar was added 2,3,4,6-tetra-*O*-methyl-α/β-D-galactopyranose **S36** (1.06 g, 4.49 mmol, 1 equiv) and 4-dimethylaminopyridine (DMAP, 1.644 g, 13.5 mmol, 3 equiv.). The reaction flask was evacuated and backfilled with N_2 three times. To the reaction flask was added 45 mL dry CH_2Cl_2, and the reaction was cooled to 0 °C. To the cooled solution was added diphenyl phosphoryl chloride (1.1 mL, 5.38 mmol, 1.2 equiv.) dropwise. The reaction was stirred at 0 °C for 1 hour and then concentrated under reduced pressure (note: the temperature of rotary evaporator water bath should be around 10 °C). The crude mixture was

[29] Matwiejuk, M.; Thiem, J. New Method for Regioselective Glycosylation Employing Saccharide Oxyanions. *Eur. J. Org. Chem*. **2011**, 5860–5878.

purified by column chromatography (45% Et_2O/hexanes to 100% Et_2O/hexanes) on 100 g silica gel to give the product, **1**, in 44% yield (0.93 g, 1.98 mmol) as a colorless oil. ^{1}H NMR (500 MHz, $CDCl_3$) δ 7.37 – 7.27 (m, 8H), 7.22 – 7.16 (m, 2H), 6.07 (dd, *J* = 6.2, 3.4 Hz, 1H), 3.90 (dd, *J* = 8.2, 5.3 Hz, 1H), 3.72 (d, *J* = 2.7 Hz, 1H), 3.69 (dt, *J* = 10.0, 3.3 Hz, 1H), 3.55 (s, 3H), 3.50 (s, 3H), 3.49 – 3.45 (m, 2H), 3.44 (s, 3H), 3.31 (s, 3H), 3.20 (dd, *J* = 9.2, 5.4 Hz, 1H). ^{13}C NMR (101 MHz, $CDCl_3$) δ 150.8 (d, *J* = 3.3 Hz), 150.7 (d, *J* = 3.0 Hz), 129.9, 129.7, 125.5 (d, *J* = 1.1 Hz), 125.4 (d, *J* = 0.9 Hz), 120.7 (d, *J* = 4.8 Hz), 120.3 (d, *J* = 5.0 Hz), 97.2 (d, *J* = 6.7 Hz), 79.4, 77.3, 77.2, 75.1, 71.2, 70.0, 61.5, 59.2, 58.7, 58.3. ^{31}P NMR (162 MHz, $CDCl_3$) δ -13.2. HRMS (ESI) m/z calculated for $C_{22}H_{29}O_9P[M+H]^+$: 469.1622; found: 469.1613.

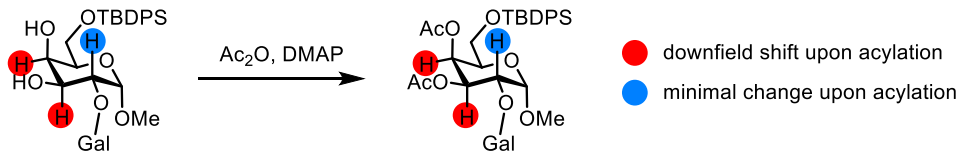
2 was prepared as previously reported.[30]

3.8.8 Anomeric Configuration and Connectivity Assignment

The assignment of anomeric configuration of galactosyl linkages was conducted by utilizing $^3J_{H1\text{-}H2}$. $^3J_{H1\text{-}H2}$ for α-products is around 3 Hz, and that for β-products is around 7 Hz.

The assignment of anomeric configuration of mannosyl linkages was conducted by following a previously reported procedure.[31] A combination of $^3J_{H1\text{-}H2}$, $^1J_{C1\text{-}H1}$, and the chemical shift of the H-5 proton data was used to determine anomeric configuration. $^3J_{H1\text{-}H2}$ for α-products is 0 Hz, and that for β-products is 2.5–3.0 Hz. The $^1J_{C1\text{-}H1}$ of α-anomers ranges from 170 to 177 Hz, while that of β-anomers ranges from 160 to 165 Hz. H-5 proton resonance in β-mannosides typically appears in the 3.3–3.4 ppm region, while in α-mannosides, the resonance is shifted downfield and appears in the 3.6–3.9 ppm region.

[30] Li, Q.; Levi, S. M.; Jacobsen, E. N. Highly Selective β-Mannosylations and β-Rhamnosylations Catalyzed by Bis-thiourea. *J. Am. Chem. Soc.* **2020**, *142*, 11865–11872.



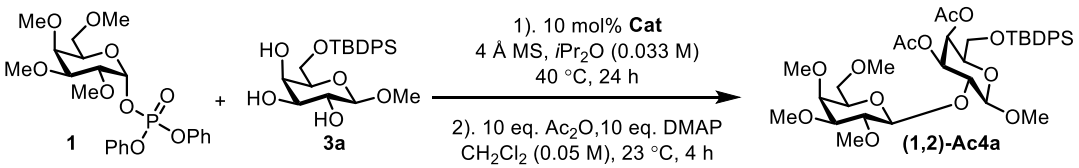
Site of glycosylation was determined by ^{1}H NMR analysis of acylated products. Upon acylation, proton resonances corresponding to unglycosylated sites shift downfield and appear above 5 ppm, while resonance corresponding to glycosylation site does not undergo significant change and appears in the 3–4 ppm. By comparing chemical shifts of proton resonances in acceptor, site of glycosylation can be easily distinguished from sites of acylation. Proton resonances in acceptor are assigned unequivocally by COSY analysis.

Site selectivities were determined using anomeric proton peaks in the crude catalytic glycosylation mixture. Peaks used in assignment will be noted in the characterization data of each compound.

3.8.9 Synthesis and Characterization of Products

General Procedure A. To a flame-dried 10 mL round bottom flask equipped with a stir bar was added acceptor (0.1–0.15 mmol, 1–1.5 equiv), Catalyst **1** (0.01 mmol, 0.1 equiv), and activated 4 Å molecular sieves (0.3 g). To the reaction mixture was added a solution of galactosyl phosphate (0.1 mmol, 1 equiv.) in 3 mL anhydrous diisopropyl ether. The flask was sealed with a yellow polyethylene cap under an atmosphere of air and parafilm was used to seal the cap tightly. The mixture was stirred at specified temperature for 24–48 hours. The mixture was cooled to room temperature, and 150 μL aliquot was diluted with diethyl ether and filtered to remove the molecular sieves. This solution was concentrated, and ^{1}H NMR analysis on the unacylated crude mixture was used to determine the site selectivity. The reaction mixture was filtered through cotton to remove molecular sieves. The filtrate was concentrated under reduced pressure. To the 20 mL scintillation

vial containing crude product was added 2 mL anhydrous CH_2Cl_2, acetic anhydride (1 mmol, 10 equiv.) and 4-(dimethylamino)pyridine (1 mmol, 10 equiv.). The reaction mixture was stirred at 23 ˚C for 4 hours. At that time, the mixture was concentrated under reduced pressure and purified by column chromatography to give the desired product.



Methyl 6-*O*-*tert*-butyldiphenylsilyl-3,4-di-*O*-acetyl-2-*O*-(2',3',4',6'-tetra-*O*-methyl-β-D-galactopyranosyl)-β-D-galactopyranoside ((1,2)-Ac4a) was synthesized according to general procedure A.

Materials: methyl 6-*O*-(*tert*-butyldiphenylsilyl)-β-D-galactopyranoside **3a** (64.9 mg, 0.15 mmol, 1.5 equiv), Catalyst **1** (11.5 mg, 0.01 mmol, 0.1 equiv), activated 4 Å molecular sieves (0.3 g), and a solution of galactosyl phosphate (46.8 mg, 0.1 mmol, 1 equiv.) in 3 mL anhydrous diisopropyl ether.

Temperature and reaction time: 40 ˚C, 24 hours

Site selectivity: 15:1, 1,2-product:1,3-product

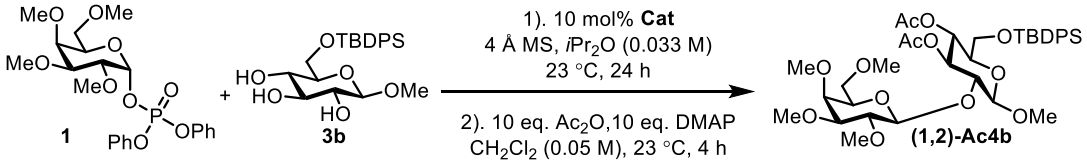
Purification conditions and yield: The crude mixture from acylation was purified by column chromatography (20% Et_2O/hexanes to 90% Et_2O/hexanes) on 10 g silica gel to give the acylated product in 81% yield over two steps (59.2 mg, 0.081 mmol) as a white solid.

^{1}H NMR (600 MHz, $CDCl_3$) δ 7.63 – 7.57 (m, 4H), 7.45 – 7.33 (m, 6H), 5.51 (d, J = 3.5 Hz, 1H), 5.03 (dd, J = 10.0, 3.4 Hz, 1H), **4.36 (dd, J = 7.7, 6.5 Hz, 2H, Gal(donor)-H-1, Gal(acceptor)-**

H-1), 3.78 – 3.70 (m, 3H), 3.64 – 3.58 (m, 3H), 3.54 (s, 3H), 3.51 – 3.49 (m, 4H), 3.48 (s, 6H), 3.47 – 3.43 (m, 1H), 3.38 (s, 4H), 3.23 (dd, *J* = 9.8, 7.8 Hz, 1H), 3.07 (dd, *J* = 9.7, 3.0 Hz, 1H), 2.00 (s, 3H), 1.98 (s, 3H), 1.01 (s, 9H). ^{13}C NMR (126 MHz, $CDCl_3$) δ 170.2, 170.1, 135.7, 135.7, 133.1, 133.0, 129.9, 129.9, 127.9, 104.2, 103.2, 84.4, 81.0, 74.8, 73.1, 73.0, 72.8, 70.7, 67.4, 61.4, 61.3, 61.1, 59.3, 58.4, 57.1, 26.8, 20.9, 20.8, 19.1. HRMS (ESI) m/z calculated for $C_{37}H_{54}O_{13}Si$ $[M+NH_4]^+$: 752.3672; found: 752.3657.

Unacylated (1,2)-product: ^{1}H NMR (600 MHz, $CDCl_3$) δ 4.43 (d, *J* = 7.9 Hz, 1H), 4.26 (d, *J* = 7.5 Hz, 1H)

Unacylated (1,3)-product: ^{1}H NMR (600 MHz, $CDCl_3$) δ 4.56 (d, *J* = 7.8 Hz, 1H)



Methyl 6-*O*-*tert*-butyldiphenylsilyl-3,4-di-*O*-acetyl-2-*O*-(2',3',4',6'-tetra-*O*-methyl-β-D-galactopyranosyl)-β-D-glucopyranoside ((1,2)-Ac4b)) was synthesized according to general procedure A.

Materials: Methyl 6-*O*-(*tert*-butyldiphenylsilyl)-β-D-glucopyranoside **3b** (64.9 mg, 0.15 mmol, 1.5 equiv), Catalyst **1** (11.5 mg, 0.01 mmol, 0.1 equiv), activated 4 Å molecular sieves (0.3 g), and a solution of galactosyl phosphate (46.8 mg, 0.1 mmol, 1 equiv.) in 3 mL anhydrous diisopropyl ether.

Temperature and reaction time: 23 ˚C, 24 hours

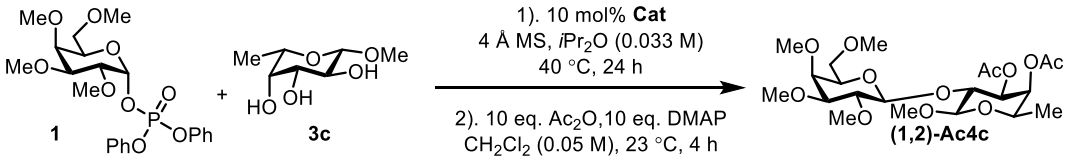
Site selectivity: 9:1, 1,2-product:1,3-product

Purification conditions and yield: The crude mixture from acylation was purified by column chromatography (20% Et_2O/hexanes to 90% Et_2O/hexanes) on 10 g silica gel to give the acylated product in 75% yield over two steps (55 mg, 0.075 mmol) as a white solid.

^{1}H NMR (500 MHz, $CDCl_3$) δ 7.71 – 7.62 (m, 4H), 7.43 – 7.33 (m, 6H), 5.19 (t, *J* = 9.3 Hz, 1H), 5.06 (t, *J* = 9.6 Hz, 1H), **4.41 (d, *J* = 7.5 Hz, 1H, Glu(acceptor)-H-1)**, **4.39 (d, *J* = 7.8 Hz, 1H, Gal(donor)-H-1),** 3.74 – 3.67 (m, 3H), 3.65 – 3.59 (m, 2H), 3.56 – 3.51 (m, 8H), 3.49 (s, 3H), 3.47 – 3.44 (m, 4H), 3.39 (s, 3H), 3.24 (dd, *J* = 9.7, 7.8 Hz, 1H), 3.06 (dd, *J* = 9.7, 3.1 Hz, 1H), 2.02 (s, 3H), 1.90 (s, 3H), 1.03 (s, 9H). ^{13}C NMR (126 MHz, $CDCl_3$) δ 170.3, 169.8, 135.8, 135.7, 133.4, 133.3, 129.8, 129.8, 127.8, 127.7, 104.1, 102.4, 84.5, 80.7, 79.2, 75.2, 74.7, 74.1, 73.1, 70.6, 69.2, 62.8, 61.3, 61.1, 59.3, 58.4, 56.4, 26.8, 21.1, 20.8, 19.3. HRMS (ESI) m/z calculated for $C_{37}H_{54}O_{13}Si$ $[M+NH_4]^+$: 752.3672; found: 752.3655.

Unacylated (1,2)-product: ^{1}H NMR (600 MHz, $CDCl_3$) δ 4.48 (d, *J* = 7.9 Hz, 1H), 4.29 (d, *J* = 7.7 Hz, 1H).

Unacylated (1,3)-product: ^{1}H NMR (600 MHz, $CDCl_3$) δ 4.37 (d, *J* = 7.9 Hz, 1H)



Methyl 3,4-di-*O*-acetyl-2-*O*-(2',3',4',6'-tetra-*O*-methyl-β-D-galactopyranosyl)-β-L-frucopyranoside ((1,2)-Ac4c) was synthesized according to general procedure A.

Materials: Methyl β-L-fucopyranoside **3c** (26.7 mg, 0.15 mmol, 1.5 equiv), Catalyst **1** (11.5 mg, 0.01 mmol, 0.1 equiv), activated 4 Å molecular sieves (0.3 g), and a solution of galactosyl phosphate (46.8 mg, 0.1 mmol, 1 equiv.) in 3 mL anhydrous diisopropyl ether.

Temperature and reaction time: 40 ˚C, 24 hours

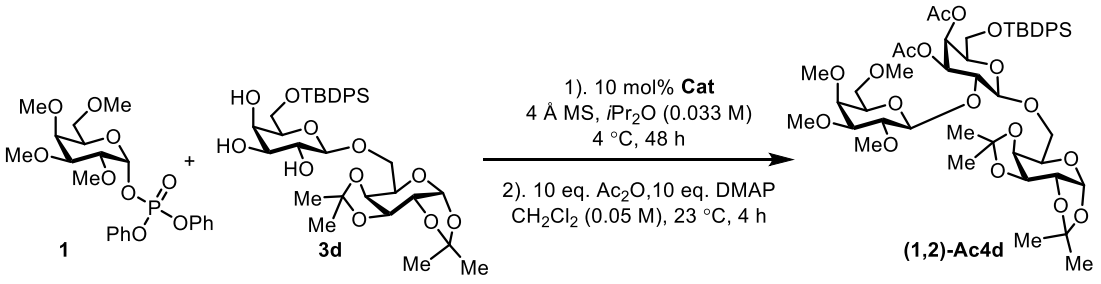
Site selectivity: 11:1, 1,2-product:1,3-product

Purification conditions and yield: The crude mixture from acylation was purified by column chromatography (20% EtOAc/hexanes to 100% EtOAc/hexanes) on 10 g silica gel to give the acylated product in 71% yield over two steps (34 mg, 0.071 mmol) as a white solid.

^{1}H NMR (500 MHz, $CDCl_3$) δ 5.18 (d, *J* = 3.3 Hz, 1H), 4.98 (dd, *J* = 10.0, 3.5 Hz, 1H), **4.46 (d, *J* = 7.6 Hz, 1H, Gal(donor)-H-1), 4.32 (d, *J* = 7.8 Hz, 1H, Fuc(acceptor)-H-1)**, 3.80 (dd, *J* = 10.0, 7.8 Hz, 1H), 3.75 (q, *J* = 6.4 Hz, 1H), 3.60 – 3.53 (m, 8H), 3.51 (s, 3H), 3.49 (s, 3H), 3.45 – 3.39 (m, 2H), 3.37 (s, 3H), 3.19 (dd, *J* = 9.8, 7.6 Hz, 1H), 3.10 (dd, *J* = 9.8, 3.1 Hz, 1H), 2.12 (s, 3H), 1.98 (s, 3H), 1.19 (d, *J* = 6.4 Hz, 3H). ^{13}C NMR (126 MHz, $CDCl_3$) δ 170.7, 170.3, 104.3, 103.3, 83.8, 80.8, 75.4, 74.9, 73.1, 71.6, 70.9, 68.9, 61.3, 60.8, 59.3, 58.4, 57.6, 20.9, 20.8, 16.3. HRMS (ESI) m/z calculated for $C_{21}H_{36}O_{12}$ $[M+NH_4]^+$: 498.2545; found: 498.2541.

Unacylated (1,2)-product: ^{1}H NMR (600 MHz, $CDCl_3$) δ 4.35 (d, *J* = 7.7 Hz, 1H), 4.24 (d, *J* = 7.7 Hz, 1H).

Unacylated (1,3)-product: ^{1}H NMR (400 MHz, $CDCl_3$) δ 4.70 (d, *J* = 7.7 Hz, 1H), 4.57 (d, *J* = 7.6 Hz, 1H).



1,2:3,4-di-*O*-Isopropylidene-6-*O*-(2'-*O*-(2'',3'',4'',6''-tetra-*O*-methyl-β-D-galactopyranosyl)-3',4'-di-*O*-acetyl-6′-*O*-*tert*-butyldiphenylsilyl-β-D-galactopyranosyl)-α-D-galactopyranoside ((1,2)-Ac4d) was synthesized according to general procedure A.

Materials: 1,2:3,4-di-*O*-Isopropylidene-6-*O*-(6′-*O*-*tert*-butyldiphenylsilyl-β-D-galactopyranosyl) -α-D-galactopyranoside **3d** (79.3 mg, 0.12 mmol, 1.2 equiv.), Catalyst **1** (11.5 mg, 0.01 mmol, 0.1 equiv.), activated 4 Å molecular sieves (0.3 g), and a solution of galactosyl phosphate (46.8 mg, 0.1 mmol, 1 equiv.) in 3 mL anhydrous diisopropyl ether.

Temperature and reaction time: 4 ˚C, 48 hours

Site selectivity: 12:1, 1,2-product:1,3-product

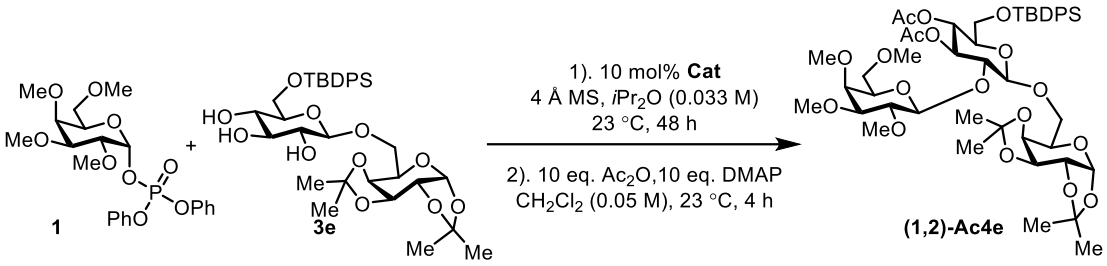
Purification conditions and yield: The crude mixture from acylation was purified by column chromatography (20% Et_2O/hexanes to 80% Et_2O /hexanes) on 10 g silica gel to give the acylated product in 64% yield over two steps (62 mg, 0.064 mmol) as a white solid.

^{1}H NMR (600 MHz, $CDCl_3$) δ 7.61 – 7.57 (m, 4H), 7.44 – 7.33 (m, 6H), 5.52 (d, *J* = 3.4 Hz, 1H), **5.47 (d, *J* = 4.9 Hz, 1H, α-Gal(acceptor)-H-1),** 5.02 (dd, *J* = 9.9, 3.4 Hz, 1H), 4.57 (dd, *J* = 7.9, 2.4 Hz, 1H), **4.45 (d, *J* = 7.7 Hz, 1H, Gal(donor)-H-1''), 4.44 (d, *J* = 7.6 Hz, 1H, β-Gal(acceptor)-H-1')**, 4.39 (dd, *J* = 8.0, 1.5 Hz, 1H), 4.26 (dd, *J* = 5.0, 2.4 Hz, 1H), 4.02 (dd, *J* = 10.9, 5.7 Hz, 1H), 3.94 (t, *J* = 5.8 Hz, 1H), 3.81 (dd, *J* = 10.0, 7.6 Hz, 1H), 3.73 – 3.68 (m, 2H), 3.67 – 3.62 (m, 2H), 3.59 – 3.56 (m, 2H), 3.56 – 3.51 (m, 6H), 3.50 (s, 3H), 3.48 (s, 3H), 3.36 (s, 3H), 3.18 (dd, *J* = 9.8, 7.7 Hz, 1H), 3.07 (dd, *J* = 9.7, 3.0 Hz, 1H), 1.99 (s, 3H), 1.98 (s, 3H), 1.48 (s, 3H), 1.41 (s, 3H), 1.32 (s, 3H), 1.30 (s, 3H), 1.01 (s, 9H). ^{13}C NMR (126 MHz, $CDCl_3$) δ 170.2, 170.0, 135.7, 135.7, 133.0, 133.0, 129.9, 127.9, 127.9, 109.1, 108.6, 103.4, 102.7, 96.4, 84.3, 81.3, 75.9, 74.5, 73.3, 72.8, 72.7, 71.2, 70.8, 70.4, 68.8, 67.3, 66.8, 61.2, 61.1, 61.0, 59.2, 58.3, 26.8,

26.4, 26.2, 25.2, 24.8, 20.9, 20.8, 19.1. HRMS (ESI) m/z calculated for $C_{48}H_{70}O_{18}Si[M+NH_4]^+$: 980.4670; found: 980.4647.

Unacylated (1,2)-product: ^{1}H NMR (600 MHz, $CDCl_3$) δ 4.37 (d, J = 7.6 Hz, 1H).

Unacylated (1,3)-product: ^{1}H NMR (600 MHz, $CDCl_3$) δ 4.44 (d, J = 7.1 Hz, 1H).



1,2:3,4-di-*O*-isopropylidene-6-*O*-(2'-*O*-(2'',3'',4'',6''-tetra-*O*-methyl-β-D-galactopyranosyl)-3',4'-di-*O*-acetyl-6′-*O*-*tert*-butyldiphenylsilyl-β-D-glucopyranosyl)-α-D-galactopyranoside ((1,2)-Ac4e) was synthesized according to general procedure A.

Materials: 1,2:3,4-di-*O*-Isopropylidene-6-*O*-(6′-*O*-*tert*-butyldiphenylsilyl-β-D-glucopyranosyl)-α-D-galactopyranoside **3e** (79.3 mg, 0.12 mmol, 1.2 equiv.), Catalyst **1** (11.5 mg, 0.01 mmol, 0.1 equiv.), activated 4 Å molecular sieves (0.3 g), and a solution of galactosyl phosphate (46.8 mg, 0.1 mmol, 1 equiv.) in 3 mL anhydrous diisopropyl ether.

Temperature and reaction time: 23 ˚C, 48 hours

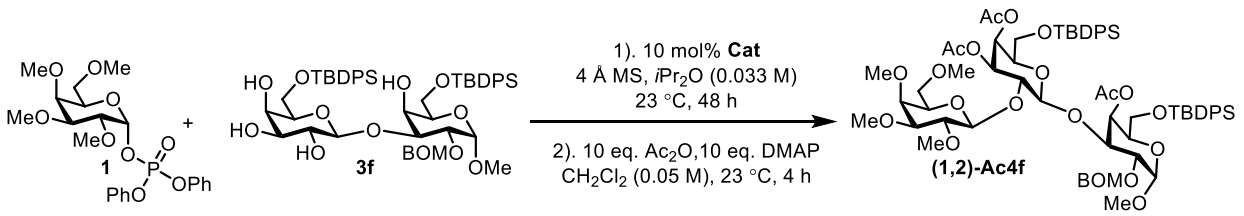
Site selectivity: 14:1, 1,2-product:1,3-product

Purification conditions and yield: The crude mixture from acylation was purified by column chromatography (20% Et_2O/hexanes to 80% Et_2O /hexanes) on 10 g silica gel to give the acylated product in 80% yield over two steps (77 mg, 0.08 mmol) as a white solid.

^{1}H NMR (600 MHz, $CDCl_3$) δ 7.69 – 7.62 (m, 4H), 7.43 – 7.34 (m, 6H), **5.50 (d, *J* = 5.0 Hz, 1H, Gal(acceptor)-H-1)**, 5.16 (t, *J* = 9.3 Hz, 1H), 5.05 (t, *J* = 9.7 Hz, 1H), 4.60 (dd, *J* = 7.9, 2.4 Hz, 1H), **4.48 (d, *J* = 7.5 Hz, 1H, Glu(acceptor)-H-1')**, 4.47 (dd, *J* = 8.0, 1.8 Hz, 1H), **4.42 (d, *J* = 7.7 Hz, 1H, Gal(donor)-H-1'')**, 4.29 (dd, *J* = 5.0, 2.4 Hz, 1H), 4.11 (dd, *J* = 10.8, 6.7 Hz, 1H), 3.97 (td, *J* = 6.3, 1.8 Hz, 1H), 3.75 – 3.67 (m, 4H), 3.64 (d, *J* = 2.7 Hz, 1H), 3.58 (d, *J* = 8.8 Hz, 1H), 3.55 – 3.52 (m, 5H), 3.51 – 3.48 (m, 4H), 3.45 (s, 3H), 3.37 (s, 3H), 3.17 (dd, *J* = 9.7, 7.7 Hz, 1H), 3.05 (dd, *J* = 9.7, 3.1 Hz, 1H), 2.02 (s, 3H), 1.89 (s, 3H), 1.53 (s, 3H), 1.43 (s, 3H), 1.35 (s, 3H), 1.32 (s, 3H), 1.03 (s, 9H). ^{13}C NMR (126 MHz, $CDCl_3$) δ 170.3, 169.8, 135.8, 135.7, 133.3, 133.3, 129.8, 129.7, 127.8, 127.8, 109.1, 108.7, 103.6, 102.0, 96.5, 84.4, 80.9, 77.9, 75.5, 74.4, 74.2, 72.7, 71.1, 70.9, 70.8, 70.3, 69.1, 68.3, 66.7, 62.7, 61.2, 61.1, 59.2, 58.3, 26.8, 26.4, 26.2, 25.1, 24.8, 21.0, 20.7, 19.3. HRMS (ESI) m/z calculated for $C_{48}H_{70}O_{18}Si[M+NH_4]^+$: 980.4670; found: 980.4644.

Unacylated (1,2)-product: ^{1}H NMR (600 MHz, $CDCl_3$) δ 5.49 (d, *J* = 5.0 Hz, 1H), 4.57 (dd, *J* = 8.0, 2.3 Hz, 1H), 4.49 (d, *J* = 7.8 Hz, 1H), 4.44 (d, *J* = 7.7 Hz, 1H), 4.35 (dd, *J* = 7.8, 1.8 Hz, 1H), 4.28 (dd, *J* = 5.0, 2.4 Hz, 1H), 4.27 – 4.23 (m, 1H).

Unacylated (1,3)-product: ^{1}H NMR (600 MHz, $CDCl_3$) δ 5.55 (d, *J* = 5.1 Hz, 1H), 4.59 (dd, *J* = 8.0, 2.4 Hz, 1H), 4.41 (d, *J* = 7.9 Hz, 1H), 4.38 (d, *J* = 7.8 Hz, 1H), 4.31 (dd, *J* = 5.1, 2.4 Hz, 1H), 4.26 (dd, *J* = 8.0, 1.3 Hz, 2H).



Methyl 4-acetyl-2-*O*-(benzyloxy)methyl-6-*O*-*tert*-butyldiphenylsilyl-3-*O*-(2'-*O*-(2'',3'',4'',6''-tetra-*O*-methyl-β-D-galactopyranosyl)-3',4'-di-*O*-acetyl-6′-*O*-*tert*-butyldiphenylsilyl-β-D-galactopyranosyl)-α-D-galactopyranoside ((1,2)-Ac4f) was synthesized according to general procedure A.

Materials: Methyl 2-*O*-(benzyloxy)methyl-6-*O*-*tert*-butyldiphenylsilyl-3-*O*-(6′-*O*-*tert*-butyldiphenylsilyl-β-D-galactopyranosyl)-α-D-galactopyranoside **3f** (95.3 mg, 0.1 mmol, 1 equiv.), Catalyst **1** (11.5 mg, 0.01 mmol, 0.1 equiv.), activated 4 Å molecular sieves (0.3 g), and a solution of galactosyl phosphate (46.8 mg, 0.1 mmol, 1 equiv.) in 3 mL anhydrous diisopropyl ether.

Temperature and reaction time: 23 ˚C, 48 hours

Site selectivity: 14:1, 1,2-product:1,3-product

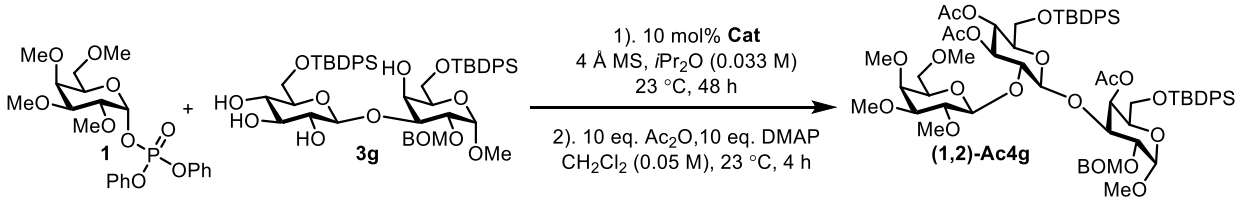
Purification conditions and yield: The crude mixture from acylation was purified by column chromatography (20% Et_2O/hexanes to 80% Et_2O /hexanes) on 10 g silica gel to give the acylated product in 55% yield over two steps (69 mg, 0.055 mmol) as a white solid.

^{1}H NMR (600 MHz, $CDCl_3$) δ 7.65 – 7.61 (m, 6H), 7.60 – 7.57 (m, 2H), 7.44 – 7.41 (m, 4H), 7.41 – 7.28 (m, 13H), 5.46 (d, *J* = 3.5 Hz, 1H), 5.34 (d, *J* = 3.2 Hz, 1H), 5.16 (d, *J* = 7.6 Hz, 1H), 4.96 (dd, *J* = 10.0, 3.5 Hz, 1H), **4.83 (d, *J* = 3.7 Hz, 1H, α-Gal(acceptor)-H-1**), 4.80 (d, *J* = 7.5 Hz, 1H), 4.78 (d, *J* = 11.9 Hz, 1H), **4.64 (d, *J* = 7.7 Hz, 1H, Gal(acceptor)-H-1'**), 4.52 (d, *J* = 11.9 Hz, 1H), **4.37 (d, *J* = 7.6 Hz, 1H, Gal(donor)-H-1''**), 4.05 (dd, *J* = 10.3, 3.3 Hz, 1H), 3.97 (dd, *J* = 10.2, 3.7 Hz, 1H), 3.90 (dd, *J* = 7.6, 4.5 Hz, 1H), 3.75 – 3.66 (m, 3H), 3.62 – 3.52 (m, 5H), 3.49 (s, 3H), 3.48 (s, 3H), 3.47 – 3.44 (m, 1H), 3.43 – 3.36 (m, 7H), 3.35 (s, 3H), 3.11 (dd, *J* = 9.7, 7.6 Hz, 1H), 3.00 (dd, *J* = 9.8, 3.0 Hz, 1H), 2.02 (s, 3H), 2.00 (s, 3H), 1.97 (s, 3H), 1.02 (s, 9H), 0.96

(s, 9H). ^{13}C NMR (126 MHz, $CDCl_3$) δ 170.4, 170.1, 169.6, 138.4, 135.7, 135.7, 135.7, 135.6, 133.4, 133.2, 133.0, 129.9, 129.8, 129.7, 128.5, 128.4, 128.0, 127.9, 127.8, 127.7, 127.6, 127.6, 103.7, 102.8, 99.9, 98.0, 84.2, 81.0, 76.3, 75.5, 74.7, 74.3, 74.0, 73.0, 72.7, 71.7, 70.7, 70.4, 69.7, 67.6, 63.2, 61.3, 61.2, 61.1, 59.2, 58.2, 55.3, 26.8, 21.0, 20.9, 20.9, 19.2, 19.2. HRMS (ESI) m/z calculated for $C_{69}H_{92}O_{20}Si_2[M+Na]^+$: 1319.5613; found: 1319.5579.

Unacylated (1,2)-product: ^{1}H NMR (600 MHz, $CDCl_3$) δ 5.11 (d, J = 7.3 Hz, 1H), 4.83 (d, J = 3.3 Hz, 1H), 4.81 (d, J = 7.3 Hz, 1H), 4.76 (d, J = 12.1 Hz, 1H), 4.73 (d, J = 6.4 Hz, 1H), 4.52 (d, J = 12.1 Hz, 1H), 4.43 (s, 1H), 4.39 (d, J = 7.8 Hz, 1H).

Unacylated (1,3)-product: ^{1}H NMR (600 MHz, $CDCl_3$) δ 4.96 (d, J = 6.9 Hz, 1H), 4.86 (d, J = 7.0 Hz, 1H), 4.83 (d, J = 3.7 Hz, 1H), 4.73 (d, J = 12.0 Hz, 1H), 4.57 (d, J = 12.1 Hz, 1H), 4.52 (d, J = 7.8 Hz, 2H).



Methyl 4-acetyl-2-*O*-(benzyloxy)methyl-6-*O*-*tert*-butyldiphenylsilyl-3-*O*-(2'-*O*-(2'',3'',4'',6''-tetra-*O*-methyl-β-D-galactopyranosyl)-3',4'-di-*O*-acetyl-6′-*O*-*tert*-butyldiphenylsilyl-β-D-glucopyranosyl)-α-D-galactopyranoside ((1,2)-Ac4g) was synthesized according to general procedure A.

Materials: Methyl 2-*O*-(benzyloxy)methyl-6-*O*-*tert*-butyldiphenylsilyl-3-*O*-(6′-*O*-*tert*-butyldiphenylsilyl-β-D-glucopyranosyl)-α-D-galactopyranoside **3g** (95.3 mg, 0.1 mmol, 1 equiv.), Catalyst **1** (11.5 mg, 0.01 mmol, 0.1 equiv.), activated 4 Å molecular sieves (0.3 g), and a solution of galactosyl phosphate (46.8 mg, 0.1 mmol, 1 equiv.) in 3 mL anhydrous diisopropyl ether.

Temperature and reaction time: 23 ˚C, 48 hours

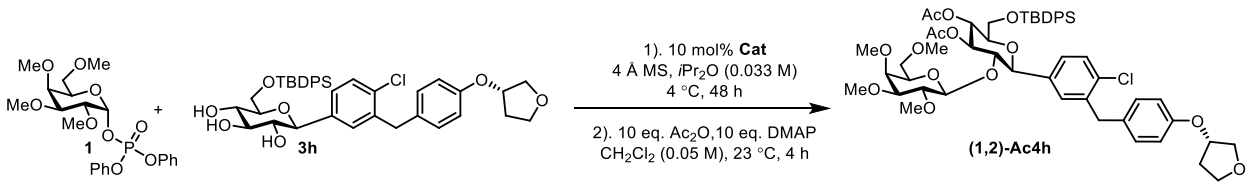
Site selectivity: 6:1, 1,2-product:1,3-product

Purification conditions and yield: The crude mixture from acylation was purified by column chromatography (20% Et_2O/hexanes to 80% Et_2O /hexanes) on 10 g silica gel to give the acylated product in 65% yield over two steps (81 mg, 0.065 mmol) as a white solid.

^{1}H NMR (600 MHz, $CDCl_3$) δ 7.69 – 7.64 (m, 6H), 7.61 – 7.57 (m, 2H), 7.41 – 7.32 (m, 14H), 7.31 – 7.27 (m, 3H), 5.50 (d, *J* = 3.4 Hz, 1H), 5.19 (d, *J* = 7.6 Hz, 1H), 5.10 (t, *J* = 9.4 Hz, 1H), **4.87 (d, *J* = 3.5 Hz, 1H, Gal(acceptor)-H-1),** 4.85 (t, *J* = 9.8 Hz, 1H), 4.82 (d, *J* = 7.2 Hz, 1H), 4.80 (d, *J* = 11.3 Hz, 1H), **4.68 (d, *J* = 7.8 Hz, 1H, Glu(acceptor)-H-1'**), 4.53 (d, *J* = 11.9 Hz, 1H), **4.31 (d, *J* = 7.6 Hz, 1H, Gal(donor)-H-1''**), 4.12 (dd, *J* = 10.2, 3.4 Hz, 1H), 4.03 – 3.98 (m, 2H), 3.71 (dd, *J* = 11.3, 6.4 Hz, 1H), 3.67 – 3.62 (m, 3H), 3.62 – 3.56 (m, 4H), 3.49 (s, 3H), 3.48 (s, 3H), 3.46 (s, 3H), 3.42 (dd, *J* = 8.8, 5.0 Hz, 1H), 3.39 – 3.36 (m, 4H), 3.35 (s, 3H), 3.09 (dd, *J* = 9.7, 7.6 Hz, 1H), 3.00 (dd, *J* = 9.7, 3.1 Hz, 1H), 2.00 (s, 3H), 1.99 (s, 3H), 1.86 (s, 3H), 1.04 (s, 9H), 0.97 (s, 9H). ^{13}C NMR (126 MHz, $CDCl_3$) δ 170.3, 169.9, 169.6, 138.5, 135.8, 135.7, 135.7, 135.6, 133.4, 133.4, 133.3, 133.1, 129.9, 129.8, 129.7, 129.7, 128.5, 127.9, 127.9, 127.8, 127.7, 127.6, 104.0, 102.8, 99.9, 98.1, 84.1, 80.7, 77.9, 76.0, 76.0, 75.6, 74.5, 74.2, 72.6, 72.0, 70.7, 70.5, 69.7, 69.5, 63.7, 63.1, 61.2, 61.2, 59.2, 58.2, 55.3, 26.8, 26.8, 21.1, 21.0, 20.7, 19.3, 19.3. HRMS (ESI) m/z calculated for $C_{69}H_{92}O_{20}Si_2[M+Na]^+$: 1319.5613; found: 1319.5578.

Unacylated (1,2)-product: ^{1}H NMR (600 MHz, $CDCl_3$) δ 5.11 (d, *J* = 7.4 Hz, 1H), 4.84 (d, *J* = 3.6 Hz, 1H), 4.82 (d, *J* = 7.4 Hz, 1H), 4.77 (d, *J* = 12.1 Hz, 1H), 4.76 (d, *J* = 7.7 Hz, 1H), 4.52 (d, *J* = 12.0 Hz, 1H), 4.44 (d, *J* = 7.8 Hz, 1H).

Unacylated (1,3)-product: ^{1}H NMR (600 MHz, $CDCl_3$) δ 5.00 (d, *J* = 7.0 Hz, 1H), 4.89 (d, *J* = 7.0 Hz, 1H), 4.89 (d, *J* = 3.6 Hz, 1H), 4.76 (d, *J* = 12.1 Hz, 1H), 4.60 (d, *J* = 12.2 Hz, 1H), 4.59 (d, *J* = 7.7 Hz, 1H), 4.33 (d, *J* = 7.8 Hz, 1H).



Galactosylated empagliflozin **((1,2)-Ac4h)** was synthesized according to general procedure A.

Materials: TBDPS-empagliflozin **3h** (68.9 mg, 0.1 mmol, 1 equiv), Catalyst **1** (11.5 mg, 0.01 mmol, 0.1 equiv.), activated 4 Å molecular sieves (0.3 g), and a solution of galactosyl phosphate (46.8 mg, 0.1 mmol, 1 equiv.) in 3 mL anhydrous diisopropyl ether.

Temperature and reaction time: 4 ˚C, 48 hours

Site selectivity: 6.4:1, 1,2-product:1,3-product

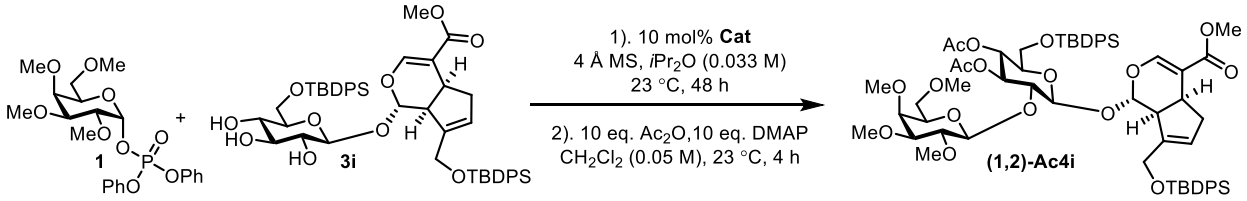
Purification conditions and yield: The crude mixture from acylation was purified by column chromatography (20% Et_2O/hexanes to 80% Et_2O /hexanes) on 10 g silica gel to give the acylated product in 65% yield over two steps (64 mg, 0.065 mmol) as a white solid.

^{1}H NMR (600 MHz, $CDCl_3$) δ 7.68 (d, *J* = 8.1 Hz, 2H), 7.62 (d, *J* = 8.1 Hz, 2H), 7.40 – 7.35 (m, 2H), 7.34 – 7.27 (m, 5H), 7.23 (dd, *J* = 8.3, 2.0 Hz, 1H), 7.16 (d, *J* = 8.3 Hz, 2H), 7.03 (s, 1H), 6.79 (d, *J* = 8.6 Hz, 2H), 5.31 – 5.24 (m, 2H), 4.88 (tt, *J* = 4.7, 2.1 Hz, 1H), **4.18 (d, *J* = 9.4 Hz, 1H, Glu(acceptor)-H-1**), **4.08 (d, *J* = 7.6 Hz, 1H, Gal(donor)-H-1**), 4.05 (d, *J* = 15.9 Hz, 1H), 4.02 – 3.94 (m, 4H), 3.89 (td, *J* = 8.1, 4.4 Hz, 1H), 3.81 (d, *J* = 11.6 Hz, 1H), 3.73 (dd, *J* = 11.6, 3.7 Hz, 1H), 3.65 – 3.57 (m, 2H), 3.47 (s, 4H), 3.45 (s, 3H), 3.42 (s, 3H), 3.24 (s, 3H), 3.07 – 3.00

(m, 2H), 2.95 (t, J = 8.8 Hz, 1H), 2.90 (dd, J = 9.8, 3.1 Hz, 1H), 2.65 (dd, J = 9.0, 5.0 Hz, 1H), 2.21 – 2.11 (m, 2H), 2.05 (s, 3H), 1.96 (s, 3H), 1.04 (s, 9H). ^{13}C NMR (126 MHz, $CDCl_3$) δ 170.6, 169.8, 156.0, 137.8, 137.3, 135.8, 135.7, 133.3, 133.3, 133.2, 132.0, 131.1, 130.5, 129.8, 129.7, 128.8, 127.8, 127.7, 126.1, 115.4, 104.1, 84.0, 80.5, 80.3, 80.2, 78.2, 77.4, 76.8, 74.3, 73.3, 72.0, 70.1, 68.9, 67.4, 62.6, 61.2, 61.1, 59.0, 58.1, 38.3, 33.2, 26.8, 21.1, 20.8, 19.4. HRMS (ESI) m/z calculated for $C_{53}H_{67}ClO_{14}Si[M+NH_4]^+$: 1008.4327; found: 1008.4309.

Unacylated (1,2)-product: ^{1}H NMR (500 MHz, $CDCl_3$) δ 4.89 – 4.85 (m, 1H), 4.16 (d, J = 9.4 Hz, 1H), 4.12 (d, J = 8.0 Hz, 1H), 2.72 (dd, J = 8.9, 4.9 Hz, 1H).

Unacylated (1,3)-product: ^{1}H NMR (600 MHz, $CDCl_3$) δ 4.86 – 4.82 (m, 1H), 4.37 (d, J = 7.9 Hz, 1H), 4.15 (d, J = 9.3 Hz, 1H).



Galactosylated geniposide **((1,2)-Ac4i)** was synthesized according to general procedure A.

Materials TBDPS-geniposide **3i** (86.5 mg, 0.1 mmol, 1 equiv.), Catalyst **1** (11.5 mg, 0.01 mmol, 0.1 equiv.), activated 4 Å molecular sieves (0.3 g), and a solution of galactosyl phosphate (46.8 mg, 0.1 mmol, 1 equiv.) in 3 mL anhydrous diisopropyl ether.

Temperature and reaction time: 23 ˚C, 48 hours

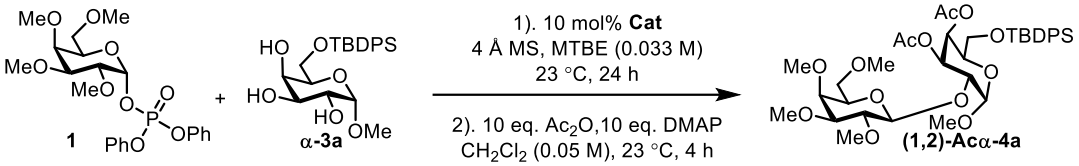
Site selectivity: 3.5:1, 1,2-product:1,3-product

Purification conditions and yield: The crude mixture from acylation was purified by column chromatography (20% Et_2O/hexanes to 80% Et_2O /hexanes) on 10 g silica gel to give the acylated product in 54% yield over two steps (63.1 mg, 0.054 mmol) as a white solid.

^{1}H NMR (600 MHz, $CDCl_3$) δ 7.70 – 7.67 (m, 4H), 7.60 – 7.57 (m, 4H), 7.47 (d, *J* = 1.2 Hz, 1H), 7.45 – 7.32 (m, 12H), 5.92 (s, 1H), 5.15 (t, *J* = 9.2 Hz, 1H), 5.04 (d, *J* = 8.0 Hz, 1H), 4.94 (t, *J* = 9.6 Hz, 1H), **4.90 (d, *J* = 7.6 Hz, 1H, Glu(acceptor)-H-1**), 4.44 – 4.39 (m, 1H), 4.28 – 4.23 (m, 1H), **4.14 (d, *J* = 7.8 Hz, 1H, Gal(donor)-H-1**), 3.74 (s, 3H), 3.65 (dd, *J* = 11.5, 2.5 Hz, 1H), 3.62 (t, *J* = 5.7 Hz, 1H), 3.56 – 3.51 (m, 2H), 3.48 (s, 3H), 3.45 (s, 3H), 3.43 (s, 3H), 3.42 – 3.37 (m, 2H), 3.35 (dd, *J* = 9.1, 7.6 Hz, 1H), 3.23 – 3.13 (m, 4H), 3.11 (s, 3H), 2.93 (dd, *J* = 9.7, 3.1 Hz, 1H), 2.90 – 2.82 (m, 1H), 2.57 (t, *J* = 8.3 Hz, 1H), 2.06 (s, 3H), 2.04 – 1.98 (m, 1H), 1.91 (s, 3H), 1.05 (s, 9H), 0.97 (s, 9H). ^{13}C NMR (126 MHz, $CDCl_3$) δ 170.2, 169.9, 167.9, 151.8, 142.7, 135.7, 135.6, 135.6, 133.8, 133.7, 133.2, 133.1, 129.9, 129.8, 127.9, 127.9, 127.9, 127.8, 127.0, 111.5, 104.0, 96.3, 96.0, 84.5, 80.5, 79.3, 75.1, 74.5, 74.3, 72.6, 70.0, 69.3, 63.1, 62.7, 61.2, 61.1, 58.9, 58.2, 51.3, 46.0, 38.8, 35.8, 27.0, 26.7, 21.1, 20.8, 19.4, 19.3. HRMS (ESI) m/z calculated for $C_{63}H_{82}O_{17}Si_2[M+Na]^+$: 1189.4983; found: 1189.4960.

Unacylated (1,2)-product: ^{1}H NMR (600 MHz, $CDCl_3$) δ 4.82 (d, *J* = 7.8 Hz, 1H)

Unacylated (1,3)-product: ^{1}H NMR (600 MHz, $CDCl_3$) δ 4.77 (d, *J* = 7.6 Hz, 1H).



Methyl 6-*O*-*tert*-butyldiphenylsilyl-3,4-di-*O*-acetyl-2-*O*-(2',3',4',6'-tetra-*O*-methyl-β-D-galactopyranosyl)-a-D-galactopyranoside ((1,2)-Ac4a) was synthesized according to general procedure A.

Materials: methyl 6-*O*-(*tert*-butyldiphenylsilyl)-a-D-galactopyranoside **3a** (71.3 mg, 0.16 mmol, 1.5 equiv), **cat-9** (12.1 mg, 0.011 mmol, 0.1 equiv), activated 4 Å molecular sieves (0.33 g), and a solution of galactosyl phosphate (51.5 mg, 0.11 mmol, 1 equiv.) in 3.3 mL anhydrous MTBE.

Temperature and reaction time: 23 ˚C, 24 hours

Site selectivity: 16:1, 1,2-product:1,3-product

Purification conditions and yield: The crude mixture from acylation was purified by column chromatography (20% Et_2O/hexanes to 90% Et_2O/hexanes) on 10 g silica gel to give the acylated product in 90% yield over two steps (72.8 mg, 0.099 mmol) as a white solid.

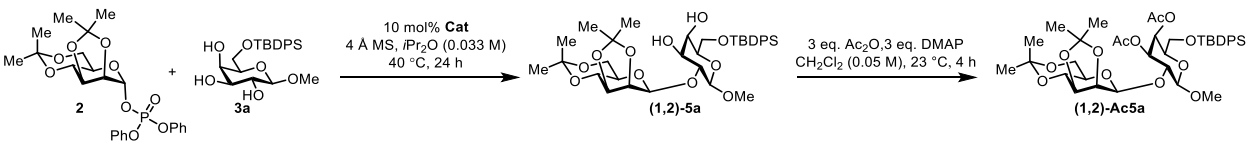
^{1}H NMR (600 MHz, $CDCl_3$) δ 7.65 – 7.58 (m, 4H), 7.46 – 7.33 (m, 6H), 5.52 (d, *J* = 2.6 Hz, 1H), 5.39 (dd, *J* = 10.6, 3.5 Hz, 1H), 4.91 (d, *J* = 3.5 Hz, 1H), 4.25 (d, *J* = 7.7 Hz, 1H), 4.04 (t, *J* = 6.8 Hz, 1H), 3.88 (dd, *J* = 10.6, 3.6 Hz, 1H), 3.65 (dd, *J* = 10.1, 6.3 Hz, 1H), 3.62 – 3.58 (m, 2H), 3.58 – 3.56 (m, 1H), 3.54 (s, 3H), 3.49 (s, 3H), 3.48 – 3.43 (m, 5H), 3.37 (s, 3H), 3.34 (s, 3H), 3.32 (dd, *J* = 9.7, 7.7 Hz, 1H), 3.06 (dd, *J* = 9.7, 3.1 Hz, 1H), 2.00 (d, *J* = 1.6 Hz, 6H), 1.02 (s, 9H). ^{13}C NMR (126 MHz, $CDCl_3$) δ 170.1, 170.0, 135.7, 133.2, 133.1, 129.9, 129.9, 127.8, 127.8, 105.9, 99.8, 84.0, 80.2, 75.8, 75.0, 73.2, 70.9, 69.3, 68.9, 68.5, 61.8, 61.4, 60.8, 59.3, 58.5, 55.5, 26.8, 20.9, 20.8, 19.1. HRMS (ESI) m/z calculated for $C_{37}H_{54}O_{13}Si[M+Na]^+$: 752.3672; found: 752.3656.

Unacylated (1,2)-product: ^{1}H NMR (600 MHz, $CDCl_3$) δ 4.84 (d, *J* = 3.5 Hz, 1H), 4.39 (d, *J* = 7.9 Hz, 1H)

Unacylated (1,3)-product: ^{1}H NMR (600 MHz, $CDCl_3$) δ 4.81 (d, J = 3.8 Hz, 1H), 4.54 (d, J = 7.8 Hz, 1H).

General Procedure B. To a flame-dried 10 mL round bottom flask equipped with a stir bar was added acceptor (0.1–0.15 mmol, 1–1.5 equiv), Catalyst **1** (11.5 mg, 0.01 mmol, 0.1 equiv), and activated 4 Å molecular sieves (0.3 g). To the reaction mixture was added a solution of mannosyl phosphate (0.1 mmol, 1 equiv.) in 3 mL anhydrous diisopropyl ether. The flask was sealed with a yellow polyethylene cap under an atmosphere of air and parafilm was used to seal the cap tightly. The mixture was stirred at specified temperature for 24 hours. The mixture was cooled to room temperature, and 150 μL aliquot was diluted with diethyl ether and filtered to remove the molecular sieves. This solution was concentrated, and ^{1}H NMR analysis on the unacylated crude mixture was used to determine the site-selectivity. The reaction mixture was concentrated under reduced pressure and purified by column chromatography to give the desired product.

General Procedure C. To the 20 mL scintillation vial equipped with a stir bar was added unacylated product (1 equiv), 2 mL anhydrous CH_2Cl_2, acetic anhydride (3–5 equiv.) and 4-(dimethylamino)pyridine (3–5 equiv.). The reaction mixture was stirred at 23 ˚C for 4 hours. At that time, the mixture was concentrated under reduced pressure and purified by column chromatography to give the acylated product.



Methyl 6-*O*-*tert*-butyldiphenylsilyl-2-*O*-(2',3':4',6'-di-*O*-isopropylidene-β-D-

mannopyranosyl)-β-D-galactopyranoside (1,2)-5a was synthesized according to general procedure B.

Materials: Methyl 6-*O*-*tert*-butyldiphenylsilyl-β-D-galactopyranoside **3a** (64.9 mg, 0.15 mmol, 1.5 equiv.), Catalyst **1** (11.5 mg, 0.01 mmol, 0.1 equiv.), activated 4 Å molecular sieves (0.3 g), and a solution of mannosyl phosphate (49.2 mg, 0.1 mmol, 1 equiv.) in 3 mL anhydrous diisopropyl ether.

Temperature and reaction time: 40 ˚C, 24 hours

Site selectivity: 13:1, 1,2-product:1,3-product

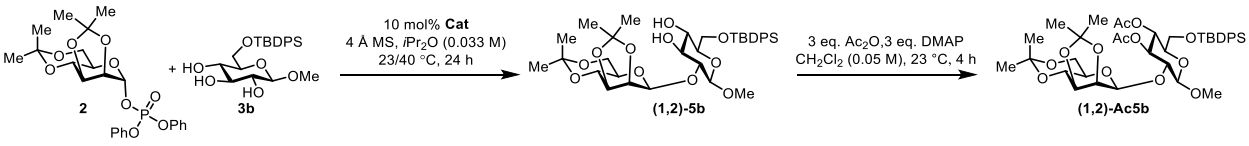
Purification conditions and yield: The reaction mixture was concentrated under reduced pressure and purified by column chromatography (10% EtOAc/hexanes to 60% EtOAc /hexanes) on 10 g silica gel to give the desired product as a mixture of 1,2 and 1,3-product in 87% yield (58.7 mg, 0.087 mmol) as a white solid.

Unacylated (1,2)-product: ^{1}H NMR (400 MHz, $CDCl_3$) δ 7.73 – 7.66 (m, 4H), 7.44 – 7.35 (m, 6H), 5.19 (d, *J* = 3.3 Hz, 1H), 4.38 – 4.31 (m, 2H), 4.29 – 4.23 (m, 2H), 4.11 (s, 1H), 4.00 – 3.94 (m, 2H), 3.94 – 3.86 (m, 2H), 3.80 (t, *J* = 10.5 Hz, 1H), 3.67 – 3.64 (m, 2H), 3.53 (s, 4H), 3.38 (td, *J* = 10.4, 5.4 Hz, 1H), 2.69 (s, 1H), 1.58 (s, 3H), 1.54 (s, 3H), 1.43 (s, 3H), 1.38 (s, 3H), 1.06 (s, 9H). ^{13}C NMR (101 MHz, $CDCl_3$) δ 135.7, 135.6, 133.3, 133.1, 129.9, 127.9, 127.8, 111.2, 102.7, 99.7, 99.5, 80.0, 75.7, 74.6, 74.1, 73.4, 71.2, 68.7, 66.0, 63.2, 63.0, 56.5, 29.1, 26.9, 26.7, 25.2, 19.3, 19.2. HRMS (ESI) m/z calculated for $C_{35}H_{50}O_{11}Si[M+NH_4]^+$: 692.3461; found: 692.3448.

Unacylated (1,3)-product (incomplete list due to peak overlap): ^{1}H NMR (400 MHz, $CDCl_3$) δ 5.16 (d, *J* = 3.6 Hz, 1H), 3.20 (td, *J* = 10.0, 5.4 Hz, 1H).

Acylation was performed following General Procedure C. The crude mixture was purified by column chromatography (10% Et_2O/hexanes to 90% Et_2O /hexanes) on 10 g silica gel.

Acylated (1,2)-product: ^{1}H NMR (500 MHz, $CDCl_3$) δ 7.65 – 7.57 (m, 4H), 7.46 – 7.34 (m, 6H), 5.51 (d, *J* = 3.0 Hz, 1H), 5.04 (d, *J* = 3.3 Hz, 1H), 4.96 (dd, *J* = 10.1, 3.3 Hz, 1H), 4.49 (dd, *J* = 10.7, 6.7 Hz, 1H), 4.35 (d, *J* = 7.7 Hz, 1H), 4.25 (t, *J* = 7.2 Hz, 1H), 4.20 (dd, *J* = 7.8, 3.3 Hz, 1H), 3.89 – 3.81 (m, 3H), 3.81 – 3.71 (m, 2H), 3.63 (dd, *J* = 9.8, 7.3 Hz, 1H), 3.55 (s, 3H), 3.46 – 3.36 (m, 1H), 2.01 (s, 3H), 1.97 (s, 3H), 1.56 (s, 3H), 1.44 (s, 3H), 1.41 (s, 3H), 1.32 (s, 3H), 1.01 (s, 9H). ^{13}C NMR (126 MHz, $CDCl_3$) δ 170.1, 169.9, 135.7, 135.7, 133.1, 133.0, 130.0, 129.9, 127.9, 111.6, 102.6, 99.5, 98.4, 75.9, 74.3, 74.2, 73.5, 73.3, 70.9, 67.7, 65.9, 63.2, 61.4, 56.8, 29.2, 26.8, 26.7, 25.7, 20.9, 20.8, 19.4, 19.1. HRMS (ESI) m/z calculated for $C_{39}H_{54}O_{13}Si[M+NH_4]^+$: 776.3672; found: 776.3657.



Methyl 6-*O*-*tert*-butyldiphenylsilyl-2-*O*-(2',3':4',6'-di-*O*-isopropylidene-β-D-mannopyranosyl)-β-D-glucopyranoside (1,2)-5b was synthesized according to general procedure B.

Materials: Methyl 6-*O*-*tert*-butyldiphenylsilyl-β-D-glucopyranoside **3b** (64.9 mg, 0.15 mmol, 1.5 equiv.), Catalyst **1** (11.5 mg, 0.01 mmol, 0.1 equiv.), activated 4 Å molecular sieves (0.3 g), and a solution of mannosyl phosphate (49.2 mg, 0.1 mmol, 1 equiv.) in 3 mL anhydrous diisopropyl ether.

Temperature and reaction time: 23 ˚C, 24 hours

Site selectivity: 6:1, 1,2-product:1,3-product

Purification conditions and yield: The reaction mixture was concentrated under reduced pressure and purified by column chromatography (10% Et_2O/hexanes to 90% Et_2O /hexanes) on 10 g silica gel to give the desired product as a mixture of 1,2 and 1,3-product in 63% yield (42.5 mg, 0.063 mmol) as a white solid.

The same procedure was repeated at 40 ˚C in an oil bath for 24 hours. ^{1}H NMR analysis on the unacylated crude mixture was used to determine the site-selectivity (5:1 1,2-product:1,3-product). The reaction mixture was concentrated under reduced pressure and purified by column chromatography (10% Et_2O/hexanes to 90% Et_2O /hexanes) on 10 g silica gel to give the desired product as a mixture of 1,2 and 1,3-product in 79% yield (53.3 mg, 0.079 mmol) as a white solid.

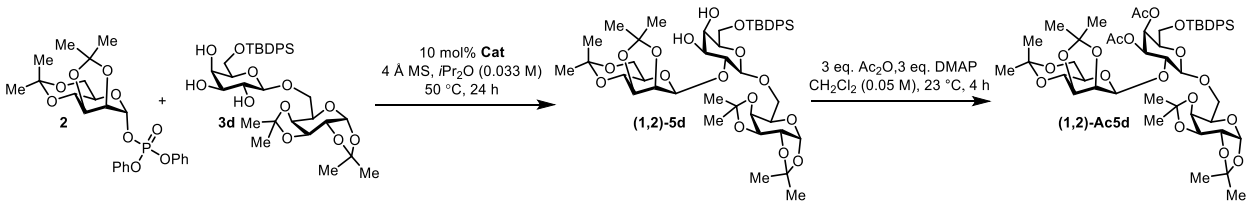
Unacylated (1,2)-product: ^{1}H NMR (400 MHz, $CDCl_3$) δ 7.74 – 7.67 (m, 4H), 7.46 – 7.34 (m, 6H), 5.17 (d, J = 3.3 Hz, 1H), 4.42 (dd, J = 10.6, 7.3 Hz, 1H), 4.35 – 4.30 (m, 2H), 4.28 (d, J = 7.4 Hz, 1H), 3.99 – 3.91 (m, 3H), 3.86 (br, 1H), 3.81 (t, J = 10.5 Hz, 1H), 3.67 (t, J = 9.1 Hz, 1H), 3.62 (t, J = 8.9 Hz, 1H), 3.54 (s, 3H), 3.46 – 3.38 (m, 2H), 3.32 (t, J = 8.2 Hz, 1H), 3.04 (br, 1H), 1.58 (s, 3H), 1.55 (s, 3H), 1.44 (s, 3H), 1.38 (s, 3H), 1.05 (s, 9H). ^{13}C NMR (101 MHz, $CDCl_3$) δ 135.8, 135.7, 133.2, 133.1, 129.9, 127.9, 127.8, 111.3, 102.1, 99.7, 99.6, 82.1, 75.6, 75.2, 73.5, 71.1, 71.0, 66.0, 64.4, 63.3, 56.6, 29.1, 26.9, 26.6, 25.1, 19.3, 19.2. HRMS (ESI) m/z calculated for $C_{35}H_{50}O_{11}Si[M+Na]^+$: 697.3015; found: 697.2988.

Unacylated (1,3)-product (incomplete list due to peak overlap): ^{1}H NMR (400 MHz, $CDCl_3$) δ 5.06 (d, J = 3.0 Hz, 1H), 3.55 (s, 3H), 1.59 (s, 3H), 1.52 (s, 3H), 1.40 (s, 3H). ^{13}C NMR (101 MHz, $CDCl_3$) δ 135.7, 133.5, 133.4, 129.8, 127.8, 127.8, 111.5, 103.4, 100.5, 99.9, 88.5, 76.1, 76.0, 73.8, 73.2, 71.5, 69.3, 66.3, 63.9, 62.7, 57.0, 29.0, 27.3, 25.6, 19.4, 19.0.

Acylation was performed following General Procedure C. The crude mixture was purified by column chromatography (10% Et_2O/hexanes to 90% Et_2O /hexanes) on 10 g silica gel.

Acylated (1,2)-product: ^{1}H NMR (400 MHz, $CDCl_3$) δ 7.72 – 7.63 (m, 4H), 7.45 – 7.33 (m, 6H), 5.11 (t, *J* = 9.3 Hz, 1H), **5.05 (d, *J* = 2.3 Hz, 1H, Man-H-1'**), 5.04 (t, *J* = 9.5 Hz, 1H), 4.48 (dd, *J* = 10.8, 6.7 Hz, 1H), **4.39 (d, *J* = 7.7 Hz, 1H, Glu-H-1**), 4.25 (t, *J* = 7.7 Hz, 1H), 4.20 (dd, *J* = 7.8, 3.4 Hz, 1H), 3.93 – 3.87 (m, 2H), 3.76 – 3.72 (m, 2H), 3.69 (dd, *J* = 9.2, 7.7 Hz, 1H), 3.62 – 3.55 (m, 4H), 3.42 (ddd, *J* = 10.7, 8.8, 6.7 Hz, 1H), 2.02 (s, 3H), 1.91 (s, 3H), 1.58 (s, 3H), 1.44 (s, 3H), 1.43 (s, 3H), 1.32 (s, 3H), 1.04 (s, 9H). ^{13}C NMR (101 MHz, $CDCl_3$) δ 170.2, 169.8, 135.8, 135.7, 133.3, 133.2, 129.9, 129.8, 127.8, 127.8, 111.7, 102.0, 99.5, 98.8, 77.3, 75.8, 75.8, 74.6, 73.3, 70.8, 69.1, 65.9, 63.1, 62.6, 56.4, 29.2, 26.8, 26.6, 25.5, 21.0, 20.7, 19.4, 19.3. HRMS (ESI) m/z calculated for $C_{39}H_{54}O_{13}Si[M+NH_4]^+$: 776.3672; found: 776.3653.

Acylated (1,3)-product: ^{1}H NMR (400 MHz, $CDCl_3$) δ 7.72 – 7.64 (m, 4H), 7.45 – 7.33 (m, 6H), 5.10 (t, *J* = 9.5 Hz, 1H), 4.98 (dd, *J* = 9.5, 7.8 Hz, 1H), **4.91 (d, *J* = 2.8 Hz, 1H, Man-H-1'**), **4.30 (d, *J* = 7.9 Hz, 1H, Glu-H-1**), 4.14 (dd, *J* = 6.3, 2.8 Hz, 1H), 4.09 (t, *J* = 6.4 Hz, 1H), 3.95 (t, *J* = 9.3 Hz, 1H), 3.91 (dd, *J* = 10.6, 5.4 Hz, 1H), 3.87 (dd, *J* = 10.5, 7.6 Hz, 1H), 3.78 – 3.70 (m, 2H), 3.64 (t, *J* = 10.4 Hz, 1H), 3.55 – 3.46 (m, 4H), 3.19 (td, *J* = 10.2, 5.4 Hz, 1H), 2.07 (s, 3H), 1.96 (s, 3H), 1.52 (s, 3H), 1.49 (s, 3H), 1.41 (s, 3H), 1.32 (s, 3H), 1.04 (s, 9H). ^{13}C NMR (101 MHz, $CDCl_3$) δ 169.4, 169.0, 135.8, 135.8, 133.4, 133.3, 129.8, 129.8, 127.8, 127.8, 111.3, 102.0, 99.8, 99.0, 80.8, 76.3, 75.2, 74.2, 72.9, 71.8, 69.0, 66.2, 63.1, 62.6, 56.7, 29.1, 27.7, 26.8, 26.0, 21.3, 21.2, 19.4, 19.1.



1,2:3,4-di-*O*-isopropylidene-6-*O*-(2'-*O*-(2'',3'':4'',6''-di-*O*-isopropylidene-β-D-mannopyranosyl)-6′-*O*-*tert*-butyldiphenylsilyl-β-D-galactopyranosyl)-α-D-galactopyranoside (1,2)-5d was synthesized according to general procedure B.

Materials: 1,2:3,4-di-*O*-isopropylidene-6-*O*-(6′-*O*-*tert*-butyldiphenylsilyl-β-D-galactopyranosyl) -α-D-galactopyranoside **5d** (66.1 mg, 0.1 mmol, 1 equiv.), Catalyst **1** (11.5 mg, 0.01 mmol, 0.1 equiv.), activated 4 Å molecular sieves (0.3 g), and a solution of mannosyl phosphate (49.2 mg, 0.1 mmol, 1 equiv.) in 3 mL anhydrous diisopropyl ether.

Temperature and reaction time: 50 ˚C, 24 hours

Site selectivity: 20:1, 1,2-product:1,3-product

Purification conditions and yield: The reaction mixture was concentrated under reduced pressure and purified by column chromatography (10% Et_2O/hexanes to 90% Et_2O /hexanes) on 10 g silica gel to give the desired product as a mixture of 1,2 and 1,3-product in 81% yield (73.2 mg, 0.081 mmol) as a white solid.

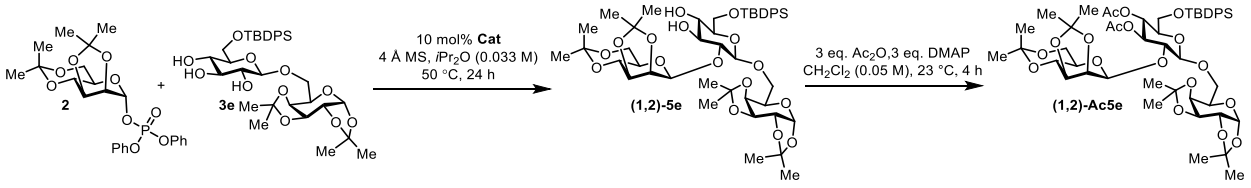
Unacylated (1,2)-product: ^{1}H NMR (400 MHz, $CDCl_3$) δ 7.73 – 7.63 (m, 4H), 7.46 – 7.34 (m, 6H), **5.52 (d, *J* = 5.0 Hz, 1H, α-Gal(acceptor)-H-1**), **5.37 (d, *J* = 2.7 Hz, 1H, Man-H-1''**), 4.56 (dd, *J* = 7.9, 2.4 Hz, 1H), **4.46 – 4.39 (m, 2H, Gal(acceptor)-H-1'**), 4.29 (dd, *J* = 5.1, 2.4 Hz, 1H), 4.22 – 4.12 (m, 3H), 4.05 (dd, *J* = 10.4, 3.3 Hz, 1H), 4.03 – 3.90 (m, 5H), 3.88 – 3.80 (m, 2H), 3.71 – 3.60 (m, 3H), 3.53 (t, *J* = 6.5 Hz, 1H), 3.38 (td, *J* = 10.2, 5.5 Hz, 1H), 2.55 (d, *J* = 1.3 Hz, 1H),

1.59 (s, 3H), 1.51 (s, 3H), 1.49 (s, 3H), 1.41 (s, 3H), 1.38 (s, 3H), 1.31 (s, 3H), 1.28 (s, 3H), 1.05 (s, 9H). ^{13}C NMR (101 MHz, $CDCl_3$) δ 135.7, 135.6, 133.5, 133.2, 129.9, 129.9, 127.9, 127.9, 110.7, 109.5, 108.6, 102.5, 99.7, 98.7, 96.4, 78.1, 76.5, 74.3, 73.2, 72.9, 72.0, 71.4, 70.9, 70.5, 69.3, 67.6, 67.4, 66.1, 62.7, 62.3, 29.2, 27.7, 26.9, 26.2, 26.1, 25.9, 25.1, 24.5, 19.4, 19.1. HRMS (ESI) m/z calculated for $C_{46}H_{66}O_{16}Si[M+NH_4]^+$: 920.4458; found: 920.4439.

Unacylated (1,3)-product (incomplete list due to peak overlap): ^{1}H NMR (600 MHz, $CDCl_3$) δ 5.34 (d, J = 3.9 Hz, 1H).

Acylation was performed following General Procedure C. The crude mixture was purified by column chromatography (10% Et_2O/hexanes to 50% Et_2O /hexanes) on 10 g silica gel.

Acylated (1,2)-product: ^{1}H NMR (400 MHz, $CDCl_3$) δ 7.63 – 7.57 (m, 4H), 7.44 – 7.33 (m, 6H), 5.55 (dd, J = 3.4, 0.9 Hz, 1H), **5.49 (d, J = 5.0 Hz, 1H, α-Gal(acceptor)-H-1**), 5.14 (d, J = 2.8 Hz, 1H, Man-H-1''), 4.97 (dd, J = 10.1, 3.4 Hz, 1H), **4.57 – 4.51 (m, 2H, Gal(acceptor)-H-1'**), 4.27 (dd, J = 5.0, 2.4 Hz, 1H), 4.24 – 4.14 (m, 4H), 4.01 – 3.95 (m, 2H), 3.94 – 3.88 (m, 2H), 3.86 – 3.78 (m, 2H), 3.77 – 3.68 (m, 2H), 3.59 (dd, J = 9.1, 7.6 Hz, 1H), 3.34 (td, J = 9.6, 5.9 Hz, 1H), 2.00 (s, 3H), 1.97 (s, 3H), 1.53 (s, 3H), 1.48 (s, 3H), 1.47 (s, 3H), 1.40 (s, 3H), 1.38 (s, 3H), 1.31 (s, 3H), 1.30 (s, 3H), 1.25 (s, 3H), 1.01 (s, 9H). ^{13}C NMR (101 MHz, $CDCl_3$) δ 170.1, 169.9, 135.8, 135.7, 133.1, 132.9, 129.9, 129.9, 127.9, 127.9, 111.0, 109.4, 108.6, 101.9 ($^1J_{C-H}$ = 161.2 Hz), 99.6, 98.6 ($^1J_{C-H}$ = 164.2 Hz), 96.3 ($^1J_{C-H}$ = 179.8 Hz), 76.1, 75.3, 73.7, 73.0, 71.5, 71.5, 70.8, 70.4, 68.9, 67.6, 67.5, 66.1, 63.2, 61.1, 29.2, 27.3, 26.8, 26.2, 26.1, 25.7, 25.1, 24.5, 20.9, 20.8, 19.5, 19.1. HRMS (ESI) m/z calculated for $C_{50}H_{70}O_{18}Si[M+NH_4]^+$: 1004.4670; found: 1004.4649.



1,2:3,4-di-*O*-isopropylidene-6-*O*-(2'-*O*-(2'',3'':4'',6''-di-*O*-isopropylidene-β-D-mannopyranosyl)-6′-*O*-*tert*-butyldiphenylsilyl-β-D-glucopyranosyl)-α-D-galactopyranoside (1,2)-5e was synthesized according to general procedure B.

Materials: 1,2:3,4-di-*O*-isopropylidene-6-*O*-(6′-*O*-*tert*-butyldiphenylsilyl-β-D-glucopyranosyl)-α-D-galactopyranoside **5e** (66.1 mg, 0.1 mmol, 1 equiv.), Catalyst **1** (11.5 mg, 0.01 mmol, 0.1 equiv.), activated 4 Å molecular sieves (0.3 g), and a solution of mannosyl phosphate (49.2 mg, 0.1 mmol, 1 equiv.) in 3 mL anhydrous diisopropyl ether.

Temperature and reaction time: 50 ˚C, 24 hours

Site selectivity: 7:1, 1,2-product:1,3-product

Purification conditions and yield: The reaction mixture was concentrated under reduced pressure and purified by column chromatography (10% Et_2O/hexanes to 90% Et_2O /hexanes) on 10 g silica gel to give the desired product as a mixture of 1,2 and 1,3-product in 75% yield (67.7 mg, 0.075 mmol) as a white solid.

Unacylated (1,2)-product: ^{1}H NMR (400 MHz, $CDCl_3$) δ 7.73 – 7.64 (m, 4H), 7.45 – 7.33 (m, 6H), **5.52 (d, *J* = 5.1 Hz, 1H, Gal(acceptor)-H-1**), **5.27 (d, *J* = 2.9 Hz, 1H, Man-H-1''**), 4.57 (dd, *J* = 7.9, 2.4 Hz, 1H), **4.48 (d, *J* = 7.7 Hz, 1H, Glu(acceptor)-H-1'**), 4.38 (dd, *J* = 6.7, 2.8 Hz, 1H), 4.29 (dd, *J* = 5.0, 2.4 Hz, 1H), 4.24 – 4.18 (m, 2H), 4.12 (dd, *J* = 10.3, 7.7 Hz, 1H), 4.04 (dd, *J* = 10.4, 3.9 Hz, 1H), 4.00 – 3.85 (m, 6H), 3.73 – 3.62 (m, 3H), 3.45 – 3.33 (m, 3H), 3.11 (s, 1H),

1.58 (s, 3H), 1.52 (s, 3H), 1.50 (s, 3H), 1.42 (s, 3H), 1.40 (s, 3H), 1.38 (s, 3H), 1.31 (s, 3H), 1.29 (s, 3H), 1.05 (s, 9H). ^{13}C NMR (101 MHz, $CDCl_3$) δ 135.7, 135.7, 133.1, 133.0, 129.9, 129.9, 127.9, 127.9, 110.9, 109.4, 108.6, 101.8 ($^1J_{C\text{-}H}$ = 160.2 Hz), 99.7, 99.0 ($^1J_{C\text{-}H}$ = 162.2 Hz), 96.4 ($^1J_{C\text{-}H}$ = 179.6 Hz), 81.0, 76.4, 76.1, 74.8, 73.2, 71.6, 71.6, 71.5, 70.9, 70.4, 69.1, 67.3, 66.2, 64.7, 63.0, 29.2, 27.3, 26.9, 26.2, 26.1, 25.5, 25.0, 24.6, 19.3, 19.2. HRMS (ESI) m/z calculated for $C_{46}H_{66}O_{16}Si[M+NH_4]^+$: 920.4458; found: 920.4448.

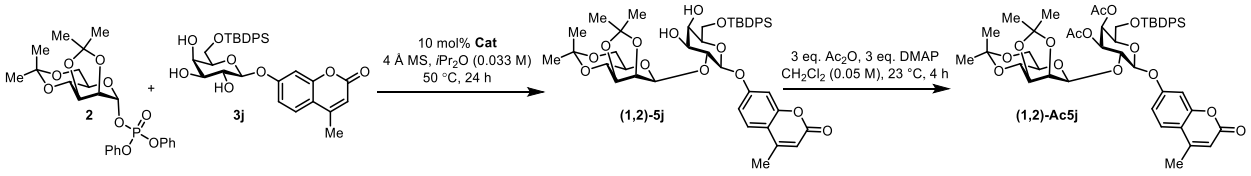
Unacylated (1,3)-product (incomplete list due to peak overlap): ^{1}H NMR (400 MHz, $CDCl_3$) δ **5.54 (d, *J* = 5.1 Hz, 1H, Gal(acceptor)-H-1**), **5.10 (d, *J* = 2.6 Hz, 1H, Man-H-1''**), 4.60 (dd, *J* = 7.9, 2.3 Hz, 1H), 4.41 (dd, *J* = 6.1, 2.7 Hz, 1H), 4.32 (dd, *J* = 5.2, 2.5 Hz, 1H). ^{13}C NMR (101 MHz, $CDCl_3$) δ 135.8, 133.5, 133.5, 129.7, 127.8, 127.7, 111.3, 109.6, 108.9, 103.8, 100.2, 99.8, 87.0, 76.0, 74.3, 71.9, 71.3, 70.8, 70.6, 69.0, 68.1, 66.3, 64.0, 62.3, 36.8, 32.0, 29.1, 27.9, 26.2, 26.1, 25.1, 24.5, 19.4, 19.0.

Acylation was performed following General Procedure C. The crude mixture was purified by column chromatography (10% Et_2O/hexanes to 50% Et_2O /hexanes) on 10 g silica gel.

Acylated (1,2)-product: ^{1}H NMR (400 MHz, $CDCl_3$) δ 7.71 – 7.63 (m, 4H), 7.43 – 7.34 (m, 6H), 5.51 (d, *J* = 5.0 Hz, 1H), 5.16 – 5.04 (m, 3H), 4.63 (d, *J* = 7.5 Hz, 1H), 4.56 (dd, *J* = 7.9, 2.4 Hz, 1H), 4.30 (dd, *J* = 5.0, 2.4 Hz, 1H), 4.24 – 4.16 (m, 4H), 4.08 – 4.01 (m, 2H), 3.95 – 3.85 (m, 3H), 3.77 – 3.68 (m, 3H), 3.59 – 3.52 (m, 1H), 3.35 (q, *J* = 8.6 Hz, 1H), 2.02 (s, 3H), 1.89 (s, 3H), 1.55 (s, 3H), 1.53 (s, 3H), 1.48 (s, 3H), 1.41 (s, 3H), 1.39 (s, 3H), 1.33 (s, 3H), 1.32 (s, 3H), 1.29 (s, 3H), 1.04 (s, 9H). ^{13}C NMR (101 MHz, $CDCl_3$) δ 170.3, 169.8, 135.8, 135.7, 133.4, 133.3, 129.8, 129.8, 127.9, 127.8, 111.1, 109.5, 108.7, 101.0, 99.6, 98.7, 96.4, 77.9, 76.1, 75.4, 74.4, 73.6, 71.7, 71.5, 70.9, 70.4, 69.2, 68.5, 68.0, 66.2, 63.1, 62.8, 29.2, 27.3, 26.8, 26.4, 26.1, 25.8, 25.1, 24.6,

21.1, 20.8, 19.5, 19.4. HRMS (ESI) m/z calculated for $C_{50}H_{70}O_{18}Si[M+NH_4]^+$: 1004.4670; found: 1004.4651.

Acylated (1,3)-product: ^{1}H NMR (400 MHz, $CDCl_3$) δ 7.71 – 7.65 (m, 4H), 7.43 – 7.35 (m, 6H), 5.51 (d, *J* = 4.9 Hz, 1H), 5.10 (t, *J* = 9.6 Hz, 1H), 5.00 (t, *J* = 8.8 Hz, 1H), 4.91 (d, *J* = 2.8 Hz, 1H), 4.58 (dd, *J* = 7.9, 2.4 Hz, 1H), 4.46 (d, *J* = 8.0 Hz, 1H), 4.29 (dd, *J* = 5.0, 2.4 Hz, 1H), 4.18 (dd, *J* = 7.9, 1.9 Hz, 1H), 4.14 (dd, *J* = 6.2, 2.7 Hz, 1H), 4.12 – 4.05 (m, 2H), 3.98 – 3.83 (m, 4H), 3.72 (d, *J* = 3.8 Hz, 2H), 3.69 – 3.59 (m, 3H), 3.52 – 3.46 (m, 1H), 3.18 (td, *J* = 10.1, 5.2 Hz, 1H), 2.09 (s, 3H), 1.95 (s, 3H), 1.53 (s, 3H), 1.52 (s, 3H), 1.49 (s, 3H), 1.42 (s, 3H), 1.41 (s, 3H), 1.33 (s, 3H), 1.32 (s, 3H), 1.31 (s, 3H), 1.04 (s, 9H).



4-methylumbelliferyl 2-*O*-(2',3':4',6'-di-*O*-isopropylidene-β-D-mannopyranosyl)-6-*O*-*tert*-butyldiphenylsilyl-β-D-galactopyranoside (1,2)-5j was synthesized according to general procedure B.

Materials: 4-methylumbelliferyl 6-*O*-*tert*-butyldiphenylsilyl-β-D-galactopyranoside **5j** (57.7 mg, 0.1 mmol, 1 equiv.), Catalyst **1** (11.5 mg, 0.01 mmol, 0.1 equiv.), activated 4 Å molecular sieves (0.3 g), and a solution of mannosyl phosphate (49.2 mg, 0.1 mmol, 1 equiv.) in 3 mL anhydrous diisopropyl ether.

Temperature and reaction time: 50 ˚C, 24 hours

Site selectivity: 17:1, 1,2-product:1,3-product

Purification conditions and yield: The reaction mixture was concentrated under reduced pressure and purified by column chromatography (20% Et_2O/hexanes to 100% Et_2O/hexanes) on 10 g silica gel to give the desired product as a mixture of 1,2 and 1,3-product in 60% yield (49.1 mg, 0.06 mmol) as a white solid.

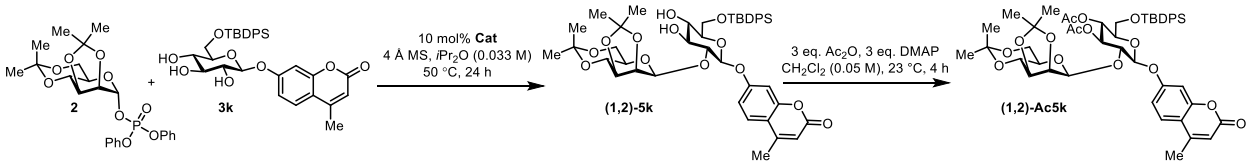
Unacylated (1,2)-product: ^{1}H NMR (400 MHz, $CDCl_3$) δ 7.68 – 7.61 (m, 4H), 7.45 (d, *J* = 8.7 Hz, 1H), 7.43 – 7.27 (m, 6H), 6.99 (dd, *J* = 8.7, 2.4 Hz, 1H), 6.95 (d, *J* = 2.4 Hz, 1H), 6.16 (d, *J* = 1.4 Hz, 1H), **5.23 (d, *J* = 3.5 Hz, 1H, Man-H-1'**), **5.08 (d, *J* = 7.5 Hz, 1H, Gal-H-1**), 4.37 (dd, *J* = 7.2, 3.5 Hz, 1H), 4.29 – 4.15 (m, 4H), 4.00 – 3.89 (m, 3H), 3.82 – 3.75 (m, 2H), 3.72 (t, *J* = 5.7 Hz, 1H), 3.47 (t, *J* = 10.5 Hz, 1H), 3.37 (td, *J* = 10.0, 5.0 Hz, 1H), 2.77 (d, *J* = 2.2 Hz, 1H), 2.38 (d, *J* = 1.2 Hz, 3H), 1.60 (s, 3H), 1.39 (s, 3H), 1.35 (s, 3H), 1.27 (s, 3H), 1.05 (s, 9H). ^{13}C NMR (101 MHz, $CDCl_3$) δ 161.0, 159.7, 155.0, 152.3, 135.7, 135.6, 133.1, 132.9, 129.9, 127.9, 127.9, 125.7, 115.0, 113.6, 113.0, 111.3, 103.7, 100.5, 99.6, 98.8 ($^1J_{C\text{-}H}$ = 161.0 Hz, Man-H-1'), 81.5, 75.5, 75.3, 73.7, 73.5, 70.9, 68.4, 66.0, 63.5, 63.0, 29.0, 26.9, 26.5, 24.8, 19.3, 19.0, 18.8. HRMS (ESI) m/z calculated for $C_{44}H_{54}O_{13}Si[M+H]^+$: 819.3406; found: 819.3393.

Unacylated (1,3)-product (incomplete list due to peak overlap): ^{1}H NMR (400 MHz, $CDCl_3$) δ 6.14 (d, *J* = 1.4 Hz, 1H), 5.32 (d, *J* = 3.3 Hz, 1H, Man-H-1'), 3.19 (td, *J* = 10.2, 5.2 Hz, 1H), 2.34 (d, *J* = 1.2 Hz, 3H).

Acylation was performed following General Procedure C. The crude mixture was purified by column chromatography (5% EtOAc/hexanes to 50% EtOAc /hexanes) on 10 g silica gel.

Acylated (1,2)-product: ^{1}H NMR (400 MHz, $CDCl_3$) δ 7.62 – 7.53 (m, 4H), 7.47 – 7.38 (m, 3H), 7.37 – 7.30 (m, 4H), 7.02 – 6.97 (m, 2H), 6.17 (d, *J* = 1.4 Hz, 1H), 5.56 (d, *J* = 3.0 Hz, 1H), 5.23 (d, *J* = 7.6 Hz, 1H), 5.11 (d, *J* = 1.8 Hz, 1H), 5.05 (dd, *J* = 10.1, 3.3 Hz, 1H), 4.27 – 4.17 (m, 3H),

4.11 (dd, *J* = 10.1, 7.6 Hz, 1H), 3.91 (t, *J* = 6.6 Hz, 1H), 3.85 (dd, *J* = 10.7, 5.4 Hz, 1H), 3.76 – 3.66 (m, 2H), 3.62 (dd, *J* = 10.3, 6.9 Hz, 1H), 3.35 (td, *J* = 10.2, 5.3 Hz, 1H), 2.36 (d, *J* = 1.3 Hz, 3H), 2.03 (s, 3H), 1.99 (s, 3H), 1.47 (s, 3H), 1.32 (s, 6H), 1.12 (s, 3H), 1.00 (s, 9H). ^{13}C NMR (101 MHz, $CDCl_3$) δ 170.0, 169.8, 160.9, 159.1, 154.9, 152.2, 135.7, 135.7, 132.9, 132.7, 130.0, 130.0, 127.9, 127.9, 125.8, 115.4, 113.4, 113.3, 111.5, 104.6, 99.6, 99.4, 98.5, 75.9, 75.6, 74.0, 73.8, 73.5, 71.0, 67.3, 65.9, 63.3, 61.5, 29.0, 27.0, 26.8, 25.5, 20.9, 20.8, 19.1, 18.9, 18.8. HRMS (ESI) m/z calculated for $C_{48}H_{58}O_{15}Si[M+NH_4]^+$: 920.3883; found: 920.3859.



4-methylumbelliferyl 2-*O*-(2',3':4',6'-di-*O*-isopropylidene-β-D-mannopyranosyl)-6-*O*-*tert*-butyldiphenylsilyl-β-D-glucopyranoside (1,2)-5k was synthesized according to general procedure B.

Materials: 4-methylumbelliferyl 6-*O*-*tert*-butyldiphenylsilyl-β-D-glucopyranoside **5k** (57.7 mg, 0.1 mmol, 1 equiv.), Catalyst **1** (11.5 mg, 0.01 mmol, 0.1 equiv.), activated 4 Å molecular sieves (0.3 g), and a solution of mannosyl phosphate (49.2 mg, 0.1 mmol, 1 equiv.) in 3 mL anhydrous diisopropyl ether.

Temperature and reaction time: 50 ˚C, 24 hours

Site selectivity: 13:1, 1,2-product:1,3-product

Purification conditions and yield: The reaction mixture was concentrated under reduced pressure and purified by column chromatography (10% EtOAc/hexanes to 80% EtOAc/hexanes) on 10 g

silica gel to give the desired product as a mixture of 1,2 and 1,3-product in 51% yield (41.8 mg, 0.051 mmol) as a white solid.

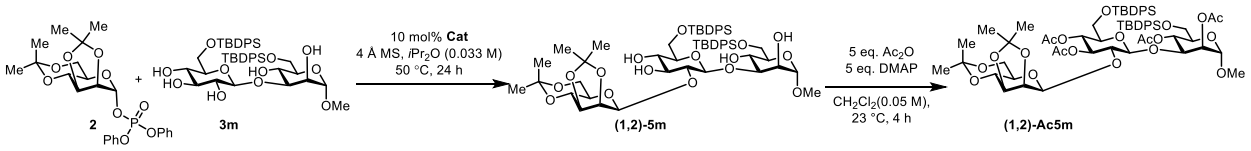
Unacylated (1,2)-product: ^{1}H NMR (400 MHz, $CDCl_3$) δ 7.66 – 7.60 (m, 4H), 7.45 (d, *J* = 8.8 Hz, 1H), 7.40 – 7.21 (m, 6H), 7.01 (dd, *J* = 8.8, 2.5 Hz, 1H), 6.95 (d, *J* = 2.4 Hz, 1H), 6.17 (d, *J* = 1.4 Hz, 1H), **5.25 (d, *J* = 3.6 Hz, 1H, Man-H-1')**, **5.13 (d, *J* = 7.6 Hz, 1H, Glu-H-1**), 4.37 (dd, *J* = 7.3, 3.6 Hz, 1H), 4.30 – 4.20 (m, 3H), 3.98 (dd, *J* = 11.1, 3.6 Hz, 1H), 3.90 (dd, *J* = 11.1, 5.2 Hz, 1H), 3.84 (dd, *J* = 10.7, 5.2 Hz, 1H), 3.77 – 3.68 (m, 2H), 3.62 – 3.58 (m, 2H), 3.54 (t, *J* = 10.5 Hz, 1H), 3.41 (tt, *J* = 10.0, 5.3 Hz, 1H), 2.96 (s, 1H), 2.38 (d, *J* = 1.2 Hz, 3H), 1.60 (s, 3H), 1.39 (s, 3H), 1.35 (s, 3H), 1.24 (s, 3H), 1.03 (s, 9H). ^{13}C NMR (101 MHz, $CDCl_3$) δ 161.0, 159.7, 155.0, 152.3, 135.8, 135.7, 133.2, 132.9, 129.9, 127.8, 127.8, 125.8, 115.1, 113.3, 113.1, 111.4, 103.9, 100.3, 99.7, 98.2 ($^{1}J_{C\text{-}H}$ = 161.6 Hz, Man-H-1'), 83.3, 76.9, 76.2, 75.5, 73.4, 70.8, 70.1, 66.0, 63.8, 63.6, 29.0, 26.9, 26.4, 24.8, 19.3, 19.0, 18.8. HRMS (ESI) m/z calculated for $C_{44}H_{54}O_{13}Si[M+H]^{+}$: 819.3406; found: 819.3389.

Unacylated (1,3)-product (incomplete list due to peak overlap): ^{1}H NMR (400 MHz, $CDCl_3$) δ 5.10 (d, *J* = 3.1 Hz, 1H, Man-H-1'), 5.02 (d, *J* = 7.9 Hz, 1H, Glu-H-1), 4.42 (dd, *J* = 6.7, 3.1 Hz, 1H), 2.36 (d, *J* = 1.3 Hz, 3H).

Acylation was performed following General Procedure C. The crude mixture was purified by column chromatography (5% EtOAc/hexanes to 50% EtOAc /hexanes) on 10 g silica gel.

Acylated (1,2)-product: ^{1}H NMR (400 MHz, C_6D_6) δ 7.74 – 7.71 (m, 2H), 7.70 – 7.66 (m, 2H), 7.15 – 7.08 (m, 6H), 6.93 (d, *J* = 2.1 Hz, 1H), 6.89 – 6.81 (m, 2H), 5.84 (d, *J* = 1.3 Hz, 1H), 5.43 (t, *J* = 9.1 Hz, 1H), 5.36 (t, *J* = 9.5 Hz, 1H), 5.07 (d, *J* = 7.4 Hz, 1H), 5.05 (d, *J* = 3.5 Hz, 1H), 4.56 (dd, *J* = 10.7, 7.0 Hz, 1H), 4.18 (t, *J* = 7.3 Hz, 1H), 4.11 (dd, *J* = 10.6, 5.4 Hz, 1H), 4.06 – 3.96

(m, 2H), 3.75 – 3.70 (m, 2H), 3.68 (dd, J = 11.6, 4.3 Hz, 1H), 3.46 – 3.34 (m, 2H), 1.86 (s, 3H), 1.72 (s, 3H), 1.65 (s, 3H), 1.55 (d, J = 1.3 Hz, 3H), 1.43 (s, 3H), 1.15 (s, 3H), 1.13 (s, 9H), 1.12 (s, 3H). ^{13}C NMR (101 MHz, $CDCl_3$) δ 170.1, 169.7, 160.9, 159.1, 155.0, 152.2, 135.7, 135.6, 133.1, 132.9, 129.8, 129.8, 127.8, 127.7, 125.8, 115.3, 113.5, 113.3, 111.6, 104.6, 99.6, 99.4, 98.0, 78.2, 75.9, 75.3, 75.1, 73.4, 71.0, 68.6, 66.0, 63.2, 62.3, 29.0, 27.0, 26.7, 25.5, 21.0, 20.8, 19.3, 19.0, 18.8. HRMS (ESI) m/z calculated for $C_{48}H_{58}O_{15}Si[M+NH_4]^+$: 920.3883; found: 920.3862.



Methyl 6-*O*-*tert*-butyldiphenylsilyl-3-*O*-(2'-*O*-(2'',3'':4'',6''-di-*O*-isopropylidene-β-D-mannopyranosyl)-6′-*O*-*tert*-butyldiphenylsilyl-β-D-glucopyranosyl)-α-D-mannopyranoside (1,2)-5m was synthesized according to general procedure B.

Materials: Methyl 6-*O*-*tert*-butyldiphenylsilyl-3-*O*-(6′-*O*-*tert*-butyldiphenylsilyl-β-D-glucopyranosyl)-α-D-mannopyranoside **5m** (83.3 mg, 0.1 mmol, 1 equiv), Catalyst **1** (11.5 mg, 0.01 mmol, 0.1 equiv.), activated 4 Å molecular sieves (0.3 g), and a solution of mannosyl phosphate (49.2 mg, 0.1 mmol, 1 equiv.) in 3 mL anhydrous diisopropyl ether.

Temperature and reaction time: 50 ˚C, 24 hours

Site selectivity: 14:1, 1,2-product:1,3-product

Purification conditions and yield: The reaction mixture was concentrated under reduced pressure and purified by column chromatography (10% EtOAc/hexanes to 80% EtOAc /hexanes) on 10 g silica gel to give the acylated product in 71% yield over two steps (76.3 mg, 0.071 mmol) as a white solid.

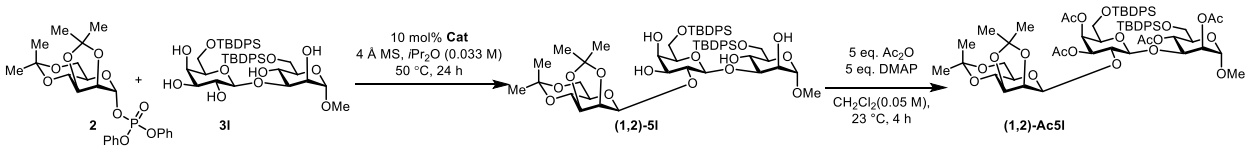
Unacylated (1,2)-product: ^{1}H NMR (400 MHz, $CDCl_3$) δ 7.77 – 7.63 (m, 8H), 7.48 – 7.30 (m, 12H), **5.19 (d, *J* = 3.1 Hz, 1H, Man(donor)-H-1'')**, **4.79 (d, *J* = 1.4 Hz, 1H, Man(acceptor)-H-1)**, **4.51 (d, *J* = 7.7 Hz, 1H, Glu(acceptor)-H-1')**, 4.38 (dd, *J* = 6.7, 3.2 Hz, 1H), 4.22 – 4.14 (m, 1H), 4.06 – 3.96 (m, 4H), 3.93 – 3.86 (m, 3H), 3.85 – 3.74 (m, 3H), 3.74 – 3.60 (m, 4H), 3.48 – 3.41 (m, 3H), 3.39 (s, 3H), 3.31 (td, *J* = 10.3, 5.5 Hz, 1H), 3.13 (s, 1H), 3.07 (s, 1H), 1.59 (s, 3H), 1.53 (s, 3H), 1.43 (s, 3H), 1.39 (s, 3H), 1.06 (s, 9H), 1.05 (s, 9H). ^{13}C NMR (101 MHz, $CDCl_3$) δ 135.8, 135.7, 133.7, 133.7, 132.6, 132.6, 130.1, 130.1, 129.6, 129.6, 128.0, 128.0, 127.7, 111.0, 100.5, 100.4, 99.9, 82.5, 82.1, 76.3, 76.0, 74.7, 73.8, 72.8, 71.9, 71.4, 68.7, 66.5, 66.2, 64.4, 64.3, 62.4, 54.6, 29.0, 27.1, 26.9, 25.4, 19.4, 19.2, 19.1. HRMS (ESI) m/z calculated for $C_{57}H_{78}O_{16}Si_2[M+NH_4]^+$: 1092.5167; found: 1092.5149.

Unacylated (1,3)-product: ^{1}H NMR (400 MHz, $CDCl_3$) δ 5.04 (d, *J* = 3.0 Hz, 1H), 4.74 (d, *J* = 1.5 Hz, 1H).

Acylation was performed following General Procedure C. The crude mixture was purified by column chromatography (5% Et_2O/hexanes to 55% Et_2O/hexanes) on 10 g silica gel.

Acylated (1,2)-product: ^{1}H NMR (400 MHz, $CDCl_3$) δ 7.71 – 7.65 (m, 8H), 7.46 – 7.32 (m, 12H), 5.29 – 5.18 (m, 3H), 5.16 (d, *J* = 2.6 Hz, 1H), 5.08 (dd, *J* = 8.8, 7.1 Hz, 1H), 4.79 (d, *J* = 1.8 Hz, 1H), 4.71 (d, *J* = 6.1 Hz, 1H), 4.51 (dd, *J* = 9.9, 3.4 Hz, 1H), 4.21 – 4.09 (m, 3H), 3.91 (dd, *J* = 10.8, 5.4 Hz, 1H), 3.81 – 3.70 (m, 5H), 3.70 – 3.61 (m, 3H), 3.32 – 3.24 (m, 4H), 2.13 (s, 3H), 2.03 (s, 3H), 1.89 (s, 3H), 1.88 (s, 3H), 1.54 (s, 3H), 1.51 (s, 3H), 1.40 (s, 3H), 1.33 (s, 3H), 1.06 (s, 18H). ^{13}C NMR (101 MHz, $CDCl_3$) δ 170.7, 170.3, 169.8, 169.6, 135.9, 135.8, 135.8, 135.8, 133.5, 133.4, 133.1, 129.9, 129.8, 129.8, 127.9, 127.9, 127.8, 127.8, 111.1, 99.8, 98.2, 97.6, 97.2, 77.0, 76.3, 75.3, 74.0, 73.8, 71.7, 71.6, 71.4, 68.9, 68.1, 67.0, 66.3, 63.5, 62.9, 62.4, 54.9, 29.2,

27.2, 26.9, 26.9, 26.8, 25.8, 21.3, 21.1, 21.0, 20.8, 19.4, 19.4, 19.2. HRMS (ESI) m/z calculated for $C_{65}H_{86}O_{20}Si_2[M+NH_4]^+$: 1260.5589; found: 1260.5566.



Methyl 6-*O*-*tert*-butyldiphenylsilyl-3-*O*-(2'-*O*-(2'',3'':4'',6''-di-*O*-isopropylidene-β-D-mannopyranosyl)-6′-*O*-*tert*-butyldiphenylsilyl-β-D-galactopyranosyl)-α-D-mannopyranoside (1,2)-5l was synthesized according to general procedure B.

Materials: Methyl 6-*O*-*tert*-butyldiphenylsilyl-3-*O*-(6′-*O*-*tert*-butyldiphenylsilyl-β-D-galactopyranosyl)-α-D-mannopyranoside **5l** (83.3 mg, 0.1 mmol, 1 equiv), Catalyst **1** (11.5 mg, 0.01 mmol, 0.1 equiv.), activated 4 Å molecular sieves (0.3 g), and a solution of mannosyl phosphate (49.2 mg, 0.1 mmol, 1 equiv.) in 3 mL anhydrous diisopropyl ether.

Temperature and reaction time: 50 ˚C, 24 hours

Site selectivity: 15:1, 1,2-product:1,3-product

Purification conditions and yield: The reaction mixture was concentrated under reduced pressure and purified by column chromatography (10% EtOAc/hexanes to 80% EtOAc /hexanes) on 10 g silica gel to give the acylated product in 64% yield over two steps (68.8 mg, 0.064 mmol) as a white solid.

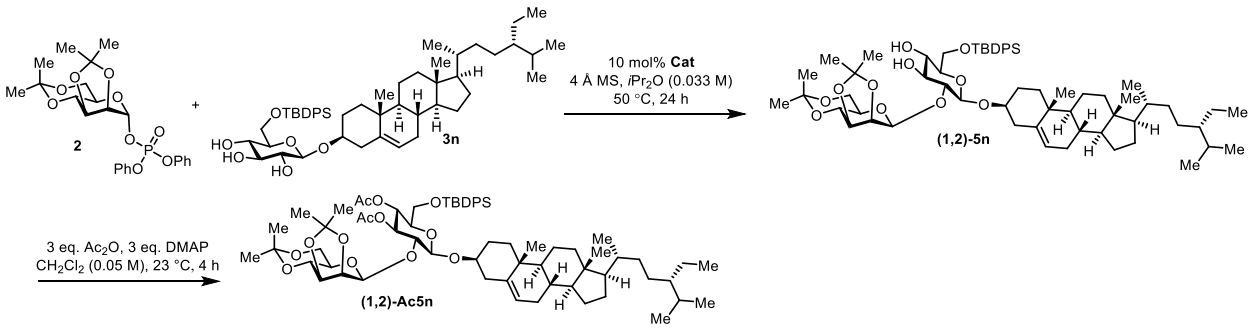
Unacylated (1,2)-product: ^{1}H NMR (400 MHz, $CDCl_3$) δ 7.76 – 7.62 (m, 8H), 7.48 – 7.29 (m, 12H), 5.18 (d, *J* = 3.2 Hz, 1H), 4.79 (d, *J* = 1.0 Hz, 1H), 4.47 – 4.42 (m, 1H), 4.39 (dd, *J* = 6.8, 3.2 Hz, 1H), 4.20 – 4.13 (m, 1H), 4.07 (s, 1H), 4.05 – 3.95 (m, 4H), 3.93 – 3.85 (m, 3H), 3.83 – 3.75 (m, 3H), 3.74 – 3.67 (m, 3H), 3.60 – 3.44 (m, 3H), 3.40 (s, 3H), 3.30 (td, *J* = 10.2, 5.4 Hz, 1H),

3.08 (s, 1H), 2.86 (s, 1H), 1.60 (s, 3H), 1.53 (s, 3H), 1.43 (s, 3H), 1.39 (s, 3H), 1.05 (s, 9H), 1.05 (s, 9H). ^{13}C NMR (101 MHz, $CDCl_3$) δ 135.8, 135.7, 135.6, 133.8, 133.7, 132.8, 132.7, 130.1, 129.6, 128.0, 128.0, 127.7, 111.0, 101.0, 100.6, 100.6, 99.9, 82.3, 81.4, 76.0, 74.4, 73.9, 73.4, 72.9, 71.4, 68.7, 68.7, 66.5, 66.0, 64.2, 63.0, 62.4, 54.6, 29.1, 27.1, 26.9, 25.4, 19.4, 19.2, 19.1. HRMS (ESI) m/z calculated for $C_{57}H_{78}O_{16}Si_2[M+NH_4]^+$: 1092.5167; found: 1092.5148.

Unacylated (1,3)-product: ^{1}H NMR (400 MHz, $CDCl_3$) δ 5.08 (d, J = 3.7 Hz, 1H)

Acylation was performed following General Procedure C. The crude mixture was purified by column chromatography (5% Et_2O/hexanes to 55% Et_2O/hexanes) on 10 g silica gel.

Acylated (1,2)-product: ^{1}H NMR (400 MHz, $CDCl_3$) δ 7.69 – 7.63 (m, 4H), 7.61 – 7.57 (m, 4H), 7.46 – 7.32 (m, 12H), 5.54 (d, J = 3.0 Hz, 1H), 5.32 (dd, J = 3.2, 1.8 Hz, 1H), 5.26 (t, J = 9.9 Hz, 1H), 5.04 – 4.98 (m, 2H), 4.78 (d, J = 1.7 Hz, 1H), 4.47 (d, J = 7.6 Hz, 1H), 4.22 (dd, J = 9.8, 3.3 Hz, 1H), 4.16 (dd, J = 5.9, 2.4 Hz, 1H), 4.11 – 4.06 (m, 1H), 4.02 (dd, J = 10.1, 7.5 Hz, 1H), 3.92 (dd, J = 10.3, 7.6 Hz, 1H), 3.82 (dd, J = 10.6, 5.4 Hz, 1H), 3.75 – 3.69 (m, 2H), 3.69 – 3.59 (m, 5H), 3.35 (s, 3H), 3.15 (td, J = 10.1, 5.5 Hz, 1H), 2.10 (s, 3H), 2.01 (s, 3H), 1.96 (s, 3H), 1.62 (s, 3H), 1.59 (s, 3H), 1.58 (s, 3H), 1.40 (s, 3H), 1.36 (s, 3H), 1.03 (s, 9H), 1.02 (s, 9H). ^{13}C NMR (101 MHz, $CDCl_3$) δ 170.8, 170.0, 169.8, 169.2, 135.9, 135.7, 135.7, 133.5, 133.4, 133.0, 132.7, 130.1, 130.0, 129.7, 127.9, 127.9, 127.7, 127.7, 111.1, 102.8 ($^1J_{C\text{-}H}$ = 158.6 Hz), 99.9, 98.4 ($^1J_{C\text{-}H}$ = 163.7 Hz), 98.0 ($^1J_{C\text{-}H}$ = 171.4 Hz), 76.2, 74.4, 73.9, 73.8, 73.3, 71.7, 71.5, 70.8, 68.0, 67.2, 66.5, 63.2, 62.2, 60.8, 54.9, 29.2, 27.4, 26.8, 26.4, 21.4, 21.1, 20.8, 20.7, 19.3, 19.1. HRMS (ESI) m/z calculated for $C_{65}H_{86}O_{20}Si_2[M+NH_4]^+$: 1260.5589; found: 1260.5562.



2,3:4,6-di-*O*-isopropylidene-β-D-mannopyranosyl-daucosterol (1,2)-5n was synthesized according to general procedure B.

Materials: TBDPS-daucosterol **3n** (81.5 mg, 0.1 mmol, 1 equiv), Catalyst **1** (11.5 mg, 0.01 mmol, 0.1 equiv.), activated 4 Å molecular sieves (0.3 g), and a solution of mannosyl phosphate (49.2 mg, 0.1 mmol, 1 equiv.) in 3 mL anhydrous diisopropyl ether.

Temperature and reaction time: 50 ˚C, 24 hours

Site selectivity: 7:1, 1,2-product:1,3-product

Purification conditions and yield: The reaction mixture was concentrated under reduced pressure and purified by column chromatography (10% EtOAc/hexanes to 60% EtOAc /hexanes) on 10 g silica gel to give the acylated product in 60% yield over two steps (63.2 mg, 0.060 mmol) as a white solid.

Unacylated (1,2)-product (impurities from commercial daucosterol could not be removed.): ^{1}H NMR (400 MHz, $CDCl_3$) δ 7.73 – 7.66 (m, 4H), 7.46 – 7.34 (m, 6H), 5.32 (d, *J* = 5.1 Hz, 1H), 5.20 (d, *J* = 3.4 Hz, 1H), 4.54 (d, *J* = 7.6 Hz, 1H), 4.36 (dd, *J* = 6.8, 3.3 Hz, 1H), 4.28 – 4.18 (m, 2H), 4.00 – 3.90 (m, 2H), 3.90 – 3.79 (m, 2H), 3.66 – 3.54 (m, 3H), 3.46 – 3.40 (m, 1H), 3.36 (td, *J* = 10.0, 5.4 Hz, 1H), 3.29 (t, *J* = 8.1 Hz, 1H), 2.98 (br, 1H), 2.42 (ddd, *J* = 13.3, 4.9, 2.2 Hz, 1H), 2.36 – 2.24 (m, 1H), 2.06 – 1.93 (m, 3H), 1.89 – 1.77 (m, 2H), 1.70 – 0.97 (m, 45H), 0.95 – 0.89

(m, 4H), 0.89 – 0.76 (m, 9H), 0.69 (d, J = 7.4 Hz, 3H). ^{13}C NMR (101 MHz, $CDCl_3$) δ 140.4, 135.7, 135.7, 133.2, 133.2, 129.9, 127.8, 127.8, 122.1, 111.1, 99.8, 99.7, 99.6, 83.1, 79.0, 75.9, 75.2, 73.3, 71.2, 66.1, 64.6, 63.3, 56.9, 56.2, 50.3, 45.9, 42.4, 39.9, 39.0, 37.3, 36.9, 36.3, 34.1, 32.1, 32.0, 29.9, 29.3, 29.1, 28.4, 26.9, 26.8, 26.2, 25.2, 24.4, 23.2, 21.2, 20.0, 19.5, 19.4, 19.3, 19.2, 18.9, 12.1, 12.0. HRMS (ESI) m/z calculated for $C_{63}H_{96}O_{11}Si[M+Na]^+$: 1079.6614; found: 1079.6591.

Unacylated (1,3)-product: ^{1}H NMR (400 MHz, $CDCl_3$) δ 5.07 (d, J = 3.0 Hz, 1H).

Acylation was performed following General Procedure C. The crude mixture was purified by column chromatography (5% Et_2O/hexanes to 55% Et_2O/hexanes) on 10 g silica gel.

Acylated (1,2)-product: ^{1}H NMR (400 MHz, $CDCl_3$) δ 7.68 – 7.62 (m, 4H), 7.44 – 7.33 (m, 6H), 5.33 (d, J = 5.1 Hz, 1H), 5.19 – 5.09 (m, 2H), 4.98 (t, J = 9.7 Hz, 1H), 4.62 (d, J = 7.6 Hz, 1H), 4.23 – 4.10 (m, 3H), 3.95 (dd, J = 10.8, 5.4 Hz, 1H), 3.85 (t, J = 10.5 Hz, 1H), 3.74 – 3.63 (m, 4H), 3.56 (ddd, J = 9.8, 4.4, 3.1 Hz, 1H), 3.30 (td, J = 10.0, 5.4 Hz, 1H), 2.43 (ddd, J = 13.1, 4.5, 1.9 Hz, 1H), 2.38 – 2.28 (m, 1H), 2.07 – 1.93 (m, 7H), 1.92 – 1.80 (m, 5H), 1.74 – 1.06 (m, 22H), 1.05 – 0.99 (m, 14H), 0.95 – 0.88 (m, 4H), 0.88 – 0.76 (m, 9H), 0.69 (d, J = 7.3 Hz, 3H). ^{13}C NMR (101 MHz, $CDCl_3$) δ 170.1, 169.8, 140.4, 135.8, 135.7, 133.3, 133.3, 129.9, 129.8, 127.8, 127.8, 122.3, 111.1, 99.9, 99.7, 99.1, 79.1, 79.0, 76.1, 75.3, 74.4, 73.8, 71.5, 69.4, 66.2, 63.2, 62.9, 56.9, 56.2, 50.3, 46.0, 42.5, 39.9, 38.8, 37.4, 36.9, 36.3, 32.1, 32.0, 29.9, 29.3, 29.1, 27.3, 26.8, 26.2, 25.8, 24.4, 23.2, 21.2, 21.1, 20.8, 20.0, 19.7, 19.6, 19.3, 19.2, 18.9. HRMS (ESI) m/z calculated for $C_{67}H_{100}O_{13}Si[M+Na]^+$: 1163.6825; found: 1163.6794.

3.8.10 Michaelis-Menten Kinetics

Preparation of Materials for Kinetic Experiments

Phosphate solution: To a 1 dram vial was added galactosyl phosphate (46.8 mg, 0.1 mmol), naphthalene (6.4 mg, 0.05 mmol), and 0.5 mL anhydrous diisopropyl ether.

Catalyst solution: To a 0.5 dram vial was added catalyst (0.01 mmol) and 0.5 mL diisopropyl ether.

Acceptor solution 1: To a 1 dram vial was added methyl 6-*O*-(*tert*-butyldiphenylsilyl)-β-D-glucopyranoside (43.3 mg, 0.1 mmol) and 1 mL diisopropyl ether.

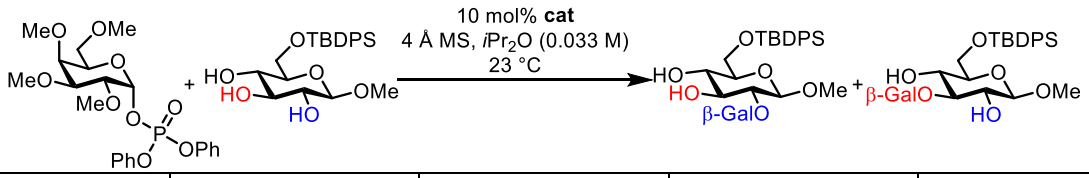
Acceptor solution 2: To a 1 dram vial was added methyl 6-*O*-(*tert*-butyldiphenylsilyl)-β-D-glucopyranoside (10.8 mg, 0.025 mmol) and 1 mL diisopropyl ether.

Kinetic Run Setup and Data Acquisition

Due to the heterogeneity and relatively slow nature of the reaction, we decided to monitor the reaction via initial rate quench kinetics, in which the reaction was aliquoted at time points and diluted into $CDCl_3$, which stopped the reaction. ^1H NMR analysis of the same sample on the same day and two days after sample collection showed no change in phosphate concentration.

To a 0.5 dram vial equipped with a stir bar and PTFE cap was added 4 Å molecular sieves (30 mg), anhydrous diisopropyl ether (amount specified in table below), acceptor solution (amount specified in table below), phosphate solution (50 μL), and catalyst solution (50 μL). The reaction was stirred at 23 °C. The PTFE cap of the 0.5 dram vial was punctured with a 25 μL glass syringe, and 20 μL of solution was removed and immediately injected into a new 0.5 dram vial containing 600 μL of $CDCl_3$. The mixture was pushed through a syringe filter into an NMR tube. The sample was analyzed by ^1H NMR analysis with 12 scans and 10 seconds of relaxation delay. We measured conversion by monitoring the disappearance of anomeric proton of galactosyl phosphate at 6.05 ppm and integrating it relative to a peak of naphthalene at 7.83 ppm as the internal standard. Peaks

were chosen because they were the cleanest and far away from the region where peaks corresponding diisopropyl ether appear. Below is a representative example of the NMR kinetics time course, with the following time points 10, 20, 30, 40 minutes (from bottom to top):



Equiv. of acceptor	Phosphate solution (μL)	Acceptor solution 1 (μL)	Catalyst solution (μL)	*i*Pr$_2$O (μL)
0.125	50	12.5	50	187.5
0.25	50	25	50	175
0.5	50	50	50	150
0.75	50	75	50	125
1	50	100	50	100
1.25	50	125	50	75
1.5	50	150	50	50
1.75	50	175	50	25
2	50	200	50	0
Equiv. of acceptor	Phosphate solution (μL)	Acceptor solution 2 (μL)	Catalyst solution (μL)	*i*Pr$_2$O (μL)
0.06	50	24	50	176
0.19	50	76	50	124
0.38	50	152	50	48

Table 3.1 Materials used for different kinetic experiments. Galactosyl phosphate (0.01 mmol), methyl 6-*O*-(*tert*-butyldiphenylsilyl)-β-D-glucopyranoside (0.0006–0.02 mmol), catalyst (0.001 mmol), and diisopropyl ether (0.3 mL).

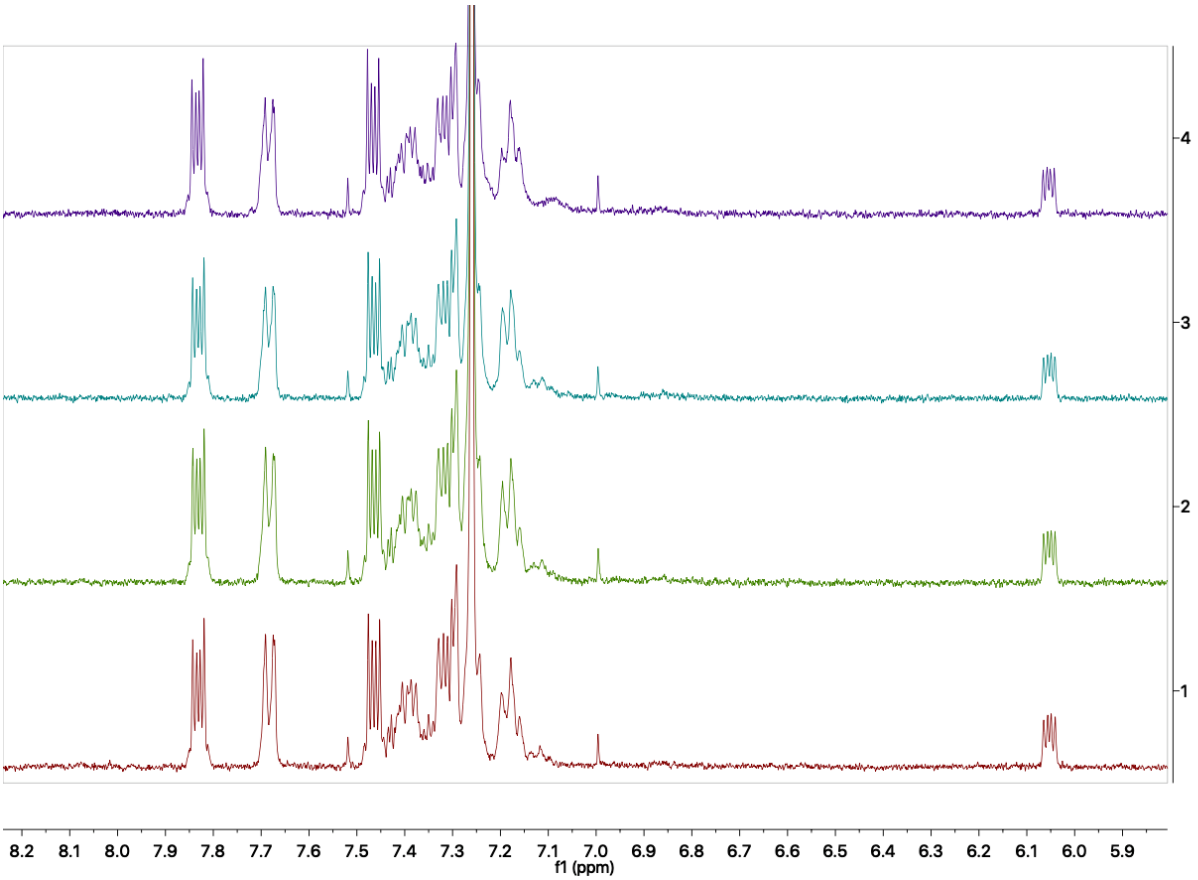
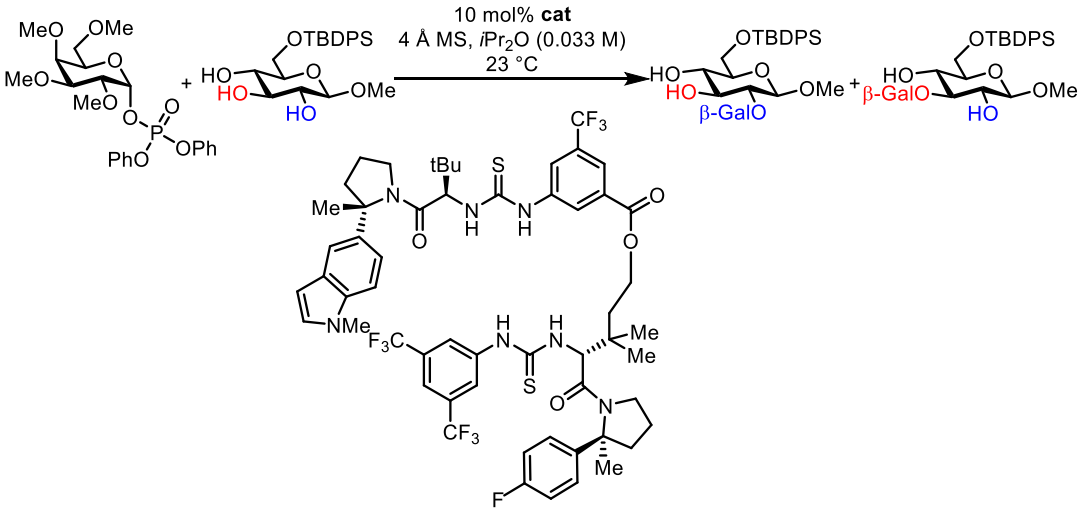


Figure 3.23 Representative ^{1}H NMR traces for kinetic data analysis.

Initial Rates Data



Time (hour)	[Phosphate] (M)		Time (hour)	[Phosphate] (M)
0.06 equiv. acceptor			0.75 equiv. acceptor	
0.13333333	0.02672669		0.16666667	0.02741837
0.26666667	0.02641349		0.33333333	0.02610309
0.4	0.02610754		0.5	0.02544582

0.53333333	0.02561308		0.66666667	0.02414313
0.19 equiv. acceptor			0.16666667	0.0266313
0.13333333	0.02641349		0.33333333	0.02493567
0.26666667	0.02523079		0.5	0.02311745
0.4	0.02458856		0.66666667	0.02234169
0.53333333	0.02432321		1 equiv. acceptor	
0.13333333	0.0258086		0.16666667	0.02619977
0.26666667	0.025137		0.33333333	0.02389844
0.4	0.02449947		0.5	0.02296733
0.53333333	0.0239782		0.66666667	0.02183314
0.38 equiv. acceptor			0.16666667	0.025508905
0.13333333	0.02561308		0.33333333	0.023525881
0.26666667	0.02441102		0.5	0.022492649
0.4	0.02380934		1.25 equiv. acceptor	
0.53333333	0.02331673		0.08333333	0.02641994
0.13333333	0.02532529		0.16666667	0.02521903
0.26666667	0.02414947		0.25	0.02429863
0.4	0.02323661		0.33333333	0.02386317
0.53333333	0.02276718		0.08333333	0.02699976
0.125 equiv. acceptor			0.16666667	0.02572341
0.16666667	0.0273125		0.25	0.02490823
0.33333333	0.02639529		0.33333333	0.02414313
0.66666667	0.02591186		1.5 equiv. acceptor	
0.16666667	0.02728616		0.08333333	0.02649415
0.5	0.02610911		0.16666667	0.02544582
0.66666667	0.02502941		0.25	0.0244773
0.25 equiv. acceptor			0.33333333	0.02397945
0.16666667	0.02741837		0.08333333	0.02621191
0.33333333	0.02610309		0.16666667	0.02541154
0.5	0.02544582		0.25	0.02484263
0.66666667	0.02414313		0.33333333	0.02369332
0.16666667	0.02717479		1.75 equiv. acceptor	
0.33333333	0.02570589		0.08333333	0.02590593
0.5	0.02550891		0.16666667	0.02541154
0.66666667	0.02493567		0.25	0.02421027
0.5 equiv. acceptor			0.33333333	0.02352588
0.16666667	0.0266313		0.08333333	0.02610309
0.33333333	0.02465861		0.16666667	0.02517416
0.5	0.02377794		0.25	0.02456229
0.16666667	0.02669411		0.33333333	0.02326953
0.33333333	0.02591186		2 equiv. acceptor	
0.5	0.02406101		0.08333333	0.02669411
			0.16666667	0.02544582
0.06 equiv. acceptor			0.25	0.02482084
0.13333333	0.02672669		0.33333333	0.02350146

0.26666667	0.026310711		2 equiv. acceptor	
0.4	0.026007126		0.08333333	0.025705885
0.53333333	0.02561308		0.16666667	0.025123865
			0.25	0.024035467
			0.33333333	0.022800768

Table 3.2 Galactosyl phosphate concentration at different time points with different loading of acceptor.

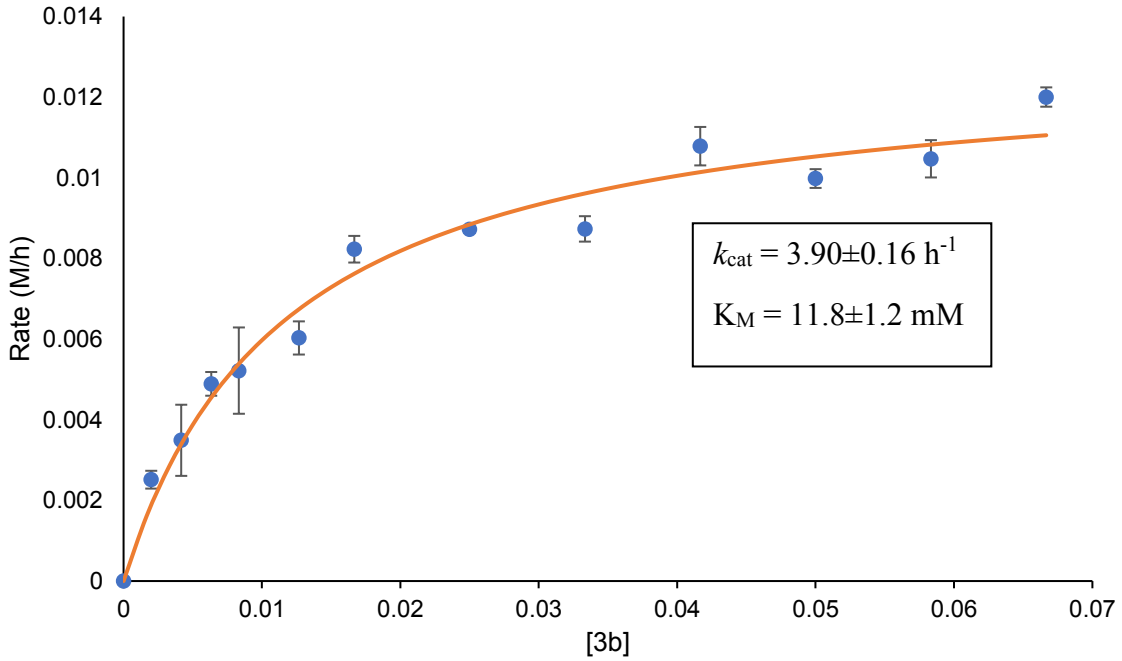
Acceptor concentration (M)	Initial Rate (M/h)	Acceptor concentration (M)	Initial Rate (M/h)
0	0 (Run 1&2)	0.025	0.00863384 (Run 1)
0.002	0.00273509 (Run 2)	0.025	0.00881222 (Run 2)
0.00416667	0.00260828 (Run 1)	0.03333333	0.0084186 (Run 1)
0.00416667	0.00437317 (Run 2)	0.03333333	0.00904877 (Run 2)
0.00633333	0.0051848 (Run 1)	0.04166667	0.01126208 (Run 1)
0.00633333	0.00459654 (Run 2)	0.04166667	0.01030885 (Run 2)
0.00833333	0.00628978 (Run 1)	0.05	0.01021515 (Run 1)
0.00833333	0.00414861 (Run 2)	0.05	0.00974959 (Run 2)
0.01266667	0.00561804 (Run 1)	0.05833333	0.01093506 (Run 1)
0.01266667	0.0064404 (Run 2)	0.05833333	0.01000971 (Run 2)
0.01666667	0.00789928 (Run 1)	0.06666667	0.01224352 (Run 1)
0.01666667	0.00856006 (Run 2)	0.06666667	0.011764 (Run 2)
0.002	0.002293397 (Run 1)		

Table 3.3 Initial rates of reactions catalyzed by 5-NMeindole-bis-thiourea with different loading of acceptor.

The above initial rates were fitted to the Michaelis-Menten equation ($Rate = \frac{V_{max} * [acceptor]}{K_M + [acceptor]}$). The fitted parameters were shown below.

	V_{max} ($M \cdot h^{-1}$)	k_{cat} (h^{-1})	K_M (mM)
Run 1	0.01352985	4.058955	12.97187
Run 2	0.01248956	3.746868	10.59028

The average of two runs was reported in the plot shown below.



Galactosyl phosphate does not undergo a measurable background reaction or side reaction such as hydrolysis; therefore, k_{cat} is a sum of the rate constants corresponding to the (1,2)- and (1,3)-pathway.

$$k_{cat} = k_{cat_{1,2}} + k_{cat_{1,3}}$$

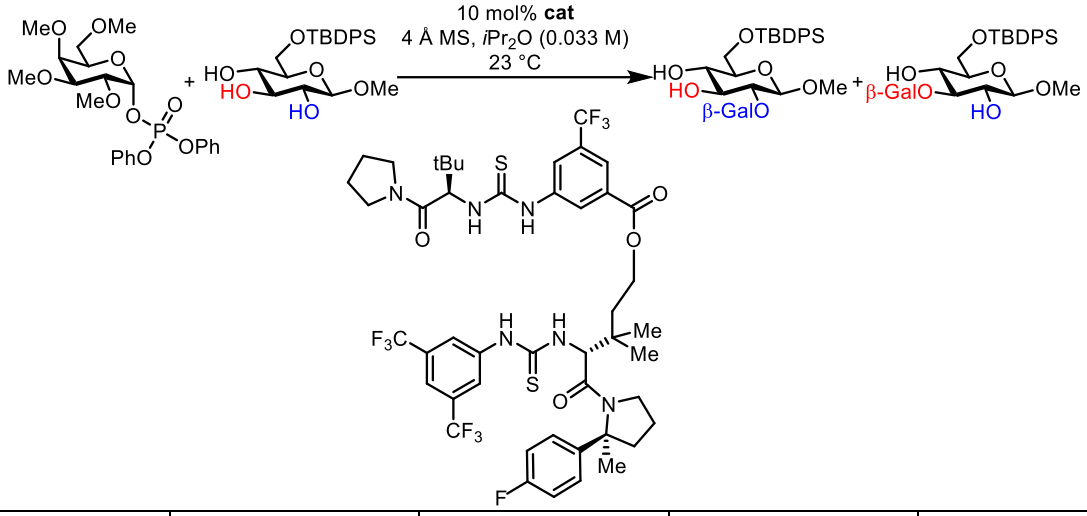
$$regioisomeric\ ratio\ (r.r.) = e^{\frac{-\left(\Delta G^{\ddagger}_{1,2} - \Delta G^{\ddagger}_{1,3}\right)}{RT}}$$

$$\frac{k_{cat_{1,2}}}{k_{cat_{1,3}}} = \frac{e^{-\frac{\Delta G^{\ddagger}_{1,2}}{RT}}}{e^{-\frac{\Delta G^{\ddagger}_{1,3}}{RT}}} = e^{\frac{-\left(\Delta G^{\ddagger}_{1,2} - \Delta G^{\ddagger}_{1,3}\right)}{RT}} = e^{\frac{-\left(\Delta G^{\ddagger}_{1,2} - \Delta G^{\ddagger}_{1,3}\right)}{RT}} = r.r.$$

$$k_{cat_{1,2}} = k_{cat}\left(\frac{r.r.}{r.r.+1}\right)$$

$$k_{cat_{1,3}} = k_{cat}\left(\frac{1}{r.r.+1}\right)$$

	r.r. (1,2:1,3)	k_{cat} (h^{-1})	$k_{cat_1,2}$ (h^{-1})	$k_{cat_1,3}$ (h^{-1})	$k_{cat_1,2}$ (h^{-1})_ average	$k_{cat_1,3}$ (h^{-1}) _average
Run 1	9	4.058955	3.6530595	0.4058955	3.51±0.14	0.39±0.02
Run 2	9	3.746868	3.3721812	0.3746868		



Time (hour)	[Phosphate] (M)		Time (hour)	[Phosphate] (M)
0.125 equiv. acceptor			0.75 equiv. acceptor	
0.25	0.02959033		0.25	0.02797405
0.5	0.02869752		0.5	0.02600713
0.75	0.02833117		0.75	0.02465861
1	0.02739845		1	0.02403547
0.25	0.02771251		0.25	0.02693965
0.5	0.02726554		0.5	0.02485975
0.75	0.02693965		0.75	0.02364284
1	0.02672669		1	0.02261489
0.19 equiv. acceptor			1 equiv. acceptor	
0.16666667	0.0275994		0.25	0.02717479
0.33333333	0.02704741		0.5	0.02590593
0.5	0.02662147		0.75	0.02429863
0.66666667	0.02600713		0.25	0.02651707
0.16666667	0.0275994		0.5	0.0239782
0.33333333	0.02715604		0.75	0.02269078
0.5	0.02651707		1	0.02239024
0.66666667	0.02590748		1.25 equiv. acceptor	
0.38 equiv. acceptor			0.16666667	0.02631071
0.16666667	0.02704741		0.33333333	0.02523079
0.33333333	0.02600713		0.5	0.0239782
0.5	0.02561308		0.66666667	0.02331673
0.66666667	0.0250439		1.5 equiv. acceptor	
0.16666667	0.02662147		0.16666667	0.02774093
0.33333333	0.02600713		0.33333333	0.02621191
0.5	0.0254205		0.5	0.02590593
0.66666667	0.02476869		0.66666667	0.02403547
0.25 equiv. acceptor			0.16666667	0.02662147
0.25	0.02932962		0.33333333	0.0254205
0.5	0.02869752		0.5	0.02432321

0.75	0.02785701		0.66666667	0.02292153
1	0.02717479		1.75 equiv. acceptor	
0.25	0.0275994		0.16666667	0.02739845
0.5	0.02662147		0.33333333	0.0266313
0.75	0.02600713		0.5	0.02475028
1	0.02532529		0.66666667	0.0244773
0.5 equiv. acceptor			0.16666667	0.02631071
0.25	0.02728616		0.33333333	0.02406353
0.5	0.02673825		0.5	0.02441102
0.75	0.02590593		0.66666667	0.02261489
1	0.02475028		2 equiv. acceptor	
0.25	0.02704741		0.16666667	0.02762583
0.5	0.02551643		0.33333333	0.02631551
0.75	0.02458856		0.5	0.02502941
1	0.02364284		0.66666667	0.02412255
1.25 equiv. acceptor			0.16666667	0.02662147
0.16666667	0.02651707		0.33333333	0.02449947
0.33333333	0.025325291		0.5	0.02356046
0.5	0.024063533		0.66666667	0.0228441
0.66666667	0.023236607			

Table 3.4 Galactosyl phosphate concentration at different time points with different loading of acceptor.

Acceptor concentration (M)	Initial Rate (M/h)	Acceptor concentration (M)	Initial Rate (M/h)
0	0 (Run 1&2)	0.025	0.00567648 (Run 2)
0.00416667	0.00277679 (Run 1)	0.03333333	0.00575233 (Run 1)
0.00416667	0.00131334 (Run 2)	0.03333333	0.00546716 (Run 2)
0.00633333	0.00342883 (Run 2)	0.04166667	0.00614072 (Run 2)
0.00633333	0.00312166 (Run 1)	0.05	0.00685343 (Run 1)
0.00833333	0.002922 (Run 1)	0.05	0.00731825 (Run 2)
0.00833333	0.00297467 (Run 2)	0.05833333	0.0063867 (Run 1)
0.01266667	0.00384275 (Run 2)	0.05833333	0.00644398 (Run 2)
0.01266667	0.00368697 (Run 1)	0.06666667	0.00707755 (Run 1)
0.01666667	0.00337599 (Run 1)	0.06666667	0.00736267 (Run 2)
0.01666667	0.00445663 (Run 2)	0.04166667	0.006661887 (Run 1)
0.025	0.00526571 (Run 1)		

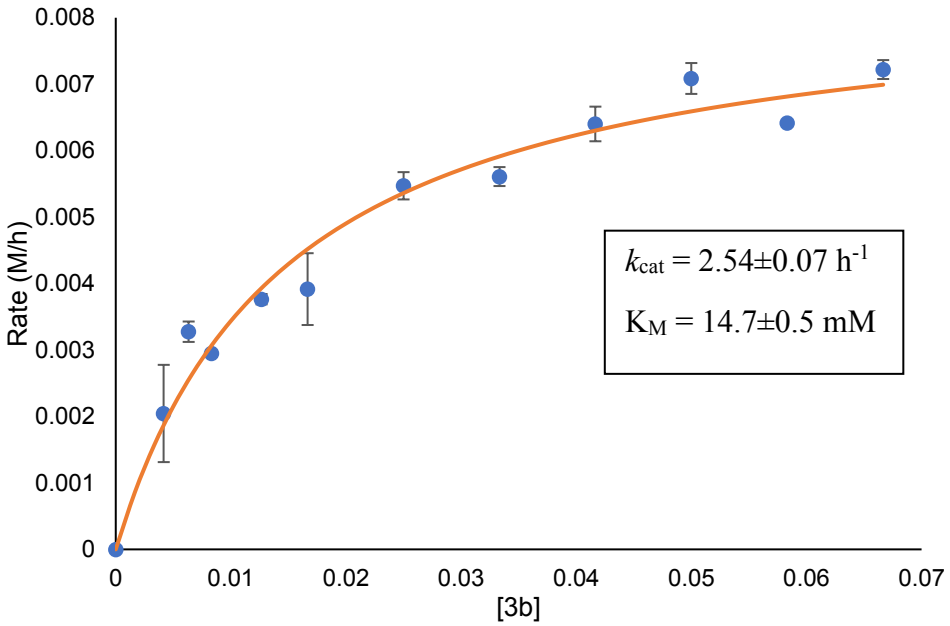
Table 3.5 Initial rates of reactions catalyzed by pyrrolidine-bis-thiourea with different loading of acceptor.

The above initial rates were fitted to the Michaelis-Menten equation ($Rate = \frac{V_{max}*[acceptor]}{K_M+[acceptor]}$). The fitted parameters were shown below.

	Vmax ($M \cdot h^{-1}$)	k_{cat} (h^{-1})	K_M (mM)

Run 1	0.00840435	2.521305	14.5626
Run 2	0.00869982	2.609946	15.19533

The average of two runs was reported in the plot shown below.



Galactosyl phosphate does not undergo a measurable background reaction or side reaction such as hydrolysis; therefore, k_{cat} is a sum of the rate constants corresponding to the (1,2)- and (1,3)-pathway.

$$k_{cat} = k_{cat_{1,2}} + k_{cat_{1,3}}$$

$$regioisomeric\ ratio\ (r.r.) = e^{\frac{-\left(\Delta G^{\ddagger}_{1,2} - \Delta G^{\ddagger}_{1,3}\right)}{RT}}$$

$$\frac{k_{cat_{1,2}}}{k_{cat_{1,3}}} = \frac{e^{-\frac{\Delta G^{\ddagger}_{1,2}}{RT}}}{e^{-\frac{\Delta G^{\ddagger}_{1,3}}{RT}}} = e^{\frac{-\left(\Delta G^{\ddagger}_{1,2} - \Delta G^{\ddagger}_{1,3}\right)}{RT}} = e^{\frac{-\left(\Delta G^{\ddagger}_{1,2} - \Delta G^{\ddagger}_{1,3}\right)}{RT}} = r.r.$$

$$k_{cat_{1,2}} = k_{cat}\left(\frac{r.r.}{r.r.+1}\right)$$

$$k_{cat_{1,3}} = k_{cat}\left(\frac{1}{r.r.+1}\right)$$

	r.r. (1,2:1,3)	k_{cat} (h^{-1})	$k_{cat_1,2}$ (h^{-1})	$k_{cat_1,3}$ (h^{-1})	$k_{cat_1,2}$ (h^{-1})_ average	$k_{cat_1,3}$ (h^{-1}) _average
Run 1	2	2.521305	1.68087	0.840435	1.71±0.03	0.86±0.01
Run 2	2	2.609946	1.739964	0.869982		

3.8.11 Initial Rate Comparison between Polyols and Mono-protected Analogs

To a scintillation vial was charged nucleophile (0.03 mmol, 1.50 equiv.), *ent*-cat-1 (2 mg, 0.002 mmol, 0.1 equiv.), and 4 Å molecular sieves (60 mg). To this, a stock solution of **1** was added (0.02 mmol, 0.60 mL at 0.033 M), 2.5 μL mesitylene (internal standard), and a stir bar. The mixture was stirred at room temperature and 25 μL aliquots were taken every 10 minutes for 100 minutes. Each aliquot was diluted directly into 500 μL $CDCl_3$ and filtered. ^1H NMR spectra were obtained for each aliquot. We measured conversion by monitoring the disappearance of anomeric proton of galactosyl phosphate at 6.05 ppm and integrating it relative to the aromatic proton resonance of mesitylene. % yield = 1 – % conversion. Initial rates were calculated by fitting the data in Table 3.6 for the initial 10-20 % of the reaction.

Time (min)	**α-3a** (% yield)	**α-3,4-diBn-3a** (% yield)	**α-2,4-diBn-3a** (% yield)
0	0	0	0
10	11	3	1
20	22	9	1
30	33	11	2
40	39	15	6
50	45	15	7
60	53	15	7
70	54	22	7
80	60	22	9
90	53	25	11
100	65	26	10

Table 3.6 Kinetics for partially protected galactose derivatives, **α-3a**, **α-3,4-diBn-3a**, and **α-2,4-diBn-3a**.

3.8.12 Interaction Energy Calculation

Computational Methods

Calculations were performed using the Gaussian 16 program[31] on the Odyssey cluster supported by Harvard University's Faculty of Arts and Sciences Research Computing group. The geometries of all ground-state structures were fully optimized at the B97-D/TZV level of theory[32] with solvent correction. Interaction energies were computed at the B97-D/TZV level of theory using counterpoise corrections. A polarization continuum model was used with either diethyl ether as the solvent.[33] Default geometric and SCF convergence criteria were used. Stationary points were verified by harmonic frequency calculations. All molecular structures were rendered in CYLView.[34]

B97-D/TZV level of theory was selected because it has been previously applied to efficiently and accurately calculate interaction energies for prototypical CH/π interactions. The B97-D energies were found to be in good agreement with the CCSD(T) data by Wheelers and coworkers.[15]

Procedure for Geometric Optimization

β-Galactose and arenes were optimized independently at the B97-D/TZV level of theory with PCM (ether). The optimized galactose and arenes were subjected to constrained optimizations at the B97-D/TZV level of theory with PCM (ether) by fixing the coordinates of arenes to optimize the

[31] Gaussian 16, Revision A.03, M. J. Frisch, G. W. Trucks, H. B. Schlegel, G. E. Scuseria, M. A. Robb, J. R. Cheeseman, G. Scalmani, V. Barone, G. A. Petersson, H. Nakatsuji, X. Li, M. Caricato, A. V. Marenich, J. Bloino, B. G. Janesko, R. Gomperts, B. Mennucci, H. P. Hratchian, J. V. Ortiz, A. F. Izmaylov, J. L. Sonnenberg, D. Williams-Young, F. Ding, F. Lipparini, F. Egidi, J. Goings, B. Peng, A. Petrone, T. Henderson, D. Ranasinghe, V. G. Zakrzewski, J. Gao, N. Rega, G. Zheng, W. Liang, M. Hada, M. Ehara, K. Toyota, R. Fukuda, J. Hasegawa, M. Ishida, T. Nakajima, Y. Honda, O. Kitao, H. Nakai, T. Vreven, K. Throssell, J. A. Montgomery, Jr., J. E. Peralta, F. Ogliaro, M. J. Bearpark, J. J. Heyd, E. N. Brothers, K. N. Kudin, V. N. Staroverov, T. A. Keith, R. Kobayashi, J. Normand, K. Raghavachari, A. P. Rendell, J. C. Burant, S. S. Iyengar, J. Tomasi, M. Cossi, J. M. Millam, M. Klene, C. Adamo, R. Cammi, J. W. Ochterski, R. L. Martin, K. Morokuma, O. Farkas, J. B. Foresman, and D. J. Fox, Gaussian, Inc., Wallingford CT, 2016.

[32] (a) Grimme, S. Semiempirical GGA-type density functional constructed with a long-range dispersion correction. *J. Comput. Chem*. **2006**, *27*, 1787−1799. (b) Becke, A. Density-functional thermochemistry. V. Systematic optimization of exchange-correlation functionals. *J. Chem. Phys*. **1997**, *107*, 8554−8560.

[33] Scalmani, G.; Frisch, M. J. Continuous Surface Charge Polarizable Continuum Models of Solvation. I. General Formalism. *J. Chem. Phys*. **2010**, *132*, 114110–114115.

[34] C. Y. Legault, CYLview, 1.0b; Université de Sherbrooke, 2009 (http://www.cylview.org).

geometries of galactose-arene complexes. All other coordinates were permitted to optimize. Because several energy minima could be located, in order to be consistent across different galactose-arene complexes, galactose(H5)-arene complexes were selected for single point energy. Single point energy calculation with counterpoise corrections was performed to calculate the interaction energies of optimized galactose-arene complexes.

Validation of Computation Protocol

The magnitude of calculated interaction energies was in good agreement with energies reported in the literature. Although computation of the exactly same galactose-arene complexes has not been reported, the interaction energies of several other carbohydrate-arene complexes have been computed at various levels of theory. Tsuzuki and coworkers computed different β-fucose-arene complexes and found that the interaction energy of the most stable CH/π contact structure was –4.5, –4.9, and –6.5 kcal/mol (CCSD(T) interaction energy at the basis set limit) for β-fucose-benzene, β-fucose-phenol and β-fucose-indole complex, respectively.[13a] Hillier and coworkers computed different β-fucose-toluene complexes at DFT-D/TZV2D, and the interaction energies range from –5.83 to –7.88 kcal/mol.[13b] A similar analysis was performed on β-glucose-3-methylindole complexes (–9.2 to –10.9 kcal/mol). Koča and coworkers performed a three-dimensional potential energy surface scan for the β-glucose-benzene complex at the DFT-D BP/def2-TZVPP level of theory.[35] Three energy minima were located and corresponded to the interaction between benzene and C-H1 (–5.07 kcal/mol), C-H3 (–4.83 kcal/mol), and C-H5 (–5.41 kcal/mol). A similar trend was observed in our computation. The interaction energies computed at

[35] Kozmon, S.; Matuška, R.; Spiwok, V.; Koča, J. Three-dimensional potential energy surface of selected carbohydrates' CH/pi dispersion interactions calculated by high-level quantum mechanical methods. *Chemistry* **2011**, *17*, 5680–5690.

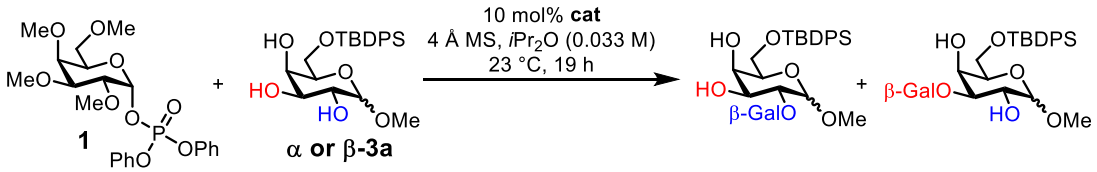
B97-D/TZV for different β-galactose-benzene complexes (benzene-H1, benzene-H3, and benzene-H5) were –5.83, –5.57, and –6.53 kcal/mol, respectively.

In order to further validate the predictability of B97-D/TZV level of theory in computing CH/π interactions between arenes and carbohydrates, we calculated interaction energies of carbohydrate-arene complexes that have been computed previously by Tsuzuki and co-workers, and the interaction energies at CCSD(T)/basis limit level of theory were reported by the authors.[13a] We then compared the energies obtained at B97-D/TZV level of theory to energies computed at CCSD(T)/basis limit (Table 3.7). An excellent correlation ($R^2 = 0.99$) was observed, suggesting that B97-D/TZV correctly predicted the relative stability of carbohydrate-arene complexes although B97-D/TZV consistently overestimated the absolute energy.

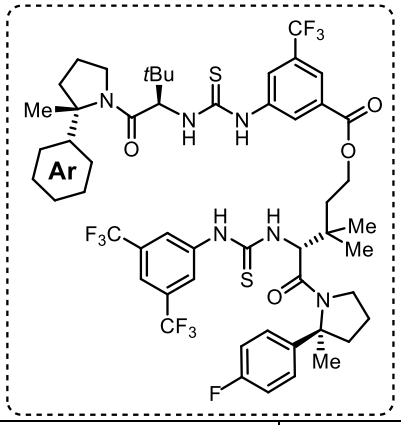
Carbohydrate-arene complex from Tsuzuki[20]	B97D/TZV (kcal/mol)	CCSD(T)/basis limit (kcal/mol)[20]	Carbohydrate-arene complex from Tsuzuki[20]	B97D/TZV (kcal/mol)	CCSD(T)/basis limit (kcal/mol)[20]
1a	-5.4	-5.114	1l	-12.72	-11.326
1b	-5.77	-5.324	2a	-7.49	-6.703
1c	-5.64	-5.188	2b	-7.31	-6.816
1d	-7.2	-6.451	2c	-7.6	-7.016
1e	-9.09	-7.996	2d	-7.67	-7.031
1f	-9.93	-8.617	2e	-9.83	-8.494
1g	-12.92	-10.786	2f	-8.68	-7.845
1h	-10.56	-9.167	2g	-9.11	-8.203
1i	-13.46	-11.177	2h	-10.13	-8.852
1j	-12.22	-10.837	2i	-9.13	-8.109
1k	-14.3	-12.174	2j	-10.09	-8.744

Table 3.7 Interaction energies of complex 1α-2j computed at B97D/TZV and CCSD(T)/basis limit.

Table of Interaction Energies and ΔΔG‡



Ar	β-3a (1,2):(1,3)	α-3a (1,2):(1,3)
p-NO_2 Ph (**cat-3**)	6.4:1	2.2:1
p-OTf Ph (**cat-S3**)	7:1	1.9:1
p-F Ph (**cat-1**)	8.8:1	2.2:1
Ph (**cat-S4**)	10:1	2.9:1
p-OAc Ph (**cat-S5**)	12:1	3.2:1
p-OMe Ph (**cat-4**)	13:1	2.7:1
2-Nap (**cat-5**)	15:1	3.6:1
5-NMeindole (**cat-6**)	17:1	2.1:1



Arene	Interaction Energies (B97D/TZV) (kcal/mol)	ΔΔG‡ (kcal/mol) derived from site selectivity (**β-3a**)	ΔΔG‡ (kcal/mol) derived from site selectivity (**α-3a**)
Ph-OTf	–5.41	–1.15	–0.38
Ph-F	–6.08	–1.28	–0.46
Ph-H	–6.53	–1.35	–0.63
Ph-OAc	–6.88	–1.46	–0.68
Ph-OMe	–7.22	–1.49	–0.58
naphthalene	–8.70	–1.61	–0.75
N-methyl indole	–9.21	–1.67	–0.44
Ph-NO_2	–5.04	–1.09	–0.45

Table 3.8 Table of interaction energies at B97D/TZV and ΔΔG‡ of site selective galactosylation of **α-3a** and **β-3a**.

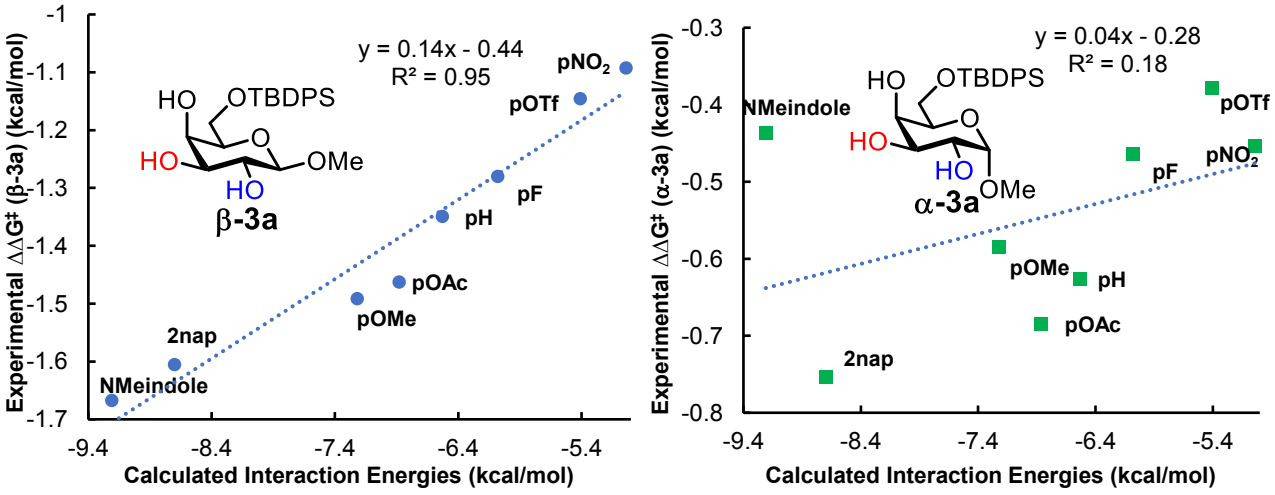


Figure 3.24 Correlation of experimental site selectivity (ΔΔG‡ = −RTln(r.r.)) with computed B97D/TZV interaction energies between substituted catalyst arenes and galactose.

The linear fit obtained in Figure S13 could be applied to convert the "raw" B97D/TZV interaction energies to the estimated CCSD(T)/basis limit energies.

$$Estimated\ CCSD(T) = 0.79 * B97D\ energy - 0.86$$

Arene	Interaction Energies (B97D/TZV) (kcal/mol)	Estimated Energies (CCSD(T)/basis limit) (kcal/mol)
Ph-OTf	–5.41	–5.13
Ph-F	–6.08	–5.66
Ph-H	–6.53	–6.02
Ph-OAc	–6.88	–6.30
Ph-OMe	–7.22	–6.57
naphthalene	–8.70	–7.74
N-methyl indole	–9.21	–8.14
Ph-NO_2	–5.04	–4.84

Table 3.9 Table of estimated interaction energies at CCSD(T)/basis limit.

A similar linear free energy relationship correlation can be plotted against the estimated CCSD(T) energies. Because B97D/TZV energies linearly correlate with reported CCSD(T)/basis limit energies, we expect the linear correlation between experimental site selectivity and interaction energies is maintained when estimate CCSD(T) energies are used. Indeed, the same level of correlation (R^2 = 0.95) was observed in site selective galactosylation of **β-3a**. Therefore, the conclusion that the strength of CH/π interactions is crucial for controlling site selectivity in glycosylation of β-carbohydrate nucleophiles remains unchanged whether the "raw" B97D/TZV energies or the estimated CCSD(T)/basis limit energies are used.

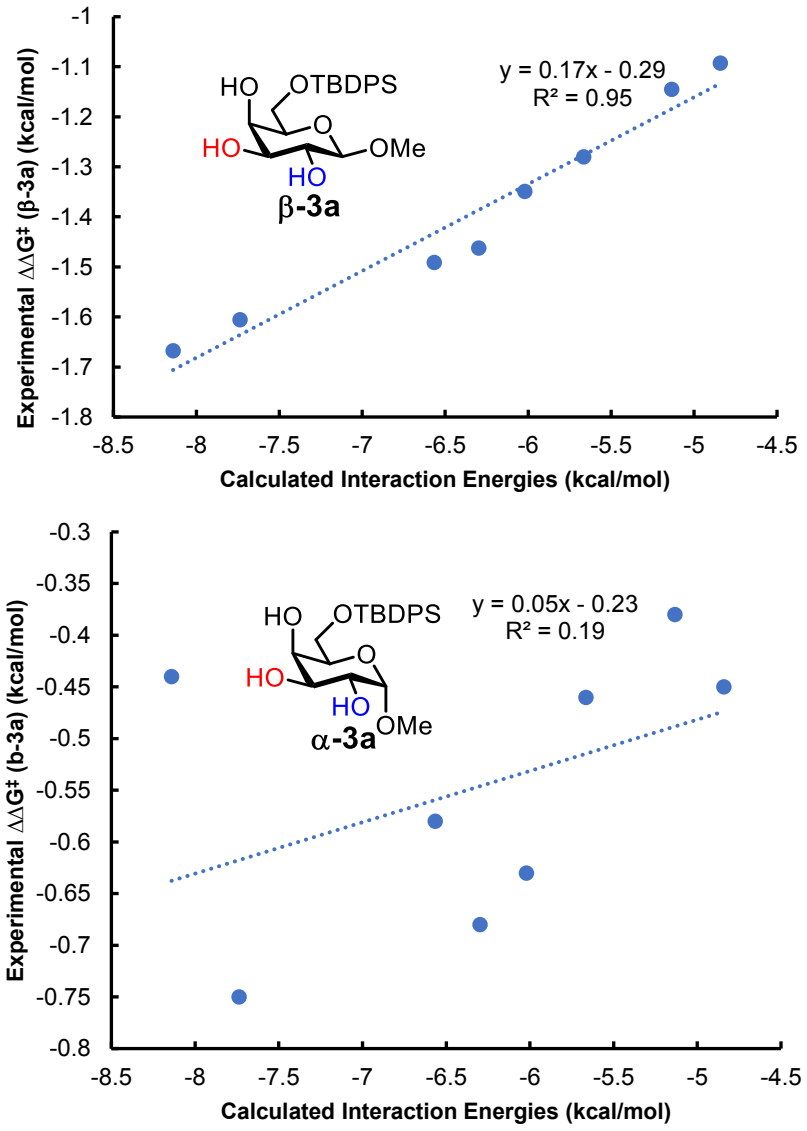
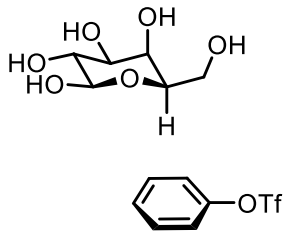
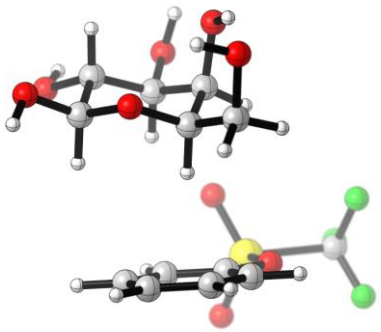


Figure 3.25 Correlation of experimental site selectivity ($\Delta\Delta G^{\ddagger} = -RT\ln(r.r.)$) with estimated CCSD(T)/basis limit interaction energies between substituted catalyst arenes and galactose.

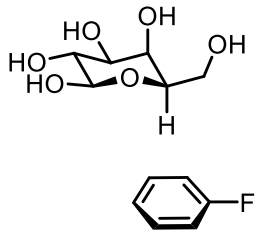
Optimized Structures of Galactose-Arene Complexes

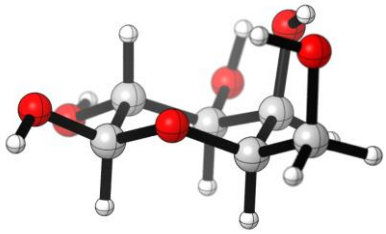


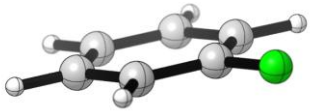


C(Fragment=1)	3.33815200	-0.16995100	-1.07313400
C(Fragment=1)	2.90184500	-1.63462000	-1.00499500
C(Fragment=1)	1.55256800	-1.76959200	-0.26510500
C(Fragment=1)	1.58189600	-1.09848800	1.11608900
C(Fragment=1)	2.08769300	0.35197300	0.97587700
H(Fragment=1)	2.61866000	0.42465700	-1.65619400
H(Fragment=1)	0.75962600	-1.32357100	-0.87147900
H(Fragment=1)	0.56085400	-1.06799300	1.52476500
H(Fragment=1)	1.35025800	0.91048600	0.38751400
H(Fragment=1)	3.66893800	-2.20053000	-0.46107600
O(Fragment=1)	3.39691600	0.39606500	0.29314700
O(Fragment=1)	4.65400800	-0.09002800	-1.61385800
H(Fragment=1)	4.87134700	0.84701200	-1.80946800
O(Fragment=1)	2.76002700	-2.12945300	-2.37868700
H(Fragment=1)	2.31142500	-3.00357500	-2.31703500
O(Fragment=1)	1.20042500	-3.19416600	-0.17033700
H(Fragment=1)	1.75223700	-3.57703100	0.55068500
O(Fragment=1)	2.42874900	-1.93525500	1.97870700
H(Fragment=1)	2.87680000	-1.34122800	2.63726500
C(Fragment=1)	2.29400900	1.06527100	2.31190400
H(Fragment=1)	2.56911600	2.11111700	2.13573300
H(Fragment=1)	1.38309900	1.01574400	2.91290400
O(Fragment=1)	3.34610300	0.39869700	3.11686500
H(Fragment=1)	4.18754300	0.47954700	2.61462200
C(Fragment=2)	-0.55726400	2.77856200	0.68829800
C(Fragment=2)	-1.02737000	1.82080400	-0.22680700
C(Fragment=2)	-0.43619100	1.66084700	-1.48590600
C(Fragment=2)	0.64955900	2.48015700	-1.83232500
C(Fragment=2)	1.13540000	3.44212400	-0.93578000
C(Fragment=2)	0.52762100	3.58570500	0.32181700
H(Fragment=2)	-1.03654200	2.87846000	1.65646500
H(Fragment=2)	-0.80064100	0.92072600	-2.19113300
H(Fragment=2)	1.11048500	2.35836200	-2.80885200
H(Fragment=2)	1.97618200	4.07172300	-1.21261800

H(Fragment=2)	0.89432200	4.32768300	1.02660600
O(Fragment=2)	-2.13275900	1.06412600	0.26268000
S(Fragment=2)	-2.91684000	-0.28297000	-0.82145000
C(Fragment=2)	-4.28138300	-0.67944900	0.73234800
F(Fragment=2)	-3.58140200	-1.07237000	1.83766800
F(Fragment=2)	-5.00722800	0.45218400	0.97452600
F(Fragment=2)	-5.09725100	-1.69256400	0.29063300
O(Fragment=2)	-1.93195100	-1.54216000	-1.01192100
O(Fragment=2)	-3.69784000	0.34600300	-2.08092500

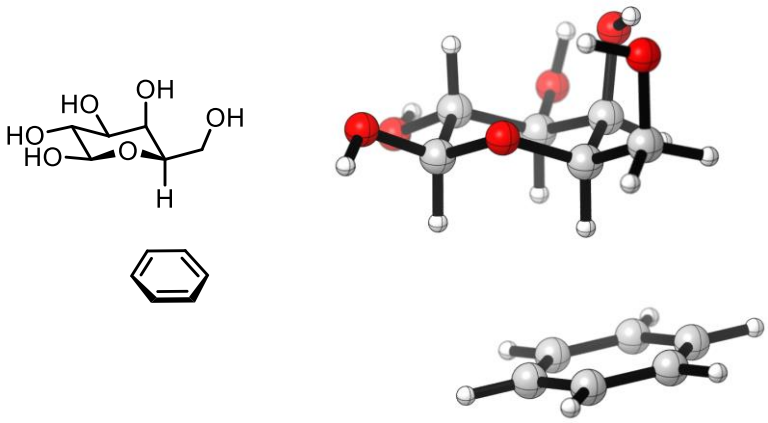






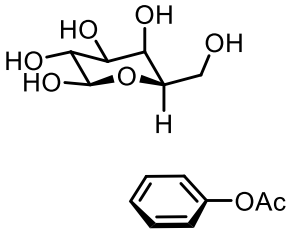
C(Fragment=1)	-1.61955400	-0.51383000	1.40210600
C(Fragment=1)	-2.41881200	-0.80160400	0.12854400
C(Fragment=1)	-1.52413900	-0.62163000	-1.11687000
C(Fragment=1)	-0.85640900	0.75903600	-1.15425500
C(Fragment=1)	-0.12262100	1.00737700	0.17857600
H(Fragment=1)	-0.79355500	-1.23357000	1.51268800
H(Fragment=1)	-0.75311700	-1.39562700	-1.10860900
H(Fragment=1)	-0.11002000	0.77831100	-1.96203700
H(Fragment=1)	0.69176200	0.27674700	0.25118300
H(Fragment=1)	-3.26179000	-0.10081800	0.07807700
O(Fragment=1)	-1.03679700	0.84483200	1.32866400
O(Fragment=1)	-2.49376000	-0.53260400	2.52712500
H(Fragment=1)	-1.96491200	-0.51420900	3.35389000
O(Fragment=1)	-2.89115500	-2.18929200	0.19311900
H(Fragment=1)	-3.25333400	-2.40363600	-0.69676500
O(Fragment=1)	-2.31655900	-0.87930000	-2.32854300
H(Fragment=1)	-2.86924300	-0.07900700	-2.48587600
O(Fragment=1)	-1.91314700	1.73941900	-1.44038000
H(Fragment=1)	-1.67321100	2.58859100	-0.98321600
C(Fragment=1)	0.46086800	2.41424500	0.30856800
H(Fragment=1)	1.03921500	2.49431900	1.23624400
H(Fragment=1)	1.09990700	2.64068400	-0.54779100
O(Fragment=1)	-0.61095100	3.43901800	0.29487200

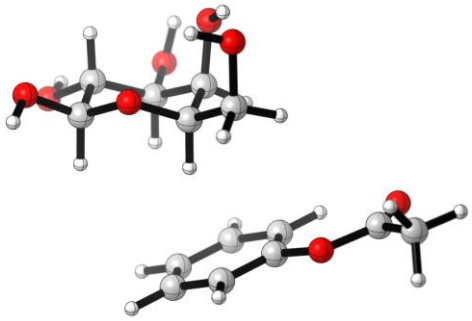
H(Fragment=1)	-1.16386200	3.28930000	1.09399300
C(Fragment=2)	3.32966500	-0.02529100	-0.03489200
C(Fragment=2)	2.86160900	-0.47779400	-1.26357700
C(Fragment=2)	3.02347200	-0.66470000	1.16376300
F(Fragment=2)	4.11684700	1.08364200	-0.00150300
C(Fragment=2)	2.05320500	-1.61915500	-1.28760400
H(Fragment=2)	3.12773900	0.05475700	-2.17155300
C(Fragment=2)	2.21413100	-1.80382600	1.12036900
H(Fragment=2)	3.41326700	-0.27275900	2.09826600
C(Fragment=2)	1.72811200	-2.28280100	-0.10045000
H(Fragment=2)	1.67767500	-1.98763500	-2.23890200
H(Fragment=2)	1.96411900	-2.31647600	2.04575400
H(Fragment=2)	1.09953200	-3.16848400	-0.12635200



C(Fragment=1)	-1.26107000	-0.67383100	1.39717500
C(Fragment=1)	-2.04548800	-1.05211000	0.13859200
C(Fragment=1)	-1.21808200	-0.72742700	-1.12405200
C(Fragment=1)	-0.75704600	0.73563400	-1.15163700
C(Fragment=1)	-0.03425100	1.06902700	0.16810900
H(Fragment=1)	-0.33635900	-1.26612300	1.47286400
H(Fragment=1)	-0.34294100	-1.38110100	-1.15176200
H(Fragment=1)	-0.04115100	0.87304800	-1.97533100
H(Fragment=1)	0.88099000	0.46762000	0.20834000
H(Fragment=1)	-2.97798000	-0.47361900	0.12138200
O(Fragment=1)	-0.88581200	0.75638700	1.33666500
O(Fragment=1)	-2.09197500	-0.83823000	2.54354000
H(Fragment=1)	-1.54913200	-0.74627300	3.35624000
O(Fragment=1)	-2.32036500	-2.49213500	0.18726300
H(Fragment=1)	-2.66555700	-2.74115200	-0.70044700
O(Fragment=1)	-1.99875200	-1.07713700	-2.32077300
H(Fragment=1)	-2.66325200	-0.36103300	-2.44867900
O(Fragment=1)	-1.95083300	1.55781400	-1.39958600
H(Fragment=1)	-1.82898900	2.42311000	-0.92634700

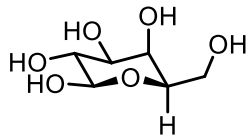
C(Fragment=1)	0.33715500	2.54394600	0.31255900
H(Fragment=1)	0.92220000	2.69271200	1.22744400
H(Fragment=1)	0.91183900	2.87705400	-0.55458700
O(Fragment=1)	-0.87443500	3.39962200	0.34779700
H(Fragment=1)	-1.38016800	3.14885100	1.15294200
C(Fragment=2)	2.62711500	-1.40956100	1.05234700
C(Fragment=2)	2.24448100	-1.87959400	-0.20914300
C(Fragment=2)	3.28511500	-0.18159000	1.17100000
H(Fragment=2)	2.41253300	-1.99978700	1.93973100
C(Fragment=2)	2.52027100	-1.12018000	-1.35119900
H(Fragment=2)	1.73311800	-2.83425100	-0.30129900
C(Fragment=2)	3.56147000	0.57778600	0.02843600
H(Fragment=2)	3.58243600	0.18381300	2.15109400
C(Fragment=2)	3.17872300	0.10814200	-1.23230900
H(Fragment=2)	2.22344300	-1.48556600	-2.33123000
H(Fragment=2)	4.07271600	1.53262000	0.12110800
H(Fragment=2)	3.39328400	0.69807500	-2.11997700

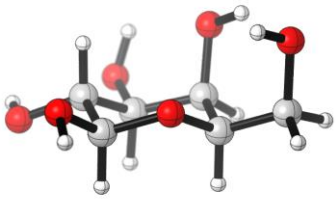


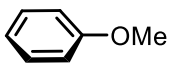


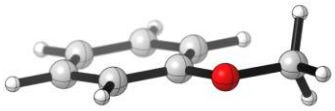
C(Fragment=1)	2.69268700	-0.16097900	-1.24542600
C(Fragment=1)	3.30733600	-0.06434300	0.15382800
C(Fragment=1)	2.20815300	-0.17198900	1.23304400
C(Fragment=1)	1.09236400	0.85837500	1.02145500
C(Fragment=1)	0.55613100	0.73743500	-0.41852800
H(Fragment=1)	2.22397000	-1.14648000	-1.39682300
H(Fragment=1)	1.78176100	-1.17795200	1.20423200
H(Fragment=1)	0.26447900	0.64455800	1.71234200
H(Fragment=1)	0.09243300	-0.25095600	-0.52096700
H(Fragment=1)	3.81380500	0.90465900	0.24620700
O(Fragment=1)	1.64778000	0.87494100	-1.40606300
O(Fragment=1)	3.69440600	0.10411300	-2.22383700
H(Fragment=1)	3.35053400	-0.12105000	-3.11523000
O(Fragment=1)	4.25669600	-1.17198500	0.31056300
H(Fragment=1)	4.50987700	-1.19093100	1.26166600

O(Fragment=1)	2.81987400	-0.05226800	2.56511000
H(Fragment=1)	3.00769500	0.90376500	2.71082000
O(Fragment=1)	1.66295600	2.17732400	1.33133400
H(Fragment=1)	1.20109100	2.84990100	0.76491400
C(Fragment=1)	-0.47160300	1.80819200	-0.78351300
H(Fragment=1)	-0.87914600	1.61059600	-1.78169900
H(Fragment=1)	-1.27796700	1.82306200	-0.04763600
O(Fragment=1)	0.13129100	3.16225100	-0.74566400
H(Fragment=1)	0.83644100	3.18298300	-1.43074900
C(Fragment=2)	-1.92548500	-1.78623100	-1.38051200
C(Fragment=2)	-2.43756900	-1.13897700	-0.24469300
C(Fragment=2)	-1.90253800	-1.37511300	1.03140200
C(Fragment=2)	-0.83522300	-2.28197400	1.15030000
C(Fragment=2)	-0.31040000	-2.93681500	0.02652000
C(Fragment=2)	-0.86150400	-2.68449100	-1.24146900
H(Fragment=2)	-2.36674200	-1.57640100	-2.34982500
H(Fragment=2)	-2.30013300	-0.87427000	1.90200600
H(Fragment=2)	-0.41456300	-2.46936100	2.13473000
H(Fragment=2)	0.51520700	-3.63440800	0.13533000
H(Fragment=2)	-0.46558100	-3.18629300	-2.12078500
O(Fragment=2)	-3.51826600	-0.25436600	-0.54651600
C(Fragment=2)	-4.23815400	0.53203200	0.35722800
O(Fragment=2)	-4.03899100	0.57688500	1.57589100
C(Fragment=2)	-5.29077400	1.31096700	-0.39785500
H(Fragment=2)	-4.81865700	1.94800900	-1.15552300
H(Fragment=2)	-5.96830300	0.62380900	-0.91891800
H(Fragment=2)	-5.85268100	1.92506300	0.30869000



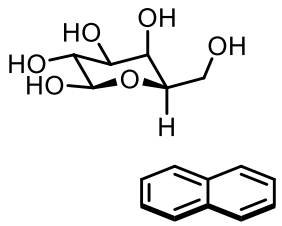


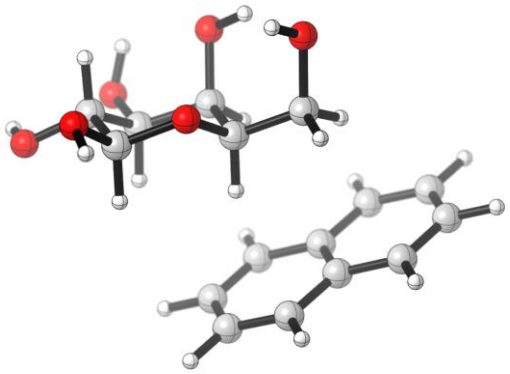




C(Fragment=1)	-1.74202300	-0.32198200	1.48918300
C(Fragment=1)	-2.73056900	-0.53924100	0.34117900
C(Fragment=1)	-1.98499800	-0.52645600	-1.01104900
C(Fragment=1)	-1.15431700	0.74981400	-1.20138000
C(Fragment=1)	-0.23501400	0.94894500	0.01934700

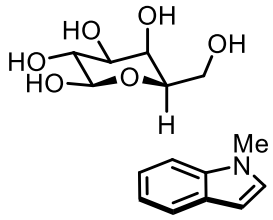
H(Fragment=1)	-1.00453000	-1.13805900	1.52648700
H(Fragment=1)	-1.32459600	-1.39579400	-1.05724200
H(Fragment=1)	-0.51742600	0.63584400	-2.09105300
H(Fragment=1)	0.48648700	0.12430700	0.03114700
H(Fragment=1)	-3.47114400	0.27048200	0.35822600
O(Fragment=1)	-1.01091400	0.94716300	1.27783100
O(Fragment=1)	-2.45518600	-0.19270100	2.71602900
H(Fragment=1)	-1.82309900	-0.22258700	3.46632200
O(Fragment=1)	-3.37369400	-1.84411800	0.53318700
H(Fragment=1)	-3.86196100	-2.04021500	-0.29886100
O(Fragment=1)	-2.95254000	-0.71587000	-2.10285800
H(Fragment=1)	-3.41034900	0.14697100	-2.23215700
O(Fragment=1)	-2.10313400	1.85268900	-1.41657700
H(Fragment=1)	-1.70886700	2.67580300	-1.02339000
C(Fragment=1)	0.52699500	2.27333500	0.00957100
H(Fragment=1)	1.22356700	2.30822500	0.85504300
H(Fragment=1)	1.07255000	2.38900500	-0.92966200
O(Fragment=1)	-0.40384800	3.42645900	0.07859400
H(Fragment=1)	-0.86999300	3.36864500	0.94243300
C(Fragment=2)	4.61498300	1.16684300	0.04640600
O(Fragment=2)	3.88614400	0.25473700	0.87008300
H(Fragment=2)	5.24333000	1.74720500	0.72665200
H(Fragment=2)	5.24571200	0.62955800	-0.67715800
H(Fragment=2)	3.93504400	1.83863800	-0.49803300
C(Fragment=2)	3.01398700	-0.59824500	0.24602900
C(Fragment=2)	2.31612800	-1.47973800	1.08974400
C(Fragment=2)	2.79005600	-0.63582000	-1.13884000
C(Fragment=2)	1.40698000	-2.38539300	0.55056700
H(Fragment=2)	2.50230600	-1.43635900	2.15921300
C(Fragment=2)	1.87172800	-1.55347300	-1.66421800
H(Fragment=2)	3.31780000	0.03530300	-1.80733800
C(Fragment=2)	1.17701600	-2.42996300	-0.83123700
H(Fragment=2)	0.87338400	-3.06205700	1.21364300
H(Fragment=2)	1.70489300	-1.57516400	-2.73853400
H(Fragment=2)	0.46655700	-3.13838900	-1.24787000

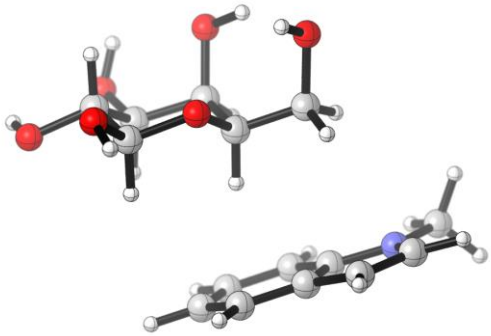




C(Fragment=1)	-2.51709700	-0.18858600	1.27963200
C(Fragment=1)	-3.08086000	-0.27882400	-0.14114100
C(Fragment=1)	-1.93307300	-0.41601300	-1.16437600
C(Fragment=1)	-0.89911600	0.70678300	-1.02223600
C(Fragment=1)	-0.41558800	0.76966700	0.44031700
H(Fragment=1)	-1.98443500	-1.11641600	1.54460300
H(Fragment=1)	-1.44032100	-1.38021100	-1.01650200
H(Fragment=1)	-0.03178300	0.48516900	-1.65782500
H(Fragment=1)	0.10335100	-0.17100700	0.66413800
H(Fragment=1)	-3.64873700	0.63647400	-0.35038000
O(Fragment=1)	-1.55695200	0.93339700	1.36726200
O(Fragment=1)	-3.57438200	0.09452100	2.19254500
H(Fragment=1)	-3.24928400	-0.00945800	3.11289200
O(Fragment=1)	-3.94576300	-1.46215200	-0.21272200
H(Fragment=1)	-4.15496900	-1.59795400	-1.16500900
O(Fragment=1)	-2.49496500	-0.47459100	-2.52298600
H(Fragment=1)	-2.74498600	0.44589800	-2.76946500
O(Fragment=1)	-1.54291200	1.94517000	-1.48545600
H(Fragment=1)	-1.14112900	2.70051100	-0.97975400
C(Fragment=1)	0.52882800	1.93572700	0.72587400
H(Fragment=1)	0.89168200	1.87789000	1.75804800
H(Fragment=1)	1.37360600	1.91672000	0.03560600
O(Fragment=1)	-0.14960700	3.23781700	0.50609400
H(Fragment=1)	-0.87902000	3.29710200	1.16263600
C(Fragment=2)	4.18615100	1.09162800	0.30909900
C(Fragment=2)	3.60051600	0.19088300	1.18272100
C(Fragment=2)	2.69317300	-0.80363800	0.70968100
C(Fragment=2)	2.39272400	-0.85672300	-0.70316100
C(Fragment=2)	3.01378900	0.08652300	-1.57568000
C(Fragment=2)	3.89019600	1.03900000	-1.08255900
H(Fragment=2)	2.30058100	-1.70365700	2.64474800
H(Fragment=2)	4.87607000	1.84474900	0.68235000
H(Fragment=2)	3.82452900	0.22802900	2.24759000

C(Fragment=2)	2.07234200	-1.74682000	1.58090200
C(Fragment=2)	1.48546900	-1.85123100	-1.17723700
H(Fragment=2)	2.78531200	0.04339300	-2.63888500
H(Fragment=2)	4.35721400	1.75253400	-1.75730700
C(Fragment=2)	0.89982700	-2.75196600	-0.30330700
C(Fragment=2)	1.19587400	-2.69922200	1.08812000
H(Fragment=2)	1.26146800	-1.88834300	-2.24184500
H(Fragment=2)	0.20989600	-3.50500400	-0.67657500
H(Fragment=2)	0.72867400	-3.41284100	1.76315100

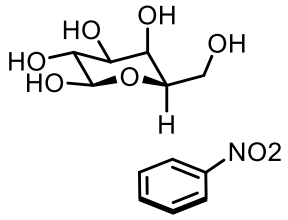


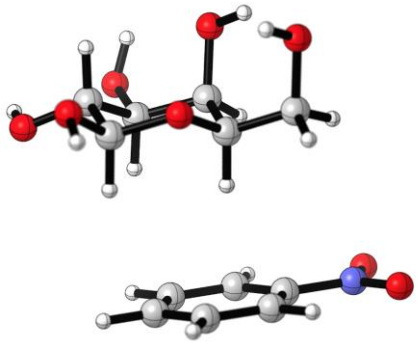


C(Fragment=1)	-2.17805100	-0.66450100	1.25682800
C(Fragment=1)	-3.13543800	-0.35605100	0.10274900
C(Fragment=1)	-2.33762400	-0.03715900	-1.18106300
C(Fragment=1)	-1.31295700	1.08399500	-0.96207500
C(Fragment=1)	-0.43221900	0.73415200	0.25094300
H(Fragment=1)	-1.57130200	-1.55548700	1.03252600
H(Fragment=1)	-1.81689700	-0.94244400	-1.50699500
H(Fragment=1)	-0.66223100	1.15436300	-1.84626200
H(Fragment=1)	0.13071100	-0.16940200	0.00034300
H(Fragment=1)	-3.74570600	0.51361800	0.37814000
O(Fragment=1)	-1.25890000	0.47848600	1.45098100
O(Fragment=1)	-2.91900500	-0.81608900	2.46522700
H(Fragment=1)	-2.33183000	-1.17708000	3.16405600
O(Fragment=1)	-3.97714700	-1.53627500	-0.12409000
H(Fragment=1)	-4.45245100	-1.38210000	-0.97231500
O(Fragment=1)	-3.27467000	0.28268000	-2.26949200
H(Fragment=1)	-3.58959000	1.20324500	-2.11439900
O(Fragment=1)	-2.06440200	2.33878100	-0.80734200
H(Fragment=1)	-1.55836500	2.91806400	-0.17808100
C(Fragment=1)	0.54600300	1.83750900	0.64438800
H(Fragment=1)	1.20660100	1.48408200	1.44303000
H(Fragment=1)	1.14072900	2.14065800	-0.21944800
O(Fragment=1)	-0.17788500	3.05832800	1.08368300

H(Fragment=1)	-0.68061100	2.81729000	1.89350100
C(Fragment=2)	0.83056800	-2.68588700	-0.49639500
C(Fragment=2)	1.09188600	-1.98907400	-1.70330700
C(Fragment=2)	2.00083600	-0.92641300	-1.74578000
C(Fragment=2)	2.64710300	-0.57254400	-0.54987700
C(Fragment=2)	2.39724600	-1.26507600	0.68434800
C(Fragment=2)	1.47413300	-2.33276700	0.69249500
H(Fragment=2)	0.11766000	-3.50702200	-0.50062000
H(Fragment=2)	0.57665100	-2.28520100	-2.61405900
H(Fragment=2)	2.19285500	-0.39978800	-2.67721200
H(Fragment=2)	1.26772100	-2.87277500	1.61405900
C(Fragment=2)	3.22212200	-0.64266300	1.68963600
H(Fragment=2)	3.28543700	-0.91209500	2.73524200
C(Fragment=2)	3.92515000	0.37137200	1.07013500
H(Fragment=2)	4.64551000	1.06987100	1.47502100
N(Fragment=2)	3.58746800	0.42613600	-0.28650500
C(Fragment=2)	4.13995500	1.37890000	-1.24917800
H(Fragment=2)	3.90815700	2.41154300	-0.95437500
H(Fragment=2)	5.22980700	1.26601800	-1.32959200
H(Fragment=2)	3.69866800	1.19163600	-2.23183300

pNO2-galactose





C(Fragment=1)	-2.17015700	-1.32084800	1.09786100
C(Fragment=1)	-2.80670200	-0.59959200	0.07688000
C(Fragment=1)	-2.60458400	-0.89540400	-1.27932900
C(Fragment=1)	-1.73972500	-1.94384700	-1.61606400
C(Fragment=1)	-1.09226900	-2.67880500	-0.60859100
C(Fragment=1)	-1.30858400	-2.36612700	0.74436900
H(Fragment=1)	-2.35300700	-1.06076900	2.13382400
H(Fragment=1)	-3.11531900	-0.31432000	-2.03816000
H(Fragment=1)	-1.57267500	-2.18538300	-2.66191400
H(Fragment=1)	-0.42205800	-3.49150800	-0.87626500
H(Fragment=1)	-0.80773600	-2.93435900	1.52304700
N(Fragment=1)	-3.72280600	0.51140600	0.44316700
O(Fragment=1)	-4.29892500	1.16338900	-0.50064200
O(Fragment=1)	-3.89925100	0.77207000	1.68771700
C(Fragment=2)	2.16589500	-0.66485900	-1.11118700

C(Fragment=2)	2.79577100	-0.60878900	0.28270500
C(Fragment=2)	1.73212500	-0.22957200	1.33585700
C(Fragment=2)	1.01225900	1.07756800	0.98099100
C(Fragment=2)	0.44470800	0.97194700	-0.44930500
H(Fragment=2)	1.40669700	-1.46070700	-1.15868000
H(Fragment=2)	1.00164700	-1.03992900	1.40215600
H(Fragment=2)	0.16994800	1.22750500	1.67294000
H(Fragment=2)	-0.32511900	0.18890400	-0.44468300
H(Fragment=2)	3.59285100	0.14503700	0.27893000
O(Fragment=2)	1.50169000	0.62207800	-1.41929700
O(Fragment=2)	3.18678500	-0.84826400	-2.08752100
H(Fragment=2)	2.77825800	-1.04751300	-2.95753300
O(Fragment=2)	3.32984000	-1.94069200	0.58845100
H(Fragment=2)	3.58123700	-1.93020200	1.54011400
O(Fragment=2)	2.35926300	-0.16815800	2.66383500
H(Fragment=2)	2.84980200	0.68476400	2.71258900
O(Fragment=2)	1.98667800	2.16223100	1.15246600
H(Fragment=2)	1.76385800	2.87828900	0.49986400
C(Fragment=2)	-0.17571100	2.27126000	-0.96558700
H(Fragment=2)	-0.62205000	2.10423900	-1.95293600
H(Fragment=2)	-0.93644800	2.63352300	-0.27022700
O(Fragment=2)	0.84018000	3.34687100	-1.04940500
H(Fragment=2)	1.50152600	3.06879600	-1.72166700

3.8.13 Transition State Calculation

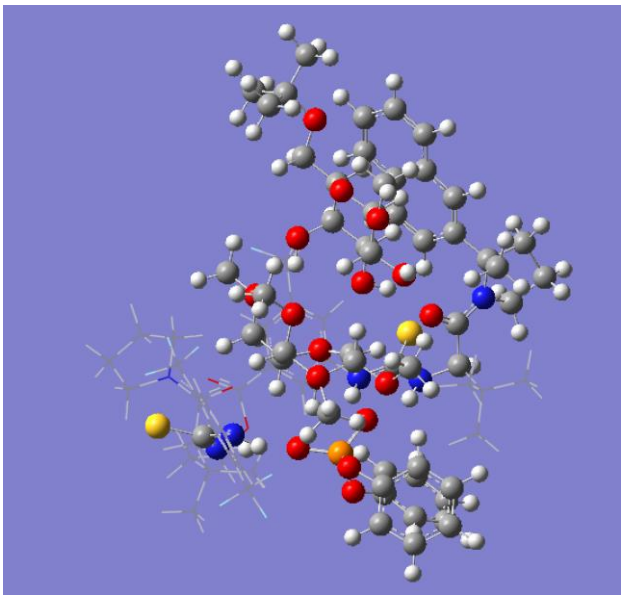
Computational Methods and Results

All computations were performed on the Cannon cluster at Harvard University. Images of the 3D structures were visualized using CYLView unless otherwise stated.[36] Gaussian 16[32] was used for DFT calculations. Transition states were located using the following route card: "#p opt=(ts,calcfc,noeigentest,maxstep=5) freq=noraman m062x/6-31g(d)". Ground and transition state geometries were validated by vibrational analysis at the same level, showing zero and one imaginary frequencies respectively. Computed energies are reported in Hartrees unless otherwise specified. Due to the large size of the system, it was necessary to use at least 120 GB memory for

[36] Legault, C. Y. CYLView20. University of Sherbrooke, Quebec, Canada (**2020**).

frequency/Hessian calculations. (*t*-Bu was used on the acceptor C6 hydroxyl in place of TBDPS to reduce the size of the system by a few atoms.)

The initial geometry (using 2-naphthalene on the "northern" arylpyrrolidine) was found by iteratively modifying the previously reported transition state for HBD-catalyzed substitution of glycosyl chlorides.[37] Transition state searching was initiated using ONIOM QM/QM' calculations (Figure 3.26). The "high" layer (comprising both sugars, the "northern" arylpyrrolidine and amide, and both thioureas) employed the M06-2X/6-31G(d) level of theory, while the "low" layer (comprising the rest of the catalyst backbone) employed the PM7 level of theory.[38] (Use of an ONIOM model helped speed optimization of the overall ternary complex geometry.) Once the complex appeared to be close to a transition state (as assessed by low gradients and forces during optimization), the transition state was then located using M06-2X/6-31G(d) for the entire structure. This functional/basis set combination have been used previously to analyze similar systems.[38]



[37] Park, Y.; Harper, K. C.; Kuhl, N.; Kwan, E. E.; Liu, R. Y.; Jacobsen, E. N. Macrocyclic Bis-thioureas Catalyze Stereospecific Glycosylation Reactions. *Science* **2017**, *355*, 162−166.
[38] Zhao, Y.; Truhlar, D. G. The M06 suite of density functionals for main group thermochemistry, thermochemical kinetics, noncovalent interactions, excited states, and transition elements: Two new functionals and systematic testing of four M06-class functionals and 12 other functionals. *Theor. Chem. Acc.* **2008**, *120*, 215–241.

Figure 3.26 Illustration of an intermediate ONIOM-based structure as depicted in GaussView. The "high" layer is shown with spheres, whereas the "low" layer is shown in wireframe.

Subsequent transition states were found by modifying the above geometry while constraining acceptor–donor–phosphate bond distances using "opt=modredundant." Once the constrained geometries were minimized, scans along the forming C–O bond and full transition state calculations were initiated until the appropriate transition states were located. Attempts to use Grimme's *crest*[39] with constrained forming and breaking bond distances to locate alternate transition states were unsuccessful. However, the high conformational complexity of this system means that the possibility of alternate lower-energy conformations cannot be ruled out.

Single point electronic energies were computed at the B97/TZP level, as employed for the cation–π interaction study. For these calculations the PCM solvation model for diisopropyl ether was employed.[34] Since the Hessian matrix was not calculated at the B97/TZP level of theory, the "Final ΔG Estimate" was computed as **E**(B97/TZP/PCM(*i*-Pr_2O)) – **E**(M06-2X/6-31G(d)) + **G**(M06-2X/6-31G(d)), where **E** represents the electronic energy and **G** the Gibbs free energy. The computations were shown to favor the (1,3)-transition state by 4.98 kcal/mol, in contrast to the 15:1 (1,2):(1,3) experimental selectivity observed with this catalyst (Table 3.10). Analysis of the transition states revealed that the (1,3)-transition state contained additional stabilization from donor–acceptor hydrogen bonds, which was hypothesized to be anomalous on the basis of semiempirical molecular dynamics simulations (as described in the main text and below). Accordingly, the 4' hydroxyl on the acceptor was replaced with F and OMe to preclude unphysical hydrogen-bonding interactions. Full (1,2)- and (1,3)-transition states were found for both 4-

[39] Pracht, P.; Bohle, F.; Grimme, S. Automated exploration of the low-energy chemical space with fast quantum chemical methods. *Phys. Chem. Chem. Phys.* **2020**, *22*, 7169–7192.

substituted compounds, and the (1,2) transition state was found to be favored in both cases. Full results are shown in Table 3.10.

Structure	**E** (B97/TZP/PCM)	**E** (M06-2X/6-31G(d))	**G** (M06-2X/6-31G(d))	**Final ΔG Estimate**
4OH (1,2) TS	-7386.81389	-7387.99130	-7386.14631	-7384.96890
4OH (1,3) TS	-7386.81893	-7387.99106	-7386.14897	-7384.97684
Delta (kcal/mol)	–3.16	+0.15	–1.67	–4.98
4F (1,2) TS	-7410.85175	-7412.00442	-7410.17485	-7409.02218
4F (1,3) TS	-7410.83740	-7411.99429	-7410.16439	-7409.00750
Delta (kcal/mol)	+9.00	+6.36	+6.56	+9.21
4OMe (1,2) TS	-7426.08872	-7427.27104	-7425.43810	-7424.25578
4OMe (1,3) TS	-7426.07480	-7427.25887	-7425.42271	-7424.23864
Delta (kcal/mol)	+8.73	+7.64	+9.66	+10.76

Table 3.10: Comparison of (1,2)- and (1,3)-Transition State Energies

"Delta" represents $E_{(1,3)} - E_{(1,2)}$, so a positive value indicates that the (1,2)-transition state is favored.

Information and Cartesian Coordinates for DFT Structures

C4-OH (1,2) TS
Number of Atoms: 239
Stoichiometry: $C_{90}H_{111}F_{10}N_6O_{19}PS_2$
Charge: 0
Multiplicity: 1
Imaginary Frequencies (cm-1): -127
Energy: -7387.99130255
Enthalpy: -7385.891243
Gibbs Free Energy: -7386.176271
Dipole Moment (Debye): 7.7257
Cartesian Coordinates (Å):

C	-0.52256399	-2.61908889	-4.43624306
C	0.58991200	-1.78445804	-4.45691919
C	0.50379199	-0.48341000	-3.95621800
C	-0.68162102	-0.03319800	-3.38195395
C	-1.79950500	-0.87534398	-3.34174395
C	-1.71621597	-2.14583397	-3.89539790
N	-0.69651401	1.24203002	-2.77966905
C	1.88463700	-2.33501101	-4.95742416
O	2.14409709	-3.51703501	-4.98037577
O	2.72749209	-1.37016201	-5.35379887
C	-1.69402301	2.17109895	-2.84496403
N	-1.51569998	3.20380807	-1.99958301
C	-2.58256412	4.12783003	-1.69858897
C	-2.06020594	5.29185486	-0.80017602
C	-3.09213305	6.42503691	-0.76083797
C	-0.75716299	5.83480692	-1.40403998
C	-1.79342401	4.82109785	0.63211697
C	4.58767414	3.60323191	4.87792683
C	4.65927696	2.27377796	4.18323708
C	5.03414011	2.22010899	2.84735990
C	4.97442102	1.01086104	2.15856791
C	4.53041315	-0.14105900	2.80998111
C	4.16482687	-0.06909700	4.15070105
C	4.24135590	1.12972200	4.85288000
N	5.21003485	1.02914095	0.76774800
C	5.89181614	0.10415100	0.03835900
N	5.55856895	0.15364499	-1.27950799
C	5.81991720	-0.97262198	-2.15823507
C	5.34472513	-0.64329201	-3.63186407
C	6.54734898	-0.05806300	-4.38171482
C	4.21405411	0.39557001	-3.63558006
C	4.85936785	-1.94062698	-4.32386923
C	4.08457184	-1.76768899	-5.62825584
C	5.05809689	-2.18109012	-1.59069300
C	-3.71525002	3.32912707	-1.00433099
O	-3.42356110	2.39558291	-0.24285699
N	-4.99134684	3.72321010	-1.18662405
C	-5.46901512	4.64253712	-2.22866797
C	-6.75715685	5.18646193	-1.62507105
C	-7.34265518	3.94242501	-0.96115702
C	-6.12052107	3.17024708	-0.38512200
O	3.91052103	-2.00282907	-1.18845201
N	5.62724495	-3.40626907	-1.64510298
C	7.06128407	-3.66561294	-1.82904303
C	7.23133421	-5.05912304	-1.22495997
C	5.91230917	-5.73846292	-1.58419001
C	4.84238911	-4.63858318	-1.37221599
C	3.68007588	-1.30736995	4.85151100
F	2.94699597	-1.01320195	5.93333721

F	4.70447302	-2.07400489	5.26466990
F	2.92949390	-2.07693410	4.04864120
C	-2.92308807	-3.04209900	-3.97321296
F	-3.99669909	-2.53658891	-3.34615302
F	-2.67862105	-4.25751686	-3.46468806
F	-3.27935195	-3.23533511	-5.25510693
H	-0.44681999	-3.62634301	-4.83511686
H	1.37109399	0.16793001	-3.99792600
H	-2.71674109	-0.53454697	-2.87611198
H	0.10461800	1.47018003	-2.19050503
H	-0.67815900	3.21143293	-1.40819800
H	-2.93707609	4.54347277	-2.64501500
H	-2.73060203	7.21855783	-0.09899100
H	-3.24375296	6.86640406	-1.75287199
H	-4.05834579	6.08472919	-0.37033299
H	-0.84781998	5.99595022	-2.48410296
H	-0.50588298	6.78984594	-0.92928398
H	0.08194100	5.15474081	-1.22976005
H	-1.13975501	3.94245505	0.65995097
H	-2.72858596	4.57573414	1.14746106
H	5.35673618	3.11473608	2.32672310
H	4.45503521	-1.07307506	2.25463104
H	3.95090508	1.17834496	5.89660215
H	4.52952099	1.58707297	0.25130999
H	4.64291620	0.58163702	-1.42685997
H	6.89515305	-1.16055799	-2.16811991
H	6.26763582	0.26218301	-5.39151382
H	6.93372011	0.81706899	-3.84906101
H	7.35677910	-0.79195601	-4.46738720
H	3.87190104	0.58192098	-4.65692520
H	3.36062694	0.05436800	-3.03894901
H	4.55011988	1.35471201	-3.23208809
H	4.17971802	-2.48538089	-3.66475701
H	5.71595097	-2.60386300	-4.50766420
H	4.06309080	-2.70639300	-6.18541384
H	4.48289394	-0.97693098	-6.26785898
H	-4.74306202	5.42217112	-2.44318295
H	-5.65785885	4.07880497	-3.15211105
H	-7.42025709	5.62227201	-2.37527609
H	-6.52060509	5.95780087	-0.88315600
H	7.32623005	-3.66419792	-2.89616489
H	7.65025187	-2.90743804	-1.30702305
H	7.33607292	-4.97805214	-0.13811800
H	8.10694122	-5.58009720	-1.61798203
O	-2.41795993	-0.17784300	0.02376500
H	-3.02247405	0.59248900	-0.10317200
C	-0.46969199	0.74666297	1.83915997
C	0.90591699	0.21825600	2.27043104
C	1.06042504	-1.15312004	1.61544001
C	1.21078801	-0.95978302	0.11663500
C	-0.61545098	0.63900900	0.32834101
H	1.68658698	0.91040498	1.90134299
H	-1.23757100	0.13106699	2.32495403
H	2.13558698	-0.40944600	-0.09546700
O	0.15064800	-0.07721500	-0.40623501
O	-0.59701502	2.09917092	2.18641996
O	1.01119399	0.04865500	3.65342212
C	1.23453701	-2.20697188	-0.73812997
H	1.55348206	-1.94280696	-1.75593400
H	2.00665092	-2.86921310	-0.32220200
O	-0.01446500	-2.85035300	-0.77698398
C	-1.82312906	2.45385289	2.80213308
H	-1.70557296	3.48798203	3.13484311
H	-2.65503597	2.37765002	2.09426594
H	-2.01975203	1.80585396	3.66552591
C	1.03868103	1.23999906	4.41876507
H	1.66916502	2.00726390	3.94899702
H	0.03521400	1.65135503	4.56853104
H	1.45905304	0.96539098	5.38759518
C	0.08777900	-4.10373402	-1.43068302
H	-0.92658103	-4.47353411	-1.58390403
H	0.58716398	-3.99786806	-2.40332603
H	0.66601503	-4.80484819	-0.81152099
S	7.05438519	-0.92269099	0.68504101
S	-3.00740290	2.06547594	-3.89726305
F	4.84695292	3.49266601	6.18953609
F	5.44970894	4.48853397	4.36338520
F	3.35911298	4.13515997	4.76675987
H	-1.29448402	5.62307787	1.18884301
H	-7.83778000	3.32445407	-1.71630096
H	-8.07106304	4.15859699	-0.17490600
C	-6.34173203	1.67807603	-0.61676300
C	-7.22549009	0.96808898	0.16324399
C	-5.75498199	1.04008806	-1.74335003
C	-7.54631519	-0.38870901	-0.12300200
H	-7.71558094	1.43141103	1.01696801
C	-6.04951286	-0.26118299	-2.05036592
H	-5.06363916	1.58963203	-2.37363505
C	-8.42795181	-1.14533699	0.69350600
C	-6.94549513	-1.01791298	-1.24884498
H	-5.58480787	-0.73277003	-2.91307902
C	-8.69459438	-2.46047401	0.40495601
H	-8.86783409	-0.67547500	1.56926596
C	-7.23482609	-2.38025308	-1.52246904
C	-8.09288502	-3.08563900	-0.71454197
H	-9.34741306	-3.03517604	1.05376899
H	-6.75120878	-2.85225296	-2.37467694
H	-8.30664253	-4.12898922	-0.92560500
C	-5.89257717	3.52496004	1.08867204
H	-5.79984808	4.61127901	1.19484103
H	-6.73462105	3.19760609	1.70404994
H	-4.98017216	3.05043793	1.45679402
H	5.92012501	-6.02948713	-2.64176512
H	5.69400215	-6.62594986	-0.98572803
H	1.97186303	-1.63667405	1.99118304
C	0.14340501	-3.26243210	2.25123811
H	-0.83508199	-3.69486809	2.47316599
H	0.58906198	-3.79538798	1.40329099
H	0.79951203	-3.35292411	3.12564301
O	-0.08846900	-1.90105498	1.94185805
H	-1.07863700	1.48062694	-0.17632601
O	2.96837497	1.48430002	-1.02273405
P	2.31057692	2.76738191	-0.61199200
O	3.07304597	3.19758105	0.75834101
O	2.79813194	4.01894808	-1.54948902
O	0.81419599	2.79475188	-0.46933499
C	2.22039390	4.21738911	-2.78597689
C	2.06065607	5.53103495	-3.21613598
C	1.81604898	3.15191007	-3.58698201
C	1.45529997	5.77473116	-4.44461823
H	2.39348888	6.33679199	-2.56998110
C	1.18450201	3.40831494	-4.80084801
H	2.01402593	2.13672709	-3.25562501
C	0.99831802	4.71870899	-5.23243093

H	1.32499504	6.79923677	-4.78002882
H	0.83754700	2.57596111	-5.40700197
H	0.50556803	4.91561222	-6.17856407
C	2.77964211	4.36074114	1.45736301
C	3.77280593	5.32825518	1.55717099
C	1.55121398	4.50700378	2.09125710
C	3.53546906	6.46345615	2.32691908
H	4.71084309	5.18012524	1.03126395
C	1.32543004	5.65499878	2.84679103
H	0.80711597	3.72295094	1.99292803
C	2.31212306	6.63039303	2.97140408
H	4.31045103	7.21745682	2.42152691
H	0.37263799	5.77850294	3.35431099
H	2.13149309	7.51504707	3.57350707
C	-3.03979993	-1.24896896	0.74479699
C	-4.17385721	-0.76589602	1.63627994
C	-3.60491300	-2.26808310	-0.24150500
H	-2.26311803	-1.70992696	1.36373305
H	-4.98157978	-0.32939801	1.01158595
C	-4.32775593	-3.38675404	0.52000600
H	-4.31813622	-1.75153303	-0.89959401
C	-5.31548214	-2.80162001	1.51875997
H	-4.88276386	-3.99584198	-0.21216600
H	-6.11417198	-2.30057406	0.95834500
C	-4.72365093	0.69972098	3.35070109
H	-5.03699112	-0.04700600	4.08445787
H	-4.31800508	1.57808006	3.85756207
H	-5.59158278	0.99611402	2.74610305
C	-5.94127512	-3.85171890	2.40976191
H	-6.30462980	-4.68175793	1.78422296
H	-5.16807508	-4.24032688	3.08256793
O	-4.67379618	-1.85418105	2.36153507
O	-7.00167990	-3.23476410	3.10265207
O	-3.69663811	0.18844999	2.51735997
O	-2.60143209	-2.88488889	-1.00770199
H	-1.76097095	-2.38940406	-0.95497698
O	-3.37450910	-4.16912603	1.20667100
H	-2.64516711	-4.27561283	0.57074201
C	-7.42048502	-3.84017611	4.32623100
C	-7.77589417	-5.31283188	4.11484003
H	-8.50901031	-5.41024923	3.30708790
H	-6.89286518	-5.90585995	3.85623503
H	-8.20675564	-5.73536301	5.02773809
C	-6.34088182	-3.68018603	5.39981604
H	-6.72458410	-3.99818611	6.37435579
H	-5.45230389	-4.27957392	5.18254805
H	-6.03943205	-2.63051510	5.46315813
C	-8.66354275	-3.04545498	4.71474886
H	-9.07707310	-3.40428805	5.66180420
H	-8.40805531	-1.98675394	4.81899881
H	-9.42791939	-3.14104509	3.93742490
C	3.71390605	-4.78497124	-2.39711809
H	3.24428701	-5.76989317	-2.32196403
H	2.94864893	-4.01786280	-2.25736189
H	4.11523724	-4.69431591	-3.41009212
C	4.32379389	-4.66744184	0.06771900
C	3.26094508	-5.50262308	0.42640099
C	4.93337107	-3.90882492	1.07102597
C	2.79526711	-5.55895090	1.73854804
H	2.77712488	-6.12714386	-0.31801501
C	4.49111080	-3.96015406	2.38927388
H	5.75252199	-3.24017191	0.82295001
C	3.41507101	-4.77750492	2.70013094
H	1.96513903	-6.19764900	2.02218795
H	4.96816683	-3.37836695	3.17044711
F	2.95323610	-4.81136084	3.95990992

C4-OH (1,3) TS

Number of Atoms: 239

Stoichiometry: $C_{90}H_{111}F_{10}N_6O_{19}PS_2$

Charge: 0

Multiplicity: 1

Imaginary Frequencies (cm-1): -132

Energy: -7387.9910567

Enthalpy: -7385.891418

Gibbs Free Energy: -7386.182031

Dipole Moment (Debye): 8.2328

Cartesian Coordinates (Å):

C	1.02487898	-2.10842490	4.38898182
C	-0.03399100	-1.25473702	4.68690586
C	-0.09770700	0.01372300	4.10603380
C	0.86595201	0.41117299	3.18719006
C	1.92590106	-0.44200501	2.87393308
C	2.00871897	-1.68351603	3.49896789
N	0.71511900	1.65456295	2.52183509
C	-1.12172902	-1.75344598	5.58034992
O	-1.22030199	-2.90105700	5.94966602
O	-1.99530900	-0.78674501	5.89291191
C	1.65832901	2.63677096	2.50797105
N	1.45296800	3.57564402	1.56695497
C	2.45069194	4.56334686	1.22902405
C	1.84868801	5.64236784	0.28090200
C	2.86135793	6.78199100	0.11472200
C	0.57456702	6.19540882	0.93332797
C	1.49950099	5.08109188	-1.10457301
C	-5.98631620	2.88116002	-4.35703087
C	-5.72779417	1.53934896	-3.73496199
C	-5.56865978	1.45775604	-2.35437107
C	-5.16764784	0.25870299	-1.77344704
C	-4.92076588	-0.85589898	-2.57824492
C	-5.09905195	-0.75949103	-3.94922304
C	-5.51232719	0.43253699	-4.54272223
N	-4.90960407	0.23271801	-0.38934901
C	-5.38233519	-0.65401900	0.52796799
N	-4.92285109	-0.38192099	1.77477098
C	-4.93969917	-1.36743200	2.83931088
C	-4.64975882	-0.67425501	4.22063112
C	-5.97148895	-0.08791400	4.73361206
C	-3.65950799	0.48606399	4.03034782
C	-4.12904310	-1.73122895	5.23485422
C	-3.27858996	-1.20573199	6.38722897
C	-3.88348198	-2.43173599	2.48569989
C	3.63688302	3.82303810	0.57393003
O	3.40401793	2.93185306	-0.25767601
N	4.89582109	4.18003178	0.86227900
C	5.29871416	5.14866590	1.89209199
C	6.70375586	5.54588890	1.45244706
C	7.25593901	4.22777319	0.91576397
C	6.06857395	3.56978607	0.16420101
O	-2.78733110	-2.05949712	2.06947303
N	-4.18946123	-3.73469710	2.68247008
C	-5.53613091	-4.23643398	3.00987601
C	-5.42372894	-5.74215794	2.76918793
C	-3.95987511	-6.02286291	3.09034300

C	-3.20720911	-4.82531500	2.46524405
C	-4.79000998	-1.92912900	-4.83893681
F	-3.98457503	-1.56449103	-5.84877205
F	-5.89699316	-2.44151998	-5.39273882
F	-4.17807102	-2.92340398	-4.17503405
C	3.19886208	-2.55778909	3.23034406
F	3.56773996	-2.52801895	1.93555903
F	2.96983790	-3.83912301	3.55024910
F	4.27755690	-2.16661501	3.93228793
H	1.06160903	-3.09155703	4.84678984
H	-0.90434903	0.69053698	4.36186981
H	2.66293907	-0.13288200	2.13674212
H	-0.02274000	1.70036995	1.81728697
H	0.59717900	3.51780295	1.00533402
H	2.76975012	5.04956913	2.15521193
H	2.46894002	7.52022600	-0.59182501
H	3.03960609	7.29778385	1.06550705
H	3.82097006	6.42403078	-0.27866399
H	0.73828202	6.45333290	1.98583496
H	0.25071499	7.09734106	0.40209699
H	-0.24635300	5.47424984	0.88532501
H	0.82288200	4.21967220	-1.04664099
H	2.39629698	4.78409004	-1.65650201
H	-5.73901606	2.32642889	-1.72825503
H	-4.58197117	-1.77956903	-2.12369800
H	-5.62555313	0.50341702	-5.61998081
H	-4.30134487	0.97361702	-0.03909800
H	-4.10386515	0.23061199	1.78275895
H	-5.93737221	-1.80658495	2.86824393
H	-5.81435204	0.46258599	5.66849184
H	-6.38925219	0.60725701	3.99863195
H	-6.71058798	-0.87486100	4.92078781
H	-3.36657310	0.91342902	4.99204302
H	-2.76112199	0.16005000	3.49874091
H	-4.11940098	1.29201198	3.45253706
H	-3.51316404	-2.49092007	4.74495983
H	-4.98557997	-2.26968503	5.66191578
H	-3.13118410	-1.98364902	7.13933086
H	-3.70181608	-0.31819600	6.86277199
H	4.61750698	5.99719286	1.92512202
H	5.29528189	4.65747213	2.87372494
H	7.29457903	5.95543003	2.27438498
H	6.64694881	6.30047321	0.66020501
H	-5.77577209	-4.02189398	4.06002808
H	-6.28482723	-3.76679206	2.36603308
H	-5.63066816	-5.96696520	1.71809101
H	-6.12124777	-6.31136084	3.38690305
O	4.27665377	1.57034397	-2.94735193
H	4.61162615	1.69351494	-3.85079908
C	0.17768700	0.78585303	-2.19368792
C	-1.26397002	0.24929599	-2.15310597
C	-1.22106898	-1.08530295	-1.41666698
C	-0.79264402	-0.88524902	0.03154100
C	0.72714800	0.87024301	-0.77731699
H	-1.90904403	0.96334398	-1.61415899
H	0.77376699	0.07987600	-2.78893590
H	-1.63375700	-0.45762900	0.58807701
O	0.26074001	0.12714100	0.17780600
O	0.16328500	2.07201505	-2.74631691
O	-1.75355399	-0.00529600	-3.43694305
C	-0.32679400	-2.12821102	0.75915301
H	-0.25969601	-1.91880298	1.83603895
H	-1.09538198	-2.90243101	0.62769699
O	0.92315298	-2.54812694	0.26234400
C	1.39836895	2.49274111	-3.29828405
H	1.22153902	3.48178911	-3.72700810
H	2.18613410	2.56075096	-2.54224205
H	1.72052896	1.80179405	-4.08885717
C	-2.27905989	1.11991704	-4.12088013
H	-2.99225903	1.66527796	-3.48763490
H	-1.49147499	1.80878198	-4.43765783
H	-2.79841805	0.72359699	-4.99464607
C	1.22116196	-3.87316394	0.64233899
H	2.19263911	-4.12273598	0.21042401
H	1.27199495	-3.96941495	1.73552501
H	0.45882201	-4.56825495	0.26327601
S	-6.45041418	-1.90544498	0.16502900
S	2.93383408	2.68436098	3.61230803
F	-6.61208200	2.77352095	-5.53787422
F	-6.73294592	3.66622090	-3.56849599
F	-4.83146286	3.52956796	-4.58005619
H	0.98138702	5.85813284	-1.67884398
H	7.55272007	3.58747911	1.75300598
H	8.11933804	4.34058809	0.25497100
C	6.15372181	2.05611897	0.35164100
C	6.95079994	1.28077900	-0.45872399
C	5.52532101	1.44757700	1.47172999
C	7.15596581	-0.10266800	-0.19481499
H	7.45409489	1.70746100	-1.32249105
C	5.68223000	0.11240700	1.73826301
H	4.90393019	2.04879594	2.12736106
C	7.98250103	-0.91340297	-1.02136803
C	6.50322485	-0.70454299	0.91622102
H	5.19170380	-0.32972500	2.60208201
C	8.13054180	-2.25334191	-0.76855803
H	8.48352814	-0.45256600	-1.86996996
C	6.68447685	-2.09268188	1.16331697
C	7.47394514	-2.85041904	0.33653399
H	8.73696804	-2.86996603	-1.42402899
H	6.17574215	-2.53695607	2.01392293
H	7.58776617	-3.91537690	0.51194102
C	6.03291893	3.99119496	-1.30914199
H	5.95623493	5.08148479	-1.37653995
H	6.95203304	3.69154310	-1.81928205
H	5.18195581	3.52808595	-1.81272697
H	-3.80132294	-6.00993299	4.17575788
H	-3.59461999	-6.97516823	2.69832802
H	-2.23210907	-1.51839101	-1.39738703
C	-0.77662599	-3.22947407	-2.36281705
H	0.01903800	-3.72843409	-2.91956496
H	-0.94741201	-3.76003003	-1.41814303
H	-1.70104098	-3.23431897	-2.95430493
O	-0.33747199	-1.90697002	-2.14015603
H	0.97251803	1.87715697	-0.44331899
O	-2.74320698	1.42635000	1.17904401
P	-2.38780594	2.74538994	0.55905098
O	-3.35644102	2.86579108	-0.74588501
O	-3.00919199	3.99943900	1.40413105
O	-0.94608200	2.99679399	0.21584199
C	-2.31845593	4.54239988	2.46698189
C	-2.39651990	5.91971016	2.64791298
C	-1.57445002	3.74746609	3.33382607
C	-1.69189203	6.50556993	3.69484091
H	-2.99066210	6.50607395	1.95481205

C	-0.84253001	4.34825993	4.35424089
H	-1.57701194	2.66980290	3.20468402
C	-0.89942503	5.72775888	4.53885603
H	-1.74820602	7.58030701	3.83925509
H	-0.22706001	3.73012495	5.00205994
H	-0.33330500	6.19345999	5.33882713
C	-3.35044909	3.99570799	-1.55699694
C	-4.47715378	4.80920887	-1.55669796
C	-2.26102090	4.25389099	-2.38149095
C	-4.52473497	5.89675617	-2.42423010
H	-5.29510212	4.58349895	-0.87951303
C	-2.32169008	5.35032701	-3.23755503
H	-1.39787698	3.59561896	-2.34606600
C	-3.44916105	6.16866779	-3.26583290
H	-5.40735197	6.52817822	-2.44267297
H	-1.48124397	5.55994177	-3.89294696
H	-3.49109507	7.01439190	-3.94467902
C	3.91621208	0.20710100	-2.86164999
C	5.09306002	-0.63863897	-3.35313511
C	3.63781810	-0.16450600	-1.41664696
H	3.04512906	-0.03315700	-3.48681998
H	5.99418783	-0.35577500	-2.77380610
C	3.42745805	-1.66832495	-1.29891098
H	4.50311804	0.13037400	-0.80905598
C	4.68968105	-2.34499097	-1.83968103
H	3.29199505	-1.91781402	-0.23900101
H	5.55878305	-1.99486804	-1.26902497
C	6.42625999	-0.92346799	-5.24993277
H	6.34162903	-2.01322198	-5.23334694
H	6.50286388	-0.56994599	-6.27870893
H	7.32419777	-0.62488401	-4.69084692
C	4.63092184	-3.85099101	-1.73329401
H	4.36925411	-4.11605597	-0.69561201
H	3.84225106	-4.21768713	-2.40077305
O	4.85734510	-2.00843191	-3.21061993
O	5.90448093	-4.34868288	-2.06927800
O	5.27095985	-0.32216501	-4.69339323
O	2.53430009	0.57291901	-0.82760102
H	2.89024496	1.46239901	-0.54591697
O	2.33933711	-2.09170008	-2.07847905
H	1.53278804	-2.09113693	-1.53160095
C	5.97906303	-5.70388222	-2.51317191
C	5.33201218	-6.64859200	-1.49886298
H	5.76656580	-6.48941612	-0.50626302
H	4.25066090	-6.48912811	-1.43469298
H	5.49920511	-7.69048405	-1.78862202
C	5.33578205	-5.84769297	-3.89466095
H	5.52806711	-6.84531307	-4.30198002
H	4.25171089	-5.70690012	-3.85970092
H	5.75588703	-5.10005617	-4.57367086
C	7.47820902	-5.97183514	-2.60406709
H	7.67353678	-6.98805094	-2.95880699
H	7.93943691	-5.26140404	-3.29659104
H	7.94174099	-5.84665585	-1.62043095
C	-1.89284098	-4.58327103	3.21432710
H	-1.29738498	-5.50176620	3.21930099
H	-1.30670798	-3.78110504	2.76455688
H	-2.09783697	-4.32233477	4.25621319
C	-2.99111509	-5.08478594	0.97009498
C	-2.03045797	-6.01625013	0.55748397
C	-3.79668999	-4.49062681	-0.00578600
C	-1.87255096	-6.34828377	-0.78544098
H	-1.39660299	-6.50671291	1.29143500
C	-3.65893602	-4.81531811	-1.35355401
H	-4.55636311	-3.76769805	0.27724299
C	-2.69483209	-5.73884678	-1.72119498
H	-1.12856901	-7.06626320	-1.11349201
H	-4.28320312	-4.35806084	-2.11445594
F	-2.52372193	-6.02623701	-3.02094293

C4-OH Precomplex

Number of Atoms: 239
Stoichiometry: $C_{90}H_{111}F_{10}N_6O_{19}PS_2$
Charge: 0
Multiplicity: 1
Imaginary Frequencies (cm-1): none
Energy: -7388.00049443
Enthalpy: -7385.90009
Gibbs Free Energy: -7386.194669
Dipole Moment (Debye): 5.7481
Cartesian Coordinates (Å):

C	-0.88833600	-2.06663108	-4.44676113
C	0.27251700	-1.33681798	-4.68896580
C	0.42854300	-0.06347600	-4.13703489
C	-0.54704499	0.45763099	-3.29419398
C	-1.70160902	-0.27976099	-3.02194405
C	-1.87533498	-1.51962399	-3.63072610
N	-0.32297701	1.70175505	-2.65621901
C	1.35708404	-1.97557795	-5.49214792
O	1.35442400	-3.13802004	-5.82540083
O	2.35232806	-1.11932099	-5.76704502
C	-1.15676999	2.77844405	-2.71437311
N	-0.84864402	3.75283003	-1.83392704
C	-1.80368197	4.78386402	-1.48982596
C	-1.16297305	5.82517576	-0.52363402
C	-2.08604193	7.04509592	-0.41804600
C	0.18587901	6.26628304	-1.10591996
C	-0.93564099	5.25382423	0.88228899
C	5.93418312	2.48396993	4.66664886
C	5.58193111	1.16954303	4.03153419
C	5.63098383	1.05441499	2.64683008
C	5.15832710	-0.10083300	2.02939892
C	4.62942886	-1.13406503	2.80394912
C	4.59158707	-1.00288796	4.18468714
C	5.07889891	0.13941100	4.81499100
N	5.10121679	-0.12948300	0.62341899
C	5.45494318	-1.14367902	-0.21303201
N	5.09257412	-0.88383800	-1.49408197
C	5.06592321	-1.90604401	-2.52296400
C	4.91083193	-1.23816705	-3.93998694
C	6.30806494	-0.81408602	-4.41042614
C	4.04041910	0.02445600	-3.83861589
C	4.32008123	-2.26895690	-4.94114304
C	3.60889506	-1.69519103	-6.16353512
C	3.89325595	-2.85108805	-2.20475411
C	-3.02305198	4.08858824	-0.83696401
O	-2.80120707	3.14554906	-0.06622400
N	-4.26626682	4.54430819	-1.06757200
C	-4.63158703	5.54430199	-2.07964993
C	-5.90815210	6.14655304	-1.50694299
C	-6.60131693	4.91701794	-0.92625600
C	-5.46194601	4.05170584	-0.31670099
O	2.80937195	-2.35897398	-1.89158595
N	4.08433104	-4.18337584	-2.33198810

C	5.39477682	-4.83174276	-2.51386595
C	5.11017418	-6.29346609	-2.17261696
C	3.66910195	-6.46619511	-2.64042091
C	2.97514105	-5.16018677	-2.18997192
C	3.97046900	-2.08572698	5.02033281
F	3.26725793	-1.56784403	6.03822708
F	4.88843918	-2.90144491	5.55425978
F	3.13343906	-2.85227609	4.29949379
C	-3.17189288	-2.25161099	-3.43436909
F	-3.61980295	-2.15443206	-2.16990495
F	-3.06637907	-3.55647802	-3.72372508
F	-4.14682722	-1.75420702	-4.21417093
H	-1.00055599	-3.05157995	-4.88781309
H	1.31716299	0.51636600	-4.35806179
H	-2.43703294	0.11142200	-2.32249904
H	0.47266799	1.75701594	-2.02264810
H	-0.07660500	3.58006096	-1.18471897
H	-2.09055710	5.28889990	-2.41490889
H	-1.66345298	7.76358223	0.29163599
H	-2.18904710	7.55409479	-1.38363099
H	-3.08368897	6.76936388	-0.05528400
H	0.10608200	6.51396704	-2.17033291
H	0.54698598	7.14982080	-0.56778401
H	0.94242698	5.48312998	-0.99867803
H	-0.35756901	4.32254696	0.86592901
H	-1.88416803	5.06026077	1.39321601
H	6.01994801	1.86466801	2.04054594
H	4.23743200	-2.01910400	2.31566405
H	5.02478600	0.24188800	5.89392185
H	4.62007904	0.66276002	0.19940101
H	4.34411097	-0.19170800	-1.57025599
H	6.01645517	-2.43968701	-2.48739195
H	6.25129414	-0.28539300	-5.36896181
H	6.76684093	-0.13977700	-3.68034506
H	6.96555614	-1.68128705	-4.53744316
H	3.84674597	0.44755700	-4.82718277
H	3.08410501	-0.19079500	-3.35222912
H	4.55203581	0.79852903	-3.26006794
H	3.58231497	-2.91672707	-4.46025610
H	5.12302494	-2.93248105	-5.28910208
H	3.42137694	-2.47939992	-6.89979315
H	4.15815210	-0.87840098	-6.63713980
H	-3.84375596	6.28208780	-2.21463609
H	-4.80884981	5.04283524	-3.03994012
H	-6.50634718	6.65754795	-2.26434588
H	-5.65694809	6.86720610	-0.72032201
H	5.73086214	-4.72879601	-3.55483007
H	6.13576698	-4.38436604	-1.84677398
H	5.17730999	-6.43950891	-1.08949494
H	5.81088305	-6.97592783	-2.65780902
O	-4.18247986	1.72516501	3.07936096
H	-4.43627691	1.83110797	4.01040792
C	-0.01317100	1.03191996	1.95781004
C	1.27243304	0.22992399	2.20400405
C	0.99844402	-1.14013600	1.56862700
C	0.86532098	-1.00545001	0.05406800
C	-0.34335700	1.04595196	0.49914101
H	2.13676906	0.71784103	1.72164500
H	-0.82603002	0.44897401	2.42010999
H	1.82827902	-0.74204499	-0.39673999
O	-0.00835600	0.13994899	-0.30389401
O	0.01743400	2.33409095	2.45511198
O	1.51371098	0.01396900	3.56163597
C	0.28290799	-2.18833399	-0.69149500
H	0.38268900	-2.01321197	-1.77276897
H	0.89657998	-3.06838799	-0.44457501
O	-1.06579196	-2.37338400	-0.34237900
C	-1.22388303	2.73721600	3.02477908
H	-1.07240903	3.74912691	3.40516210
H	-2.02686906	2.73205900	2.28144598
H	-1.50049603	2.06525493	3.84741712
C	2.02657700	1.13513100	4.26366615
H	2.83985806	1.61431599	3.70062900
H	1.25039804	1.87926304	4.46172619
H	2.41609597	0.74811298	5.20614195
C	-1.53947997	-3.64490891	-0.73171401
H	-2.57346702	-3.71547103	-0.39256701
H	-1.49134099	-3.76710296	-1.82262897
H	-0.94185299	-4.43939495	-0.26370901
S	6.29139090	-2.51893401	0.27882999
S	-2.43131709	2.88712001	-3.81043911
F	6.38274479	2.32824898	5.92033577
F	6.87339592	3.14182711	3.97407699
F	4.85663986	3.28340197	4.73010588
H	-0.36882100	5.98271513	1.47373605
H	-7.08846092	4.35843182	-1.73152602
H	-7.35829020	5.14889288	-0.17228501
C	-5.77999115	2.57802105	-0.56877202
C	-6.81487989	1.97359598	0.11241600
C	-5.11397600	1.84545898	-1.58554006
C	-7.20438099	0.63414598	-0.16009900
H	-7.36486006	2.51339698	0.88041800
C	-5.46139717	0.54879200	-1.86629105
H	-4.32378292	2.31723690	-2.15967894
C	-8.25743484	-0.00874400	0.54846001
C	-6.50432110	-0.10086400	-1.15731895
H	-4.94838285	0.01006800	-2.65837097
C	-8.57921600	-1.31717503	0.29143700
H	-8.79204178	0.55234599	1.31141198
C	-6.86012220	-1.45498395	-1.40406096
C	-7.86971617	-2.05109406	-0.69272900
H	-9.36426640	-1.80804706	0.85760897
H	-6.30379486	-2.00503206	-2.15865397
H	-8.12063599	-3.09310389	-0.86397398
C	-5.27345610	4.35675097	1.17533898
H	-5.07223701	5.42569590	1.30843306
H	-6.18141890	4.11064100	1.73168600
H	-4.45396614	3.77023292	1.59435797
H	3.63305306	-6.52767992	-3.73506904
H	3.17128897	-7.34718418	-2.22834301
H	1.85078299	-1.80606997	1.76958299
C	-0.14811601	-2.98607993	2.56050897
H	-1.10150301	-3.17725301	3.05364203
H	-0.05470600	-3.64754796	1.69074297
H	0.68307298	-3.16651392	3.25201392
O	-0.17691199	-1.62708402	2.16626906
H	-0.93490398	1.85990000	0.07754000
O	3.03691792	1.10038304	-1.04251599
P	2.74700999	2.46124101	-0.48266301
O	3.67023206	2.57588410	0.85019398
O	3.45808196	3.65031004	-1.34299505
O	1.30080402	2.79749393	-0.21301600
C	2.91804099	4.08233500	-2.53936291
C	2.98148608	5.44400787	-2.81602597

C	2.35039997	3.19256997	-3.44644308
C	2.43064189	5.92014885	-4.00122690
H	3.44150901	6.10565519	-2.08929706
C	1.77272606	3.68507910	-4.61371517
H	2.37202907	2.12915111	-3.22882795
C	1.80823803	5.04816198	-4.89381981
H	2.47293210	6.98305893	-4.21895981
H	1.29094899	2.99702907	-5.30291510
H	1.35770297	5.42823410	-5.80448198
C	3.76122999	3.74862194	1.59544003
C	4.98407221	4.40806103	1.62488604
C	2.66813993	4.19788885	2.32680893
C	5.12355804	5.53519011	2.42916703
H	5.80341101	4.03680706	1.01715302
C	2.82252789	5.33293819	3.11913705
H	1.72899103	3.65555501	2.27122808
C	4.04461479	5.99894905	3.17772102
H	6.07920885	6.04798603	2.47049809
H	1.97909904	5.69219780	3.70153403
H	4.15737915	6.87576389	3.80716109
C	-4.08901787	0.32845500	2.86587811
C	-5.34961891	-0.35052100	3.39135098
C	-3.98286700	0.05706200	1.37470496
H	-3.22318196	-0.10883400	3.38515902
H	-6.23507023	0.09550700	2.88867211
C	-4.04258585	-1.44447005	1.11524498
H	-4.84887600	0.52385801	0.89220798
C	-5.31385899	-1.99628901	1.75237405
H	-4.09380102	-1.59511995	0.02630400
H	-6.17718220	-1.50320804	1.28580797
C	-6.60188007	-0.58134800	5.35207605
H	-6.67764378	-1.66799402	5.25862503
H	-6.56560183	-0.29918900	6.40505600
H	-7.47926903	-0.11876000	4.87867880
C	-5.46715784	-3.48739910	1.56008804
H	-5.23427916	-3.73476100	0.51172698
H	-4.74624491	-4.00072718	2.20724010
O	-5.32487011	-1.72947395	3.15049911
O	-6.80349493	-3.81525898	1.86824501
O	-5.40766716	-0.10815400	4.75776386
O	-2.79806304	0.59517097	0.81389499
H	-3.02062511	1.48700404	0.48114201
O	-2.94231391	-2.12326097	1.67526197
H	-2.13192797	-1.83164895	1.21639001
C	-7.08096409	-5.17261124	2.20994496
C	-6.56059980	-6.12880087	1.13493299
H	-6.94624901	-5.83605099	0.15251400
H	-5.46673489	-6.12901402	1.09248698
H	-6.88772821	-7.15164995	1.34560096
C	-6.48820496	-5.50677109	3.58123398
H	-6.82132292	-6.49621201	3.91039705
H	-5.39460087	-5.51286888	3.56350493
H	-6.81429386	-4.76129913	4.31234121
C	-8.60453796	-5.22653294	2.27137804
H	-8.95031643	-6.22545815	2.55322289
H	-8.97063828	-4.50475502	3.00738692
H	-9.02771282	-4.96879482	1.29540801
C	1.80432296	-4.83093882	-3.12233996
H	1.10399604	-5.67118502	-3.15124106
H	1.26920295	-3.93526912	-2.80162001
H	2.16785502	-4.67529011	-4.14149523
C	2.52535796	-5.28531599	-0.73164803
C	1.42021704	-6.08441401	-0.41721201
C	3.21309400	-4.66555309	0.31507900
C	0.99369401	-6.24804783	0.89753097
H	0.87357700	-6.59358311	-1.20625603
C	2.80263996	-4.81850481	1.63784206
H	4.08633184	-4.05335712	0.10878200
C	1.69369602	-5.60347891	1.90550995
H	0.13242599	-6.85786915	1.14854896
H	3.33000803	-4.34308910	2.45806193
F	1.26266301	-5.71921206	3.17159200

Free Catalyst

Number of Atoms: 139

Stoichiometry: $C_{57}H_{60}F_{10}N_6O_4S_2$

Charge: 0

Multiplicity: 1

Imaginary Frequencies (cm-1): none

Energy: -4631.05263384

Enthalpy: -4629.857654

Gibbs Free Energy: -4630.040749

Dipole Moment (Debye): 3.5018

Cartesian Coordinates (Å):

C	-0.89157897	4.40561008	0.90974802
C	-0.44880900	3.23479104	1.53146005
C	0.82258898	2.72338891	1.29208195
C	1.67821896	3.39586306	0.41268200
C	1.25503397	4.58158684	-0.18507300
C	-0.02556500	5.06918621	0.05639500
N	2.89411092	2.85435510	-0.03172400
C	-1.34323704	2.47249103	2.45279908
O	-1.00975597	1.47081697	3.04771209
O	-2.55303192	3.03651595	2.53659391
C	3.74415708	1.98164296	0.60001600
N	4.52132511	1.32205796	-0.30215999
C	5.44420815	0.27302700	0.08919700
C	6.44576979	-0.00450200	-1.07033503
C	7.37804985	-1.15821099	-0.67943299
C	7.28500891	1.25869000	-1.29626799
C	5.72473288	-0.37505400	-2.37537289
C	1.91380703	2.14738703	-3.21397209
C	1.35532403	0.98919302	-2.44595790
C	0.35027701	1.18207204	-1.50420403
C	-0.11610000	0.08012300	-0.78319502
C	0.43290401	-1.18070304	-1.01000905
C	1.41671896	-1.34961402	-1.97537005
C	1.89260805	-0.27001899	-2.70143604
N	-1.12649202	0.18639700	0.20090599
C	-2.36223412	0.73930597	0.03883200
N	-3.19528008	0.50247103	1.09355700
C	-4.64262915	0.61968899	0.96067101
C	-5.35553789	0.99397600	2.28112197
C	-5.19117498	-0.05120500	3.39355111
C	-6.85043383	1.11675894	1.94461000
C	-4.88167477	2.37662196	2.78647399
C	-3.50386310	2.47066808	3.44639492
C	-5.11428595	-0.74098301	0.41309100
C	4.61336517	-0.97379398	0.45460701
O	3.67302108	-1.28633106	-0.26978800
N	4.96739817	-1.69844306	1.54074204
C	6.01913595	-1.36813402	2.50585294
C	6.26866388	-2.70497704	3.19831300
C	4.86426783	-3.30492091	3.26637602

C	4.20207024	-2.91841102	1.91762102
O	-4.82227802	-1.75258696	1.04823101
N	-5.75368595	-0.81122702	-0.77551597
C	-6.19210911	0.29521400	-1.63263094
C	-6.17696524	-0.32820499	-3.02708602
C	-6.61435318	-1.76874900	-2.75899506
C	-5.98766804	-2.14623904	-1.38925600
C	1.88856900	-2.73315501	-2.31649995
F	3.17142105	-2.75230503	-2.70479703
F	1.16802597	-3.23398805	-3.33603597
F	1.75683606	-3.58505607	-1.29336095
C	-0.43483001	6.34122181	-0.62994701
F	0.24924500	7.39462423	-0.15599699
F	-1.73667800	6.60473919	-0.47214100
F	-0.18534499	6.28267288	-1.94714296
H	-1.89439297	4.77397585	1.08172905
H	1.11876500	1.78832197	1.75539505
H	1.91186202	5.10572577	-0.87381399
H	3.14745808	3.09547901	-0.98328298
H	4.07185602	1.15855503	-1.19869602
H	5.99671412	0.64429998	0.95507401
H	8.06194782	-1.37368906	-1.50660706
H	7.99163723	-0.89821899	0.19017801
H	6.82323217	-2.07630301	-0.45528999
H	7.83336401	1.53504002	-0.38872799
H	8.01446438	1.08689797	-2.09504008
H	6.65555477	2.10572910	-1.58348799
H	5.13544321	0.46206099	-2.76886201
H	5.06257391	-1.23423195	-2.24538493
H	-0.07109500	2.16429806	-1.33213997
H	0.06000900	-2.03593111	-0.45502999
H	2.66793299	-0.40555599	-3.44991207
H	-0.98977500	-0.40831000	1.01853001
H	-2.90586710	-0.25677401	1.70972800
H	-4.82061577	1.42913997	0.25438601
H	-5.61330509	0.34304401	4.32562780
H	-5.70255280	-0.98168498	3.14306593
H	-4.14211321	-0.29870999	3.58778000
H	-7.42404985	1.36866605	2.84237409
H	-7.02490997	1.90242302	1.19966400
H	-7.24769020	0.17436901	1.55008602
H	-5.62149906	2.70136499	3.52863193
H	-4.92070198	3.10943699	1.97069395
H	-3.12910604	1.50824797	3.79483008
H	-3.54042792	3.15262294	4.30110598
H	6.91166496	-0.98872900	2.00812602
H	5.66405678	-0.60169202	3.20871091
H	6.73242998	-2.58607697	4.17994785
H	6.92763281	-3.32386208	2.57968998
H	-7.20690918	0.61067599	-1.35315204
H	-5.51318979	1.14571798	-1.55742598
H	-5.16206884	-0.29281700	-3.43413305
H	-6.83938599	0.19385400	-3.72112894
S	-2.79969311	1.65449405	-1.30343604
S	3.86907911	1.81944394	2.25464201
F	1.78802097	2.00332499	-4.53309107
F	1.36790001	3.31711292	-2.86676192
F	3.25599289	2.27442002	-2.98036289
H	6.47050619	-0.61763400	-3.13994098
H	4.31125116	-2.85166192	4.09504604
H	4.85455179	-4.38831615	3.41010404
C	2.72897601	-2.58374310	2.13309908
C	1.70765197	-3.34694791	1.62932301
C	2.41138911	-1.44965994	2.93292403
C	0.34839901	-3.03480005	1.90435398
H	1.91144300	-4.19814110	0.98953599
C	1.11644697	-1.13789904	3.24527311
H	3.21608496	-0.81116498	3.28715897
C	-0.72246599	-3.75635099	1.30466700
C	0.04750300	-1.94059205	2.76131606
H	0.88420999	-0.26557800	3.85043597
C	-2.02687311	-3.44116092	1.59274197
H	-0.48645499	-4.53571177	0.58245599
C	-1.31037796	-1.68223405	3.09871697
C	-2.32059002	-2.42956710	2.54133797
H	-2.84701610	-3.95689201	1.10223603
H	-1.52428901	-0.87261999	3.79327893
H	-3.35935807	-2.23853302	2.78572392
C	4.43669605	-4.01035023	0.87077999
H	5.51130009	-4.19655609	0.77607799
H	3.96001005	-4.94573021	1.17803597
H	4.03997803	-3.70922995	-0.10070300
H	-7.70663404	-1.80955195	-2.67169094
H	-6.31148577	-2.47097802	-3.53876305
C	-6.98922682	-2.95719790	-0.56247902
H	-7.33894110	-3.82426500	-1.13207400
H	-6.54831791	-3.28979206	0.37774101
H	-7.85946798	-2.32922697	-0.34687999
C	-4.64442015	-2.86302996	-1.57159698
C	-4.51275682	-4.24068785	-1.38626397
C	-3.51236892	-2.13894796	-1.96485102
C	-3.28607297	-4.88137197	-1.55957603
H	-5.36570883	-4.83615685	-1.07890606
C	-2.28609991	-2.76260900	-2.16141701
H	-3.56939006	-1.06113398	-2.09264398
C	-2.18810296	-4.12641096	-1.93553805
H	-3.17365193	-5.94798422	-1.39734495
H	-1.41153204	-2.20869899	-2.48346996
F	-0.99122697	-4.72552395	-2.06681895

C4-F (1,2) TS

Number of Atoms: 238
Stoichiometry: $C_{90}H_{110}F_{11}N_6O_{18}PS_2$
Charge: 0
Multiplicity: 1
Imaginary Frequencies (cm-1): -119
Energy: -7412.00442118
Enthalpy: -7409.91767
Gibbs Free Energy: -7410.208479
Dipole Moment (Debye): 8.4772
Cartesian Coordinates (Å):

C	-0.45297399	-2.28611302	-4.74349594
C	0.64033198	-1.42577004	-4.72691488
C	0.53741097	-0.17161401	-4.11898088
C	-0.64283001	0.20169701	-3.48143601
C	-1.74209094	-0.66357100	-3.48545098
C	-1.64418495	-1.88379896	-4.14280987
N	-0.67353100	1.42971396	-2.78039408
C	1.91632402	-1.89145005	-5.34513712
O	2.16753411	-3.05076909	-5.58259010
O	2.75958991	-0.87688297	-5.59329510
C	-1.68810499	2.34308100	-2.75950289
N	-1.50645101	3.32398391	-1.85384595
C	-2.54866791	4.26816607	-1.52471602

C	-1.98740697	5.40625000	-0.61715800
C	-3.00068307	6.55441713	-0.54108202
C	-0.68898797	5.93605709	-1.24282503
C	-1.69732594	4.90894508	0.80307502
C	4.89375877	3.20096397	5.07103395
C	4.89619398	1.89102995	4.33734608
C	5.15897703	1.88082898	2.97373700
C	5.00264311	0.70281398	2.24559402
C	4.56740284	-0.45477200	2.88843799
C	4.31751013	-0.42819700	4.25583982
C	4.49535799	0.73451799	4.99741983
N	5.14301109	0.76023400	0.84528297
C	5.73795223	-0.16023800	0.03549000
N	5.36912918	0.00091000	-1.25970900
C	5.58355904	-1.02721298	-2.26047611
C	5.26404905	-0.45789599	-3.69451308
C	6.53735018	0.21725900	-4.21894693
C	4.15347004	0.60162300	-3.62204003
C	4.86114693	-1.62262702	-4.63501883
C	4.11716795	-1.23164296	-5.90865993
C	4.66429520	-2.20917296	-1.90735102
C	-3.69237089	3.49322510	-0.82660300
O	-3.41128397	2.56586194	-0.05698100
N	-4.96514893	3.89890289	-1.00935495
C	-5.43395710	4.83564901	-2.03891301
C	-6.72616100	5.37044907	-1.43484199
C	-7.31428003	4.11765385	-0.78973699
C	-6.09459877	3.34331107	-0.21115801
O	3.49687195	-1.97137702	-1.60012996
N	5.15047312	-3.46668911	-2.01054001
C	6.57290316	-3.81533790	-2.15768290
C	6.61365318	-5.28154802	-1.72942305
C	5.25923109	-5.80052185	-2.20179105
C	4.27786303	-4.65744591	-1.85101998
C	3.81466889	-1.68083894	4.91478682
F	3.29840112	-1.43880606	6.12473392
F	4.79199219	-2.58974600	5.06669092
F	2.86055589	-2.27338910	4.17531300
C	-2.82873893	-2.80692506	-4.26305008
F	-3.96394110	-2.27778101	-3.79164100
F	-2.62169003	-3.97791004	-3.64362311
F	-3.04730701	-3.10620189	-5.55840778
H	-0.36772200	-3.25020504	-5.23585606
H	1.38393998	0.50614202	-4.14061213
H	-2.65092206	-0.39193001	-2.96487403
H	0.13068300	1.62540996	-2.18531489
H	-0.65467203	3.31725001	-1.28434002
H	-2.90337300	4.70667219	-2.46090889
H	-2.61720610	7.33047199	0.12909999
H	-3.16069198	7.01568794	-1.52272904
H	-3.96632695	6.22169495	-0.14225800
H	-0.80034900	6.11621284	-2.31823492
H	-0.40889999	6.87928915	-0.76062799
H	0.14108799	5.23870707	-1.09892094
H	-1.05902398	4.01928186	0.80449200
H	-2.62447190	4.66989613	1.33597100
H	5.46761799	2.78671098	2.46427894
H	4.40962601	-1.35892606	2.30746889
H	4.28475714	0.75054300	6.06101799
H	4.48654413	1.39563203	0.39303800
H	4.47569084	0.48936599	-1.35816395
H	6.63291121	-1.32323694	-2.22284389
H	6.35665894	0.69490403	-5.18862486
H	6.86984682	0.99177599	-3.52028394
H	7.35051823	-0.50705898	-4.34101820
H	3.88255811	0.94702399	-4.62260103
H	3.25905609	0.20517600	-3.13095403
H	4.48848915	1.48034000	-3.06374407
H	4.19742918	-2.32600403	-4.12635422
H	5.75867510	-2.19186497	-4.91301489
H	4.10620880	-2.06368494	-6.61555290
H	4.53381777	-0.34755099	-6.39663315
H	-4.70504618	5.61886311	-2.23155594
H	-5.61493206	4.29077816	-2.97517705
H	-7.38580990	5.81559706	-2.18261600
H	-6.49419880	6.13196611	-0.68145901
H	6.89084291	-3.70186996	-3.20333099
H	7.18792820	-3.17693591	-1.51879501
H	6.68598986	-5.34494209	-0.63862199
H	7.46017408	-5.81738615	-2.16368604
O	-2.57149410	-0.00353000	0.05825900
H	-3.19870400	0.75341803	0.03843600
C	-0.44429201	0.79512399	1.80724597
C	0.93341601	0.24261799	2.20117402
C	0.99754697	-1.16746497	1.61321402
C	1.04278195	-1.06388497	0.09075200
C	-0.61125600	0.71370798	0.31057599
H	1.73079395	0.87062401	1.76600397
H	-1.19799900	0.15005200	2.27969098
H	1.99290800	-0.61636502	-0.22336300
O	0.04159700	-0.09705700	-0.42035800
O	-0.59375501	2.12976289	2.20181203
O	1.07713795	0.15031999	3.58797789
C	0.87018198	-2.34249902	-0.69603401
H	0.95595402	-2.11418009	-1.76971197
H	1.71038496	-2.99967098	-0.43107101
O	-0.36056799	-2.96967411	-0.41802701
C	-1.77853203	2.40449905	2.92995906
H	-1.68298900	3.43244696	3.28823495
H	-2.66143107	2.31128812	2.28831506
H	-1.86861598	1.72075200	3.78387094
C	1.41498005	1.36479402	4.23486185
H	2.19913697	1.90149605	3.68339491
H	0.55126703	2.02780199	4.34620619
H	1.79112899	1.09176505	5.22283220
C	-0.46529400	-4.23190308	-1.05991304
H	-1.43392098	-4.64238119	-0.77657998
H	-0.41902599	-4.11746693	-2.15144610
H	0.34560201	-4.88863993	-0.72263497
S	6.84585381	-1.30344605	0.57921100
S	-3.02635407	2.28419089	-3.78381395
F	5.20487499	3.04881096	6.36632299
F	5.75562620	4.07828999	4.54209900
F	3.67503095	3.76647091	5.02412796
H	-1.17445195	5.69600916	1.35951304
H	-7.80012083	3.50655198	-1.55661702
H	-8.05076790	4.32234192	-0.00803300
C	-6.31957388	1.85281706	-0.45436099
C	-7.15503216	1.12065697	0.35731000
C	-5.79965115	1.24439704	-1.63075602
C	-7.50632381	-0.22344500	0.04501100
H	-7.58724594	1.55668199	1.25501704
C	-6.13051319	-0.04093300	-1.96617103
H	-5.12764406	1.80471098	-2.27353191

C	-8.34102917	-1.00172198	0.89058000
C	-6.99489403	-0.81347799	-1.14352798
H	-5.71181393	-0.49106899	-2.86368608
C	-8.65540695	-2.29815197	0.56708097
H	-8.71554375	-0.55864501	1.80985999
C	-7.33337212	-2.15690088	-1.45451200
C	-8.14934444	-2.88180208	-0.62064803
H	-9.26970100	-2.89041090	1.23694301
H	-6.92383480	-2.59842896	-2.36038709
H	-8.40223122	-3.90955091	-0.86261499
C	-5.87559891	3.69084406	1.26586902
H	-5.75757122	4.77437401	1.37334394
H	-6.73407888	3.38718605	1.87030494
H	-4.97967100	3.19584608	1.64672899
H	5.26921988	-5.93917513	-3.28986692
H	4.95799303	-6.74236917	-1.73696804
H	1.92610204	-1.65513694	1.94298995
C	0.09657600	-3.20367193	2.46383691
H	-0.88356501	-3.62696791	2.69150710
H	0.54571003	-3.78073311	1.64826000
H	0.74351603	-3.24587202	3.34678602
O	-0.13242801	-1.85987902	2.08267593
H	-1.08582795	1.54229105	-0.20040201
O	2.87789702	1.39527202	-0.87995100
P	2.33010006	2.71574402	-0.43040600
O	3.08605695	3.00878811	0.98317200
O	2.96877599	3.96019292	-1.28107095
O	0.83841097	2.86901402	-0.33253700
C	2.39538002	4.34716082	-2.47384810
C	2.35597396	5.70767403	-2.76066208
C	1.87821603	3.41332507	-3.36758804
C	1.76116502	6.13285112	-3.94449806
H	2.77251291	6.40652609	-2.04277110
C	1.25737596	3.85099292	-4.53381920
H	1.98511803	2.35572290	-3.14422894
C	1.19532800	5.21149397	-4.82529593
H	1.72469795	7.19415188	-4.17095804
H	0.82384098	3.12229705	-5.21310616
H	0.71385199	5.55119610	-5.73618507
C	2.90014505	4.18092918	1.70527005
C	3.97736406	5.05034018	1.83102095
C	1.68514299	4.42716694	2.33427811
C	3.84288597	6.18172884	2.63070107
H	4.89915085	4.83244324	1.30055499
C	1.56399405	5.56878996	3.12252903
H	0.87033200	3.72113609	2.20532990
C	2.63784099	6.44260216	3.27845502
H	4.68356323	6.85834885	2.74657607
H	0.62266999	5.76922512	3.62658501
H	2.53741097	7.32324123	3.90464306
C	-3.09015703	-1.16523194	0.68010402
C	-4.15936518	-0.84541398	1.71425700
C	-3.69090390	-2.09652710	-0.37130499
H	-2.24987888	-1.66446400	1.18086803
H	-5.02795315	-0.36767301	1.21525395
C	-4.25258303	-3.32832003	0.32510000
H	-4.53440714	-1.57801104	-0.84272200
C	-5.21730900	-2.92315292	1.43028998
H	-4.74088383	-3.98346090	-0.40595499
H	-6.07665205	-2.42092800	0.96562397
C	-4.61718416	0.50044799	3.55675602
H	-5.00575113	-0.30249500	4.18899679
H	-4.13749790	1.25944602	4.17772579
H	-5.44631910	0.95664197	2.99747396
C	-5.72219801	-4.10658216	2.22976303
H	-6.02928591	-4.90670013	1.53998005
H	-4.89103794	-4.48345518	2.83537507
O	-4.57824802	-2.03580999	2.33857799
O	-6.82125521	-3.69147706	3.00615406
O	-3.63337302	0.01040500	2.66444802
C	-6.85934496	-4.10118389	4.37630177
C	-6.77423477	-5.62423992	4.49618196
H	-7.54506207	-6.09166813	3.87531900
H	-5.79690695	-6.00309086	4.18160105
H	-6.93071508	-5.93207979	5.53457022
C	-5.74418783	-3.41347194	5.16487122
H	-5.80209398	-3.68463898	6.22382879
H	-4.75200081	-3.69009995	4.79702520
H	-5.84497786	-2.32883596	5.06990480
C	-8.22180462	-3.61394405	4.85926819
H	-8.35845470	-3.83160210	5.92261696
H	-8.30349922	-2.53377199	4.70612812
H	-9.01917267	-4.10488510	4.29334116
C	3.11324000	-4.62993097	-2.84773111
H	2.60037088	-5.59637308	-2.85751009
H	2.39074707	-3.84793305	-2.60735011
H	3.49083996	-4.45224619	-3.85868597
C	3.79837298	-4.80497694	-0.40323400
C	2.81349301	-5.74699497	-0.08540800
C	4.35827684	-4.06160498	0.63915300
C	2.36443591	-5.91552114	1.22183800
H	2.37848091	-6.36573982	-0.86547899
C	3.93284011	-4.22488403	1.95587301
H	5.14052820	-3.33674002	0.43306899
C	2.92707896	-5.13893604	2.22344398
H	1.58979201	-6.63278580	1.47172499
H	4.38303089	-3.67114305	2.77235389
F	2.47762895	-5.27462292	3.48080802
F	-3.19334292	-4.03901815	0.88985300
O	-2.78276491	-2.42059207	-1.37835598
H	-1.87773597	-2.39142108	-1.00741303

C4-F (1,3) TS

Number of Atoms: 238

Stoichiometry: $C_{90}H_{110}F_{11}N_6O_{18}PS_2$

Charge: 0

Multiplicity: 1

Imaginary Frequencies (cm-1): -115

Energy: -7411.99429049

Enthalpy: -7409.907437

Gibbs Free Energy: -7410.197507

Dipole Moment (Debye): 9.4813

Cartesian Coordinates (Å):

C	0.98087800	-2.42127609	4.19103479
C	-0.03353200	-1.53320396	4.53819990
C	-0.05452000	-0.24326000	4.00254679
C	0.91748202	0.14652400	3.08986092
C	1.93407798	-0.73977798	2.72812891
C	1.96889806	-2.00746989	3.30068898
N	0.83398801	1.42663205	2.48282504
C	-1.11096096	-2.01531005	5.45319605
O	-1.24540806	-3.17003894	5.78711510
O	-1.92385495	-1.02305901	5.83990812
C	1.86472404	2.31853700	2.45689607

N	1.75983405	3.25688100	1.49218500
C	2.79481101	4.23083210	1.22706199
C	2.30110097	5.23903084	0.13917699
C	3.43422890	6.21326590	-0.20677701
C	1.12969899	6.03730011	0.72751701
C	1.83111596	4.53530979	-1.14404094
C	-5.96310377	3.39704704	-4.01332188
C	-5.77524281	2.01067400	-3.46878505
C	-5.61469603	1.84216702	-2.09691000
C	-5.26806116	0.59317797	-1.58902895
C	-5.07635117	-0.48149300	-2.45933104
C	-5.24723291	-0.29601100	-3.82277393
C	-5.61050797	0.94495600	-4.34250307
N	-4.99673510	0.47850999	-0.21348500
C	-5.45878315	-0.46317399	0.65416598
N	-4.93380022	-0.30227700	1.89256203
C	-4.99507999	-1.33300495	2.91096306
C	-4.64407301	-0.72150898	4.31785393
C	-5.93089914	-0.12057200	4.89835978
C	-3.62303996	0.41634101	4.15620184
C	-4.13014603	-1.84290600	5.26549578
C	-3.19631910	-1.40520704	6.38925695
C	-4.01034307	-2.44136190	2.49594903
C	4.05358601	3.48353410	0.74727201
O	3.93056297	2.57294893	-0.09337200
N	5.26715803	3.86086106	1.16028595
C	5.53627777	4.83132696	2.23369694
C	7.03102207	5.11055183	2.09462905
C	7.57652187	3.77026391	1.60728896
C	6.51747322	3.25385094	0.60370398
O	-2.89147592	-2.11942101	2.09940004
N	-4.40225077	-3.72995210	2.62515807
C	-5.77844095	-4.16200495	2.92687392
C	-5.76204300	-5.65291882	2.59026599
C	-4.32361794	-6.04881191	2.90527010
C	-3.48880291	-4.86832809	2.35882306
C	-4.98404789	-1.43006694	-4.77230310
F	-4.29556990	-1.00829506	-5.84395790
F	-6.11803722	-1.97748804	-5.22903299
F	-4.27240896	-2.41174507	-4.19487715
C	3.11991596	-2.91869092	2.98855495
F	3.51287007	-2.81713390	1.70345402
F	2.82717609	-4.20570421	3.21653795
F	4.20513487	-2.63017011	3.73099899
H	0.98228598	-3.42006493	4.61537695
H	-0.82820201	0.45761201	4.29259396
H	2.68293595	-0.42976701	2.00364995
H	0.05684500	1.57095397	1.83550704
H	0.84757799	3.36899209	1.03846598
H	3.01528811	4.78257322	2.14763188
H	3.07572603	6.93414783	-0.94793200
H	3.75757289	6.78399611	0.67130297
H	4.30380678	5.70288801	-0.63601202
H	1.42574406	6.56292582	1.64175904
H	0.79171902	6.78164196	-0.00187200
H	0.27007899	5.40094090	0.96353900
H	0.93261701	3.93281388	-0.97820401
H	2.60268593	3.89683390	-1.58544004
H	-5.73757410	2.68086600	-1.42070603
H	-4.78163481	-1.44456005	-2.05951190
H	-5.71677685	1.08652496	-5.41329288
H	-4.33888578	1.16249895	0.15954800
H	-4.07637501	0.25574401	1.90675199
H	-6.01727676	-1.71169496	2.93623400
H	-5.72926521	0.37403500	5.85580492
H	-6.34519386	0.62582803	4.21314716
H	-6.69089413	-0.89190000	5.06620216
H	-3.28903604	0.78340501	5.12908220
H	-2.75151896	0.09143500	3.58300710
H	-4.07401180	1.26403904	3.63404608
H	-3.57789207	-2.61218309	4.71889019
H	-4.99068403	-2.35501409	5.71617413
H	-3.04431105	-2.22074199	7.09938812
H	-3.55143595	-0.52153301	6.92397499
H	4.93591499	5.73251581	2.10986495
H	5.28613710	4.37219620	3.19839907
H	7.47488689	5.43408585	3.03817797
H	7.20140123	5.89681387	1.35224700
H	-6.00359106	-4.00005722	3.98990202
H	-6.49524593	-3.60581589	2.31704593
H	-5.96794415	-5.79383087	1.52425003
H	-6.50406313	-6.21369123	3.16221499
C	0.10677600	0.78302699	-2.16314006
C	-1.35430706	0.29690400	-2.22582293
C	-1.34463894	-1.12179196	-1.65390205
C	-0.99704701	-1.05389297	-0.16185600
C	0.51379102	0.79452902	-0.71584702
H	-1.99719203	0.95050198	-1.61001205
H	0.71239698	0.05927300	-2.72057199
H	-1.87683904	-0.69024003	0.38166600
O	0.00400200	-0.01458000	0.14235701
O	0.24207500	2.09407401	-2.63890505
O	-1.81021094	0.25136501	-3.54657292
C	-0.53881902	-2.31980896	0.52468002
H	-0.47656301	-2.12767291	1.60715795
H	-1.32450497	-3.07812691	0.37932700
O	0.70256001	-2.74915099	0.02697000
C	0.95949900	2.23860192	-3.85751295
H	0.69423300	3.22276402	-4.25236320
H	2.03955007	2.20156789	-3.68327308
H	0.65556699	1.47091699	-4.57909584
C	-2.38460112	1.45796394	-4.01742601
H	-3.09034204	1.86882102	-3.28332710
H	-1.63048196	2.22086000	-4.23555899
H	-2.92020893	1.20283997	-4.93335199
C	0.99211901	-4.05210304	0.46955600
H	1.98579097	-4.31380415	0.09876700
H	0.98974401	-4.11371613	1.56779301
H	0.25524500	-4.77161694	0.08239200
S	-6.58612585	-1.64669502	0.24588700
S	3.13459396	2.26904607	3.56118894
F	-6.62424707	3.39176989	-5.17934608
F	-6.63580704	4.18565893	-3.16452599
F	-4.77381182	3.98106790	-4.23715591
H	1.56015503	5.30050278	-1.88113701
H	7.64590788	3.07140803	2.44749188
H	8.56126690	3.83340096	1.13766098
C	6.50177813	1.72763205	0.63027698
C	7.14025021	0.96573800	-0.31807300
C	5.89473200	1.07393503	1.73844600
C	7.21212196	-0.45312801	-0.20189600
H	7.61300278	1.42164099	-1.18397796
C	5.91258192	-0.28879401	1.85934496
H	5.38044500	1.66999495	2.48501301

C	7.88040304	-1.25246704	-1.16884506
C	6.58061695	-1.09561396	0.89751297
H	5.42145109	-0.76784497	2.70274401
C	7.90167284	-2.61955905	-1.05614603
H	8.36139297	-0.76026601	-2.01113605
C	6.62938309	-2.51205993	0.99811202
C	7.27032280	-3.25669193	0.04034700
H	8.38361454	-3.22359490	-1.81770301
H	6.13884306	-2.98777509	1.84240305
H	7.28216410	-4.34011889	0.10502700
C	6.75854778	3.83737111	-0.79231101
H	6.74492979	4.93010616	-0.74488503
H	7.73500681	3.53368998	-1.17772603
H	5.99009418	3.51219010	-1.49919295
H	-4.17760181	-6.11196184	3.99069190
H	-4.01705694	-6.99790716	2.45896602
H	-2.35747194	-1.54978800	-1.72835600
C	-0.73895401	-3.19426394	-2.65454602
H	0.07307300	-3.59472990	-3.26416206
H	-0.78878403	-3.75999188	-1.71706402
H	-1.68906403	-3.30004907	-3.19478798
O	-0.43732899	-1.83854604	-2.43849111
H	0.74427199	1.76994205	-0.30755600
O	-2.64188409	1.37425697	1.31232595
P	-2.26459098	2.73077989	0.80445999
O	-3.24400592	2.96782398	-0.48289201
O	-2.82808709	3.91096497	1.78274703
O	-0.82990801	3.00754690	0.45662501
C	-1.96903300	4.71467590	2.50445890
C	-2.12127495	6.09251022	2.39460993
C	-1.00160897	4.16363192	3.34044909
C	-1.29068303	6.92729521	3.13751006
H	-2.87994695	6.48377180	1.72452295
C	-0.15844899	5.00717783	4.05824900
H	-0.91727501	3.08418202	3.42945290
C	-0.30604601	6.39006615	3.96488595
H	-1.40872097	8.00377941	3.05962205
H	0.60919601	4.57449293	4.69352484
H	0.34457901	7.04657507	4.53405190
C	-3.18165994	4.14668512	-1.21558297
C	-4.23897505	5.04355717	-1.11691296
C	-2.10314894	4.37825108	-2.06320500
C	-4.22788477	6.19051313	-1.90676606
H	-5.05095720	4.83319998	-0.42743799
C	-2.10344696	5.53343678	-2.83983397
H	-1.29333198	3.65511394	-2.10675311
C	-3.16249800	6.43672514	-2.76885104
H	-5.05756378	6.88795996	-1.84942806
H	-1.27024400	5.72384882	-3.51025891
H	-3.15920401	7.32898617	-3.38663697
C	3.78319311	0.39217600	-2.68934298
C	4.95673418	-0.41304401	-3.25988197
C	3.48216891	-0.13645799	-1.28695297
H	2.92677212	0.20732699	-3.34795189
H	5.86421585	-0.21127400	-2.65647602
C	3.23461008	-1.62580705	-1.32981896
H	4.35807896	0.04274400	-0.64206898
C	4.47326088	-2.29031205	-1.92160904
H	2.97298598	-2.00581789	-0.33835399
H	5.33526993	-2.05460596	-1.28482497
C	6.30679417	-0.60007900	-5.14185381
H	6.24966383	-1.69281399	-5.15333509
H	6.37443495	-0.21974100	-6.16170788
H	7.20249701	-0.29486501	-4.58133888
C	4.33117294	-3.79467010	-2.00191402
H	4.08587694	-4.17379189	-0.99658298
H	3.50009894	-4.02980709	-2.67870593
O	4.67842293	-1.79735005	-3.23067594
O	5.55609083	-4.31785917	-2.45056701
O	5.14510679	-0.03284400	-4.57076693
O	2.39618111	0.54848200	-0.64195800
H	2.74921393	1.43631899	-0.35626999
C	5.52713203	-5.60623312	-3.06867003
C	4.86843777	-6.63694477	-2.15046310
H	5.35771418	-6.63548708	-1.17066598
H	3.80355096	-6.42554283	-2.00777197
H	4.95447016	-7.63944912	-2.58052111
C	4.81616306	-5.53209114	-4.42208195
H	4.94234991	-6.47189522	-4.96866512
H	3.74222398	-5.35466290	-4.31426096
H	5.24037886	-4.71644020	-5.01468086
C	7.00165701	-5.94094896	-3.27022290
H	7.11892796	-6.91298819	-3.75799489
H	7.47315121	-5.17466497	-3.89286494
H	7.51564312	-5.96767712	-2.30409408
C	-2.17200708	-4.74644279	3.13248205
H	-1.63126397	-5.69719982	3.09236789
H	-1.53538895	-3.95727396	2.72914195
H	-2.37337804	-4.52947187	4.18479204
C	-3.25485992	-5.05134821	0.85640699
C	-2.35312009	-6.02554703	0.41299200
C	-3.95855808	-4.31525993	-0.10072500
C	-2.14391088	-6.25591803	-0.94346201
H	-1.80059302	-6.62362814	1.13260102
C	-3.76486611	-4.53306818	-1.46328497
H	-4.67607689	-3.56034303	0.20805100
C	-2.85651588	-5.49946117	-1.86070204
H	-1.44278896	-7.00475883	-1.29602504
H	-4.30663013	-3.96669888	-2.21415496
F	-2.63071489	-5.68791008	-3.17114091
F	2.16650105	-1.86710799	-2.17547607
O	4.05759478	1.77145100	-2.70212293
H	4.36557722	2.04546094	-1.82057405

C4-OMe (1,2) TS

Number of Atoms: 242
Stoichiometry: $C_{91}H_{113}F_{10}N_6O_{19}PS_2$
Charge: 0
Multiplicity: 1
Imaginary Frequencies (cm-1): -94
Energy: -7427.27104155
Enthalpy: -7425.141531
Gibbs Free Energy: -7425.438098
Dipole Moment (Debye): 8.2879
Cartesian Coordinates (Å):

C	-0.70391101	-2.00683403	-4.72450686
C	0.48017099	-1.27767897	-4.75981188
C	0.56005597	-0.03441600	-4.12468815
C	-0.53213900	0.46080700	-3.42033410
C	-1.73204303	-0.25760299	-3.39654994
C	-1.80906606	-1.47822797	-4.05774021
N	-0.38197899	1.65503204	-2.67447090
C	1.65852797	-1.86980402	-5.45852804
O	1.75022697	-3.03831506	-5.75801086

O	2.61221600	-0.95724601	-5.69817591
C	-1.24196899	2.71203804	-2.65690708
N	-0.96401697	3.61767101	-1.69805801
C	-1.91366303	4.64193201	-1.32882500
C	-1.28414202	5.64030695	-0.30904901
C	-2.18089390	6.87824917	-0.18746001
C	0.09150100	6.07451916	-0.83200198
C	-1.11551297	5.01669502	1.08056295
C	5.46951008	2.60162091	4.98850584
C	5.27222300	1.32630599	4.22076893
C	5.52089977	1.31016099	2.85497594
C	5.20892477	0.17713700	2.10626698
C	4.63795805	-0.93057901	2.73104310
C	4.39953995	-0.89783698	4.10005093
C	4.73015881	0.21770500	4.86155176
N	5.33890820	0.25105500	0.70549101
C	5.77523422	-0.72570199	-0.13714600
N	5.40811300	-0.48009801	-1.42079401
C	5.42989016	-1.51570499	-2.43662405
C	5.17838287	-0.88045400	-3.85408401
C	6.52284813	-0.35554600	-4.37325287
C	4.21063805	0.30782101	-3.74206305
C	4.63495016	-1.96597302	-4.81980181
C	3.90977407	-1.45846903	-6.06252909
C	4.33875084	-2.53799701	-2.06764793
C	-3.15728092	3.93585801	-0.73796803
O	-2.99551702	2.93172503	-0.03466800
N	-4.37882280	4.46917009	-0.93676198
C	-4.71568203	5.51639080	-1.90913796
C	-5.98251915	6.12159681	-1.31720197
C	-6.70394611	4.88464117	-0.78659302
C	-5.58245277	3.97078395	-0.21393099
O	3.24255991	-2.11982989	-1.69785595
N	4.60738182	-3.85574389	-2.21935105
C	5.94975615	-4.42124081	-2.43437505
C	5.76696920	-5.89592695	-2.07700801
C	4.32718992	-6.16316700	-2.50379992
C	3.56357408	-4.89720106	-2.04853702
C	3.75421691	-2.08863997	4.74970722
F	3.19221807	-1.77370095	5.92337179
F	4.64175606	-3.07042003	4.98076820
F	2.79855204	-2.62144804	3.96959400
C	-3.09021997	-2.27067804	-4.06457281
F	-4.16267395	-1.52714801	-3.77112603
F	-3.06476593	-3.29657102	-3.19454598
F	-3.30278301	-2.81647396	-5.27475977
H	-0.75495201	-2.96584010	-5.23102283
H	1.47834206	0.53952903	-4.17623520
H	-2.58147812	0.12206900	-2.84361506
H	0.37180901	1.66476202	-1.98812997
H	-0.17352299	3.43520689	-1.07192695
H	-2.17849803	5.18862200	-2.23729992
H	-1.75751495	7.56179619	0.55550700
H	-2.24586892	7.42133808	-1.13761997
H	-3.19358492	6.61741114	0.14248499
H	0.05524700	6.34282923	-1.89369595
H	0.44187301	6.94366503	-0.26395401
H	0.83518797	5.28197289	-0.70629001
H	-0.55331302	4.07708311	1.04705501
H	-2.08541012	4.82625484	1.55196297
H	5.94114017	2.17850494	2.36038995
H	4.36410999	-1.79684496	2.13596606
H	4.53577089	0.23782900	5.92820692
H	4.77862692	0.98968101	0.28002000
H	4.59205198	0.13304099	-1.48371506
H	6.41745806	-1.97906196	-2.42704511
H	6.39646292	0.16126101	-5.33149719
H	6.95163393	0.35668799	-3.66118693
H	7.24010611	-1.17137003	-4.51701021
H	3.95995688	0.70279598	-4.72934294
H	3.28732610	0.01788900	-3.23094702
H	4.66656399	1.12765598	-3.18063307
H	3.91708302	-2.62038112	-4.31815100
H	5.46408892	-2.61142397	-5.13967800
H	3.78375793	-2.26399398	-6.78871584
H	4.41454220	-0.61579198	-6.54049921
H	-3.91167688	6.24144411	-2.01231599
H	-4.90009499	5.06004906	-2.89083195
H	-6.56779289	6.67364120	-2.05563092
H	-5.72010994	6.80622292	-0.50252301
H	6.25195217	-4.30586386	-3.48431897
H	6.67864990	-3.92300510	-1.78999901
H	5.87392998	-6.03043318	-0.99568701
H	6.49496794	-6.53688192	-2.57846904
O	-2.60608792	0.50609303	1.01244605
H	-3.14696789	1.06697094	0.41874999
C	-0.21062900	0.89866102	2.15241408
C	1.13772202	0.20206399	2.37090111
C	1.01266897	-1.14021504	1.63602102
C	0.91525900	-0.89852601	0.13465500
C	-0.55606002	0.94690198	0.68130898
H	1.96163797	0.80491900	1.94938803
H	-0.95713902	0.26262501	2.64814806
H	1.84992301	-0.45806900	-0.23724900
O	-0.10558500	0.12547000	-0.17766500
O	-0.24526601	2.19939208	2.66767597
O	1.37099397	-0.09033200	3.71799397
C	0.59045303	-2.08962893	-0.73709202
H	0.69253898	-1.80103898	-1.79458702
H	1.34433997	-2.86354399	-0.53679800
O	-0.71053499	-2.57300806	-0.48939800
C	-1.51243901	2.55761600	3.20313311
H	-1.38539302	3.54321599	3.65540195
H	-2.27412510	2.60372305	2.41668105
H	-1.82484198	1.82870102	3.96107411
C	1.63850296	1.02459598	4.54975080
H	2.35810089	1.71105599	4.08237791
H	0.72714800	1.57978404	4.79074717
H	2.06821394	0.61792701	5.46696377
C	-0.93049800	-3.79282093	-1.17281902
H	-1.98234200	-4.03442383	-1.04158604
H	-0.70892900	-3.68535304	-2.24315405
H	-0.29413000	-4.58131886	-0.74844998
S	6.71399784	-2.03354311	0.35124800
S	-2.50749207	2.89609694	-3.75697398
F	5.80029202	2.36674595	6.26698685
F	6.42683411	3.36955094	4.45258617
F	4.34059477	3.32998490	5.00425482
H	-0.55439597	5.71005011	1.71851802
H	-7.20173693	4.37009001	-1.61441803
H	-7.45731878	5.09985781	-0.02409800
C	-5.93084908	2.52283311	-0.55185598
C	-6.85358381	1.82889199	0.19699501
C	-5.44112587	1.93716502	-1.75226200

C	-7.33526087	0.55397499	-0.21093901
H	-7.26577377	2.25215912	1.10951996
C	-5.87652111	0.70654899	-2.16653204
H	-4.70333195	2.46833396	-2.34644794
C	-8.29330540	-0.16778401	0.55043501
C	-6.83586407	-0.02176500	-1.41208303
H	-5.47589016	0.27045000	-3.07651806
C	-8.71404934	-1.41159904	0.15051700
H	-8.66918468	0.26937300	1.47202206
C	-7.28253222	-1.31229997	-1.79862595
C	-8.19908524	-1.99290299	-1.03422403
H	-9.42516804	-1.96393502	0.75670701
H	-6.87062788	-1.75218999	-2.70375800
H	-8.53369522	-2.98114991	-1.33586001
C	-5.39225817	4.21157885	1.28846502
H	-5.15998888	5.26744986	1.46311700
H	-6.30435991	3.97493410	1.84134603
H	-4.57545805	3.59821510	1.67444003
H	4.26729012	-6.24029922	-3.59629107
H	3.89666104	-7.06861496	-2.06946611
H	1.91475201	-1.73905802	1.82576203
C	-0.03167400	-3.17126012	2.32890391
H	-1.04057395	-3.52686501	2.54942608
H	0.32870901	-3.67719507	1.42658603
H	0.63883299	-3.39363694	3.16617298
O	-0.13830800	-1.77413297	2.13549900
H	-1.03997302	1.83095300	0.27163199
O	3.15840697	1.27327096	-0.94981599
P	2.68812203	2.56081700	-0.34360600
O	3.55854297	2.72571111	1.02097094
O	3.28555107	3.85916996	-1.13700902
O	1.21099496	2.72736907	-0.09803700
C	2.78582311	4.24683380	-2.36316991
C	2.83389997	5.60468578	-2.66551900
C	2.26482391	3.33181310	-3.27364492
C	2.31576490	6.04964685	-3.87668300
H	3.25541592	6.28785276	-1.93529499
C	1.71990502	3.79306293	-4.46943903
H	2.30057001	2.27208591	-3.04259610
C	1.74006903	5.15073919	-4.77442598
H	2.34718895	7.10915089	-4.11234713
H	1.27625501	3.08195901	-5.16093302
H	1.31447399	5.50594902	-5.70686817
C	3.49013996	3.85907006	1.82257199
C	4.63786077	4.63264084	1.95178795
C	2.32291508	4.16319418	2.51346111
C	4.62309694	5.72656822	2.81196499
H	5.52008581	4.37249899	1.37526000
C	2.32253194	5.26730394	3.36286092
H	1.44487405	3.53734589	2.38798308
C	3.46640706	6.04654217	3.51870608
H	5.51936579	6.32752609	2.92866707
H	1.41890299	5.51061678	3.91458106
H	3.45884204	6.89791584	4.19169617
C	-3.16440392	-0.77789497	1.23864496
C	-4.08454990	-0.71518099	2.45352197
C	-3.92645597	-1.25269699	0.01067400
H	-2.33186412	-1.45563805	1.46530902
H	-4.84577179	0.08011300	2.29407191
C	-4.67291689	-2.55115104	0.31341100
H	-4.69124508	-0.49574700	-0.21135101
C	-5.55418205	-2.29719996	1.54056096
H	-5.29536581	-2.79631090	-0.55945599
H	-6.23190403	-1.46309304	1.30085301
C	-4.07893896	-0.21315400	4.73262691
H	-4.66106415	-1.10223496	4.99081421
H	-3.37480807	0.01413000	5.53422785
H	-4.76192713	0.63702899	4.59385395
C	-6.41540718	-3.46735811	1.96176195
H	-6.90375805	-3.89387703	1.07088399
H	-5.77101803	-4.23454094	2.41306496
O	-4.73582983	-1.94645703	2.64620090
O	-7.37136793	-2.97643399	2.86981392
O	-3.31125498	-0.43076199	3.56419802
C	-8.03370380	-3.93397403	3.69896889
C	-8.64587307	-5.05769491	2.86060405
H	-9.27922058	-4.63774490	2.07165599
H	-7.87523890	-5.67964411	2.39350891
H	-9.26167870	-5.70727491	3.48990893
C	-7.06503820	-4.49017906	4.74538612
H	-7.60260010	-5.11058378	5.46931696
H	-6.28437090	-5.10963202	4.29425907
H	-6.58374310	-3.66397810	5.27651787
C	-9.13222027	-3.12464809	4.38088703
H	-9.70514488	-3.74947691	5.07219124
H	-8.68893337	-2.29494596	4.93879509
H	-9.81353855	-2.71061301	3.63139009
C	2.36387992	-4.64010096	-2.96643209
H	1.67981505	-5.49399710	-2.94381094
H	1.81782401	-3.74086499	-2.67603707
H	2.70200205	-4.52127981	-3.99956894
C	3.15739703	-5.04229403	-0.57801801
C	2.08869100	-5.87457323	-0.22497600
C	3.88109589	-4.42978191	0.44836500
C	1.72998405	-6.06961823	1.10627902
H	1.52314901	-6.39232779	-0.99514699
C	3.54611397	-4.62174177	1.78687704
H	4.72912598	-3.79377103	0.21221000
C	2.46409202	-5.42975521	2.09370494
H	0.89687902	-6.70550823	1.38651597
H	4.12059689	-4.16911793	2.58750701
F	2.10666609	-5.59199286	3.37703705
O	-3.10357308	-1.33011901	-1.11736298
H	-2.23975706	-1.70941401	-0.85317802
O	-3.72554111	-3.57702804	0.54918802
C	-4.10404921	-4.83070898	0.02785600
H	-3.30282497	-5.53312588	0.26945400
H	-5.03736019	-5.20094299	0.47169501
H	-4.22710085	-4.78254890	-1.06340206

C4-OMe (1,3) TS

Number of Atoms: 242
Stoichiometry: $C_{91}H_{113}F_{10}N_6O_{19}PS_2$
Charge: 0
Multiplicity: 1
Imaginary Frequencies (cm-1): -129
Energy: -7427.25886937
Enthalpy: -7425.129136
Gibbs Free Energy: -7425.42271
Dipole Moment (Debye): 6.889
Cartesian Coordinates (Å):

C	1.00397801	-2.27791190	4.19360924
C	0.01211500	-1.36516798	4.54215622
C	0.00639200	-0.08354700	3.98574901

C	0.97348100	0.27582300	3.05560708
C	1.97180402	-0.63302702	2.69872689
C	1.98755097	-1.89503896	3.28413701
N	0.89510202	1.54088104	2.41808510
C	-1.06309903	-1.81123900	5.47819710
O	-1.22163498	-2.95878792	5.82657909
O	-1.84339201	-0.79446900	5.86692715
C	1.93572199	2.42114305	2.35628796
N	1.84078598	3.31796193	1.35396099
C	2.88497806	4.27035189	1.05393505
C	2.40543699	5.25139618	-0.06228100
C	3.50322008	6.28939486	-0.32897800
C	1.15322399	5.98540020	0.43818101
C	2.07256293	4.52649689	-1.37460101
C	-5.97710896	3.45718288	-3.96467090
C	-5.82277107	2.06784391	-3.41679502
C	-5.57404900	1.90901899	-2.05614996
C	-5.27140808	0.64898401	-1.54979897
C	-5.21820688	-0.45176101	-2.40846205
C	-5.48397923	-0.27618000	-3.75700307
C	-5.79586411	0.97996801	-4.27650213
N	-4.92084599	0.53452998	-0.19072101
C	-5.44597483	-0.31696799	0.73334599
N	-4.90712118	-0.12078900	1.96148503
C	-4.98386002	-1.11582899	3.01482606
C	-4.59232807	-0.47484499	4.39787722
C	-5.85470390	0.16869400	4.98629713
C	-3.55166101	0.63629001	4.18598080
C	-4.08230877	-1.58060801	5.36666584
C	-3.11034799	-1.13571405	6.45456314
C	-4.04075718	-2.26581502	2.61528993
C	4.13232613	3.48563600	0.59966600
O	3.99634790	2.53331494	-0.18756500
N	5.35220289	3.87927604	0.98639601
C	5.63224506	4.89706278	2.01127601
C	7.12598801	5.16596699	1.84443104
C	7.66502714	3.80128288	1.42146003
C	6.59432697	3.23509693	0.45737699
O	-2.92554903	-1.98739505	2.17757297
N	-4.46319008	-3.53715897	2.80098391
C	-5.83674383	-3.91020894	3.18500495
C	-5.87567711	-5.42303705	2.96198392
C	-4.42746782	-5.83582687	3.20103693
C	-3.60464001	-4.71504402	2.52408504
C	-5.37500620	-1.43160999	-4.70989799
F	-4.52167082	-1.15044904	-5.70744324
F	-6.55312586	-1.71900403	-5.27994299
F	-4.93676615	-2.54808497	-4.10765791
C	3.10514998	-2.83903193	2.94908500
F	3.46125007	-2.75779390	1.65252399
F	2.78392506	-4.11592817	3.19714999
F	4.21591377	-2.57406902	3.66231990
H	0.99026000	-3.27189398	4.62889910
H	-0.75232702	0.63492501	4.27219105
H	2.71889091	-0.34649101	1.96240604
H	0.13090400	1.66287804	1.75131702
H	0.93597698	3.40617490	0.88145697
H	3.11129403	4.84785223	1.95724404
H	3.18348002	6.95576811	-1.13605702
H	3.68490505	6.91139889	0.55498803
H	4.44818306	5.82622623	-0.63606101
H	1.32516503	6.44601011	1.41681504
H	0.88872898	6.77698898	-0.27167401
H	0.28597501	5.32256079	0.51951200
H	1.27136600	3.78793502	-1.24873996
H	2.94589710	4.02754879	-1.80560303
H	-5.59977722	2.76350594	-1.38914096
H	-4.96328592	-1.42814302	-2.01340199
H	-5.98165512	1.10826802	-5.33831596
H	-4.23385811	1.20950603	0.14732300
H	-4.03592014	0.41426101	1.94878197
H	-6.01671410	-1.46099699	3.06514502
H	-5.62424707	0.68393397	5.92618513
H	-6.26681995	0.90519202	4.28915310
H	-6.62709904	-0.58168799	5.18896294
H	-3.19393611	1.02474701	5.14204597
H	-2.69558907	0.27741501	3.60967207
H	-3.99387908	1.47688103	3.64544606
H	-3.56425905	-2.38091707	4.83125591
H	-4.94346380	-2.05557990	5.85516024
H	-2.95851207	-1.93723500	7.18062592
H	-3.43284392	-0.23186500	6.97602081
H	5.03297901	5.79313278	1.85095799
H	5.39196110	4.48511887	2.99971700
H	7.57953596	5.53729200	2.76556301
H	7.28964090	5.91262484	1.06066406
H	-6.01457119	-3.66211104	4.23995590
H	-6.56464720	-3.37956905	2.56443501
H	-6.16550922	-5.64023781	1.92922294
H	-6.58407497	-5.91855001	3.62889290
C	0.03029500	0.69001597	-2.20497799
C	-1.46001101	0.30695000	-2.13997197
C	-1.54631102	-1.04750597	-1.43711102
C	-0.99712402	-0.96355599	-0.01313600
C	0.54821599	0.76637900	-0.79334700
H	-2.01605701	1.06551397	-1.56231904
H	0.55871201	-0.10422800	-2.74856305
H	-1.76601899	-0.50922298	0.62102002
O	0.12022500	-0.01192700	0.13619500
O	0.17634900	1.95149195	-2.79918790
O	-2.00774908	0.15014499	-3.41480994
C	-0.58832699	-2.26316500	0.63849300
H	-0.39002699	-2.07361507	1.70523596
H	-1.45545304	-2.93757105	0.59416902
O	0.54041702	-2.82480597	0.01864200
C	1.31310904	2.10226202	-3.63621712
H	1.20537305	3.07318306	-4.12458992
H	2.24835300	2.08799791	-3.06670189
H	1.33406901	1.31355405	-4.39919615
C	-2.46538401	1.34178698	-4.03004694
H	-3.08156109	1.93097401	-3.33732700
H	-1.63721097	1.96506298	-4.37889910
H	-3.07481790	1.02661002	-4.87876511
C	0.79485899	-4.11142397	0.52815598
H	1.72321999	-4.46856785	0.07402900
H	0.91532600	-4.09558678	1.62103105
H	-0.02580000	-4.80110979	0.27802199
S	-6.65430880	-1.44202495	0.39876601
S	3.19564509	2.40762591	3.47269511
F	-6.67723799	3.47018099	-5.10753012
F	-6.59308290	4.27305412	-3.09791493
F	-4.77698183	3.99913692	-4.23016787
H	1.70610094	5.26370811	-2.09851694
H	7.74360323	3.14737701	2.29629707

H	8.64444637	3.83886290	0.93798000
C	6.56555700	1.71352506	0.57769197
C	7.19337511	0.88496703	-0.32106099
C	5.95438623	1.13923705	1.72652304
C	7.25086021	-0.52341002	-0.11041000
H	7.66623402	1.27820694	-1.21721900
C	5.94951582	-0.21327300	1.93121898
H	5.45269203	1.78825295	2.43621397
C	7.92503977	-1.38942897	-1.01360202
C	6.60389614	-1.08811200	1.02147901
H	5.44941521	-0.63099700	2.80145001
C	7.92049503	-2.74664688	-0.82027900
H	8.43164253	-0.95475203	-1.87247503
C	6.62807512	-2.49674797	1.20734704
C	7.26370001	-3.30752301	0.30254099
H	8.41073227	-3.40230489	-1.53232706
H	6.12344503	-2.91387010	2.07352710
H	7.25173521	-4.38521719	0.42698801
C	6.82825279	3.73809695	-0.97108603
H	6.85974121	4.83174610	-0.97467798
H	7.78388691	3.37835312	-1.36034298
H	6.03248310	3.41572499	-1.64828598
H	-4.20450115	-5.83355522	4.27518606
H	-4.17457294	-6.81892920	2.79652095
H	-2.61090899	-1.31001306	-1.33247101
C	-1.56172597	-3.21321797	-2.36201406
H	-0.99556202	-3.83236694	-3.06125212
H	-1.61947203	-3.73394489	-1.39759302
H	-2.57586908	-3.06955194	-2.75864506
O	-0.89011502	-1.98021603	-2.25322390
H	0.82136899	1.75413406	-0.44265801
O	-2.60043406	1.52503300	1.31544602
P	-2.18268108	2.84222293	0.73753703
O	-3.17844701	3.06348205	-0.53745699
O	-2.67983007	4.08822823	1.66490197
O	-0.74516898	3.03165507	0.34252700
C	-1.79772103	4.87508821	2.37677312
C	-1.92307198	6.25518417	2.25681710
C	-0.84077799	4.31125498	3.21515298
C	-1.07818401	7.07889986	2.99517202
H	-2.67525101	6.65585613	1.58499098
C	0.01793900	5.14384413	3.92799401
H	-0.77781200	3.23151302	3.31459999
C	-0.10422800	6.52859116	3.82722306
H	-1.17687094	8.15686703	2.91097307
H	0.77680898	4.70024681	4.56621695
H	0.55693698	7.17619896	4.39436817
C	-3.09381104	4.21711779	-1.30841506
C	-4.12029123	5.14931679	-1.21267796
C	-2.02856112	4.38841391	-2.18644595
C	-4.09183788	6.27216291	-2.03554797
H	-4.92271709	4.98371696	-0.50025302
C	-2.01183009	5.52024412	-2.99703312
H	-1.24247801	3.63960600	-2.22820997
C	-3.03962302	6.45894480	-2.92820692
H	-4.89781284	6.99702597	-1.98026597
H	-1.19045997	5.66311598	-3.69313788
H	-3.02270007	7.33237600	-3.57215190
C	4.08090115	0.14991900	-2.68646407
C	5.15292883	-0.83262402	-3.17760897
C	3.51804900	-0.29063699	-1.33116806
H	3.27151489	0.12720200	-3.42114902
H	6.05702782	-0.71607399	-2.55477810
C	3.07045293	-1.73884594	-1.41653800
H	4.28953505	-0.19130400	-0.55081999
C	4.35433817	-2.51797700	-1.77560496
H	2.64648795	-2.07932591	-0.46279600
H	5.14222813	-2.17547393	-1.08391798
C	6.59096622	-1.17553103	-4.97342587
H	6.51201487	-2.26534510	-4.89573479
H	6.70399284	-0.88962400	-6.01993084
H	7.47389507	-0.84176701	-4.41012287
C	4.31158876	-4.03047514	-1.59005702
H	4.08145714	-4.21965694	-0.53078097
H	3.52878809	-4.49581718	-2.19143200
O	4.72255182	-2.18315911	-3.09779000
O	5.58123493	-4.55677605	-1.89905405
O	5.42442799	-0.53843898	-4.49747086
O	2.43679094	0.56963599	-0.93194902
H	2.82754302	1.42350996	-0.60071898
C	5.64568901	-5.64556980	-2.82447696
C	5.04123688	-6.90152597	-2.19539595
H	5.56093216	-7.14323807	-1.26314104
H	3.97888494	-6.75597095	-1.97103906
H	5.12498188	-7.75486994	-2.87589407
C	4.95831394	-5.30363798	-4.15020800
H	5.25772381	-6.02131081	-4.92042112
H	3.86663103	-5.34443617	-4.07705879
H	5.24168777	-4.29500484	-4.46360588
C	7.14300919	-5.82859516	-3.05142593
H	7.33769512	-6.68681479	-3.70118499
H	7.55963802	-4.93039417	-3.51797295
H	7.64815617	-5.99040508	-2.09388304
C	-2.22633290	-4.60979509	3.18404102
H	-1.74247003	-5.59184599	3.17712808
H	-1.58042705	-3.89043307	2.67994404
H	-2.33334994	-4.30687189	4.22909117
C	-3.51885509	-4.98947906	1.01850998
C	-2.66796994	-5.99309301	0.53924698
C	-4.35155678	-4.33732319	0.10447400
C	-2.64709306	-6.34196997	-0.80830097
H	-2.01566005	-6.52736807	1.22476006
C	-4.35286093	-4.67990494	-1.24576700
H	-5.02186823	-3.55124402	0.43982700
C	-3.49700904	-5.67794704	-1.68046105
H	-1.98982406	-7.11671400	-1.18814099
H	-4.99829912	-4.17514181	-1.95793700
F	-3.46293497	-5.99182892	-2.98498392
O	4.59742785	1.46127295	-2.64132690
H	4.84167099	1.67254400	-1.72345197
O	2.07485390	-1.71956205	-2.41701102
C	1.71089196	-2.93771410	-3.01958704
H	2.53748894	-3.33903408	-3.61594796
H	1.37652004	-3.66869092	-2.27005792
H	0.87312901	-2.70587301	-3.67718792